INTERCONNECTIVITY AND WATER QUALITY OF SHALLOW AQUIFER AND THE RIVER SYSTEM IN THE KATHMANDU VALLEY

A THESIS SUBMITTED TO THE

CENTRAL DEPARTMENT OF GEOLOGY

INSTITUTE OF SCIENCE AND TECHNOLOGY

TRIBHUVAN UNIVERSITY

NEPAL

FOR THE AWARD OF

DOCTOR OF PHILOSOPHY

IN GEOLOGY

BY

RAMITA BAJRACHARYA

MARCH 2022

TRIBHUVAN UNIVERSITY

Institute of Science and Technology

DEAN'S OFFICE

Kirtipur, Kathmandu, Nepal

Reference No.:

EXTERNAL EXAMINERS

The Title of Ph.D. Thesis: " Interconnectivity and Water Quality of Shallow Aquifer and the River System in the Kathmandu Valley"

Name of Candidate: Ramita Bajracharya

External Examiners:

(1) Dr. Rajendra Bhandari
Ministry of Industry, Commerce and Supply
Kathmandu, NEPAL

(2) Prof. Dr. Sangam Shrestha
Asian Institute of Technology
Bangkok, THAILAND

(3) Prof. Dr. Futaba Kazama
University of Yamanashi
Yamanashi, JAPAN

October 12, 2023

(Dr. Surendra Kumar Gautam)
Asst. Dean

DECLARATION

Thesis entitled **"Interconnectivity and water quality of shallow aquifer and the river system in the Kathmandu valley"** which is being submitted to the Central Department of Geology, Institute of Science and Technology (IOST), Tribhuvan University, Nepal for the award of the degree of Doctor of Philosophy (Ph.D.), is a research work carried out by me under the supervision of Associate Prof. Dr. Naresh Kazi Tamrakar, Central Department of Geology, Tribhuvan University, Nepal and co-supervised by Associate Prof. Dr. Subesh Ghimire, Central Department of Geology, Tribhuvan University, Nepal and Associate Prof. Dr. Takashi Nakamura, University of Yamanashi, Japan.

This research is original and has not been submitted earlier in part or full in this or any other form to any university or institute, here or elsewhere, for the award of any degree.

Ramita Bajracharya

RECOMMENDATION

This is to recommend that **Ramita Bajracharya** has carried out research entitled **"Interconnectivity and water quality of shallow aquifer and the river system in the Kathmandu Valley"** for the award of Doctor of Philosophy (Ph.D.) in **Geology** under our supervision. To our knowledge, this work has not been submitted for any other degree.

She has fulfilled all the requirements laid down by the Institute of Science and Technology (IOST), Tribhuvan University, Kirtipur for the submission of the thesis for the award of a Ph.D. degree.

.....

Dr. Naresh Kazi Tamrakar

Supervisor (Associate Prof.)

Central Department of Geology, Tribhuvan University

Kirtipur, Kathmandu, Nepal

.....

Dr. Subesh Ghimire

Co-Supervisor (Associate Prof.)

Central Department of Geology, Tribhuvan University

Kirtipur, Kathmandu, Nepal

中村 高志 Takashi Nakamura

.....

Dr. Takashi Nakamura

Co-Supervisor (Associate Prof.)

University of Yamanashi, Japan

December 2023

Tel No.: 977-01-4332449
977-01-4333085
977-01- 4330405

TRIBHUVAN UNIVERSITY

CENTRAL DEPARTMENT OF GEOLOGY

OFFICE OF THE HEAD OF DEPARTMENT

Kirtipur, Kathmandu, Nepal

Ref No.

LETTER OF APPROVAL

18/12/2023

On the recommendation of Associate Prof. Dr. **Naresh Kazi Tamrakar**, Dr. **Subesh Ghimire** and Dr. **Takashi Nakamura**, this Ph.D. thesis submitted by **Ramita Bajracharya** entitled **"Interconnectivity and water quality of shallow aquifer and the river system in the Kathmandu Valley"** is forwarded by the Central Department Research Committee (CDRC) to the Dean, IOST, T.U.

Prof. Dr. Khum Narayan Paudayal

Professor and Head,

Central Department of Geology

Tribhuvan University

Kirtipur, Kathmandu

Nepal

Website: www.cdgltu.edu.np, Email: head@cdgl.tu.edu.np

ACKNOWLEDGEMENTS

I would first like to express my sincere gratitude to my supervisor Associate Prof. Dr. Naresh Kazi Tamrakar, and my co-supervisors Associate Prof. Dr. Subesh Ghimire and Associate Prof. Dr. Takashi Nakamura for their enormous support, suggestions, and guidance for each and every step of the research.

I express my sincere thanks to Prof. Dr. Khum Narayan Paudayal, Head of the Central Department of Geology, for his valuable suggestions and for providing the necessary information regarding this research.

I am grateful to the Institute of Science and Technology (IOST) and the Central Department of Geology, Tribhuvan University, Kirtipur for providing leave for the research. I would like to thank the members of the Central Department Research Committee (CDRC) Prof. Dr. Prakash Chandra Adhikary, Prof. Dr. Vishnu Dangol, Prof. Dr. Suresh Das Shrestha, Prof. Dr. Dinesh Pathak and Former Head Prof. Dr. Lalu Paudel for evaluating the progress and providing suggestions for the research. I express my deep gratitude to Prof. Dr. Megh Raj Dhittal, Former Head of, the Central Department of Geology, for providing necessary materials of the sedimentological map of the Kathmandu Valley.

My special thanks go to JICA, SATREPS project and project members for providing me with the opportunity to visit the University of Yamanashi, Japan. I would like to acknowledge the Interdisciplinary Center for River Basin Environment (ICRE) management committee, University of Yamanashi for supporting, valuable suggestion and all laboratory facilities for isotopic and chemical analysis during my stay in Japan. I like to express my thanks to Dr. Bijay Man Shakya and all lab members of the laboratory for their help and support in laboratory work.

I am very much thankful to the University Grants Commission (UGC), Nepal for providing me with partial financial support for the research.

I would like to thank my friends Ms Mamata Sayemi, and Mrs Anjita Joshi for their continuous support throughout the research. I am also thankful to my students Mr. Manish Shrestha, Mr. Bimal Bohara, Mrs. Bhawana Niraula, Mr. Ishwor Gyawali, Mr. Raj Kumar Lama, Mr. Dinesh Sharma, Mr. Ashish KC, Mr. Suman Maharjan, Mr.

Rhythm Rai, Mr. Bishal Maharjan and Mr. Indrajeet Kohar for their help during field survey.

I am very much thankful to Dr. Sarmila Tandukar, Dr. Rajani Ghaju Shrestha, Dr. Sadhana Malla Shrestha, and Dr. Amit Kumar Maharjan, for their continuous support in the research field. I am grateful to Dr. Bhesh Raj Thapa, Dr. Anil Aryal, Dr. Bikash Malla, Dr. Khadga Bahadur Shrestha and Dr. Rajit Ojha, for continuous help during my stay in Japan.

I would like to thank Dr. Upendra Baral and Dr. Ramesh Raj Pant for guiding with statistical analytic methods for data interpretation. I am also grateful to Mr. Nir Shakya for his continuous support.

I express my sincere thanks to external examiners Dr. Rajendra Bhandari, Prof. Dr. Sangam Shrestha and Prof. Dr. Futaba Kazama for their valuable comments and suggestions to improve this thesis. I am very much thankful to internal examiner Dr. Ranjan Kumar Dahal for managing time for format checking and his valuable suggestions. I am grateful to Prof. Dr. Binil Aryal, Dr. Surendra Kumar Gautam and all research committee members of the Dean's Office for their positive response and comments.

I would like to acknowledge Dr. Kamala Kant Acharya, Dr. Kabiraj Paudyal, Dr. Suman Panthee, Dr. Moti Rijal and Mr. Narayan Gopal Ghimire for their encouragement and support. I am very much thankful to Mr. Nir Shakya for his continuous support for this research. I am also thankful to all staff of the Central Department of Geology for their official support.

Last but not least I am very grateful to my husband and all my family members for their continuous support, cooperation, and suggestion from the beginning to the end of the studies to make it achievable.

Ramita Bajracharya

December 2023

शोध सार

भूमिगत र सतहको पानी जलस्रोत प्रणालीसँग सम्बन्धित छ । भूमिगत पानीको सम्बन्ध विभिन्न जलाशय जस्तै पोखरी, ताल, समुद्र र नदीमा देख्न सकिन्छ । तर मुख्य रूपमा नदीहरूसँगको सम्बन्धबारे धेरै अनुसन्धान भएको देखिन्छ । नदी र भूमिगत पानीको अन्तरसम्बन्ध एक प्राकृतिक प्रकृया हो जसमा नदी र भूमिगत पानी बिचमा पानी आदानप्रदान हुन्छ । पानी आदानप्रदानका प्रवाह नदीमा पानीको सतह र भूमिगत पानीको सतह, भूमिगत र नदीको सतह तथा किनारामा भएको sediment को hydraulic conductivity तथा नदीको प्रकारमा निर्भर गर्दछ । पानीको प्रवाह प्रकृयालाई विभिन्न गतिविधिहरू जस्तै ढलहरू सिधै नदीमा मिसाउने, भूमिगत पानीको सतह तलतल जाने, नदी तथा भूमिगतमा भएका sediment को आकार, आदिले असर गर्न सक्छ । यस्ता प्रकृयाहरूले नदी र भूमिगत पानीको अन्तरसम्बन्धलाई असर पार्ने तथा भूमिगत पानीलाई दुषित बनाउन सक्छ । तसर्थ नदी र भूमिगत पानीको अन्तरसम्बन्धको अनुसन्धान गर्न अति आवश्यक देखिन्छ । यस्ता अनुसन्धानले जलस्रोत व्यवस्थापन, विकास तथा नीतिनिर्माण गर्न प्रभावकारी भूमिका निर्वाह गर्दछ । हाम्रो देशको परिप्रेक्षमा यस विषयमा गरिने अनुसन्धानहरू निकै कम छन् । तसर्थ यो अध्ययन अनुसन्धान काठमाडौं उपत्यकाका नदी तथा खोलाहरू र नदी आसपासका भूमिगत पानीको अन्तरसम्बन्धमा केन्द्रित रहेको छ ।

यो अनुसन्धानको लागि हाइड्रोजन र अक्सिजनका stable isotope (δD and $\delta^{18}O$), पानीको रसायनिक आयन (cation and anion), नदी किनाराका sediment distribution pattern लाई मुख्य विधिको रूपमा प्रयोग गरिएको थियो । यसका साथसाथै तथ्याङ्क विश्लेषणका रूपमा Hierarchical Cluster Analysis (HCA) पनि प्रयोग गरिएको थियो । HCA विश्लेषण गर्नको लागि δD, $\delta^{18}O$, Na^+ र Cl^- को प्रयोग गरिएको थियो । HCA विश्लेषण गर्दा नदी र भूमिगत पानीको

नमुना एउटै समूहमा जम्मा भएमा नदी र भूमिगत पानीको अन्तरसम्बन्ध भएको मानिन्छ । यो अनुसन्धानको लागि नदी र भूमिगत पानीको नमुना सङ्कलन वर्षा (August 2017-165 नमूना) र सुख्खा (Februrary 2018- 162 नमूना) मौसममा गरिएको थियो ।

नदीबाट सङ्कलित पानीको दुवै मौसमको आइसोटीपिक संरचनाबाट नदीमा हुने बहाब आकाशे पानीकै कारणले भएको देखिन्छ । बागमती नदी, हनुमन्ते र गोदावरी खोलाबाट सङ्कलित पानीको आइसोटोपिक संरचनाबाट यो खोलाहरूमा सुख्खा मौसममा बाष्पीकरण हुन सक्ने सम्भावना देखिन्छ । त्यस्तै गरी भूमिगत पानीको आइसोटोपिक संरचना नदीको पानी भन्दा धेरै नै ठाउँ अनुसार परिवर्तनशील भएको देखिन्छ । भूमिगत पानीको आइसोटेपिक संरचना GMWL तथा LMWL सँग तुलना गर्दा भूमिगत पानी पनि आकाशे पानीले नै पूनर्भरण गरेको देखिन्छ । तर केही सङ्ख्यामा सङ्कलित नमूनामा वाष्पिकरण भएको पनि देखाउँछ ।

नदी र भूमिगत पानीको अन्तरसम्बन्धको अवस्था HCA को प्रयोग गरी पहिचान गरिएको छ । नदी र भूमिगत पानीको अन्तरसम्बन्ध स्थान र मौसम अनुसार परिवर्तनशील छ । वर्षा मौसमको विश्लेषणले लगभग ६८ प्रतिशत स्थानहरूमा नदी र भूमिगत पानीको सम्बन्ध नरहेको देखाउँछ । यी स्थानहरू विशेष गरी काठमाडौँको मुख्य शहरी क्षेत्रहरूमा रहेका छन् । तर सुख्खा मौसममा जम्मा ११ प्रतिशत स्थानहरूमा मात्र नदी र भूमिगत पानीको सम्बन्ध नरहेको देखाउँछ साथै ५४ प्रतिशत स्थानहरूमा नदीले भूमीगत पानीलाई पूनर्भरण (recharge) गरेको देखाउँदछ । दुवै मौसमको तुलना गर्दा जम्मा ९ प्रतिशत स्थानहरूमा मात्र नदी र भूमिगत पानीको अन्तरसम्बन्ध नरहेको देखाउँछ । यसबाट प्रमाणित हुन्छ कि काठमाडौं उपत्यकाका सबै नदीहरू आसपास रहेका भूमिगत पानीसँग अन्तरसम्बन्धित छन् ।

नदीको पानीको रसायनिक विश्लेषणले वर्षा मौसमको पानीलाई $Ca\text{-}HCO_3$ प्रकारमा छुटाइएको छ । तर सुख्खा मौसममा गोदावरी खोला र केही अन्य नदीका केही स्थानहरू बाहेकका अरू

स्थानहरू Na-K-HCO_3, Ca-SO_4 र Na-Cl-SO_4 प्रकारमा परिवर्तन भएको छ । यसले सुख्खा मौसममा नदीको पानीमा प्रदूषणको वृद्धि भएको सङ्केत गर्छ । रसायनिक आयनहरू बिचको सकारात्मक सम्बन्धले मानवीय क्रियाकलाप जस्तै ढलको सिधै मिसावट तथा नदीको किनारामा जम्मा गरिने फोहोरहरूको प्रभावलाई सङ्केत गर्दछ । त्यसका साथसाथै PO_4^- -P र SO_4^{2-} को सकारात्मक सम्बन्धले नदी आसपासका कृषि क्षेत्रमा प्रयोग हुने मल तथा किटनाशकहरूको प्रभाव देखाउँछ । सुख्खा मौसमको HCA विश्लेषणबाट गोदावरी खोला सबैभन्दा कम र हनुमन्ते सबैभन्दा बढी प्रदूषित भएको देखिन्छ ।

भूमिगत पानीको गुणस्तरको स्थिति NDWQS को सीमासँग तुलना गरी निर्धारण गरिएको छ । यसरि तुलना गर्दा NH_4^+-N र EC को मात्रा सुख्खा मौसममा वर्षामा भन्दा दोब्बर स्थानहरूमा वृद्धि भएको छ भने pH दश गुणाले NDWQS को सिमाभन्दा बाहिर परेको छ । मनहरा नदी तथा हनुमन्ते र बल्खु खोला आसपासबाट लिइएका भूमिगत पानीको करिब ८० प्रतिशत पानीमा NH_4^+-N वृद्धि भएको छ । नदी र भूमिगत पानीको अन्तरसम्बन्धले सुख्खा मौसममा धेरै नै प्रदूषित नदीको पानी मिसिएर भूमिगत पानी प्रदूषित भएको देखाउँछ ।

Keyword: नदी-भूमिगत पानीको अन्तरसम्बन्ध, रसायनिक विश्लेषण, आइसोटोपिक विश्लेषण, काठमाडौं उपत्यका

ABSTRACT

The groundwater and surface water are connected systems of single water resources. The connection condition can be noticed in different lands such as ponds, lakes, seas, and reservoirs but is mainly investigated at the stream reach scale. Interconnection of river-groundwater is a natural process that exchanges water between the river channel and water in subsurface areas. The exchange flow of water is dependent on the hydraulic conductivities of the river bed and aquifer sediments; the difference in water level in the river channel and adjacent groundwater; and the geometry of the river channel within the alluvial plain. The flow direction of water exchange is dependent on the hydraulic head between the river channel and the aquifer. The exchange process can be affected by anthropogenic activities such as sewage load in rivers, and a decline in the water table, which can alter the exchange condition, reduce connectivity, and contaminate aquifers chemically or biologically. Thus, the research related to interconnection is very essential to develop effective water resource management and policy as it can change the water quality and quantity of both water systems. However, there is a lack of such research in the case of Nepal. Hence, this study is focused to identify spatial and temporal interconnectivity between contaminated rivers of the Kathmandu Valley with peripheral groundwater.

The isotopic analysis of δD and $\delta^{18}O$, chemical analysis of cations and anions along with sediment distribution patterns on the surface and subsurface were major utilized methods of the research. Hierarchical cluster analyses were used for grouping water samples into clusters depending on isotopic and chemical composition (Na^+ and Cl^-). The combination of river and groundwater samples into a single cluster indicated the presence of interconnection. For this research, Water samples were collected in August 2017 (wet) and Feb 2018 (dry). A total of 165 and 162 samples were collected from rivers, dug wells and shallow tube wells in the wet and dry seasons respectively.

The isotopic composition (δD and $\delta^{18}O$) of the river presents a meteoric source for river discharge in both seasons. Samples from the Bagmati River, and Hanumante and Godawari Khola with enriched isotopic composition exhibit the possibility of evaporation during the dry season. The isotopic composition of groundwater shows spatially variable. Compared to GMWL and LMWL, groundwater is recharged through precipitation with some evaporation effect on samples.

Interconnection condition of the groundwater and river water has been identified using HCA. River-groundwater interconnection is spatially and temporally variable. Wet season analysis shows that about 68% of sites are non-connected with river water which is especially located at the center of core urban areas of the Kathmandu Valley. The percentage of non-connection sites is reduced to 11% in the dry season showing a dominant influent condition (54%) as the exchange process. Only 9% of sites which shows non-connected in both seasons imply that the rivers of the Kathmandu Valley are connected with adjacent shallow groundwater.

Chemical analyses of river water classify wet season as Ca-HCO_3 type. Except for Godawari Khola and a few other river sections; others are changed to Na-K-HCO_3, Ca-SO_4, and Na-Cl-SO_4 type, which indicates an increment of contamination during the dry season. The presence of a significant positive correlation between chemical ions indicates the influence of anthropogenic activities such as untreated municipal and industrial sewage discharge and leachate of solid waste disposal in river water. Additionally, a strong positive correlation of PO_4^--P with SO_4^{2-} suggests the effect of fertilizer and pesticides used in the river's peripheral agricultural land. Cluster analysis of dry season river water signifies that the Godawari Khola is the least polluted and the Hanumante Khola is a seriously contaminated river of the valley.

The quality status of groundwater is determined by comparing it with the limit of NDWQS. The percentage of dug wells exceeding NH_4^+-N and EC becomes doubled (60.9% and 8.5% respectively) in the dry season, whereas dug wells exceeding pH has become increased up to ten times (10.4%). About 80% of dug wells exceed the limit of NH_4^+-N from the Manahara River and Hanumante and Balkhu Khola in the dry season showing severe anthropogenic contamination in the shallow aquifers. The presence of river-groundwater interconnection as a dominant influent condition again indicates that the higher contamination in shallow groundwater is the result of groundwater recharge by heavily contaminated river water during the dry season.

LIST OF ACRONYMS AND ABBREVIATION

BAR : Balkhu River Water

BAW : Balkhu Groundwater

BMR : Bishnumati River Water

BMW : Bishnumati Groundwater

BR : Bagmati River Water

BW : Bagmati Groundwater

DR : Dhobi River Water

DW : Dhobi Groundwater

DO : Dissolved Oxygen

EC : Electrical Conductivity

ERT : Electrical Resistivity Tomography

GIS : Geographic Information System

GMWL : Global Meteoric Water Line

GR : Godawari River Water

GW : Godawari Groundwater

HCA : Hierarchical Cluster Analysis

HR : Hanumante River Water

HW : Hanumante Groundwater

ICS : Ion – Chromatograph

JICA : Japan International Co-operation Agency

KR : Kodku River Water

KW : Kodku Groundwater

KUKL : Kathmandu Upatyaka Khanepani Limited

LMWL : Local Meteoric Water Line

MR : Manahara River Water

MW : Manahara Groundwater

NDWQS : Nepal Drinking Water Quality Standard

NR : Nakhu River Water

NW : Nakhu Groundwater

SPSS : Statistical Package for Social Studies

USGS : United States Geological Survey

VSMOW : Vienna Standard Mean Ocean Water

LIST OF SYMBOLS

δD	: Stable Isotope of Hydrogen
$\delta^{18}O$	: Stable Isotope of Oxygen
Ω	: Unit of Resistivity
µS	: Micro Siemens

LIST OF TABLES

Page No.

LIST OF FIGURES

Page No.

LIST OF APPENDICES

TABLES OF CONTENTS

Page No.

CHAPTER 1

INTRODUCTION

1.1 Introduction

The interconnection of groundwater and river water is a natural process of the hydrological cycle. It indicates water exchange between the river bed/channel and water in the subsurface area by the lateral flow. The hydrologic exchange of these water bodies is controlled by the relative water stage of the river channel and adjacent aquifer head; hydraulic conductivities of both river channel and aquifer sediments; and geometry and position of the river channel within the alluvial plain (Sophocleous, 2002; Woessner,1999). The exchange direction of water is essentially dependent on the hydraulic head while the flow rate depends on geological materials or the hydraulic conductivity of sediments. Two types of flow conditions are distinguished in the river and groundwater interaction: (1) the influent condition- river water infiltrates into the aquifer; and (2) the effluent condition- groundwater exfiltration into the river (Ezugwu and Apeh, 2017; Winter *et al*., 1998; Woessner,1999). The flow condition can be changed with the alteration of the hydraulic head by different precipitation events, evapotranspiration and seasonal precipitation patterns (Sophocleous, 2002; Winter *et al*., 1998; Barrie *et al.*, 2022). Based on the exchange flow condition, numerous studies specify that exfiltration from shallow groundwater is the source of base flow in the dry season (Lee and Kim, 2007; Li *et al*., 2016; Menció and Mas-Pla, 2008; Winter *et al*., 1998; Zhang *et al*., 2016).

The river and aquifer interconnection can vary in space and time. The occurrence of interconnection is specifically observed in the peripheral areas of river channels. The dimension of the area is determined by hydrology, geology, geomorphology, and climatic and anthropogenic condition of the catchment area (Brunke and Gonser, 1997). Human activities like irrigation development, river channel modification, reservoir construction, over-extraction of groundwater, removal of natural vegetation and road extension along river channels can alter exchange conditions and reduce/increase connectivity between rivers and aquifers (Winter *et al*., 1998). The presence of clogging layers on a riverbed or bank can also reduce or stop the water exchange process (Derx *et al*., 2010). Clogging layers are generally characterized by tightly packed with

compact texture, low porosity and permeability showing high strength against river discharge (Brunke and Gonser, 1997; Sophocleous, 2002). Natural clogging layers are formed by the siltation of fine sediments during low discharge while external clogging layers are developed by sedimentation of an organic layer or dense algal mats on the river bed due to continuous sewage loading into the rivers.

The hydrological connectivity of rivers and groundwater was first given by Hynes in 1983, emphasizing the significance of the water balance and metabolism of streams (Brunke and Gonser, 1997). The research activities on interaction have increased gradually since the 1990s in different disciplines of hydrology, hydrogeology, ecology, biogeochemistry and environmental management and law (Fleckenstein *et al*., 2010). Maximum research has been carried out to evaluate areas of interconnection and the existence of exchange flow between river and aquifer on a regional as well as local scale (Guggenmos *et al*., 2011; Epting *et al*., 2018; Ali and Ajeena, 2016; Song *et al*., 2006; Huang and Han, 2016; Vrzel *et al.,* 2018; Quichimbo *et al.*, 2020: Modie *et al*., 2022). Some research also conducted to differentiate the effect of steady and dynamic flow condition on river-aquifer interconnection (Barrie *et al*., 2022).

In the advanced research development, the hydraulic connection of river water and groundwater is analyzed in the laboratory by using the sandbox experiments. This experiment can be used to find out the changing condition from the river-aquifer connection condition to disconnection (Wang *et al.,* 2016) as well as to analyze the river-aquifer hydraulic connection in different particle sizes of homogeneous sand (Gao *et al.,* 2022). Furthermore, interconnection research also focused on the deterioration of shallow aquifers by the transfer of toxic chemical and biological contaminations from polluted river water (Brindha *et al*., 2014; Zhu *et al*., 2019).

Understanding of interconnection between rivers and groundwater is very essential to improve effective water resource management and policy development as interaction can change the quality and quantity of both river and aquifer systems (Ezugwu and Apeh, 2017; Winter *et al*., 1998). Additionally, the study of river-aquifer interconnection needs to include before any river restoration. Removing clogging materials from the riverbed/bank during river channel widening can improve river-groundwater connectivity. At the same time, groundwater adjacent rivers has possibility to be contaminated by intrusion of polluted river water (Hoehn and Scholtis, 2011).

In the context of Nepal, water resource research is still focused on surface water or groundwater, treated as separate bodies. Numerous studies on the quality of Kathmandu Valley rivers have reported strong deterioration in downstream sections (Moog and Sharma, 1996; Devkota and Watanabe, 2005; Bajrachaya and Tamrakar, 2007; Kannel *et al*., 2007; Davids *et al*., 2018; Bajracharya *et al*., 2018; and Giri *et al.*, 2022), producing various water-borne viruses of diarrhoea, cholera, and dysentery (Pandey, 2006: Shrestha *et al.*, 2015: Shrestha *et al.*, 2015). Additionally, shallow groundwater quality studies of the valley also present a higher concentration of coliform bacteria, nitrate, EC, chloride and turbidity exceeding Nepal standards (Pathak *et al*., 2009; Diwakar *et al*., 2010; Pant, 2011; Prasai *et al*., 2010; Tamrakar and Shakya, 2013; Warner *et al*., 2008; Koju *et al*., 2014; Shrestha *et al*., 2015; Ito *et al.*, 2020; Sarkar *et al.*, 2022). Shrestha *et al*., (2016) also reported vulnerable groundwater pollution by nitrate in more than 50% of the groundwater basin of the Kathmandu valley. The high concentration of arsenic, iron and manganese is recently reported from the water sources associated with floodplain deposits (Sarkar *et al.*, 2022). Meanwhile, numbers of research also reported a decline in shallow aquifer water levels by over-extraction (Gautam and Prajapati, 2014; Pandey *et al*., 2012; Metcalf and Eddy, 2000), exceeding the rate of groundwater discharge that of recharge (Pandey *et al*., 2010). In such conditions, river water can recharge shallow aquifers and can contaminate groundwater by transferring toxic materials (Gautam *et al*., 2013).

However, research on the interaction of rivers and aquifers already developed since 1990's in developing countries, but it has just started in Nepal (Prajapati *et al.*, 2021; Neupane *et al.*, 2019; Hada *et al.*, 2019; Bajracharya *et al*., 2018; Malla *et al*., 2015). Only fewer research has concentrated on the river and aquifer interconnection of the Kathmandu Valley (Prajapati *et al.*, 2021; Bajracharya *et al*., 2018; Malla *et al*., 2015). The study conducted by Bajracharya *et al*. (2018) and Malla *et al*. (2015) include only a certain portion of the Bagmati, Bishnumati and Manahara rivers. There is still a lack of research which can present the interconnection of the whole river system with the aquifer within the valley.

This research attempts to present a scenario of interconnection between major rivers (the Bagmati, Bishnumati, Dhobi, Manahara, Hanumante, Godawari, Kodku, Nakhu and Balkhu Rivers) of the Kathmandu Valley with surrounding aquifers. This study also depicts a temporal and spatial variation in interconnection; and the effects of

interconnection on river and groundwater quality. A finding of the water quality status of the river, as well as groundwater nearby rivers channel, are the additional goals of this study. Information on river-aquifer interconnection is primarily very important for the government as well as local people to be aware of the linkage between two water systems; the impact of linkage in maintaining water quality; and activities of humans to impair these water systems. Identifying areas of interaction is useful for developing effective water resource management and policy-making by authorized organizations. Information on groundwater water quality can be useful for the local government to aware of people who are using that groundwater without treatment.

1.2 Geology of the Kathmandu Valley

The geology of the Kathmandu basin was early mapped by Stocklin and Bhattarai (1977) and Stocklin (1980). They included these rocks in the Kathmandu Complex which is divided into the Phulchoki Group and the underlying Bhimphedi Group. The hills to the north and the northeast are mainly composed of gneiss and schist belonging to the Bhimphedi Group whereas the southern and western hills are made up of the lower Phulchoki Group.

The Kathmandu basin comprises Plio-Pleistocene fluvial, fluvio-lacustrine, and fluvio-deltaic sediments (Yoshida & Igarashi, 1984; and Sakai *et al*., 2008). The Tokha Formation, Thimi Formation, Patan Formation, Gokarna Formation, Chapagaon Formation and Lower Terrace Deposit (Figure 1) are dominant formations around the river corridors (Dhital, 2015). The northern part of the river corridors is composed of the Tokha Formation, containing silt or silty sand and some gravel lenses. The central area of the study area is composed of the Patan Formation and Thimi Formation. The Thimi Formation consists of clay, peat, silt, sand, and gravel composed of gneiss and granite of the Shivapuri Range. Likewise, Patan Formation contains deposits of fluvial-lacustrine composed of sand, silt, clay, and peat.

The southern section is covered by the Gokarna Formation and Chapagaon Terrace Deposit. The Gokarna Formation mainly contains dark brown coloured, laminated arkosic sand, silty clay, and peat. The Chapagaon Terrace Deposit contains pebbles and cobbles of limestone and metasandstone. The Lower Terrace Deposit is mainly observed along the river corridors containing micaceous sand, pebbles, and granules (Dhital, 2015).

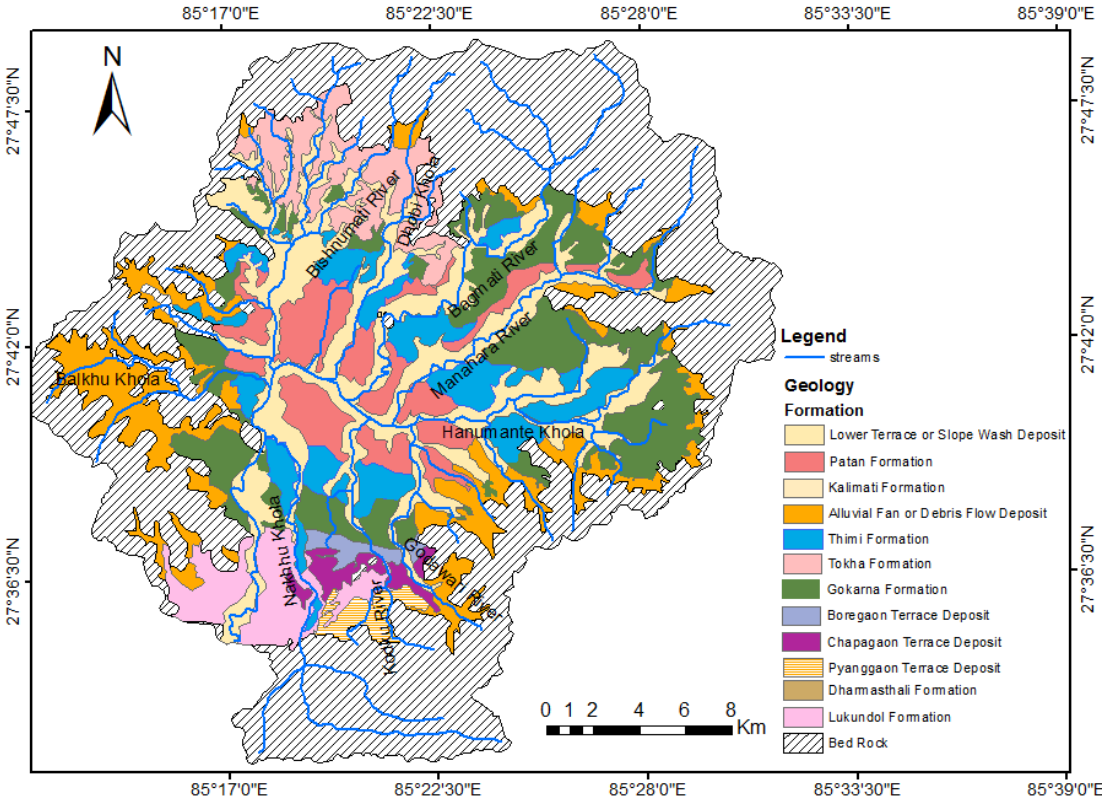

Figure 1: Sedimentological map of the Kathmandu Valley (Dhital, 2015)

1.3 Fluvial morphology

The Bagmati River is the mainstream of the Kathmandu Valley having numerous tributaries such as the Bishnumati River, the Manahara River, the Dhobi Khola, the Hanumante Khola, the Godawari Khola, the Kodku Khola, the Nakhu Khola and the Balkhu Khola possessing a centripetal drainage pattern (Figure 2). It is 7th order, a sinuous perennial stream originating from the eastern hill Nagarkot and stretches for about 51 km (Shrestha and Tamrakar, 2011). Anthropogenic activities such as direct effluent discharge from municipal and domestic, excavation of construction materials and urban encroachment are major sources of river contamination.

The Bishnumati River is one of the major tributaries of the Bagmati River from the northern part of the Kathmandu Valley. It is 6th order perennial stream that originates from the Shivapuri hills stretching for about 16.34 km (Shrestha and Tamrakar, 2011). It has a low sinuosity and low gradient in the main section with a high-gradient head (Tamrakar, 2009). Generally, upstream riverbank materials consisted of thick gravel with thin clay layers. Thick clay layers are dominant in the middle section which is decreased in the downstream section (Adhikari and Tamrakar, 2006). River bed

materials consist of gravel, sandy gravel and muddy gravel showing decreasing grain size downstream (Tamrakar, 2009). It is one of the most deteriorated rivers in the Kathmandu basin (Tamrakar, 2004).

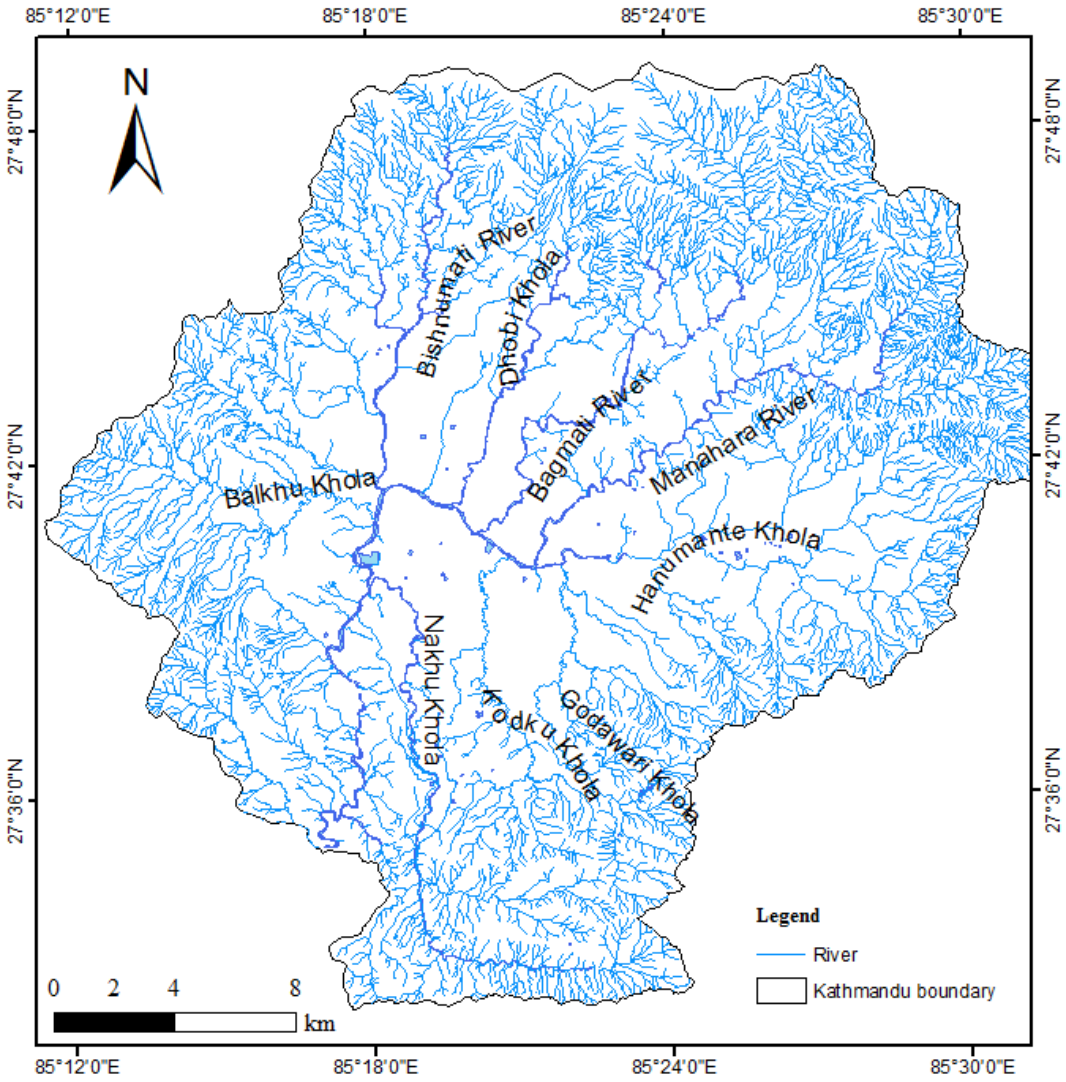

Figure 2: Drainage map of the Kathmandu Valley

The Bishnumati River is one of the major tributaries of the Bagmati River from the northern part of the Kathmandu Valley. It is 6th order perennial stream that originates from the Shivapuri hills stretching for about 16.34 km (Shrestha and Tamrakar, 2011). It has a low sinuosity and low gradient in the main section with a high-gradient head (Tamrakar, 2009). Generally, upstream riverbank materials consisted of thick gravel with thin clay layers. Thick clay layers are dominant in the middle section which is decreased in the downstream section (Adhikari and Tamrakar, 2006). River bed materials consist of gravel, sandy gravel and muddy gravel showing decreasing grain

size downstream (Tamrakar, 2009). It is one of the most deteriorated rivers in the Kathmandu basin (Tamrakar, 2004).

Dhobi Khola is a 5^{th} order stream stretching for about 17.82 km with a 30.74 km^2 watershed area (Shrestha and Tamrakar, 2011). River channelization and direct disposal of sewers are major disturbances in this river. Road extension along the river reduces river width creating flooding problems even in a small duration of rainfall.

The Manahara River is one of the longest tributaries of the Bagmati River from the northeast of the Kathmandu basin. It is 5^{th} order meandering river with cobble to sand-sized riverbed material (Bajracharya and Tamrakar, 2007). It extends for about 25.24 km covering 74.13 km^2. Bank erosion with channel shifting is a frequently occurring problem in this river.

The Hanumante Khola is one of the utmost contaminated tributaries that drain from the eastern part of the Kathmandu basin to the Bagmati River (Sada, 2014). It is a 6^{th} order stream extending up to 18.29 km with a 97 km^2 watershed area. Direct disposal of sewage and solid waste effluent from industries converts the Hanumante Khola into an open sewer during the dry season (Pathak *et al*., 2015).

The Godawari Khola is a southern tributary of the Bagmati River stretching for about 16.08 km with a 46.65 km^2 watershed area. It is 5^{th} order sinuous stream (Tamrakar and Bajracharya, 2013) with dominant riverbed materials of pebble to sand size particles (Karki and Tamrakar, 2016).

The Kodku River is also a southern tributary of the Bagmati River covering a length of 15.86 km with a 35.67 km^2 watershed area. It is 5^{th} order sinuous stream with riverbed material of coarse pebble to silt and clay (Tamrakar *et al*., 2013).

The Nakhu Khola is one of the longest southern tributaries of the Bagmati River covering a length of 25.98 km with a 58 km^2 watershed area. It is 5^{th} order meandering river with low sinuosity. Riverbed material is usually composed of pebble-grade material and fine sands in upstream and downstream sections respectively showing decreasing trends in grain size (Maharjan and Tamrakar, 2010). Human-induced activities such as the removal of riparian vegetation, quarrying of gravels, and construction of roads at the right bank along the river are major disturbing activities to the river corridors (Maharjan and Tamrakar, 2011).

The Balkhu River is one of the major tributaries of the Bagmati River from the western part of the Kathmandu basin. It is a 6^{th} order stream covering a length of 16.44 km with a 43.95 km^2 watershed area. The downstream section of the river is polluted by the disposal of solids and sewage and by various chemical effluents from nearby factories (Dhakal, 2006).

Natural as well as anthropogenic activities are responsible for changing the morphological features of rivers. The trend of precipitation in the Kathmandu Valley can change the slope and sinuosity of rivers. Generally, the decreasing trend of precipitation indirectly decreases discharge in perennial rivers reducing slope with increasing sinuosity (Shrestha and Tamrakar, 2011). The activities such as excavation of construction materials, channelization, road extension along the river channels, urban encroachment and reduction in the floodplain are common anthropogenic activities observed in all rivers (Bajrcharya and Tamrakar, 2007; Maharjan and Tamrakar, 2011; Sada, 2014).

1.3 Rational

The river system of the Kathmandu Valley originates from the surrounding Hills and collects at the centre of the basin (amphitheatre basin), where rivers are alluvial rivers as soon as they leave the bedrock at the surrounding portion of the Kathmandu basin. Along the river course in the alluvial portion of the channel, the riverbeds may or may not have connections with the shallow groundwater aquifer. The interconnectivity between the river and the shallow aquifer depends on geologic materials and their hydraulic conductivities; differences in the water stage of the river channel and well.

The connectivity of groundwater and surface water can show spatial and temporal variation throughout a river. The existence of river-groundwater connection specifies river reaches as losing (Influent- infiltration to groundwater) and gaining (effluent-exfiltration from groundwater). The river can change connectivity status from losing to gaining, or from gaining to losing, or connected to non-connected within the same river reach depending on the head difference between the river and the well. The hydraulic head can be changed depending on precipitation events and duration (single or multiple seasons); groundwater extraction and irrigation use of river water. The connectivity can only be present in certain segments of the river reaches also. In the case of Kathmandu Valley, previous research signify that the river water qualities of most of the rivers are

in deteriorating condition. In the name of restoration, different organizations remove surficial solid waste along the channel and bank from rivers like the Bagmati and Manahara. However, these activities can only improve the aesthetic appearance of river channels; they cannot improve the chemical and biological conditions of a river which has already deteriorated due to the direct disposal of sewer and leachate from solid waste deposited on or near river banks. Meanwhile, research on shallow groundwater also reported unsuitable quality from urbanized areas of the Kathmandu Valley. Consequently, if there is the presence of any interaction of the river section with adjacent groundwater, they can not only contaminate the shallow aquifer or river but also can affect water quantity in both water systems.

Thus for the enhancement of the river and adjacent shallow groundwater, it is very essential to study about river-groundwater interconnection. Additionally, transferring information about interaction to local government as well as people can develop alertness about the effects of human activities on the deterioration of both water systems.

1.4 Objectives

1.4.1 General objectives

The general objectives of the research are:

i. To understand the river and adjacent shallow groundwater interconnection in the Kathmandu Valley,
ii. To compare the seasonal variation of interconnection, and
iii. To establish a status of shallow groundwater along major rivers of the Kathmandu Valley.

1.4.2 Specific objectives

The specific objectives of the research are:

i. To prepare inventory data of wells, including data on well dimension; distance from the river channel and in-situ parameters of water
ii. To analyze physio-chemical parameters of water samples from groundwater and river water
iii. To analyze the isotopic composition of groundwater and river water samples

iv. To prepare a sediment distribution pattern map along river channels of five rivers
v. To analyze subsurface lithology by using ERT

1.4 Limitation:

i. Inventory data includes only those dug wells data which can easily measure during a survey and located within 100 m from the river channel. The interaction of river-groundwater is typically concentrated on the peripheral part of the channel so that limitation of 100 m is utilized for this research.
ii. The geology of Kathmandu valley depends on the map prepared by Dhital, 2015 and the map generated by DMG of 1:50,000 scales and other compilation of reports.
iii. Include only such chemical parameters of water which can be analyzed in the Ion Chromatography Machine available at the University of Yamanashi, Japan.
iv. Survey for ERT on only fewer location, as it is difficult to get open spaces to conduct resistivity survey due to dense urbanization along river corridors.

1.5 Layout of the dissertation

The dissertation includes six chapters. The description of the chapters are given below:

Chapter 1 - Introduction: This chapter presents the general background, needs of research and objectives of the research.

Chapter 2 - Literature review: This chapter presents reviewed literature on the interconnection of groundwater and river water using stable isotopes and chemical analysis, statistical analysis used to identify interconnection and quality analyses of Kathmandu Valley groundwater and river water.

Chapter 3 – Materials and methods- The material uses in the sample collection and resistivity survey is presented in this chapter. The specific analytic methods used for isotopic and chemical as well as for statistical methods for the interpretation of analyzed data are also included in this section.

Chapter 4 - Results and discussion: Finding about inventory of dug wells, prepared sediment distribution map, results of resistivity survey and isotopic as well as the chemical composition are included in this chapter. The interconnection condition of

groundwater and river water along major rivers is also included in this section. The quality status of dug wells are additional part observed in this chapter.

Chapter 5 – Conclusion and recommendation: This section includes overall research findings and their related recommendation.

Chapter 6 – Summary: This chapter summarizes the overall research including the introduction, methods and results.

CHAPTER 2

LITERATURE REVIEW

Relevant literatures were reviewed in different phases of the research to achieve objectives using appropriate methodology. The first phase of the review was focused to develop a methodology for the research, the second on data analyses and the third phase on data interpretation. The review was carried out on stable water isotope, chemical water quality analysis, resistivity survey for subsurface lithology, the geology of the related area, interconnection of river and groundwater and statistical analysis for data interpretation.

2.1 Stable isotopes

The study of stable isotopes began in the 1950s (Epstein and Mayeda, 1953; Darling *et al*. 2005). A study related to stable isotopes was carried out for rainfall by Craig, (1961). Generally, stable isotopes are one of the major indications of water movement. It is widely used to investigate the origin of water, recharge sources, groundwater age, and recharge processes in groundwater hydrology.

Water has two atoms of hydrogen and one atom of oxygen. Normal hydrogen atoms have one atomic mass (^{1}H), but a stable isotope of hydrogen has two atomic masses (^{2}H = D) which is commonly known as deuterium. Similarly, isotopes of oxygen have 17 and 18 atomic masses. A combination of $HD^{16}O$, and $H_2{}^{18}O$ presents heavy isotopic components of water. The composition of an isotope is expressed as parts per thousand or parts per mill (‰) of the isotopic ratio, R = D/H or $^{18}O/^{16}O$ to that of standard. Vienna Standard Mean Ocean Water (VSMOW) is used as standard water for isotopic analysis and the isotopic composition is expressed as delta (δ), defined by Craig, (1961):

$$\delta = \frac{\mathrm{R} - \mathrm{RVSMOW}}{\mathrm{RVSMOW}} * 1000\ ‰$$

Analysis of precipitation at a global and regional scale defines a linear relationship of the δD and $\delta^{18}O$, and is known as Global Meteoric Water Line (GMWL) and is given by:

$$\delta\mathrm{D} = 8\delta 18\mathrm{O} + 10$$

The excess of deuterium or d-excess can vary depending on the location of sample collection. The water lying below GMWL with a slope of less than 8 is mostly an indication of evaporation (Terwey, 1984). The relationship between δD and $\delta^{18}O$ can be changed depending on the isotopic composition of local precipitation. The relation defined by local precipitation isotopic composition is commonly known as Local Meteoric Water Line (LMWL) and is defined for individual countries. In the case of Nepal, isotopic composition in hydrogeology is in starting phase. Regional scale LMWL has still not been developed but the local scale was defined by fewer authors for far western Nepal especially for Banlek and Shikarpur (Matheswaran *et al*., 2019) and for the Kathmandu Valley (Chhetri *et al*., 2014 and Adhikari *et al*., 2020).

Chhetri *et al*., (2014) define an LMWL for Kathmandu based on rainfall samples collected from February 2011 to July 2012. They give a relation for LMWL as:

$$\delta D = 7.77\ \delta^{18}O + 3.10$$

This relation shows a lower slope with a lower intercept. Their research also presents the amount of effects in δD and $\delta^{18}O$ during the summer season and temperature effects in the winter season. Similarly, Adhikari *et al*., also determine LMWL for Kathmandu using the isotopic composition of rainfall collected from May 2016 to September 2018. They define LMWL as:

$$\delta D = 7.52 \pm 0.11\ \delta^{18}O + 4.92 \pm 0.76$$

These LMWLs defined by Chhetri *et al*., and Adhikari *et al*., have a lower slope with a smaller intercept compared to GMWL which indicates the evaporation of raindrops at Kathmandu. Results of Adhikari *et al*. indicate the influences of moisture source on the composition of isotope rather than the amount effect as suggested by Chhetri *et al*. They reported that the precipitation resulting from the Indian monsoon depletion in $\delta^{18}O$ during the mid-June to end of September as compared to rainfall created from the southern branch of the westerlies.

The temperature and amount effect of precipitation on oxygen isotope values of precipitation was also studied by Lachniet and Patterson (2009). They show an inverse correlation between rainfall amount and $\delta^{18}O$. The $\delta^{18}O$ values are decreased with an increase of 1.24‰ per 100 mm of monthly rainfall. The $\delta^{18}O$ of surface water is variable with distance from the coast and mean catchment altitude. About 84% of $\delta^{18}O$ surface

water is dependent on these two variables. The composition of $\delta^{18}O$ presents -1.9 to -2.4 ‰ km^{-1} and 0.69‰ per 100 km as an altitude effect and a continental effect respectively.

Liu and Yamanaka (2012) also present the altitude effect in the isotopic composition of precipitation. They reported -0.25 ‰ per 100m for $\delta^{18}O$ and -1.7‰ per 100m for δD. The isotopic composition of precipitation can be modified during the transition from precipitation to river water and groundwater (Gat, 1995). The isotopic modification is the result of isotope fractionation that includes the evaporation process, utilization of rainfall as runoff creation and groundwater recharge. The modification in a composition is controlled by morphological, climatic and ecological parameters.

Stable isotopes are taken as one reliable method in hydrogeology to identify: recharge sources of groundwater (Vanderzalm *et al*., 2011; Shakya *et al*., 2019; Nakamura *et al*., 2016; Zhou *et al*., 2017). Chemical and stable isotopes of hydrogen and oxygen were used to identify sources of groundwater recharge in the Nile aquifer system, in Upper Egypt (Awad *et al.*, 1997). The values of stable isotope were plotted on δoxygen-18 versus δ deuterium. From this plot, the sources of groundwater were determined. A combination of the chemical and isotopic composition of groundwater was also investigated using the plot of oxygen-18 and deuterium versus chlorinity of water. The variation of the isotopic data with chloride ion (Cl^-) concentration was used to identify different possible recharge sources.

The concentration of tritium (^3H), helium (^3He) and isotopic abundances of hydrogen ($^2H/^1H$) and oxygen ($^{18}O/^{16}O$) were analyzed to identify groundwater recharge sources, estimate groundwater movement rate and measure aquifer vulnerability (Kay *et al.*, 2002). The isotopic data on helium and tritium was used to find out the age of water whereas the isotopic content of deuterium and oxygen-18 was used to identify sources.

Stable water isotope (to identify the sources of water), sodium and chloride ratio (to distinguish between recharge sources and quantify their relative contribution) and boron (to identify the presence of effluent) are used by Vanderzalm *et al*., (2011) in alluvial basins in arid central Australia. This study used aqueous geochemistry to create the hydrogeochemical condition by 1) refining the contribution of multiple natural and anthropogenic recharge sources estimated from hydraulic data and 2) defining the methods leading to the hydrogeochemical development of groundwater following the

recharge. They explained that the value of Na/Cl ratio greater than 1 has a high influence on wastewater and groundwater throughflow on the groundwater. The plot of deuterium versus oxygen 18 and oxygen 18 versus boron was used to find out potential sources of recharge.

Physio-chemical and water isotopes of the Bagmati and Bishnumati Rivers and surrounding groundwater were studied by Malla *et al.*, (2015). The physio-chemical values indicate severe contamination in river water along the Bishnumati River and adjacent shallow groundwater due to untreated sewage discharge into the river. The clustering of river water and shallow groundwater together indicates a possible interrelationship between them. The fractional contribution of the river water to groundwater was also calculated using the isotope mass balance approach and gives the result that about 30% -40% of river water is mixed in the Bagmati river corridor well and 45%-50% mixed in the Bishnumati river corridor wells indicating possible harms due to mixing of polluted river water.

Stable isotopic composition is widely used for the identification of the connection conditions of surface and groundwater. Numerous studies used δD and $\delta^{18}O$ to determine the connection condition of surface and groundwater (Terway, 1984; Yang *et al*., 2018; Li *et al*., 2016; Yang *et al*., 2012; Mohammed *et al*., 2016; Ali and Ajeena, 2016; Derx *et al*., 2010;).

2.2 Groundwater and surface water interaction

The study on groundwater and surface water interaction was first started in the 1980s and has then grown steadily over the last two decades (Fleckenstein *et al.*, 2010). The interaction of surface water and groundwater can be affected by the geology of subsurface areas, topography and climatic condition. Geological information about the areas can give information about hydraulic conductivities. Additional information on topography and configuration of water tables provides the pattern of groundwater flow (Sophocleous, 2002). The direction of groundwater flow in hydraulically connected river-groundwater interaction is distinguished into two types: 1) influent condition: infiltration from riverbed indicating recharge of the aquifer; and 2) effluent condition: exfiltration or drain of groundwater into rivers indicates aquifer-fed rivers (Brunke and Gonser, 1997; Sophocleous, 2002). The condition of effluent can be changed influent depending on the climatic condition. Normally, base flow in the river is contributed by

groundwater in low precipitation conditions (effluent). But in the case of high precipitation, interflow and surface runoff are increased which has increased hydraulic pressure at the riverbed to infiltrate into the subsurface changing conditions from effluent to influent.

The interaction of rivers and groundwater can play an important role to reduce the flood level and recharge the aquifer during high precipitation conditions. During flooding, the river loses water by infiltrating the bank, which diminishes the water level. The capacity of bank storage depends on the storage capacity and transmissivity of the aquifer; and the duration and intensity of precipitation events. In a dry season, stored water on the bank is released into the river, contributing to river discharge (Brunke and Gonser, 1997; Sophocleous, 2002).

The amount and direction of water exchange can also be dependent on the type of stream segment.

1. A straight or gorge stream normally flows in a single and stable channel. This type of river section shows insignificant lateral and vertical exchange processes.
2. The meandering river shows a sinuous pattern with low velocity containing a fine suspended load which can cause the formation of a clogging layer at the riverbed and reduce the interaction rate of river-groundwater.
3. A braided river has multiple channels with high permeable sediments, indicating an exchange process both horizontally and vertically.
4. Anastomosed rivers also having multiple channels with low permeable fine-grained sediments shows manifold river-groundwater interaction.

Exchange flow condition in river-groundwater interaction can be affected by numerous human activities such as agricultural development, urban and industrial development, modification to the river channel, construction of reservoirs and removal of natural vegetation from river channels (Ezugwu and Apeh, 2017; Winter *et al*., 1998). Exchange flow conditions can be measured by 1) measuring water level in river channels as well as in wells or piezometers; 2) installing stream gauging; 3) comparing discharge, and 4) conducting tracers on stream channels (Woessner (1999).

The connection of GW-SW can appear in three different conditions such as gaining, losing and losing disconnected. Losing disconnected conditions in a stream is possible when there is the presence of an unsaturation zone between the river bed and the

groundwater table. This condition occurs when certain hydraulic conditions combine to control the water movement down from the river into the saturation zone of an aquifer.

Different methods are used to determine the connection condition of river-groundwater status. Connection status can find out by estimating different parameters such as hydraulic conductivity of the streambed (including the presence of a clogging layer); rate of infiltration through the streambed (by using the Darcy flux method); source of recharge to the alluvial aquifer (using environmental tracer); and reach-scale infiltration rate (by using differential gauging) (Brownbill *et al.,* 2011).

The vertical hydraulic conductivity (K_v) of the streambed was measured by using constant-head and falling-head tests. These values were divided into low (with K_v ranging from 10^{-10} to 10^{-6} ms^{-1}) and high hydraulic conductivity sites (with K_v ranging from 10^{-5} to 10^{-3} ms^{-1}). The low Kv streambeds were lined with clays while the high K_v was generally a mixture of silt, sand and coarser sediments. The source of recharge was evaluated by using salinity and stable isotope of water.

Kalbus *et al*., (2006) reviewed different types of measuring methods for the groundwater–surface water interactions. They provide various methods that are currently used for measuring the interaction between groundwater and surface water. The methods are grouped into heat tracer methods, direct water flux measurement, methods based on Darcy's Law, and mass balance approach.

Physio-chemical and microbial analysis was also used to find out the connection conditions of groundwater and surface water. Gautam *et al.,* (2013) used physio-chemical and microbial parameters to find out the possibility of penetration of the Bagmati River towards groundwater. For this study, they collected samples from five stations such as Gokarna, Tilganga, Sankhamul, Teku and Sundarighat in the winter season, monsoon and post-monsoon. From each station, one river water sample with six groundwater samples from both banks, located within 50 m, 50-100 m and 100-150 m distances from the collected river sample. Analysis of river water indicates minor contamination in the winter season and got severely degraded in urban areas. Groundwater samples were analyzed by using the regression method using parameters such as pH, conductivity, chlorides, free carbon dioxide, alkalinity, hardness, nitrate, ammonia, iron and orthophosphate and showed that these parameters decreased as the distance from the river bank increased. Microbial analysis, mainly focused on the

coliform count presented that 88% of contaminated samples. This study suggests that groundwater along the Bagmati River could not be used for consumptive purposes without treatment. This study also reveals the possibility of polluted river water intrusion towards groundwater. A similar type of research was conducted in Budha Nullah, India by Singh *et al.,* (2013). Analysis of surface water reveals high values of total dissolved solids, chlorides, chemical oxygen demand and many heavy metals such as Cr, Mn, and Ni. The presence of high TDS and heavy metals suggests unsuitability for drinking purposes. Analysis of soil indicates good condition for leaching and water percolation. Thus they concluded that the presence of impurities and heavy metals in groundwater is due to the intrusion of surface water of Budha Nullah.

Topographic survey of river and groundwater level is also used to identify losing and gaining stream. Prajapati *et al*. (2021) performed topographic survey in the river corridors of the Kathmandu valley in 2018 and 2019. They concluded that the pre-monsoon wells has only 12% (2018) and 44% (2019) higher water level than nearby rivers presenting dominantly as a losing stream. Contrarily, in the case of post-monsoon, wells has 69% (2018) and 70% (2019) higher water level than adjacent river and indicate dominant of gaining river.

A dominant and reliable method for river-groundwater interaction studies is stable isotopes of hydrogen and oxygen. Numerous research conducted in different countries used this method for the investigation of river-groundwater interaction (Ali and Ajeena, 2016b; Brenot *et al*., 2015; Hunt *et al*., 2005; Liu *et al*., 2006; Song *et al*., 2006; Banks *et al*., 2011; Yang *et al*., 2012; Li *et al.*, 2016; Zhang *et al*., 2016a; Krishna *et al.*, 2017; Vrzel et al., 2018; Modie *et al*., 2022).

A multivariate method such as Hierarchical Cluster Analysis (HCA) is also a widely used method in the study of river-groundwater interaction (Guggenmos *et al*., 2011; Sakakibara *et al*., 2016; Huang and Han, 2016). HCA is a tool used to reduce datasets by dividing a set of observations into number of clusters depending on the statistical similarity of selected parameters. Observation encloses within a single cluster shows statistically similar while those grouped in different clusters indicate different values. Squared Euclidian Distance is used to measure statistical similarity between sampling sites and a distance can be represented by variation between values of samples. The Wards method is used to categorize samples (Huang and Han, 2016).

2.3 Hyporheic zone

The hyporheic zone represents the area under and adjacent to the streambed which has mix water of groundwater and surface. The definition of the hyporheic zone is a little bit different based on the academic discipline. The review of the hyporheic zone by different academic disciplines was combined in the Science report of Environmental Agency UK (2005). Based on the hydrogeologists, the hyporheic sediments are carbon and microbial community rich as compared to the aquifer sediments. The hyporheic zone can be delineated by ecology and community structure (microbial, macroinvertebrate fauna); tracer tests (chloride, chromium, nitrate); geophysical investigation (ground-penetrating radar, GPR, electrical conductivity and resistivity methods); and temperature profiling.

Hyporheic exchange mechanics and their environmental effects on mountain rivers were given in detail by Tonina and Buffington (2009). According to this research, the hyporheic exchange can be formed by transmitting surface and groundwater through permeable sediments in the peripheral areas of the river. The exchange process is variable depending on hydraulic conductivity streambed pressure, bed mobility, and alluvial volume. They studied multiple effects on the riverine ecosystem and different factors for the delineation of the hyporheic zone.

Characteristics of the hyporheic transport process were studied by Ward *et al*., (2010) during solute tracer studies and interpretion of electrical geophysical data. Stream tracer experiments coupled with solute transport modelling are frequently used to characterize mobile subsurface storage and immobile subsurface dynamics. They couple simulations of near-surface electrical resistivity (ER) methods with conservative solute transport to directly compare solute transfer with ER interpretation, and determine the ability of ER to predict spatial and temporal trends of solute distribution and transport in stream-hyporheic systems. Results showed that temporal moments from both ER and solute transport data are well correlated for locations where advection is not the dominant solute transport process.

2.4 Groundwater recharge

Groundwater management of the Kathmandu Valley was studied by JICA (1990). They studied about availability of groundwater recharge in the valley and found two main

problems to recharge: (1) the extensive spreading of the lacustrine layer interbedded with impermeable black clay which prevents easy access to the recharged groundwater (2) the poor quality of groundwater in the central part of the valley is caused by an excessive accumulation of decaying organic matter. This would appear to be the source of ammonia and nitrogen which are found in the valley. In this study, Kathmandu valley is divided into three groundwater districts based on the chemical properties of groundwater and geological structure.

Table 1: Division of groundwater districts (JICA, 1990)

Northern Groundwater District (NGD)	Central Groundwater District CGD)	Southern Groundwater District (SGD)
Areas: Bansbari, Dhobi Khola, Manohara, Bhaktapur and Gokarna Materials: Highly permeable unconsolidated materials which are interbedded with several impermeable fine sediments	Areas: Central Kathmandu Materials: Very thick (200 m) black clay with some lignite	Areas: Along the Bagmati river between Chobhar and Farping area Materials: Combination of thick impermeable clay with low permeable basal gravel.

The shallow aquifer mapping of Kathmandu Valley was conducted by Groundwater Resources Development Board (GRDB, 2014) (Figure 3). This study was based on secondary data. In this study, secondary data available on geology, hydrogeology, precipitation, discharge, aquifer thickness and landuse are used to prepare thematic maps which were then overlaid in ArcGIS to prepare shallow aquifer potential maps. According to this report, the valley was divided into three potential zones:

1. The good potential area is mostly extended to the northern and northeastern part of the valley covering the areas of Tokha, Gongabu, Dhapasi, Jorpati and Mulpani. These areas fall mostly under Tokha Formation and Gokarna Formation and the aquifer thickness is more than 10 m.
2. The fair potential area is distributed in the northern and southern parts covering areas of Sunakothi, Harisiddhi, Kamalpokhari, Sinamangal and Lazimpath. This area has less build-up area and falls in the northern groundwater district.
3. The poor potential area is distributed around the central part of the valley covering Bhaktapur, Balkot, Balkumari, Sanepa and Balambu. Geologically this area consists of Kalimati Formation and covers most of the build-up areas of the three cities of Kathmandu, Lalitpur and Bhaktapur.

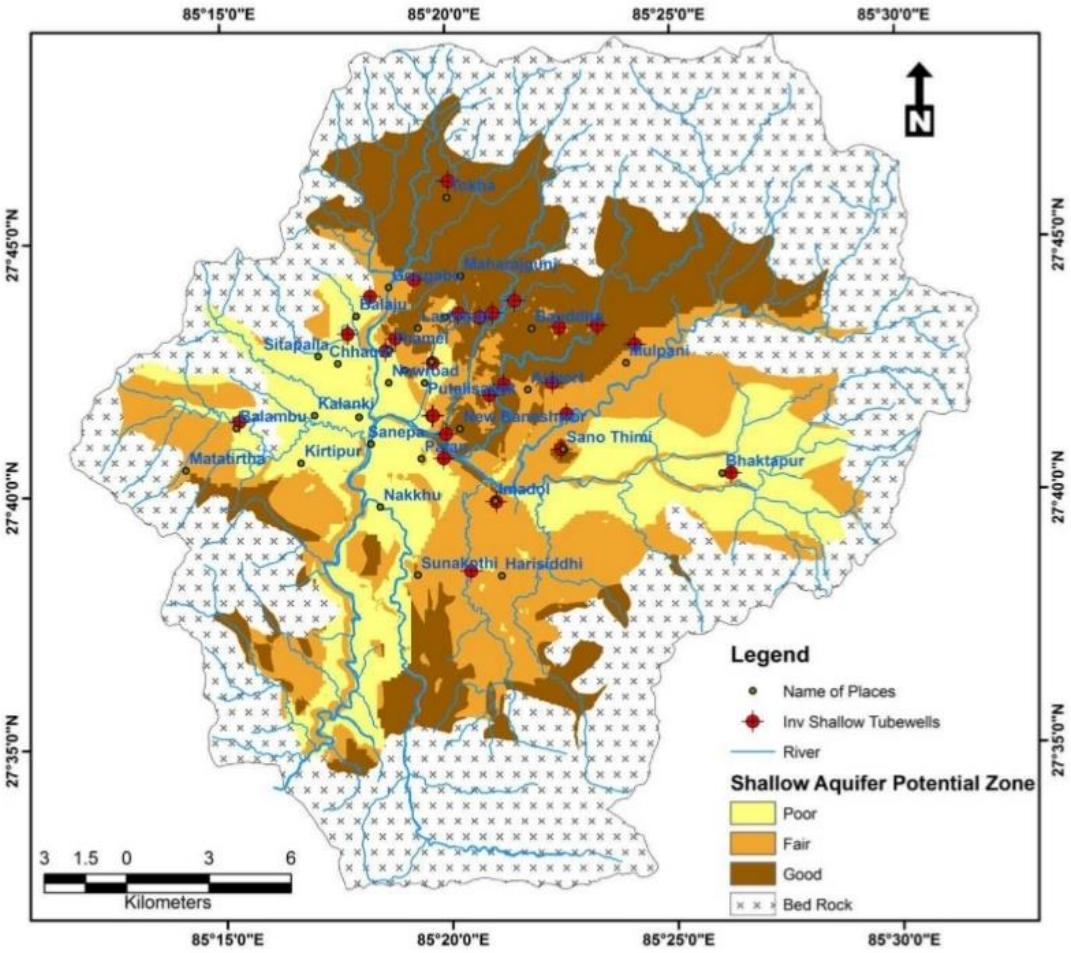

Figure 3: Shallow aquifer potential map of the Kathmandu Valley (Source: GWRDB, 2014)

Pandey *et al.*, (2010) focused their study to evaluate the groundwater environment of Kathmandu valley. In this research, the groundwater environment is evaluated by using natural and social systems together to define the origin of stress and expected impacts and responses to restore a healthy environment. This research presents that the increase in population density, urbanization and increasing hotels are responsible to exceed groundwater extraction over recharge (extraction=21.56 and recharge=9.6 million m^3/y), decrease in water level (13-33m during 1980-2000 and 1.38-7.5m during 2000-2008), the decline in well yield (4.97-36.17l/s during 1980 to 1998) and degrading in water quality.

2.5 Water quality:

Table 2 presents some of researches related with groundwater quality of the Kathmandu Valley. The quality of groundwater especially depends on the composition of recharging water, mineralogical composition in the aquifer, and the impact of human

activities. The quality of water is determined by using different physical, chemical and biological analyses. The contamination in shallow aquifers shows seasonal variation as more contaminations were found in the wet season compared to the dry season (Pathak *et al*., 2013).

Table 2: Summary of studies on the Kathmandu valley's groundwater quality

Author/year	Water source	Major Ions	Results
Bittener, 2000	Shallow and deep well	Nitrate	Higher Nitrate and lower ammonia at shallow depth (less than 50 feet)
Prasai *et al*., 2007	tube wells, wells, taps and stone spots	total plate and coliform bacteria	82 to 92% of drinking water samples cross the WHO guidelines
Warner *et al.*, 2008	Deep and shallow tube wells, tap water and dhunge dhara	nitrate, ammonia, heavy metals, total coliform and E-coli	Coliform and E-coli exceeds in 94 and 72% of samples; nitrate, ammonia exceeds in 11 and 45% samples
Pathak *et al.*, 2009	shallow tube well, dug wells and stone spouts	Nitrate	16% of the sampled wells exceeded WHO guidelines
Panta, B.R. (2011)	shallow wells, tube wells and deep tube wells	coliform and physical parameters	Iron and total coliform exceeds WHO guidelines in shallow wells
Tamrakar and Shakya, 2013	deep groundwater	turbidity,total alkalinity, total hardness, iron and ammonia	Dominant sites exceeds NDWQS
Nakamura *et al*., 2014	Dug wells, river water, sewage water	Nitrate compounds, chloride, stable isotopes of nitrogen, oxygen and hydrogen	Higher concentration of nitrate-nitrogen and ammonia-nitrogen,
Shakya *et al.*, 2019	Shallow dug wells	Nitrogen, chloride and iron	Lower fluctuation of nitrogen compounds in the clay-bearing areas than in the gravel-bearing areas
Bhandari *et al.*, 2021	dug wells, tube wells, deep tube wells and tap water	chloride, total hardness, copper, nitrate, sulfate, and total coliform	Total coliform exceeds NDWQS in 84.6% samples

Groundwater vulnerability assessment and its risk of groundwater pollution were studied by Shrestha *et al*., (2016). This research indicates that more than 50% of the Kathmandu basin, especially from the Northern district is susceptible to groundwater pollution and low vulnerable areas are located in the Central and Southern groundwater districts.

Spatial-temporal variation of river water qualities of the Kathmandu Valley is studied by Kannel *et al*., (2007) and Pathak *et al*., (2015). Both of the research presented an increased chemical load in the core urban areas of the valley due to untreated municipal sewage. Cluster analyses represent river water into two major clusters 1) a highly contaminated zone and 2) a less contaminated zone. Table 3 present some researches related to water quality of the Kathmandu Valley's river water.

Table 3: Summary of reseaarches on river water quality of the Kathmandu Valley

Authors/Year	River Name	Major parameters	Results
Moog and Sharma, 1995	Bagmati river and tributaries	Biological assessment	Deterioration of water quality
Devkota and Watanabe, 2005	Bishnumati River and adjacent groundwater	Solid waste and water quality	High conductivity, nitrate, nitrite, and COD concentrations in river and shallow wells
Kannel *et al*., 2007	Bagmati River and tributaries	Physical and chemical parameters	Urban water qualities were significantly poor as compared with rural. The main river and its tributaries were equally polluted in urban areas.
Paudyal *et al.*, 2016	Bagmati river and tributaries	Major ions (Na^+, NH_4^+, Mg_2^+, Ca_2^+, Cl^-, SO_4^{2-}, and NO_3^-) and elements (Mn, Cd, Cr, Co, Zn)	Ionic and elemental concentration higher in lower sections
Mishra *et al*., 2017	Bagmati River	DO, BOD, Water evaluation and planning model (WEAP)	Inefficiencies of current practice of discharging untreated sewage into the surface water to improve river water
Davids *et al*., 2018	Bagmati river and tributaries	Rapid steam assessment (RSA), water quality, landuse	Downstream in deteriorating condition
Ghimire *et al.*, 2022	Bagmati River	Water quality control technologies	Descriptive Solution Model

The influence of bedrock on the water flow and quality in the Jhikhu Khola watershed was explained by Nakarmi and Li (1998). They used data which are derived from the monitoring of rainfall variation, temperature fluctuation, and measurement of discharge and electrical conductivity of the stream. Discharge was measured at 18 spots and conductivity at about 100 sites. They used these data to compare with geology and found that more than 75% of the annual rainfall occurring between June and September recharges the groundwater. The area composed of carbonate rock shows higher conductivity whereas the area composed of mica schist and quartzite has little flow with low conductivity.

2.6 Electrical resistivity tomography (ERT)

Electrical surveys are one indirect method to determine subsurface lithology by using resistivity variation beneath the surface. The resistivity can be measured by injecting current through two current electrodes into the ground and measuring the resulting voltage difference at two potential electrodes. From the current (*I*) and voltage (*V*) values, an apparent resistivity value is determined:

$$p_a = K\mathrm{V} / \mathrm{I}$$

where K is the geometric factor depending on the four electrodes arrangement. The calculated resistivity value is not the true resistivity of the subsurface, but an apparent value which is the resistivity of a homogeneous ground which will give the same resistance value for the same electrode arrangement. The true subsurface resistivity can be determined from the measured apparent resistivity values using a computer program (Loke, 2000).

Binnie and Partners first studied the resistivity of the Kathmandu Valley in 1973. Similarly, JICA (1990) also studied resistivity by vertical electrical sounding. They correlated resistivity with the sediment type of the valley. They divided valley sediments into five categories: 1) clay and silt (<15 Ωm); 2) sandy clay (15-50 Ωm); 3) clayey sand (50-100 Ωm); 4) sand and gravel (100-500 Ωm) and 5) Basement rock (>500 Ωm).

Electrical Resistivity Tomography (ERT) is one geophysical imaging technique which is extensively used to investigate subsurface lithological variations, geological structure, and groundwater conditions. It is being increasingly used in environmental

and engineering site investigations. It is also used as a tool for assessing groundwater/ surface water interactions within streams (Nyquist *et al.*, 2007).

2D ERT is also used to investigate groundwater pollution or contamination of shallow aquifers (Uchegbulam & Ayolabi, 2014; Gardi, 2014; Chambers *et al.*, 2006)**.** They used Wenner array methods with different electrode spacing. This 2D ERT gave information about the changes of resistivity in the vertical direction as well as in the horizontal direction along the survey line. The variation in value depends on subsurface lithology and fluid type. The high resistivity formations are due to the presence of hydrocarbon within the subsurface.

CHAPTER 3

MATERIAL AND METHODS

3.1 Materials

A variety of materials was used for the collection of primary and secondary data to analyze the interconnection conditions of groundwater and river water. Details are described in the following sections.

3.1.1 Maps

The geological map of Kathmandu Valley published by the Department of Mines and Geology (1998) (Shrestha, *et al*., 1999) and the geological map of Kathmandu Valley prepared by Dhital (2015) were used to collect information about fluvial-lacustrine deposits. Similarly, topographic maps were used to prepare base maps for the preparation of sediment distribution pattern maps along river corridors. Google maps from Google earth were used as additional information.

3.1.2 Reports and articles

Reports and articles related to the water quality and geology of Kathmandu Valley were collected from Ground Water Resource Development Board, Nepal Geological society and different journals. Additionally, reports and papers about the river-groundwater interconnection of different countries were also collected for the development of methodology.

3.1.3 Equipment

Portable devices, namely, a DO meter (Mettler Toledo SG3-ELK, Greifensee, Zurich, Switzerland) and a pH/EC meter (Mettler Toledo Duo, Greifensee, Zurich, Switzerland) used for in-situ parameter measurement of water (Figure 4). A water depth logger was deployed for the water depth measurement. Measuring tape, plastic buckets and plastic sample bottles were used for sample collection.

A fully automatic instrument, SYSCAL R1 Plus SWITCH 48 was used for the ERT survey to measure the apparent resistivity of the subsurface materials (Figure 5). The list of equipment and needed accessories for this instrument is presented in Table 4.

Figure 4: DO and pH/EC meter

Table 4: List of equipment for 2D- accessories ERT survey using SYSCAL R1PLUS SWITCH 48

S. N.	Description	Quantity	Country of Origin	Style/Part No.
1	Resistivity meter	1 set	France	SYSCAL R1 PLUS SWITCH 48
2	Multicore cable	4 reels	France	Each reel with 12 electrodes; separated at 10m spacing
3	Electrodes	96 pieces	France	Stainless steel electrodes
4	Connecting box	2 set	France	Connecting boxes to connect two multicore cables
5	External Battery	1 set	India	80 Ah DC battery to supply electricity to the transmitter

3.1.4 Software

ArcGIS software was used for the preparation of different types of maps while SPSS was used for the statistical analysis of chemical and isotopic data.

The ELECTRE PRO software manufactured and distributed by IRIS was used to generate sequence files in the instrument SYSCAL R1 Plus SWITCH 48. Another software PROSYS was used to upload a sequence file into the instrument and to download data from the instrument. PROSYS is also used for data preprocessing to

filter high-quality data before tomographic inversion. The measured and preprocessed apparent resistivity data was used to obtain the resistivity models after inversion. For inversion or forward modelling, RES2DINV software (Loke, 1994; Loke, 1997; Saad *et al*., 2012; Ozel *et al*., 2017) manufactured and distributed by GEOTOMO was used.

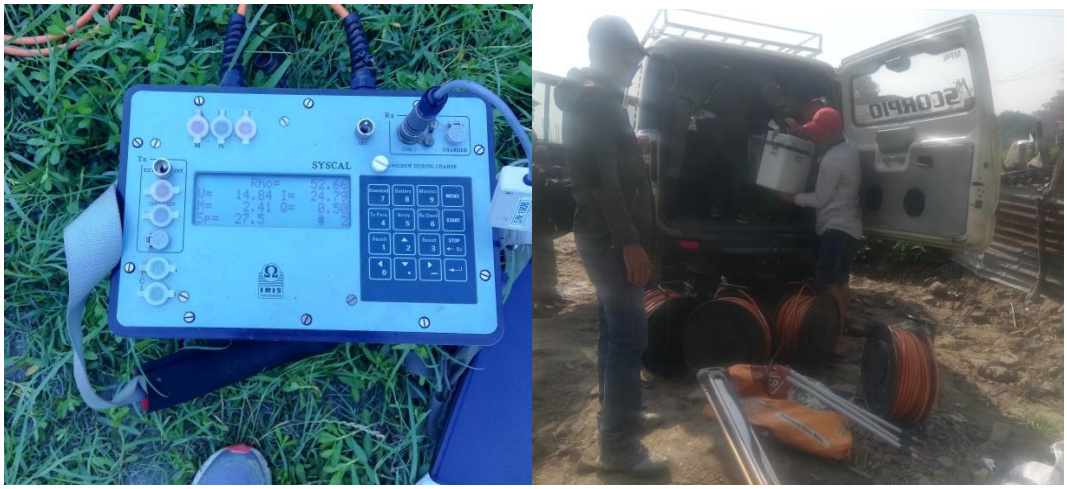

Figure 5: Equipment for ERT survey a) Resistivity meter and b) Necessary accessories

3.2 Methods

The research was focused on the shallow aquifer (specially dug wells) which is located close to major tributaries of the Bagmati River. Field surveys and laboratory analyses were alternatively conducted to complete the research (Figure 7). Details of each field survey and analysis are described in the following sections.

3.2.1 Field Survey

3.2.1.1 Preparation of Inventory data

Initially, field survey was conducted for the preparation of inventory data from dug well adjacent to the Bagmati River and its tributaries. Tributaries include the Bishnumati, and the Manahara Rivers and the Dhobi, Hanumante, Godavari, Kodku, Nakhu and Balkhu kholas. All these rivers shows centripetal river system and flow on relatively similar elevation as they leave bedrock at the peripheral areas of the Kathmandu basin. The groundwater collection from the wells which are located far from the river channel may have combined effects from other watershed. Schematic diagram (Figure 6) shows the relationship between river and groundwater; and possibility of mixing of two river water in single well (well 3 and 4). In other hand, the groundwater collection far from the river channel may also show low possibility of river-groundwater interaction (well

5) (Krishna *et al.*, 2017; Hoehn and Scholtis, 2011). The research conducted by Gautam *et al.* (2013) also observed higher chemical concentration (chloride, nitrate, and ammonia) on groundwater which are near to river channel (0-100 m) comparing to groundwater collected from 100 to 150 m distance. They concluded that the higher concentration in nearby groundwater is the effects of polluted river water intrusion. The research on Jialu River basin (Yang *et al.*, 2012) also shows the occurrences of river water intrusion in only adjacent well (30 m). However, the lateral distance of interconnection is dependable on the subsurface material and can vary with space and time. Thus in the present study, the wells which are located within 100 m (both banks) from the channel was included in the inventory data. But the 100 m distance is not taken as boundary for river-groundwater interaction.

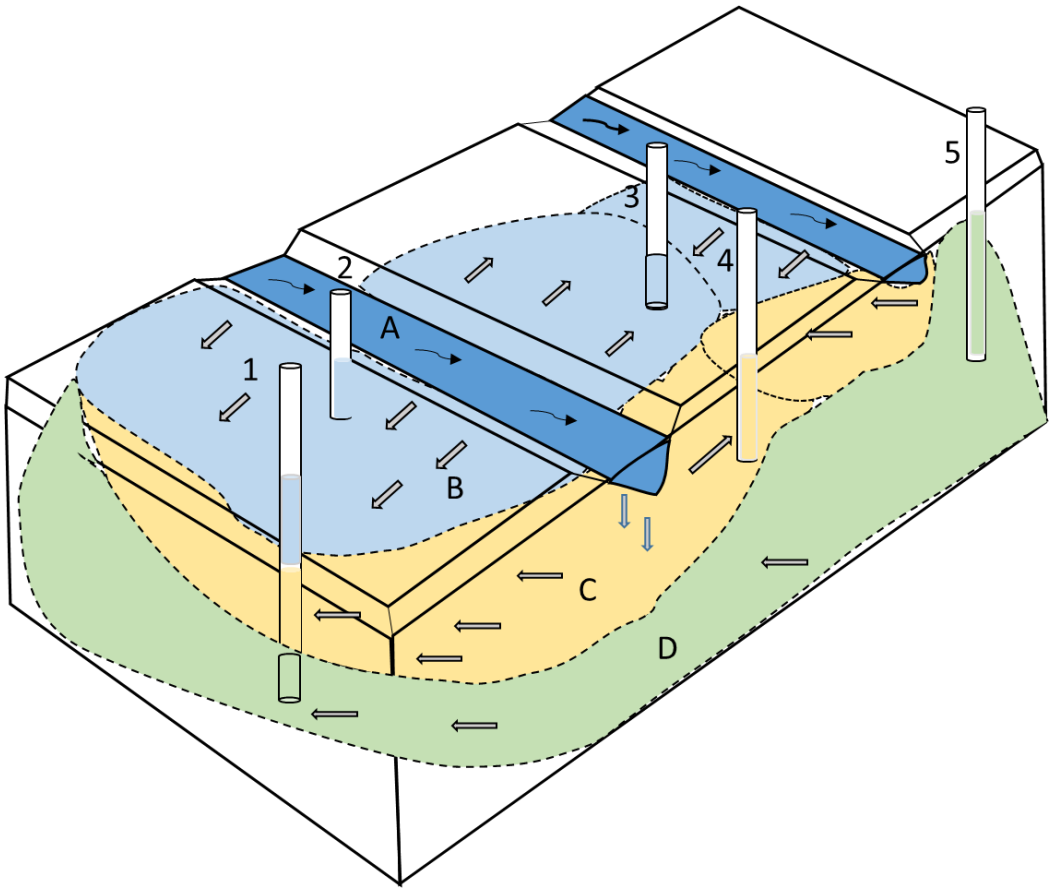

Figure 6: Schematic block diagram presenting rivers and groundwater relationship: (A) River, (B) & (C) Groundwater of river bank/bed infiltration origin (well 1, 2, 3, &4) and (D) groundwater without river water infiltration (well 5)

During inventory of dug wells, GPS location, well dimension (depth, diameter and water level depth), distance from the river channel, and in-situ parameters such as dissolved oxygen (DO), pH, electrical conductivity (EC) and temperature of the water

were measured. In-situ parameters were measured at the field immediately after removing three purge water, using DO and pH/EC meters. The fieldwork was conducted in two successive seasons of 2017 (April and August) for the analyses of seasonal variation in water level depth and in-situ parameters in dry and wet seasons.

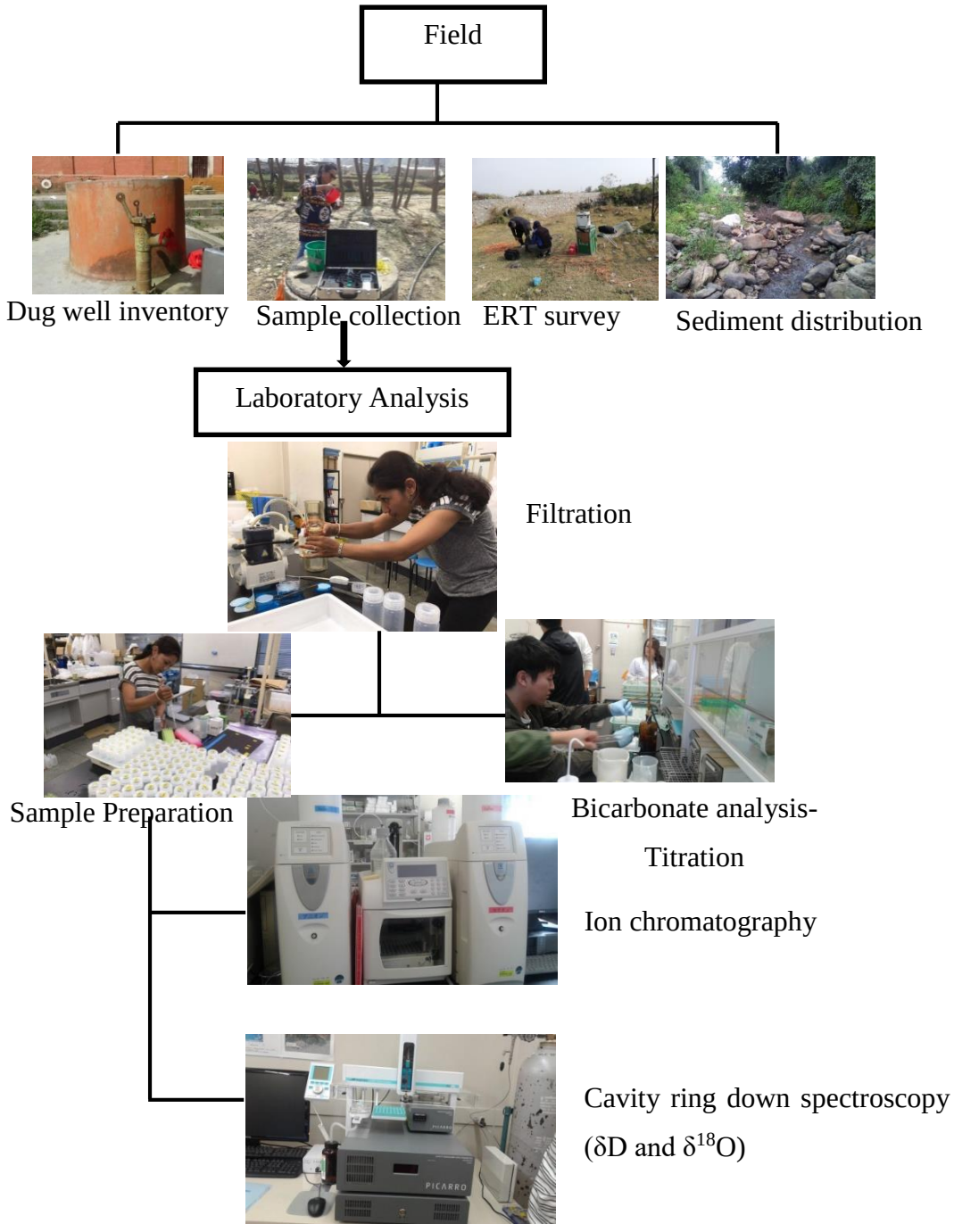

Figure 7: Flowchart of methodology

3.2.1.1.1 Selection of wells for detailed study:

Sample collection and analysis of all wells incorporated within inventory were impossible in this research. Thus with the help of inventory from each river, 10 well locations were selected for detailed analysis except in the Kodku and Nakhu Khola. The selection was based on distance from the river channel; geological information; and the possibility of assessable. Well located at different distances such as from 2 to 100 m were tried to include in well selection from each river reaches.

3.2.1.2 Sample collection from groundwater and river water

Groundwater was collected from the wells selected from the inventory data whereas river water was collected from the nearby rivers of selected wells. Sampling was carried out in two seasons –August 2017 (wet season) and February 2018 (dry season). Water samples were collected in 100 mL polyethene bottles. Each bottle was rinsed three times with the same water before sample collection. Groundwater samples were collected after removing a quantity of water using an installed hand pump or with the help of rope and a plastic bucket.

3.2.1.2.1 Sample Id

Sample Id for each water sample was given based on the name of rivers from which the sample was collected such as BM for Bishnumati; D for Dhobi; B for Bagmati; M for Manahara; H for Hanumante; G for Godawari; K for Kodku; N for Nakhhu and BA for Balkhu corridor samples. Again, sample Id was separated for river water and groundwater water as BMR for the Bishnumati river sample and BMW for Bishnumati well sample; DR for Dhobi river and DW for Dhobi well; and so on for all other rivers.

3.2.1.2.2 Sample transportation and storage

During sample collection in the field, samples were stored in a cooler bags with ice packs. Then at the end of each collection day, samples were transferred to the Central Department of Geology (CDG) and stored in a deep freezer (-4°C) to maintain their chemical constituents constant. These samples were then transferred to the University of Yamanashi, Japan for chemical and isotope analysis. Sample bottles of each river were packed in double zipped locked plastic packets and then kept in cooler bag for transportation. After reaching at University of Yamanashi, these samples were immediately stored in a deep freezer (-4°C) until chemical and isotope analysis.

3.2.1.3 Electrical resistivity (ERT) survey

Electrical resistivity tomography (ERT) was applied to record the resistivity structure of sub-surface materials. The resistivity of the ground was measured by injected currents and the resulting potential difference at the surface. A multi-electrode resistivity meter (SYSCAL R1 PLUS SWITCH 48) was used to carry out ERT survey. During this survey, a number of electrodes (15 to 48, depending on site condition) arranged in a straight line with a constant spacing (1 and 2 m, depends on site). A computer-controlled system was used to select automatically the active electrodes for each measure using Wenner (Schlumberger in one profile) array (Figure 8). The response of current on geological formations such as clay, silt, sand, gravel, boulders, and bedrock are different. The electrical resistivity of a geological material depends both on the matrix (rock and/or sediments) and on the salinity of the fluids (water) and the degree of saturation of pore spaces.

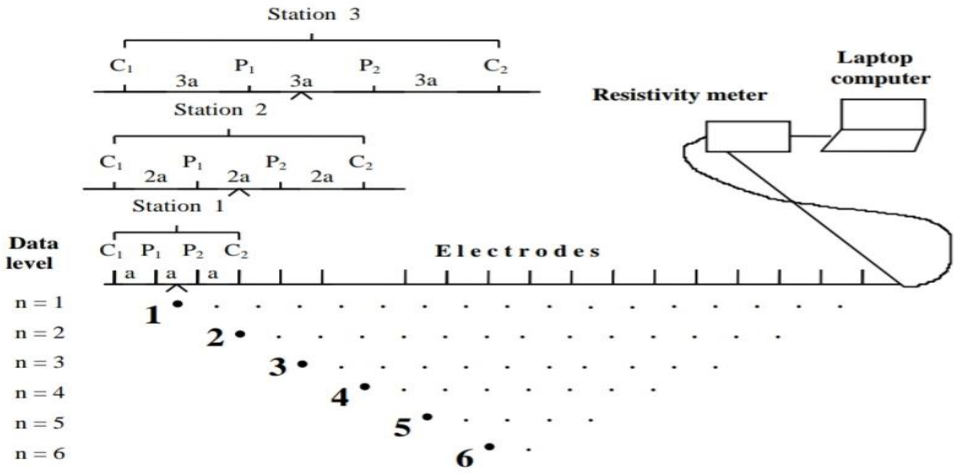

Figure 8: A schematic diagram showing arrangement of electrodes (Wenner array) and measurement sequences to build up a pseudosection. C1 and C2 are current electrodes, P1 and P1 are potential 'a' is spacing between electrodes and 'n' is number of measurement level

3.2.1.4 Preparation of sediment distribution pattern map along river channels

A sediment distribution pattern map was prepared along the river corridors of the Bishnumati, the Bagmati and the Manahara Rivers and the Kodku and Nakhu kholas. It was prepared in the 1:10,000 base maps created from a topographic maps, using the grain size scale given by Blair and McPherson (1999). A manually prepared map was digitized to bring digitally by using ArcGIS.

3.2.2 Laboratory analysis

Water sample collected from groundwater and river water was chemically and isotopically analyzed in the laboratory of University of Yamanashi, Japan.

3.2.2.1 Sample preparation

Before analyses for chemical and isotope, water samples were first filtered using filter paper of 0.2 µm to remove suspended materials. The sample of only 1 mL was required for chemical and isotope analysis and about 30 mL for HCO_3 analysis.

The material used for sample preparation was:

1. 1 mL of plastic and glass sample bottles (plastic for chemical and glass for isotope)
2. 1 mL of a pipette
3. Label tape & marker

Sample preparation procedure (Figure 9)

1. The sample number was written in all 1 mL sample bottles before sample filling
2. 1 mL of sample bottle was ringed with sample 2 times which has to be filled in the bottle
3. Then the sample was filled using 1 mL of pipette but it need to be free of gas bubbles in a pipette and then tight with a bottle cover

Figure 9: Sample preparation a) 1 mL of sample bottles with labels and b) Pipette

3.2.2.2 HCO_3 analysis

HCO_3^- is one of the major anion of chemical analysis which could not be measured from ion chromatography. The concentration of it was calculated through titration with 0.01N H_2SO_4. (Figure 10)

Indicator for titration:

- 0.01 g of Bromocresol green (pH range 3.8-5.4) and 0.01 g of methyl red (pH 4.4-6.3) were mixed in 100 mL of ethanol to make a solution for the indicator.

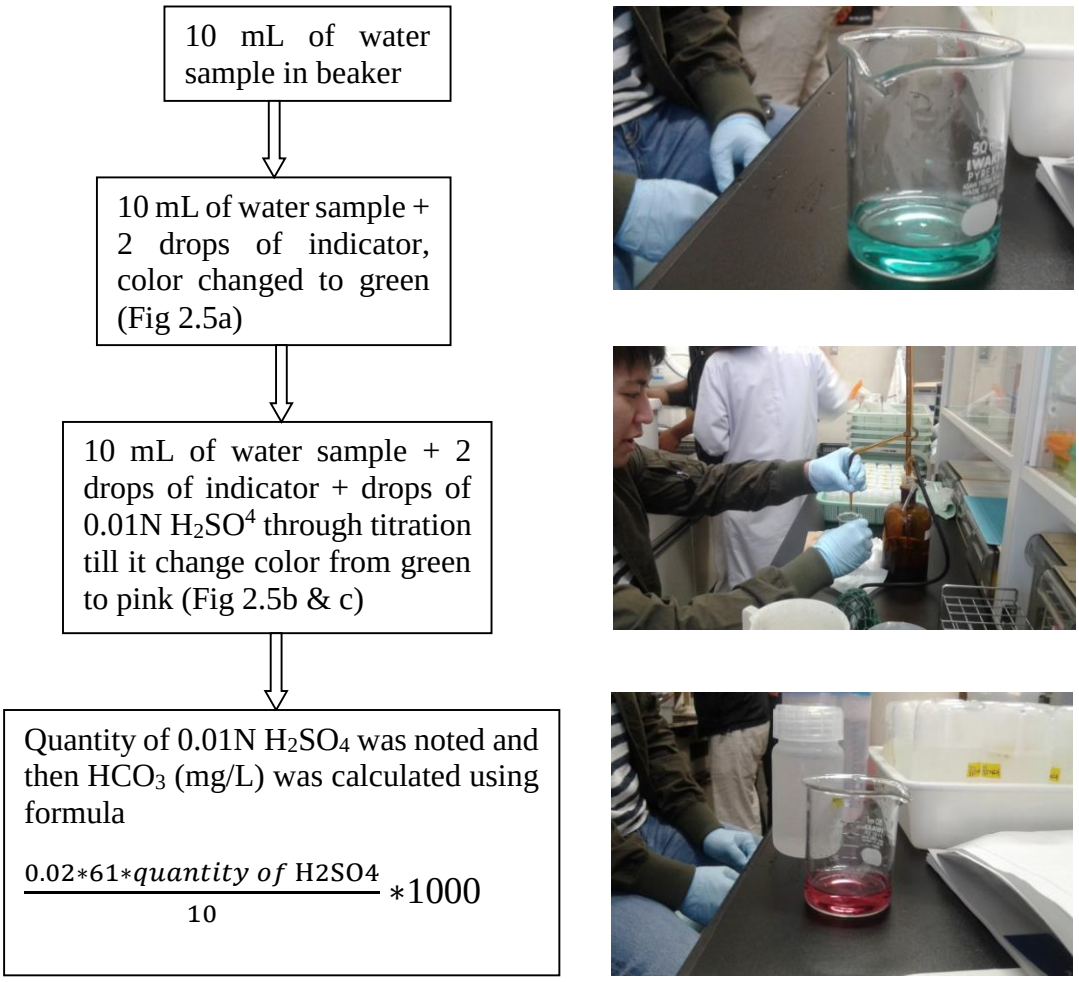

Figure 10: Procedures of bicarbonate analysis by titration method

3.2.2.3 Chemical analysis

Groundwater and river water samples collected from the wet and dry seasons were chemically analyzed by using an ion chromatography (ICS-1100 Dionex, USA) system. It was used to find out the chemical concentration of different types of anions and cations. Basically, cations include Li^+, Na^+, NH_4^+- N, K^+, Mg^{2+} and Ca^{2+}; and include F^-, Cl^-, NO_2^--N, Br^-, NO_3^--N, PO_4^--P and SO_4^{2-}. Normally, an ion chromatography system contains a liquid eluent, a high-pressure pump, a sample injector, a guard and separator column, a chemical suppressor, a conductivity cell, and a data collection system. A standard solution was used to calibrate the ion chromatography system. Sample ions were recognized by comparing the data obtained from a known solution to that of a sample (Manual Dionex ICS-1100 Ion chromatograph).

3.2.2.4 Isotope Analysis:

Cavity ring-down spectroscopy (L1102-I, Picarro, Santa Clara, CA, USA) was deployed to analyze stable water isotopes of hydrogen (δD) and oxygen ($\delta^{18}O$). Vienna Standard Mean Ocean Water (VSMOW) was the standard water utilized for the calculation of isotopic ratios of hydrogen (δD) and oxygen ($\delta^{18}O$) in water samples. The results were presented in per mill (parts per thousand) with respect to these standards with a precision of 0.5% for δD and 0.1% for $\delta^{18}O$. The isotopic ratios of δD and $\delta^{18}O$ were presented relative to the VSMOW given by Craig, (1961):

$$\delta D \text{ or } \delta 18O = \frac{Rsample - RVSMOW}{RVSMOW} \times 1000 \ (‰)$$

Where R is an isotopic ratio of D and ^{1}H or ^{18}O and ^{16}O of water samples

3.2.3 Statistical analysis

Statistical Package for Social Studies (SPSS) version 25 was used for analysis.

3.2.3.1 Hierarchical cluster analysis (HCA)

Hierarchical cluster analysis (HCA) was used to group water samples with similar properties to selected parameters. It is a widely used multivariate method for river-groundwater interaction. HCA was implemented based on Ward's linkage method (Ward, 1963) with squared Euclidean distances as a measure of similarity in selected parameters of samples (Mencio and Mas-Pla, 2008; Pathak *et al*., 2015). For the present research, chemical (Na^{+} and Cl^{-}) and isotopic composition (δD and $\delta^{18}O$) were used as major parameters for HCA. Using HCA, water samples with similar selected parameters were grouped into single cluster. Occurrences of combined water samples from river and groundwater into a single cluster indicated existence of river-groundwater interconnection.

3.2.4 Connectivity of groundwater and river water

Chemical and isotope analyses were two major methods applied in this research. ERT and sediment distribution survey were additionally used in selected areas for sub-surface sediment and surficial sediment distribution pattern sequentially along the river corridors. However, HCA was the principle method to identify interconnection between groundwater and river water, information from sub-surface materials again clarifies the

presence of interconnectivity in those areas where ERT was conducted. Figure 11 presents a flowchart of the whole methodology of this research. The connection between chemical, isotope and ERT methods to distinguish river segments as connected and disconnected with surrounding shallow wells.

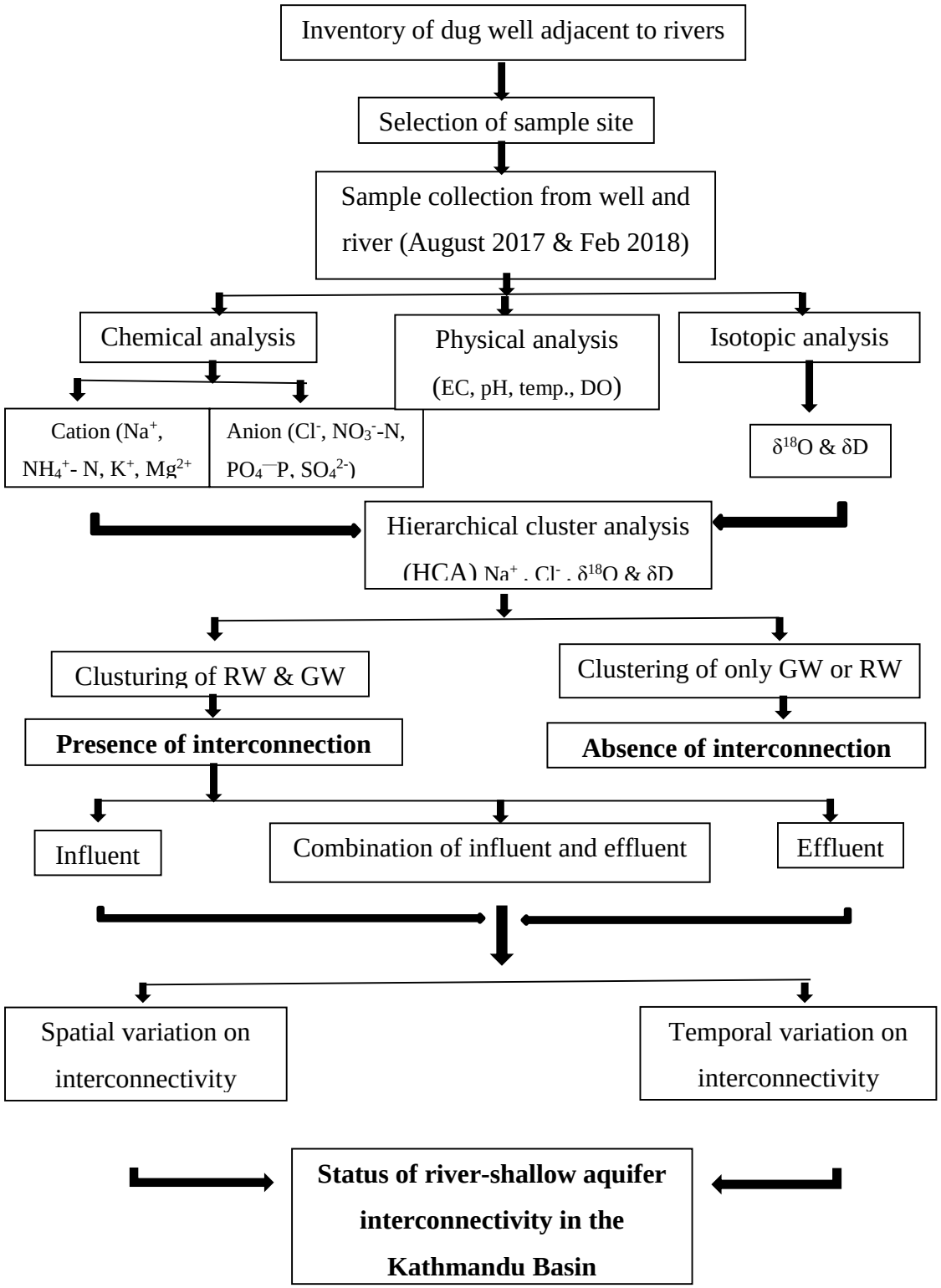

Figure 11: Connection of methods used to identify interconnection of GW and RW

CHAPTER 4

RESULTS AND DISCUSSION

4.1 Sediment distribution pattern along rivers

Surface sediments along rivers exhibited variation in particle size depending on the maturity of rivers and depositional features. Initially, sediment distribution pattern was planned to prepare in all nine selected rivers. But at the time of preparation along the Bagmati and Bishnumati, it was difficult to observe natural sediment deposition on river bed and banks. Most of all rivers are channelized by making retaining structures on both banks. Road corridors are constructed on both banks of the Dhobi Khola and road under construction in the Nakhu Khola. Due to these human activities, sediments along the bank and riverbed was highly alter. Thus, spatial distribution patterns of sediment was only prepared along the five rivers: the Bagmati, the Bishnumati and the Manahara Rivers and the Godawari and Kodku Khola. The distribution pattern was prepared on the 1:10,000 base maps by traversing from upstream to downstream. During this traverse, sediment size along the river channel and both banks were noted using the grain size scale given by Blair and McPherson (1999) as silt, sand and gravel. About 100 m from the river channel in both banks were incorporated for mapping. The purpose of the preparation of maps was to understand the capacities of water percolation through surficial materials to recharge groundwater.

4.1.1 Bishnumati River

Figure 12 presents the sediment distribution patterns along the Bishnumati River. Sandy gravel, gravelly sand, muddy sand and sandy mud are dominantly observed along this river. In the upstream section, sandy gravel and gravelly sand occurred as channel material (Figure 13a) showing a maximum gravel size of 7 to 15 cm while sandy mud was observed as bank material. The proportion of sandy gravel and gravelly sand was nearly absent in downstream from the Gongabu area. Bank material was also hardly visible between Gongabu and Banasthali area. But from downstream of Banasthali area, muddy sand and sandy mud with a granule of 4 to 6 mm were observed as channel and bank material respectively in a narrow zone (Figure 13b). The road along river corridor with dense settlement area observed in these areas. River training works and dumping of sewer and solid wastes were common throughout the river (Figure 13 c & d).

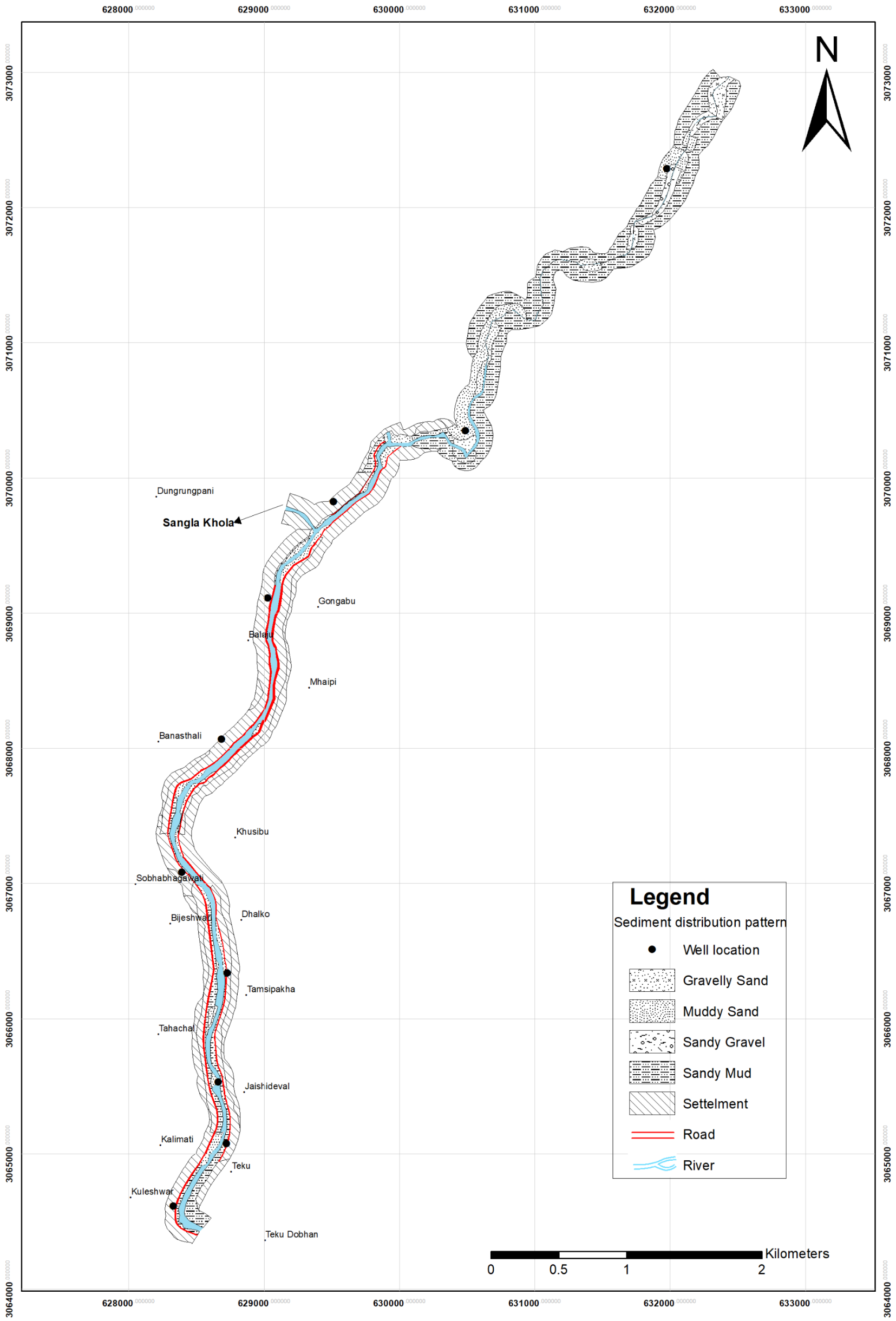

Figure 12: Sediment distribution pattern along the Bishnumati River

Figure 13: Sediment pattern along the Bishnumati River a) Channel material at upstream section b) Channel material at downstream section c) Channelization, dense settlement and road along river, source-Setopati.com and d) River training works in river channel

4.1.2 Bagmati River

The sediment distribution pattern along this river (Figure14) clearly showed five variations of materials. Except in the upstream section from the Gokarna area, a road corridor was constructed mostly on both banks which reduced sediment exposure and increased settlement along this river. The World Heritage Site, Pashupati and Guheshori temples are also located at the banks of the river. Generally, gravelly sand dominantly occurred at the channel and point bar areas in the upstream section up to the Gokarna area (Figure 15a). The size of gravel varied from 1 to 7 cm. Sand and muddy sand as channel and bank materials were dominant in between Jorpati to Tilganga area. A very narrow zone of sandy mud exposed downstream of Tilganga to Sinamangal area (Figure 15b). The width of the river channel as well as the bank was increased downstream from the Shankhamul area (downstream from the confluence with the Manahara River) exposing sand and muddy sand as channel material (Figure 15c). Mud dominantly occurred as bank material in the uppermost and downstream sections of the river.

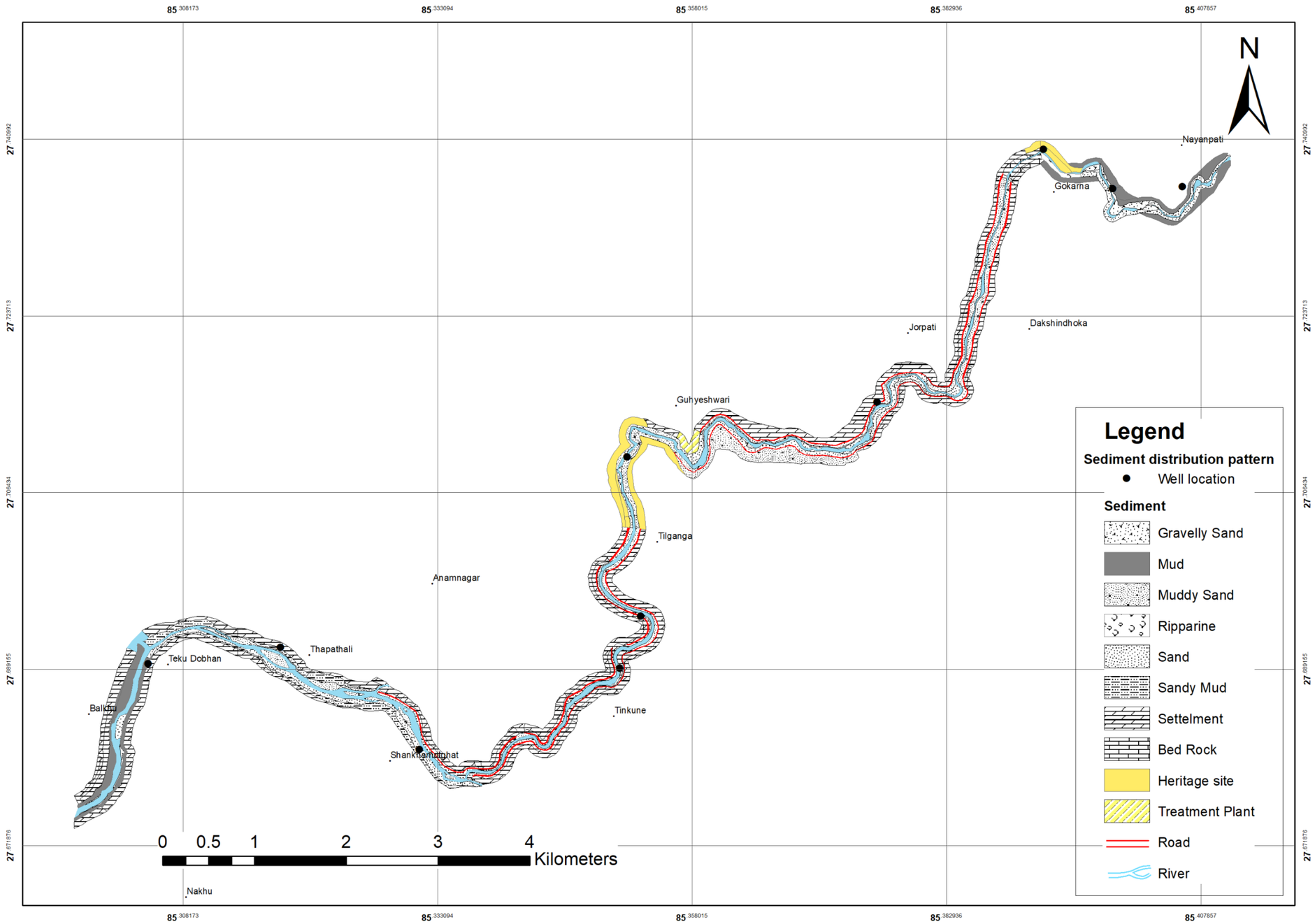

Figure 14: Sediment distribution pattern along the Bagmati River

The bed rock of Kulikhani Formation, composed of quartzite was also exposed in Gokarna and Gaurighat area (Figure 15d). Channelization, sewer and solid waste disposal were common disturbing activities along this river (Figure 15e & f).

Figure 15: Sediment pattern along the Bagmati River a) Sediment pattern at upstream b) Narrow channel and bank c) Sediment pattern at downstream d) Bed rock exposed at Gokarna area e) Channelization and d) Solid waste disposal at bank

4.1.3 Manahara River

The sediment distribution along this river is presented in Figure16. Dominant materials were gravelly sand, gravelly mud, muddy sand and sandy mud. Gravelly mud dominantly occurred as river bank materials while gravel and gravelly sand as channel materials in the upstream section. The gravel size of channel material had a variation of 1.5 to 32 cm (Figure 17a).

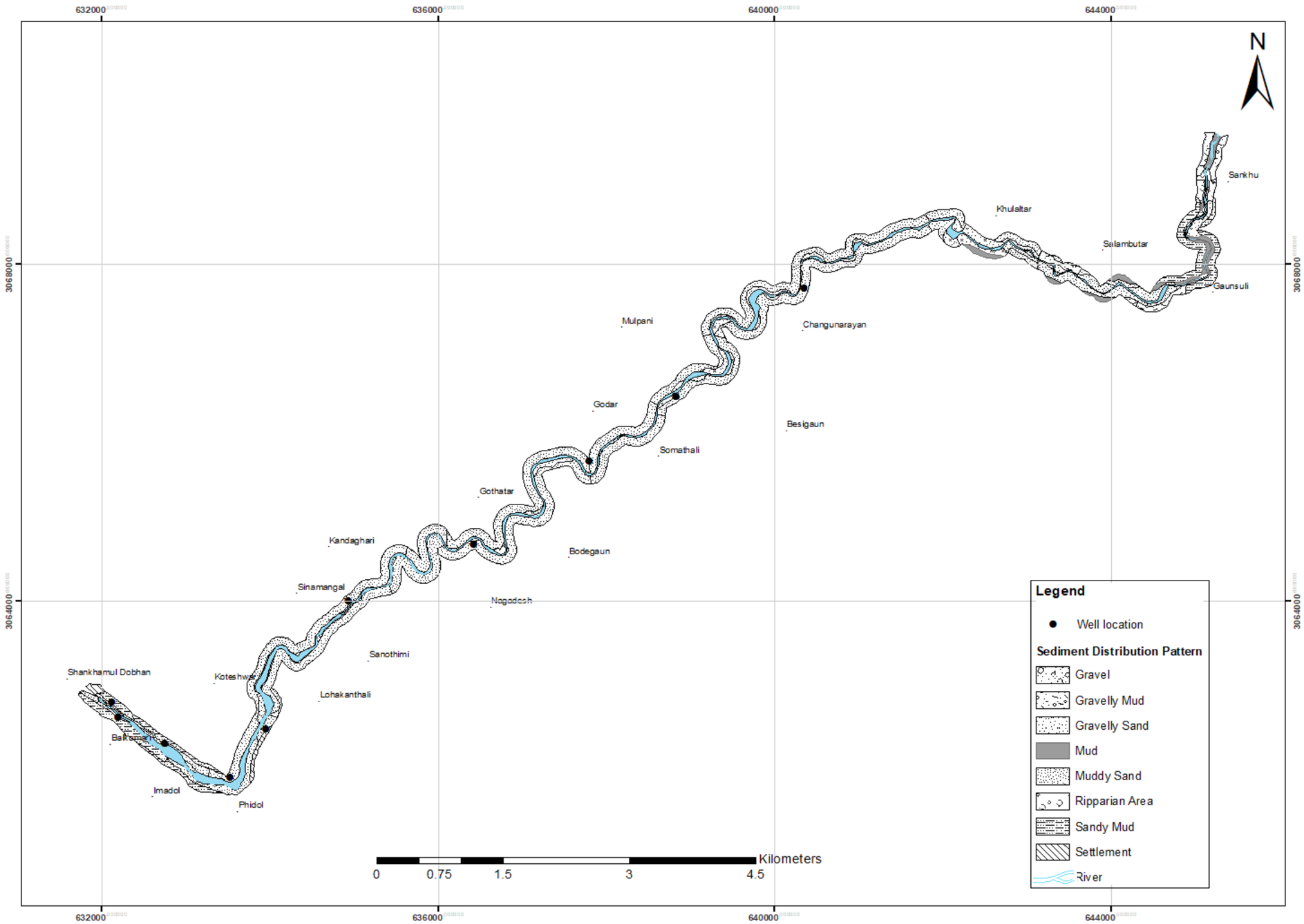

Figure 16: Sediment distribution pattern along the Manahara River

Figure 17: Sediment pattern along the Manahara river a) Coarse sediment deposit at upstream b) Fine sediment at downstream c) Cultivation on river banks and d) Channelization

Muddy sand occurred as bank material (Figure 17b) throughout the whole river except the uppermost section from the Gaunsuli area. However, gravelly sand dominantly occurred as a point bar and channel material up to the Sanothimi area, gravel size showed gradual decrement towards the downstream section. Sandy mud as bank material dominated at downstream section from the Phidol area. Cultivation commonly occurred throughout the river preserving natural sediment distribution patterns in the upstream section (Figure 17 b & c). River training works, road corridor construction and bank encroachment were usually concentrated at the downstream of the Jadibuti

area (Figure 17d, e & f). Due to these activities, natural sediment pattern was highly alter at the downstream section whereas the upstream section possess natural sediment distribution.

4.1.4 Godawari Khola

Figure 19 presents the sediment distribution pattern along the Godawari Khola. Dominant materials were muddy gravel, gravelly mud, and sandy mud. Generally, muddy gravel was dominant in the upstream section as channel and bank material. The channel material had size variation form boulders with 1.5 m of b-axis to 3 cm of pebbles (Figure 18a).

Figure 18: Sediment pattern along the Godawari Khola a) Channel material at upstream section b) Channel as well as bank material c) Grain size decrement in channel and bank near Bishnudol area d) Fine sediments at the downstream section e) Channelization using pipe at Bishnudol area and f) Local scale solid waste disposal

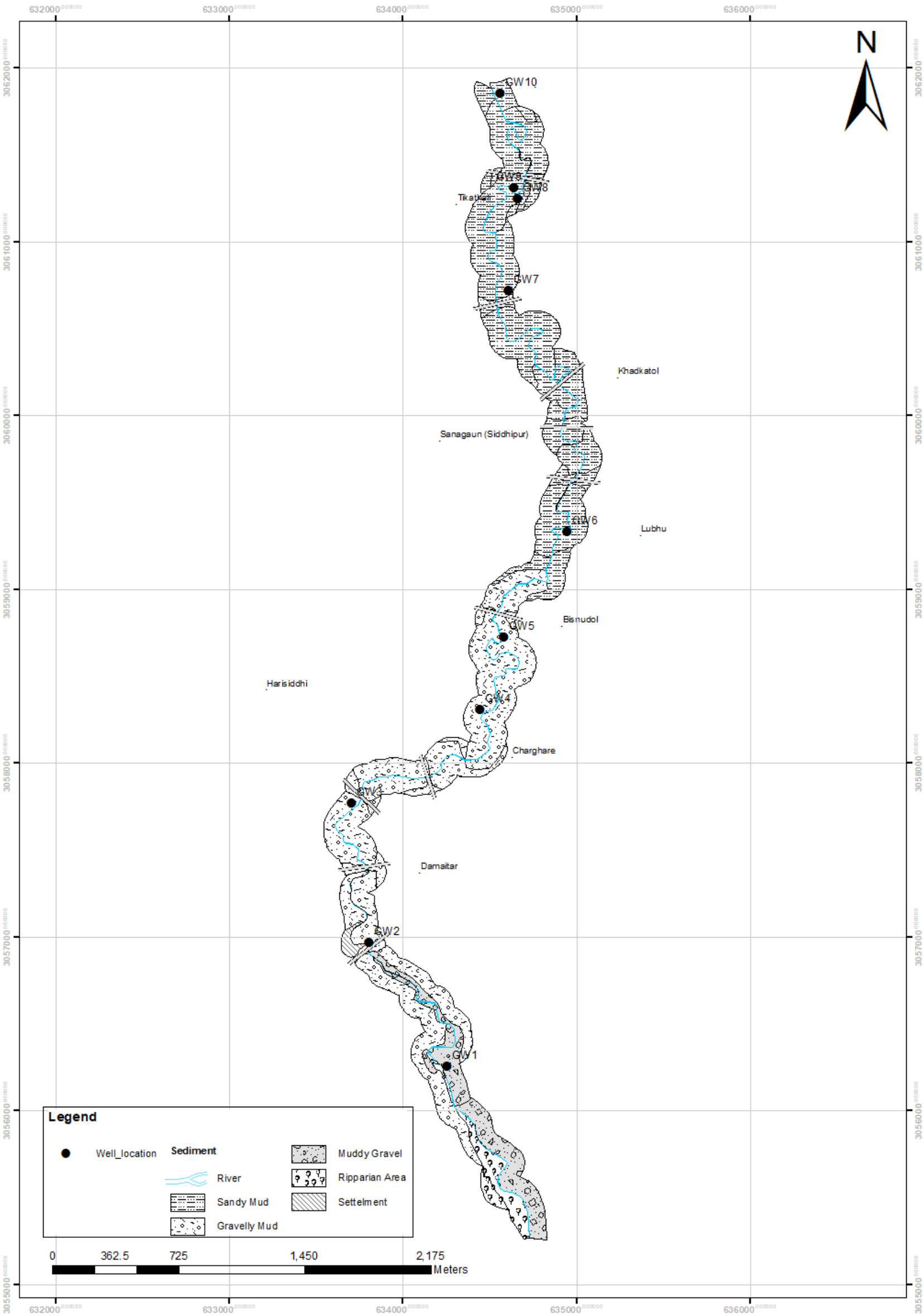

Figure 19: Sediment distribution pattern along the Godawari Khola

River bank material consisted of gravelly mud, gravel size varied from 25 cm to 5 cm (Figure 18b). However, gravelly mud dominantly occurred up to the Bishnudol area as channel and bank material, gravel size showed gradual decrement towards downstream sections (Figure 18c). Sandy mud with occasional gravels (10 to 0.3 cm) was observed as channel and bank material in the downstream section from the Bishnudol area. Although a riparian zone was noticed in most of part of the river, a dense riparian zone was only observed in the upstream areas (Figure 18d). Except for some downstream sections, the rest of the river bank was used for cultivation. This may be the river in which road extension along the river was not still developed. But channelization and local scale pollution occurred along the river (Figure 18e &f).

4.1.5 Kodku Khola

The sediment distribution pattern along the Kodku Khola is presented in Figure 21. Sediment consisted of five variations as mud, muddy sand, sandy gravel, gravel and the bed rock. Sandy gravels were the dominant sediment deposited in the point bar and river channel while muddy sand was observed as river bank material in the upstream section. Sandy gravels mainly consisted of cobble to pebble size particles with a maximum of 12 cm (Figure 20a&b). Mud as dominated bank material was observed at the mid-section between Subbagaun and Dhapakhel area. Channel material dominated by muddy sand occurred downstream from the Khumaltar area (Figure 20c). Heavy settlement along the river channel was noticed in the downstream section near Imadol and Gwarko areas (Figure 20d & Figure 21). Bedrock was exposed only at the upstream section near the Thaiba area.

4.1.6 Comparison of sediment distribution pattern among rivers

The sediment distribution pattern map prepared along five major rivers exhibited nine types of sediments varying from gravel to mud size particles. Coarse-grained sediments such as gravel, sandy gravel, muddy gravel, gravelly sand and gravelly mud were dominant in the upstream section of all rivers. Largest size of boulders and gravels commonly observed as channel material in the upstream of the Godawari Khola (Figure 18a) whereas smallest one noted in the Bagmati River (Figure 15a). Sand, muddy sand and sandy mud was dominant sediment type observed as channel and bank material in the middle to downstream of the rivers. Mud dominantly occurs in the downstream section of the Bagmati River as channel and bank material. In overall rivers, grain size

decrement occurred towards downstream and away from the river channel. The natural condition of the river bank was only preserved in the river section of the Godawari Khola and upstream sections of the Manahara River and Kodku Khola.

Figure 20: Sediment pattern along the Kodku Khola a) & b) Channel and bank material at upstream section c) Channel material at downstream section and d) Settlement area along river

These conditions enhanced water percolation capacity through surficial sediment to sub-surface. But in the case of the Bagmati and the Bishnumati Rivers, road corridors constructed on both banks narrower bank material exposure and increased settlement (Figure 13c). These activities may indirectly affect infiltration capacity and increased urban flooding during rainy seasons.

4.2 Inventory of dug wells

The purpose of preparation of inventory is to get ideas about spatially distribution of wells along river corridors. Thus, wells located close to channels (around 100 m) of major 9 rivers of the Kathmandu Valley were included within the inventory map. Data collection from dug wells was tried to incorporate overall numbers of wells however it could not be possible due to the absence of the well owner at the time of the survey.

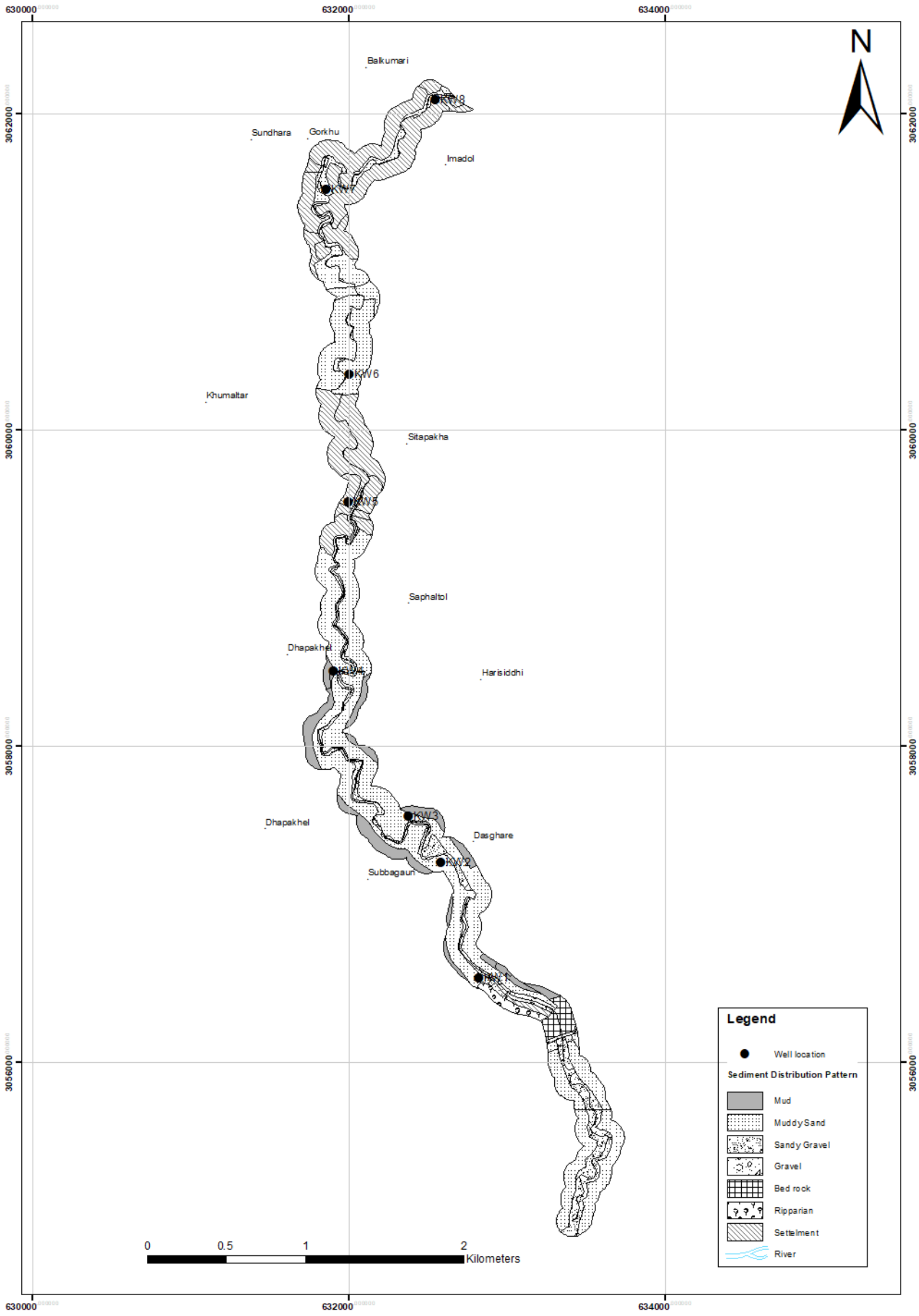

Figure 21: Sediment distribution pattern along the Kodku Khola

GPS position, well dimension (well depth, well diameter and water level depth) and some in-situ parameters such as dissolved oxygen (DO), pH, electrical conductivity (EC), and water temperature measured at each well location. Measurement of well dimension and in-situ parameters were carried out in dry (April 2017) and wet (August 2017) seasons.

Total of 237 wells were recorded from nine river corridors. Figure 22 presents the dug wells location and Appendix 3 presents details of dug wells along different rivers. The numbers of wells recorded for different river corridors is presented in Table 5.

Table 5: Total number of wells in each river

SN	River Name	Total number of wells
1	Bishnumati (BMW)	34
2	Dhobi (DW)	27
3	Bagmati (BW)	28
4	Manahara (MW)	28
5	Hanumante (HW)	30
6	Godawari (GW)	26
7	Kodku (KW)	18
8	Nakhhu (NW)	23
9	Balkhu (BAW)	23
	Total wells	237

4.2.1 Inventory on nine rivers

4.2.1.1 Bishnumati River

Details of 34 dug wells recorded from the Bishnumati River are presented in Appendix 3A. The wells were located within 1 to 230 m from the river channel. Wells observed from the Tokha area had the shallowest well depth (2.2 to 2.9 m) while well recorded from Gongabu (BMW24) had the deepest well depth (9.5 m). Water level depth varied from 0.9 to 6.8 m and 0.4 to 4.2 m in the dry and wet seasons respectively. Almost all wells had shallow water depth during the wet season, with a maximum fluctuation of 4.8 m and minimum fluctuation of 0.4 m at BMW24 and BMW33 respectively.

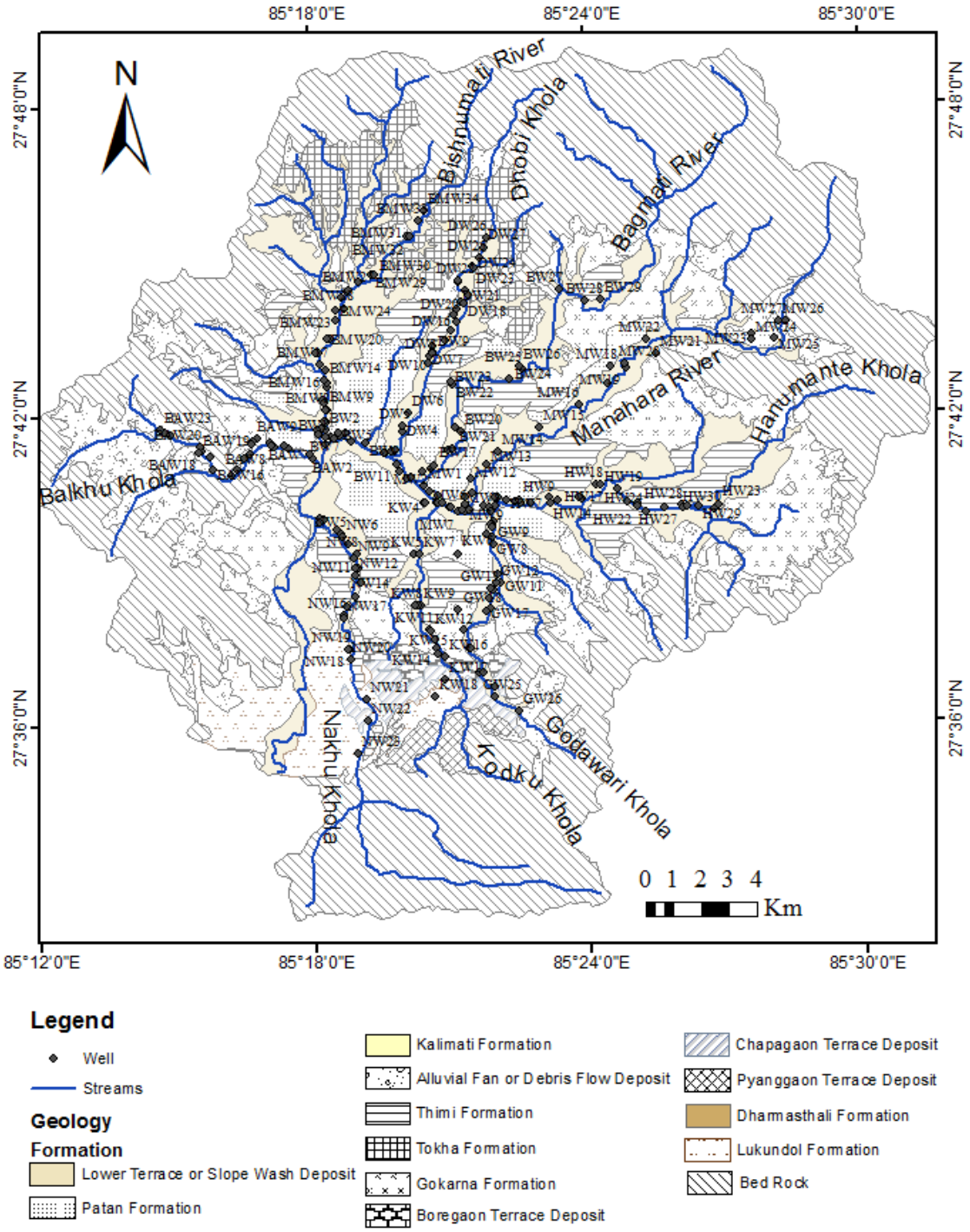

Figure 22: Inventory map of dug wells located within 100 m from river channel

The range of temperature was 16.2 to 21.6 ^{o}C in the dry season and 21.6 to 25.8 ^{o}C in the wet season. The pH value ranged from 6.5 to 8.5 and 5.3 to 7.7 in the dry and wet seasons respectively. The pH of BMW27 had drastically changed from neutral (7.5) to acidic (5.3) water during the wet season. EC measured in both dry and wet seasons exhibited wide spatial variation with a value range of 260 to 2150 µS/cm and 334 to

2090 µS/cm respectively. In both seasons, higher EC was recorded from core settlement areas of the Dallu and lower EC from the Budhanilkantha area. Comparatively, EC recorded was lower in the wet season except in a few wells such as BMW7, BMW27 and BMW28. EC was increased by more than double in these wells during the wet season (Annex 3A). The water level depth was also decreased in these wells which indicates that the increased in EC may be the result of point source contamination near to these wells. During wet season, higher concentration of contaminants transport with rainfall infiltration to groundwater. The value of DO varied from 0.3 to 5.9 mg/L in the dry season and 0.3 to 6.34 mg/L in the wet season.

4.2.1.2 Dhobi Khola

Details of dug wells observed from the Dhobi Khola are presented in Appendix 3B. Recorded 27 wells located within 5 to 80 m from the river channel. A wide spatial variation in well depth was noticed with the shallowest of 2.3 m and the deepest of 12.2 m. Water level depth ranged from 1.1 to 11.8 m in the dry season and 0.1 to 3.1 m in the wet season. Maximum water level fluctuation of 9 m was detected at DW27 and minimum fluctuation of 0.1 at DW11. Shallower water depth observed in the wet season indicated precipitation as one of the major recharge sources for these dug wells.

The temperature ranged from 18.4 to 21.2 ^{o}C and 21.8 to 24.8 ^{o}C in the dry and wet seasons respectively. The pH values in both seasons showed more or less neutral in all water of wells except in DW2 and DW22 having pH value greater than 8. EC value varied from 231 to 1481 µS/cm in the dry and 162 to 1199 µS/cm in the wet season. Lower EC was noted from the upstream section while higher from the downstream section in both seasons. DO value fluctuated from 0.37 to 6.1 mg/L in the dry season and 0.5 to 4.9 in the wet season.

4.2.1.3 Bagmati River

Details of total of 29 dug wells from the Bagmati River are presented in Appendix 3C. Observed wells located within 2 to 80 m from the river channel with 1.9 to 9 m well depth. Comparatively, deeper water level depth was recorded in the dry season with a maximum fluctuation of 5.5 m at BW23.

The water samples showed a similar pH value ranges in both seasons (6 to 7.7). EC of dry season ranged from 149.6 to 2280 µS/cm and wet season from 121.7 to 1949 µS/cm.

In both seasons, the EC of wells located at the core settlement area measured more than ten times as compared to the upstream settlement area. DO values varied from 0.2 to 4.8 mg/L and 0.3 to 8.5 mg/L in the dry and wet season respectively.

4.2.1.4 Manahara River

Total of 28 dug wells observed from the Manahara river was located within 10 to 280 m from the river channel. The shallowest well depth was noted from MW2 (1.2 m) while the deepest was from MW6 (7.6 m) (Appendix 3D). Comparatively, almost all wells had shallow water level depth with a value variation of 0.1 to 5.0 m in the wet season. A water level of 0.1 m was measured at MW2 and MW27.

The pH of almost all wells changed to slightly basic during the wet season with a value range of 6.51 to 7.87. EC of the upstream section (Sankhu area) showed very low value whereas downstream core areas (Pepsicola area) presented the highest value in both seasons (Appendix 1D). The value range of DO slightly increased in the wet season (0.5 to 6.4 mg/L) as compared to the dry season (0.4 to 5.4 mg/L).

4.2.1.5 Hanumante Khola

Details of 30 dug wells recorded from the Hanumante Khola are presented in Appendix 3E. Observed wells were located within 2 to 90 m from the river channel with well depth variations of 1.5 to 15.7 m. The water depth ranged from 1.1 to 6.3 m and 0.1 to 5.6 m in the dry and wet seasons respectively. A maximum fluctuation of 3.3 m was recorded at HW22 and a minimum fluctuation of 0.3 m at HW8.

The range of temperature was 18.1 to 20.7 ^{o}C in the dry season and 20.7 to 24.7 ^{o}C in the wet season. The pH value slightly increased in the wet season ranging value from 5.92 to 8.05. Acidic water was only observed at HW7 in both seasons. EC ranged from 549 to 1546 µS/cm and 228 to 2158 µS/cm in the dry and wet seasons respectively. EC was drastically decreased in HW26 while it was drastically increased in HW22 during the wet season (Annex 1E). However most the wells showed temporal variation on DO, the range was more or less similar (0.5 to 4.8 mg/L) in the both dry and wet seasons.

4.2.1.6 Godawari Khola

Total of 26 dug wells documented from the Godawari Khola are presented in Appendix 3F. These wells were located within 5 to 160 m from the river channel. The shallowest

depth of 1.5 m was noted from GW24 and GW25 and the deepest depth of 10.4 m was observed at GW26. Water level depth ranged from 0.5 to 8.3 m in the dry season and 0.1 to 4.5 m in the dry season. Comparatively, all wells had shallow water depth in the wet season with a maximum fluctuation of 7.8 m and a minimum fluctuation of 0.1 m at GW16 and GW22 respectively.

The temperature of water varied from 15.3 to 24 ^{o}C and 19.6 to 25.6 ^{o}C in the dry and wet seasons respectively with a wide temporal variation of 10 ^{o}C at GW13. The pH value showed an almost similar ranges in both seasons ranging from 6.8 to 7.8. Comparatively, lower EC was exhibited in the wet season relative to the dry season. In both seasons, higher EC was recorded at GW2 and lower EC at GW26 showing increasing order towards the downstream section. The value of DO fluctuated from 0.5 to 5.8 mg/L in the dry season and 0.8 to 5.2 in the wet season.

4.2.1.7 Kodku Khola

Only 18 dug wells were recorded from the Kodku Khola and are presented in Appendix 3G. Observed wells were located very close (2 m) as well as far (160 m) from the river channel with a well depth variations of 1.3 to 13 m. The shallowest water level depth of 0.1 m was noted at around 40 percent of wells while the deepest up to 6.4 m depth was measured at KW1 during the wet season. KW2 showed a maximum fluctuation of 5.8 m whereas KW12 had a minimum fluctuation of 0.1 m.

The temperature range increased from 15.5-22 ^{o}C to 20-24.9 ^{o}C presenting warm water in almost all wells in the wet season. Wide temporal variations of 9 ^{o}C and 8.7 ^{o}C recorded at KW8 and KW9 respectively. The pH value ranged from 6.2 to 8.0 and 6.5 to 8.1 in the dry and wet seasons respectively showing the lowest value at KW18 in both seasons. The value of EC was low (230 to 180 µS/cm) in upstream sections which abruptly increased towards downstream sections (1840 to 1568 µS/cm) during both dry and wet seasons. Usually, Groundwater presented lower EC during the wet season but more than 50 percent of wells from the Kodku Khola recorded higher EC relative to the dry season (Appendix 1G). KW10 had more than double EC (1204 µS/cm) in the wet season as compared to the dry season (416 µS/cm). The range of DO varied from 0.1 to 5.45 mg/L and 0.4 to 5.0 mg/L in the dry and wet seasons respectively.

4.2.1.8 Nakhu Khola

Total 23 dug wells were recorded from the Nakhu Khola which were located within 3 to 80 m from the river channel (Appendix 3H). These wells had depth variations of 1.4 to 14.4 m and were located within 3 to 80 m from the river channel. Water level depth ranged from 0.2 to 3.8 m in the dry season and 0.1 to 2.6 m in the dry season showing a maximum fluctuation of 2.3 m at NW8.

The temperature ranged from 18.2 to 20.9 ^{o}C in the dry season and 21.6 to 25.1^{o}C in the wet season. The value range of pH was almost similar (6.8 to 7.9) in both seasons showing neutral water in all wells. Except for few wells, EC decreased in the wet season with a value ranges from 244 to 1540 µS/cm. DO value varied from 0.5 to 5.7 mg/L and 0.2 to 5.1 mg/L in the dry and wet seasons. In both seasons, a lower value was observed at NW16 and a higher value at NW23.

4.2.1.9 Balkhu Khola

Total of 23 dug wells observed from the Balkhu Khola were located within 1 to 70 m from the river channel (Appendix 3I). Shallowest well depth of 1.9 m was noted from BAW23 and the deepest depth of 10.8 m was measured at BAW20. The range of water level depth varied from 1.3 to 8.1 m in the dry season which had changed to the shallow range of 0.3 to 3.0 m in the wet season. BAW18 showed a maximum fluctuation of 6.4 m while BAW21 presented a minimum fluctuation of 0.1 m.

As in other river well, these wells also had a higher temperatures in the wet season with value variations from 21.7 to 25.2 ^{o}C. The pH value of most the wells slightly increased during the wet season. EC measured ranged from 553 to 2860 µS/cm in the wet season and from 385 to 3030 µS/cm in the wet season. In both seasons, BAW9 presented the highest EC value. The range of DO varied from 0.1 to 3.5 mg/L and 0.3 to 3.6 mg/L in the wet and dry seasons respectively.

4.2.2 Comparison of well dimensions among rivers

The variations of values for well dimension and elevation are presented in Table 6. Among rivers, the smallest well diameter varied from 60 to 90 cm whereas the highest was from 120 to 230 cm. Inventoried wells were situated at various elevations. The maximum elevation was obtained at upstream sections of the Kodku, Godavari and the Nakhu Khola (1400 to 1430 m) and the minimum at downstream sections of all rivers (1263 to 1293 m). The well depth showed wide variation along and among wells of

different tributaries. The lowest well depth was noted from the downstream of the Manahara River (1.15 m) while the highest one was measured from the upstream of the Hanumante Khola (15.7 m). The lowest well depth was noted from the wells of the Bishnumati River and the Manahara River corridors (Table 6). Wells situated at the Lower Terrace Deposit, Chapagaon Terrace Deposit and Boreaon Terrace Deposit (especially the southern part) presented lower well depth compared to wells observed at the Patan and Thimi Formation (northern part). Gravels, pebbles, and sand were dominating materials of the Terrace Deposits while sand, silt, clay and peat layers were dominated in the Patan and Thimi Formations. This indicated that subsurface lithology of well location is one of a governing factors for wells depth.

Table 6: Data range of well dimension, elevation and water level depth

River Name	Elevation (m)	Well Diameter (m)	Well Depth (m)	Water level Depth (m)	
				Dry	Wet
Bishnumati River	1280 - 1309	0.8 - 1.2	2.2-7.1	0.9 - 6.8	0.4 - 4.2
Dhobi Khola	1277 - 1329	0.9 - 1.2	2.3-12.2	1.1 - 11.8	0.1 - 3.1
Bagmati River	1267 - 1329	0.8 - 1.6	1.9-8.5	0.9 - 8.8	0.6 - 5.7
Manahara River	1276 - 1390	0.8 - 1.2	1.15-7.6	0.6 - 5.7	0.1 - 5
Hanumante Khola	1280 - 1315	0.8 - 1.2	1.5-15.7	1.1 - 6.3	0.1 - 5.6
Godawari Khola	1293 - 1429	0.9 - 1.3	1.5-10.4	0.5 - 8.3	0.1 -4.5
Kodku Khola	1288 - 1430	0.9 - 2.3	2.3-9.9	0.4 - 8.3	0.1 - 6.4
Nakhhu Khola	1263 - 1400	0.6 - 1.2	1.4-14.4	0.2 - 3.8	0.1 - 2.6
Balkhu Khola	1267 - 1345	0.8 - 1.2	2.8-10.8	1.3 - 8.1	0.1 - 3

The level of water ranged from 0.2 to 11.8 in the dry season. Shallow water level was measured from well nearby the Nakhu Khola and deeper water level from well near the Dhobi Khola.(Figure 23). Apart from a few wells, the dominancy of wells have shallow water level depths (0.1 to 6.4 m) in the wet season possessing increment in groundwater level (Appendix 3). The research conducted on shallow groundwater level variation in the Kathmandu Valley (Prajapati *et al.,* 2023; Duwal *et al.,* 2019) also presented rises in groundwater level in the monsoon season (August) during their study period 2017 to 2019. The rises of groundwater level in the wet season indicated direct influence of monsoon rainfall. Variable water level depth was noted from wells along a single river as well as among rivers. A minimum variation of 3.6 m was measured from the Nakhu Khola and a maximum of 10.7 m was recorded from the Dhobi Khola during the dry

season which had changed to the wet season with 2.5 m and 6.3 m noted from the Nakhu Khola and Kodku Khola respectively. The variation in groundwater level fluctuation may depends on infiltration capacities of rainfall by sub-surface material. The recording of shallow groundwater level from all river corridors during the wet season (Figure 23) indicated that these areas have higher infiltrating capacities (Lamichane and Shakya, 2019). At the same time, the rate of infiltration can be variable depending on the landuse practices.

Previous studies (Shrestha *et. al*., 2023; Prajapati *et. al*., 2021; Lamichane and Shakya, 2019) presented that the cultivated land had higher infiltration rate comparing to the built land areas. The present study also have similar result. The corridors along the northern (Bagmati, Bishnumati, and Dhobi) and western valley (Balkhu) had higher water level depth in comparison to southern corridors (Godawari, Kodku and Nakhhu). In the land use land cover (LULC) map of the valley by Lamichane and Shakya (2019), the area along the northern corridors are dominated by buildup while the areas along southern corridors have domination of cultivated land. Increment in buildup also increased extraction rate of water from wells which can directly impacted on the water level depth. The observation of higher water level depth in the Bagmati, Bishnumati, Dhobi and Balkhu corridors (Figure 23) may be due to higher extraction rate. The similar result was presented by Duwal et al. (2019) for the central part of the valley.

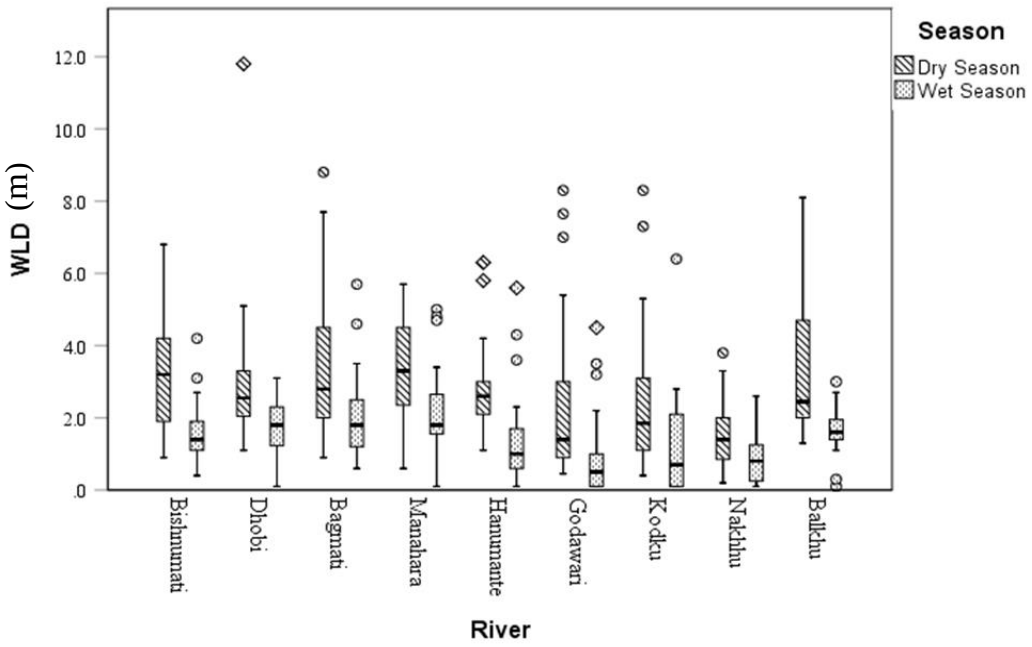

Figure 23: Water level depth (m) variation in rivers during dry and wet seasons

4.2.3 Comparison on in-situ parameters among rivers

Data range of in-situ parameters in river are presented in Table 4.

4.2.3.1 Temperature

The temperature of groundwater is one of essential factor as it can change physical, chemical and biological activities. Increment in temperature is responsible for decrease in solubility of gases such as O_2, CO_2 and N_2 (Yilmaz and Koc, 2014). Increased temperature is also responsible for increases in taste, odour, colour and corrosion problem, as it can growth microorganism (UNICEF, 2008). Temperature increment can also reduce dissolved oxygen amount, increase nitrification rate, oxidation of ammonia to nitrates and generate oxygen-deficient water environment (Ngabirano *et al*., 2016). The average temperature of groundwater varied from 17.6 to 19.8ºC measuring the lowest and highest from Kodku Khola and Dhobi Khola respectively during the dry season. Temperature variations in river corridors are presented in Figure 24. Variations may occur due to differences in water depth, change in sample collection timing and mixing of cold or warm from the surrounding rocks and soils in the plumes (Ngabirano *et al*., 2016). Temporal variation was noticed in the wet season with an average values ranging from 22.59 to 23.66ºC. (Table 7)

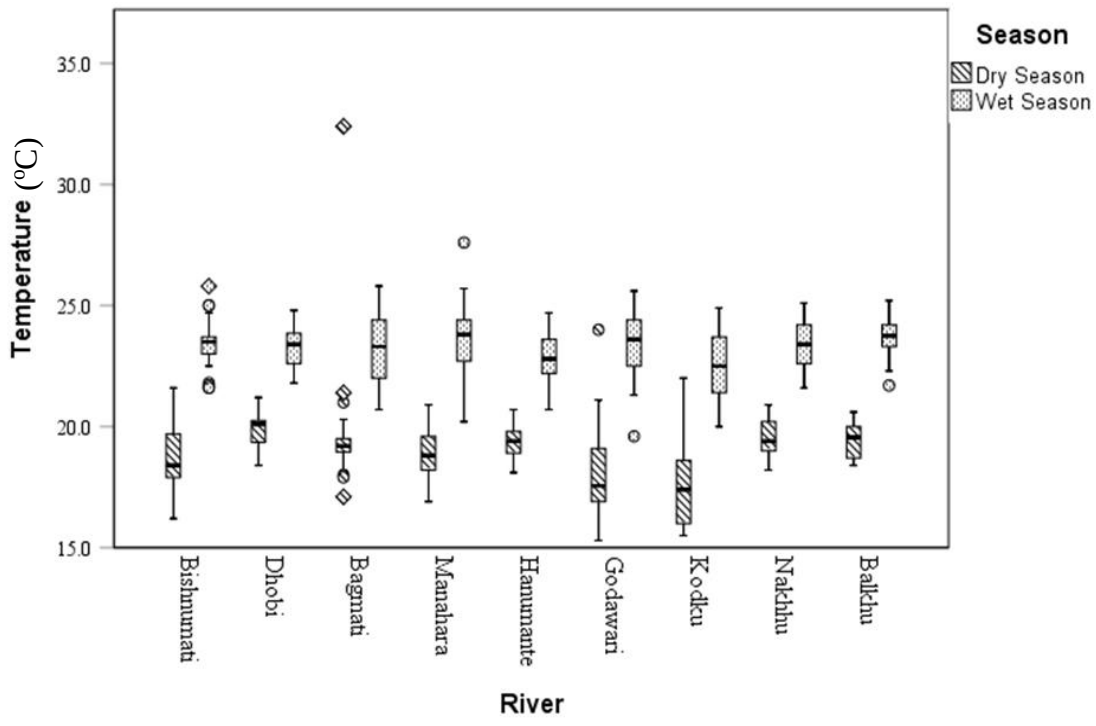

Figure 24: Temperature (ºC) range during dry and wet seasons

Table 7: Maximum and minimum values of in-situ parameters in rivers

River Name		EC (µS/cm)		pH		DO (mg/L)		Temperature (°C)	
		Dry	Wet	Dry	Wet	Dry	Wet	Dry	Wet
	Min	260	334	6.46	5.33	0.26	0.33	16.2	21.6
	Max	2150	2090	8.5	7.73	5.93	6.34	21.6	25.8
Bishnumati River	Average	1014.15	851.73	7.33	7.19	2.39	2.18	18.74	23.4
	Min	231	162.5	6.65	6.5	0.37	0.48	18.4	21.8
	Max	1481	1199	7.41	8.11	6.06	4.88	21.2	24.8
Dhobi Khola	Average	744.93	656.91	6.98	7.24	2.46	2.18	19.83	23.29
	Min	149.6	121.7	6.34	6.71	0.19	0.26	17.1	20.7
	Max	2280	1949	7.34	7.79	4.8	8.55	23.4	25.8
Bagmati River	Average	962.99	872.16	6.84	7.24	1.48	2.16	19.69	23.34
	Min	119.8	148.5	5.96	6.51	0.37	0.52	16.9	20.2
	Max	2070	1922	7.29	7.87	5.43	6.36	20.9	27.6
Manahara River	Average	691.89	666.28	6.69	7.19	2.31	2.27	18.90	23.60
	Min	549	228	5.67	5.92	0.54	0.55	18.1	20.7
	Max	1546	2158	7.69	8.05	4.67	4.88	20.7	24.7
Hanumante Khola	Average	892.17	852.90	6.96	7.26	1.72	2.53	19.37	22.82
	Min	303	299	6.88	6.96	0.5	0.77	15.3	19.6
	Max	2090	1575	7.68	7.8	5.78	5.21	24	25.6
Godawari Khola	Average	707.15	622.40	7.26	7.41	2.26	1.93	18.07	23.38
	Min	230	183	6.16	6.51	0.09	0.42	15.5	20
	Max	1840	1568	8.03	8.06	5.45	5.04	22	24.9
Kodku Khola	Average	710.72	749.44	7.18	7.29	1.67	1.94	17.67	22.59
	Min	242	244	6.8	6.92	0.5	0.19	18.2	21.6
	Max	1131	1540	7.81	7.94	5.7	5.05	20.9	25.1
Nakhhu Khola	Average	614.26	613.04	7.22	7.34	2.15	2.11	19.51	23.42
	Min	553	385	6.63	6.73	0.11	0.33	18.4	21.7
	Max	2860	3030	7.54	8.3	3.46	3.64	20.6	25.2
Balkhu Khola	Average	1123.91	916.18	7.08	7.39	1.46	1.67	19.46	23.66

4.2.3.2 pH

The pH in water represents the concentration of hydrogen ions which can be affected by dissolved gases and salts. The average pH value fluctuated from 6.69 to 7.33 in the dry season with low pH in certain wells near the Hanumante, Manahara and Kodku

kholas as 5.67, 5.96 and 6.16, respectively (Table 7 and Appendix 3) lying below the NWQDS limit (WHO Nepal, 2005). Higher pH of 8.5 noted from a nearby well to the Bishnumati River is difficult to treat with chlorine (Oyem *et al*., 2014). The study of shallow wells by Panta (2011) also showed variation in pH from 5.9 to 11.5 with average 7.1. These results indicated that the pH value was variable within a season depending on the local condition of well location.

The value range of pH is slightly increased in the wet season except in the Bishnumati River (Table 7 and Figure 25). The average value varied from 7.19 to 7.41 showed slightly basic nature (Ramamohan and Sudhakar, 2014) but lies within NDWQS limits (6.5 to 8.5). This value range was slightly increased than that of Bhandari et al. (2021). In their research, the value varied from 6.1 to 6.7 with average value of 6.45. The research conducted by Zhou *et al*. (2015) in China; and Naaz and Anshumali (2015) also presented higher pH in the rainy season comparing to the dry season. Contrarily, the research on South Africa by Edokpayi *et al*. (2015) and Nigeria by Idoko and Oklo (2010) presented higher pH value in the dry season comparing to the wet season.

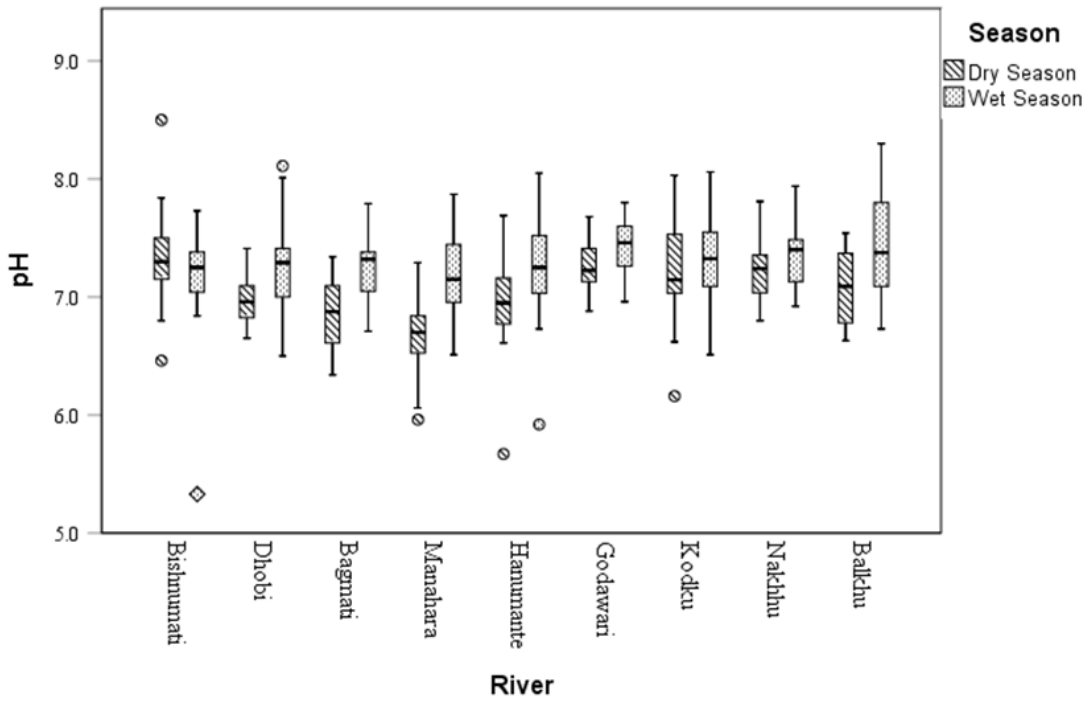

Figure 25: pH range in dry and wet seasons

Generally, a water sample showing less than 7 pH is taken as acidic water which has tendency to corrode metals such as copper, zinc, lead from pipes affecting the level of toxic metal in water (Aytekin and Bayraktaroglu, 2014). The pH can be changed

depending on presence of organic and inorganic solutes along with carbon dioxide containing in the water (EPA, CADDIS). The processes which increases dissolved carbon dioxide or dissolved organic carbon such as sewer effluent, landfill leachate can decrease the value of pH. Contrarily, the agricultural runoff with fertilizer dominated by lime, alkaline subsurface material and dissolve of carbonate or bicarbonate ions can increase pH value (EPA, CADDIS). The pH is negatively correlated to the multiple water quality parameters (ammonia, phosphate) and positively correlated with temperature and DO (Siriwardana, *et al*., 2019). The higher value of pH during the wet season shows slightly alkaline nature of water which might be due to high temperature that can reduces the solubility of carbon dioxide (Mahananda *et al*., 2010). The overall decrease in pH during the dry season may indicate the influence of sewer effluent in the shallow dug wells. But in the case of higher pH of 8.5 (near Bishnumati), there may be presence of point source to increase pH value.

4.2.3.3 Electrical Conductivity (EC)

Electrical conductivity indicates the amount of total dissolved substitution in water (Yilmaz and Koc, 2014). A wide variation of EC was observed as spatially and temporally in groundwater. The average EC value varied from 614.2 to 1123.9 µS/cm in the dry season. The value range was decreased to 613.0 and 916.1 µS/cm during the wet season. Wells from the Balkhu Khola corridor presented the highest value and from the Nakhu Khola had the lowest in both seasons (Table 7). Besides few wells, majority of wells had lower EC during the wet season compared to the dry season. Occurrences of lower EC during the wet season were the indication of dilution in dissolved ions due to infiltration of precipitation (Ngabirano *et al*., 2016). Generally, wells with lower EC were concentrated in the upstream segments of rivers and well with higher EC were dominated at the downstream urbanized area of the Kathmandu Valley (Figure 26 and Figure 27). Wells located in the downstream section of rivers, except the Nakhu and the Dhobi Khola, exceed the permissible the limit of NDWQS (1500 µS/cm) (Figure 26). The EC values exceeding limit of NDWQS indicated unsuitability for drinking purposes.

The conductivity of groundwater along the Bagmati corridor was also analyzed by Gautam *et al*. (2013) from the water sample collected in 2009/10 for three seasons as winter, monsoon and post-monsoon. During their study periods, conductivity value of

groundwater varied from 1372 µS/cm to 159 µS/cm. This range of conductivity was lower than the present range of groundwater collected from the Bagmati River (149.6 to 2280 µS/cm and 121.7 to 1949 µS/cm in dry and wet season respectively). The variation in conductivity value in a single river within 7 years (2010 to 2017) indicated that the groundwater contain more ions as year passed. The observation of higher EC represented the higher concentration of dissolved ions. These ionic substances were available to groundwater by infiltration of solid wastes, industrial wastes, agricultural wastes, and leakage of safety tanks and sewer pipes (Pant, 2011). The lower concentration of EC observed from the Nakhu Khola in both seasons indicated that this corridor was less effected by anthropogenic activities during the study periods comparing to other corridors.

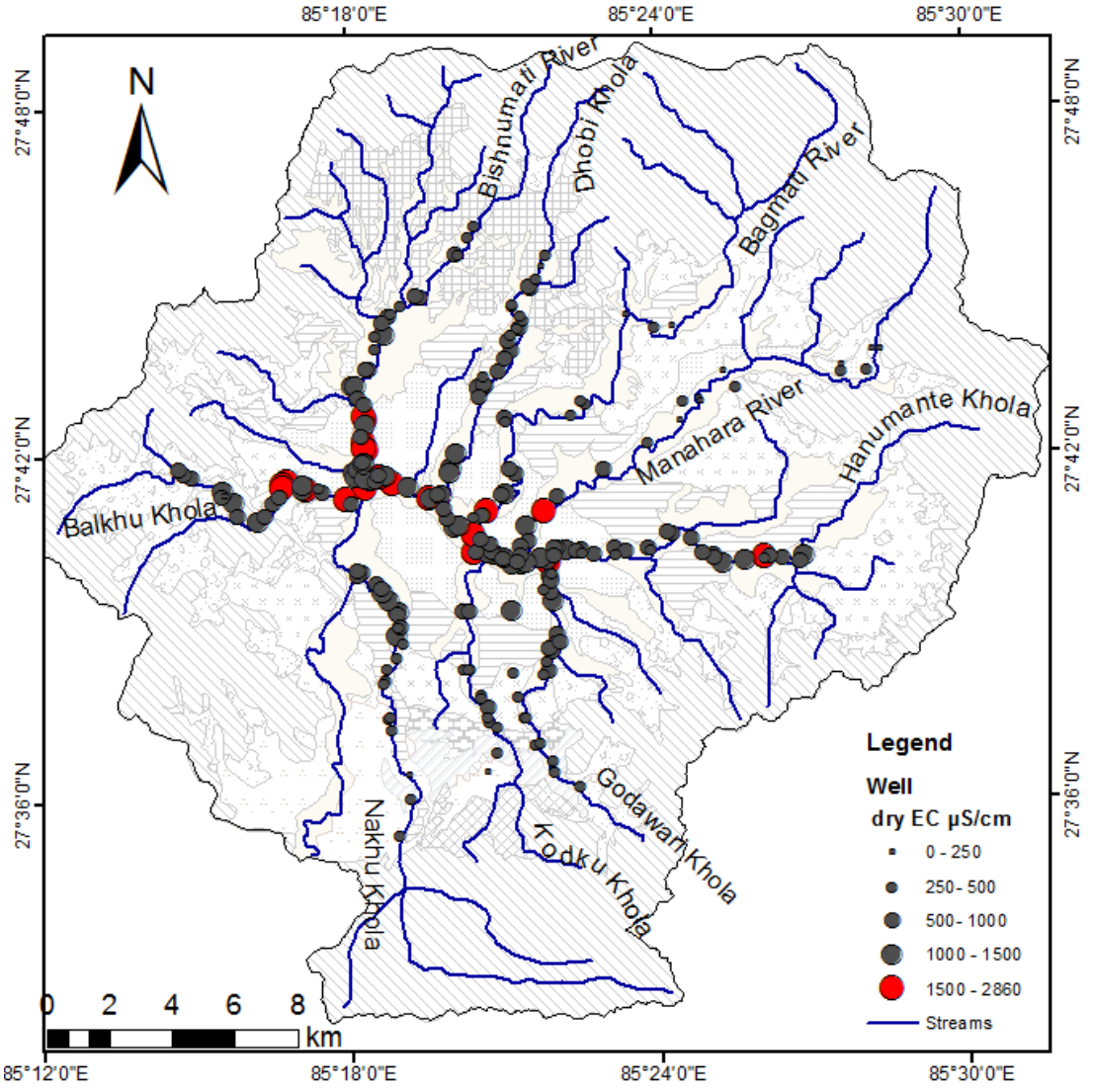

Figure 26: EC variation in the dry season

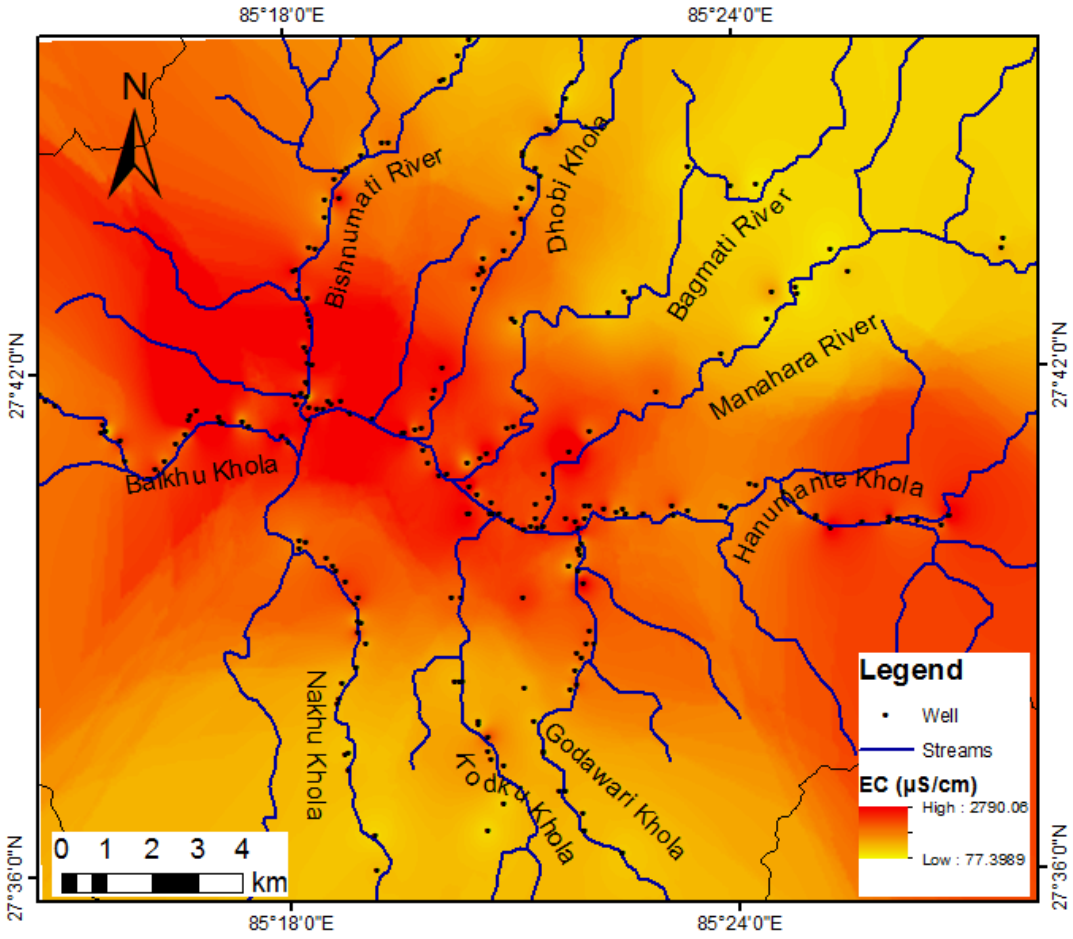

Figure 27: EC variation from upstream to downstream section in the dry season

4.2.3.4 Dissolve Oxygen (DO)

Dissolved oxygen is the indication of the level of free, non-compound oxygen present in water. It is a major parameter for assessing water quality, as it can influence the living organism within a body of water. Variations in DO depend on temperature and salinity of water (Fundamentals of Environmental Measurements, 2015). DO has an increased value range in the wet season (1.67 and 2.53 mg/L) compared to the dry season (1.46 to 2.46 mg/L). DO variation observed by Gautam et al., (2013) also showed similar increasing trend in the wet season. The highest DO was measured from wells of the upstream section and decreased in wells towards core areas of the Kathmandu Valley. Increased DO was generally observed with increased temperature and decreased EC.

Comparing among nine rivers, a minimum value obtained from the downstream of the Kodku Khola (0.09 mg/L) and a maximum value found in the sample from upstream of the Dhobi Khola (6.06 mg/L) in the dry season. But in the case of the wet season,

minimum (0.26 mg/L) and maximum (8.55 mg/L) values of DO were recorded from the downstream and the upstream segments of the Bagmati River (Figure 28 and Table 7).

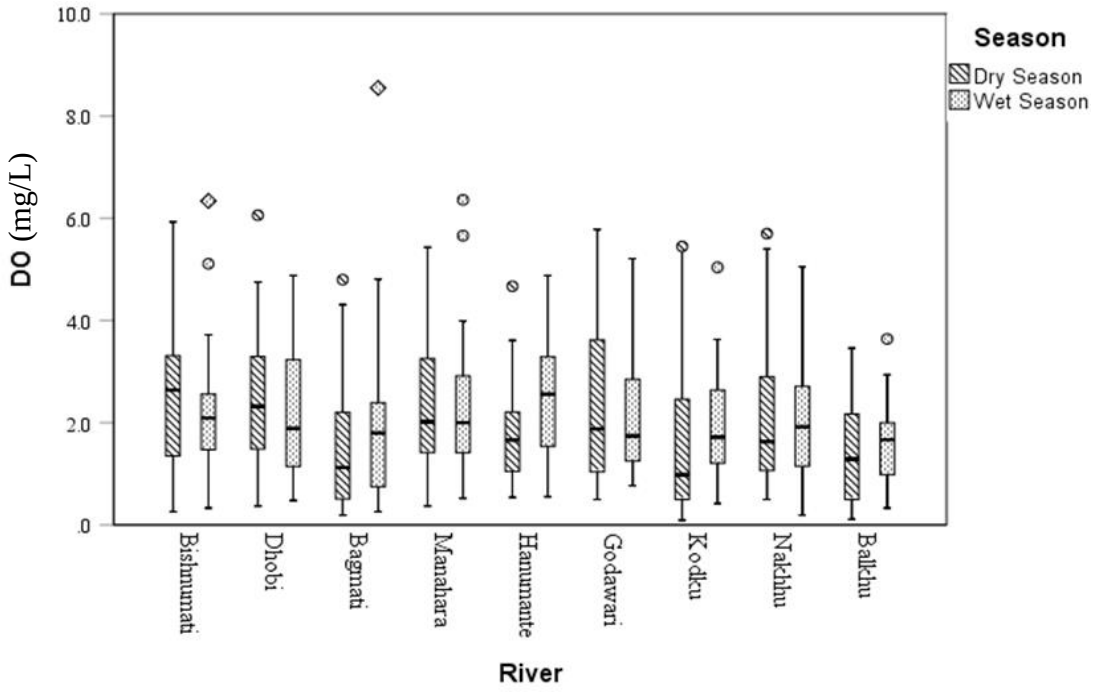

Figure 28: DO variation in dry and wet season

4.2.4 Relation between in-situ parameter of water and distance from river channel to well location

Distance from the river channel to wells was divided into 4 categories as 0–30 m, 30–60 m, 60–90 m and above 90 m. Table 8 presents ranges of EC, DO, temperature and pH of wells located at categorized distances. The highest EC was observed in the wells of the first category (0-30 m) presenting an average value of 878.2 µS/cm. Average EC gradually decreased to 858.1 µS/cm, 727.2 µS/cm and 378.1 µS/cm as the distance from the river channel increased to 30–60 m, 60–90 m and above 90 m, respectively in the dry season. But within 30 m distance also, there was a wide range of values with a minimum of 231 µS/cm and a maximum 2860µS/cm. The minimum value recorded from the upstream section whereas a maximum value was noted from the downstream section. This value variations in upstream and downstream clearly indicated that the upstream segments had lower dissolved ions compared to downstream urban section. Additionally, this result also represented higher chemical contamination in the downstream section. Previous research conducted on the groundwater along the

Bagmati river (Gautam *et al*., 2013; Maharjan, 2018) also presented similar decreasing value trend. They also reported higher EC in the groundwater located close to the river channel and towards downstream urban areas. Lower average EC was observed in the wet season in all categories except last one (<90 m) (Table 8).

Table 8: In-situ parameter and distance from river channel

Parameters		Distance from river channel							
		0 - 30 m		30 -60 m		60 - 90 m		>90 m	
		Dry	Wet	Dry	Wet	Dry	Wet	Dry	Wet
EC (µS/cm)	Min	231	121.7	126.8	160.5	169.9	190	119.8	148.5
	Max	2860	2090	2090	2158	1637	1413	1092	1142
	Average	878.2	765.6	858.1	817.0	727.2	646.0	378.1	475.0
pH	Min	6.46	5.33	6.35	6.73	5.67	5.92	5.96	6.51
	Max	8.5	8.3	7.73	7.85	8.03	7.87	7.23	7.82
	Average	7.1	7.3	7.1	7.3	7.0	7.2	6.5	7.2
DO (mg/L)	Min	0.09	0.19	0.19	0.36	0.11	0.59	0.31	1.02
	Max	5.93	8.55	6.06	4.81	4.75	3.88	4.61	6.36
	Average	1.9	2.2	2.1	2.0	2.0	1.9	2.1	2.8
Temp. (°C)	Min	15.3	19.6	15.5	21	15.4	21	18.8	20.2
	Max	21.6	25.8	23.4	25.8	24	27.6	16	24.1
	Average	19.0	23.3	19.3	23.5	18.9	23.4	19.7	23.0

The average pH and temperature were more or less similar in all categories in both seasons. But in the case of DO, near channel wells (within 30 m) showed a least average value of DO (1.9 mg/L) which had increased to 2.1 mg/L with an increased in distance from the river. The combined information on EC and DO suggested two probabilities: (1) nearby wells may be recharged by the polluted river water and contaminated groundwater (Gautam *et al*., 2013) and (2) leachate from solid waste, sewer and industrial disposal near the river banks contaminated the shallow groundwater.

4.2.5 Selection of wells for an interconnection study

Except in Kodku and Nakhu Kholas, 10 wells were selected from an inventory of each river for the detailed study about interconnection. (Figure 26). The selection was based primarily on the distance from the river channel, geology of the well location and easily assessable to the location.

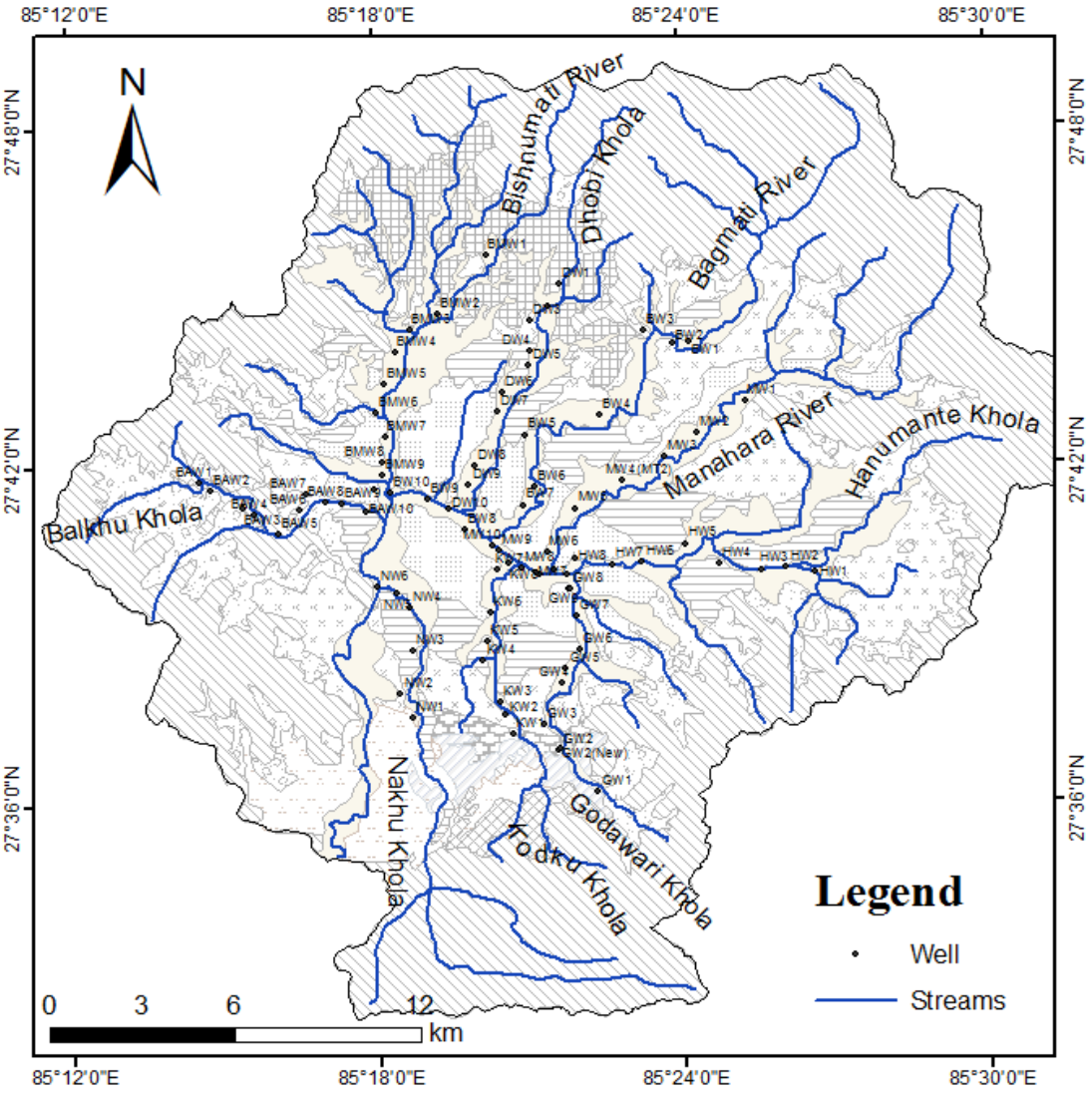

Figure 29: Location of selected well from inventory

4.2.6 Groundwater and river water sampling

Groundwater samples were collected from selected wells from inventory and river water from the river located nearby the selected wells. Samples collection was conducted in wet (August 2017) and dry (February 2018) seasons. In the wet season, Total of 165 water samples were collected among which 80 were collected from the river, 80 from shallow dug wells and 5 from shallow tube wells. Similarly, 162 water samples were collected in the dry season, 80 from river, 79 from dug well and 3 from tube well.

Except in a few locations, samples were collected from the same wells and river locations during wet and dry seasons.

4.3 In-situ and hydro-chemical parameters of groundwater and river water

In-situ parameters, namely, well depth, water level depth, electrical conductivity (EC), dissolved oxygen (DO), pH and water temperature measured at each sampling location in the wet and dry seasons. While hydro-chemical parameters were analyzed from collected water samples at the laboratory of the University of Yamanashi, Japan using Ion Chromatography. Ion chromatograph can measure the chemical concentration of cations (Li^+, Na^+, K^+, NH_4^+-N, Ca^{2+}, Mg^{2+}) and anions (F^-,Cl^-, Br^-, NO_2^--N, NO_3^--N, HCO_3^-, PO_4^--P and $SO4^{2-}$) of each sample. But in the present study, concentration of Li^+, F^-, Br^-, and NO_2^--N were nearly absent. Detailed data of hydro-chemical parameters of nine rivers are presented in Appendix 4.

4.3.1 Bishnumati River

Total of 20 samples, 10 from dug wells (BMW1 to BMW10) and 10 from their nearby river location (BMR1 to BMR10) were collected in the wet season. But in the dry season, only 17 water samples were collected. Two wells BMW3 and BMW10 became dry so water samples from these two wells as well as BMR10 were not collected. The sampling locations of the well and river are presented in Figure 30.

4.3.1.1 In-situ parameters

Table 9 presents the locations of sample points, water level depth, and in-situ parameters in the wet and dry seasons. The depth of dug wells varied from 2.2 to 7.1 m while the distance of the sample wells ranged from 5 to 50 m away from the river channel. All wells presented shallow water depth in the wet season which may imply high recharge and lower extraction rate during the wet season with a maximum fluctuation of 6.1 m and minimum fluctuation of 1.2 m at BMW9 and BMW8 respectively.

The temperature of river water was varied from 22.6^{o}C to 26.5^{o}C and 12.3.0-18.6^{o}C in the wet and dry seasons respectively. On the other hand, groundwater temperature had a fluctuation of 21.6-24.7^{o}C in the wet season and 14.2-20.3^{o}C in the dry season. River water and groundwater showed slightly decreased pH during the dry season (Table 6). EC of groundwater was varied from 334 to 1536 µS/cm in the wet season, and from 256 to 1667 µS/cm in the dry season. Except BMW1 and BMW4 (Table 9), the remaining groundwater had higher EC in the dry season relative to the wet season. But in the case of the river water, value of EC was low in the wet season (147.5 to 439 µS/cm) and

abruptly increased up to four times (364 to 1644 µS/cm) in the dry season. DO was relatively high in the river water during the wet season which was drastically reduced during the dry season.

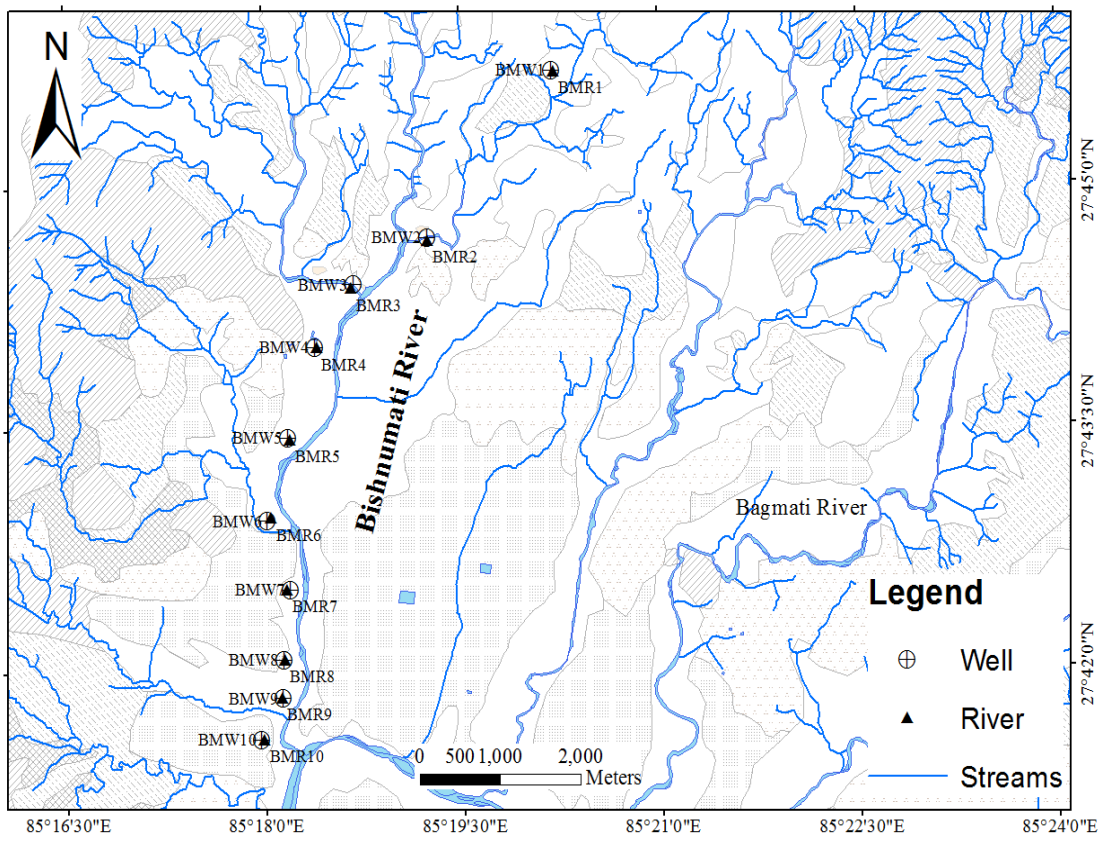

Figure 30: Sampling points of groundwater and river water in the Bishnumati River

4.3.1.2 Hydro-chemical parameters

Figure 31 and Appendix 4A present the spatial and temporal variations of the chemical parameters studied from river water and groundwater. Ca^{2+}, Na^{+}, and HCO_3^{-} were principal ions of river water in the wet season, with value variations from 9.9 to 18.5 mg/L, 7.5 to 16.8 mg/L, and 42.7 to 109.8 mg/L respectively (Figure 31). The dominant cations had an order of Na^{+}>Ca^{2+}>K^{+}> NH_4^{+}-N>Mg^{2+} in the wet season, which changed to the order of Na^{+}> NH_4^{+}> K^{+}>Ca^{2+}>Mg^{2+} in the dry season. Similarly, in the case of anion, HCO_3^{-} was dominant, followed by Cl^{-} and SO_4^{2-} in both wet and dry seasons. All chemical parameters presented strong significant seasonal variation ($p<0.01$). Concentration of all these parameters increased in the dry season with different increment rates. NH_4^{+}-N concentration was very low (<5 mg/L) in the wet season and

drastically increased in the dry season, with variations of 3.6 to 83.6 mg/L. In the same way, the concentration of Na^+, K^+, Cl^-, PO_4^--P, and HCO_3^- increased by four to six times more than in the wet season (Figure 31). Based on the results from the chemical analyses, the Bishnumati River was categorized as Ca-HCO_3 type in the wet season and Na-K-HCO_3 type in the dry season, except BMR1 (Appendix 5A).

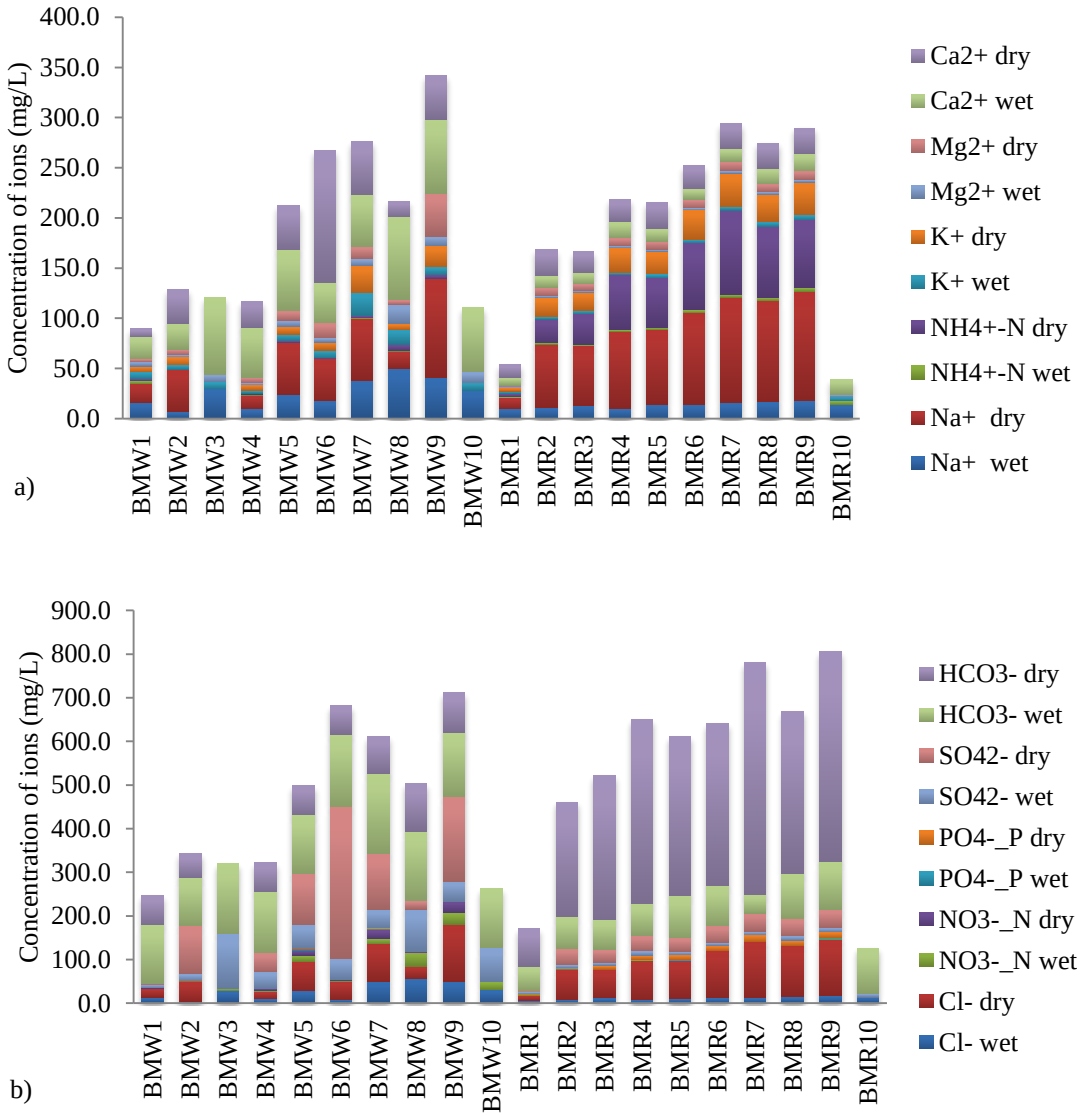

Figure 31: Bar diagram showing temporal and spatial variation of cation (a) and anion (b) in groundwater and river water of the Bishnumati River

Likewise, Ca^{2+}, HCO_3^- and SO_4^{2-} were the most dominant ions in the wet season with values ranging from 22.1 to 82.9 mg/L, 109.8 to 183 mg/L and 8.3 to 126 mg/L respectively. Except in BMW1 and BMW8, concentrations of Na^+, K^+, Mg^{2+}, Cl^-, and SO_4^{2-} were increased in the dry season (Figure 31) but statistical analysis (paired t-test within 95% confidence level) showed no significant temporal variation.

Table 9: Well information and in-situ parameters of the Bishnumati River

Sampling ID	E	N	Elevation (m)	Distance from river (m)	Bank	Well Depth (m)	Water Level Depth (m)			DO (mg/L)		EC (µs/cm)		Water Temp (°C)		pH	
							wet	dry	DWLD	wet	dry	wet	dry	wet	dry	wet	dry
BMW1	85.336611	27.761972	1303	30	Right	2.2	1.2	1.3	0.1	0.52	2.47	368	256	24.7	14.2	6.84	6.47
BMW2	85.320778	27.744778	1296	20	Right	2.2	0.4	4	3.6	2.56	5.5	468	826	23.5	15	7.29	7.61
BMW3	85.311417	27.74	1291	10	Right	4.9	2.7	WD		0.7		1074		21.6		5.33	
BMW4	85.306472	27.733556	1290	15	Right	4.6	1	2.2	1.2	2.21	1.01	740	579	23.6	16.7	7.17	6.6
BMW5	85.302972	27.72425	1289	40	Right	5.1	0.4	3.1	2.7	1.55	3.97	334	768	23.3	16.8	7.46	6.28
BMW6	85.300361	27.715667	1289	50	Right	4.85	1.4	4.1	2.7	1.5	3.18	779	1395	23.5	15.8	6.97	6.73
BMW7	85.303139	27.7085	1287	20	Left	4.2	1.3	3.1	1.8	0.33	3.67	880	1449	23.2	14.6	7.35	6.31
BMW8	85.30225	27.701278	1283	7	Right	3.2	1.1	1.2	0.1	1.08	0.72	1536	1667	23.7	20.3	7.29	6.54
BMW9	85.302167	27.697306	1288	25	Left	7.1	1.4	6.1	4.7	3.72	2.93	689	1440	24.1	16.9	7.5	7.01
BMW10	85.299387	27.693055	1285	15	Right	6.9	0.9			1.85		1139		23.2		7.29	
BMR1	85.336884	27.761842								6.37	4.77	147.5	364	22.6	12.3	7.76	7.14
BMR2	85.320821	27.744483								4.78	2.48	220	829	24.4	14	7.72	7.23
BMR3	85.311148	27.739596								3.95	0.97	255	915	24.2	14.1	7.71	7.16
BMR4	85.306729	27.733493								3.79	1.85	304	1109	25	14.3	7.75	7.32
BMR5	85.303244	27.723989								2.34	0.43	305	1285	25.9	14.7	7.86	7.29
BMR6	85.300783	27.715945								1.22	0.13	347	1341	26.5	14.6	7.9	7.21
BMR7	85.302713	27.708508								2.06	0.16	358	1510	26.1	14.3	7.99	7.25
BMR8	85.302355	27.701284								0.64	0.15	375	1551	25.8	17.8	7.88	7.16
BMR9	85.301994	27.697333								1.92	1.27	416	1644	25.6	18.6	8	7.15
BMR10	85.299699	27.693048								1.02		439		25.7		7.92	

BMW = Bishnumati well water, BMR = Bishnumati river water, DWLD = Difference in water level depth, WD = Well dry

While in the case of HCO_3^-, the concentration decreased in the dry season showing strong significant temporal variation with a p-value of 0.000. The decrement in HCO_3^- along with increment in SO_4^{2-} indicates mineral dissolution from the gneissic rock from upstream section of this river in the dry season. Chemical concentration plot on the piper diagram categorized the water type of wet season as Ca-HCO_3 except for BMW3, BMW8 and BMW10. As dominant anions change in the dry season, water type also changed to Ca-SO_4 except for BMW1 and BMW8. Water samples of BMW1 and BMW8 changed from Ca-HCO_3 and Ca-SO_4 (in the wet season) to Na-K- HCO_3 and Ca-HCO_3 respectively during the dry season (Appendix 5A).

4.3.2 Dhobi Khola

Figure 32 present sampling location of groundwater and river water. Total of 21 samples, 10 from dug well (DW1 to DW10), 10 from the river (DR1 to DR10) and 1 from shallow tube well (DT1) were collected in the wet season. But in the dry season, only 19 samples were collected. DW3 was totally dry and thus DR3 was also not collected during this season.

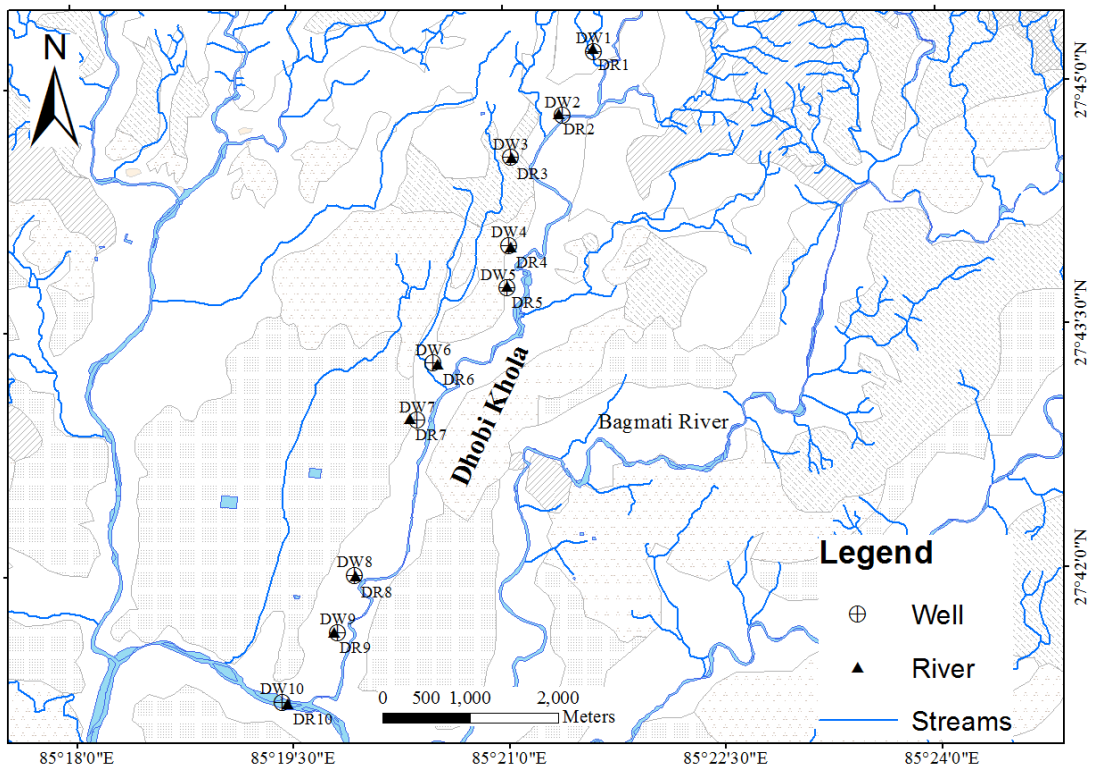

Figure 32: Sampling point of groundwater and river water in the Dhobi Khola

4.3.2.1 In situ parameters

The depth of dug wells selected from the Dhobi Khola was varied from 2.6 to 5.5 m whereas the distance of the sample wells was ranged from 5 to 80 m away from the river channel. Very shallow water depth was observed at DW9 (0.1 m) and deep at DW2 (3.1 m) during the wet season. Except DW6 and DW10, all other dug wells had the shallow water depth in the wet season (Table 7) with a maximum variation of 2 m and a minimum variation at 0.5 m at DW7 and DW8 respectively.

The wide range of river water temperature was observed in the wet season (23.4 to 27.4°C) as compared to that of the dry season (15.4 to 18.5°C). Temperature of groundwater was slightly lower than that of river water with value range from 20.7 to 24.5°C in the wet season which changed to the range between 15.5 to 19.4°C during the dry season. The pH value of both river water and groundwater slightly changed to acidic nature during the dry season. EC of river water showed increasing trend towards downstream section both in the wet and dry seasons. It was lower in the wet season (116.8 to 809 µS/cm) which was increased up to four times during the dry season (328 to 1472 µS/cm). Similarly, EC of groundwater was also increased in the dry season except at DW4 and DW7 (Table 10) with value range from 116.3 to 1274 µS/cm. The increment rate of groundwater EC in the dry season was much lower than that in the river water. Highest EC was obtained at the dug well located in the downstream section (DW10) while lowest was observed at shallow tube well DT1, located in upstream sections (Table 10) in both wet and dry seasons. DO of upstream river water was high in both wet and dry seasons with value ranged from 1.26 to 6.32 mg/L which rapidly decreased towards downstream river sites (<1 mg/L). Contrarily, DO of groundwater was relatively high in the dry season with a value variations from 1.66 to 4.76 mg/L as compared to that in the wet season (0.48 to 3.83 mg/L).

4.3.2.2 Hydro-chemical parameters

Na^+ and Ca^{2+} were dominant cations of wet season river water which was followed by NH_4^+–N, K^+ and Mg^+ (Figure 33 and Appendix 4B). All these cations significantly increased ($p < 0.001$) in the dry season with an order of $Na^+ > NH_4^+$–$N > K^+ > Ca^{2+} > Mg^{2+}$. Similarly, in the case of anion, $HCO3^-$ was most dominant, and followed by Cl^- and SO_4^{2-} in both wet and dry seasons. Except NO_3^--N, all anions showed strong significant temporal variation ($p < 0.001$). However, all these parameters showed significant

temporal increment, the rate of increment was different for different parameters. Higher concentration of Na^+, NH_4^+–N, K^+ and Cl^- in the dry season signified additional effects of anthropogenic contamination in the river water. Furthermore, all these parameters showed gradual increment of concentration towards downstream river sections in both seasons. Downstream river water had more than three times higher concentrations in relative to upper most section of river water (Figure 33). Based on the Piper plot from the chemical analysis, the river water classified as Ca-HCO_3 type and Na-K-HCO_3 in the wet and dry seasons respectively (Appendix 5B).

Alike in the river water, Ca^{2+} and Na^+ were dominant cations of groundwater in both wet and dry seasons (Figure 33). The concentration of Ca^{2+} ranged from 5.4 to 84.6 mg/L in the wet season and from 5.7 to 33.5 mg/L in the dry season. Similarly, Na^+ concentration varied from 4.0 to 31.6 mg/L in the wet season and from 6.2 to 59.5 mg/L in the dry season.

But in the case of anions, $HCO3^-$ was dominant and followed by SO_4^{2-} and Cl^-. Wells located at upstream sections; especially DT1 and DW3 showed lower ions concentration while wells of downstream river sections (DW6 to DW10) had higher ions concentration in the wet season. The concentration of Ca^{2+} and SO_4^{2-} drastically increased in DW7 with a value of 84.6 mg/L and 113.1 mg/L in the wet season. Paired T-test (within 95% confidence level) showed strong significant temporal variation ($p< 0.02$) only in K^+ and Ca^{2+}.

Concentration of Ca^{2+} decreased in all samples of dug wells except DW1 and DT1 whereas K^+ concentration increased in all water samples of dug wells except DW6 in the dry season. Generally, most the groundwater samples showed an increment of chemical concentration in the dry season. But in the case of DW4, DW6 and DW7, chemical parameters such as Na^+, K^+, Mg^+, Ca^{2+}, Cl^-, SO_4^{2-}, NO_3^--N and $HCO3^-$ decreased in the dry season relative to the wet season.

Based on these chemical concentrations, groundwater samples collected from DW1, DW4, DW6 and DW9 were classified as Ca-HCO_3 type in both wet and dry seasons. But in the remaining groundwater samples, water type changed from Ca-HCO_3 type to Na-K-HCO_3 type (DW8 and DW10) and Na-Cl-SO_4 type (DW2 and DW5). Water samples collected from DW3 and DW7 were classified as Ca-Cl-SO_4 in both wet and dry seasons (Appendix 5B).

Table 10: Well information and in-situ parameters of the Dhobi Khola

Sampling ID	E	N	Elevation (m)	Distance from river (m)	Bank	Well Depth (m)	Water Table (m)			DO (mg/L)		EC (µs/cm)		WaterTemp(°C)		pH	
							Wet	Dry	DWLD	Wet	Dry	Wet	Dry	Wet	Dry	Wet	Dry
DW1	85.3605	27.75344	1315	15	Right	2.6	0.9			1.1	3.8	283	311	23.6	16	7.0	6.3
DT1	85.35952	27.75223	1315	10	Left					2.8	2.4	113.8	116	20.7	15.5	7.1	6.2
DW2	85.3568	27.74689	1315	10	Left	5.5	3.1			3.2	4.5	357	386	22.3	18.5	6.9	6.7
DW3	85.35081	27.74264	1309	20	Right	3.7	2	WD		1.5		162.5		24.5		8.1	
DW4	85.35051	27.73362	1306	40	Right	3	1.3	2	0.7	3.0	3.7	448	418	24	15.9	7.1	6.7
DW5	85.35028	27.72925	1304	5	Left	3.5	2	3.1	1.1	2.6	3.1	515	761	21.8	17.1	7.4	6.6
DW6	85.34162	27.72163	1300	80	Right	3.1	2.2	2	-0.2	2.3	3.6	389	549	24	16.8	7.6	6.5
DW7	85.33969	27.71577	1304	60	Left	5.4	1.2	3.2	2	3.8	4.7	843	757	23.2	17.2	7.0	7.5
DW8	85.3323	27.69994	1294	20	Right	4.7	1.9	2.4	0.5	0.5	1.7	1128	1179	22.8	18.5	7.6	6.8
DW9	85.33018	27.69411	1291	40	Left	2.75	0.1	1.6	1.5	1.2	4.2	780	1098	23.6	16.3	7.4	6.6
DW10	85.32379	27.687	1283	50	Right	3.25	2.4	1.5	-0.9	0.7	2.5	1196	1274	22.4	19.4	7.5	6.9
DR1	85.36047	27.75365								6.3	4.7	116.8	328	23.4	15.9	8.1	7.4
DR2	85.3564	27.74705								6.1	3.0	141.9	439	24.4	15.4	7.9	7.3
DR3	85.35096	27.74255								5.4		168.3		25.6		8.1	
DR4	85.3507	27.73344								3.6	1.3	228	956	26.8	16.8	8.0	7.3
DR5	85.3502	27.72934								2.5	0.7	315	1037	25.9	17.3	8.1	7.4
DR6	85.34209	27.72151								1.2	0.5	330	1183	27.4	18.1	8.0	7.3
DR7	85.33885	27.71587								0.2	0.2	354	1301	26	17.5	7.9	7.3
DR8	85.33235	27.69979								0.0	0.2	445	1353	25.6	17.5	8.0	7.3
DR9	85.32983	27.69408								0.0	0.1	451	1472	26.1	17.3	7.9	7.2
DR10	85.32437	27.68679								0.3	0.1	809	1382	25	18.5	7.9	7.3

DW = Dhobi well water, DR = Dhobi river water, DWLD = Difference in water level depth, WD = Well dry

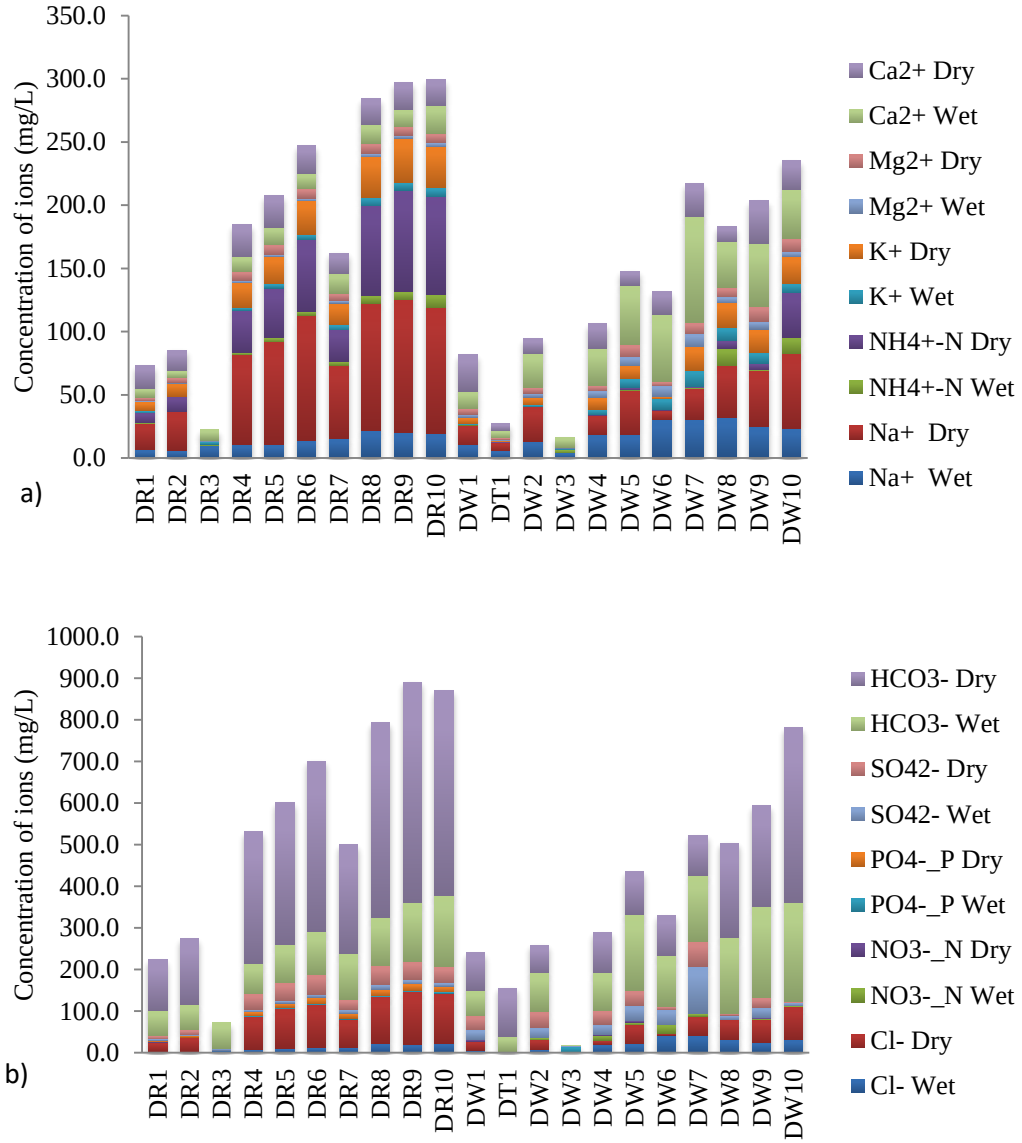

Figure 33: Bar diagram showing variation of cation (a) and anion (b) in the Dhobi Khola

4.3.3 Bagmati River

The sampling location of groundwater and river water is presented in Figure 34. Total of 21 water samples were collected, 10 from the river (BR1 to BR10), 10 from dug wells (BW1 to BW10) and 1 from shallow tube well (BT2) in the wet season. In the dry season, additional two samples BT1W and BT1R were collected along with samples from 21 wet season locations.

4.3.3.1 In situ parameters

Dug wells selected from the Bagmati River ranged in depth between 2.75 and 6.5 m while shallow tube wells depth varied from 16.76 to 36.57 m. Except for BW7, wells

presented shallow water levels in the wet season with a higher variation of 3.6 m and a lower variation of 0.16 m at BW4 and BW1 respectively (Table 11).

The temperature of river water varied from 22.1 to 28.4°C in the wet season and 16.6 to 22.1°C in the dry season. Temperature range of groundwater was 21.7 to 25.7 in the wet season and 15 to 20.4°C in the dry season (Table 11). Both river water and groundwater showed slightly reduced pH values during the dry season. EC measures in groundwater varied from 94.2 to 1413 µS/cm in the wet season which changed to the range between 157.6 and 1351 µS/cm in the dry season. Except for BW5, BW8 and BW10, all other groundwater had greater EC in the dry season compared to the wet season (Table 11). But in the case of river water, low EC (41.2–290 µS/cm) was recorded in the wet season which drastically increased up to eight times (150.6–1369 µS/cm) in the dry season. Comparing the EC of river water and groundwater in both seasons, highest EC was noted at BW10 (1413 µS/cm), located in the downstream section of the river. DO of groundwater ranged from 0.6 to 4.7 mg/L in the wet season while it changed to the range of 0.33 to 4.46 mg/L in the dry season. DO of upstream river water (BR1 to BR3) was high in both seasons while the value lay below 1 in the remaining downstream section in the dry season (Table 11). However, in the case of groundwater, the value range of DO was more or less similar in both seasons.

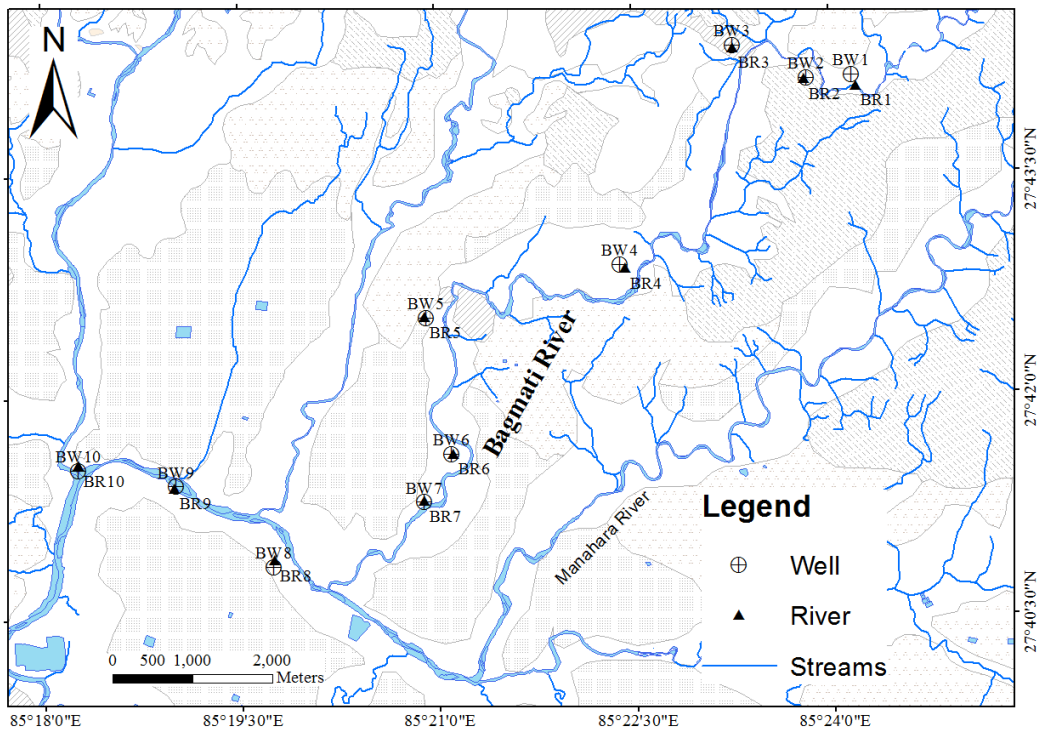

Figure 34: Sampling points of groundwater and river water in the Bagmati River

4.3.3.2 Hydro-chemical parameters

Spatial and seasonal variations of chemical concentrations are presented in Figure 35. Ca^{2+}, Na^{+} and $HCO3^{-}$ were the most dominant river water ions in the wet season with a value ranging from 2.3 to 15.1 mg/L, 3.4 to 15.7 mg/L and 18.3 to 97.6 mg/L respectively. Except for NO_3^{-}–N, all other parameters showed strong significant temporal variation ($p < 0.01$). The concentration of Na^{+}, K^{+} and Cl^{-} increased more than ten times in the dry season while the concentration of Ca^{2+}, Mg^{+}, SO_4^{2-} and HCO_3^{-} increased up to 5 times (Figure 35 and Appendix 4C). But in the case of NH_4^{+}–N and PO_4^{-}–P, the concentration of these parameters is very less (< 3 mg/L) in the wet season and abruptly increased in the dry season ranging from 0.08 to 69.13 mg/L and 0.37 to 17.8 mg/L respectively. All these chemical parameters had the lowest concentration in the upstream section and highest in downstream urbanized areas in both seasons. Piper plots from the chemical analysis classified river water as Ca-HCO_3 type and Na-K-HCO_3 type in the wet and dry season respectively. (Appendix 5C).

Alike in river water, Ca^{2+}, Na^{+} and $HCO3^{-}$ were the most dominant groundwater ions in the wet season with a value ranges from 2.6 to 49.2 mg/L, 2.7 to 30.7 and 30.5 to 201.3 mg/L respectively. The range of these parameters was nearly double the range observed in the river samples during the wet season. It indicated that groundwater had a higher chemical concentration than river sample in this season. Concentrations of ions were mostly increased in all groundwater samples during the dry season, except at BW3 and BW4. But the increment rate was much lower as compared to the river samples. Paired T-test (within 95% confidence level) showed strong significant temporal variation ($p < 0.03$) in Na^{+}, NH_4^{+}–N, Mg^{+} and Cl^{-}. Groundwater collected from BW1, BW2, BW3, BW9 and BW10 was categorized as Ca-HCO_3 in both seasons. The water types of BW4 and BW5 changed from Ca-HCO_3 to Ca-Cl-SO_4, and BW6 and BW7 changed from Ca-HCO_3 to Na-K-HCO_3 and Na-K-SO_4-HCO_3 respectively (Appendix 5C). But in the case of BW8, groundwater is classified as Ca-Cl-SO_4 in both wet and dry seasons.

4.3.4 Manahara River

Figure 36 presents the sampling location of groundwater and river water. Total of 21 samples, 10 from river water (MR1 to MR10), 9 from dug well (MW1 to MW10, MW4

not collected) and 2 from boring (MB1 and MB2) were collected in the wet season. But in the case of the dry season, MB1 and MB2 could not be collected and thus new sample MW4 was collected.

4.3.4.1 In-situ parameters

Table 12 presents in-situ parameters measured in the wet and dry seasons.

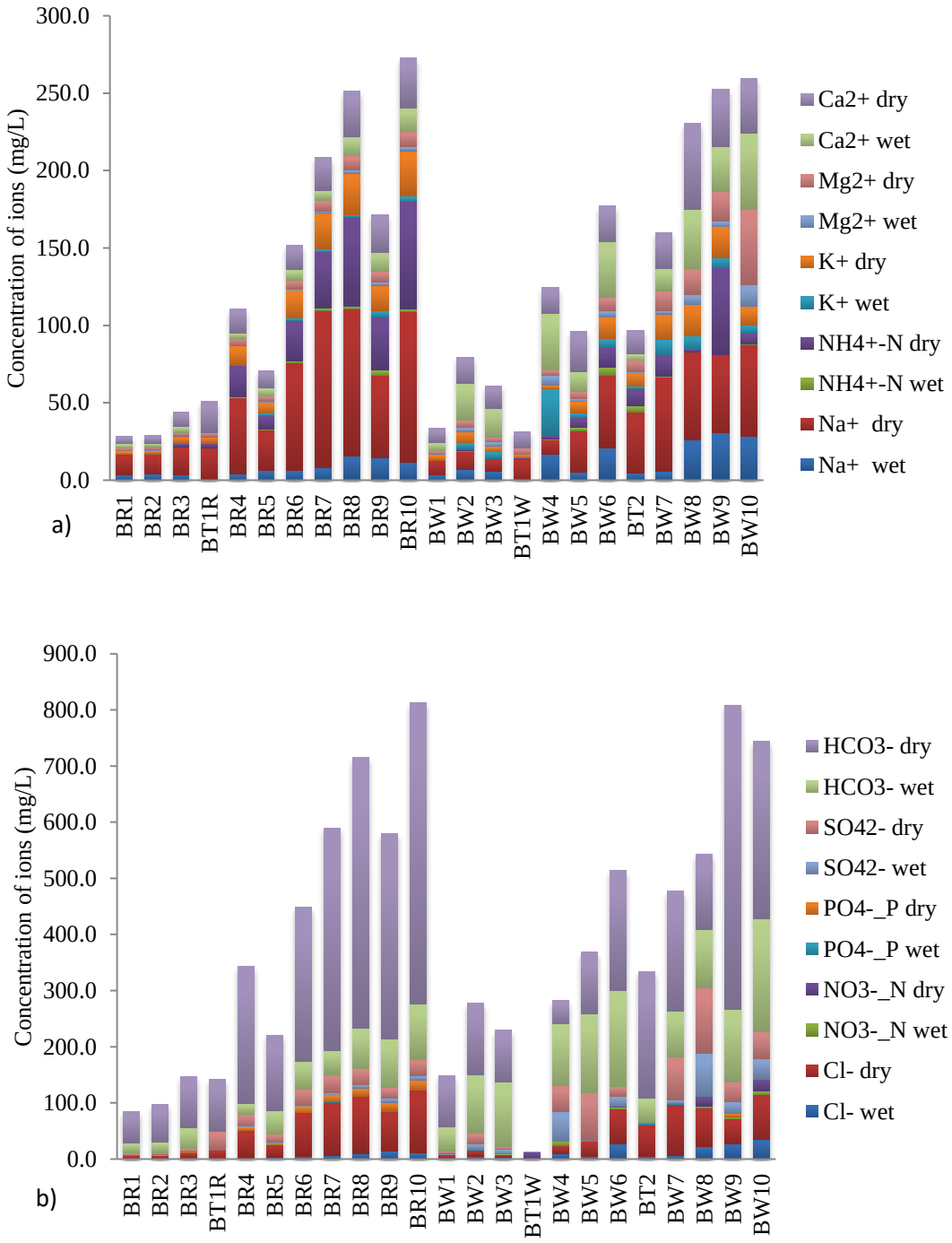

Figure 35: Bar diagram showing variation of cation (a) and anion (b) in the groundwater and river water of the Bagmati River.

Table 11: Well information and in-situ parameters of the Bagmati River

Sampling ID	E	N	Elevation (m)	Distance from river (m)	Bank	Well Depth (m)	Water Table (m)			DO (mg/L)		EC (µS/cm)		Water Temp (°C)		pH	
							Wet	Dry	DWLD	Wet	Dry	Wet	Dry	Wet	Dry	Wet	Dry
BW1	85.40282	27.735906	1322	80	Right	3.2	1.8	2.0	0.2	1.6	2.8	94.2	158	22.7	17.7	7.4	6.1
BW2	85.39717	27.735536	1324	40	Right	4.3	2.4	3.7	1.3	0.6	1.3	113	295	24.3	18.9	7.4	6.1
BW3	85.38779	27.739308	1323	20	Right	6.5	1.6	4.7	3.1	4.4	0.8	193	316	21.7	17.6	7.0	6.7
BW4	85.34866	27.708889	1308	40	Right	4.3	0.6	4.2	3.6	1.3	2.6	243	321	25.7	19.1	7.8	5.9
BT1W	85.38426	27.730428			Right	16.8					2.5		279		20.3		6.2
BW5	85.37321	27.714681	1300	5	Left	3.5	2.5	3.2	0.7	1.8	1.9	922	591	23.3	17.9	7.5	6.8
BW6	85.35163	27.69355	1295	30	Right	4.9	1.7	4.3	2.6	0.5	1.1	207	826	25.1	20.4	7.5	6.5
BT2	85.35175	27.69353		7	Right				0.0	2.4	2.4	234	777	22.8	17.7	7.8	6.8
BW7	85.34818	27.68815	1290	10	Left	4.9	2.8	2.1	-0.7	4.7	0.3	793	1161	22.8	16.7	7.3	6.5
BW8	85.32898	27.681	1288	65	Left	6.5	1.6	4.5	2.9	1.9	0.9	1155	1033	24.7	18.9	7.3	6.7
BW9	85.31674	27.690161	1282	20	Right	3.2	1.8	5.1	3.3	1.4	2.1	701	1351	24.5	20.2	7.1	6.5
BW10	85.30436	27.69204	1281	50	Left	2.8	2.2	2.4	0.2	2.4	4.5	1413	1290	22.6	15	7.1	7.1
BR1	85.40335	27.734623								6.4	9.9	41.2	151	22.3	17.5	7.1	7.3
BR2	85.3968	27.735445								6.2	6.4	42.2	159	22.1	16.6	7.4	7.3
BR3	85.38785	27.739033								5.9	6.5	64.3	206	22.9	18	7.4	7.1
BT1R	85.38415	27.73035									5.8		311		18.7		6.9
BR4	85.3739	27.71424								5.8	0.6	72.9	607	24.6	18.8	7.8	7.0
BR5	85.34844	27.708931								5.1	1.4	75	386	25.5	22.1	7.6	7.0
BR6	85.35186	27.69352								3.9	0.0	122	852	24.3	19.8	7.7	7.0
BR7	85.34815	27.688227								3.5	0.2	136	1188	25.5	17.3	7.7	7.0
BR8	85.32913	27.681718								3.1	0.0	227	1222	27.9	19.2	8.0	7.1
BR9	85.31652	27.689923								2.4	0.0	290	1321	28.4	20.1	7.9	7.1
BR10	85.30434	27.692603								3.3	0.0	231	1369	26.7	18.1	7.8	7.2

DW = Bagmati well water, DR = Bagmati river water, DWLD = Difference in water level depth

The depth of dug wells ranged in between 1.15 to 7.6 m while the distance from the river channel ranged from 10 to 120 m. All sample wells had the shallow water depth in wet season with a maximum fluctuation of 4.4 m and a minimum fluctuation of 0.1 m at MW8 and MW5 respectively.

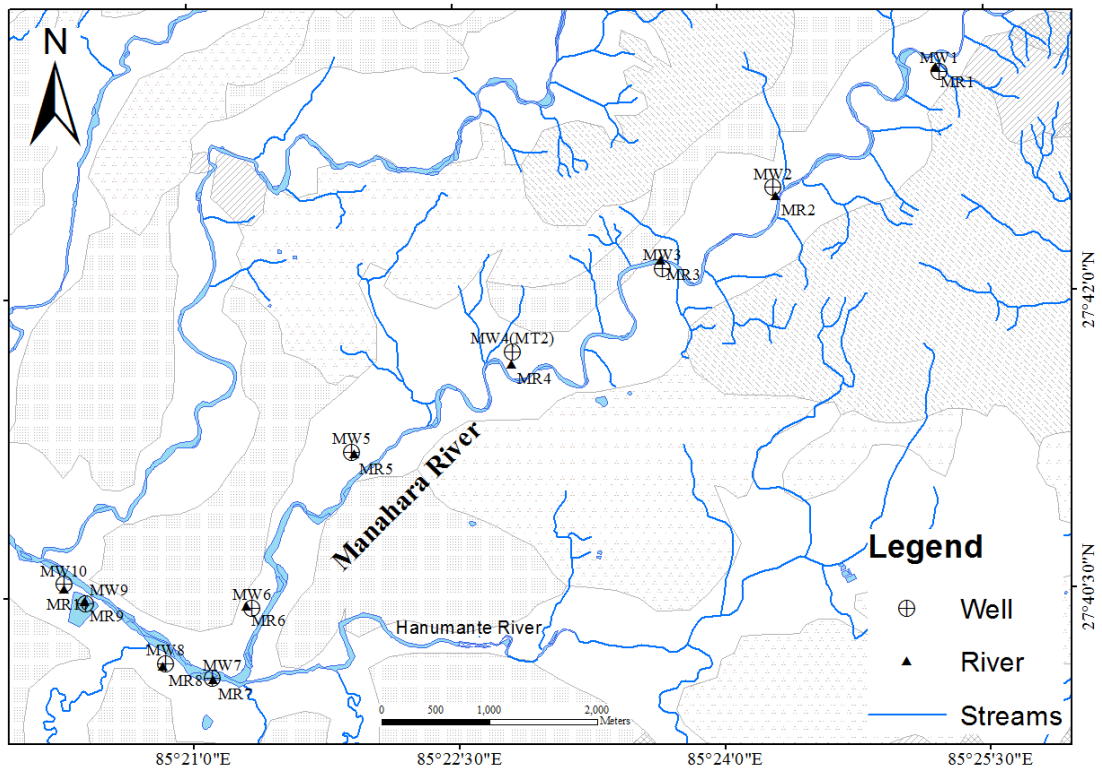

Figure 36: Sampling point of groundwater and river water in the Manahara River

The temperature of river water ranged from 23.4 to 27.2 ºC in the wet season and 16.8 to 20.7 ºC in the dry season. On the other hand, temperature range of groundwater was 21ºC to 24.7º C and 16.5 to 20.9 ºC in the wet and dry seasons respectively. Value of pH was slightly decreased during the dry season in both the river water and groundwater (Table 12). The EC measured in groundwater ranged from 160 to 1656 µS/cm in the wet season, and from 219 to 1573 µS/cm in the dry season. About 50% of groundwater samples had reduced EC during the dry season. Similarly, EC of river water was varied from 62.2 to 892 µS/cm in the wet season and 118 to 1364 µS/cm in the dry season. Except for MR7, all river water showed an increment of EC up to six times during the dry season. DO was relatively high in the river water during the wet season which abruptly decreases up to zero at the downstream section during the dry season (Table 12).

4.3.4.2 Hydro-chemical parameters

Table 12: Well information and in-situ parameters of the Manahara River

Sampling ID	E	N	Elevation (m)	Distance from river (m)	Bank	Well Depth (m)	Water Level Depth (m)			DO (mg/L)		EC (µS/cm)		Water Temp (℃)		pH	
							Wet	Dry	DWLD	Wet	Dry	Wet	Dry	Wet	Dry	Wet	Dry
MW1	85.420814	27.71848	1321	30	Left	5.35	4.7	5.5	0.8	2.0	7.38	620	294	21.9	17.4	7.0	6.9
MW2	85.40503	27.708881	1317	90	Right	2.3	2	2.3	0.3	1.9	0.78	235	313	24.2	18.1	6.7	6.1
MB1	85.40501	27.70896	1317	120	Right				0.0	1.5		160		21.6		7.5	
MW3	85.39455	27.702189	1313	50	Left	2.6	1.5	2.6	1.1	2.9	3.59	681	402	24.2	17.6	7.0	6.2
MB2	85.38039	27.69539	1310	45	Right	33.5			0.0	1.2		205		22.3		7.1	
MW4	85.380381	27.695314	1309	20	Right	5.1		3.0	3.0		2.07		574		20.1		6.3
MW5	85.36514	27.687031	1296	15	Right	5.4	4.8	4.9	0.1	1.2	0.83	612	867	21.9	20.9	7.2	6.2
MW6	85.3556	27.674039	1292	40	Left	4.8	3.4	3.8	0.4	0.5	1.6	1123	974	21.7	18.8	7.0	6.7
MW7	85.35181	27.668161	1287	10	Right	3.9	1.6	2.1	0.5	1.6	0.58	740	419	24.5	19.1	7.7	6.2
MW8	85.34741	27.669439	1287	20	Right	7.65	2	6.4	4.4	0.8	0.46	724	847	24.7	21	7.4	6.8
MW9	85.33992	27.674569	1283	10	Left	1.15	0.1	0.5	0.4	2.2	0.7	768	772	24.5	16.5	7.2	6.7
MW10	85.33791	27.6762	1286	35	Right	7.1	5	5.0	0.0	1.5	1.95	1656	1573	21	19.8	7.6	7.4
MR1	85.420458	27.718792								6.1	8.5	62.2	118	23.4	19.6	7.7	7.7
MR2	85.405338	27.708159								5.8	8.0	64.9	119	25.4	19.9	7.7	7.4
MR3	85.394442	27.702835								5.4	7.5	88	300	27.2	19.2	7.9	7.2
MR4	85.3803	27.694265								5.8	2.9	76.2	199	26.8	19.7	7.6	6.9
MR5	85.365353	27.686843								5.3	1.1	101	566	26.1	18.6	7.5	7.1
MR6	85.355068	27.67419								5.0	0.4	110	629	26	16.8	7.6	7.1
MR7	85.351837	27.668017								4.7	0.2	892	630	24.5	20.7	7.7	7.0
MR8	85.347188	27.66919								3.5	0.0	194	1177	25.1	20.2	7.8	7.0
MR9	85.339838	27.674724								4.0	0.0	230	1364	25.5	18.8	7.9	7.3
MR10	85.337921	27.675728								3.6	0.0	270	1355	25.3	18.9	7.8	7.1

MW = Manahara well water, MR = Manahara river water, DWLD = Difference in water level depth

Figure 37 presents spatial and temporal variation on chemical parameters of river water and groundwater along the Manahara River.

Na^+, Ca^{2+} and HCO_3^- were principal ions of river water with a value ranging from 4.3 to 12.2 mg/L, 3.7 to 12 mg/L, and 24.4 to 73.2 mg/L respectively in the wet season. The major cations had an order of Na^+>Ca^{2+}>K^+>Mg^{2+}> NH_4^+-N in the wet season which had changed to Na^+> NH_4^+-N>Ca^2> K^{++}>Mg^{2+} order in the dry season. Similarly, in the case of anion, HCO_3^- was dominant, followed by Cl^- and SO_4^{2-} in both wet and dry seasons. All chemical ions presented strong significant seasonal variation ($p<0.01$). The concentration of all these parameters increased with different increment rates in the dry season (Figure 37). NH_4^+-N concentration was very low (<1.9 mg/L) in the wet season and drastically increased in the dry season ranging from 0.1 to 63.6 mg/L. In the same way, the concentration of Na^+, K^+, Cl^-, PO_4^--P, and HCO_3^- increased two to more than ten times during the wet season (Figure 37). Based on the piper plot, the Manahara River can be categorized as Ca-HCO_3 and Na-K-HCO_3 types in both wet and dry season (Appendix 5D).

Similarly, Ca^{2+}, Na^+ and HCO_3^- were most governing ions of groundwater in both seasons. The concentration of Ca^{2+} varied from 6.2 to 65.6 mg/L and 11.6 to 58.2 mg/L in the wet and dry season respectively. Similarly, range of Na^+ lies between 6 to 29.6 mg/L in the wet season and 16.6 to 87.4 mg/L in the dry season. In the case of HCO_3^-, 30.5 to 408.7 mg/L was the range in the wet season, which changed to 48.8 -402.6 mg/L in the dry season. Statistical analysis (paired t-test within 95% confidence level) showed no significant temporal variation in Na^+, K^+, Ca^{2+}, Cl^- and HCO_3^-. However, Mg^{2+}, PO_4^--P and NH_4^+-N showed significant temporal variation with $p<0.01$. Chemical concentration plot on the piper diagram categorized groundwater as Ca-HCO_3 in the wet season. But in the case of the dry season, MW1 and MW5 changed to Ca-Cl-SO_4 type while remaining were plotted at the boundary of Ca^{2+} and Na^+ type with dominancy of HCO_3 (Appendix 5D).

4.3.5 Hanumante Khola

Figure 38 presents sampling points of groundwater and river water. In both seasons, 20 water samples were collected among which 10 were collected from river (HR1 to HR10) and 10 from dug well (HW1 to HW10).

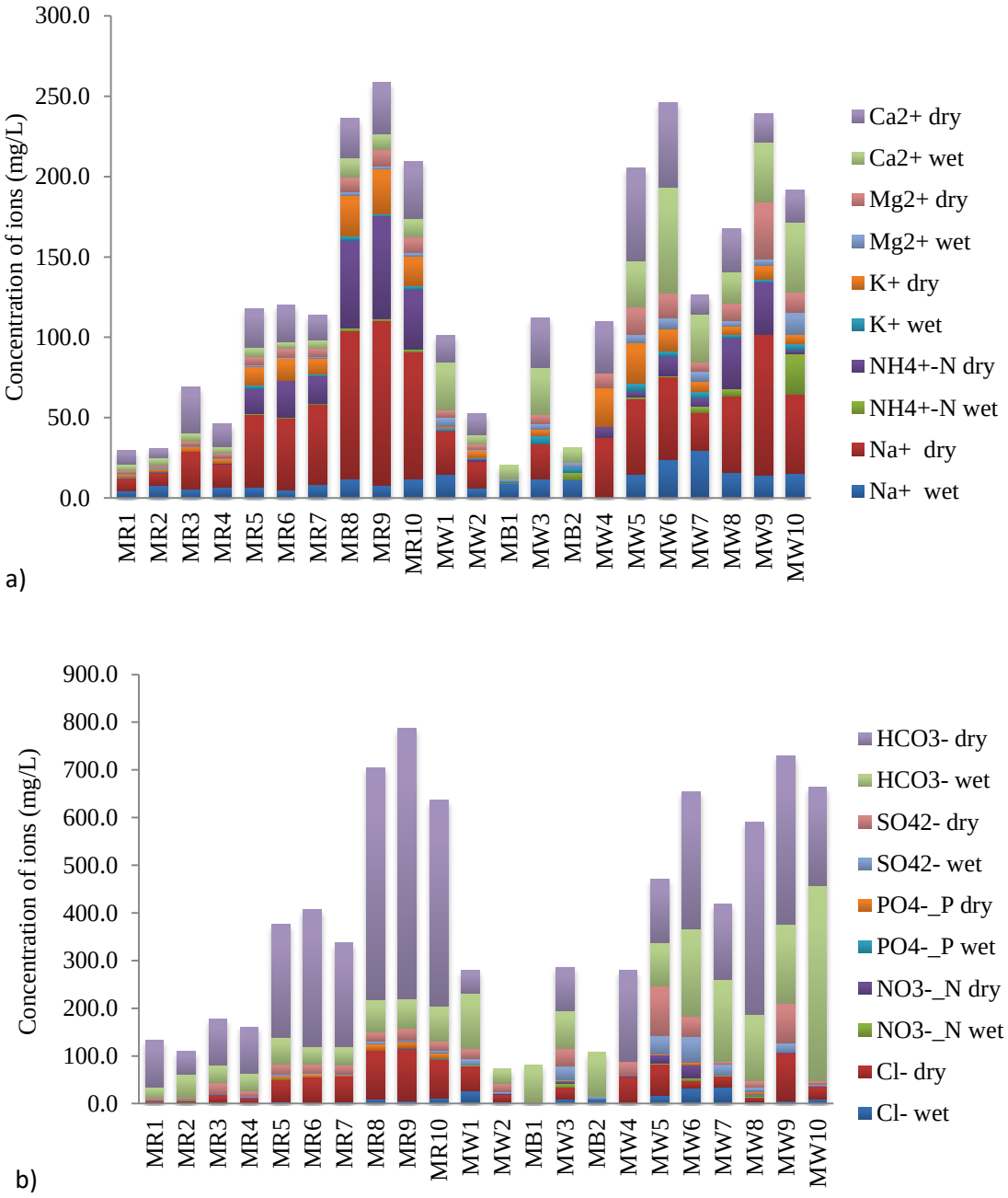

Figure 37: Bar diagram showing variation of cation (a) and anion (b) in the groundwater and river water in the Manahara River

4.3.5.1 In-situ Parameters

Table 13 presents locations of the sample points along with in-situ parameter measured in the wet and dry seasons. Dug wells were located within 10 to 100 m with well depth ranged of 1.5 to 15.7 m. All wells had the shallow water depth in the wet season, with a maximum fluctuation of 3.60 m and a minimum fluctuation of 0.65 m at HW9 and HW6, respectively (Table 13).

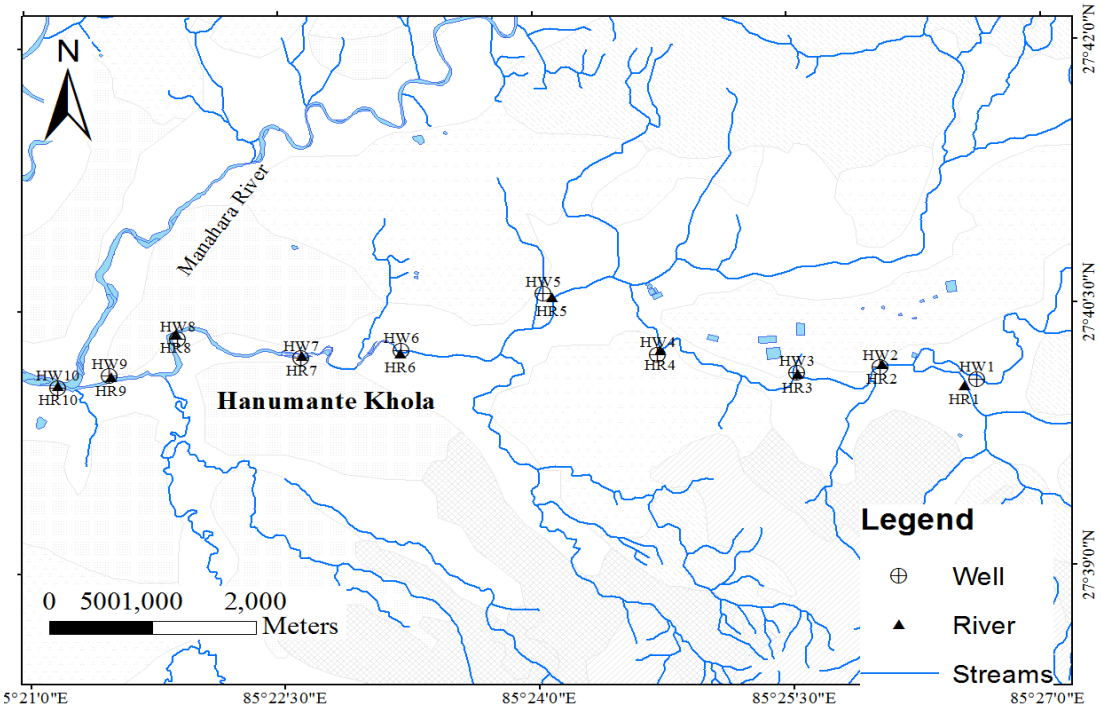

Figure 38: Sampling point of groundwater and river water in the Hanumante Khola

The temperature of river water varied from 22.3 °C to 24.3 °C and 14.0–17.9 °C in the wet and dry season respectively. Range of groundwater temperature was 20.7 to 24.1°C in the wet season while in the dry season, the range was 13.4–20.5 °C. (Table 13). Slightly decreased pH value was observed both in river water and groundwater during the dry season. The range of EC of groundwater was varied from 290 to 934 µS/cm and 576 to 1323µS/cm in the wet and dry season respectively. Groundwater exhibited higher EC in the dry season relative to the wet season, except for HW1, HW2, and HW4 (Table 13). However, in the case of river water, the value of EC was low (164.2 to 247 µS/cm) in the wet season and abruptly increased by up to eight times (604 to 2060 µS/cm) in the dry season. High DO was noted in wet season river water which was drastically reduced below the value measured in groundwater during the dry season (Table 13).

4.3.5.2 Hydro-Chemical Parameters

Figure 36 presents variations in chemical ions of river water and groundwater. Ca^{2+} and HCO_3^- were the leading ions of river water in the wet season, with values variation of 7.3 to 17.0 mg/L and 24.4 to 73.2 mg/L, respectively.

Dominant cations had an order of $Ca^{2+} > Na^+ > K^+ > Mg^{2+}$ in the wet season, which changed to the order $Na^+ > NH_4^+$-N $> Ca^{2+} > K^+ > Mg^{2+}$ in the dry season.

Table 13: Well information and in-situ parameters of the Hanumante Khola

Sampling ID	E	N	Elevation (m)	Distance from river (m)	Bank	Well Depth (m)	Water Level Depth (m)			DO (mg/L)		EC (µS/cm)		Water Temp (°C)		pH	
							Wet	Dry	DWLD	Wet	Dry	Wet	Dry	Wet	Dry	Wet	Dry
HW1	85.44028	27.66936	1302	90	Right	3.3	1	2.8	1.8	2.1	0.4	839	797	22.3	20.5	7.0	6.4
HW2	85.43617	27.6696	1306	10	Left	15.7	1	2.0	1.0	1.5	0.5	934	820	20.7	18.9	8.1	7.4
HW3	85.42796	27.66915	1300	15	Right	8.2	0.9	4.1	3.2	1.1	0.5	784	1323	23.6	19	7.2	6.8
HW4	85.41425	27.67104	1309	60	Left	1.5	0.6	1.7	1.1	2.4	2.3	681	576	22	13.4	7.2	6.4
HW5	85.4007	27.676	1305	80	Right	5	1	3.4	2.4	3.2	1.3	290	637	24.1	17.5	7.8	6.1
HW6	85.38907	27.67166	1288	20	Right	2.8	1.7	2.4	0.7	2.6	1.3	520	611	22.8	17.5	7.1	6.1
HW7	85.37917	27.67103	1284	30	Left	7	4.3	5.8	1.5	2.5	2.0	591	856	22.7	17.6	7.5	6.5
HW8	85.36717	27.673	1296	35	Left	5	3.6	4.5	0.9	4.1	1.8	889	1192	22.6	20.4	7.3	6.4
HW9	85.3619	27.67027	1283	20	Right	2.8	0.8	4.4	3.6	3.0	2.1	769	964	21	18.3	6.7	6.3
HW10	85.35531	27.66843	1280	10	Left	2.4	0.1	1.9	1.8	3.3	1.7	623	1168	22.8	16.2	7.6	6.7
HR1	85.44194	27.66722								6.5	5.5	164	604	22.3	14.9	8.0	7.5
HR2	85.43388	27.66916								6.3	1.7	172	1340	22.4	16.5	8.1	6.8
HR3	85.42555	27.66833								5.5	0.5	187	2010	23	16.6	7.2	7.0
HR4	85.41222	27.67083								4.4	0.7	226	1780	23	14	7.8	6.9
HR5	85.40166	27.67583								4.6	0.6	224	2060	23.9	15.6	7.9	6.8
HR6	85.38666	27.67083								4.3	0.2	227	1924	24.3	17.2	7.8	7.0
HR7	85.37694	27.67055								4.0	0.3	240	1998	23.5	16.7	8.0	7.0
HR8	85.36472	27.67277								4.0	0.2	237	1955	23.5	17.1	7.8	7.0
HR9	85.35805	27.66861								4.1	0.1	247	1960	23	17.9	6.7	7.0
HR10	85.35305	27.66805								4.3	0.4	239	1985	23.4	16.4	8.0	7.0

HW= Hanumante well water, HR= Hanumante river water, DWLD = Difference in water level depth

Similarly, for anions, HCO_3^- was dominant, followed by SO_4^{2-} and Cl^- in the wet season, and Cl^- and SO_4^{2-} in the dry season. Except for NO_3^--N, strong significant seasonal variation ($p < 0.01$) was observed in all other parameters. Minor concentration (<1 mg/L) of NH_4^+-N and PO_4^--P was noted in the wet season which had significantly increased in the dry season, ranging from 10.3 to 102.9 mg/L (for NH_4^+-N) and from 2.4 to 31.7 mg/L (for PO_4^--P). Similarly, concentrations of Na^+, K^+, Cl^-, and HCO_3^- increased by more than ten times than in the wet season (Figure 36). Piper plots from the chemical analyses classified the Hanumante River water as Ca-HCO_3 type and Na-K-HCO_3 type in the wet and dry seasons respectively (Appendix 5E).

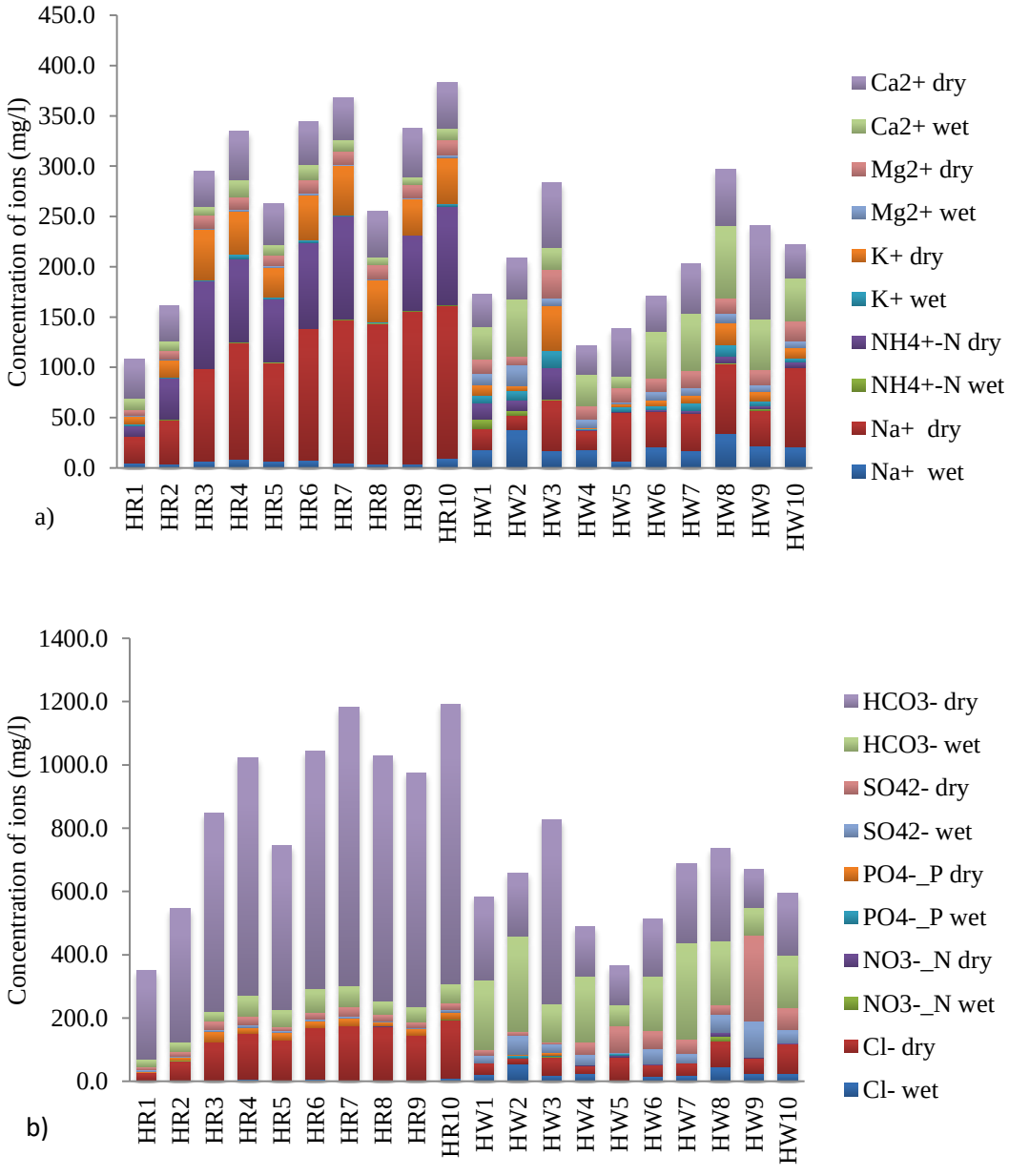

Figure 39: Bar diagram showing variation of cation (a) and anion (b) of the Hanumante Khola

Likewise, groundwater of both seasons had dominancy of Ca^{2+} and HCO_3^- ions. Values of Ca^{2+} fluctuated from 11.7 to 72.5 mg/L and 28.4 to 93.7 mg/L in the wet and dry seasons respectively. In the case of HCO_3^-, concentration ranged from 67.1-305.0 mg/L in the wet season and 122.0–579.5 mg/L in the dry season. K^+, NH_4^+-N, Ca^{2+}, HCO_3^-, NO_3^--N, and SO_4^{2-} of groundwater had an absence of significant temporal variation. Conversely, Na^+, Mg^{2+}, and Cl^- showed significant temporal variation (p-value of 0.03). Generally, groundwater presented minor chemical increments compared to river water during the dry season (Figure 36). The groundwater of the Hanumante River .was categorized as Ca-HCO_3 type in both seasons, except at HW5, HW9, and HW10. Water samples collected from HW5 and HW10 changed slightly from Ca-HCO_3 (in the wet season) to Ca-SO_4, and Na-Cl-SO_4, respectively, during the dry season (Appendix 5E). Groundwater collected from HW9 in both seasons is of Ca-SO_4 type.

4.3.6 Godawari Khola

Sampling points of groundwater and river water are presented in Figure 40. Total of 19 water samples, 10 from the dug well (GW1 to GW10) and 9 from the river (GR1 to GR10) were collected in the wet season. Water sample of GR8 and GR9 was collected from the same location and thus considered a single (GR8/GR9). However, only 18 samples, 10 from dug well and 8 from the river were collected in the dry season. GW2 of the dry season was collected from different location (new) as the well from the wet season was impossible to collect water sample. This new GW2 located nearby location of wet season GW2. Similarly, GR10 was also unable to collect due to the dryness of the river.

4.3.6.1 In situ parameters

The dug wells selected from the Godawari River were located within 4 to 90 m from the river channel with variations in well depth from 1.75 to 10.4 m. Most the dug wells (GW3 to GW8) had very shallow water level depth (0.1 to 0.9 m) during the wet season (Table 14) which was increased in the dry season showing a maximum range of 6.3 m and a lower range of 0 m at GW9 and GW10 respectively. The deep water level depth was occurred at GW1 and GW9 in the wet and dry season respectively.

Relatively, wider and higher range of river water temperature was observed in the wet season (19.4 to 27.7°C) as compared to the dry season (13.8 to 18.2°C). Groundwater

also showed similar temperature ranges as that of river water in the wet (19.6 to 25.2°C) and dry (13.2 to 19.6°C) seasons. The pH value of river water lied within 7.3 to 8.6 showing basic nature in both seasons. However all groundwater shows basic nature in the wet season which changed to a slightly acidic nature with a value variation from 6.37 to 6.86 in most the groundwater (GW3 to GW7, GW10) during the dry season (Table 14). EC varied from 277 to 388µS/cm and from 343 to 574µS/cm during the wet and dry seasons respectively.

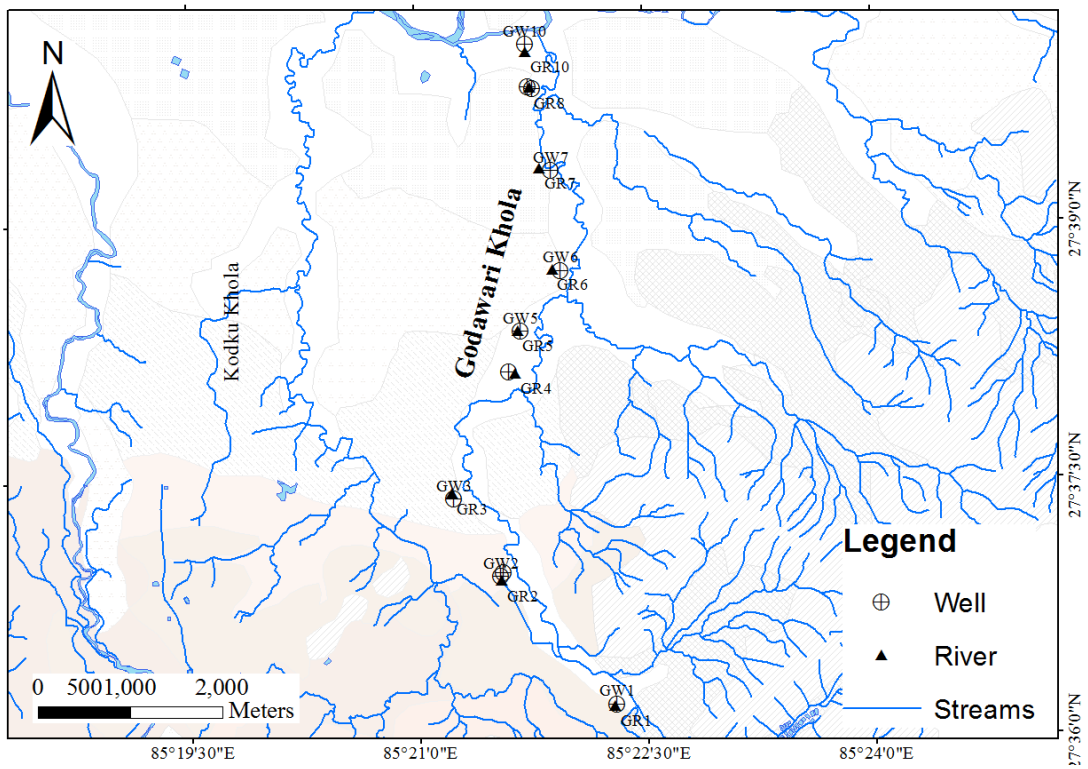

Figure 40: Sampling points of groundwater and river water in the Godawari Khola

Compared to river water, groundwater showed higher EC in both seasons. It showed an increasing trend toward downstream dug well sites with value variation from 299 to 1575µS/cm and from 326 to 1980µS/cm in the wet and dry seasons respectively. Generally, river water presented lower DO in the dry season. But in the case of Godawari Khola, higher DO was noted relative to the wet season showing values range of 3.79 to 11.66 mg/L. High DO was measured from groundwater of the upstream section (GW1) in both wet (5.21 mg/L) and dry (5.74 mg/L) seasons from the upstream section.

4.3.6.2 Hydro-chemical parameters

Table 14: Well information and in-situ parameters of the Godawari Khola

Sampling ID	E	N	Elevation (m)	Distance from river (m)	Bank	Well Depth (m)	Water Level Depth (m)			DO (mg/L)		EC (µS/cm)		Water Temp (°C)		pH	
							Wet	Dry	DWLD	Wet	Dry	Wet	Dry	Wet	Dry	Wet	Dry
GW1	85.37146	27.60316	1429	10	Right	10.4	5.2	5.8	0.6	5.2	5.7	299	326	19.6	17.8	7.7	7.1
GW2	85.35894	27.61571	1370	15	Right	4.2	2.2			1.8	WL	322		23.6		7.3	
GW2 (new)	85.35922	27.61609	1370	30	Right			2			1.0		560		14.1		7.1
GW3	85.35387	27.62329	1343	4	Left	1.8	0.1	0.5	0.4	1.5	2.3	405	402	24	13.2	7.6	6.7
GW4	85.36008	27.6356	1307	80	Left	2.9	0.8	2.5	1.7	1.7	0.6	331	448	22.9	16.1	7.3	6.5
GW5	85.36137	27.63959	1297	35	Right	1.9	0.1	1.2	1.1	2.1	1.9	405	502	25.2	15.6	7.7	6.9
GW6	85.36578	27.64546	1303	90	Right	4.1	0.1	2	1.9	1.0	1.9	809	807	23.7	15.8	7.4	6.5
GW7	85.36491	27.65522	1293	65	Right	8.5	0.9	1.3	0.4	1.5	1.1	515	873	23.5	17.1	7.1	6.5
GW8	85.36292	27.6632	1293	10	Left	3.3	0.9		-0.9	1.9	WL	923		24.4		7.5	
GW9	85.36247	27.66341	1301	80	Right	9.2	1.7	8	6.3	1.3	2.8	1099	1980	22	19	7.2	7.3
GW10	85.36217	27.66752	1298	50	Right	8.5	4.5	4.5	0	2.9	0.4	1575	1961	21.9	19.6	7.5	6.4
GR1	85.37132	27.60296								6.7	6.3	277	343	19.4	14.2	8.3	7.3
GR2	85.35901	27.61526								6.6	7.5	307	363	22.3	14.2	8.4	7.7
GR3	85.35366	27.6238								6.5	7.2	315	367	23.8	13.8	8.6	7.5
GR4	85.36075	27.63545								6.9	8.6	303	429	25.6	15.5	8.6	7.6
GR5	85.36103	27.63959								6.2	11.7	355	393	25	16.2	8.2	8.0
GR6	85.36491	27.64554								7.0	7.6	311	429	27.7	17.1	7.7	7.3
GR7	85.3636	27.65542								5.3	10.9	382	494	25	17.4	8.2	7.3
GR8/GW9	85.3626	27.66327								5.9	3.8	376	574	25	18.2	8.3	8.5
GR10	85.36214	27.66679								4.3	RD	388		25.5		8.1	

GW=Godawari well water, GR=Godawari river water, DWLD = Difference in water level depth, WL = Well locked, RD = River dry

Ca^{2+} was the most dominant cation of both wet and dry season river water with values ranging from 9.3 to 19.2 mg/L and from 12.6 to 23.6 mg/L respectively. It was followed by Na^{+}, Mg^{2+}, K^{+} and NH_4^{+}-N in both seasons. Similarly, in the case of anion, $HCO3^{-}$ was most dominant, followed by Cl^{-} and SO_4^{2-} in both seasons (Figure 41). However, the concentration of all ions had increased only Na^{+}, Mg^{2+}, K^{+} and Cl^{-} showed significant increment ($p < 0.005$) during the dry season. The absence of PO_4^{-}-P concentration in overall river water indicated minor contamination through anthropogenic activity. Drastic increment of Na^{+}, NH_4^{+}-N, Cl^{-} and SO_4^{2-} concentration at GR7 and GR8/GR9 indicated contamination through point source on these river sites. Based on the piper plot, the Godawari river water can be categorized as Ca-HCO_3 type in both seasons (Appendix 5F).

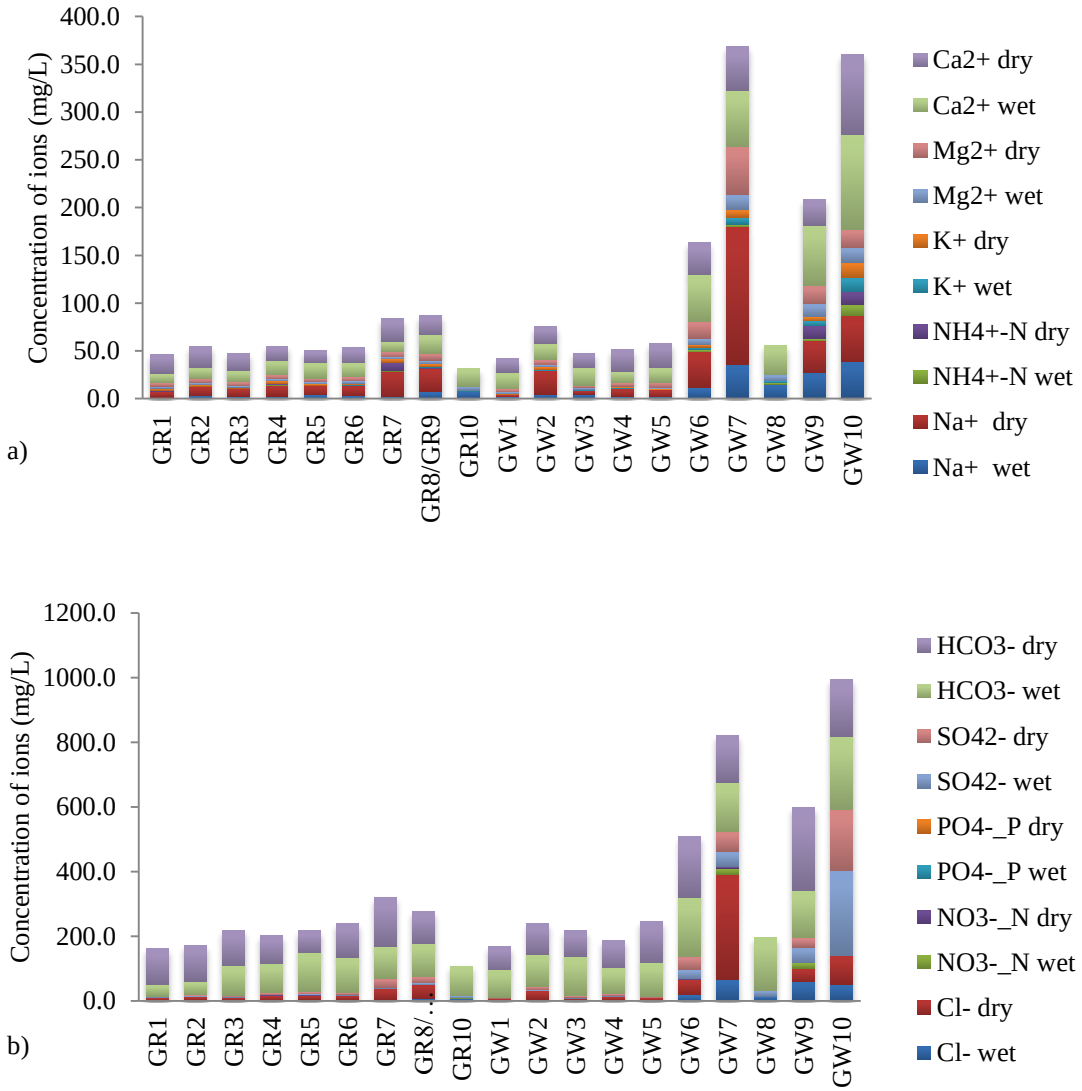

Figure 41: Bar diagram showing variation in cation (a) and anion (b) in the Godawari Khola

Alike in river water, Ca^{2+} was the dominant cation, of the groundwater varying from 12.2 to 99.2 mg/L and from 14.5 to 84.1 mg/L during the wet and dry seasons respectively. It was followed by Na^{+}, Mg^{2+}, K^{+} and NH_4^{+}-N in both seasons. Similarly, HCO_3^{-} was dominant and followed by SO_4^{2-} and Cl^{-}. Based on paired t-test (within 95% confidence level), none of ions showed significant temporal variation ($p > 0.05$). Meanwhile, it showed significant spatial variation in both seasons. The concentration of NH_4^{+}-N, Mg^{2+}, K^{+} and SO_4^{2-} was very low in the upstream five well sites (GW1 to GW5) which was drastically increased in the downstream well sites in both seasons (Figure 41). Especially, GW10 showed an extreme increment of SO_4^{2-} (262.47 mg/L) and NH_4^{+}-N (11.94 mg/L) during the wet season possessing a very bad smell. Similarly, GW7 and GW9 show an excessive concentrations of NO_3^{-}-N (17 to 20.4 mg/L) in the wet season indicating influences of anthropogenic activities. Drastic increment of Na^{+} (144.2 mg/L) and Cl^{-} (323.5 mg/L) concentration at GW7 during the dry season also pointed towards point source contamination. The chemical concentration plot on the piper diagram classified Godawari groundwater as Ca-HCO3 type in both seasons except for GW7, GW9 and GW10. Samples from GW7 and GW10 were categorized as Ca-Cl-SO4 type in both seasons (Appendix 5F).

4.3.7 Kodku River

Figure 42 shows the sampling point of groundwater and river water. Total 16 water samples, 8 from river (KR1 to KR8) and 8 from the dug well (KW1 to KW2) were collected in the wet season. Samples from KW6 and KR6 were not collected in the dry season, thus only 14 samples in the dry season.

4.3.7.1 In situ parameters

The depth of dug wells varied from 1.25 to 13 m and was located within 5 to 90 m from the river channel. All wells had shallow water level depth in the wet season with a maximum fluctuation of 1.45 m (KW8) and a minimum fluctuation of 0.4 m (KW4). The shallowest water level depth was observed at KW3 and the deepest at KW8 in both seasons (Table 15).

The temperature of river water and groundwater presented narrow spatial variation as compared to temporal variation (Table 15). River water showed a maximum spatial variation of 3.1°C and a maximum temporal variations of 8.2°C (KR7). Similarly,

groundwater also had maximum of 4.8°C spatial variation and of 10.4°C (KW3) maximum temporal variation. The pH value of both river and groundwater exhibited a slightly basic nature with values ranging from 7 to 8.3 in the wet season which slightly decreased with ranges of 7.16 to 7.73 and 6.46 to 7.25 in the river and groundwater respectively during the dry season. Lower EC was observed in the wet season river water (282 to 521 µS/cm) which increased by three times in the downstream section (KR7 and KR8) during the dry season. In the case of groundwater, it presented more conductive groundwater in the wet season (341 to 1204 µS/cm) relative to the dry season (369 to 1040 µS/cm). The highest temporal variation of 671 µS/cm was observed at KW4 and the lowest one was noted from KW1 (8µs/cm). Most the groundwater showed lower EC during the dry season except at KW1, KW2 and KW5 (Table 15). Higher DO was noted from the upstream section (KR1 to KR4) in both seasons while lower DO observe in the downstream sections (KR5 to KR8) during the dry season. DO of groundwater was higher at the downstream section KW8 and lower at KW4 in both the wet and dry seasons. Except in KW2, KW7 and KW8, the remaining groundwater had lower DO during the dry season.

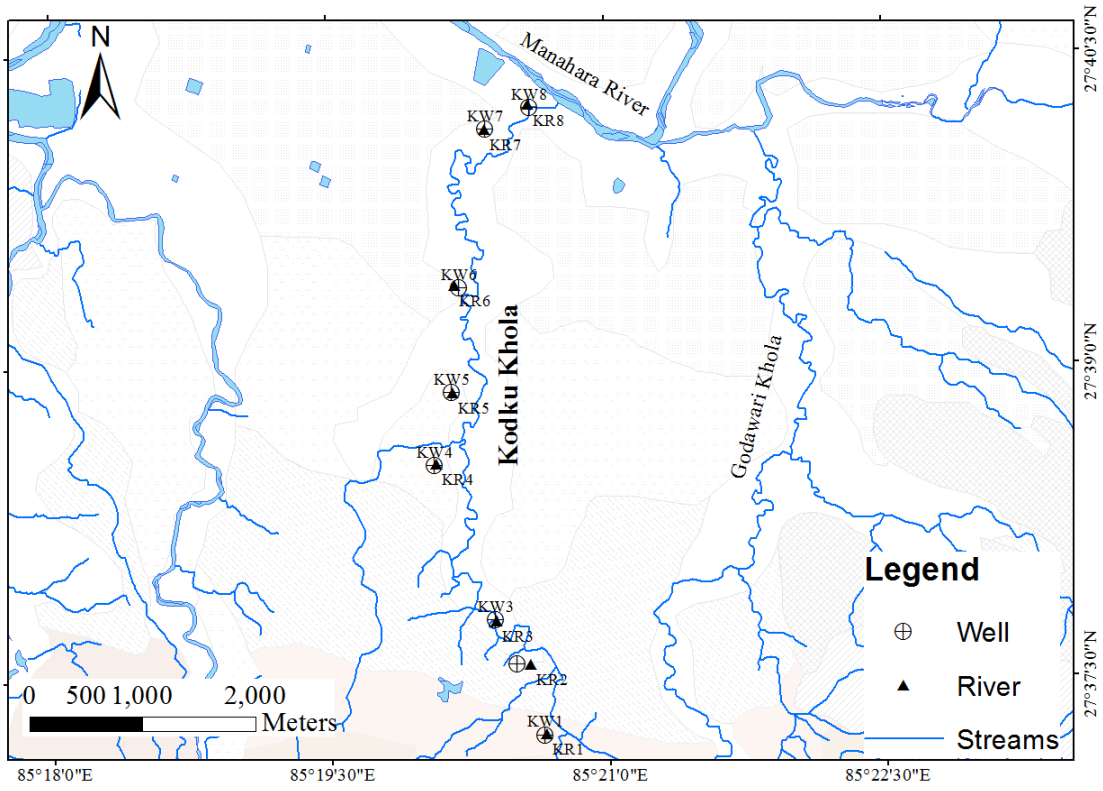

Figure 42: Sampling point of groundwater and river water in the Kodku Khola

4.3.7.2 Hydro-chemical parameters

Ca^{2+} and Na^{+} were dominant cations of wet season river water which was followed by Mg^{+}, K^{+} and NH_4^{+}-N (Figure 43). The order of dominancy was changed to $Na^{+}>Ca^{2+}>NH_4^{+}$-$N>K^{+}>Mg^{2+}$ with an increment of ions during the dry season. Similarly, in the case of anion, $HCO3^{-}$ was the dominant followed by Cl^{-} and SO_4^{2-} in both the wet and dry seasons (Figure 43).

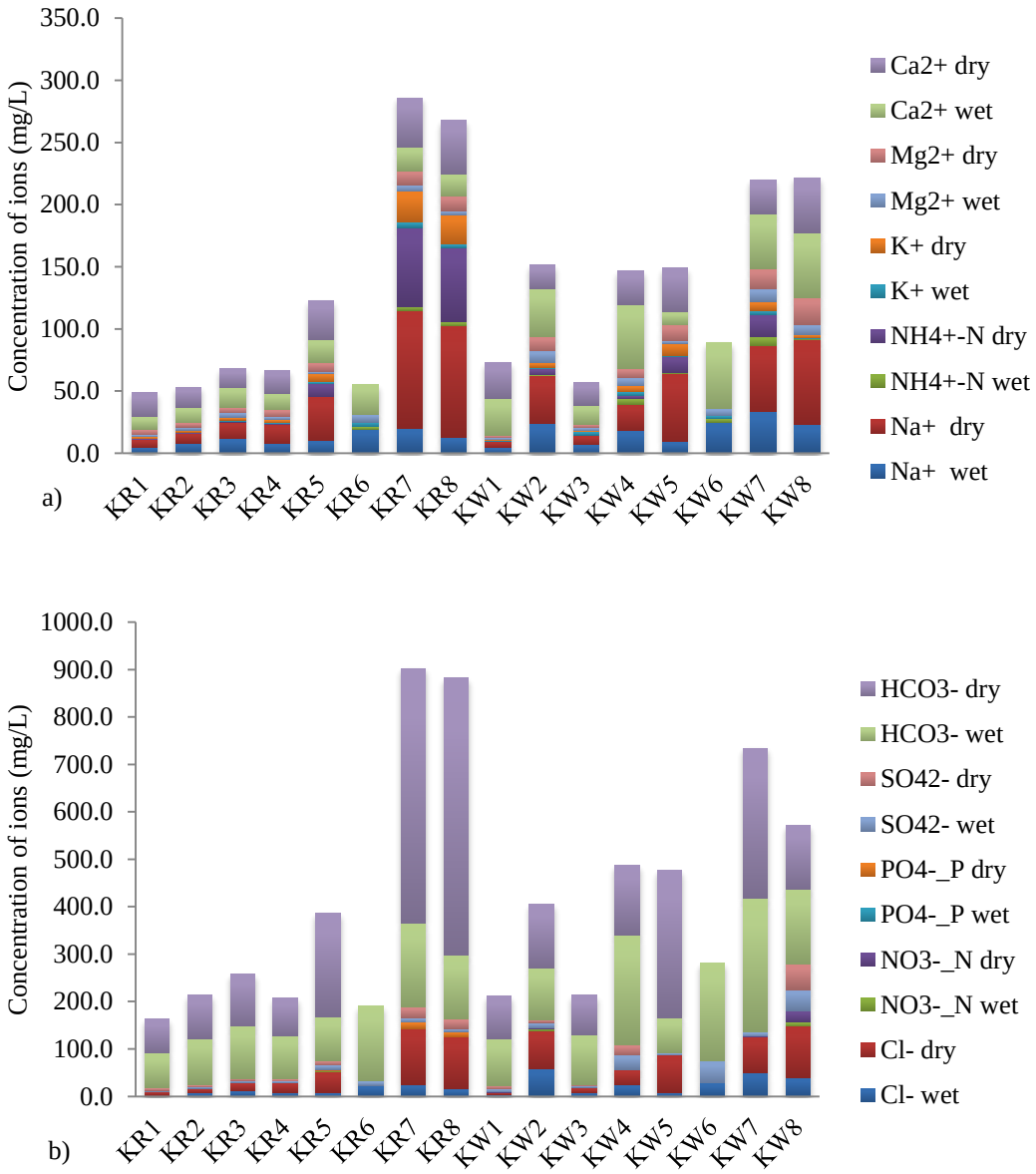

Figure 43: Bar diagram showing variation of cation (a) and anion (b) in the Kodku Khola

The wide spatial variation on chemical concentration was observed in both seasons. Specifically, Na^{+} and Cl^{-} increased more than 10 times in the downstream section with value variations from 4.5 to 20.3 mg/L and from 2.3 to 25.4 mg/L in the wet season; and from 6.66 to 94.48 mg/L and from 7.87 to 116.88 mg/L in the dry season respectively.

Table 15: Well information and in-situ parameters of the Kodku Khola

Sampling ID	E	N	Elevation (m)	Distance from river (m)	Bank	Well Depth (m)	Water Level Depth (m)			DO (mg/L)		EC (µS/cm)		Water Temp (℃)		pH	
							Wet	Dry	DWLD	Wet	Dry	Wet	Dry	Wet	Dry	Wet	Dry
KW1	85.3441	27.620581		15	Left		1.5	2.5	1.0	3.9	3.3	434	442	20.8	19.4	7.8	7.0
KW2	85.3417	27.626311	1321	90	Left	4	2.8	4.0	1.2	2.9	4.5	796	1035	21	20	7.1	6.5
KW3	85.3398	27.629818	1316	10	Right	1.25	0.3	1.1	0.8	2.6	2.3	421	369	23.7	13.3	7.6	7.0
KW4	85.3344	27.642224	1315	20	Left	3.6	2.1	2.5	0.4	0.5	0.4	1204	587	22	17.8	7.4	6.6
KW5	85.336	27.648062	1312	15	Left		1.5		-1.5	4.4	2.4	341	993	23.6	18.9	8.2	7.0
KW6	85.3368	27.6564	1296	20	Right	6	1.6		-1.6	0.4	WL	945		23.3		7.3	
KW7	85.3393	27.669103	1294	10	Right	13	1.2	1.8	0.6	1.1	2.3	1187	1036	24.8	17.5	7.6	6.7
KW8	85.3433	27.670768	1288	7	Right	8.5	6.4	7.9	1.5	5.0	5.8	1072	1040	20	18.5	7.6	7.3
KR1	85.3443	27.620667								6.4	7.9	375	320	23.1	15.4	8.3	7.6
KR2	85.3429	27.62621								6.6	8.5	282	352	22.6	17.7	8.2	7.5
KR3	85.3398	27.629738								5.3	7.8	298	377	23	16.9	8.0	7.4
KR4	85.3346	27.64232								6.2	8.8	315	371	24.8	18.2	8.1	7.7
KR5	85.3361	27.648009								3.6	1.2	371	602	24.9	17.4	8.1	7.2
KR6	85.3363	27.656603								3.0		422		24.1		8.0	
KR7	85.3392	27.66905								1.0	0.1	512	1494	25.7	17.5	8.0	7.2
KR8	85.3431	27.670993								1.1	0.1	521	1471	24.8	18.2	8.0	7.2

KW = Kodku well water, KR = Kodku river water, DWLD = Difference in water level depth, WL = Well locked

Statistical analysis showed significant temporal variation only in Ca^{2+} and Mg^{2+} with a p- value of 0.02. The concentration of NH_4^+-N was low in the wet season (0.0 to 2.8 mg/L) and significantly increased in the dry season with value variation from 0.29 to 63.38 mg/L. In the same way, PO_4^--P was only noticed from the downstream section (KR5, KR7 and KR8) during the dry season (Figure 43). The piper plot classified upstream river section (KR1 to KR5) as Ca-HCO_3 type in both the wet and dry season Similarly, downstream river sites KR7 and KR8 categorized as Ca-HCO_3 type (in the wet season) and Na-K-HCO_3 type in the dry season (Appendix 5G). Increments of chemical concentration along with change of water type especially on the downstream section during the dry season thus indicate increment of contamination towards downstream.

In the case of groundwater, Ca^{2+} was the dominant cation with values range of 10.2 to 53.1 mg/L and was followed by Na^+, Mg^{2+}, K^+ and NH_4^+-N in the wet seasons (Figure 43). Dominance of ion was changed to Na^+ and followed by Ca^{2+}, Mg^{2+}, NH_4^+-N and K^+ during the dry season. In the case of anion, HCO_3^- was dominant and followed by Cl^- and SO_4^{2-} in both the wet and dry seasons (Figure 43). PO_4^--P was absent in both seasons. NO_3^--N had a low value range (0.2 to 8.1mg/L) in the wet season and increase to 0.1 to 24.9 mg/L range during the dry season. Well from downstream (KW8) showed the highest value of NO_3^--N in both seasons. Only Na^+ and Cl^- showed significant increments ($p < 0.05$) while Ca^{2+}, SO_4^{2-} and HCO_3^- decreased in most the groundwater during the dry season. Groundwater from KW1 and KW3 presented lower concentrations in both seasons. Based on these chemical concentrations, groundwater was classified as Ca-HCO_3 in both seasons, except for KW8. The water type of KW8 changed from Ca-HCO_3 to Ca-Cl-SO_4 type during the dry season (Appendix 5G).

4.3.8 Nakhu Khola

The sampling locations of dug wells and rivers are presented in Figure 44. Only 6 water samples, 3 from dug wells and 3 from the river were collected during the wet season. The number of samples was increased by double, with 12 samples in the dry season, including 6 from the dug well (NW1 to NW6) and 6 from the river (NR1 to NR6).

4.3.8.1 In situ parameters

Dug wells selected from the Nakhu Khola corridor lie within 20 to 90 m away from the

river channel with a well depth range of 1.5 to 8 m. Very shallow water level depth was observed at NW4 (0.1 m) in the wet season which changed to deeper in the dry season (7.56 m) with maximum fluctuation of 7.4 m. In the same way, NW1 also presented shallow depth (0.2 m) even in the dry season (Table 16).

The temperature of wet season river water showed a tentative similar value (25 to 26.4°C) which was decreased to the range of 16 to 18 .3°C during the dry season. Similarly, the temperature of groundwater was also high (21 to 25.6°C) in the wet season and decreased with the same value range as in river water during the dry season (Table 16). The pH value of river water showed basic nature with a value ranging from 8.6 to 8.8 and 7.4 to 8.2 in the wet and dry seasons respectively. In the case of groundwater, pH exhibited a slightly acidic nature (6.3 to 7.1) during the dry season. EC of river water showed an increasing trend towards the downstream section with value variation from 225 to 321 µS/cm (wet season) and 264 to 1348 µS/cm (dry season). In the case of groundwater, EC varied from 666 to 937 µS/cm and from 282 to 1222 µS/cm in the wet and dry season respectively. Higher DO was observed in both seasons of river water than that in groundwater. But river water itself presented lower DO during the dry season (Table 16).

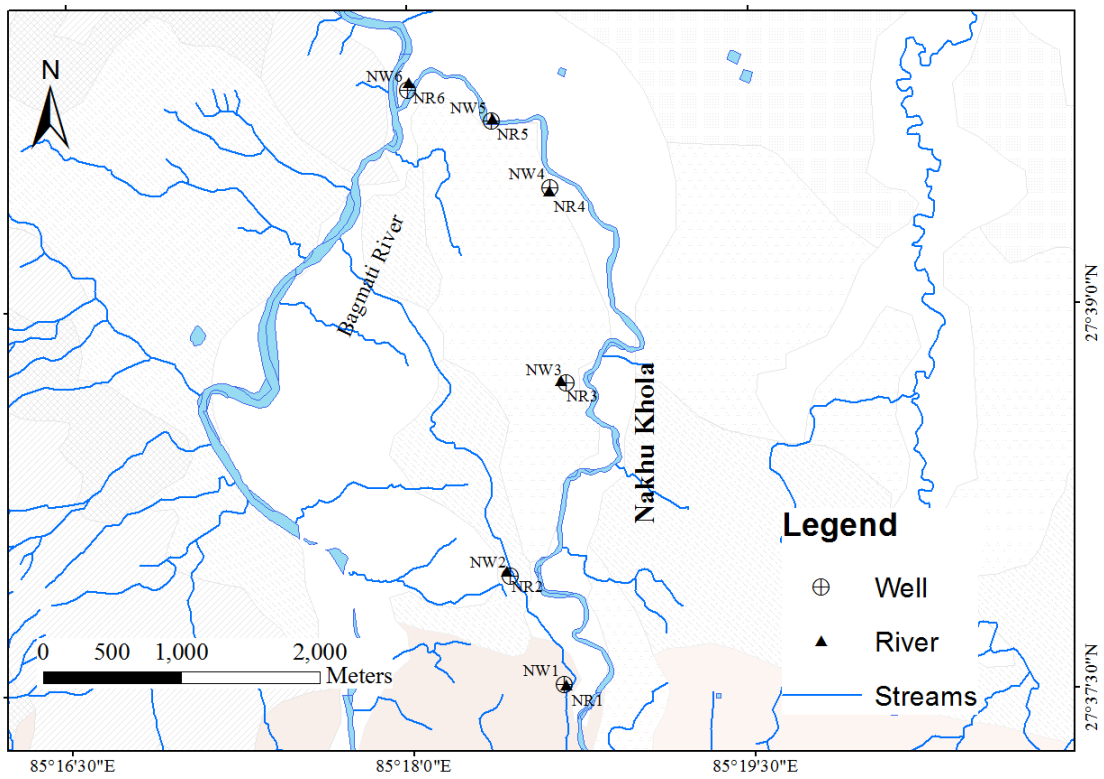

Figure 44: Sampling point of groundwater and river water in the Nakhu Khola

Table 16: Well information and in-situ parameters of the Nakhu Khola

Sampling ID	E	N	Elevation (m)	Distance from river (m)	Bank	Well Depth (m)	Water Level Depth (m)			DO (mg/L)		EC (µS/cm)		Water Temp (°C)		pH	
							Wet	Dry	DWLD	Wet	Dry	Wet	Dry	Wet	Dry	Wet	Dry
NW1	85.311065	27.625552	1324	20	Left	1.5		0.2			2.3		282		17.1		6.3
NW2	85.307206	27.632658	1307	25	Right	4.8		1.8			0.5		341		16.1		6.8
NW3	85.31145	27.645139	1318	90	Right	3.7		1.1			1.7		414		14.6		6.7
NW4	85.310385	27.657883	1272	30	Right	8	0.1	7.6	7.5	2.5	1.4	937	1222	24.6	18.4	7.9	7.1
NW5	85.30616	27.662241	1270	20	Left	7.2	1.8	3.9	2.1	1.9	2.0	867	1114	21.8	17.5	7.4	6.9
NW6	85.300043	27.664348	1263	90	Left	2.7	1.3	2.4	1.1	1.0	1.5	666	613	21.6	16.5	6.9	6.3
NR1	85.311195	27.625482									7.8		264		16.8		8.0
NR2	85.3069	27.632932									7.1		285		16.1		8.2
NR3	85.31101	27.645299									8.3		296		16.5		8.1
NR4	85.31028	27.65766								6.2	4.7	225	360	25.6	17.3	8.8	7.5
NR5	85.306187	27.662382								6.0	3.2	264	596	25.1	18.3	8.8	7.5
NR6	85.30007	27.664803								5.6	1.2	321	1348	26.4	17.9	8.6	7.4

NW Nakhu well water, NR = Nakhu river water, DWLD = Difference in water level depth

4.3.8.2 Hydro-chemical parameters

Ca^{2+} and Na^{+} were dominant cations of river water which was followed by Mg^{2+}, K^{+} and NH_4^{+}-N in both seasons. Similarly, $HCO3^{-}$ was the dominant anion and followed by Cl^{-} and SO_4^{2-} in both the wet and dry seasons (Figure 42).

The concentration of Ca^{2+}, Na^{+} and Cl^{-} were relatively high in NR5 indicating more mineralized water in the wet season. But in the case of the dry season, wide spatial variation was observed with drastic increment of chemical concentration in downstream section NR6 (Figure 42).

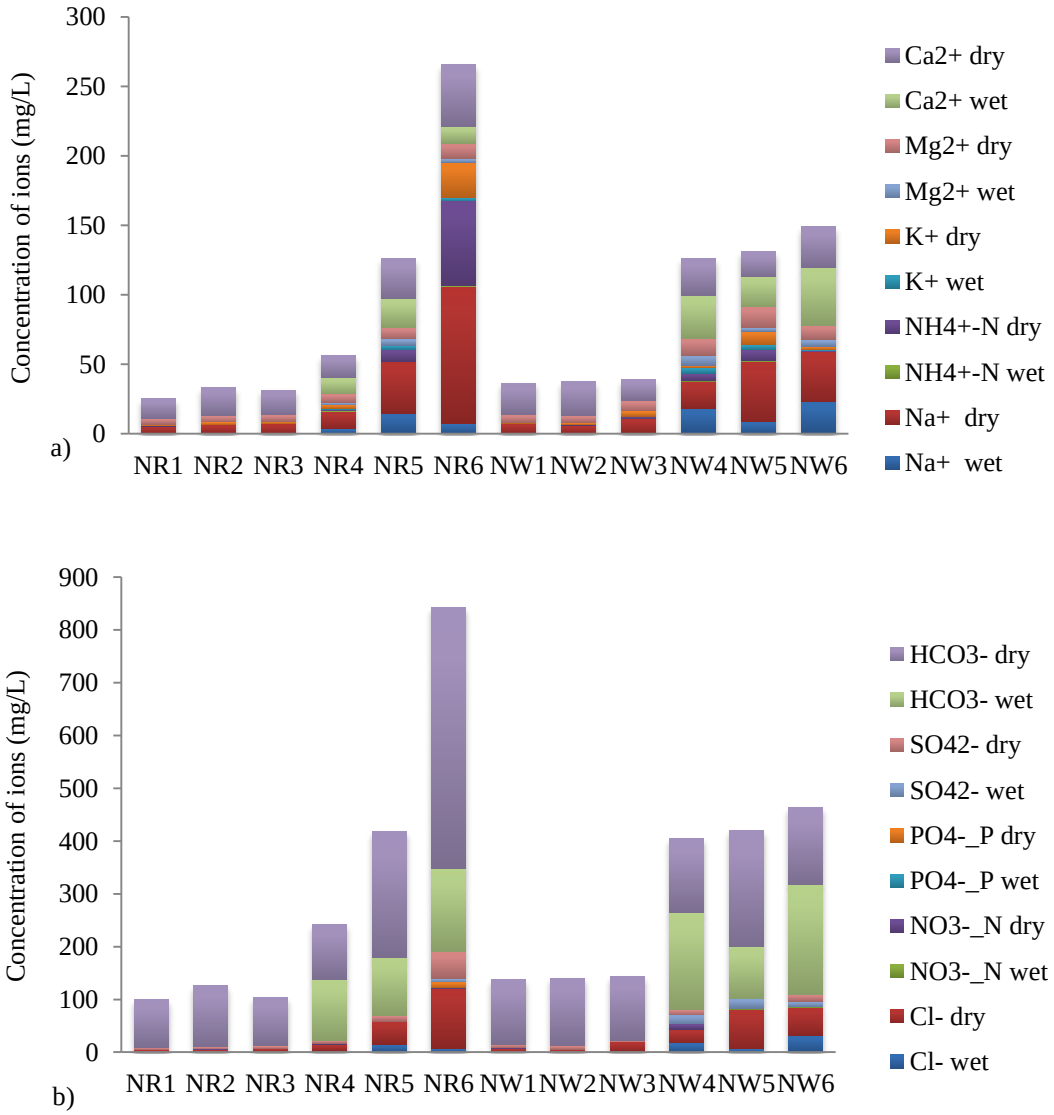

Figure 45 : Bar diagram showing variation of cation (a) and anion (b) of the Nakhu Khola

The concentration of PO_4^--P was only detected in NR6 with a drastic increment of NH_4^+-N. In the same way, the concentration of Na^+, K^+, Cl^- and SO_4^{2-} also increased more than ten times than in the wet season. Piper plot based on these chemical ions classified all river sites as Ca-HCO_3 type in both seasons, except NR6 (Appendix 5H). While the water type of NR6 changed from Ca-HCO_3 type (wet season) to Na-K-HCO_3 type (dry season).

Alike in river water, Ca^{2+}, Na^+ and $HCO3^-$ were dominant ions of groundwater in both wet and dry seasons. The range of Ca^{2+} concentration lies within 21 to 41.6 mg/L in the wet season which was decreased in the dry season with a value range of 15 to 29.3 mg/L. But in the case of Na^+, its value varied from 8.8 to 23 mg/L in the wet season and 6 to 43.1 mg/L in the dry season. Concentrations of Na^+, Ca^{2+}, Mg^{2+}, Cl^- and HCO_3^- were relatively higher in NW4 and NW6 during the wet season (Figure 42). Concentrations of Na^+, NH_4^+-N, Mg^{2+}, Cl^- and HCO_3^- were drastically increased in NW5 indicating the presence of point source contamination. In the same way, the concentration of NO_3^--N was significantly increased (9.4 mg/L) in NW4 during the dry season. Based on chemical analysis, the piper plot classified groundwater as Ca-HCO_3 type in both the wet and dry seasons (Appendix 5H).

4.3.9 Balkhu Khola

Figure 46 presents the sampling location of the well and river. In both seasons, 20 water samples, 10 from the river (BAR1 to BAR10) and 10 from dug wells (BAW1 to BAW10) were collected.

4.3.9.1 In-situ parameters

Table 17 presents well information and in-situ parameters of wet and dry seasons. Depth of dug wells varied from 1.9 m (BAW1) to 9.4 m (BAW8). Dug wells presented shallow water depth in the wet season with a higher range of 4.62 m and a lower range of 0.1 m observed at BAW9 and BAW2 respectively. All sample wells were located within 2 to 70 m from the river channel.

The higher temperatures of river water and groundwater were noted during the wet season with variations from 22^{o}C to 26^{o}C and decreased to the range of 14^{o}C to 18^{o}C during the dry season (Table 17). The value of pH indicated a slightly basic nature of river water and groundwater (7.8 to 8.6) in the wet season which decreased during the

dry season in both river and groundwater. EC in the groundwater varied from 272 to 1239 µS/cm in the wet season and from 571 to 2270 µS/cm in the dry season. EC increased up to 4 times in all groundwater during the dry season (Table 17). The highest EC was observed at BAW7 and BAW8 in both wet and dry seasons. While in the case of river water, EC ranged from 168 to 779 µS/cm and 504 to 1810 µS/cm in the wet and dry seasons respectively. DO of river water is relatively high (1.51 to 6.12 mg/L) in the wet season and abruptly decreased (<1 mg/L) at downstream sections during the dry season. Similarly, DO of groundwater was also high in the wet season and abruptly decreased in BAW5, BAW6 and BAW8 during the dry season.

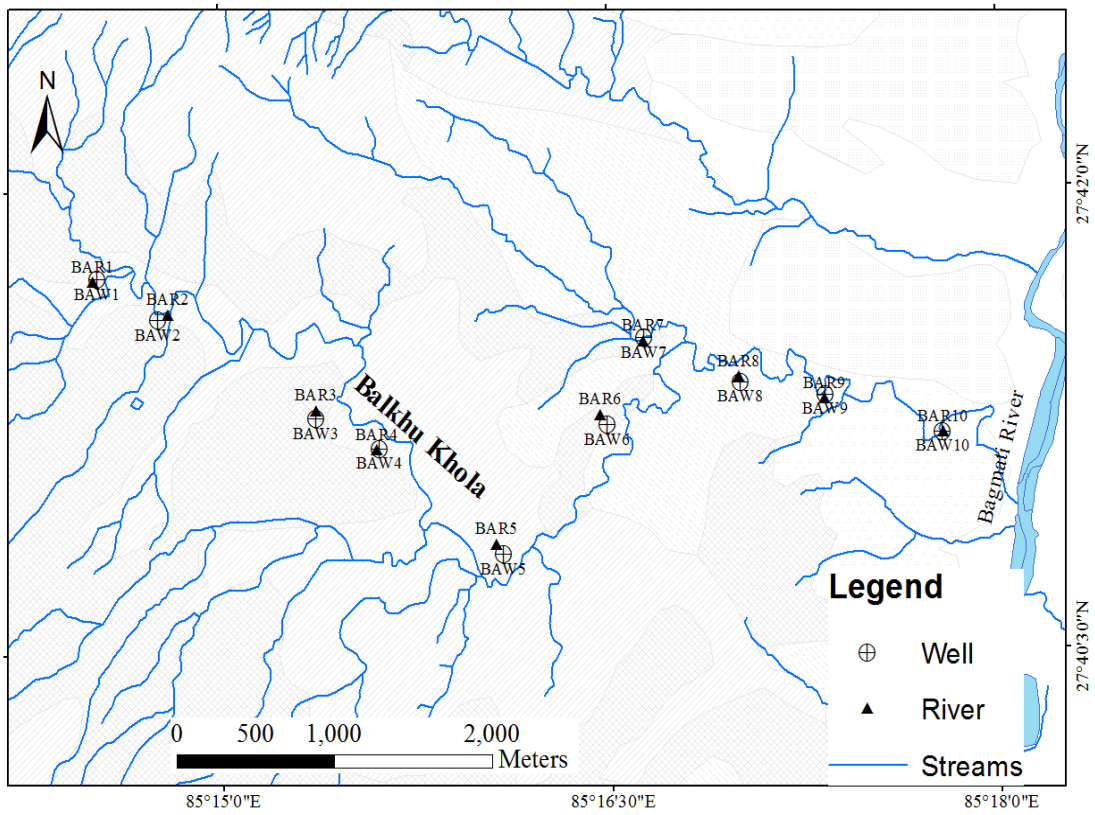

Figure 46: Sampling points of groundwater and river water in the Balkhu Khola

4.3.9.2 Hydro-chemical parameters

Figure 47 presents variations on the chemical parameters in river water and groundwater. Ca^{2+} was the most dominant cation of river water in the wet season which was followed by Na^{+}, K^{+} and Mg^{2+}. The dominancy of cations changed during the dry season with a significant increase of ions ($p < 0.001$) making an order of $Na^{+}>NH_4^{+}$–$N>Ca^{2+}>K^{+}>Mg^{2+}$. Similarly, HCO_3^{-} was the dominant anion and followed by Cl^{-} and SO_4^{2-} in both wet and dry seasons.

Table 17: Well information and in-situ parameters of the Balkhu Khola

Sampling ID	E	N	Elevation (m)	Distance from river (m)	Bank	Well Depth (m)	Water Level Depth (m)			DO (mg/L)		EC (μS/cm)		Water Temp (°C)		pH	
							Wet	Dry	DWLD	Wet	Dry	Wet	Dry	Wet	Dry	Wet	Dry
BAW1	85.24213	27.695339	1338	25	Left	1.9	1.1	1.3	0.2	4.3	3.4	273	571	25.1	16	8.2	6.8
BAW2	85.24597	27.6931	1339	40	Right	5.9	1.4	1.5	0.1	1.6	1.2	416	791	23.8	17.1	7.5	7.9
BAW3	85.25607	27.6877	1324	20	right	7.2	1.5	4.8	3.3	2.9	3.1	582	943	23	16.7	8.0	7.3
BAW4	85.26016	27.686039	1324	10	Left	4.8	2.6	4.0	1.4	3.5	2.4	289	1159	23.1	17.3	8.4	6.9
BAW5	85.26805	27.680269	1316	70	Right	2.8	1.4	2.5	1.1	5.6	1.7	366	929	24.9	14.1	8.4	6.5
BAW6	85.27479	27.687211	1284	50	Right	3.4	0.3	2.5	2.2	6.4	0.8	366	625	24.9	18	8.6	6.2
BAW7	85.27722	27.6919	1285	2	Left	4.7	1.7	3.6	1.9	3.2	1.7	1239	2270	23.1	17.1	8.0	6.8
BAW8	85.28338	27.689461	1278	20	Right	9.4	2.7	5.7	3.1	2.7	0.9	1168	1634	22.2	18.4	8.0	6.6
BAW9	85.28885	27.688731	1277	15	Left	7.7	3.0	7.6	4.6	3.0	1.8	592	900	23.4	18.3	7.6	6.9
BAW10	85.29633	27.686681	1271	7	Right	7.2	1.8	2.7	0.9	1.7	0.5	470	1754	24.4	15.7	7.9	6.8
BAR1	85.24182	27.69519								6.1	8.3	353	504	24.4	15.1	8.2	7.5
BAR2	85.24661	27.693375								5.7	5.5	369	529	24.2	15.6	7.5	7.3
BAR3	85.2561	27.688123								5.8	6.4	385	872	24.2	14.3	8.3	7.5
BAR4	85.26	27.685975								5.3	1.8	384	1085	24.3	14.1	8.4	7.3
BAR5	85.26761	27.680813								1.5	4.3	779	1182	22.8	14.2	7.6	7.3
BAR6	85.27433	27.68777								6.1	3.3	169	1065	24.3	16.5	8.2	7.6
BAR7	85.27715	27.691731								5.9	0.8	380	1178	25.3	17.1	8.6	7.4
BAR8	85.28331	27.689739								4.8	0.3	534	1413	25.2	16.5	8.5	7.2
BAR9	85.28878	27.688537								5.2	0.0	424	1569	26.2	17.0	8.6	7.2
BAR10	85.29638	27.686662								5.1	0.0	426	1810	26.2	15.6	8.6	7.1

BAW = Balkhu well water, BAR = Balkhu river water, DWLD = Difference in water level depth

The concentration of NH_4^+-N and PO_4^--P was minor (<1 mg/L) during the wet season and significantly amplified in the dry season, varying from 0.8 to 81.52 mg/L (for NH_4^+-N) and 2.81 to 13.49 mg/L (for PO_4^--P). Except SO_4^{2-}, all anions showed significant temporal variation ($p < 0.01$) with different increment rate. However, spatial variation of chemical concentration was different in two seasons. Downstream river sample showed increment in concentration more than 8 times as compared with upstream river samples (Figure 47). River samples from BAR1 to BAR3 was classified as Ca-HCO_3 type in both the wet and dry season whereas remaining river samples (BAR4 to BAR10) was classified as Ca-HCO_3 type and Na-K-HCO_3 type in the wet dry season respectively (Appendix 5I).

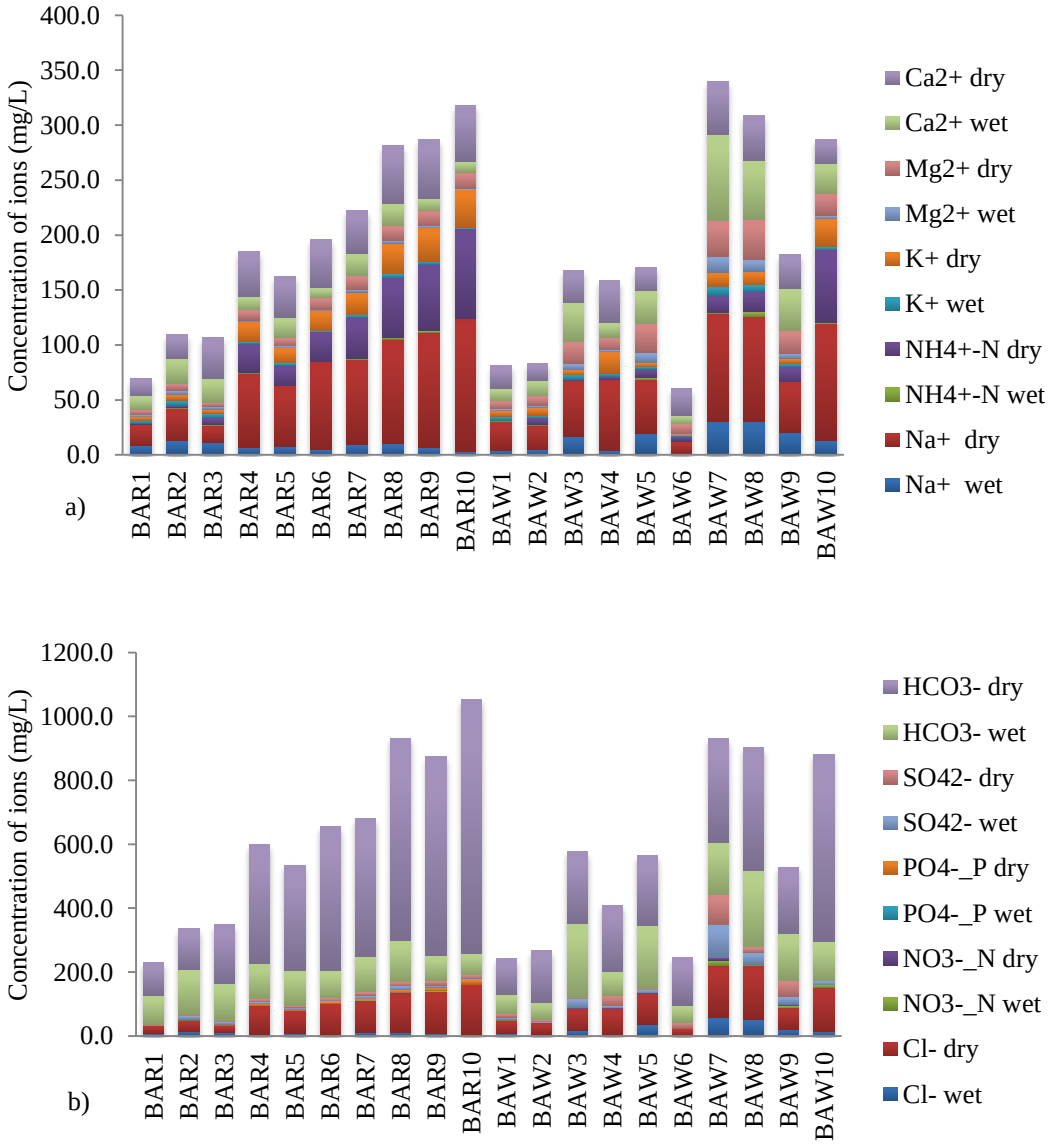

Figure 47: Bar diagram showing variation of cation (a) and anion (b) in the Balkhu Khola

Alike in river water, Ca^{2+} was the dominant cation in the groundwater and followed by Na^{+}, Mg^{2+} and K^{+} in the wet season. The dominancy of ion transformed to Na^{+} with a value ranging from 11.0 to 106.1 mg/L and followed by NH_4^{+}–N, Ca^{2+}, Mg^{2+} and K^{+} during the dry season. In the case of anion, HCO_3^{-} was dominant and followed by Cl^{-} and SO_4^{2-}. Paired t-test (within 95% confidence level) exhibited significant temporal variation ($p < 0.01$) in Na^{+}, K^{+}, Mg^{2+}, Cl^{-} and HCO_3^{-}. BAW1, BAW2 and BAW6 presented lower ion concentrations in both seasons and BAW5, BAW7, BAW8 and BAW9 had higher ions concentration. Except for Ca^{2+}, SO_4^{2-} and NO_3^{-}-N in some wells, almost all ions increased in the dry season (Figure 47). The concentration of NH_4^{+}-N was very low (0.1 to 4.6 mg/L) in the wet season and abruptly increased during the dry season with a value variation from 0.1 to 66.0 mg/L. Based on the Piper plot, groundwater was classified as Ca-HCO_3 type in both wet and dry seasons except BAW4, BAW7 and BAW10. Water from BAW4 and BAW10 were categorized as Ca-HCO_3 type (wet season) and Na-K-HCO_3 type (dry season) whereas water type of BAW7 felled on Ca-Cl-SO_4 in both seasons (Appendix 5I).

4.4 Isotopic analysis of groundwater and river water

Isotope analysis of water samples collected from wet and dry seasons was conducted in the laboratory of the University of Yamanashi, Japan.

In the case of Nepal, the global scale of the Local Meteoric Water Line (LMWL) for the whole of Nepal has not been defined to date. Only a fewer studies concerning an isotopic analysis of meteoric water had been carried out on a local scale (Gajurel *et al*., 2006; Chhetri *et al*., 2014; Matheswaran *et al*., 2019; Adhikari *et al*., 2019). The meteoric water of the Kathmandu Valley was studied by Chhetri *et al*. (2014) and Adhikari *et al*. (2019). The sampling period of Adhikari *et al*. (2019) and this study was similar (2016 to 2018). Thus for the present study, LMWL defined by Adhikari *et al*. (2019) for Kathmandu was used as the reference for meteoric water. In addition, Global Meteoric Water Line (GMWL) reported by Craig (1961) is also used

4.4.1 River wise isotopic analysis

Detailed data of isotope analysis of groundwater and river water are presented in Appendix 6. Isotopic composition of river and groundwater from individual river is described in following sections.

4.4.1.1 Bishnumati River

The δD verses $\delta^{18}O$ plot (Figure 48) presents variations in stable isotopic compositions of groundwater and river water during both wet and dry seasons.

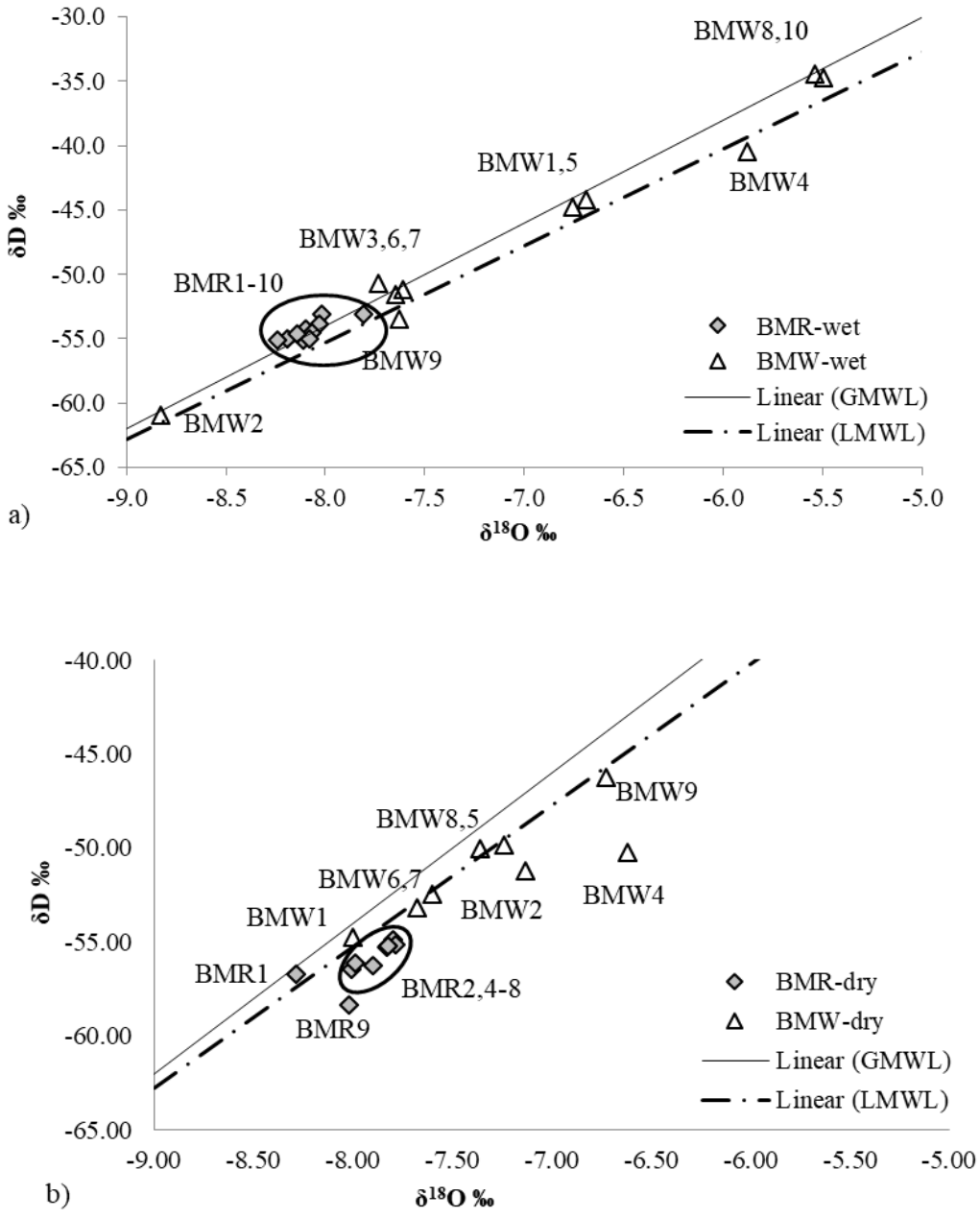

Figure 48: δD verses $\delta^{18}O$ plots of Bishnumati groundwater and river water in (a) wet season and (b) dry season

In river water, the composition of $\delta^{18}O$ had a similar value range in both wet and dry seasons (-7.8 to 8.2‰). But in the case of δD, it had a narrow range in the wet season (-53.1 to 55.1‰) and had a slightly increased the range in the dry season (-54.87 to 58.36‰). Except in BMR1, $\delta^{18}O$ slightly changed to heavier during the dry season,

while the composition of δD changed to lighter during the dry season in all the river samples. Wet season river samples ploted on the GMWL and LMWL (Figure 48a) indicate meteoric water as a major source of river discharge (Liu and Yamanaka, 2012; Sakakibara *et al*., 2016; Ali and Ajeena, 2016; Shakya *et al*., 2019a). Ca-HCO_3 water type defined from the piper diagram also suggests similar water source (Al-Khatib and Al-Najar, 2011). Conversely, dry season river samples plotted below GMWL and LMWL (Figure 48b) except BMR1 indicate the presence of other sources instead of the dry season rainfall. Water type change from Ca-HCO_3 to Na-K- HCO_3 indicates a dominancy of water source from industrial and municipal effluent for river discharge.

Wide spatial variations of $\delta^{18}O$ and δD in water from dug wells were observed in both wet and dry seasons (Figure 48). The $\delta^{18}O$ of groundwater ranged from -5.5 to -8.8 ‰ in wet and -6.61 to -8.0 ‰ in the dry season whereas range of δD varied from -34.4 to 60.9‰ in wet and -46.24 to 54.73‰ in the dry season. Meanwhile, dry season dug wells showed lighter isotopic composition except for BMW2 and BMW9. Groundwater samples plotted on or near the GMWL and LMWL in the wet season (Figure 48a) signifies precipitation as dominating recharge source for these dug wells (Li *et al*., 2016). Similarly, groundwater samples from the dry season plotted on the LMWL (Figure 48b) except for BMW2 and BMW4, suggested meteoric water as main recharge source even in the dry season. BMW2 and BMW4 plotted below LMWL indicate presence of other recharge sources such as industrial or municipal effluent besides meteoric water. Water type shifted from Ca-HCO_3 to Ca-Cl-SO_4 also suggest the presence of mix type of sources, which may be dry season rainfall, bank infiltration through river as well as from anthropogenic input to recharge these dug wells.

4.4.1.2 Dhobi Khola

In the river water, the δD range varies from -53.5 to -56.1‰ in the wet season and from -53.1 to -57.4‰ in the dry season. While in the case of $\delta^{18}O$, it ranges from -7.8 to -8.5‰ in the wet season and from -7.59 to -8.3‰ in the dry season. However, the value range of δD and $\delta^{18}O$ are similar in both the wet and dry season, each river sample shows slightly lither isotopic composition in the wet season except in DR7 and DR10 (Figure 49). All river samples, plotted as a cluster close to GMWL and LMWL suggest meteoric water as a dominating source for river discharge in the wet season (Figure 49a). But in the case of the dry season, river samples plot in three different clusters. The

first cluster has the heaviest isotopic composition and includes DR2, DR4 to DR6; the second cluster encloses DR1, DR8 to DR10; and the third cluster has only one river sample DR7 with the lightest isotopic composition (Figure 49 b). Cluster one plot slightly below the LMWL suggests the possibility of the presence of other recharge sources.

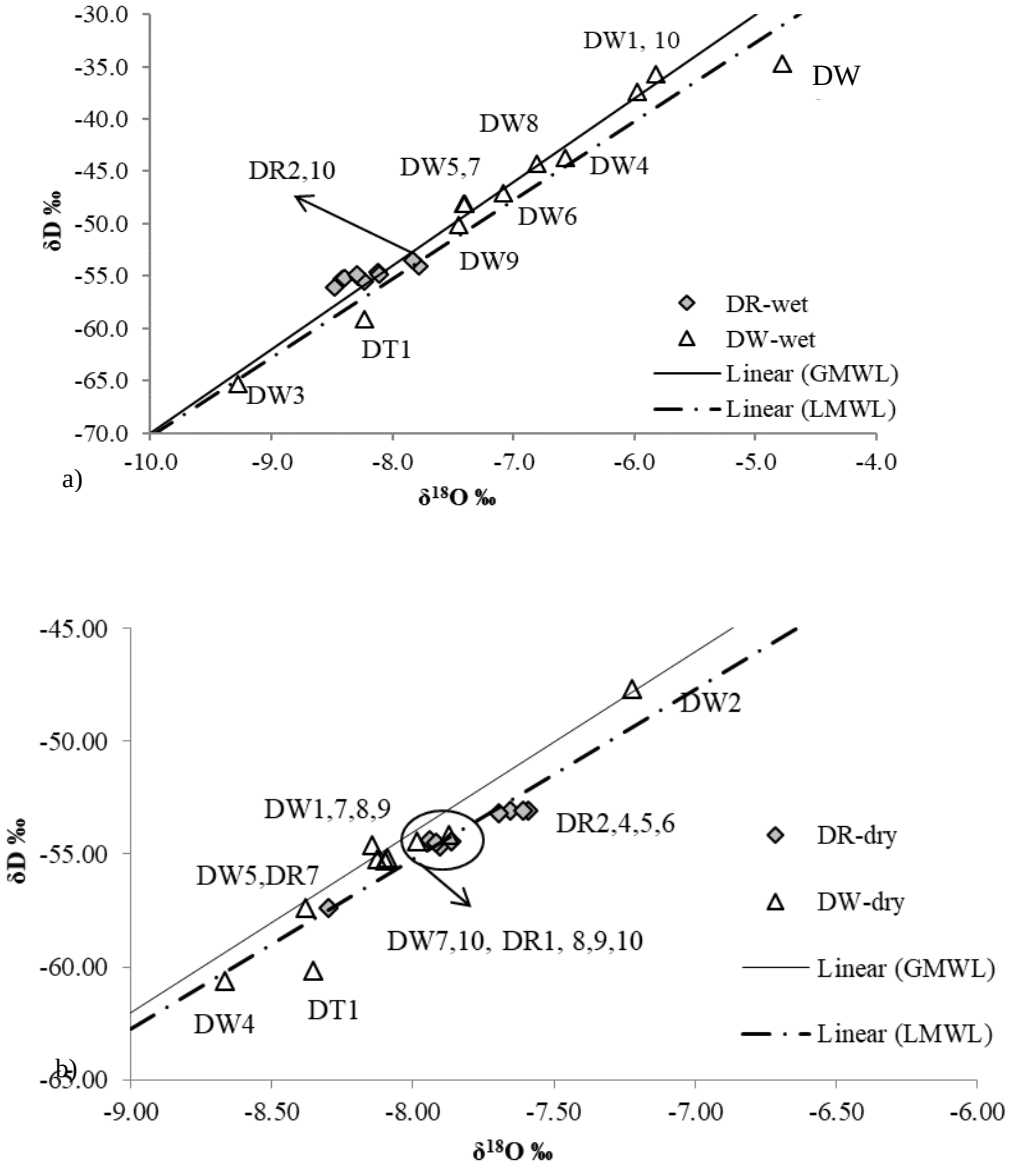

Figure 49 : δD verses $\delta^{18}O$ plots of Dhobi Khola groundwater and river water in (a) wet season and (b) dry season

Contrarily to river water, a wide spatial and temporal variations in δD and $\delta^{18}O$ of groundwater from dug wells are noticeable (Figure 49). Groundwater has the heavier isotopic composition of δD and $\delta^{18}O$ with a value ranging from -34.7 to -65.3‰ and from -4.8 to -9.3‰ respectively in the wet season. The value of δD and $\delta^{18}O$ change to

the range of -47.7 to -60.6‰ and -7.22 to -8.66‰ respectively in the dry season. Small temporal variation of δD (1.09‰) and $\delta^{18}O$ (0.12‰) is noted at DT1 whereas a large variation of δD (-18.8‰) and $\delta^{18}O$ (-2.44‰) is observed at DW10 and DW2 respectively. In both seasons, the heaviest isotopic composition is noted from DW2 and the lightest isotopic composition is observed in DW3 and DW4 during the wet and dry seasons respectively (Figure 49). Except for DW2 and DT1 in the wet and dry seasons respectively, all groundwater samples plot near the GMWL and LMWL indicating rainfall as a main source of recharge for these dug wells. However, meteoric water is a major source, and spatial variation in groundwater is visible.

4.4.1.3 Bagmati River

In the wet season, almost all river samples show the similar isotopic composition of δD and $\delta^{18}O$ with value variation from -58.1 to -63.5‰ and from -8.9 to -9.1‰ respectively. Composition of isotope changes to heavier during the dry season showing value ranging from -52.32 to -57.31‰ for δD and -7.55 to -8.32‰ for $\delta^{18}O$. Large temporal variation of 11.18‰ and 1.49‰ in δD and $\delta^{18}O$ is noted at BR8 and BR10 respectively while small variation of 0.79‰ and 0.59‰ in δD and $\delta^{18}O$ respectively is noted at BR1. River samples, except BR10, plot near or in between GMWL and LMWL in both the wet and dry seasons indicate meteoric water as one of the major sources of river discharge (Figure 50). BR10 plot below LMWL suggests the possibility of evaporation. Further, large spatial variation present in river samples shows the possibility of different sources for river discharge.

Wide spatial variation of δD and $\delta^{18}O$ in water samples from dug wells are noticed in both the wet and dry seasons (Figure 50). The $\delta^{18}O$ of groundwater varies from -6.4 to -9.2‰ in the wet season and changes to the range of -6.91 to -8.57‰ in the dry season. Large temporal variation is observed at BW1 (2.25‰) changing to heavier while small variation is obtained at BW8 (0.22‰) and changes to lighter isotopic composition during the dry season. Similarly, the value of δD of groundwater range from -40.3 to -66.2‰ in the wet season and -47.86 to -57.60‰ in the dry season with large temporal variation at BW1 (15.16‰) and small variation at BW8 (2.04‰). BW1 has the lightest isotopic value in the wet season which has changed to the heaviest isotopic in the dry season. All groundwater samples plotted near or in between the GMWL and LMWL in the wet season indicates meteoric water as a major source of groundwater recharge

(Figure 50 a). But in the case of the dry season, except BW1, BW2, BT1, BW4 and BW7, all other groundwater plotted above the GMWL. This indicates that the groundwater collected from basically downstream section lies above the GMWL and have additional recharge source rather than meteoric water. The additional source may be from agricultural runoff, surface runoff or leakage of sewer. But in the present condition, isotopic analysis of such source are not available. Hence it is difficult to point out recharge sources of those groundwater which are plotted above the GMWL. This may need to analyze detail isotopic study of other water sources.

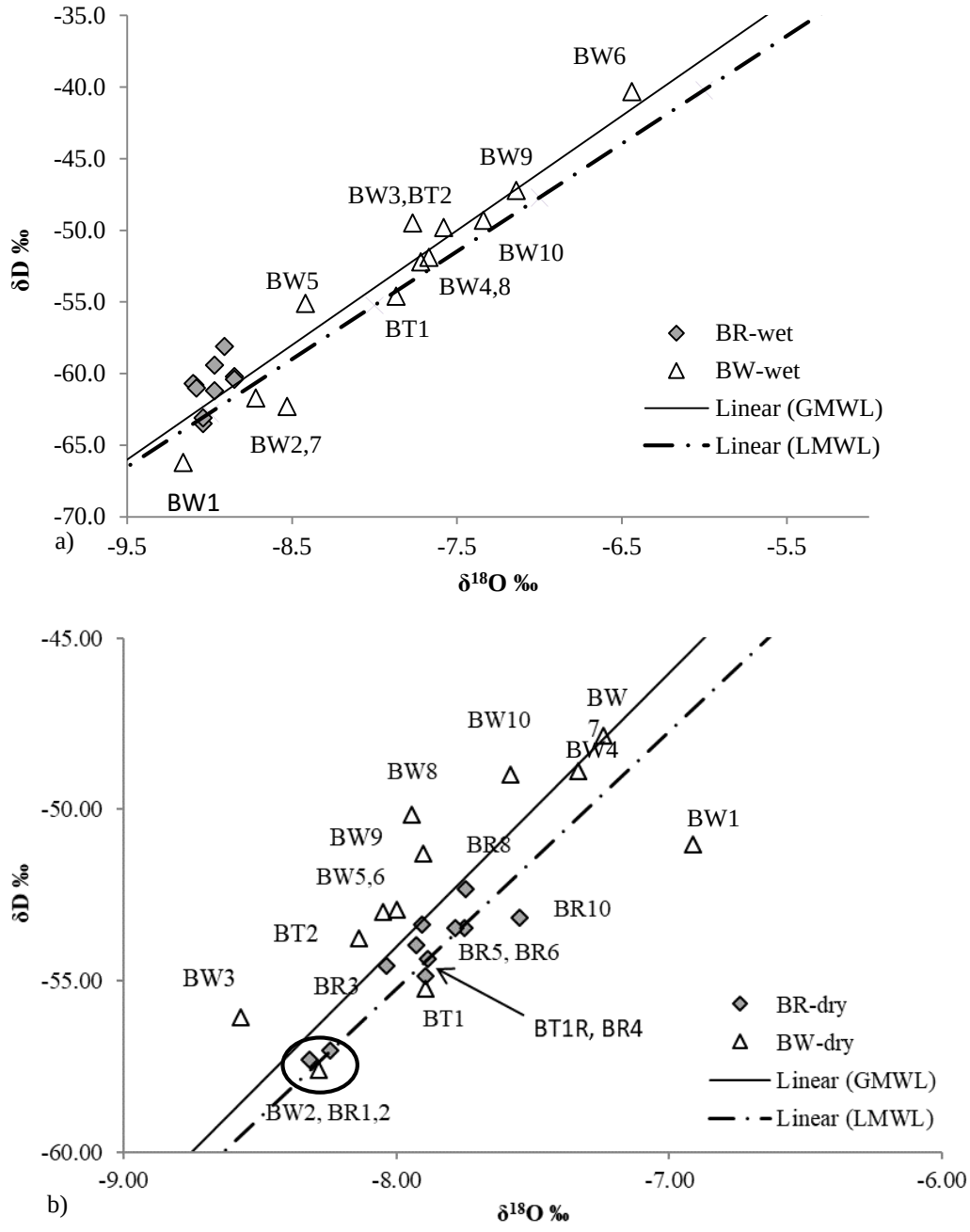

Figure 50: δD verses $\delta^{18}O$ plots of Bagmati groundwater and river water in (a) wet season and (b) dry season

4.4.1.4 Manahara River

Figure 51 presents δD versus $\delta^{18}O$ plots showing isotopic composition variations in groundwater and river water.

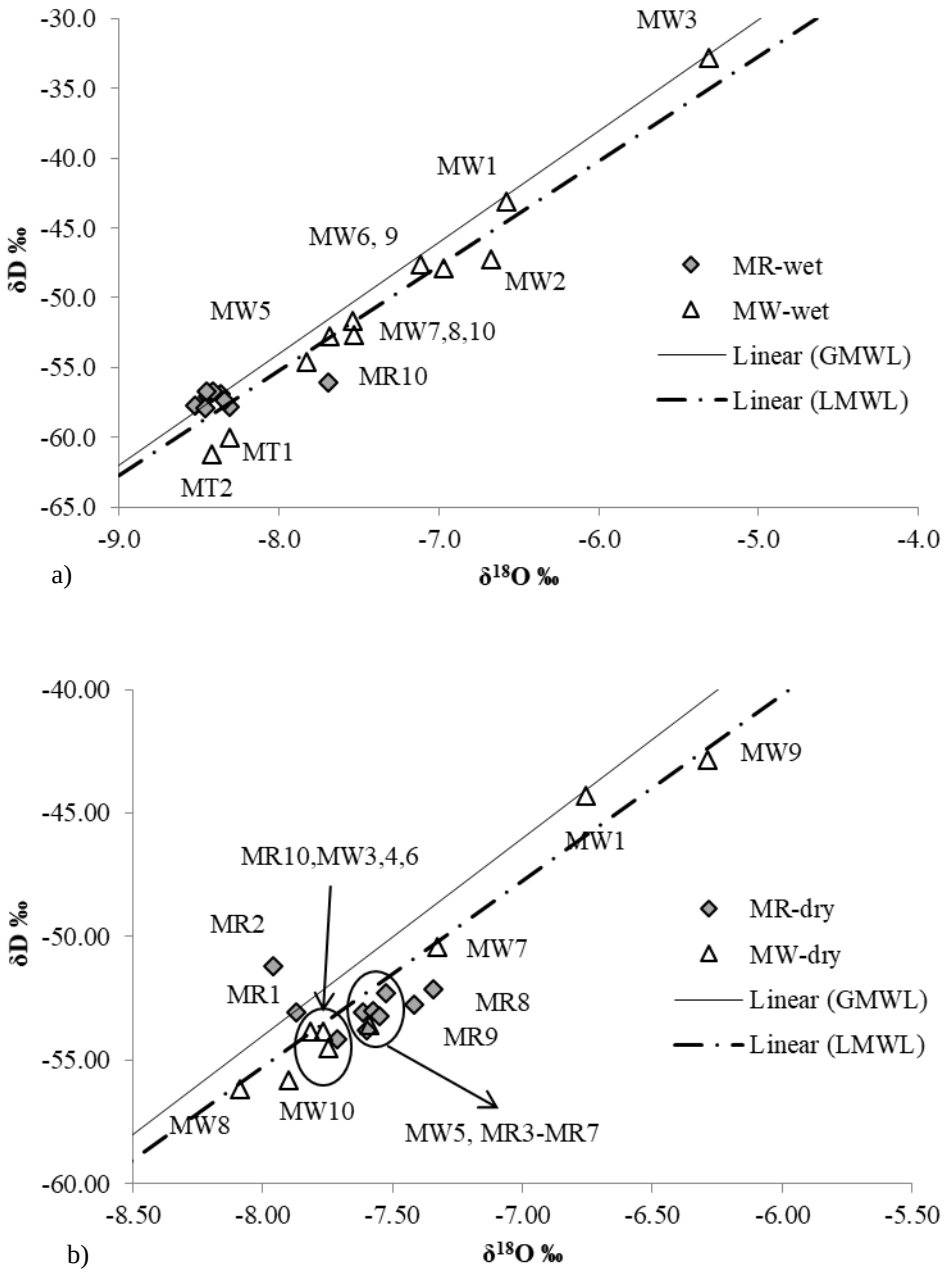

Figure 51: δD verses $\delta^{18}O$ plots of Manahara groundwater and river water in (a) wet season and (b) dry season

The $\delta^{18}O$ and δD composition of river water have tentative similar values in the wet season, except MR10 and plotted as a single cluster in the δD versus $\delta^{18}O$ plot (Figure 51a). Similarly, $\delta^{18}O$ and δD also has a narrow range in the dry season with value

variation of -7.34 to -7.96‰ and -51.19 to -54.14‰ respectively showing slightly heavier during the dry season. Wet season river samples, except MR10, plotted on the GMWL and LMWL (Figure 51a) indicate meteoric water as a major source of river discharge. In the case of the dry season, scatter plotting of river water can be seen in the Figure 51b indicating presence of different source of river discharge. In addition, river samples plotted below LMWL, except for MR1 and MR2, suggest possibility other recharge sources.

In the case of groundwater, wide spatial variations of $\delta^{18}O$ and δD are obtained in both seasons (Figure 51). The composition of $\delta^{18}O$ ranges from -5.3 to -8.4 ‰ in wet and -6.29 to -8.09 ‰ in the dry season whereas the range of δD varies from -32.8 to 61.2‰ and -42.86 to 56.18‰ in the wet and dry season respectively. Groundwater samples plotted on or near the LMWL in both seasons (Figure 51a) indicates rainfall as dominating recharge source for these dug wells.

Meanwhile, two shallow tube wells MT1 and MT2 plotted below LMWL with the lightest isotopic composition. These two tube wells have greater water depth compared to the remaining dug wells. It indicates that the recharge source of shallow tube wells are different from that of the dug wells.

4.4.1.5 Hanumante Khola

The $\delta^{18}O$ versus δD plot (Figure 52) shows variations in stable isotopic compositions in the wet and dry seasons.

In the wet season, almost all river samples have a similar isotopic composition of $\delta^{18}O$ (-8.0 to -8.1‰) and δD (-54.3 to -55.7‰) except HR8 which has the heavier isotopic composition (Figure 52a). The composition of isotope slightly changes to heavier during the dry season presenting value ranges from -6.91 to -7.73‰ for $\delta^{18}O$ and -48.75 to -54.41‰ for δD. Wet season river samples plotted near or in between GMWL and LMWL indicate meteoric water as a major source of river discharge. In the dry season, most the river samples are plotted below LMWL indicating chances of evaporation.

Groundwater shows a wide spatial variation in $\delta^{18}O$ and δD in both seasons (Figure 52). Composition of $\delta^{18}O$ ranges from -6.1 to -8.2 ‰ and -6.68 to -8.85 ‰ in the wet and dry seasons respectively. However, the overall range of $\delta^{18}O$ is similar in both seasons, samples from HW3, HW5, HW6, HW7, HW8 and HW10 show lighter composition in

the wet season. Except for HW10 from the wet season, groundwater samples plotted close to LMWL (Figure 52) signify meteoric water as the main recharge source for these dug wells. However meteoric water is the main recharge source, a wide variation in isotopic composition is noticeable. HW1 presents the heaviest isotopic value while HW2 shows the lightest isotopic composition in both seasons. Laterally, these two dug wells are very close (Figure 38) but their well depths are variable (Table 13). Wide value variation between these two wells indicates that the recharge area is different for different aquifer depths whenever they are laterally close. The lightest isotopic value in HW2 in both seasons may indicate that the higher depth wells recharged from high elevated recharge zone compared to shallow depth wells.

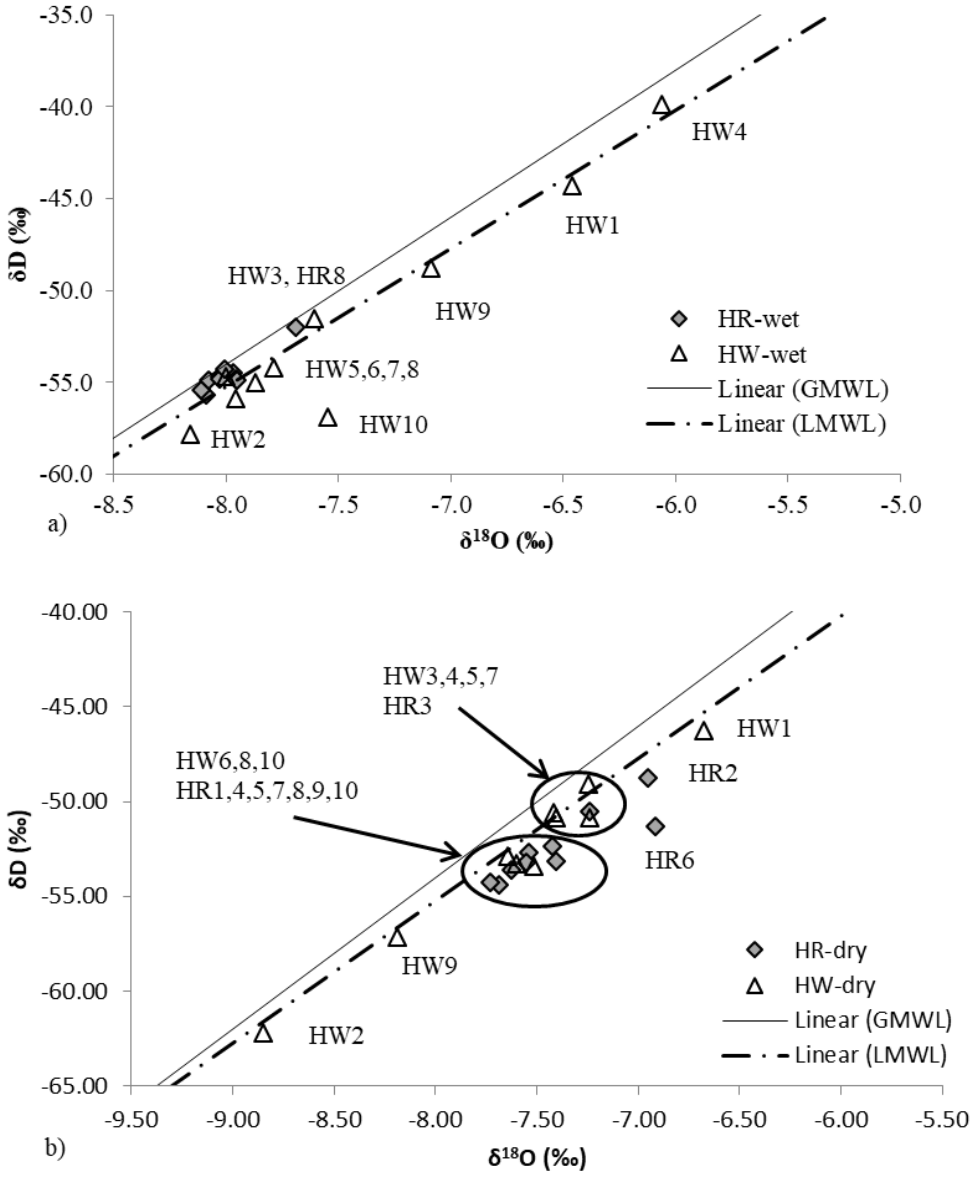

Figure 52: δD verses $\delta^{18}O$ plots of Hanumante groundwater and river water in (a) wet season and (b) dry season

4.4.1.6 Godawari Khola

The δD of river water varies from -55.5 to -60.4‰ in the wet season and from -45.9 to -58.5‰ in the dry season. Similarly, $\delta^{18}O$ ranges from -8.0 to -8.8‰ in the wet season and from -6.2 to -8.8‰ in the dry season. Compared to the wet season, wide spatial variation is noticeable showing a gradual decrease in δD and $\delta^{18}O$ towards downstream river sites during the dry season (Appendix 6F). But in the case of temporal variation, three upstream river sites show similar isotopic composition while the remaining downstream river sites have enriched isotopic composition during the dry season. Especially, GR7 and GR8/GR9 show 1.9‰ heavier composition in $\delta^{18}O$ and 9.9‰ in δD during the dry season. Existence of all river water on or close to the LMWL and GMWL on the δD versus $\delta^{18}O$ plot with a similar trend indicates meteoric water as a major source for river discharge during the wet season (Figure 53a). At the same time, the occurrence of lighter isotopic value at high elevated upstream rive sites (GR1) as compared to lower elevation downstream river sites (GR10) suggests altitude effects (Shakya *et al*, 2019). A similar type of result is also obtained in the dry season. But plotting below of LMWL with enriched isotopic composition of GR7 and GR8/GR9 indicates possible evaporation during the dry season (Figure 53b). Very minor discharge on these river sites also signifies the possibility of evaporation.

In the case of groundwater, wide spatial variation is noticeable on δD and $\delta^{18}O$ in both seasons. The value of δD varies from -50.1 to -62.4‰ in wet and from -48.4 to -62.1‰ in the dry season. Likewise, $\delta^{18}O$ ranges from -7.4 to -9.2‰ and from -7.0 to -9.2‰ in the wet and dry seasons respectively. In both seasons, the lighter isotopic composition is observed at GW1 while the heavier one is noticed at GW9 and GW10 in the wet and dry seasons respectively. Minor enrichment of isotopic composition is noticeable in most the groundwater but significant enrichment of 1.5‰ in $\delta^{18}O$ and 10.2‰ in δD is observed at GW10 during the dry season. Except for GW2 and GW5 of the wet season, all other groundwater plotted on or near to the LMWL and GMWL indicate meteoric water as a possible recharge source in both seasons (Figure 53).

But plotting of GW2 and GW5 below LMWL again signifies possible evaporation during the wet season (Figure 53a). Occurrences of lighter isotopic composition at upstream high elevated dug well with meteoric water sources suggest for the presence of altitude effects as in the river site.

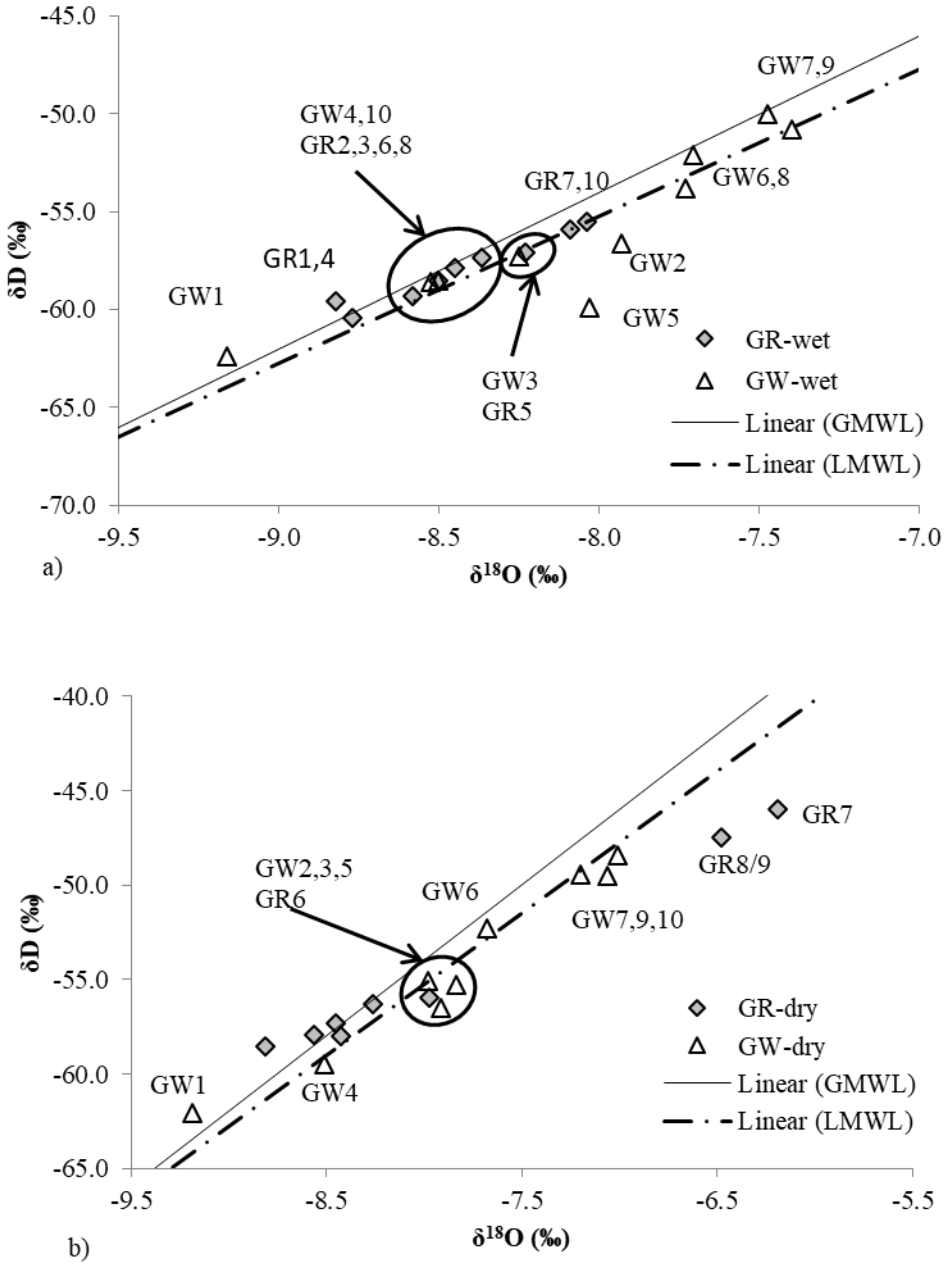

Figure 53: δD verses $\delta^{18}O$ plots of Godawari groundwater and river water in (a) wet season and (b) dry season

4.4.1.7 Kodku Khola

River isotopic composition of δD ranges from -55.5 to 58.3‰ and $\delta^{18}O$ varies from-7.9 to -8.4‰ in the wet season (Appendix 6G). These values are relatively lighter during the dry season in most the river water except KR7 and KR5 with a wide range from -54.55 to -60.71‰ (for δD) and -7.86 to -8.77‰ (for $\delta^{18}O$). In both seasons, KR1 shows comparatively lightest isotopic composition while KR7 has the heaviest isotope during the dry season. Both seasons' river samples plotting close to LMWL (Figure 54)

indicate meteoric water as a major source of river discharge. However, a spatial variation on δD and $\delta^{18}O$ during the dry season presents the possibility of additional recharge sources besides rainfall.

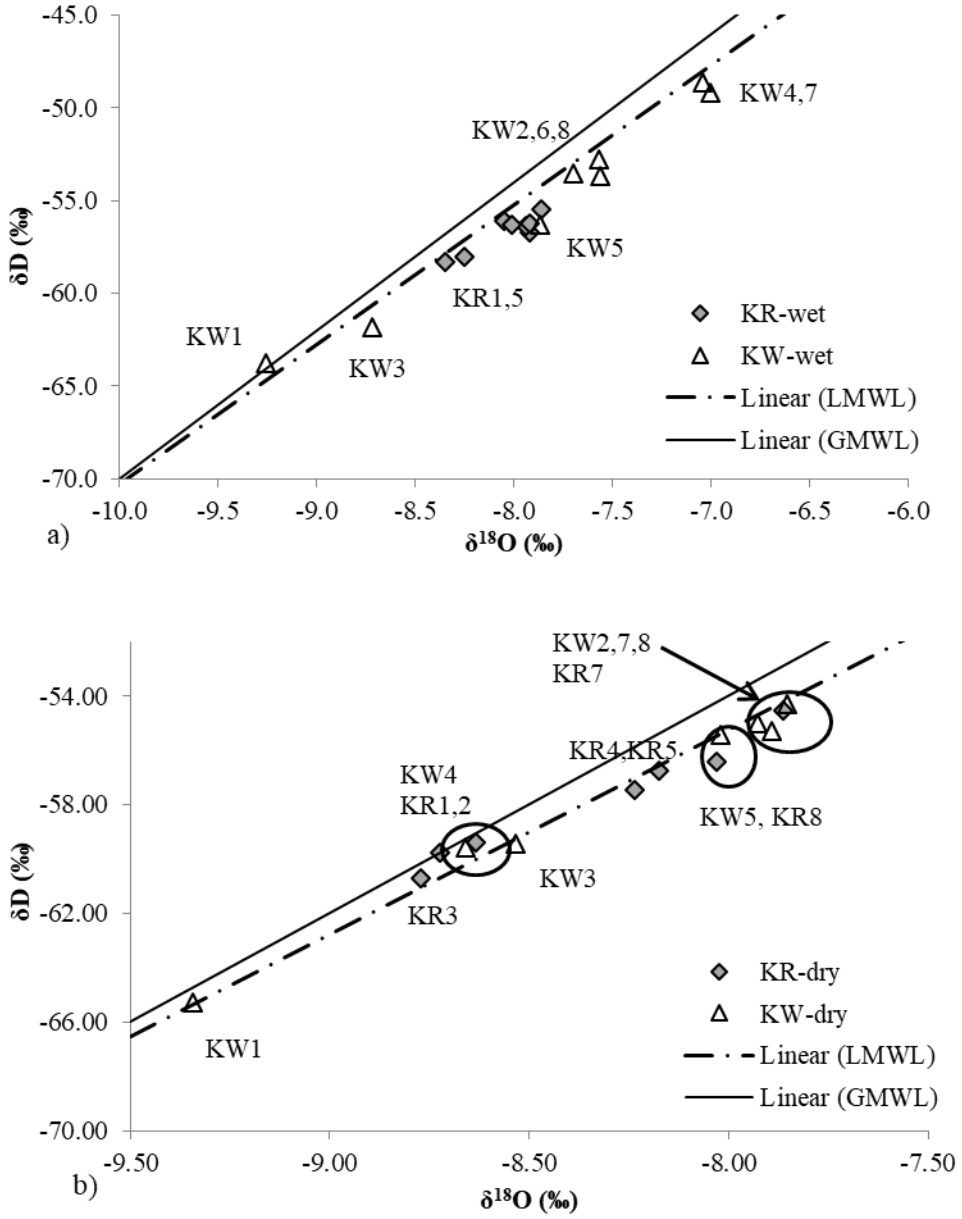

Figure 54: δD verses $\delta^{18}O$ plot of Kodku groundwater and river water in (a) wet season and (b) dry season

In the case of groundwater, δD and $\delta^{18}O$ shows a wide range of isotopic variation from -48.6 to -63.8‰ and from -7.0 to -9.3‰ respectively in the wet season. Same as in river water, almost all groundwater show relatively lighter isotopic composition during the dry season except KW3 with variation from -54.32 to -65.26‰ for δD and from -7.85 to -9.34‰ for $\delta^{18}O$. Both seasons have lighter isotopic composition at KW1, and heavier

at KW4 and KW7 in the wet and dry seasons respectively. Plotting of groundwater samples close to LMWL in δD versus $\delta^{18}O$ plots (Figure 54) signifies meteoric water as one of the recharging sources for selected dug wells in both seasons. But spatial variations observed in isotopic composition in both seasons again indicate the possibility of other additional recharge sources.

4.4.1.8 Nakhhu Khola

The river water shows minor spatial variation in wet season isotopic composition with value variation from -61.6 to -62.4‰ and from -8.9 to -9.0‰ for δD and $\delta^{18}O$ respectively (Figure 55).

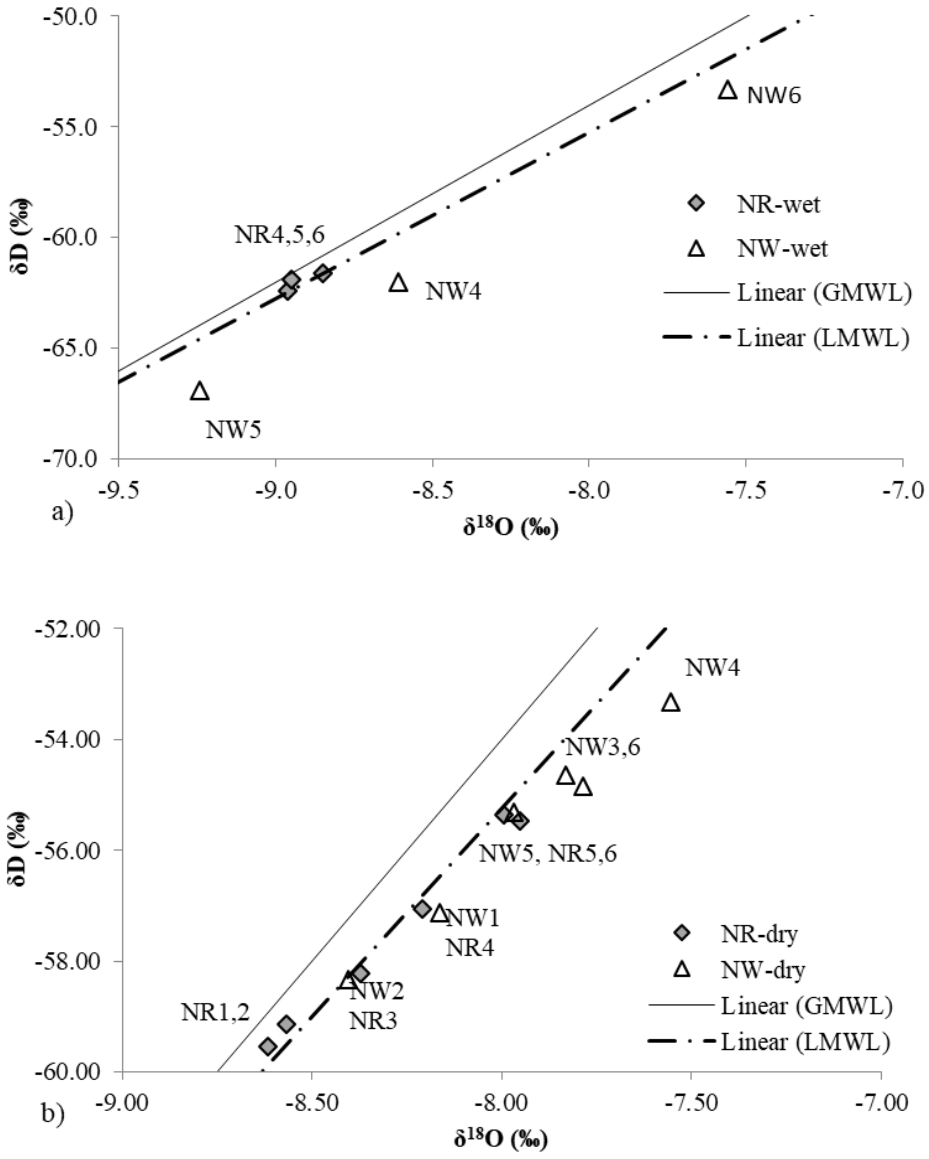

Figure 55: δD verses $\delta^{18}O$ plot of Nakhu groundwater and river water in (a) wet seson and (b) dry season

Isotopic composition of river water enriched during the dry season shows a value range of -55.36 to -59.53‰ for δD and of -7.95 to -8.62‰ for $\delta^{18}O$. The heaviest isotopic composition is observed in NR5 (Appendix 6H) during the dry season showing a maximum temporal variation of 6.43‰ (δD) and 1.05‰ ($\delta^{18}O$). The occurrence of all river water close to LMWL (Figure 55) suggests meteoric water as a major source for river discharge in both wet and dry seasons. At the same time, a clear decreasing trend of isotopic value towards the downstream river section (Figure 55) again indicates the presence of altitude effects (Shakya *et al*., 2019) in precipitation.

A wide range of isotopic composition is noticeable in the groundwater. The value of δD ranges from -53.3 to -66.9‰ and -53.3 to -58.3‰ in the wet and dry seasons respectively. Similarly, the range of $\delta^{18}O$ varies from -8.9 to -9.0‰ in the wet season and from -7.6 to -9.2‰ in the dry season. All three groundwater plots below the LMWL in the δD versus $\delta^{18}O$ suggests another recharge source rather that the rainfall during the wet season. But in the case of the dry season, upstream groundwater sites (NW1, NW2 and NW3) are plotted on LMWL while downstream sites are plotted below the LMWL (Figure 55).

4.4.1.9 Balkhu Khola

In the river samples, the isotopic composition of $\delta^{18}O$ and δD varies from -8.2 to -9.0‰ and -56.9 to -61.6‰ respectively during the wet season. Almost all river samples are plotted as a single cluster in δD versus $\delta^{18}O$ except BAR9 which has the lightest isotopic composition (Figure 56). During the dry season, the composition of isotope changes to heavier with a value ranging from -7.2 to -8.24‰ for $\delta^{18}O$ and -50.14 to -56.46‰ for δD. The river sample collected from uppermost section (BAR1) shows the lightest isotopic composition which gradually decreases towards downstream sections presenting the heaviest one at BAR10 (Appendix 6I Figure 56b) in the dry season. River samples from both the wet and dry seasons plot near LMWL with a similar trends (Figure 56) indicate meteoric water as a major source of river discharge.

Wide spatial variations of $\delta^{18}O$ and δD in water from dug wells are observed in the wet season having value variation from -7.7 to -11.4 ‰ and -53.0 to -81.7‰ respectively. The lightest isotopic composition is observed at BAW6 while the heaviest one is obtained from BAW5 (Figure 56a). Alike in river water, groundwater shows heavier isotopic composition in the dry season with a narrow value range of $\delta^{18}O$ (-6.83 to -

8.08‰) and δD (-47.09 to -55.3‰). Groundwater samples plot near LMWL with a similar trend in both wet and dry seasons (Figure 56) signifies rainfall as the main recharge source for these wells.

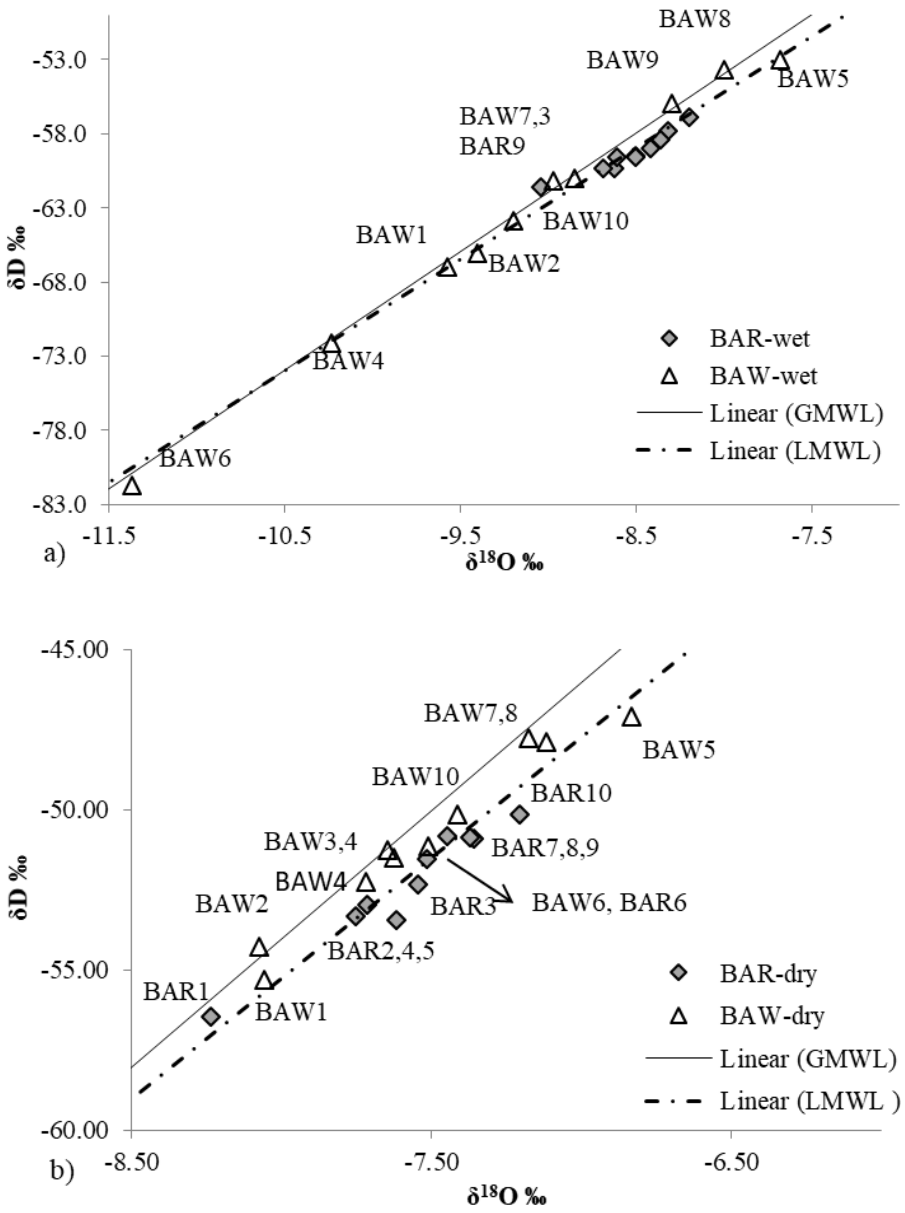

Figure 56: δD verses $\delta^{18}O$ plot of Balkhu groundwater and river water in (a) wet season and (b) dry season

4.4.2 Comparison on river water isotopic composition

A narrow spatial variation of δD and $\delta^{18}O$ is noticeable in each river corridor during both seasons (Table 18). Comparing to the nine rivers, the Godawari Khola possess a higher variation of 5 to 12.5‰ for δD, and 0.9 to 2.6‰ for $\delta^{18}O$ in the wet and dry seasons respectively. The elevation of sampling sites located in this river varies from

1429 to 1298 m (Table 14). The upstream sections of rivers especially from the Bagmati (from northern site), Godawari and Kodku (from southern site) Khola have lightest isotopic composition (Figure 57).

The elevation of these sections varies from 1429 to 1322 m. On the other side, the downstream sections from the Hanumante, Dhobi and Balkhu Khola (centre sites with elevation 1270 to 1290 m) present heavier isotopic composition. This result signifies that the isotopic composition of river water is affected by altitude variation. Lachniet and Patterson (2009), and Shakya *et al*., (2019a) also present similar type of results from the surface water study of the northern Central America and Kathmandu respectively.

Table 18: δD and δ18O value range in groundwater and river water along nine corridors

River water		δD (‰)		$\delta^{18}O$ (‰)		Groundwater	δD (‰)		$\delta^{18}O$ (‰)	
		Wet	Dry	Wet	Dry		Wet	Dry	Wet	Dry
BMR	Max	-53.1	-54.9	-7.8	-7.8	BMW	-34.4	-46.2	-5.5	-6.6
	Min	-55.1	-58.4	-8.2	-8.3		-60.9	-54.7	-8.8	-8.0
	Average	-54.4	-56.1	-8.1	-7.9		-46.2	-51.0	-6.9	-7.3
DR	Max	-53.5	-53.1	-7.8	-7.6	DW	-34.7	-47.7	-4.8	-7.2
	Min	-55.5	-57.4	-8.4	-8.3		-65.3	-60.6	-9.3	-8.7
	Average	-54.8	-54.2	-8.2	-7.8		-46.7	-55.5	-7.0	-8.1
BR	Max	-58.1	-52.3	-8.9	-7.5	BW	-49.3	-47.9	-7.3	-6.9
	Min	-63.5	-57.3	-9.1	-8.3		-66.2	-57.6	-9.2	-8.6
	Average	-60.8	-54.4	-9.0	-7.9		-56.6	-52.2	-8.1	-7.8
MR	Max	-56.1	-51.2	-7.7	-7.3	MW	-32.8	-42.9	-5.3	-6.3
	Min	-57.9	-54.1	-8.5	-8.0		-61.2	-56.2	-8.4	-8.1
	Average	-57.1	-52.9	-8.3	-7.6		-49.2	-51.7	-7.2	-7.5
HR	Max	-52.0	-48.8	-7.7	-6.9	HW	-39.9	-46.2	-6.1	-6.7
	Min	-55.7	-54.4	-8.1	-7.7		-57.8	-62.2	-8.2	-8.9
	Average	-54.6	-52.4	-8.0	-7.4		-51.9	-52.6	-7.5	-7.6
GR	Max	-55.4	-46.0	-7.9	-6.2	GW	-50.8	-48.4	-7.4	-7.0
	Min	-60.4	-58.5	-8.8	-8.8		-62.4	-62.1	-9.2	-9.2
	Average	-58.0	-54.7	-8.4	-7.9		-56.2	-54.2	-8.1	-7.8
KR	Max	-55.5	-54.5	-7.9	-7.9	KW	-48.6	-54.3	-7.0	-7.9
	Min	-58.3	-60.7	-8.4	-8.8		-61.8	-65.3	-8.7	-9.3
	Average	-56.7	-57.9	-8.0	-8.3		-53.7	-57.8	-7.7	-8.3
NR	Max	-61.6	-55.4	-8.9	-8.0	NW	-53.3	-53.3	-7.6	-7.6
	Min	-62.4	-59.5	-9.0	-8.6		-66.9	-58.3	-9.2	-8.4
	Average	-62.0	-57.5	-8.9	-8.3		-60.7	-55.6	-8.5	-8.0
BAR	Max	-56.9	-50.1	-8.2	-7.2	BAW	-53.0	-47.1	-7.7	-6.8
	Min	-60.3	-56.5	-8.7	-8.2		-81.7	-55.3	-11.4	-8.1
	Average	-59.0	-52.3	-8.5	-7.6		-63.6	-50.9	-9.2	-7.5

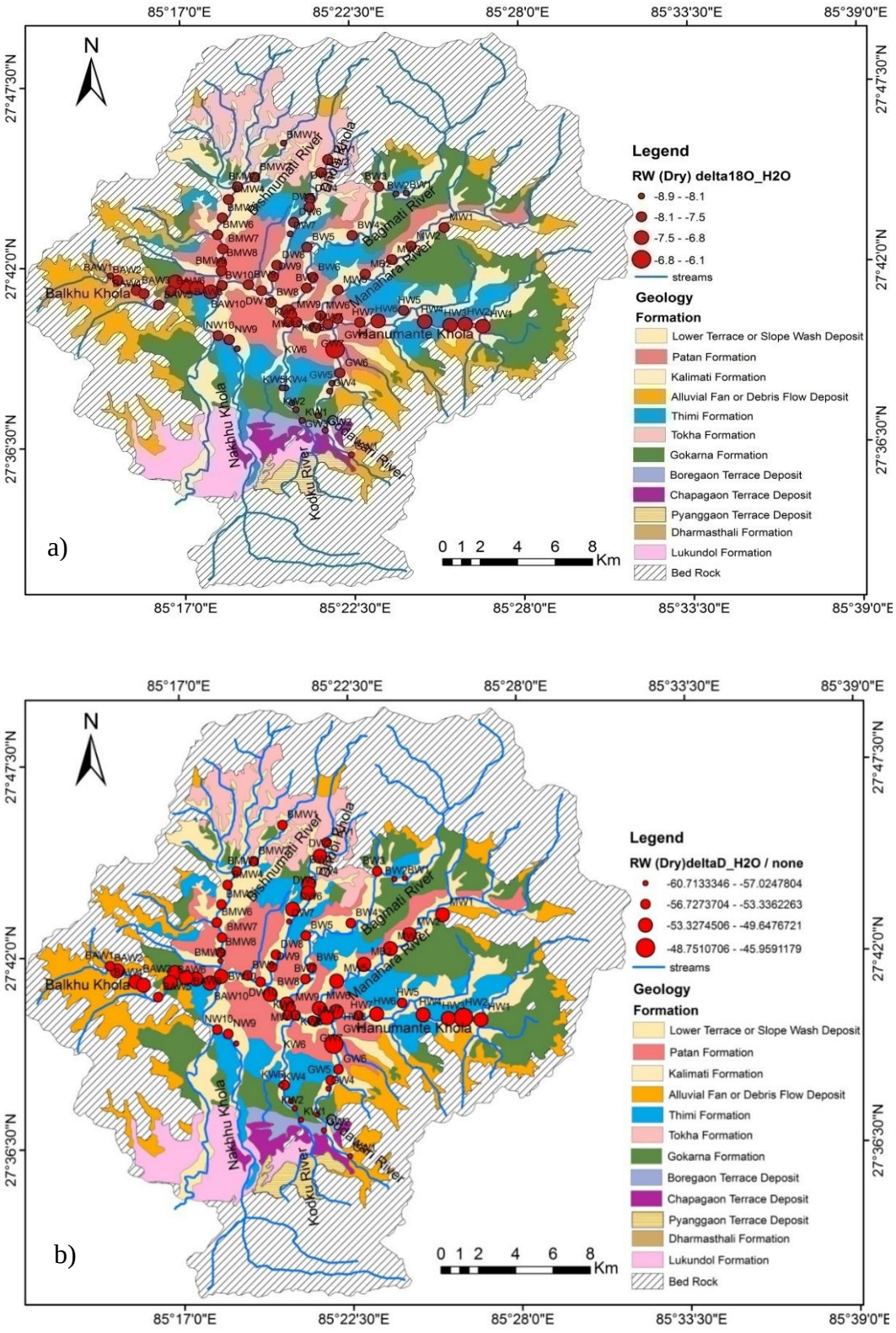

Figure 57: Spatial distribution of a) $\delta^{18}O$ and b) δD of river water in the dry season

The isotopic study of precipitation from the Kathmandu valley by Chhetri *et al*. (2014) and Adhikari *et al*. (2020) show depleted isotopic values during the wet season. During the study period of Chhetri *et al*. (Feb 2011 to July 2012), overall mean value of δD and

$\delta^{18}O$ are -27.29 and -3.91‰ respectively with annual average precipitation of 1438 mm. But in the study period of Adhikari *et al*. (May 2016 to Sep 2018), overall mean values of δD and $\delta^{18}O$ are -23.39 and -3.76‰ respectively with annual average precipitation of 1023.93 mm. Compared in these two study periods, the δD and $\delta^{18}O$ values of precipitation show slightly enriched in lower annual precipitation. The temporal variations observed in the wet and dry seasons are commonly termed as the amount effect by Chhetri *et al*. (2014). Contrarily, Adhikari *et al*. (2020) suggested this variation is due to the moisture sources and their transport processes. The wet season precipitation is characterized by moisture sources from the Bay of Bangal and shows depleted isotopic composition while the dry season precipitation is the result of moisture from the westerlies (Mediterranean Sea) presenting enriched isotopic values. The research on the western part of Nepal (Matheswaran *et al*., 2019) as well as on the Kathmandu valley (Yu *et al*., 2016) also suggested that the source of water vapour from the Indian monsoon and westerlies are main controlling factors for precipitation stable isotopes in Nepal. The local meteoric water line defined by Chhetri *et al*. (2014) and Adhikari *et al*. (2020) present lower slopes and smaller intercepts compared to GMWL, suggesting re-evaporation of raindrops at the Kathmandu Valley. The sampling period of precipitation by Adhikari *et al*. (2020) and the sampling period of this research is similar. Thus precipitation values of δD and $\delta^{18}O$ and the LMWL analyzed by Adhikari *et al*. (2020) is used as reference for precipitation of the Kathmandu Valley. According to their study, wide temporal variation on the δD and $\delta^{18}O$ is noticeable with range from -120.07 to 53.93‰ and -16.33 to 9.9‰ respectively.

River water of present study also shows wide temporal variation on isotopic composition. The δD and $\delta^{18}O$ varies from -63.5 to -52.0 and -9.1 to -7.7‰ in the wet season and -60.7 to -46.0‰ and -8.8 to -6.2‰ in the dry season respectively (Table 18). The range of river isotope lies within the range of the precipitation analyzed by Adhikari *et al*. (2020). The δD versus $\delta^{18}O$ plots from previous sections shows that all river water from the wet season lies on or close to the LMWL defined by Adhikari *et al*. (2020). It indicates that precipitation is the main source of river discharge in the Kathmandu Valley rivers during the wet season (Liu and Yamanaka, 2012; Sakakibara *et al*., 2016; Ali and Ajeena, 2016; Shakya *et al*., 2019a). But in the case of the dry season, most the river water changes to heavier during the dry season except for the Kodku Khola. The values of δD and $\delta^{18}O$ is heavier as an effect of rainfall amount suggested by Chhetri *et*

al. (2014) and by moisture source from the westerlies (Mediterranean Sea) suggested by Adhikari *et al*. (2020). The research on the Jiulong River, southeast China by Yang *et al*. (2018) also presented amount effect and source of vapour as controlling factor for seasonal variation. Most the samples especially from the Bishnumati, Manahara and Hanumante are plotted close to or just below the LMWL. This indicates that there is the presence of other additional sources of river discharge along with dry season rainfall. A fewer samples from the Bagmati (Figure 50b), Hanumante (Figure 52 b) and Godawari (Figure 53b) presents heavier isotopic value and plotted below LMWL. This suggest that the water samples from these locations has undergone evaporation or it may be mixture of evaporated water (Terwey, 1997; Gat, 1995; and Mohammed *et al*., 2016).

4.4.3 Comparison on groundwater isotopic composition

A Wide spatial variation of δD and $\delta^{18}O$ is observed in both wet and dry seasons. The variation range of δD and $\delta^{18}O$ is high in the wet season (-81.7 to -34.7‰ for δD and -11.4 to -4.8‰ for $\delta^{18}O$) compared to the range of the dry season (-65.3 to -42.9‰ for δD and -9.3 to -6.3‰ for $\delta^{18}O$). The depleted isotopic values are measured from the dug wells along the Balkhu and Kodku corridors while enriched isotopic values obtain from wells along the Dhobi Khola and the Manahara River corridors in the wet and dry seasons respectively (Table 18).

Mostly, groundwater from southern corridors such as the Kodku, Godawari and Nakhu khola exhibit lighter isotopic composition as similar as in the river water (Figure 58). This indicates that the lighter isotopic value of groundwater is the indication of recharge from greater elevation while heavier isotopic composition is from lower elevation. The value range of dry season isotopic composition is more or less similar to the range observed by Shakya *et al*. (2019a) for the shallow as well as deep aquifer of the Kathamandu valley. However, in the case of shallow tube wells and bore holes (DT1, BT1, BT1W, BT2, MB1 and MB2; Appendix 6), which generally have higher depth compared to dug wells show narrow spatial variation with value range of -7.6 to 8.4‰ in the wet and -7.8 to -8.3‰ in the dry season for $\delta^{18}O$.

The isotopic composition of groundwater samples also exhibit temporal variation. Almost all groundwater from the Dhobi corridor has changed to lighter isotope during the dry season. Conversely, all samples from the Balkhu corridor has changed to heavier isotopic value. The samples from remaining corridors show mix type of changes.

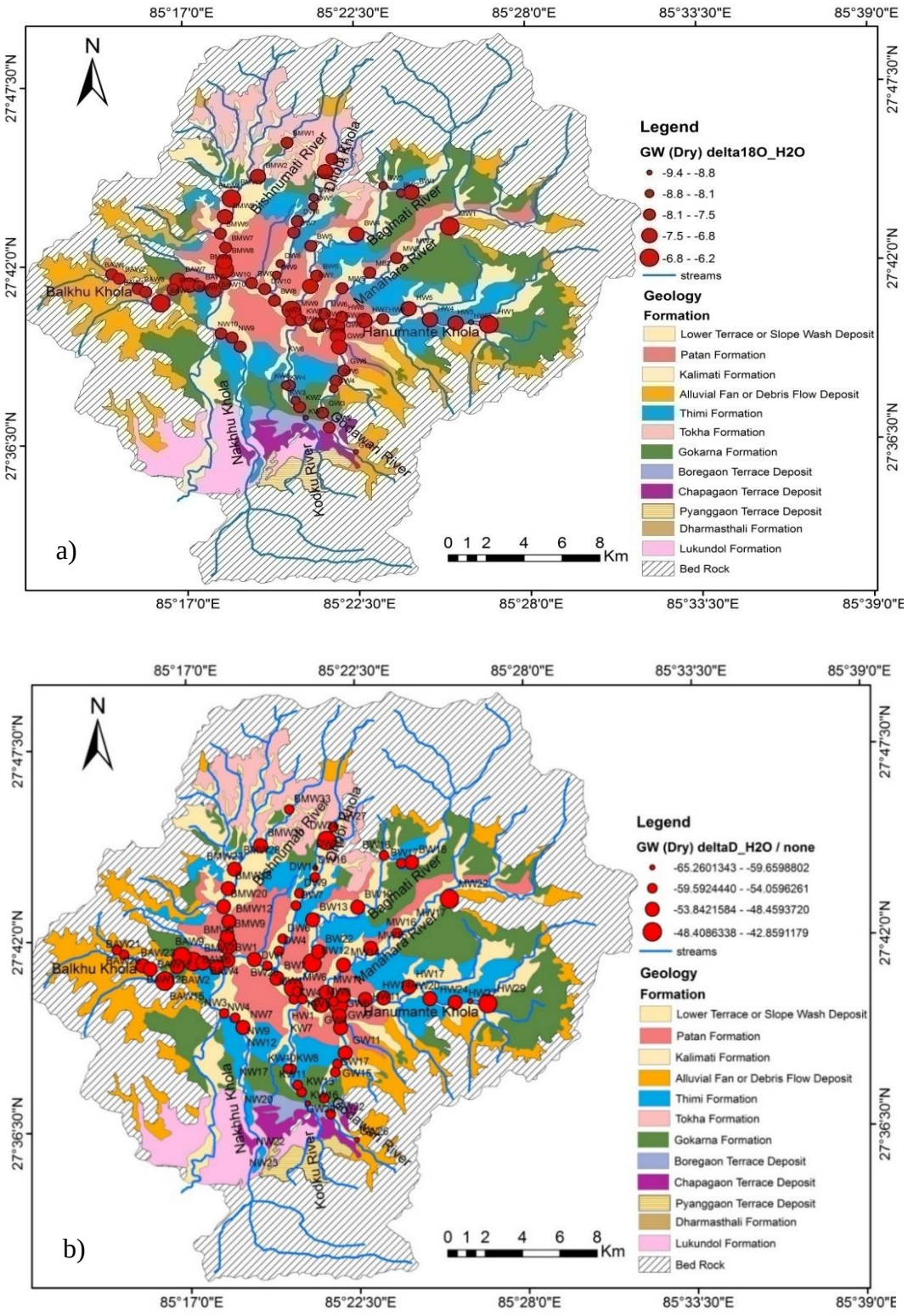

Figure 58: Spatial distribution of a) $\delta^{18}O$ and b) δD of groundwater in the dry season

The plots of δD versus $\delta^{18}O$ on previous sections show that most of the groundwater samples from both seasons plotted close to the LMWL, presenting meteoric water as a major recharge source for groundwater. The groundwater samples which are plotted

below or above the LMWL, especially in the dry season, indicate the possibility of recharge by other sources along with rainfall. In the present study, isotopic analysis of other water sources such as agricultural runoff and sewer could not be included and thus it is difficult to define exact recharge source for those groundwater which plotted below or above the GMWL.

The dominancy of Ca-HCO_3 water type classified from the piper plots for both seasons also represents freshwater infiltration from the rainfall. The temporal variation on groundwater, especially lighter isotopic composition in the wet season, is the reflection of recharge from the lighter value of precipitation (Lachniet and Patterson, 2009 and Matheswaran *et al.*, 2019). The samples from the Balkhu corridor along with other section is the result of recharge from recent rainfall. Shakya *et al*. (2019a) also presents similar recharge source for the shallow aquifer of the Kathmandu Valley. But in the case of the samples from the Dhobi corridor, they have lighter isotope in the dry season. On the other hand, they also plot close to the LMWL, indicating meteoric source. These two consequences together signifies that the groundwater of the Dhobi corridor has mixed type of recharge sources, dominantly from additional source beside of dry season rainfall.

4.5 Electrical resistivity study

The electrical resistivity method is an indirect method to get lithological information of subsurface area. At the initial phase of the research, it was planned to do resistivity survey in all areas of selected wells from the inventory data. The main purpose of ERT survey is to find out tentative subsurface lithological variation in the selected well location. Based on the resistivity variation, it tried to interpreted lateral and vertical variation of subsurface materials. But it could not be possible as these wells were located on dense settlement area. Roads are also constructed adjacent to river channels in core areas of the corridors which makes impossible in electrodes arrangements for ERT survey. Thus only 12 ERT profiles of lengths between 15 to 96 m were acquired in the corridors of the Bishnumati River, Manahara River and Nakhu Khola (Table 19)**.** It was carried out in the month of November. Except in few profile line, 48 electrodes with 2 m electrode spacing were used. Wenner array was used in all profile lines except BMW5A, as it was very short profile and thus used Schlumberger array to get information of even thin layers.

Table 19: Summary of acquisition parameter and inversion for profiles of river corridors

River Name	Profile ID	Length (m)	No. of electrodes	Electrode spacing (m)	Array	Inversion (RMS)%
Bishnumati	BMW1	96	48	2	Wenner	1.6
	BMW4	96	48	2	Wenner	1.9
	BMW5	96	48	2	Wenner	2.4
	BMW5A	15	15	1	Schlumberger	3.4
	BMW5B	96	48	2	Wenner	5.3
	BMW7	96	48	2	Wenner	5.4
Manahara	MW3	72	36	2	Wenner	1.8
	MW10	96	48	2	Wenner	2.9
Nakhu	NW1	96	48	2	Wenner	5.5
	NW2	72	36	2	Wenner	2.5
	NW3	96	48	2	Wenner	1.7
	NW6	72	36	2	Wenner	2.4

The subsurface lithology can be verified by comparing to the borehole logs located as close as ERT profiles. But in the case of this study, there is unavailability of borehole logs that are much closed to these ERT profile for comparison of resistivity value with subsurface lithology. Thus, the interpretation of subsurface materials has been done by correlation between modeled resistivity value with standard resistivity values and field observation. The range of resistivity value and their general lithology was estimated based on JICA (1990) which are presented on Table 20. As all the ERT surveys carried out in the month of November, the range of resistivity assumed for subsurface lithology is taken as similar for all the river corridors. The assumption used in this research is somehow similar as in the research conducted at Combodia by Uhlemann *et al.* (2017) for spatial distribution of clay layers along the river peripheral areas. They used borehole logs and laboratory analysis for subsurface lithology and particle size verification respectively.

4.5.1 Electrical resistivity tomography (ERT) of river corridors

4.5.1.1 Bishnumati River

Total 6 profiles were acquired on the Bishnumati river corridor (Table 19). BMW1 is located towards upstream section and BMW7 (nearby Teku area) at downstream section.

ERT Profile 1 - BMW1:

This ERT profile conducted along upstream section of the Bishnumati River from where BMW1 groundwater sample was collected. The profile line was situated in cultivated land at the right bank across to the river channel. It was stretched up to 96 m covering about 20 m depth. The BMW1 well is located at the 48 m of this profile with water level depth at 1.3 m. In this profile, 48 electrodes with 2 m spacing were used at where electrode 1 was located at river side. The tomogram of this profile is presented in Figure 60 and area around this profile is presented in Figure 59.

Table 20: Expected lithology and resistivity values (Modified from JICA, 1990)

Expected Lithology	Resistivity (Ωm)	Description
Clay and silt	<50	Silt increase towards higher value
Sandy clay with silt	50-75	Sand and silt proportion increases with higher value
Clayey sand with silt	75-100	Sand and silt proportion increases with higher value
Fine sand with occasional gravel	100-150	Proportion of gravel increases towards higher value
Medium-Coarse sand with occasional gravel	150-300	Higher value represent presence of coarse sand with gravel
Gravelly sand	300-750	Proportion of gravel increases with higher value
Sandy gravel	750-1500	Proportion of gravel increases with higher value
Fill materials	30-400	Lower value indicates presence of organic materials while higher value indicate presence of coarser materials

Figure 59: Photographs of BMW1 profile a) towards first electrode, river channel and b) towards last electrode

Resistivity imaged along this profile range between 20 to nearly 900 Ωm. Higher resistivity was imaged close to the river channel around profile position 0 to 12 m (at surface) and 14 to 20 m (4 to 10 m depth) indicating coarse-grained deposits of gravelly sand (Figure 59 a and Figure 60). A small patch of lower resistivity was observed in between these higher resistivity at around 8 to 12 m profile position within elevation 1317 to 1313 m. Thin top layer of uniform resistivity (57 to 100 Ωm) reflecting moist clayey sand along with small patch of sandy clay imaged around profile position 20 to 24 and 28 to 52 m. While high resistivity (163 to 276 Ωm) imaged at top position between 52 to 94 m which may indicates presence of medium to coarse-grained dry sand (Figure 59b). Thin horizontal layer of resistivity 163 Ωm (medium-grained sand with gravels) observed at 4 m depth which was underlain by conductive layer (97 to 160 Ωm) at the bottom of the profile.

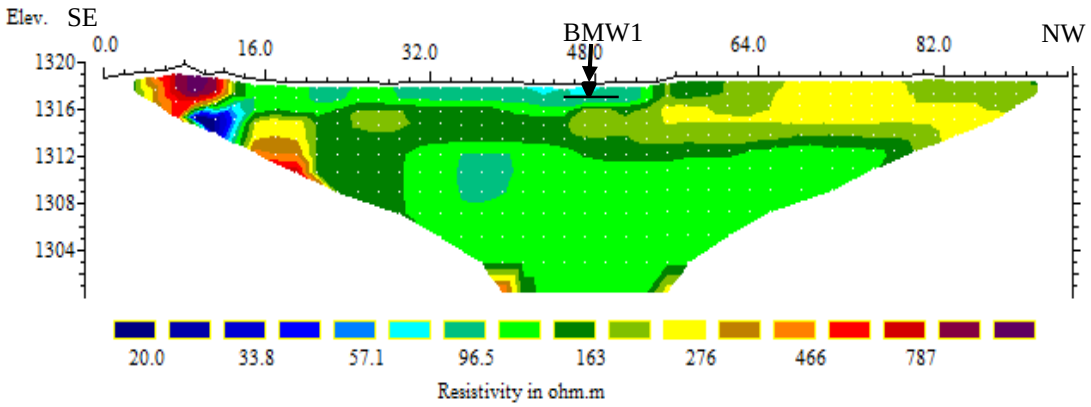

Figure 60: Resistivity model of Profile BMW1

The BMW1 has a very shallow well depth (2.2 m) with a 1.3 m water level depth. In the ERT profile (Figure 60), the resistivity within this depth at well location varied between 60 to around 130 Ωm. The resistivity of this range generally represents clayey sand or find sand which is capable to transmit water from river to aquifer or vice-versa.

ERT Profile 2 – BMW4:

This profile was situated in dry gravelly road and stretch 96 m along the right bank of the river covering about 20 m depth. It was stretched about 15 m East (electrode 24, 48 m of profile) from the Well No. BMW4. First electrode indicates upstream section of river. Solid waste and sewer disposal were dominating anthropogenic activities along this profile section (Figure 61).

Resistivity imaged along this profile section ranged from 20 to 163 Ωm and indicated two distinct horizontal layers (Figure 62). Bottom section below elevation 1278 m presented thick lower resistive layer (20 Ωm) reflecting fine-grained deposits of clay while top layer imaged as discontinuous patches of higher resistivity ranged above 34 to 163 Ωm. A distinct patch of high resistivity was imaged around 16 to 27 m profile position at elevation 1284 presenting deposits of fine-grained sand with less gravel which was embedded by lower resistive sandy clay and clayed sand with some gravel of fill sediments (Figure 62).

Figure 61: Photographs of BMW4 a) towards first electrode, upstream section and b) towards last electrode, downstream section

The BMW4 well has 4.6 m well depth with 2.2 m water level depth. Within this well depth in the ERT profile, lower resistivity varies between 20 and 50 Ωm is observed showing presence of fine sediments with lower permeability. Hence, in this case the infiltrating capacity through this layer may minimized. The anthropogenic activities as seen in the Figure 61b along this profile may has lower influences in the resistivity value. It indicates that lower scale solid disposal and sewer in the river channel does not directly effects on the resistivity of subsurface materials. If there exist such effects, the resistivity of the surficial layer may be reduced.

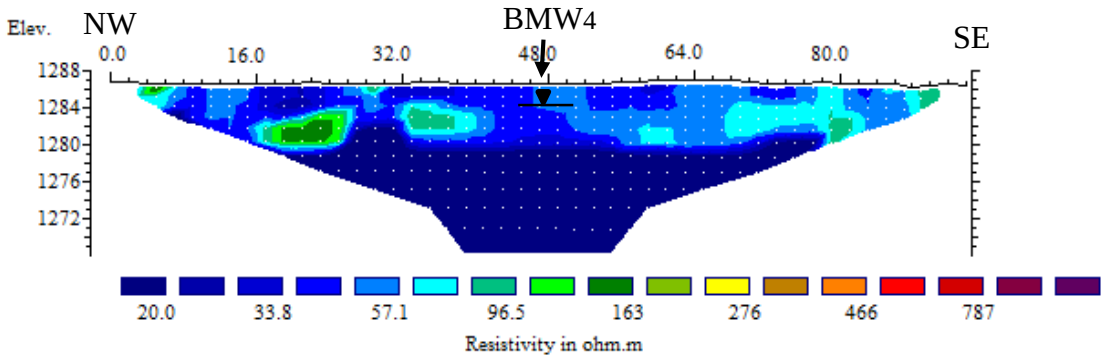

Figure 62: Resistivity model of BMW4

ERT Profile 3 – BMW5:

This profile was developed along the right bank of river channel, used as a park, and stretched upto 96 m. It was located 35 m SE from the Well No. BMW5. First electrode indicated upstream section of the river.

Three distinct layers of resistivity were imaged in this profile with value variation from 20 to 276 Ωm (Figure 63). Lower resistive of thick layer (20 Ωm) was observed at the bottom of the profile at elevation below 1279 m, indicates clay deposits. This layer was overlain by resistive layers of silt, sandy clay, clayey sand and fine-grained sand with gravel at top respectively (Figure 63 and Figure 64).

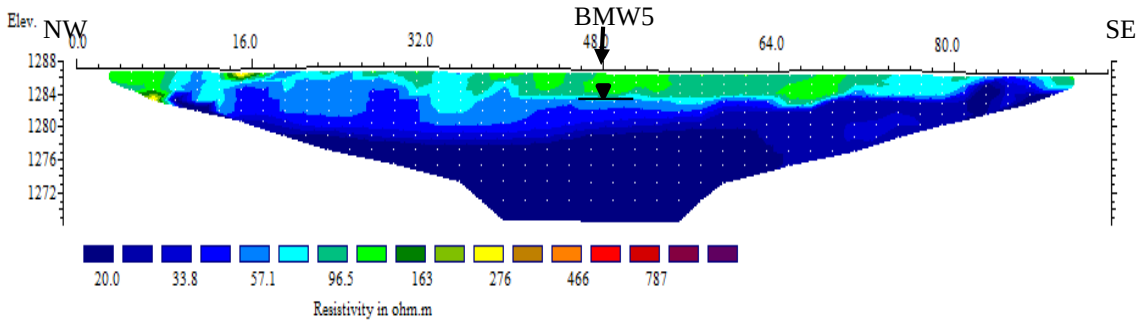

Figure 63: Resistivity model of BMW5

Figure 64: Photographs of BM profile a) towards first electrode, upstream and b) towards last electrode, downstream

ERT Profile 4 – BMW5A:

This profile was very short and stretch only for 15 m covering 3 m depth. Schlumberger array with 1 m electrode spacing was used. This profile stretched across the river channel and crosses ERT Profile 3 at 38 m and 8.5 m of this profile section respectively.

It was located 20 m NE from the Well No. BMW5. First electrode lies towards road section and last electrode towards river channel.

Thin undulating layers of different resistivity imaged in this profile section (Figure 65). Thin patch of higher resistivity (300-650 Ωm) observed towards SE direction at 9.5 to 12.5 m profile position representing gravelly sand which underlied thin layers of medium to coarse-grained sand and fine-grained sand. These sand layers were extended throughout the whole profile section. Discontinuous layer of lower ressistivity was ranged from around 14 to 75 Ωm imaged in between fine-grained sand at elevation 1287-1285 m reflecting fine deposits of clay, silt and sandy clay. The bottom section consisted of fine-grained sand with small patches of clayey sand. The overall profile showed fining towards center section.

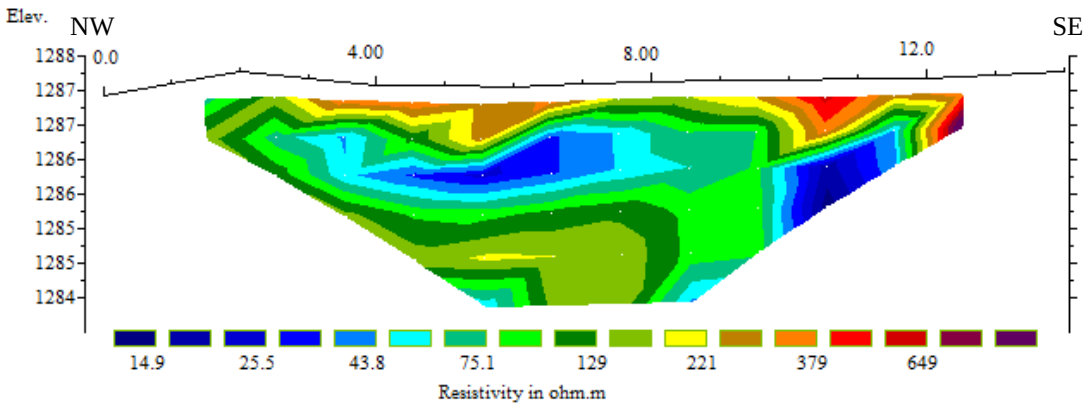

Figure 65: Resistivity model of BMW5A

ERT Profile 5 – BMW5B:

This profile section was situated on the right bank of river channel, on the gravelly road and stretched for 96 m (Figure 66) across river channel. It was 50 m South from Well No. BMW5. Electrode 1 was located 35 m away from river channel.

Resistivity imaged along this profile section ranged from 3 to about 900 Ωm and showed coarsening upward layers (Figure 67). Thick bottom section below elevation 1285 m had lower resistivity of 50 Ωm representing fine deposits of clay and silt. This layer overlaid by thin layers of sandy clay, clayey sand and fine-grained sand. Top layer indicated higher resistivity presenting medium to coarse-grained sand layer with patches of gravelly sand. The proportion of gravel increased at profile position 68 to 76 m in between elevation 1285 to 1281 m.

Figure 66: Photographs of BMW5B a) towards first electrode and b) towards last electrode

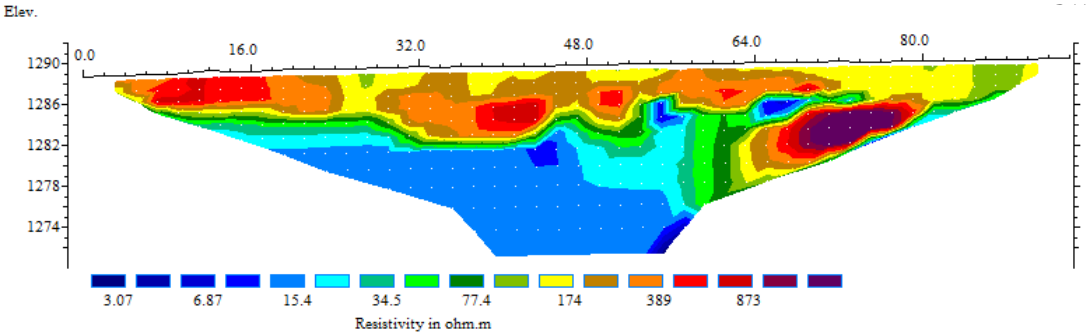

Figure 67: Resistivity model of BMW5B

Three profiles BMW5, BMW5A and BMW5B are located near to the well BMW5.The direction and distance of these profiles from the well BMW5 is presented in Figure 68. The BMW5 profile is stretched along the river channel while other two profiles BMW5A and BMW5B are stretched across the river channel. Due to presence of road and absence of open spaces for electrodes arrangement, the BMW5A and BMW5B is separately survey in different profiles.

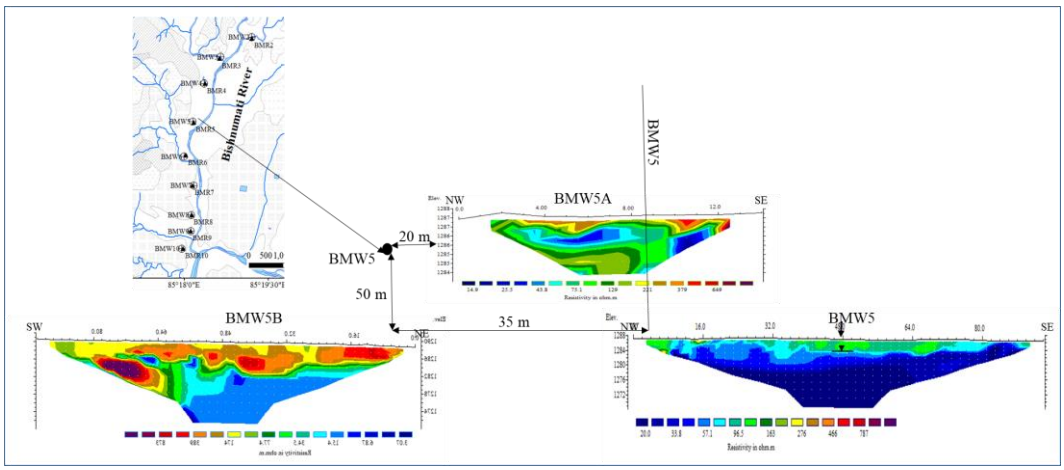

Figure 68: Relation of profiles BMW5, BMW5A and BMW5B with respect to well BMW5

The well BMW5 has 5.1 m well depth with 3.1 m water level depth. In Figure 68, it can be clearly observed that a high resistive layer is extended vertically (BMW5) and laterally (BMW5A and BMW5B) within this depth. This indicates that there is higher possibility of water transfer from river to aquifer or vice-versa.

ERT Profile 6 – BMW7:

This profile was situated at recently prepared park area located between left river channel and road (Figure 69). It was stretched for 96 m along river channel covering about 20 m depth. First electrode was located towards upstream section. This profile was about 100 m upstream from Well No. BMW7.

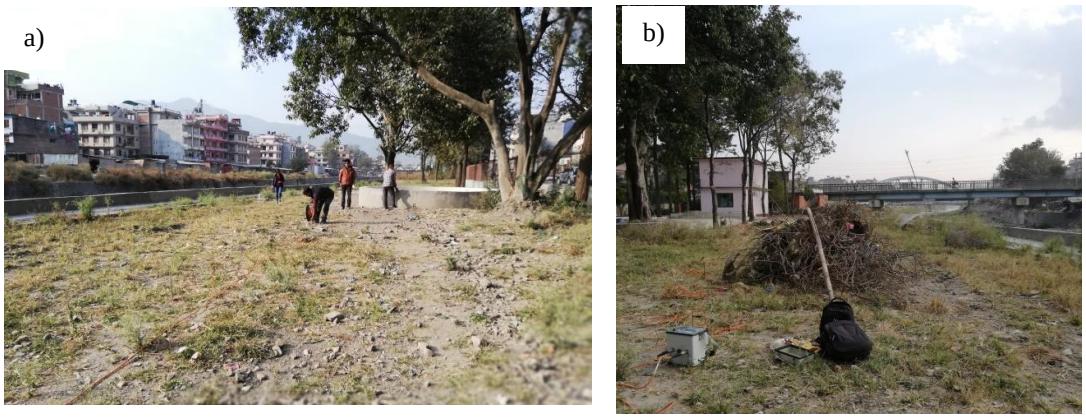

Figure 69: Photographs of BMW7 profile a) towards first electrode, upstream and b) towards downstream

Resistivity imaged along this profile showed lowest range as compared to upstream profile section with value variation from 1 to about 80 Ωm (Figure 70). As in other upstream profiles, this section had also thick bottom clay and silt layer presenting lowest resistivity (2 to 40 Ωm). The upper layer existing filled up materials composed of silt, sand and gravels (Figure 69) and indicated by resistivity of 40 to nearly 80 Ωm. Lower resistivity value range at top layer in this profile section may be indication of presence of organic material in the fill sediment.

The resistivity values from upstream section profiles BMW1 to the BMW7 of downstream section clearly presents decreasing trend towards downstream sections. In the previous 4.3 section, the chemical parameters as well as EC are increasing towards downstream. This indicates that the areas having higher chemical ions concentration with high EC possesses lower resistivity values.

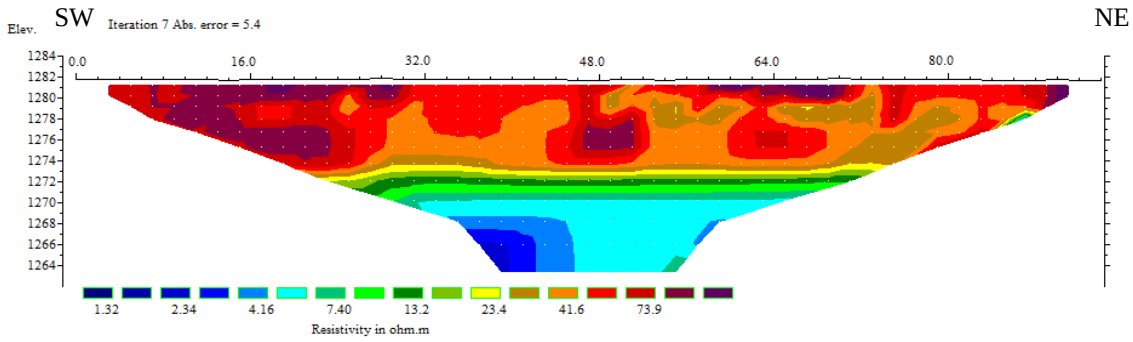

Figure 70: Resistivity model of BMW7

4.5.1.2 Manahara River

Only two profile line, one at upstream (MW3) and another at downstream section (MW10) was conducted in the Manahara River section.

ERT Profile 7-MW3

This profile located on left bank of the river channel at the cultivated land and stretched for 72 m covering 14 m depth along river channel (Figure 71). Total 36 electrodes with 2 m spacing were used with Wenner array. It was 10 m north from the well MW3. First electrode was located towards downstream section.

Figure 71: Photographs of MW3 profile a) towards first electrode, downstream and b) towards last electrode, upstream

Resistivity observed in this profile ranged from 40 to nearly 1500 Ωm showing coarsening upward layers within elevation 1304 to 1316 m (Figure 72). The overall profile section presented horizontal layers with different resistivity. Bottom layer had lower resistivity of 40 Ωm representing clay and silt which overlaid by thin layers of

sandy clay, clayey sand, fine-grained sand and medium to coarse-grained sand sequentially. These sequence was again overlaid by high resistive layers of gravelly sand (about 2 m thick) and sandy gravel (4 m thick) successively. The top layer within elevation 1316 to 1318 m presented resistivity variation from 187 to 521 Ωm showing fining upward section from gravelly sand to medium to coarse-grained sand at the surface.

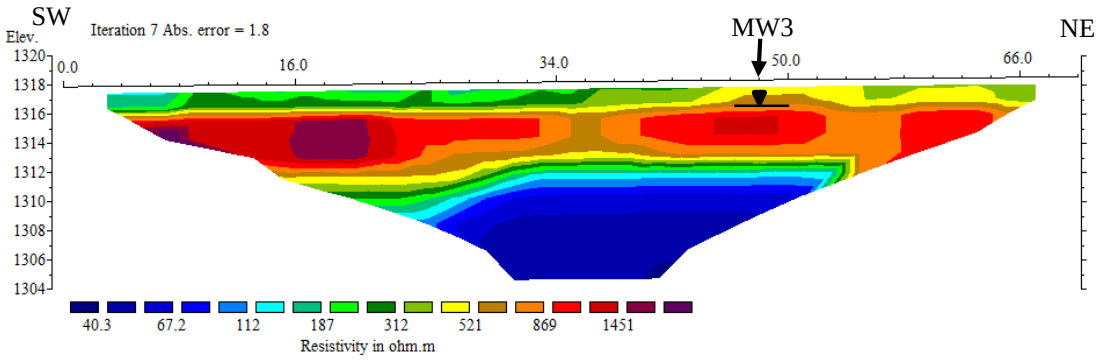

Figure 72: Resistivity model of MW3

The well close to this profile has 2.6 m water level depth. Within this depth, the BMW3 profile shows high resistive layers ranging from 521 to 869 Ωm. This value is indication of higher possibility of water transfer from river to aquifer if the water level in the river channel is greater than the water level in the well.

ERT Profile 8-MW10

This profile section was stretched for 96 m covering around 20 m depth along the river channel. The area where this profile prepared consisted of fill up materials (Figure 73). Schlumberger array with 2 m spacing was used. The first electrode lied towards upstream section. It was 21 m SW from the well MW10.

The profile section presented very low resistivity value ranged from 1.99 to aroun 150 Ωm (Figure 74). Thick bottom layer below elevation 1274m showed lower resistivity of 1.99 to 40 Ωm representing clay and silt layer. The silt layer of 38.2 Ωm value pinched out up to surface at profile position 60 to 64m. A small patch of clay deposit was also observed in between upper resistive layer of filled up materials containing clayey sand with silt and gravels. The well MW10 has 7.1 m well depth with 5 m water level depth. Within this depth, resistivity varies from 45 to 100 Ωm. This value generally indicates presence of clayey sand.

Figure 73: Photographs of MW10 profile a) towards first electrode, upstream and b) towards last electrode, downstream

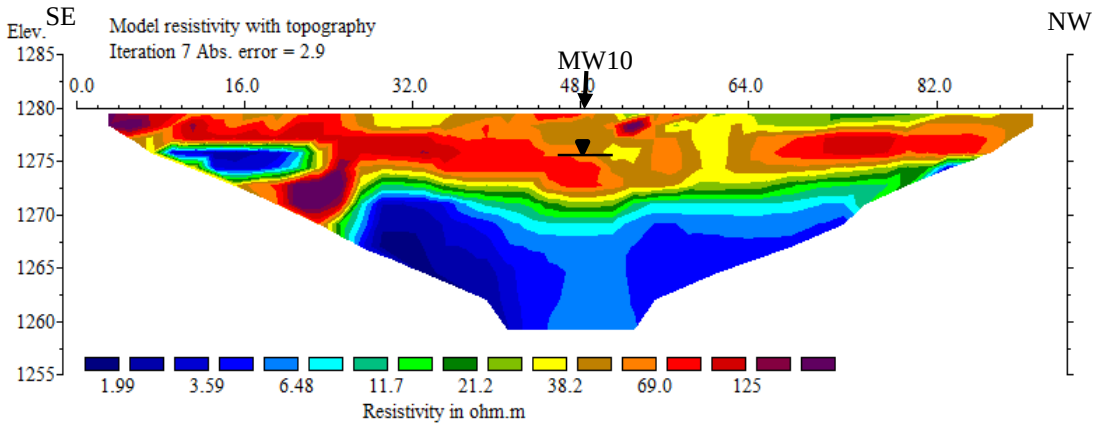

Figure 74: Resistivity model of profile MW10

4.5.1.3 Nakhu Khola

Total 4 profile lines were stretched in this river section. Wenner array with 2 m spacing was used in all profile lines. NW1 was profile line stretched at upstream section and NW6 at downstream section.

ERT Profile 9-NW1

This profile was located at cultivated land along river channel and stretched for 94 m covering about 20 m depth (Figure 75). It was 2.5 m NW from well NW1. The first electrode was located towards downstream section. In this profile, 4 electrodes were skipped due to occurrence of some problems. The information of upstream section towards SW was lost due to skipped electrodes.

Resistivity imaged in this section ranged from 7.85 to around 700 Ωm showing increasing towards upper surface part **(**Figure 76**).** Thick bottom layer presenting resistivity from 7.85 to 50 Ωm consisted of clay and silt deposit which was overlaid by sandy clay and clayey sand sequentially**.** A small patch of medium to coarse-grained sand with resistivity of 193 to around 250 Ωm imaged at profile position of 20 to 24 m. Similarly, resistive small patch with greater than 365 Ωm observed at position of 58 to 60 m representing deposit of gravelly sand.

The NW1 well has a very shallow well depth and water level depth at 0.2 m. The surficial material is composed of saturated clay (Figure 75) and thus the vertical resistivity value varied from only 30 to 53.5 (Figure 76) within this depth.

Figure 75: Profile NW1 with well and river location

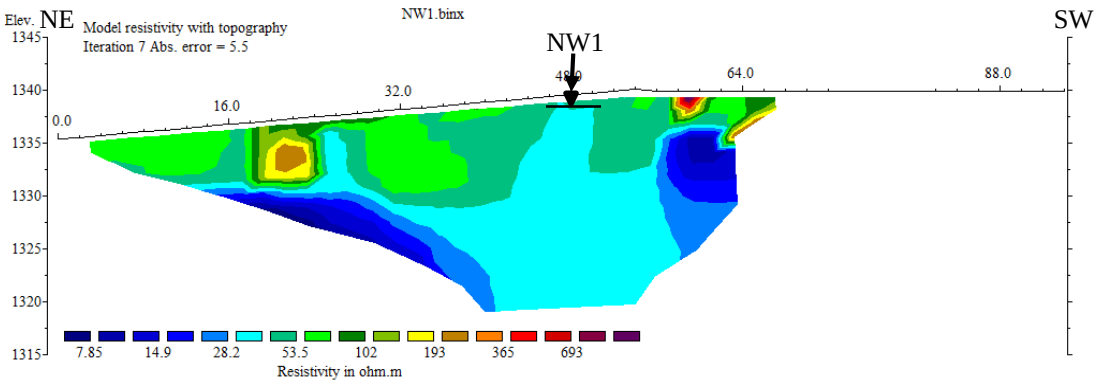

Figure 76: Resistivity model of profile NW1

ERT Profile 10-NW2

This profile line was also situated at the cultivated land at right bank of river channel. It was stretched along river channel for 70 m covering 14 m depth. It was situated 6 m NW from well NW2 (Figure 77). NW2 has a 4.8 m well depth with 1.8 m water level depth. First electrode placed towards downstream section.

Figure 77: Profile NW2 with well

Resistivity observed in this section varied from 12.4 to around 250 Ωm showing increasing value towards top part (Figure 78). As in other section, it had also thick bottom clay and silt deposit which was overlaid by sandy clay and clayey sand successively. High resistive layer greater than 150 Ωm noticed within 32 to 46 m profile position indicated presence of medium to coarse sand with gravels. A small upper section towards north at profile position 3 to 7 m imaged as fine-grained sand.

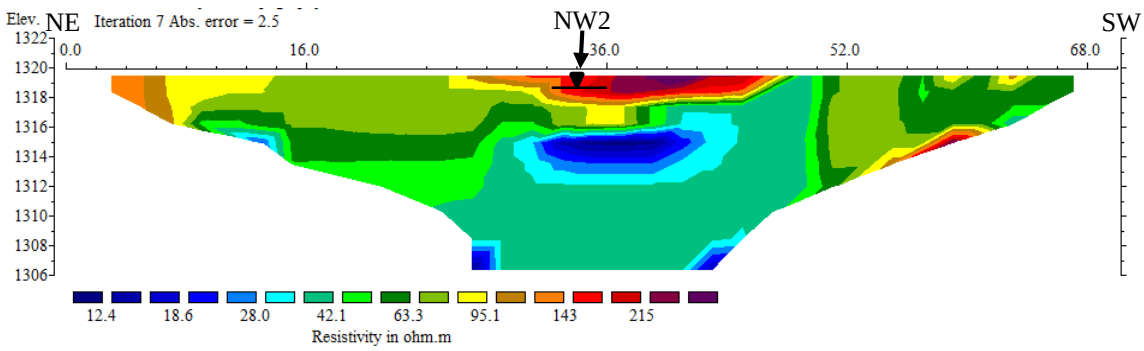

Figure 78: Resistivity model of profile NW2

ERT profile 11-NW3

The NW3 profile situated at right bank of the river channel stretching for 96 m with 20 m depth. The area consisted of fill up materials. It was stretched 9 m NW from well NW3 (Figure 79) which has 3.7 m well depth along with 1.1 m water level depth. First electrode placed towards downstream section skipping two electrodes.

The resistivity value ranged from 5.7 to around 250 Ωm indicating increasing towards top surface (Figure 80). About 15 m thick clay and silt layer with resistivity up to 50 Ωm observed at the bottom presenting clay dominancy towards NW section at profile position 72 to 80 m. Thin layers of sandy clay, clayey sand and fine-grained sand successively overlaid this bottom layer. Top layer consisted of filled up materials containing medium to coarse-grained sand with gravels presenting resistivity greater than 120 Ωm.

Figure 79: NW3 profile a) well location with profile line and b) surficial material

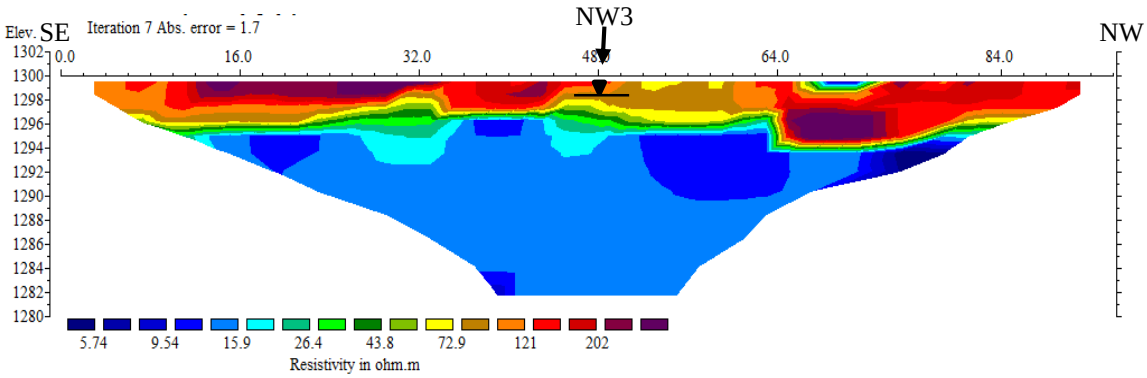

Figure 80: Resistivity model of NW3

ERT profile 12-NW6

This profile section was located at open grass land and stretched 70 m across river channel covering 14 m depth (Figure 81). It was 3 m NE from well NW6. This well is 2.7 m deep with 2.4 m water level depth. Last electrode placed towards river channel.

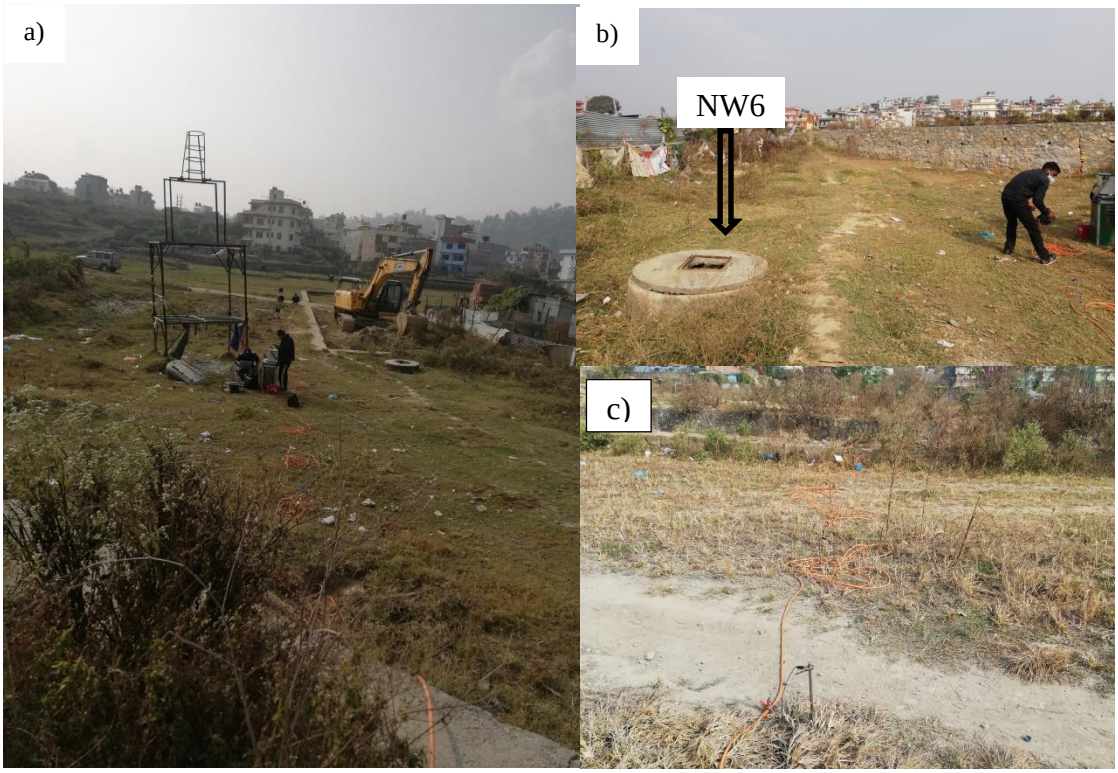

Figure 81: NW6 profile line a) towards first electrode, b) towards last electrode and c) filled up material towards river channel

Resistivity imaged in this profile ranged from 4 to around 500 Ωm (Figure 82). Clay and silt deposits were dominant lithology of this section covering about 11 m thickness. Clay was basically observed at the bottom section. Thin layers of sandy clay and clayey sand sequentially overlaid clay and silt deposits. High resistive layer noticed towards river channel at 57 to 62 m profile position represented filled up material (Figure 81c).

4.5.2 Comparison of resistivity values among rivers

The resistivity value range and general lithology in river corridors are presented in Table 21. Thick lower resistive layers are commonly observed in all profiles except in BMW1. However, the elevation of upper surface of this layer is different. Highest elevation of around 1332 m is existed in the upstream profile NW1 and lowest elevation of around 1275 m occurs in the downstream profile MW10. Profiles from the Bishnumati River exhibits tentative similar elevation of 1284 m. Generally, clay possess low resistivity. Thus these thick layers with low resistivity is termed as clay and silt in this study.

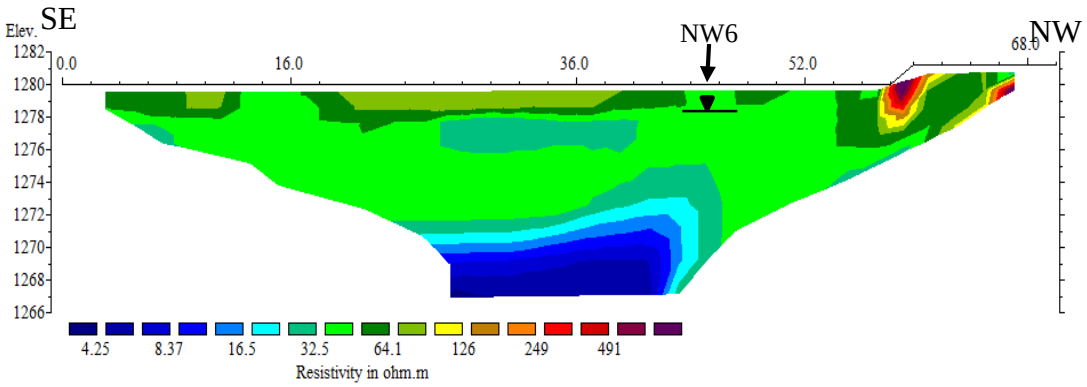

Figure 82: Resistivity model of NW6

Among three rivers, the narrow resistivity range is measured from the Nakhu khola and the wide range in the Manahara River. The resistivity value varied from 1.32 to 1500 Ωm. The lowest resistivity value is obtained from downstream profile BMW7 of the Bishnumati River while the highest value was measured from upstream profile MW3 of the Manahara River.

In overall rivers, resistivity decreases towards downstream section. This result indicates two possibilities: 1) the grain size decreases towards downstream and 2) dominating of chemical ions with higher conductivity towards downstream. Figure 27 and bar diagrams of each rivers in previous section also presented higher conductivity and chemical ion concentration respectively towards downstream section. This variations in chemical, conductivity and resistivity along these corridors clearly indicates the increased in contamination load towards urban core areas. The resistivity values is also tried to compare laterally in those profile which was stretched across the river channel (BMW1, BMW5A, BMW5B and NW6). In these profiles, there is slightly lateral variation. But this variation may occur due to lateral grain size variation instead of contamination load variation as presented by Gautam *et al*. (2013) and Maharjan (2018).

The upper layer of BMW4, BMW5B, BMW7, MW10 and NW3 consist of filled up materials as these profiles were located at gravelly road or recently prepared park at river banks. However, these layers exhibited different range of resistivity value depending on moisture content or clay and organic material presented in filled up material (Uhleman *et al*., 2017). The lowest value range is observed (1.32 to nearly 80 Ωm) in downstream profile section from the Bishnumati River (BMW7). The drastic decrease in resistivity values may indicate presence of organic material in the filled up material (Figure 70).

Based on general lithology modified from the JICA, subsurface material categorizes from clay to sandy gravel. During the ERT survey, sediment size patterns along the profiles was also observed. Based on these observations, resistivity can be correlated with lithology. However it is not sufficient to verify, but can be used to define general lithology. For example, the ERT profile BMW1 possess a high resistive layer towards the river channel (Figure 60) and the Figure 79a shows deposits of gravelly sand in this high resistive area. Similarly, MW3, the upstream ERT profile of the Manahara River also presents resistive layer at top of the surface (Figure 72) and Figure 83b represents the sediment size of gravelly sand and medium to coarse-grained sand.

Figure 83: Sediment size variation on a) BMW1 and b) MW3

Table 21: Resistivity value range and observed lithology in different river corridors

River Name	Resistivity value range (Ωm)	Observed lithology
Bishnumati	Max- 900 Min- 1.32	Clay and silt, sandy clay, clayey sand, fine to coarse sand, gravelly sand, filled up material
Manahara	Max- 1500 Min- 1.99	Clay and silt, sandy clay, clayey sand, fine to coarse sand, gravelly sand, sandy gravel, filled up material
Nakhu	Max- 700 Min- 4.25	Clay and silt, sandy clay, clayey sand, fine to coarse sand, gravelly sand, filled up material

4.6 River wise interconnection condition between groundwater and river water

Isotopic composition is a reliable source to identify recharge sources of groundwater, while the concentration of Na^+ and Cl^- can be used as an indicator of the presence of contamination through increased urbanization (Yang *et al*, 2012). Thus, for Hierarchical Cluster Analysis (HCA), isotope (δD and $\delta^{18}O$) and chemical (Na^+ and Cl^-) parameters

are used as major factors to identify the similarity or interconnection between groundwater and river water (Liu and Yamanaka, 2012; Mohammed *et al*., 2016). HCA is performed separately for each river as well as for both wet and dry season analysis data to recognize river-wise and temporal changes in interconnection conditions.

This study is unable to measure the water stage in the river channel. Thus, the water exchange process is analyzed by comparative values of isotopes and chemical concentration in the river and groundwater. These parameters are used in most the similar research (Xianfang *et.al.,* 2006; Yang *et. al.*, 2012; Ali and Ajeena, 2016; Li *et. al.,* 2016; Zhang *et.al.*, 2016).

4.6.1 Bishnumati River

4.6.1.1 Clustering of river water and groundwater

All 20 and 17 water samples from river water and groundwater of wet and dry seasons respectively are performed separately to HCA. In the wet season, two clusters namely A, and B are observed in the dendrogram (Figure 84a). Both Cluster A and B are composed to two subgroups A1 and A2; and B1 and B2 respectively. Cluster A1 consist of two dug well site (BMW2 and BMW6) with all river sites whereas Clusters A2, B1 and B2 enclose entirely groundwater locations (Figure 84a) indicating the presence of different isotopic composition; and Na^+ and Cl^- concentration compared to that of river water (Guggenmos *et al*., 2011).

Two major clusters C and D are categorized from the dendrogram of the dry season (Figure 84b). Both clusters contain a combination of river and groundwater sites indicating similarity in selected parameters (Shrestha and Kazama, 2007; Zhong *et al*., 2018). Cluster C has two subgroups C1 and C2. Four river sites and one groundwater (BMW9) site are enclosed in cluster C1. Similarly, four river sites and two groundwater sites (BMW5 and BMW7) are grouped in cluster C2. Concentrations of Na^+ and Cl^- within these two clusters are widely variable indicating the presence of most contaminated water samples within Cluster C1. These three groundwater samples which are clustered with river water in cluster C are located in the middle and downstream sections of the river. But in the case of Cluster D, it has also two subgroups D1 and D2. Cluster D1 grouped only two groundwater sites whereas D2 has a combination of three groundwater sites and one river site (BMR1). Clusters having a combination of river

water and groundwater, Cluster A1 from the wet season (Figure 84a) and Cluster C and D2 from the dry season (Figure 84b) show similarity in selected parameters indicating interconnection between two water systems (Menció and Mas-Pla, 2008; Guggenmos *et al*., 2011; Huang and Han, 2016).

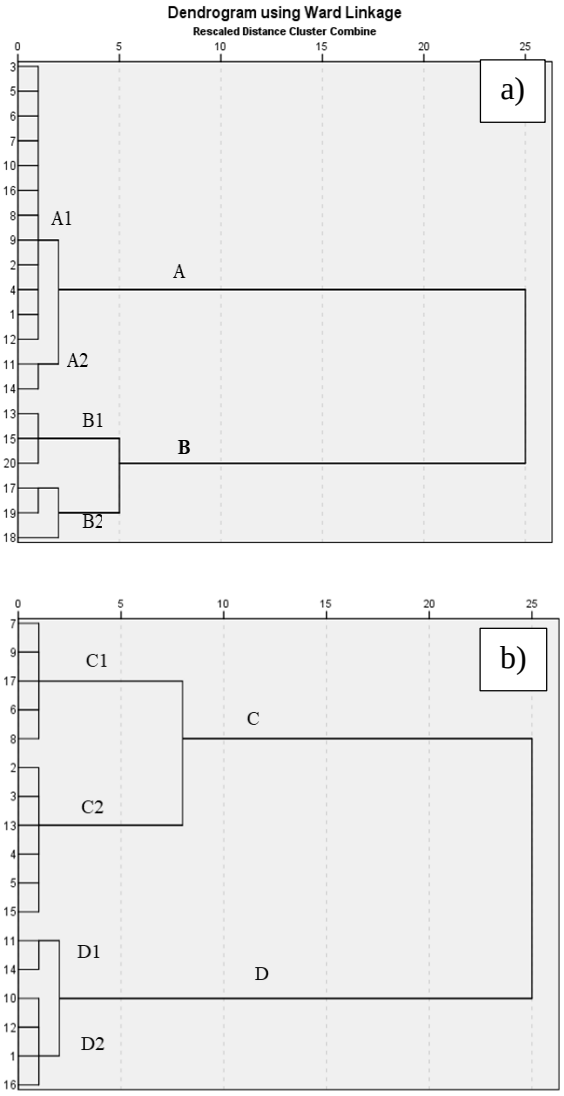

c)

Sample ID	Cluster No.	Sample ID	Cluster No.
BMR1	1	BMW1	11
BMR2	2	BMW2	12
BMR3	3	BMW3	13
BMR4	4	BMW4	14
BMR5	5	BMW5	15
BMR6	6	BMW6	16
BMR7	7	BMW7	17
BMR8	8	BMW8	18
BMR9	9	BMW9	19
BMR10	10	BMW10	20

d)

Sample ID	Cluster No.	Sample ID	Cluster No.
BMR1	1	BMW1	10
BMR2	2	BMW2	11
BMR3	3	BMW4	12
BMR4	4	BMW5	13
BMR5	5	BMW6	14
BMR6	6	BMW7	15
BMR7	7	BMW8	16
BMR8	8	BMW9	17
BMR9	9		

Figure 84: Dendrogram based on hierarchical clustering in a) wet season b) dry season and c) and d) relation of BMW and BMR with cluster number in wet and dry season respectively

4.6.1.2 Identifying areas of river water and groundwater interconnection

Results from hierarchical cluster analysis imply interconnection between river water and groundwater in both wet and dry seasons. Cluster A1 from the wet season combines all river water with two groundwater (BMW2 and BMW6) showing a similar water type as Ca-HCO_3. Well depths of these two groundwater sites are more or less the same (4.2 and 4.8m, Table 9) with diluted concentration of Na^+ and Cl^- in the wet season (Figure

31). Both wells are located in the settlement area and are used for domestic purposes. However, BMW2 and BMW6 are two groundwater sites which are grouped with all river sites in Cluster A1, BMR2 and BMR6 are the closest sites from these groundwater sites respectively (20 to 50 m away, Figure 30). Meanwhile, BMW2 is the site which has the lightest isotopic composition among all water samples (Figure 48a) with shallow water level depth (0.4 m). Field visit evidence confirms that this water level depth is above the water level in the river Na^+ and Cl^- channel at the BMR2. Thus it indicates that BMW2 can be a source of river discharge in the wet season. At the same time, lighter isotopic composition and diluted chemical ions are indicative of direct rainfall infiltration as a mechanism of recharge BMW2 during the wet season. Likewise, BMW6 has a water level depth of 1.4 m with drastic dilution on Na^+ and Cl^- (Figure 31). The isotopic composition of BMR6 is slightly lighter than that of BMW6 showing a narrow range (-7.7 to 8.0‰ for $\delta^{18}O$ and 50.7 to 53.1‰ for δD) presents a higher possibility of groundwater recharge at BMW6 from nearby BMR6 during in the wet season. Mall *et al* (2015) also present a similar type of interconnection in the northern part of the Bishnumati River for the wet season.

In the dry season, sampling sites grouped in three clusters C1, C2 and D2 indicate the presence of interconnection (Figure 84b). In Cluster C1, one dug well BMW9 is grouped with four river sites from BMR6 to BMR9. However, BMW9 grouped with these four river sites, BMR9 is the closest one (only 25 m away). The BMW9 has a higher water level depth (6.1) and is located at the downstream section of the river with higher concentrations of Na^+ (98.6 mg/L) and Cl^- (133.1 mg/L). The dug well location and its higher water level depth indicate that BMW9 cannot be a source for river discharge and thus suggest all these river sites, basically BMR9 a recharge source for BMW9. Similarly, Cluster C2 encloses two dug wells BMW5 and BMW7 with four river sites from BMR2 to BMR5. Alike in Cluster C1, BMW5 is nearest to BMR5 (40 m away). Two dug wells BMW5 and BMW7 have the same water level depth (3.1 m) and are located at settlement areas of the downstream section as compared to the river sites (Figure 30) indicating river water is a major source for these dug well recharge, especially BMR5. In the same way, Cluster D2 combine one river site BMR1 with three downstream dug wells BMW1, BMW4 and BMW8, among which BMW1 is the nearest to BMR1 (30 m). This cluster also shows river water as a recharge source for these three dug well during the dry season.

The connection condition of BMW1 and BMW5 can also be discussed with the help of resistivity variation observed on the ERT profile lines. The BMW1 and BMW5 wells have a shallow well depths of 2.2 and 5.1 m with water level depths of 1.3 and 3.1 m respectively. The resistivity range observed within these well depths at these two locations on ERT profiles is nearly similar with value variation of 100 to 163 Ωm (Figure 57 and Figure 63). According to the resistivity range modified from the JICA (1990), these resistivities are higher than the range of clay and silt. Thus it can be considered a permeable layer which can transmit water to the well through bank infiltration. The sediment distribution pattern map presented in Figure 12 also verifies the high possibility of water transmission from the top surface at BMW1, as it consists of coarse-grained material (muddy sand) at the top surficial part.

But in the case of BMW4, it has a 4.6 m well depth with a 2.2 m water level depth. The resistivity range within this depth at the well location shows low-value range from 40 to 57 Ωm (Figure 62). This value range can be considered as a clay and silt layer from which water is difficult to transmit through bank infiltration. The grouping in separate clusters of samples BMW4 and BMR4, which are only 15 m apart, also signifies the presence of such lower permeable layer in-between these two locations. However, there is the presence of interconnection between rivers and groundwater in three clusters from the dry season, the concentrations range of Na^+ and Cl^- are different. Cluster D2 has lowest value of Na^+ (10.8 – 19.3 mg/L) and Cl^- (12.2–27.5 mg/L) whereas Cluster C1 has highest value of Na^+ (91.7–108.2 mg/L) and Cl^- (107.8–133.1 mg/L). This result clearly shows that low flow highly contaminated river water recharges all groundwater, except BMW2 and BMW6 in the dry season, polluting nearby shallow groundwater.

4.6.2 Dhobi Khola

4.6.2.1 Clustering of river water and groundwater

Total of 21 and 19 samples of river water and groundwater collected from the wet and dry seasons respectively are performed separately for HCA. Four clusters namely A, B, C and D (D1 and D2 sub-clusters) are formed in the dendrogram during the wet season (Figure 81a). Cluster A and C completely encloses groundwater sites while sub-cluster D1 entirely includes water samples of river sites. Two upstream groundwater sites (DW1 and DW2) with lower Na^+ (10.5 to 13.5 mg/L) and Cl^- (6.5 to 8.0 mg/L) concentrations are grouped in Cluster C. Similarly, four downstream groundwater sites

(DW6 to DW8, DW10) having highest Na^+ (23.6 to 31.6 mg/L) and Cl^- (31.1 to 42.8 mg/L) concentration are grouped in the Cluster A. While in sub Cluster D1, it encloses five river sites (DR3 to DR7) which are located in the middle section of the river channel (Figure 32) with a medium concentrations of Na^+ (9.7 to 15.5 mg/L) and Cl^- (6.1 to 13.8 mg/L). Contrarily, two clusters B and D2 enclose combined water samples from river and groundwater sites. Upstream two river sites DR1 and DR2 are grouped with upstream groundwater sites DT1 and DW3 in the sub Cluster D2 whereas downstream river sites (DR8 to DR10) are combined with three groundwater sites (DW4, DW5 and DW9) in Cluster B (Figure 46). The water samples grouped in the sub Cluster D2 show lowest concentration of Na^+ (4.0 to 6.4 mg/L) and Cl^- (0.5 to 3.2 mg/L).

In the dry season, three major clusters E, F and G are categorized from the dendogram (Figure 81b) wherein Cluster F has two subclusters F1 and F2. Clusters E and subcluster F2 contains combined samples from river and groundwater sites. Two river sites (DR1 and DR2) comprising the lowest concentration of Na^+ (21.1–30.0 mg/L) and Cl^- (21.7–34.3 mg/L) are grouped with five groundwater sites (DW1, DT1, DW2, DW4 and DW6) in Cluster E. Similarly, Cluster F2 encloses river sites DR4 and DR7 with one groundwater site DW10 of Na-K-HCO_3. However, only groundwater sites are grouped in the Clusters F1 (DW5, DW7 to DW9) and downstream river sites in Cluster G (DR5, DR6, DR8 to DR10). River sites enclose in Cluster G have highest concentration of Na^+ (81.1–105.4 mg/L) and Cl^- (96.0–127.0 mg/L) among all river and groundwater sites indicating a more contaminated sections of the Dhobi Khola. Absence of cluster combining these downstream river sites and dug well sites indicate the presence of a clogging layer at the river channel and beds which may create a restriction for water infiltration and exfiltration.

4.6.2.2 Identifying areas of river water and groundwater interconnection

Combining water samples from river and groundwater sites in clusters of both the wet and dry seasons signifies the interconnection of river and groundwater along the Dhobi Khola. Cluster B from the wet season combine three downstream river sites DR8, DR9 and DR10; and three dug well sites DW4, DW5 and DW9. Water samples from all these sites are categorized as Ca-HCO_3 type. DW4 and DW5 are located at the upstream section of the river as compared to other sites indicating a higher possibility of downstream river recharge through these two dug wells. But in the case of DW9, it is

located at the settlement area of the downstream section (Bijuli Bazar) nearby DR9 (40 m). It has a very shallow water level depth (0.1m) and has a slightly heavier isotopic composition as compared to the dry season which suggests that DW9 has a higher tendency to recharge nearby river sites (DR9) and downstream rivers (DR10).

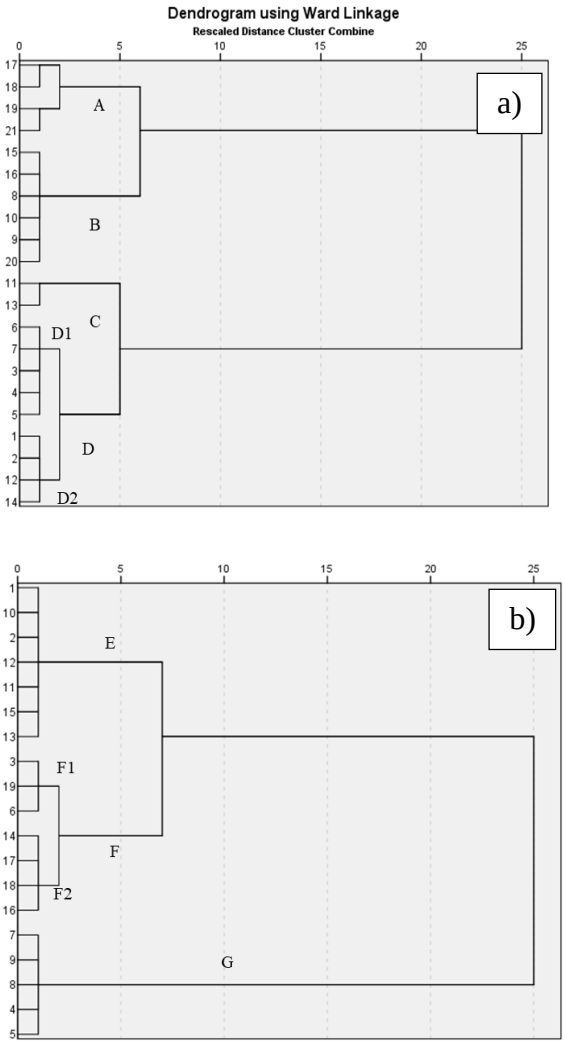

c)

Sample Id	Cluster No.	Sample Id	Cluster No.
DR1	1	DW1	11
DR2	2	DT1	12
DR3	3	DW2	13
DR4	4	DW3	14
DR5	5	DW4	15
DR6	6	DW5	16
DR7	7	DW6	17
DR8	8	DW7	18
DR9	9	DW8	19
DR10	10	DW9	20
		DW10	21

d)

Sample Id	Cluster No.	Sample Id	Cluster No.
DR1	1	DW1	10
DR2	2	DT1	11
DR4	3	DW2	12
DR5	4	DW4	13
DR6	5	DW5	14
DR7	6	DW6	15
DR8	7	DW7	16
DR9	8	DW8	17
DR10	9	DW9	18
		DW10	19

Figure 85: Dendrogram based on hierarchical clustering in a) wet season b) dry season and c) and d) relation of DW and DR with cluster number in wet and dry season respectively

Similarly, Cluster D2 groups two upstream river sites DR1 and DR2 with one shallow tube well DT1 and one dug well DT3. DT1 is very close to the river channel (10 m) and just located downstream of DR1 but upstream of DR2. As it is a tube well, water level depth cannot be measured but having a similar isotopic composition and chemical concentration of Na^+ and Cl^- as with DR1 (Appendix 4B and 5B) suggests the probability of groundwater recharge through DR1. However, in the case of DW3, it is located at the downstream section as compared to DR1 and DR2 (Figure 32) with having water level depth of 2 m indicating the possibility of recharge through upstream DR1

and DR2. The lightest isotopic composition and lowest chemical concentration of DW3 as compared to whole sampling sites; and the totally dried up DW3 during the dry season are suggestive of combined recharge from direct rainfall infiltration as well as from bank/bed infiltration through river water.

Alike in the wet season, two clusters E and F1 combine water samples from the river and groundwater sites during the dry season. Cluster E encloses two upstream river sites DR1 and DR2 together with four dug well sites DW1, DW2, DW4, DW6 and one shallow tube well DT1. Among these sampling sites, DW1 and DT1 are located at the uppermost section of the river and close to DR1 (Figure 32). DW1 has a shallow water level depth (1.5 m) and has a 2.09‰ lighter isotopic composition as compared to the wet season. Further, it plots near GMWL (Figure 46b) suggesting dry season rainfall as one of the major recharge sources of DW1 and has a higher possibility of groundwater exfiltration to nearby river site DR1. In the case of DT1, it has much lower chemical concentration of Na^+ and Cl^- but has more or less similar isotopic composition as that of DR1 supporting for the possibility of recharge through river water infiltration from DR1. Similarly, dug well site DW2 are located just downstream of DR1 and nearby to DR2 (10 m). Similar isotopic composition and chemical concentration of Na^+ and Cl^- to that of DR2; having deeper water level depth (4 m) than river level help to suggest groundwater recharge through bank infiltration at DR2. However, DW4 and DW6 are located downstream of DR1 and DR2 and plot near GMWL with lighter isotopic composition indicating upstream river water as well as dry season rainfall as a source of groundwater recharge.

Likewise, Cluster F also combines two river sites (DR4 and DR7) and one dug well DW10 of Na-K-HCO_3 water type. Existence of river sites at the upstream section as compared to DW10 (Figure 32) signify the possibility of groundwater recharge through upstream river water. Further, the plotting of DW10 near GMWL (Figure 46) supports dry season rainfall as an additional recharge source for this dug well.

4.6.3 Bagmati River

4.6.3.1 Clustering of river water and groundwater

Total of 22 and 23 samples of river water and groundwater collected from the wet season and dry season respectively are performed separately for HCA. In the wet

season, three distinct clusters namely A, B and C are observed in the dendrogram (Figure 82a). Cluster A has two subclusters as A1 and A2. Clusters of A2, and C entirely contain samples from groundwater locations. Mostly, downstream groundwater sites (BW6, BW8 to BW10) with higher Na^+ (20.6 to 30.7mg/L) and Cl^- (22.3 to 35.9 mg/L) concentrations are grouped in Cluster C while upstream groundwater sites (BW3, BW5, BT1 and BT2) with lower Na^+ and Cl^- concentration are enclosed in Cluster A2. Contrarily, clusters A1 and B enclose combined samples from river and groundwater sites. Almost all upstream river sites (BR1 to BR7) are grouped with three groundwater sites (BW1, BW2 and BW7) in Cluster A1 while downstream river sites (BR8 to BR10) are gathered with one groundwater site (BW4) in Cluster B indicating similarity in selected parameters during wet season.

Alike in the wet season, water samples of dry season are also divided into three clusters D, E and F (Figure 82b). Clusters D and F contain combined samples from river and groundwater sites while Cluster E encloses only three river sites (BR7, BR8 and BR10) which have the highest Na^+ and Cl^- concentrations (Appendix 4C). Cluster D encloses mostly an upstream section of river and groundwater sites and shows the lowest concentration of Na^+ and Cl^-. But in the case of Cluster F, it has two subgroups, F1 and F2 which combine a mixture of samples from the middle and downstream sections. Na^+ and Cl^- concentration of Cluster F2 are higher than clusters D and F1 but much lower as compared to Cluster E.

4.6.3.2 Identifying areas of river water and groundwater interconnection

The presence of combined water samples in clusters indicates the interconnection of river and groundwater in the Bagmati River in both the wet and dry seasons. Cluster B from the wet season contains three river sites (BR8 to BR10) and one groundwater site (BW4) of similar water type Ca-HCO_3. BW4 is located at the upstream section as compared with grouped river sites (Figure 34) and has a very shallow water level depth (0.6 m) indicating a higher possibility of groundwater discharge into downstream river sites. Similarly, Cluster A includes seven river sites (BR1 to BR7) with three groundwater sites (BW1, BW2 and BW7). Two groundwater sites (BW1 and BW2) are located at cultivated land of the uppermost section whereas BW7 is located in the river riparian zone and is very close to the river channel (10 m). Water level depth is 1.8, 2.4 and 2.8 m in BW1, BW2 and BW7 respectively. However these three groundwater sites

are grouped with seven river sites, BR1, BR2 and BR7 are the closest river sites to BW1 (80 m), BW2 (40 m) and BW7 (10 m) respectively. All these three groundwater sites have a lighter isotopic composition with drastic dilution of Na^+ and Cl^- concentration in the wet season which suggests possible recharge of groundwater from nearby river sites.

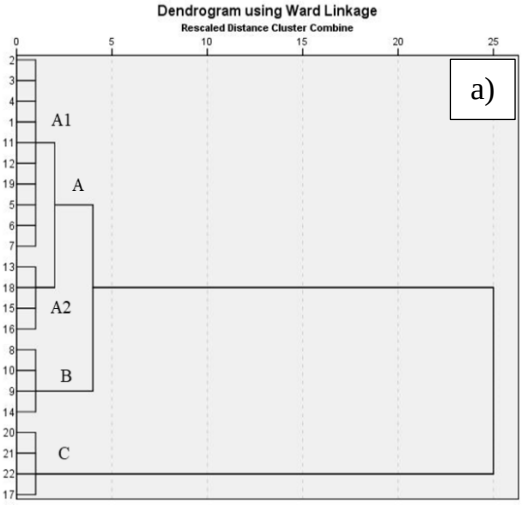

c)

Sample ID	Cluster no.	Sample ID	Cluster no.
BR1	1	BW2	12
BR2	2	BW3	13
BR3	3	BW4	14
BR4	4	BT1	15
BR5	5	BW5	16
BR6	6	BW6	17
BR7	7	BT2	18
BR8	8	BW7	19
BR9	9	BW8	20
BR10	10	BW9	21
BW1	11	BW10	22

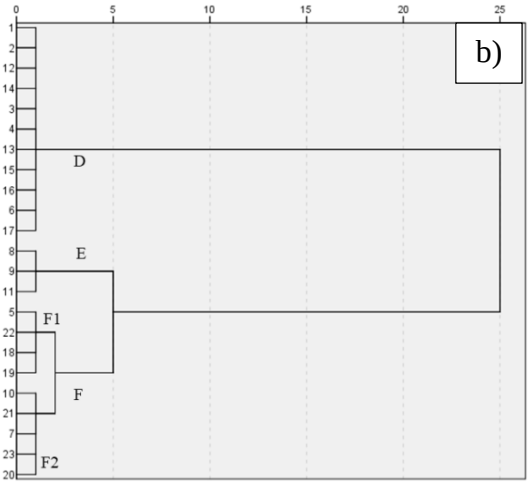

d)

Sample ID	Cluster no.	Sample ID	Cluster no.
BR1	1	BW2	13
BR2	2	BW3	14
BR3	3	BT1	15
BTR1	4	BW4	16
BR4	5	BW5	17
BR5	6	BW6	18
BR6	7	BT2	19
BR7	8	BW7	20
BR8	9	BW8	21
BR9	10	BW9	22
BR10	11	BW10	23
BW1	12		

Figure 86: Dendrogram based on hierarchical clustering in a) wet season b) dry season and c) and d) relation of BW and BR with cluster number in wet and dry season respectively

In the dry season, water samples from five river sites (BR1 to BR3, BT1R & BR5) are grouped with samples of five dug wells (BW1 to BW3, BW4 & BW5) and one shallow tube well (BT1W) in Cluster D. Except BW4, groundwater sites of BW1, BW2, BW3, BT1W and BW5 are close to river sites of BR1 (80 m), BR2 (40 m), BR3 (20 m), BT1R (30 m) and BR5 (5m) respectively. Similar isotopic composition and chemical concentration of Na^+ and Cl^- with drastic increment in these concentrations observed at BR2 & BW2; BT1R & BT1W; and BR5 & BW5 suggests possible recharge of these

groundwaters from the nearby river water. Similar chemical concentration with different isotopic composition at BW1 implies the possibility of other recharge sources besides river water. But in the case of BW3, it has a lower chemical concentration with more or less similar isotopic composition. The water level depth is 4.74 m which may be at a higher elevation as compared with the water stage in the river channel at the time of the field survey. This result reveals that BW3 can recharge river water at BR3.

Similarly, Cluster F also combines water samples from rivers and groundwater. One river site BR4 grouped with three groundwater sites (BW6, BT2 & BW9) in sub-cluster F1 whereas two river sites (BR6 & BR9) grouped with three groundwater sites (BW7, BW8 & BW10) in sub-cluster F2. When comparing sites of overall Cluster F, two river sites BR4 and BR6 are located at the uppermost section and have a higher possibility to recharge all grouped downstream groundwater sites. But the similarity in isotopic composition and chemical concentration of Na^+ and Cl^- of water samples grouped in sub-Cluster F1 imply that BR4 is a major contributing source to recharge BW6, BT2 and BW9 groundwater. In the same way, sub Cluster F2 have also two possibilities for recharge process. BR6 is located at the upstream section and can recharge all downstream groundwater through bank infiltration. But in the case of BR9, it is located at the downstream section as compared to BW7 and BW8 and has lower chemical concentration as compared to these groundwater. Thus it indicates that BW7 and BW8 have a higher possibility to recharge BR9. The overall process within this sub-Cluster F2 presents that there is river bank infiltration from BR6 to BW7 and BW8, which then change to bank exfiltration at BR9. This result presents that however combining samples from river and groundwater sites within clusters indicates the presence of interconnection, there is a difference in exchange flow direction.

4.6.4 Manahara River

4.6.4.1 Clustering of river water and groundwater

HCA is used to distinguish clusters from 21 and 19 water samples collected in the wet and dry seasons respectively. Four clusters namely A, B (subclusters B1 and B2), C and D are categorized in the dendrogram of the wet season (Figure 87a). Clusters A and B1 comprise combine water samples from river and dug/tube well sites. Eight river sites (MR1 to MR7, MR9) group with one tube well site (MT1) in Cluster A while two river sites (MR8 and MR10) combine with one dug well (MW5) and one shallow tube well

site (MT2) in Cluster B1. However, Clusters of B2, C and D enclose entirely of groundwater. The lowest concentration of Na^+ (4.3 to 9.1 mg/L) and Cl^- (1.5 to 6.4 mg/L) is observed in Cluster A and the highest value is obtained in Cluster D.

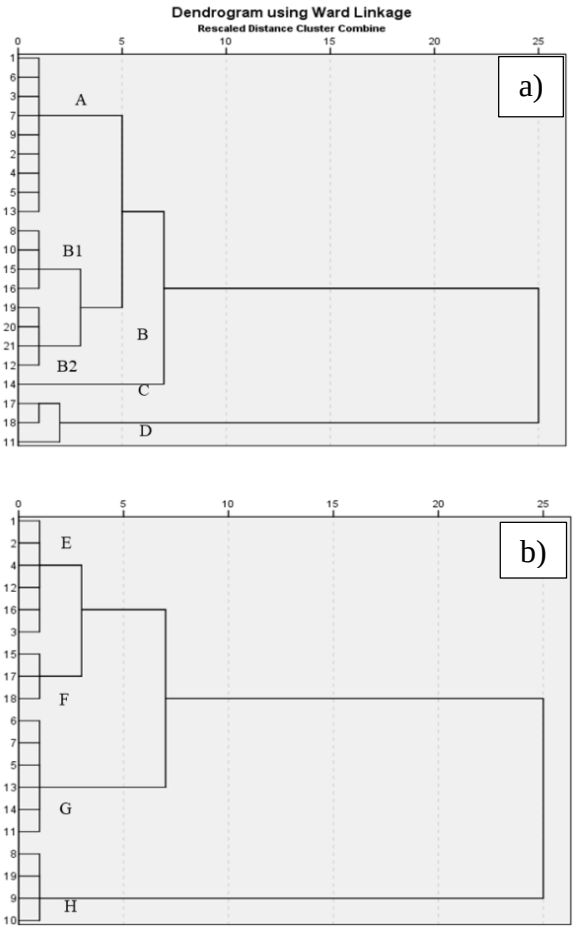

c)

Sample Id	Cluster No.	Sample Id	Cluster No.
MR1	1	MW1	11
MR2	2	MW2	12
MR3	3	MB1	13
MR4	4	MW3	14
MR5	5	MB2	15
MR6	6	MW5	16
MR7	7	MW6	17
MR8	8	MW7	18
MR9	9	MW8	19
MR10	10	MW9	20
		MW10	21

d)

Sample Id	Cluster No.	Sample Id	Cluster No.
MR1	1	MW1	11
MR2	2	MW3	12
MR3	3	MW4	13
MR4	4	MW5	14
MR5	5	MW6	15
MR6	6	MW7	16
MR7	7	MW8	17
MR8	8	MW9	18
MR9	9	MW10	19
MR10	10		

Figure 87: Dendrogram based on hierarchical clustering in a) wet season b) dry season and c) and d) relation of MW and MR with cluster number in wet and dry season respectively

Alike in the wet season, four clusters E, F, G and H are observed in the dendrogram of the dry season (Figure 87b). Except for Cluster F, all three clusters contain water samples from the river and dug well sites. Four upstream river sites (MR1 to MR4) are grouped with two dug well sites MW3 and MW7 in Cluster E whereas three river sites (MR5 to MR7) combine with three dug well sites (MW1, MW4 and MW5) in Cluster G. Similarly, three river sites from downstream section (MR8 to MR10) group with one dug well site (MW10) in Cluster H. But in the case of Cluster F, it only includes three dug well sites MW6, MW8 and MW9. Among these four clusters, the lowest chemical concentration is noted from Cluster E showing a value range from 7.9 to 23.8 mg/L and 3.7 to 23.8 mg/L for Na^+ and Cl^-.

4.6.4.2 Identifying areas of river water and groundwater interconnection

Clusters A, B1, E, G and H having combined water samples from river and groundwater sites indicate the existence of interconnection along the Manahara River in both the wet and dry seasons. Groundwater site (MT1) and most river sites except MR2, MR4 and MR7 of Cluster A are categorized as Ca-HCO_3 water type. MT1 is a shallow tube well and is located at the river upstream section nearby MR2 (120 m). Geologically, the well site is situated at a permeable lower terrace deposit which is specially used for cultivation. Previous research on the Manahara River (Tamrakar and Bajracharya, 2007) presents lateral instability of river channel which cover large floodplain area and has tendency to create small scale Ox Bow lake. Such a small lake is also generated between river sites (MR2) and this well site. On the other side, MT1 is spatially located downstream of MR1 with more or less similar chemical concentrations indicating a higher possibility of MT1 recharge through bank or bed infiltration of river water from MR1 and MR2. But in the case of Cluster B1, two river sites MR8 and MR10 are located at the downstream section compared to grouped well sites MW5 and MT2 (Figure 36). This represents that there are greater chance of groundwater exfiltration from these two dug well sites to the downstream river sites during the wet season.

In the dry season, upstream four river sites (MR1 to MR4) grouped with two well sites (MW3 and MW7) in Cluster E. The well site MW3 is closest to MR3 and located downstream from MR1 and MR2. The isotopic and chemical composition is more or less similar in this well and river site. MW3 is located at the cultivated land and is mainly composed of coarse sand with gavels (Figure 79b) presenting a shallow well depth of 2.6. The ERT profile of this site (Figure 72) also possesses a high resistive layer (312 to 700 Ωm) at the well location suggesting the presence of a permeable layer. This indicates that there is a higher possibility of the bank infiltration through MR3 to recharge MW3. While in the case of MW7, it is located downstream from all grouped well and rive sites. Thus, it has a higher possibility of recharge from upstream groundwater and river water.

In Cluster G, river sites from the middle section (MR5 to MR7) combine with well sites MW1, MW4 and MW5. The MW1 and MW4 are located at the upstream sections compared to other well and river sites which indicate possibilities of water exfiltration from these sites to downstream sections. In the case of MW5, it is closest to river site

MR5 (15 m). It has a 5.4 m well depth with a 4.9 m water level depth. The concentration of Na^+ and Cl^- is drastically increased in the dry season which is similar to that of the nearest river site MR5 (Appendix 4D). This suggests that MR5 is contributing water to recharge MW5.

Cluster H combine the downstream river sites (MR8 to MR10) with the downstream well site MW10. In this cluster, MR8 and MR9 can infiltrate water to recharge MW10 as these are located at the upstream section compared to it. But MR10 is located just 35 m apart from it. The MW10 has a 7.1 m well depth with a 5 m water level depth. Based on the field observation, this water level lies below the water stage in the river channel. The concentration of Na^+ and Cl^- is increased by three times during the dry season which is less than the river site MR10. This well is mainly located in the modified river channel section over the filled-up material. The ERT profile shows resistivity variation of 40 to 70 Ωm within the well depth (Figure 74) which is generally high as compared to the bottom of the profile. The overall condition reveals that MW10 can be recharged by all grouped river sites.

4.6.5 Hanumante Khola

4.6.5.1 Clustering of river water and groundwater

HCA is performed individually for wet and dry seasons river and groundwater samples. Mainly, three clusters of A, B and C are noted in a wet season (Figure 88a). Water samples having minor values of Na^+ and Cl^- are grouped in cluster A, including all river sites with one dug well HW5. Grouping of all river water with a lower chemical concentrations in a single cluster represents the minimum influence of sewage discharge during wet season. Clusters B and C enclose a totally groundwater sites with different isotopic composition and greater concentration of Na^+ and Cl^- relative to river water.

In the dry season, two distinct clusters D and E are observed in a dendrogram (Figure 88b). Cluster D entirely contains river sites (8 sites) while Cluster E presents a mixture of river and groundwater sites signifying similarity in selected parameters (Zhong *et al.*, 2018; and Shrestha and Kazama, 2007). E1 and E2 are two sub-clusters of cluster E. E1 enclose six groundwater sites along with one river site HR1 whereas E2 contains four groundwater sites and one river site HR2. The two river samples grouped in cluster E are situated at the upstream areas of the river (Figure 38), representing a minor values of Na^+ and Cl^- and classified as Ca- HCO_3 type. Conversely, river sites

grouped in cluster D have the highest concentration of Na^+ and Cl^- and are classified as Na-K-HCO_3 water type (Appendix 5E) representing noticeable effects of sewage discharge. Continual loading of sewage in the river can deposit an organic layer on the riverbed (Sophocleous, 2002) which will decrease exchange flow from the river to well sites (Derx *et al.*, 2010). The nonexistence of cluster containing downstream river sites with groundwater sites in cluster D may be the indication of the presence of a clogging layer in the riverbed.

4.6.5.2 Identifying areas of river water and groundwater interconnection

The presence of clusters grouping river and groundwater sites in both seasons indicates the interconnection between river and groundwater (Mencio and Mas-Pla, 2008; Guggenmos *et al.*, 2011; and Huang and Hans, 2016). Cluster A from the wet season combine all river sites with one groundwater site HW5 of the same type of water (Ca-HCO_3). HW5 is a well with a shallow water level (1 m) with shallow well depth (5 m). It is situated at a permeable lower terrace deposit which is mostly utilized for cultivation. Frequent flooding events were recorded for the Hanumante River (Poudel, 2013), with a major one recently in July 2018 (Bhatta and Pandey, 2020) which flooded the whole area from Jagati to Madhyapur Thimi along with HW2, HW5 and HW6 (Figure 38). However, groundwater site HW5 is the only site clustered with all river sites in cluster A (Figure 88), HR5 is the closest site to HW5 (80 m away). Similar Na^+ and Cl^- concentration and isotopic composition of $\delta^{18}O$ (-8.0‰) and δD (-54.7‰) along with abrupt reduction in chemical concentration at HW5 indicate bank infiltration (Liu and Yamanaka, 2012; Malla *et al.*, 2015 and Nakamura *et al.*, 2017) as the process of recharging HW5 during the wet season.

During the dry season, cluster E1 encloses HR1 with groundwater sites HW1, HW2, HW4, HW6, HW7 and HW9 while cluster E2 grouped HR2 along with groundwater sites HW3, HW5, HW8 and HW10 (Figure 88b). Both river sites HR1 and HR2 situated at upstream areas of the river compared to grouped groundwater sites, indicates a maximum probability of groundwater recharge by these river sites. But the presence of different isotopic compositions in the river and nearby groundwater sites (Figure 52) suggests chances of other recharge sources besides river water. Additionally, groundwater sites plotting close to LMWL indicate dry season meteoric water as alternative source to recharge these groundwater sites.

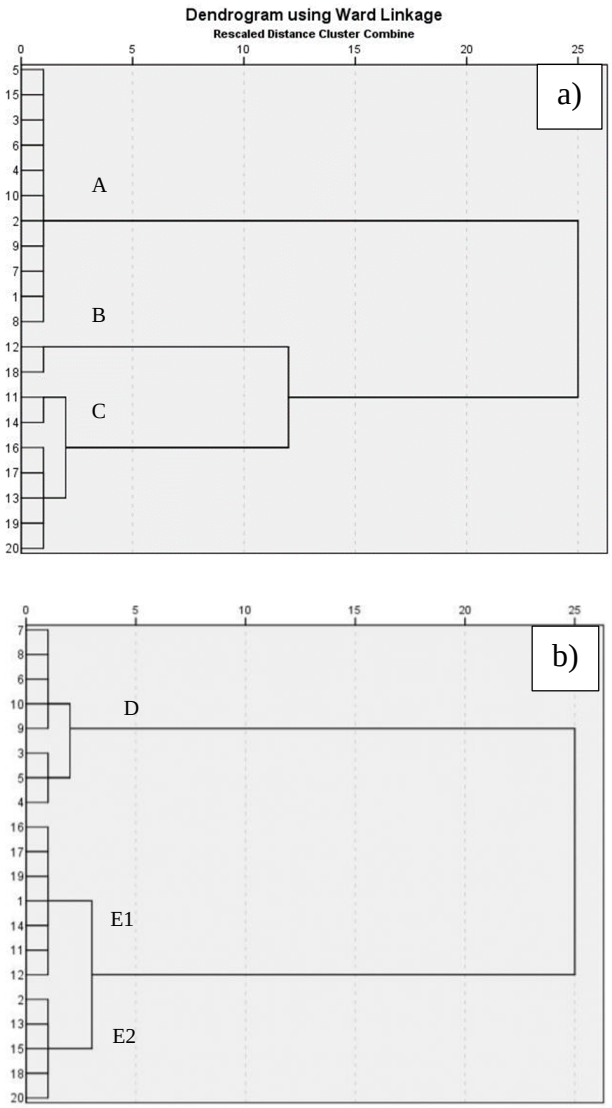

c)

River water		Groundwater	
Sampling Id	Cluster No.	Sampling Id	Cluster No.
HR1	1	HW1	11
HR2	2	HW2	12
HR3	3	HW3	13
HR4	4	HW4	14
HR5	5	HW5	15
HR6	6	HW6	16
HR7	7	HW7	17
HR8	8	HW8	18
HR9	9	HW9	19
HR10	10	HW10	20

Figure 88: Dendrogram based on hierarchical clustering in a) wet season b) dry season and c) relation of HW and HR with cluster number in wet and dry season respectively

Dug wells HW2, HW3, HW9 and HW10 are located within 20 m from river sites HR2, HR3, HR9 and HR10 respectively (Figure 38). Though these wells and river sites are closely located, there is the absence of a cluster containing these sites. These results imply that the river water-groundwater interaction is not only relying on distance from the river channel to groundwater site, but also depends on the water stage of the river channel and wells; topography of well location; and sub-surface lithological variation of the areas.

4.6.6 Godawari Khola

4.6.6.1 Clustering of river water and groundwater

In the wet season HCA, major two clusters A and B are distinguishable in the dendrogram (Figure 89a). Cluster A has two subgroups A1 and A2. Sub-cluster A1 encloses entire river sites (GR1 to GR10) along with five dug well sites (GW1 to GW5) showing a lower concentrations of Na^+ (1.6 to 7.9 mg/L) and Cl^- (1.0 to 9.3 mg/L). While clusters A2 and B only contain samples from dug well sites. Two dug wells GW6 and GW8 are grouped in sub-cluster A2, and three dug wells GW7, GW9 and GW10 are included in Cluster B. Samples from Cluster B shows the highest concentration of Na^+ (27.7 to 39.1 mg/L) and Cl^- (51.5 to 67.2 mg/L) indicating more contaminated water among all groundwater.

Alike in the wet season, the dry season has also two major clusters C and D in the dendrogram (Figure 89b). Cluster C has two sub-groups C1 and C2, and both contain combine samples of river and dug well sites. Especially, upstream samples from the river (GR1 to GR6) and dug wells (GW1, GW3 to GW5) are grouped in Cluster C1 presenting a lower concentration range from 2.6 to 9.9 mg/L and 4.8 to 14.3 mg/L for Na^+ and Cl^- respectively. Contrarily, samples from downstream river sites (GR7 and GR8/GR9) are enclosed with four dug well sites (GW2, GW6, GW9 and GW10) in Cluster C2 and possess a higher concentrations of Na^+ (24.1 to 47.5 mg/L) and Cl^- (28.2 to 87.8 mg/L) as compared to C1. But in the case of Cluster D, it has only one dug well site (GW7) which has a very highest concentration of Na^+ (144.2 mg/L) and Cl^- (323.5 mg/L) indicating higher influences of anthropogenic activities.

4.6.6.2 Identifying areas of river water and groundwater interconnection

Formation of Clusters A1, C1 and C2 including combine water samples from the river and dug well sites signify the existence of interconnection along the whole Godawari Khola in both seasons. Cluster A1 from the wet season encloses all river sites from GW1 to GW10 along with five upstream dug well sites (GW1 to GW5). Dug well GW1 is located at the uppermost section of the river (Figure 40), and very near to river site GR1 (10 m). It has deepest well (10.4 m) depth among other wells and has a 5.2 m water level depth. It is situated at an uphill slope adjacent to the river channel (Figure 90a). It is a private well used to fill in tanker (to sell as drinking water) after collecting water from the well to the artificial pond, made near this well. The water in this well shows a lighter composition of δD and $\delta^{18}O$ (Figure 53) with a very low and similar concentrations of Na^+ (1.7 mg/L) and Cl^- (1.7 mg/L) to GR1 (Appendix 4F). The

occurrence of lighter isotopic composition in GW1 indicates that water from groundwater exfiltration may be one of the source of river discharge.

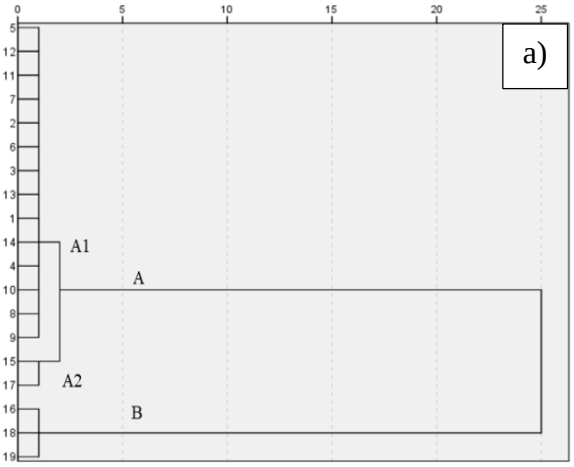

c)

Sample Id	Cluster No.	Sample Id	Cluster No.
GR1	1	GW1	10
GR2	2	GW2	11
GR3	3	GW3	12
GR4	4	GW4	13
GR5	5	GW5	14
GR6	6	GW6	15
GR7	7	GW7	16
GR8/GR9	8	GW8	17
GR10	9	GW9	18
		GW10	19

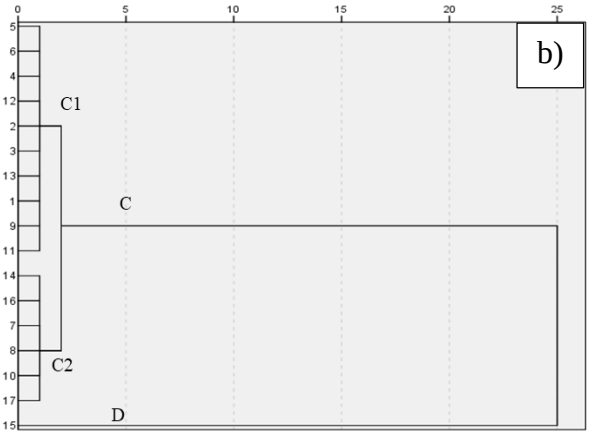

d)

Sample Id	Cluster No.	Sample Id	Cluster No.
GR1	1	GW1	9
GR2	2	GW2	10
GR3	3	GW3	11
GR4	4	GW4	12
GR5	5	GW5	13
GR6	6	GW6	14
GR7	7	GW7	15
GR8	8	GW9	16
		GW10	17

Figure 89: Dendrogram based on hierarchical clustering in a) wet season b) dry season and c) and d) relation of GW and GR with cluster number in wet and dry season respectively

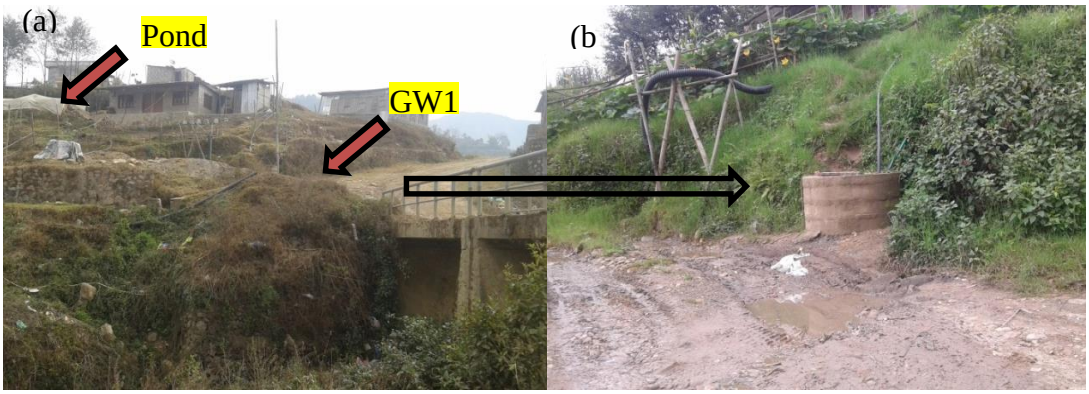

Figure 90: Photographs of GW1 well location

Same as in GW1, GW2 is also located close to river site GR2 (15 m) but situated at about 7-8 m uphill slope from the river channel. It has a 4.2 m well depth with a 2.2 m water level depth. A slightly higher concentration of Na^+ and Cl^- along with the heavier

composition of δD and $\delta^{18}O$ compared to GR2 is observed in GW2. As GW2 is located at a high elevation compared to the river channel (Figure 91); and has only a 4.2 m well depth, there is no any possibility of recharge from river water. As a result, it shows a higher probability of groundwater exfiltration to the river channel. But the occurrence of heavier composition in GW2 again discards the result. Therefore there is other mechanism of interconnection, through bank infiltration from upstream river site GR1 which is grouped in Cluster A1.

Figure 91: Well GW2 and river location

In the case of GW3, it is nearby river site GR3 (4 m) and located downstream from GR1 and GR2. It has only a 1.7 m well depth with a very shallow 0.1 m water level depth which is above the water level in the river channel (Figure 92). A relatively similar composition of δD and $\delta^{18}O$ along with a slightly higher concentrations of Na^+ and Cl^- is observed in GW3. This result directly indicates that groundwater exfiltration from GW3 can contribute to water for river discharge.

Dug well GW4 is located 80 m away from the river site GR4. It has also a shallow well depth (2.9 m) with a 0.8 m water level depth. Comparatively, the dug well and the river channel is situated at the same altitude (Figure 93). A slightly lighter composition of δD and $\delta^{18}O$ with relatively similar chemical concentration observed in GR4 thus indicate the possibility of groundwater recharge through bank infiltration during the wet season.

Figure 92: Well GW3 and rivel locaion

Figure 93: Well GW4 and river location

Similarly, dug well GW5 is near to GR5 which is about 35 m away from the river channel (at the time of sample collection, 2017-2018). The river bank and channel in this area are excessively encroached on by human activity making a very narrow river channel (Figure 94a) which is naturally increased by bank erosion during the monsoon flooding of 2020 (Figure 94b). GW5 has only a 1.8 m well depth with a very shallow water level depth (0.1 m) and is located at a permeable lower terrace deposit (Figure 95), generally used for cultivation. Comparatively, it shows a lower concentration of Na^+ and Cl^- and similar isotopic composition. But the occurrence of 0.1 m water level depth in GW5 directly indicates higher potential of groundwater contribution to river discharge during the wet season.

But in the dry season, river sites are divided into two sub-cluster C1 and C2. All upstream river sites from GR1 to GR6 are grouped with upstream dug well sites GW1,

GW3, GW4 and GW5 in Cluster C1. The locations condition of these dug wells related to nearby river sites are already discussed earlier in the wet season. As GW1 is located at a higher elevation as compared to GR1 with a 5.8 m water level depth, it has a higher possibility to recharge nearby river sites through groundwater exfiltration. Occurrences of lighter isotopic composition at GW1 as compared to GR1 also signify similar results. But in the case of GW3 and GR3, groundwater from GW3 shows heavier isotopic composition than that of GR3. Water level depth is observed at only 0.5 m which lies above the water level in the river channel (Figure 92) suggesting recharge of river water through groundwater exfiltration. But the occurrence of heavier isotopic composition pointed towards opposite chances of recharge from river water (Li *et al.*, 2016). Thus these results pointed towards two possibilities: 1) the upstream river water (GR1 and GR2) can recharge the downstream dug well (GW3), and 2) the upstream dug well (GW1) can recharge the downstream dug well (GW3) as well as the river site (GR3) also.

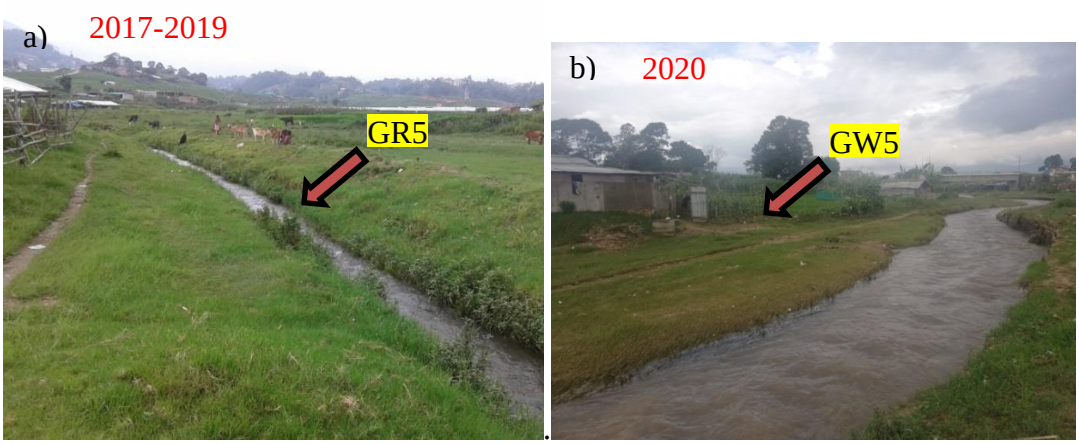

Figure 94: Well GW5 and river in a) 2017 to 2019 and b) 2020

Figure 95: River bank material at GW5

In the case of GW4, it shows a relatively similar isotopic composition (Appendix 6F) with a slightly lower concentrations of Na^+ and Cl^- (Appendix 4F), indicating a higher possibility of groundwater recharge by nearby river water (GR4) through bank infiltration. Similarly, the water level condition in GW5 (1.2 m) is also located at a deeper depth as compared to the water level in the nearby river channel at GR5 (Figure 94) presenting a higher possibility of groundwater recharge by nearby river water. Observation of lighter composition of δD and $\delta^{18}O$ in GR5 also suggests for a similar type of result.

Cluster C2 from the dry season includes two downstream river sites (GR7 and GR8/GR9) with four dug well sites (GW2, GW6, GW9 and GW10). Dug wells GW2 and GW6 are located at the upstream section (Figure 40) compared to grouped river sites; indicating greater potential to recharge downstream river as well as dug well sites. Contrarily, GW10 is located at the downstream section and has no chance to recharge the upstream river and dug well sites, thus presenting only the possibility of recharge from the upstream river and dug well sites. But in the case of GW9, it is located downstream of GW2, GW6 and GR7; and near GR8/GR9 (80 m). It has a 9.1 m well depth with a deep water level depth (8 m) compared to the water level in the river channel (Figure 96) which directly indicates the potential of groundwater recharge by nearby river water.

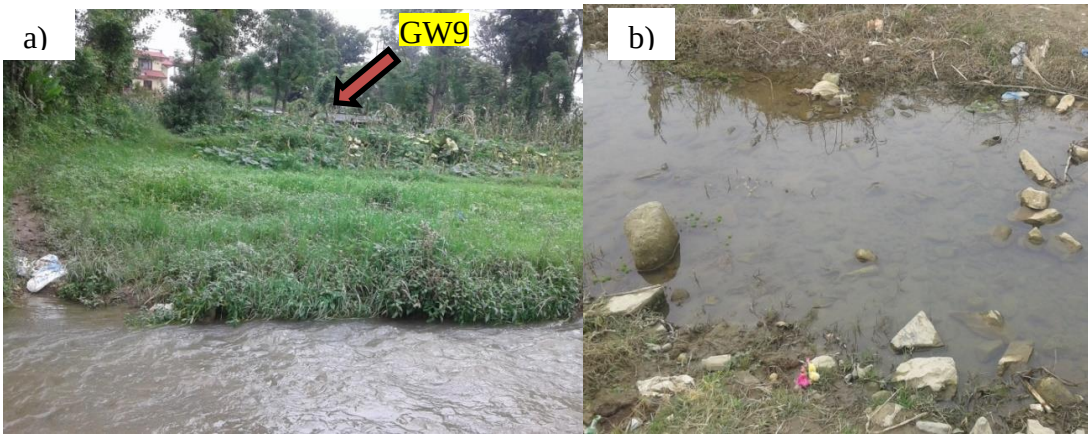

Figure 96: Well GW9 and water level in the river channel at a) wet season and b) dry season

But occurrences of heavier isotopic composition in GR8/GR9 compared to GW9 discard this possibility. The presence of very minor discharge in the river channel (Figure 96b) with an evaporation effect also suggests for impossibility to recharge surrounding groundwater during the dry season. Thus, this well has two other additional

possibilities for recharge: 1) it has the possibility of recharge through dry season rainfall as it is plotted close to LMWL (Figure 53b), and 2) can recharge by upstream dug wells GW2 and GW6.

4.6.7 Kodku Khola

4.6.7.1 Clustering of river water and groundwater

Wet season samples performed by HCA show three distinct clusters of A, B and C (C1 and C2) in the dendrogram (Figure 97). Clusters A and C1 enclose combined samples from the river and dug well sites. Cluster A includes six river samples (KR1 to KR5, and KR8) containing a lower concentrations of Na^+ (4.5 to 13.1 mg/L) and Cl^- (2.3 to 15.4 mg/L) and groundwater from three dug well sites (KW1, KW3 and KW5). Similarly, Cluster C1 consists of two river sites KR6 and KR7 with dug well sites KW4 and KW6. But Cluster B and C2 enclose entirely groundwater. Dug well sites KW2 and KW7 are grouped in Cluster B which has a highest concentrations of Na^+ (23.6 to 33.5 mg/L) and Cl^- (51.1 to 58.3 mg/L); and only KW8 is included in Cluster C2.

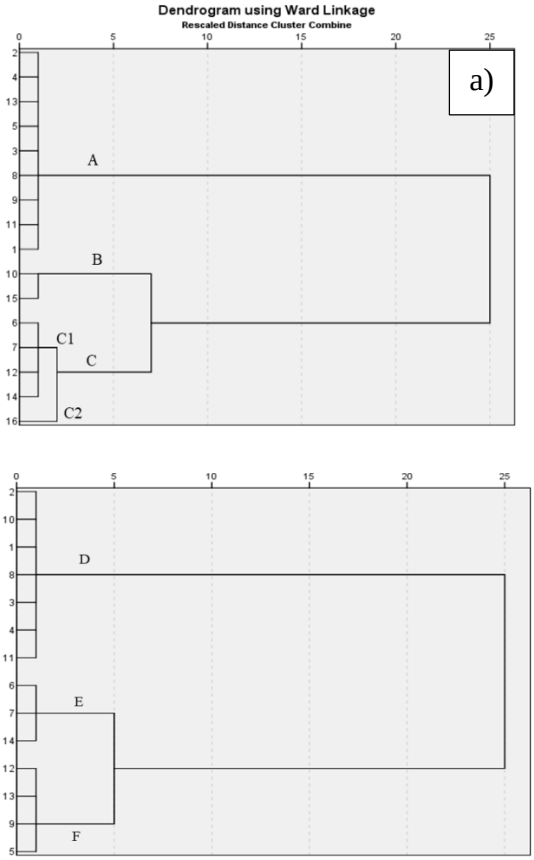

c)

Sample Id	Cluster No.	Sample Id	Cluster No.
KR1	1	KW1	9
KR2	2	KW2	10
KR3	3	KW3	11
KR4	4	KW4	12
KR5	5	KW5	13
KR6	6	KW6	14
KR7	7	KW7	15
KR8	8	KW8	16

d)

Sample Id	Cluster No.	Sample Id	Cluster No.
KR1	1	KW1	8
KR2	2	KW2	9
KR3	3	KW3	10
KR4	4	KW4	11
KR5	5	KW5	12
KR6	6	KW6	13
KR8	7	KW8	14

Figure 97: Dendrogram based on hierarchical clustering in a) wet season b) dry season and c) and d) relation of KW and KR with cluster number in wet and dry season respectively

Dendrogram of the dry season also presents three clusters D, E and F (Figure 97b) containing combine sites from the river and dug well sites. Most of the upstream river sites (KR1 to KR4) are grouped with upstream dug well sites (KW1, KW3 and KW4) in Cluster D showing a lowest concentration of Na^+ (6.6 to 20.8 mg/L) and Cl^- (4.7 to 32.2 mg/L). Similarly, downstream river sites (KR7 and KR8) are gathered with dug well KW8 in Cluster E and present the highest concentration of Na^+ (68.4 to 94.5 mg/L) and Cl^- (108.7 to 116.9 mg/L). One river (KR5) and three dug well sites (KW2, KW5 and KW6) are enclosed in Cluster F whose concentrations of Na^+ and Cl^- lies in between clusters D and E.

4.6.7.2 Identifying areas of river water and groundwater interconnection

Clusters A, C1, D, E and F presenting combined water samples from the river and dug well sites suggest interconnection along the Kodku River in both wet and dry seasons. Five upstream river sites (KR1 to KR5) along with one downstream site (KR8) are gathered with three dug well sites (KW1, KW3 and KW5) in cluster A during the wet season. These samples show lower chemical concentrations and are classified as Ca-HCO_3 water type. As KR8 is located at the downstream section as compared to all grouped sites (Figure 42), it has higher probability to gain water from the upstream river and dug well sites as a recharge sources. But in remaining river sites, these are close to dug well sites.

Specifically, dug well KW1 is very close to KR1 (5 m) and is located at the river floodplain area as well as situated at the base of a steep uphill slope (Figure 98b). This well has a wider diameter (2.5 m) with a shallow well depth (4.6 m) and 1.5 m water level depth. It is used as a community well, and distributed water to the public in the morning and evening time. Based on personal communication and field verification, this well is used to continuously collect water from the uphill side area. KW1 shows lighter isotopic composition than KR1 with a tentatively similar concentrations of Na^+ and Cl^-. Field observation and the figure (Figure 98a) of the well location may verify that the water level depth and level of the river channel are nearly at the same depth indicating the possibility of groundwater recharge through bank infiltration from KR1. But the presence of lighter isotopic groundwater than river water differs from that result. In the meantime, there is also the possibility of a higher contribution of collected uphill side water which may have lighter isotopic composition.

Figure 98: Photographs of KW1 a) well and river channel and b) uphill side adjacent to KW1

Alike in KW1, KW3 is also near to KR3 (10 m) and also located at the flood plain area (Figure 99) and situated at the base of an uphill slope. It has a very shallow well depth (1.25 m) with only 0.3 m water level depth. Comparatively, KW3 has a lower concentrations of Na^+ and Cl^- (Appendix 4G) with lighter isotopic composition as compared to KR3 (Appendix 6G). This result implies that groundwater exfiltration is the process of interconnection between the river and groundwater during the wet season. In the same way, KW5 is nearby river site KR5 (15 m) and is located in the settlement area. Unfortunately, the depth of this dug well cannot be measured but able to measure water level depth as 1.5 m. Tentatively similar Na^+ and Cl^- concentration along with slightly heavier isotopic composition in KW5 as compared with KR5 support for the bank infiltration as a mechanism of recharge KW5 during the wet season.

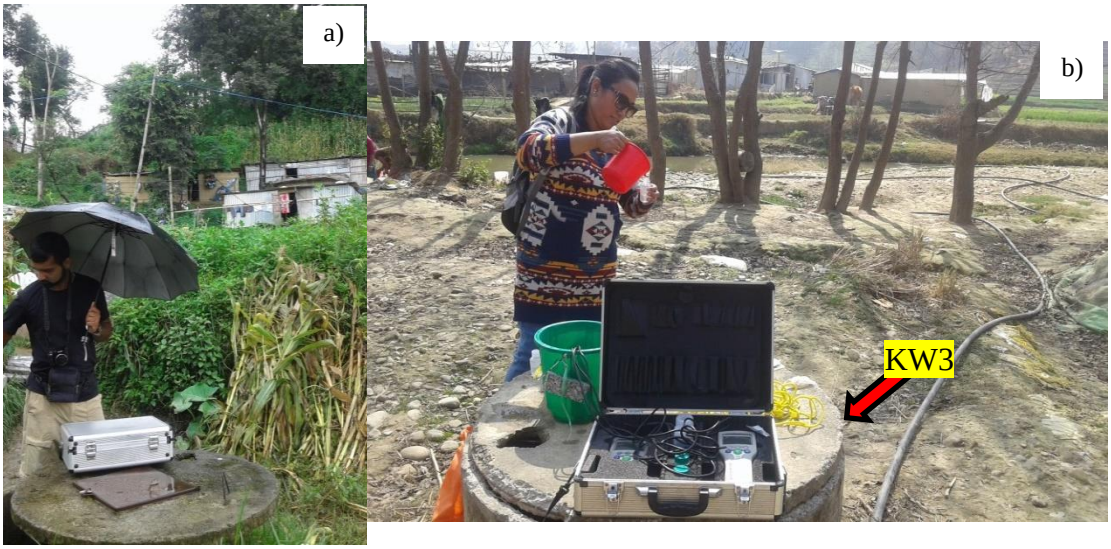

Figure 99: Photographs of well KW3 a) well and its adjacent uphill slope and b) well and river channel

Cluster C1 groups samples from two river sites (KR6 and KR7) and two dug well sites (KW4 and KW6). KW4 is located at the upper section comparing among the grouped samples (Figure 42) and thus presents a higher capacity to recharge downstream river sites as well as dug well site. But in the case of KW6, it is near river site KW6 (20 m) and is located at the new settlement area. It has a 6 m well depth with a 1.6 m water level depth. It shows a slightly heavier isotopic composition as compared to KR6 which supports for recharge of groundwater at KW6 through bank or bed infiltration during the wet season.

In the dry season, cluster D encloses four upstream river sites (KR1 to KR4) along with nearby dug well sites KW1, KW3 and KW4. As previously described the condition of KW1 in Cluster A, it is one of the closest dug well sites to the river channel. It has a 2.5 m water level depth in the dry season which is obviously at a higher depth than the water level in the river channel (Figure 98). It shows similar isotopic composition (-9.3‰) as that in the wet season which is lighter than the composition of dry season KR1 (-8.73‰). Concentration of Na^+ and Cl^- at KW1 is also lower than at the related river site (Appendix 4G). These results present two consequences: 1) Higher water level depth of well directly indicates that there is a higher possibility of groundwater recharge through bank infiltration and 2) Lighter isotopic composition of KW1 than that of KR1 exhibits a lower contribution of river water to recharge groundwater as compared with the water which is artificially used to store from an uphill slope.

In the same way, KW3 which is close to KR3 has a 1.05 m water level depth in the dry season which may be beneath the water level of the river channel (Figure 95b). The heavier isotopic composition (-8.53‰) with lower chemical concentration observed at KW3 supports bank infiltration as the mechanism of groundwater recharge from KR3 during the dry season. But in the case of KW4, it is close to KR4 and has a 2.5 m water level depth within a 3.6 m well depth. It shows lighter isotopic composition (-8.66‰) than that of KR4 (-8.24‰) with slightly higher chemical concentration. These results imply that there is the possibility of groundwater exfiltration from KW4 to recharge the river site at KR4 during the dry season.

Cluster E (dry season) only includes river sites KR7 and KR8 with only one dug well KW8. This dug well is very close to KR8 (7 m) and located at the dense settlement area. It has a 8.5 m well depth with a 7.8 m water level depth. Relatively, similar isotopic

composition and Cl^- concentration observed in KW8 and KR8 is an indication of possible groundwater recharge in KW8 through bank infiltration during the dry season.

In Cluster F, only one river site (KR5) is grouped with three dug well sites (KW2, KW5 and KW7) during the dry season. KW2 is located at the uppermost section while KW7 is at the downstream section as compared to the KR5 which indicates that KW2 may be the recharge source for the river site and KW7 has higher chances of recharge through the upstream river and dug well sites. However, in the case of KW5, it is near KR5 (15 m) which well information is previously presented in Cluster A. Due to some circumstances, the water level depth of the dry season cannot be measured in KW5. But the presence of slightly heavier isotopic composition with heavier chemical concentration in KW5 suggests bank infiltration as a mechanism of groundwater recharge at KW5 during the dry season.

4.6.8 Nakhhu Khola

4.6.8.1 Clustering of river water and groundwater

As there are only six samples in the wet season, only two clusters A and B are formed in the dendrogram (Figure 100a). Cluster A encloses one river site (NR5) and two dug wells (NW4 and NW6) showing a higher concentrations of Na^+ (14.8 to 23.0 mg/L) and Cl^- (15.2 to 31.6 mg/L). Similarly, Cluster B includes two river sites (NR4 and NR6) and one dug well NW5 with a lower concentration of Na^+ (3.7 to 8.8 mg/L) and Cl^- (2.3 to 6.8 mg/L).

In the dry season, two clusters C and D are categorized from the dendogram (Figure 100b). Cluster D has two sub-groups as D1 and D2. Clusters C and D1 contain combine samples from the river and dug well sites. Cluster C includes upstream river (NR1 to NR4) and dug well sites (NW1 to NW4) presenting lower concentrations of Na^+ (5.73 to 19.0 mg/L) and Cl^- (4.78 to 25.7 mg/L) while Cluster D1 encloses one rive site with two dug well sites. But in the case of Cluster D2, it includes only one river site NR6 with extreme concentrations of Na^+ (98.1 mg/L) and Cl^- (114.05 mg/L) showing higher contamination in downstream river section.

4.6.8.2 Identifying areas of river water and groundwater interconnection

Formation of clusters A, B, C and D1 with combined samples from the river and dug well sites signify interconnection along the Nakhu River in both seasons. Upstream dug

well NW4 groups with downstream sites NR5 and NW6 in cluster A (Figure 44) which indicates groundwater exfiltration from dug well NW4 as a recharge source for downstream river and dug well sites. In the same way, NR5 located at the upstream section compared to NW6 has also a higher possibility to recharge downstream dug well NW6 during the wet season. A similar case of recharging condition is also observed in cluster B in which upstream river site NR4 combines with downstream sites NW5 and NR6. These conditions indicate that the alternation of groundwater exfiltration and river water infiltration is a major mechanism for interconnection in the wet season.

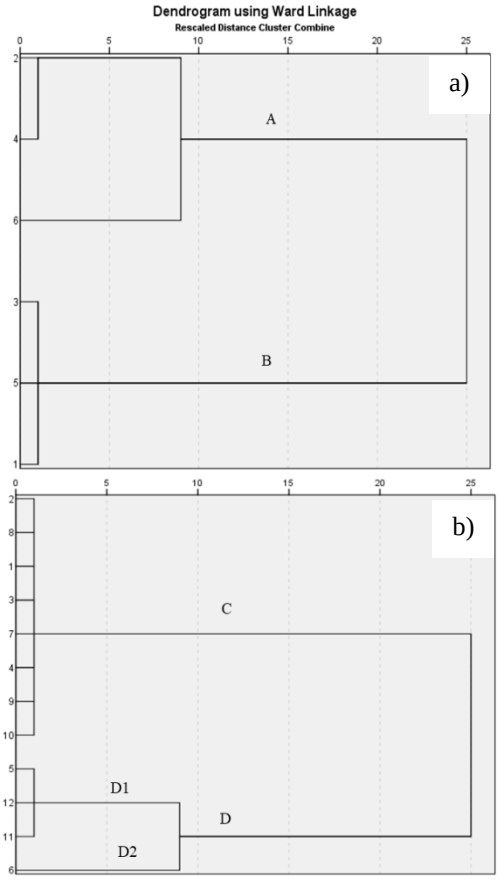

c)

Sample Id	Cluster No.	Sample Id	Cluster No.
NR4	1	NW4	4
NR5	2	NW5	5
NR6	3	NW6	6

d)

Sample Id	Cluster No.	Sample Id	Cluster No.
NR1	1	NW1	7
NR2	2	NW2	8
NR3	3	NW3	9
NR4	4	NW4	10
NR5	5	NW5	11
NR6	6	NW6	12

Figure 100: Dendrogram based on hierarchical clustering in a) wet season b) dry season and c) and d) relation of NW and NR with cluster number in wet and dry season respectively

In the case of the dry season, upstream river sites NR1 to NR4 are grouped with upstream dug wells NW1 to NW4 in which river sites are close to relative dug well sites. NW1 is very close to NR1 (20 m) having a very shallow well depth (1.5 m) with the water level depth of only 0.2 m. It is located in lower terrace deposit which is generally used for cultivation. As it has a shallow water level depth, it shows a higher

possibility of groundwater exfiltration to recharge nearby river site NR1 and downstream river as well as dug well sites. In the meantime, occurrence of heavier isotopic composition in NW1 compared to NR1 (Appendix 6H) indicate minor chances to recharge NR1. The lower resistive layer (30 to 50 Ωm) observed at the well location in the ERT profile and material obtained in the field also implies the presence of low permeable layers in this site (Figure 75 and Figure 76) The occurrences of such material signify the lower contribution of surrounding wells to recharge river recharge.

Alike in NW1, NW2 is also located only 25 m away from the river site NR2. It has a 4.8 m well depth with a 1.7 m water level depth which is below the water level in the river channel (Figure 101). A similar concentration of Na^+ and Cl^- with NW2 along with the presence of lighter isotopic composition in NR2 supports bank infiltration as a mechanism to recharge NW2. The ERT profile also presents a layer with a resistivity of 70 to 150 Ωm (Figure 78) which may present coarser materials up to the well depth.

In the case of NW3, it is located 90 m away from river site NR3 having a 3.7 m well depth with the water level depth of 1.1 m. Comparatively, it has a heavier isotopic composition of δD (-53.3 ‰) and $\delta^{18}O$ (-7.8‰) along with a higher concentration of Na^+ and Cl^- than that of NR3. This heavier isotopic value lies below LMWL in δD verses $\delta^{18}O$ plot (Figure 55b) indicating a minor possibility of recharge through meteoric water. Thus it has a higher potential of recharge from upstream river water as well as by nearby river site NR3.

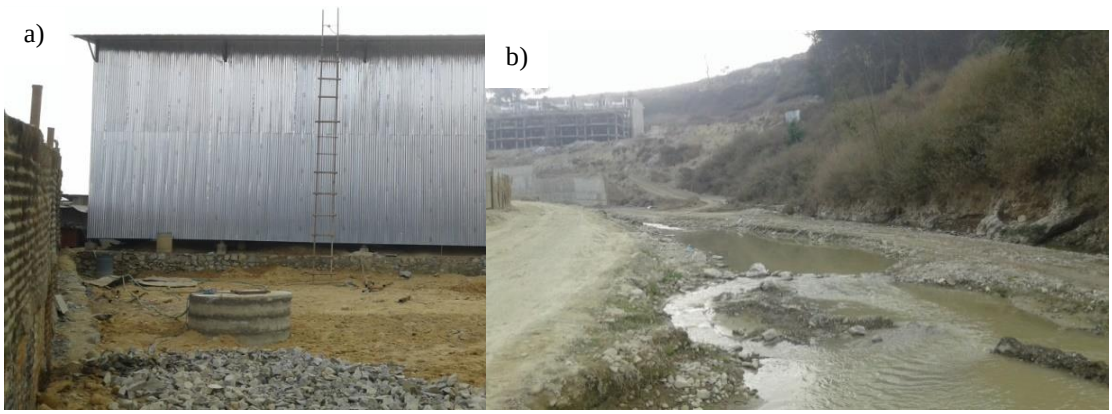

Figure 101: Photographs of a) NW2 and b) NR2 close to NW2

Heavier isotopic composition and higher chemical concentrations are also observed in NW4 which is very near to river site NR4 (30 m). It has 8 m well depth with the water level depth of 7.5 m which is deeper than the water level in the river channel (Figure

102). It has a very minor possibility of recharge by dry season rainfall as it is plotted below LMWL (Figure 55), presenting a higher potential of recharge by the upstream river/dug well site as well as nearby river site NR4.

Figure 102: Photographs of a) NW4 and b) NR4 close to NW4

In Cluster D1, one river site NR5 is grouped with its nearby dug well NW5 and downstream dug well NW6. As NW6 is located at the downstream section, it has a greater chance of recharge by the upstream river as well as dug well sites. But in NW5, it is close to NR5 (20 m) having a 7.2 m well depth with the water level depth of 3.8 m. It is located at dense settlement area showing a higher concentrations of Na^+ and Cl^-. Identical isotopic composition of δD (-55‰) and $\delta^{18}O$ (-7.9‰) observed in NW5 and NR5 with deeper water level depth than that of the river channel (Figure 103) indicate bank infiltration as the mechanism of recharge NW5 during the dry season.

Figure 103: Well NW5 and its nearby river channel

4.6.9 Balkhu Khola

4.6.9.1 Clustering of river water and groundwater

Three clusters A, B and C are distinguished in a dendrogram of the wet season (Figure 104a). Clusters A and C have two subgroups A1, A2 and C1, C2 respectively. Only Cluster A1 has combined water samples from the river and dug well sites. Cluster A2 contains entirely samples from six river sites (BAR1, BAR4 to BAR6, BAR9 and BAR10). Similarly, Cluster B and C enclose entirely groundwater samples from dug well sites. Groundwater samples BAW1, BAW2, BAW4 & BAW6 containing a very lower concentrations of Na^+ (1.4 to 5.0 mg/L) and Cl^- (0.8 to 6.6 mg/L) are grouped in Cluster B whereas groundwater samples (BAW5, BAW7 to BAR9) having a higher concentration of Na^+ (20.0–30.5 mg/L) and Cl^- (21.8–57.4 mg/L) are gathered in Cluster C.

In the dry season, all three clusters D, E and F consist of combined samples from the river and dug well sites (Figure 104b) indicating the presence of interconnection between all river and dug well sites. Cluster E contains three river sites from upstream sections (BAR1 to BAR3) and three dug well sites (BAW1, BAW2 and BAW6), which presents the lowest concentration of Na^+ and Cl^- and is classified as Ca-HCO_3 water type. Similarly, Cluster D comprises four middle section river sites (BAR4 to BAR7, Figure 46) and four dug well sites (BAW3 to BAW5, BAW9) and Cluster F encloses three downstream river sites (BAR8 to BAR10) with three dug well sites BAW7, BAW8 and BAW10. The concentration of Na^+ and Cl^- is successively increases from water samples gather in Cluster E to samples of Cluster D and Cluster F.

4.6.9.2 Identifying areas of river water and groundwater interconnection

Combining water samples from river and groundwater sites in cluster A1 (wet season) and clusters D, E and F of the dry season (Figure 104) imply the presence of interconnection between river water and groundwater along the Balkhu Khola. Only two dug well sites, one from the upstream section (BAW3) and one from the downstream section (BAW10) are grouped with four river sites (BAR2, BAR3, BAR7 and BAR8) in Cluster A1 during the wet season. Water samples of this group are categorized as Ca-HCO_3 type. As BAW10 is located at the downstream section compared to all grouped river sites (Figure 46), it has a higher possibility of recharge

from upstream river sites. Further, it is plotted on LMWL (Figure 56a), suggesting that BAW10 has a mixed water source of upstream river water and precipitation of the wet season. However, in the BAW3, it is located just downstream of BAR2 and very near to BAR3 (20 m), in the cultivated land. It has a 7.2 m well depth with a shallow water level depth of 1.5 m. Slightly heavier isotopic composition and higher Na^+ and Cl^- concentration than BAR3 along with shallow water level depth at BAW3 indicate that groundwater exfiltration may be one of the recharging processes for BAR3 during the wet season.

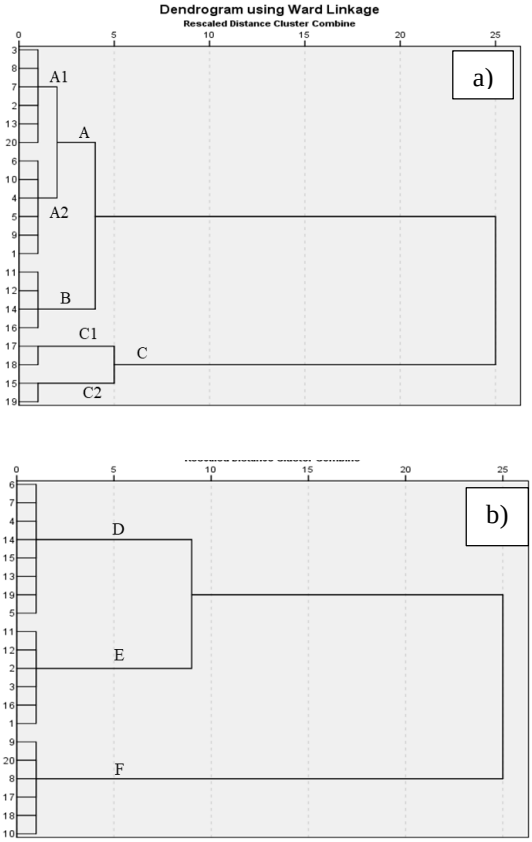

c)

Sample Id	Cluster No.	Sample Id	Cluster No.
BAR1	1	BAW1	11
BAR2	2	BAW2	12
BAR3	3	BAW3	13
BAR4	4	BAW4	14
BAR5	5	BAW5	15
BAR6	6	BAW6	16
BAR7	7	BAW7	17
BAR8	8	BAW8	18
BAR9	9	BAW9	19
BAR10	10	BAW10	20

Figure 104: Dendrogram based on hierarchical clustering in a) wet season b) dry season and c) and d) relation of BAW and BAR with cluster number in wet and dry season respectively

In the dry season, three upstream river sites (BAR1 to BAR3) are gathered with dug well sites BAW1, BAW2 and BAW6 in Cluster E. BAW6 is located at the downstream section as compared with all other gather sites and thus has a higher potential of recharge from upstream river sites. While in BAW1, it is close to river site BAR1 (25 m) which has a very lower well depth (1.9 m) along with a shallow water level of 1.3 m. It is situated at a permeable lower terrace deposit which is generally used for cultivation. A slightly lighter isotopic composition observed at BAR1 compared to

BAW1, indicates river water can be one of the recharge sources for BAW1. Similarly, BAW2 is close to BAR2 (40 m) and just located downstream of BAR1. It has also shallow depth (5.8 m) with a shallow water level of 1.5 m, situated on cultivated land. The similar chemical concentrations of Na^+ and Cl^- observed in BAW2 and BAR2 support for the presence of exchange flow between river and groundwater. But lighter isotopic composition observed at BAW2 than that of BAR2 signifies that the direction of exchange flow is towards river sites presenting as a recharge source for BAR2 (Li *et al*., 2016). In cluster D, it combines water samples from the middle section of river sites (BAR4 to BAR7) and dug well sites (BAW3 to BAW5, BAW9). BAW3 is located at the uppermost section compared to other grouped water samples, thus existing as a recharging source for downstream rive sites. Contrarily, BAW9 is situated at the downstream section and indicates upper river sites as a recharge source for it. But in the case of BAW4 and BAW5, they are close to river sites BAR4 (10 m) and BAR5 (70 m) respectively. Both dug wells have shallow well depths (2.8 to 4.8 m) with water level depths of 4 m (BAW4) and 2.5 m (BAW5). BAW4 has very similar isotopic as well as a chemical concentrations of Na^+ and Cl^- to that of BAR4, supporting for a higher proportion of groundwater recharge through bank infiltration from BAR4. While in BAW5, it has a slightly heavier isotopic composition and different chemical concentration to that of BAR5. Further, it is plotted close to LMWL which indicates that BAW5 has a mixed type of recharge source from river water and dry season rainfall.

Alike in other clusters, Cluster F gather samples from downstream sections of the river (BAR8 to BAR10) and dug well (BAW7, BAW8, BAW10) sites. BAW7 is located upstream section as compared to other grouped sites (Figure 46) and thus has the potential to recharge downstream river sites. While in BAW8 and BAW10, they are very close to river sites of BAR8 (20 m) and BAR10 (7 m) respectively. BAW8 has the deepest well depth among the selected wells (9.4 m) with a 5.7 m water level depth. The identical concentrations of Na^+ (95 mg/L) observed in BAW8 and BAR8 with similar isotopic composition suggest a higher potential of groundwater recharge through bank infiltration. Similarly, BAW10 has a 7.2 m well depth with a 2.7 m water level depth. This well is located on cultivated land and shows a heaviest chemical concentration of Na^+ and Cl^- as compared to other upstream dug wells which are also similar to that of BAR10 indicating a higher possibility of BAW10 recharge by bank infiltration from upstream and nearby river water.

4.7 Interconnectivity of river and shallow groundwater in the Kathmandu Valley

The earlier discussion in the interconnectivity of individual rivers signifies that the Kathmandu Valley's river and shallow groundwater show a spatial-temporal variation in interconnection. Areas or locations of interconnection are identified specifically based on the HCA (Guggenmos *et al*., 2011). As this research is unable to measure the water stage on river channel, the exchange flow condition is mainly discussed based on the isotopic and chemical composition of river and groundwater, the water level on dug wells and field verification on comparison of water level in well and river. Using these criteria, the exchange flow conditions on interconnected areas are categorized as influent; effluent; influent and effluent; influent from upstream; effluent from upstream; and effluent to downstream.

Generally, influent and effluent are used to indicate areas of water infiltration (losing) from the river and water exfiltration from groundwater (gaining) to adjacent river site respectively. The combination of influent and effluent is used for the groups which combine samples from the up and downstream sections of the river as well as groundwater indicating combined effects of infiltration and exfiltration during the course of the river. The condition of influent from upstream is used for those areas where upstream river sites are grouped with downstream groundwater representing upstream river water as a recharge source for downstream groundwater. Conversely, effluent from upstream is used for the areas which have grouped upstream groundwater sites with the downstream rivers as well as groundwater sites. In the same way, effluent to downstream is also a grouping of upstream groundwater with downstream river sites which indicates groundwater exfiltration is the source for downstream river sites.

The rivers of the Kathmandu Valley are alluvial rivers at the centre of the basin after leaving bedrocks at the surrounding portions of the Kathmandu basin. These rivers have narrow valley and surrounded by hillslopes in the upstream section. While they have wider alluvial valley at the centre of the basin where the hillslope flows insignificantly influenced on groundwater water table. The river-groundwater interconnection on these areas can be affected by the morphological conditions surrounding the studied areas. Generally, effluent condition (gaining rivers) is dominant in the narrow valley and influent condition (losing rivers) is dominant in wider alluvial valley (Guzman *et.al.*, 2016).

The exchange processes in river-groundwater interconnection can also determine by streambed topography, discontinuities in river slope and depth, changes in flow direction, riffle-pool sequences and obstacles into the channel (Brunke and Gonser, 1997). The Kathmandu Valley Rivers are sinuous perennial rivers. There are numbers of small and large riffles-pool sequences along these course. The formation of convexities and concavities in riverbed topography control the exchange flow between river and groundwater. Naturally, the stream depth is decreased at the end of the pool with increasing pressure of water. At this site, the river water infiltrates into bank sediments as influent condition. The infiltrate water travels for some distances as underflow and recharge groundwater. But at the end of the riffle, the river depth increases and reduce water pressure which causes water exfiltration from river bank to river channel (Brunke and Gonser, 1997). The schematic diagram (Figure 105) shows the water movement in the riffle-pool sequences. The observation of exchange process as influent from upstream, effluent from or to downstream in this study may represent the influence of riffle-pool sequences in the river course.

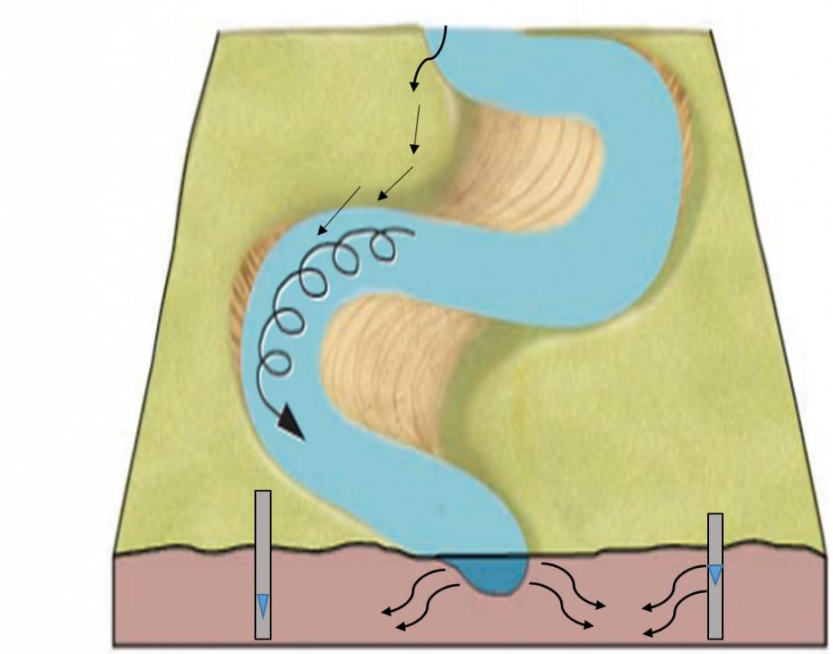

Figure 105: Schematic diagram showing water movement in riffle-pool sequence

Previous research on morphological studies indicate that most the rivers are disturbed by human activities by creating obstacles into the channel and banks (Bajracharya and Tamrakar, 2007; Maharjan and Tamrakar, 2011). These activities changes the natural morphology such as riffle-pool sequences into straight section which directly effects on

the streambed slope and depth. The external activities also influences for river water infiltration and groundwater exfiltration on the river course.

4.7.1 Spatial variation on interconnectivity in the wet season

Spatial variation in river-groundwater interconnection can be determined by the subsurface lithology, hydraulic conductivities and hydraulic head gradients of groundwater and river water, river morphology and riverbed topography (Flekenstein *et al*., 2010; Derx *et al*., 2010; Guzman *et al*., 2016; Epting *et al*., 2017). Spatial variation on river- groundwater interconnection is noticeable along and among the rivers (Figure 106). However there is presence of interconnection, the exchange flow condition is changed with locations. The presence of spatial variation with different exchange processes are also observed in previous research (Li *et al*., 2016; Zhang *et al*., 2016; Epting *et al*., 2017).

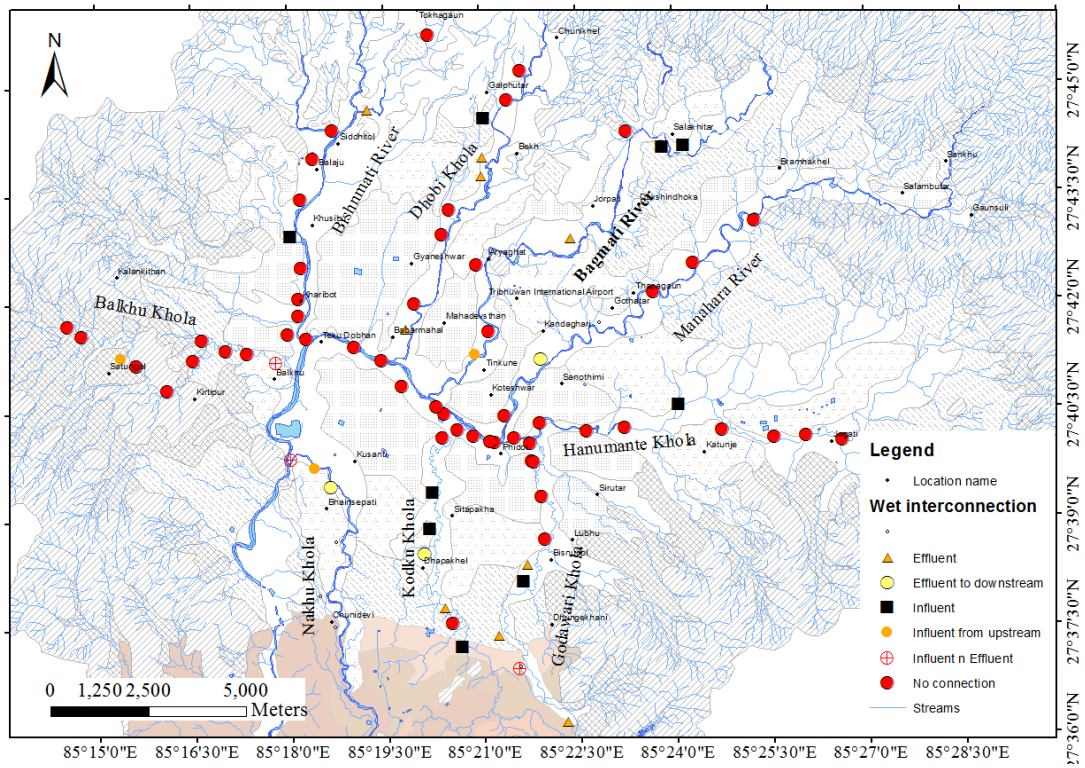

Figure 106: River-groundwater interconnection of the Kathmandu valley in the wet season

In the wet season, rivers as well as dug wells have higher water levels. The research conducted by Prajapati et al. (2021b) presented similar results from Kathmandu valley's river and their adjacent dug wells. During this season, groundwater is mainly recharged by direct infiltration of rainfall (Prajapati et. al., 2021a). The plots of δD versus $\delta^{18}O$ in

the previous section also signifies about meteoric origin of groundwater and river water in the wet season.

In spatial variation map of the wet season (Figure 106), dominant locations (68% of total location) shows absence of interconnection as they are grouped in separate cluster than that of river sites presenting different chemical and isotopic composition (Guggenmos *et al*., 2011). These locations are concentrated at the center of the basin (Figure 106). Mostly, higher urbanized areas along rivers like the Bishnumati (Balaju to Teku Dobhan), Balkhu (Balambu to Balkhu), Hanumante (Jagati to Phidol), Dhobi, Bagmati (Tilganga to Balkhu) and Manahara (up and downstream areas) rivers show lack of interconnection. The research on the Hanjiang River in China also indicates less interaction between river-groundwater in mid-lower reaches of the river during the wet season (Li *et al*., 2016).

The areas especially from southern rivers of the valley like Kodku Khola, Nakhu Khola, upstream of the Godawari Khola and the Bagmati River along with fewer sites from remaining rivers show presence of interconnection (Figure 106). In the case of connected areas, the exchange flow condition is variable. The Godawari Khola presents dominancy of effluent condition representing groundwater exfiltration contribution for river discharge in upstream reaches. In case of influent condition, it is mostly occurred at areas of the Kodku Khola and upstream section of the Bagmati River. Morphologically, upstream section of the Godawari Khola presents narrow river valley surrounded by hillslope. Whereas the downstream sections of rivers show wider valley. According to the Guzman *et al*. (2016), the effluent condition is dominant exchange process in narrow valley and influent condition in wider alluvial valley. The remaining connected areas show just contribution of river water to recharge downstream groundwater or upstream groundwater contribution for downstream river discharge.

The non-connected sites are generally observed from the Central Groundwater District which has dominant of sand and silty sand as aquifer materials with around 10 m aquifer thickness (Shrestha and Shah, 2014). These materials has lower hydraulic conductivity (Pandey and Kazama, 2011). In the other side, the connected sites are located at the Northern and Southern Groundwater District. Usually, these two districts have coarser aquifer material such as sand, gravel and coarse sand (Shrestha and Shah, 2014) with high hydraulic conductivity (Pandey and Kazama, 2011). Comparing to the Central

Groundwater District, these districts have higher permeability. The presence of connected sites located in these two district imply influence of aquifer materials and their hydraulic conductivity in river-groundwater interconnection.

Additionally, the non-connected sites are especially occurred from the core urban areas of the Kathmandu Valley. Channelization is common human activity found in all corridors. Due to this reason, rivers flows with high discharge and velocity during the wet season. This may diminishes vertical and lateral infiltration through riverbed and bank (Figure 107) and do not improve connection condition (Epting et al., 2017).

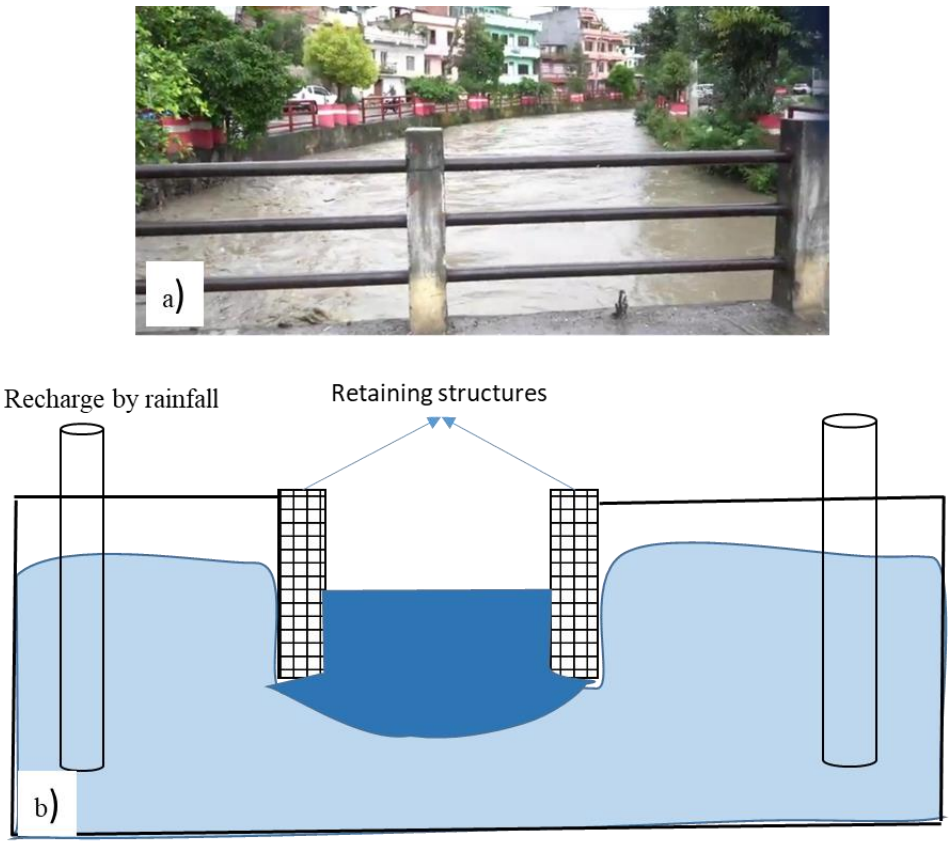

Figure 107: Relative water stage in a) During flooding on Dhobi Khola and b) Schematic diagram showing relative water level in river channel and well

Peak urban flooding recorded in each year in these rivers may be one of problem occurred by absence of river-groundwater interconnection in the center of the basin. Generally, storing of river water in banks are natural process in hydraulically connected river-groundwater areas which can reduce level of flooding during high precipitation (Brunke and Gonser, 1997; Sophocleous, 2002). But channelization of river into narrow channel; construction of rigid retaining structure on river bank; and unmanaged urbanization along river corridors disturbs natural process of interaction and restricts

storing of flooding water in banks. Absence of interaction mainly in the core urbanized areas along with frequently observed peak flooding on the rivers of the Kathmandu Valley signifies this condition. This result indicates that unmanaged urbanization is also one of effectible parameter for non-connection condition of river-groundwater.

But in the study of Prajapati et al. (2021b), the river sites located at valley floor are in gaining condition during the post monsoon (September). They concluded this results from the observation of water level difference between river channels and dug well, located within 100 m from river. In their study, they mainly focused on the water level difference. Contrarily, in the present study, there is lack of water level data of river channel. But the isotopic and chemical along with statistical analysis are widely adopted methodology for river-groundwater interconnection. Thus these combining results indicate importance of detail site specific information such as sub-surface lithology, calculation of hydrogeological parameters along with chemical, isotopic and water level differences for more specific result. Because only difference in water level doesn't indicate direct influent and effluent condition. The subsurface material is also major parameter which can restrict such movement.

4.7.2 Spatial variation on interconnectivity in the dry season

River-groundwater interconnection is spatially more variable in the dry season compared to the wet season (Figure 108). Only certain areas from the Dhobi Khola, downstream section of the Manahara River, Kodku and Godawari Khola along with one location from the Bishnumati River show absence of interconnection.

Generally, rivers are supposed to be recharged by adjacent groundwater in the dry season (Xianfang *et al*., 2006; Menció and Mas-Pla, 2008; Li *et al*., 2016). But in the case of Kathmandu Valley, influent condition is observed as dominant exchange flow (Figure 108), indicating very low discharge rivers can also contribute to recharge adjacent (35%) or downstream groundwater (19%). Prajapati et al. (2021b) also presented dominant of losing stream or influent condition in the pre monsoon period. However, Infiltration mechanism shows two distinct processes as: 1) infiltration to recharge adjacent groundwater- especially along the Nakhu Khola, certain areas of the Balkhu, Kodku, Godawari Khola and the Bishnumati, Bagmati and Manahara rivers; and 2) infiltration from upstream river section to recharge downstream groundwater- especially observe at the center of the valley from Jagati to Teku Dhobhan areas along

the Hanumante Khola and the Bagmati River. Similarly, exfiltration from groundwater also present two processes as: 1) exfiltration immediately to nearby river channel and 2) exfiltration to downstream river section. Only certain areas from the upstream section of most of rivers, except the Bishnumati, Manahara and Hanumante rivers (Figure 108) shows exfiltration to nearby river channel. The remaining mechanism for interconnection is combination of influent and effluent which is mostly occurred at downstream of the Bishnumati and certain areas of other rivers.

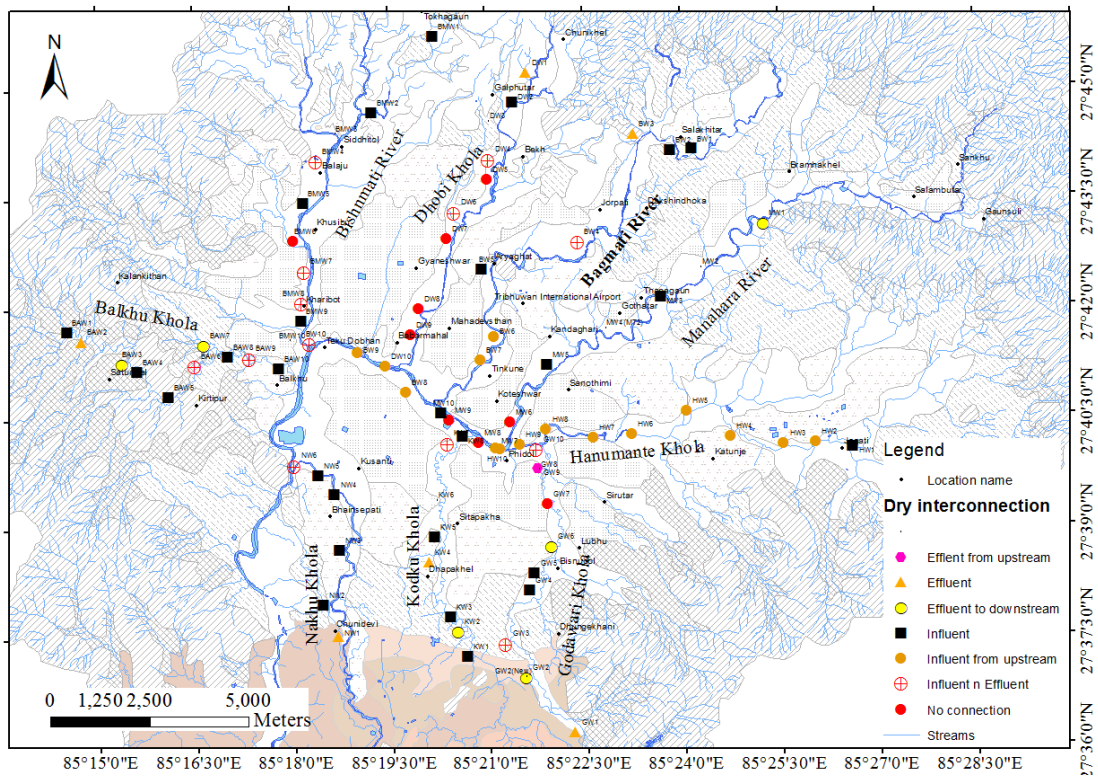

Figure 108: River-groundwater interconnection of the Kathmandu Valley in the dry season

4.7.3 Temporal variation on interconnectivity

Figure 106 and Figure 108 presents condition of river-groundwater interconnection in the wet and dry seasons respectively. The occurrence of only certain areas such as Jadibuti to Balkumari; Gyaneshwor to Babarmahal; and Tikathali area, covering nearly 9% from total sample of the valley shows absence of interconnection in both seasons. This result indicates that river and aquifer are interconnected within 100 m distance in the Kathmandu Valley. But depending on the water stage on river channel and wells, condition of interconnection is temporally variable for the same area. The areas which show absence of interconnection in the wet season (Figure 106), especially from Jagati (upstream of the Hanumante Khola) to Teku Dobhan have changed to influent from the

upstream condition during the dry season (Figure 108). As discussed earlier in wet season, the core areas located in the Central Groundwater District has finer aquifer material. They have lower permeability as well as hydraulic conductivity which can prevent direct connection to river channel. At the same time, the stream bed may also be seal by clogging layer (Derx *et al*., 2010) which are formed by continuous disposal of untreated municipal sewage (Kannel *et al*., 2007). The results obtained in the wet and dry seasons indicates that there is absence of direct influent and effluent relation between river and adjacent groundwater.

Influent from upstream condition implies the similarity in chemical and isotopic composition of groundwater with only those of river water of the upstream section. Presence of influent from upstream condition in these areas indicate influence of riffle-pool sequence in these river reaches. The downstream aquifer is recharged by infiltration of river water through upstream pool areas and extends towards downstream as shown in the schematic diagram (Figure 105). The observation of influent condition in the upstream section of the Bagmati river and Hanumante Khola signifies (Figure 106 and Figure 108) that upstream aquifers are recharge through direct infiltration of river water which then laterally transfer towards downstream aquifers. This type of connection is especially influenced by morphological features of river. The connection status of this type can be change if: 1) the morphological features of river has changed (naturally due to flooding or channel modification); and 2) water level variations in river and dug wells. The connection status of these areas changed to non-connected in the wet season indicate influences of water level variations. During the wet season, the groundwater is mainly recharge from direct infiltration of precipitation (signifies from isotopic analysis in earlier section). Thus water level is increased in groundwater comparing to the river channel (Prjapati *et al*., 2021b) which can be seen in the schematic diagram (Figure 107b) also. During this time, rate of river water infiltration through bank or bed is also low due to high velocity and discharge. Thus these areas has shown absence of interconnection during the wet season.

The connection condition of areas especially from the Nakhu, Balkhu, Kodku, Dhobi, Bishnumati, Bagmati rivers has also changed from non-connected to influent condition during the dry season. During this season, water discharge in river is very low (Figure 109) with low velocity. In the meantime, groundwater level is also lowered by high extraction rate with lower recharge rate. Thus groundwater level is comparatively lower

than river water stage (Prajapati *et al.* 2021b) (Figure 109) which indicate that river water can contribute to recharge adjacent groundwater in these areas. But plotting of most of groundwater samples close to GMWL or LMWL in δD versus $\delta^{18}O$ in earlier section signifies that the dug wells are also recharge by dry season rainfall. Thus the area which possess influent condition have mix type of water both from river infiltration and rainfall percolation. The influent condition is mainly concentrated towards upstream section of northern and sourthern rivers. Generally aquifers of these areas have coarser material and is capable of transmitting river water.

The existence of effluent condition at certain locations, mainly from the upstream sections (Figure 108), shows that these areas are influenced by surrounding hill slope flow. Meanwhile, the absence of effluent condition at wider river valley, especially center of the basin signifies that these areas has less influenced of hillslope flows as suggested by Guzman *et al*. (2016). The numbers of location which have combined effects of influent and effluent is increase in the dry season.

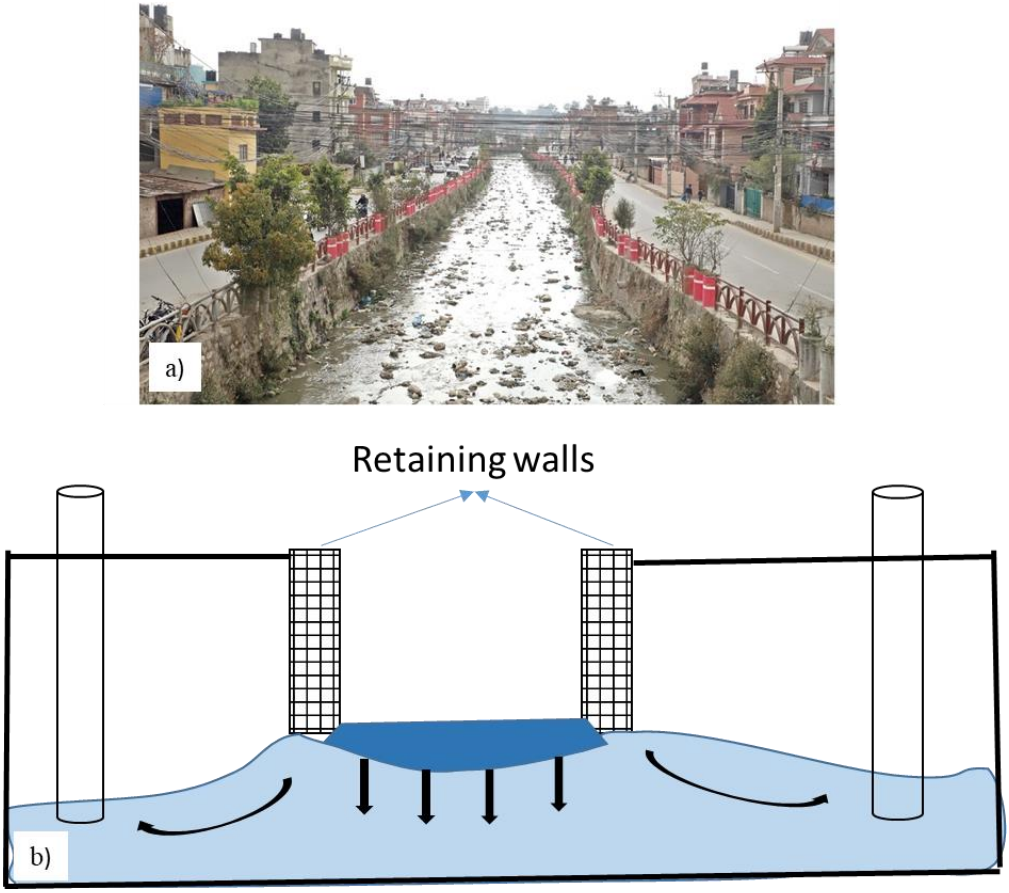

Figure 109: Water level in a) Dhobi Khola during dry season and b) schematic diagram showing water level in river channel and adjacent well

The areas of connection sites is important to identify within each river reaches. The connection condition can change water quantity and quality of both river and aquifers. It will be difficult to control quality of aquifer if it gets contaminated through polluted river water intrusion or vice-versa. Thus it need to study about interconnection condition of each river. From this present study, tentative areas of interconnection sites are identified. Mainly, aquifers located at the northern, southern and western part has tendency to interconnect with river in both seasons as they composed of coarse-materials. But in the case of central core urban areas, they possesses distinct condition in the wet and dry seasons.

The aquifer located upstream areas of the Bagmati river (upstream from Gokarna area), Dhobi, Godawari (Bishnudol area) and Nakhu Kholas shows influent condition in both seasons. Thus these areas can be used as bank storage during the wet season (Winter et al., 1998). Different engineering structures can be constructed in the riverbed and bank to reduce river velocity or to sustain river water long time in river channel so that the water can infiltrate more through the vertical and lateral infiltration. These activities can increase storing quantity of flooded water which indirectly increase the water level of that area and reduce peak discharge during wet season. Good management of storing flooded water in connected areas can be able to manage local scale water deficiency problem. But before planning these activities, it should know the quality of river water as it is directly related with human health.

The river-aquifer interconnection is also important for river restoration. Generally, river restoration is done to improve the river-aquifer connectivity by enlarging river channel and removing clogging material from riverbed (Hoehn and Scholtis, 2011). These activities can spatially and temporally changes the connection status. The groundwater near to rivers can suffer from contamination following river restoration activities. Thus before restoration operation in polluted rivers like of the Kathmandu valley, it need to improve river channel as well as bank environment to minimize anticipated contamination.

4.8 Status of water quality in the Kathmandu Valley

Quality condition of river as well as groundwater is studied by using chemical concentration of different ions. Analyses of water samples on wet and dry seasons provide chemical quality status on these seasons.

4.8.1 Status of river water quality

Amount of chemical concentration dissolved in water indicates the quality condition or pollution of the river. Generally, water temperature, pH, DO, ions of sodium and chlorine, compounds of phosphorous and nitrogen is responsible for degradation of river water. Table 22 presents minimum and maximum value ranges of rivers in the wet and dry seasons. The water from all rivers of the Kathmandu Valley shows similar range of temperature in the wet (22 to 28°C) and dry season (12 to 18°C), except than few sites. River water has slightly high pH value, ranging from 6.7 to 8.8 during the wet season (Table 22) showing basic nature of water. Basically, water from southern tributaries as Godawari, Kodku, Nakhu and Balkhu Kholas presented high pH (>8) values in the wet season. The correlation tables given in Appendix 7 clearly showed that the pH values are significantly positively correlated with temperature but negatively correlated with all the chemical ions of water except NO_3^- -N. The relationship revealed that the value of pH of Kathmandu Valley river water is controlled by the climatic condition and mineralization of river from different sources (Ling *et al.*, 2017). The value of pH may also influenced by discharge rate of rivers and rates of contamination (Islam *et al.*, 2015).

The DO is one of essential parameter for preserving aquatic life (Chang, 2005). Depending on aquatic organism, levels of DO can be changed. Minimum level of DO for fisheries type is at 3 mg/L (US EPA, 1986). Commonly, upstream section of all valley rivers possesses good environment for aquatic lives as they possess high DO in both wet and dry seasons. But in the case of downstream section, they present insignificant (<1 mg/L) value except in the Godawari Khola, during the dry season (Tables of in-situ parameters in previous sections). The strong and negative correlation of DO with EC and dominant ions of water (Table 23), especially in the dry season, clearly signifies that the lower DO is the result of high total dissolve solids (Central water commission, 2019).

The increment in dissolve solids may occur due to human activity as dumping solid and sewer to rivers. Additionally, strongly positive correlation of DO with NO_3^- -N, (Appendix 7) in the Bagmati, Bishnumati, Manahara rivers and Dhobi Khola again indicates that the decrease in DO levels during the dry season may be the result of nitrification activity (Nienie *et al.*, 2017).

Table 22: Minimum and maximum values of in-situ and chemical ions in wet and dry season

River water		Bishnumati		Dhobi		Bagmati		Manahara		Hanumante		Godawari		Kodku		Nakhu		Balkhu	
Parameters (mg/L)		Min	Max	Min	Max	Min	Max	Min	Max	Min	Max	Min	Max	Min	Max	Min	Max	Min	Max
Wet Season	DO	0.6	6.4	0.0	6.3	2.4	6.4	3.5	6.1	4.0	6.5	4.3	7.0	1.0	6.6	5.6	6.2	1.5	6.1
	EC	148	439	117	809	41	290	62	892	164	247	277	388	282	521	225	321	169	779
	Temp	22.6	26.5	23.4	27.4	22.1	28.4	23.4	27.2	22.3	24.3	19.4	27.7	22.6	25.7	25.1	26.4	22.8	26.2
	pH	7.7	8.0	7.9	8.1	7.1	8.0	7.5	7.9	6.7	8.1	7.7	8.6	8.0	8.3	8.6	8.8	7.5	8.6
	Na^+	9.9	18.5	6.1	22.0	3.4	15.7	4.3	12.2	4.0	9.9	1.6	7.9	4.5	20.3	3.7	14.8	3.4	13.1
	$NH4^+$-N	0.9	4.5	0.3	10.2	0.1	3.5	0.1	1.9	0.3	0.9	0.0	0.1	0.0	3.3	0.2	0.8	0.4	1.9
	K^+	2.1	5.4	0.4	6.8	0.2	4.3	0.2	2.7	0.5	4.0	0.2	1.1	0.1	4.4	0.6	3.2	0.2	5.0
	Mg^{2+}	1.3	2.7	0.7	3.3	0.4	2.7	0.6	2.4	0.7	2.4	1.4	4.2	1.4	6.0	1.6	4.5	0.8	3.6
	Ca^{2+}	7.5	16.8	5.5	21.7	2.3	15.1	3.7	12.0	7.3	17.0	9.3	19.2	10.0	24.0	11.7	20.3	9.0	22.6
	Cl^-	6.4	18.0	2.9	23.5	1.1	14.1	1.2	11.8	2.2	8.7	1.2	9.3	2.3	25.4	2.3	15.2	3.0	14.8
	NO_3^--N	0.0	0.9	0.0	0.7	0.1	0.3	0.1	0.5	0.2	1.2	0.1	0.4	0.1	1.8	0.2	1.0	0.3	2.0
	PO_4^--P	0.2	2.4	0.3	3.0	0.3	1.9	0.4	1.1	0.2	0.6								
	SO_4^{2-}	3.9	9.8	1.9	11.6	0.6	7.9	1.1	6.6	2.5	9.8	1.0	6.9	1.9	10.0	1.7	6.2	3.0	12.5
	HCO_3^-	42.7	109.8	61.0	170.8	18.3	97.6	24.4	73.2	24.4	73.2	36.6	122.0	73.2	176.9	109.8	158.6	67.1	140.3
Dry Season	DO	0.1	4.8	0.1	4.7	0.0	9.9	0.0	8.5	0.1	5.5	3.8	11.7	0.1	8.8	1.2	8.3	0.0	8.3
	EC	364	1644	328	1472	151	1369	118	1364	604	2060	343	574	320	1494	264	1348	504	1810
	Temp	12.3	18.6	15.4	18.5	16.6	22.1	16.8	20.7	14.0	17.9	13.8	18.2	15.4	18.2	16.1	18.3	14.1	17.1
	pH	7.1	7.3	7.2	7.4	7.0	7.3	6.8	7.7	6.8	7.5	7.3	8.5	7.2	7.7	7.4	8.2	7.1	7.6
	Na^+	10.8	108.2	21.1	105.4	12.4	101.6	7.9	102.0	26.4	151.9	6.0	26.4	6.7	94.5	5.7	98.1	16.0	120.3
	$NH4^+$-N	3.6	83.6	7.9	80.0	0.1	69.1	0.1	63.6	10.3	102.9	0.1	8.8	0.3	63.4	0.1	61.2	0.8	81.5
	K^+	3.3	32.8	7.3	34.7	1.7	29.5	1.9	28.0	7.6	50.0	1.2	3.8	1.5	24.7	1.3	25.6	3.2	34.8
	Mg^{2+}	1.6	9.6	2.8	8.2	2.0	9.7	1.6	10.7	5.7	14.7	3.8	7.5	3.4	11.9	4.0	11.0	3.5	15.0
	Ca^{2+}	13.0	26.0	16.4	25.6	4.6	32.3	6.3	35.2	35.9	48.6	12.6	23.6	15.0	42.9	14.5	44.1	15.0	53.7
	Cl^-	12.2	129.3	21.7	127.0	4.3	112.1	3.7	110.0	23.7	186.3	9.3	42.9	7.9	116.9	4.8	114.1	20.6	158.6
	NO_3^--N	0.0	0.3	0.0	0.8	0.0	0.2	0.0	1.0	0.1	0.6	0.1	1.0	0.1	0.4	0.2	0.4	0.2	0.5
	PO_4^--P	2.7	15.2	3.7	16.2	0.4	17.8	0.0	12.5	2.4	31.7			2.3	13.3	10.8	10.8	2.6	13.5
	SO_4^{2-}	3.6	41.5	8.0	47.7	4.3	32.8	3.1	24.8	10.2	31.8	2.3	28.6	3.2	22.7	4.0	50.7	2.5	14.4
	HCO_3^-	85.4	530.7	122.0	530.7	54.9	536.8	48.8	567.3	280.6	884.5	67.1	152.5	73.2	585.6	91.5	494.1	103.7	793.0

Table 23: Correlation matrix of river water in the wet and dry seasons

River water wet season														
Parameters	DO	EC	Temp	pH	Na^+	NH_4^+-N	K^+	Mg^{2+}	Ca^{2+}	Cl^-	NO_3^--N	PO_4^--P	SO_4^{2-}	HCO_3^-
DO	1													
EC	-.470**	1												
Temp	-.414**	0.11	1.00											
pH	0.18	.278*	0.15	1										
Na^+	-.791**	.435**	.415**	0.00	1									
NH_4^+-N	-.833**	.476**	.360**	-0.04	.807**	1								
K^+	-.759**	.469**	.337**	0.02	.893**	.849**	1							
Mg^{2+}	-.349**	.529**	0.16	.317**	.644**	.363**	.563**	1						
Ca^{2+}	-.341**	.641**	0.14	.410**	.543**	.368**	.580**	.861**	1					
Cl^-	-.752**	.553**	.337**	0.10	.953**	.805**	.896**	.785**	.688**	1				
NO_3^--N	.248*	0.07	-.225*	0.05	-0.05	-.282*	0.07	0.12	.305**	-0.04	1			
PO_4^--P	-.903**	.541**	.402*	.434*	.831**	.906**	.877**	.751**	.743**	.900**	-.707**	1		
SO_4^{2-}	-.652**	.475**	.264*	0.04	.719**	.585**	.804**	.566**	.677**	.737**	.401**	.719**	1	
HCO_3^-	-.427**	.640**	.332**	.423**	.589**	.500**	.580**	.790**	.812**	.727**	0.09	.862**	.549**	1
River water dry season														
Parameters	DO	EC	Temp	pH	Na^+	NH_4^+-N	K^+	Mg^{2+}	Ca^{2+}	Cl^-	NO_3^--N	PO_4^--P	SO_4^{2-}	HCO_3^-
DO	1													
EC	-.773**	1												
Temp	-0.18	-0.05	1											
pH	.599**	-.496**	-0.16	1										
Na^+	-.813**	.941**	0.06	-.524**	1									
NH_4^+-N	-.750**	.894**	0.01	-.477**	.904**	1								
K^+	-.780**	.946**	-0.01	-.533**	.960**	.928**	1							
Mg^{2+}	-.699**	.904**	-0.05	-.354**	.885**	.797**	.859**	1						
Ca^{2+}	-.538**	.770**	-0.17	-.325**	.708**	.611**	.671**	.877**	1					
Cl^-	-.801**	.961**	0.01	-.492**	.987**	.907**	.966**	.918**	.746**	1				
NO_3^--N	.419**	-0.16	-0.16	0.18	-0.20	-0.19	-0.14	-0.06	0.11	-0.17	1			
PO_4^--P	-.664**	.888**	-0.10	-.351**	.830**	.867**	.910**	.729**	.459**	.831**	-0.06	1		
SO_4^{2-}	-.633**	.545**	0.17	-.358**	.651**	.653**	.635**	.398**	0.202	.614**	-.477**	.439**	1	
HCO_3^-	-.759**	.949**	-0.01	-.508**	.956**	.893**	.952**	.935**	.814**	.968**	-0.07	.820**	.494**	1
**. Correlation is significant at the 0.01 level (2-tailed).														
*. Correlation is significant at the 0.05 level (2-tailed).														

Generally, low range of EC, varying from 41 to 892 µS/cm is measured in the wet season. The value of EC is significantly increased in the dry season with value variation from 118 to 2060 µS/cm (Table 22). The increment rate is different for different rivers as well as for different river sections. Basically, upstream sections of all rivers have low increment rate (1.5 to 3 times) whereas downstream sections presents high rate of increment (4 to more than 9 times). The water from the Hanumante Khola shows higher

EC value as well as higher increment rate (Table 13) and the Godawari river water presents low EC with lower increment rate (Table 14). The EC has significantly positive correlation with all chemical ions (Appendix 7 and Table 23) indicating full dependency of conductivity of river water on dissolved ion concentration (Ganiyo *et al.*, 2018). The higher EC and strong correlation again signifies higher anthropogenic contamination (Bhat *et al.*, 2014).

Figure 110 presents clear picture of spatial-temporal variation of chemical parameters along and among rivers of the Kathmandu Valley. Basically, river water possesses dominancy of Ca^{2+} and HCO_3^- ions in the wet season. The dominancy of Ca^{2+} is changed to Na^+ during the dry season (Figure 110). Except few ions, most of chemical ions show significant temporal variation ($p<0.01$) (Table 22 and Figure 110). However all rivers show increment of ions toward downstream, the rate of increment is very low in the Godawari Khola. Previous research on river quality also reported increment of concentration at urbanized downstream areas (Ha and Pokhrel, 2001;Kannel *et al.*, 2007; Pathak *et al.*, 2015)

Correlation matrix shows strong positive correlation of Na^+, K^+, NH_4^+-N, Ca^{2+}, Mg^{2+}, Cl^-, HCO_3^-, PO_4^--P, and SO_4^{2-} between each other (Table 23). It indicates that river water is highly influenced by anthropogenic pollution (Figure 111) (Mencio and Mas-Pla, 2008) such as direct discharge of municipal and industrial sewage and leachate of solid waste disposal near the river channel during the dry season (Pathak *et al.*, 2015). The concentration of NH_4^+-N and PO_4^--P is drastically increased during dry season in all river water, except Godawari Khola. The PO_4^--P is completely absent in the water of the Godawari Khola (Figure 110 and Table 22). Increased concentration of phosphorous in rivers is the indication of eutrophication which decreases level of DO (Davie, 2003). Negative and strong correlation of DO and PO_4^--P signifies process of eutrophication in the rivers. Strong positive correlation existence of PO_4^--P with SO_4^{2-} in most of rivers also suggests the influence of fertilizer and pesticides used in the cultivated land of river peripheral areas (Baht *et al.*, 2014; El Alfy and Merkel, 2004 and Zhong *et al.*, 2018).

Based on dominant ions, river waters from the wet seasons are classified as Ca-HCO_3^-. The water type remains same for the southern rivers like Godawari, Kodku and Nakhu Khola except few location (Appendix 5F,5G and 5H) during the dry season. But in the case of northern rivers, dominancy of river waters are changed to Na-K-HCO_3 type during the dry season (Figure 112 and Appendix 5).

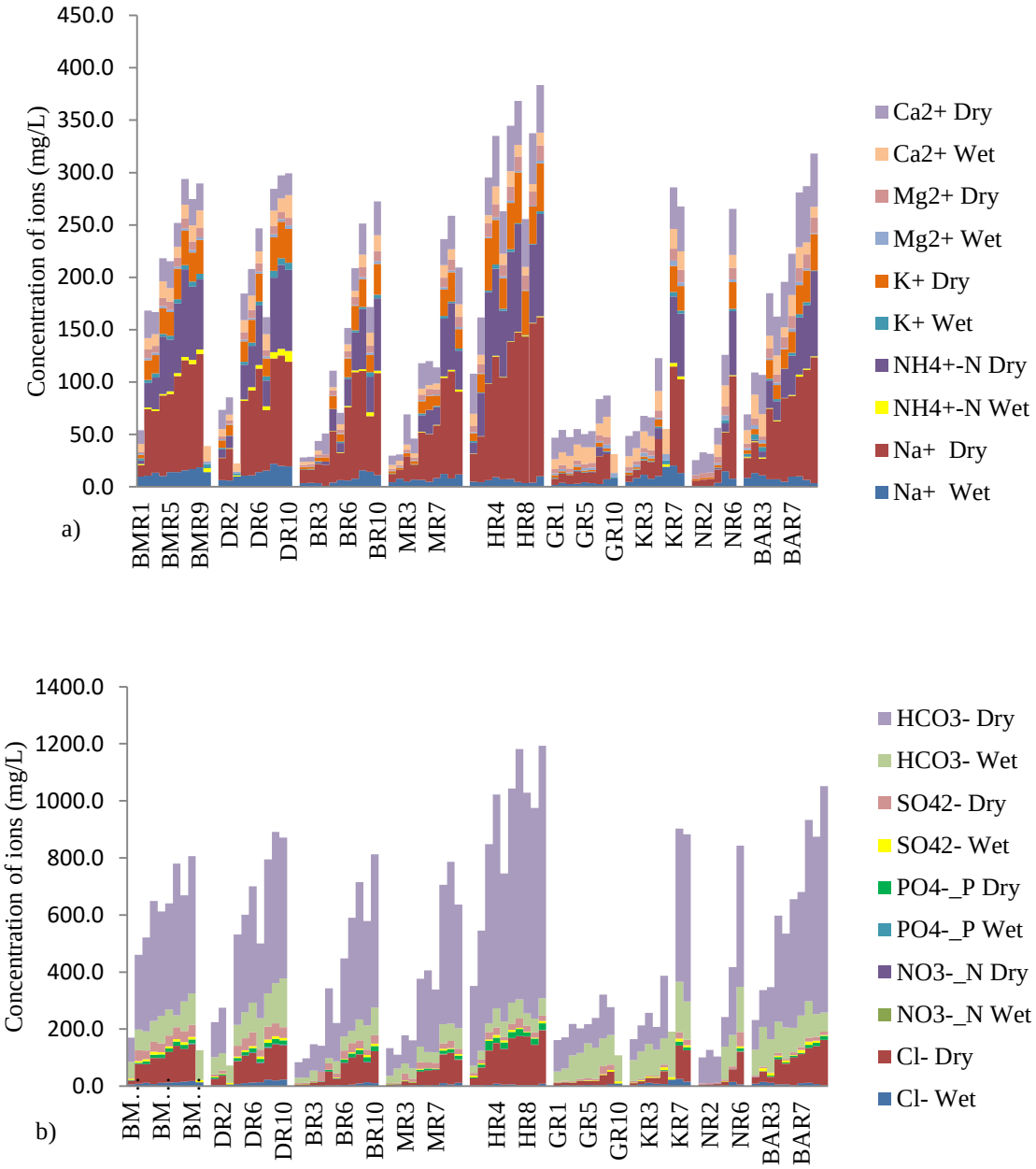

Figure 110: Spatial-temporal variation of cation (a) and anion (b) in Kathmandu Valley Rivers

Determination of water type using piper diagram also suggests the origin of water (Singh and Kumar, 2015). Ca-HCO_3 type represents recent infiltration of freshwater, whereas Na-K-HCO_3 types indicate water exhibiting simple dissolution or mixing (Al-Khatib and Al-Najar, 2011). River water from the wet season of Ca-HCO_3 type thus represents recent rainfall and runoff as a major contributing source for river discharge. The plotting of all river samples close or near to LMWL in δD verses $\delta^{18}O$ also signifies rainfall as major source. Changes in river water type during the dry season reflect the presence of different water sources for river discharge, including direct discharge of untreated sewage from municipal and industrial sources (Zhu *et al.*, 2019).

Figure 111: Anthropogenic pollution at a) Hanumante Khola b) Bagmati River c) and d) Bishnumati River

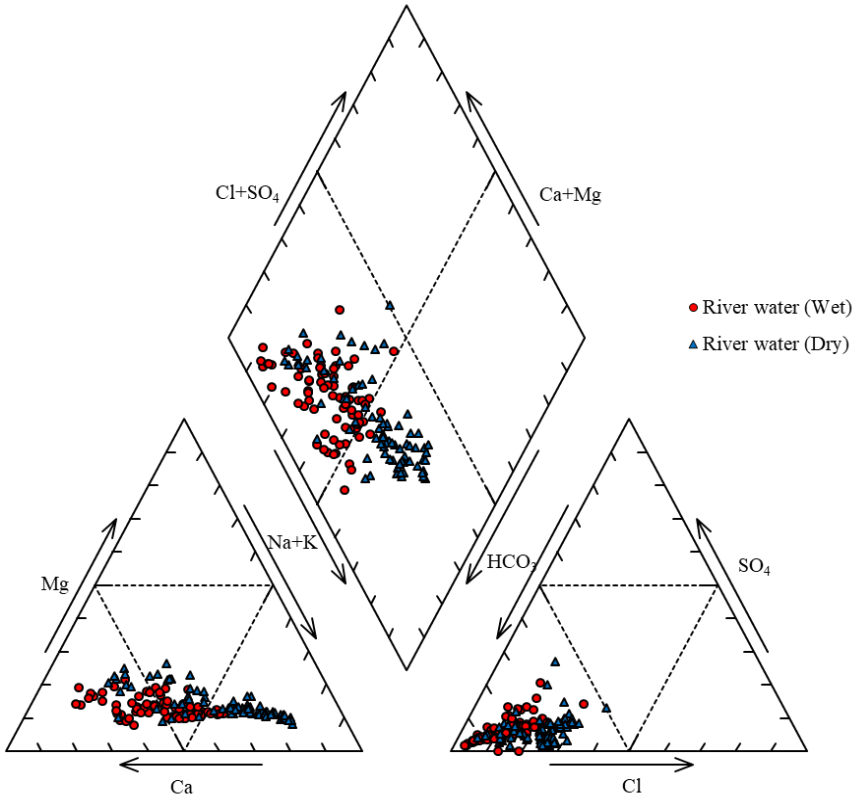

Figure 112: Piper diagram of river water in the wet and dry seasons

The HCA is carried out for the dry season data for grouping of spatially located river locations into clusters. Dominant parameters like EC, Na^+, NH_4^+–N, Cl^- and HCO_3^- are used for HCA. Mainly two major clusters are generated in the dendogram (Figure 113). Cluster A is divided into two sub-cluster A1 and A2. Sub-cluster A1 encloses sites mainly from less urban area of the upstream section of rivers except the Hanumante Khola and show least value range among clusters indicating less polluted zone of the Kathmandu valley. Similarly, Sub-cluster A2 comprises river sites from middle section of the rivers and possesses slightly increased value range comparing to A1.

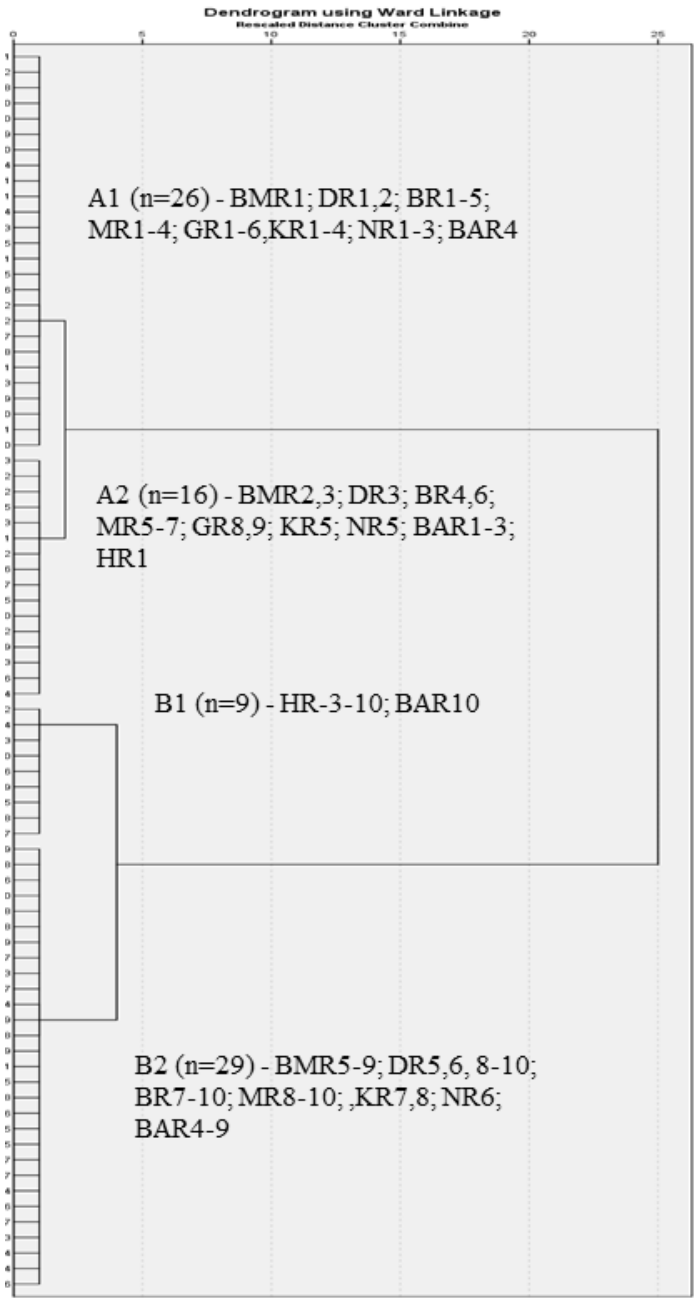

Figure 113: Dendogram with ward linkage and Euclidean distance obtained from dry season river water

Conversely, Cluster B (B1 and B2) consists of downstream river sites, especially located at highly urbanized areas of the Kathmandu valley. Sub-cluster B1 mainly contains river sites from the Hanumante Khola and presents highest value range, indicating highly polluted zone of the Kathmandu Valley. Comparing to B1, lower value range is obtained in sub-cluster B1, which consists of downstream section of the remaining rivers. This HCA clearly signifies that the Hanumante Khola is one of most polluted river in the Kathmandu Valley.

Table 24: Value range of parameters of clusters formed in dendogram

Season	RW Cluster No.		Data range	EC µc/cm	Na^+ mg/l	NH_4-N_mg/l	Cl^- mg/l	HCO_3^- mg/l
Dry	Cluster A	A1 (n=26)	Min	118.5	5.7	0.0	3.7	48.8
			Max	439.0	30.3	11.5	34.3	158.6
		A2 (n=16)	Min	264.0	5.7	0.1	4.8	91.5
			Max	956.0	71.3	33.1	79.4	329.4
	Cluster B	B1 (n=9)	Min	1780.0	92.2	63.0	120.7	518.5
			Max	2060.0	151.9	102.9	186.3	884.5
		B2 (n= 29)	Min	1037.0	43.7	18.4	63.0	262.3
			Max	1644.0	108.2	83.6	132.3	634.4

4.8.2 Status of groundwater quality

The value range of in-situ and chemical ions of groundwater is presented in Table 25. Alike in river water, the temperature of Kathmandu Valley groundwater also possesses a similar range, varying from 19 to 26°C and 14 to 20°C in the wet and dry seasons respectively. The pH value is slightly high, except in a few sites, in the wet season presenting alkaline nature. Contrarily, groundwater's pH is low, making the water slightly acidic during the dry season (Table 25). The 1.39% and 10.41% of groundwater samples collected from the wet and dry seasons respectively exceed the limit (6.5 to 8.5) set by Nepal Drinking Water Quality Standards (NDWQS) (Figure 114). Only groundwater from the Bishnumati River exceeds the NDWQS limit in the wet season while groundwater from all river corridors, except the Kodku Khola, exceeds the limit during the dry season (Figure 115) showing its acidic nature.

The range of DO varies from 0.3 to 6.4 mg/L and 0.3 to 7.4 mg/L in the wet and dry seasons respectively. DO shows random variation along each river section of the seasons. It has weak correlation conditions with chemical ions as well as with EC relative to a river (Appendix 7 and Table 26). The EC varies from 94 to 1656 µS/cm in

the wet season and from 116 to 2270 µS/cm in the dry season. Groundwater exhibits higher EC in the dry season relative to the wet season, except few sites. Furthermore, EC is high towards the downstream section in all river corridors.

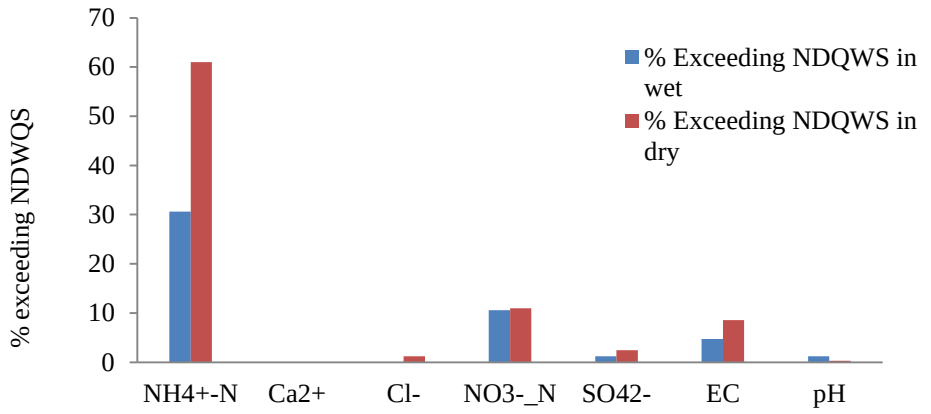

Figure 114: Dug well % and chemical ions exceeding limit of NDWQS

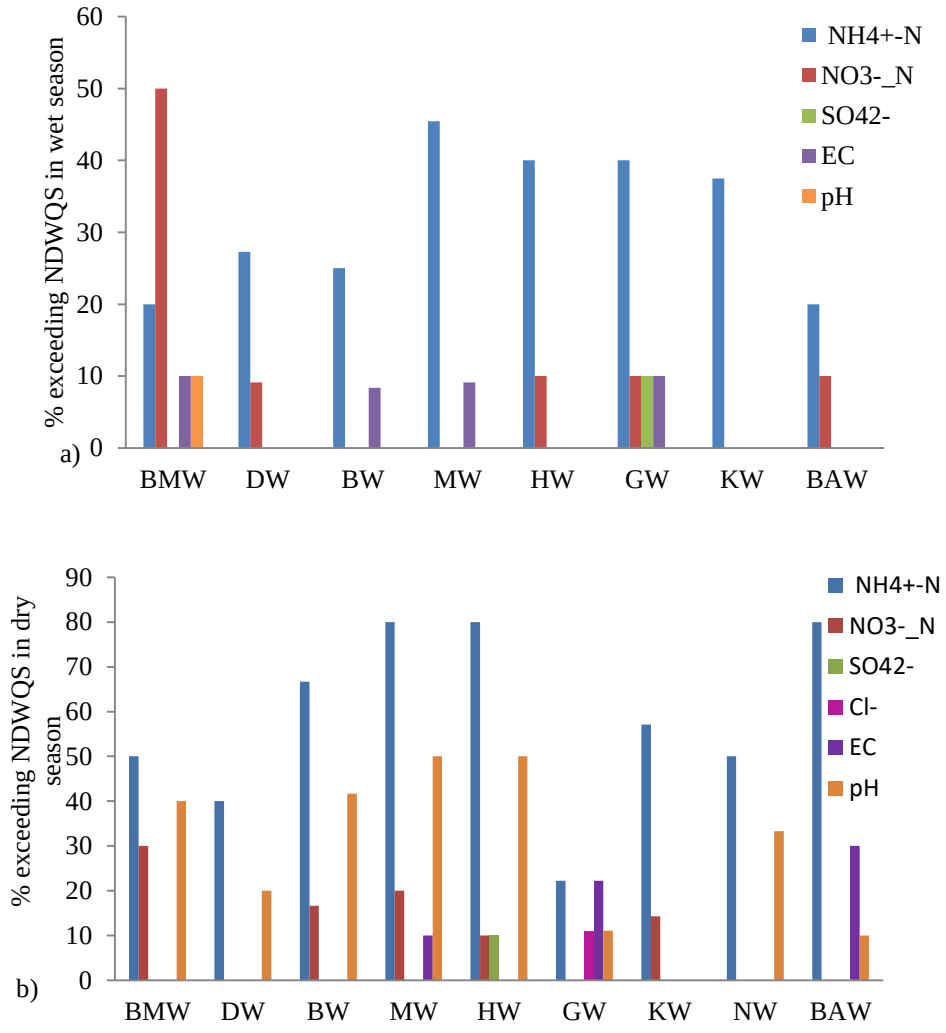

Figure 115: Bar diagram showing % of groundwater from rivers exceeding NDWQS in a) wet and b) dry season

Table 25: Minimum and Maximum values of in-situ and chemical ions in wet and dry season

Groundwater		Bishnumati		Dhobi		Bagmati		Manahara		Hanumante		Godawari		Kodku		Nakhu		Balkhu	
Parameters (mg/L)		Min	Max	Min	Max	Min	Max	Min	Max	Min	Max	Min	Max	Min	Max	Min	Max	Min	Max
Wet Season	DO	0.3	3.7	0.5	3.8	0.5	4.7	0.5	2.9	1.1	4.1	1.0	5.2	0.4	5.0	1.0	2.5	1.6	6.4
	EC	334	1536	114	1196	94	1413	235	1656	290	934	299	1575	341	1204	666	937	273	1239
	Temp	21.6	24.7	20.7	24.5	21.7	25.7	21.0	24.7	20.7	24.1	19.6	25.2	20.0	24.8	21.6	24.6	22.2	25.1
	pH	5.3	7.5	6.9	8.1	7.0	7.8	6.7	7.7	6.7	8.1	7.1	7.7	7.1	8.2	6.9	7.9	7.5	8.6
	Na^+	7.4	50.4	4.0	31.6	3.3	30.7	6.0	29.6	6.7	37.6	1.7	39.1	4.3	33.5	8.8	23.0	1.4	30.5
	$NH4^+$-N	0.0	3.3	0.1	13.6	0.0	5.4	0.1	25.4	0.1	8.7	0.0	11.9	0.0	7.1	0.3	1.0	0.1	4.6
	K^+	2.7	23.3	0.4	13.3	0.2	30.1	0.3	5.2	0.7	17.3	0.0	15.6	0.6	3.5	1.0	4.0	0.4	8.2
	Mg^{2+}	2.2	19.3	0.7	10.6	0.5	14.0	0.8	13.9	1.6	20.4	0.8	15.7	1.5	10.6	2.4	7.1	1.0	14.3
	Ca^{2+}	22.1	82.9	5.4	84.6	4.1	49.2	6.2	65.6	11.7	72.5	12.2	99.2	10.2	53.1	21.8	41.6	7.9	78.7
	Cl^-	3.3	57.2	0.5	42.8	1.0	35.9	3.3	34.6	4.8	56.6	1.0	67.2	3.5	58.3	6.5	31.6	0.8	57.4
	NO_3^-_N	0.8	32.2	0.0	19.9	0.0	8.5	0.3	7.7	0.0	14.8	0.0	20.4	0.2	8.1	0.5	1.2	0.1	16.1
	PO_4^-_P	0.7	3.0	1.0	12.7	0.2	5.3	1.7	5.0	0.0	6.3	0.4	0.7	0.0	0.0			0.3	0.9
	SO_4^{2-}	8.3	126.0	3.2	113.1	0.1	75.7	2.9	54.3	5.0	113.8	0.3	262.5	3.7	46.1	9.9	18.6	1.3	101.9
	HCO_3^-	109.8	183.0	1.2	237.9	42.7	201.3	30.5	408.7	67.1	305.0	79.3	225.7	73.2	280.6	97.6	207.4	54.9	237.9
Dry season	DO	0.7	5.5	1.7	4.7	0.3	4.5	0.5	7.4	0.4	2.3	0.4	5.7	0.4	5.8	0.5	2.3	0.5	3.4
	EC	256	1667	116	1274	158	1351	294	1573	576	1323	326	1980	369	1040	282	1222	571	2270
	Temp	14.2	20.3	15.5	19.4	15.0	20.4	16.5	21.0	13.4	20.5	13.2	19.6	13.3	20.0	14.6	18.4	14.1	18.4
	pH	6.3	7.6	6.2	7.5	5.9	7.1	6.1	7.4	6.1	7.4	6.4	7.3	6.5	7.3	6.3	7.1	6.2	7.9
	Na^+	13.3	98.6	6.2	59.5	8.1	60.8	16.6	87.4	14.4	78.8	2.6	144.2	5.4	68.4	6.3	43.1	11.0	106.1
	$NH4^+$-N	0.3	6.2	0.1	35.4	0.0	55.8	0.1	32.5	0.4	31.3	0.1	13.4	0.1	17.8	0.1	7.6	0.1	66.0
	K^+	5.4	26.7	0.7	21.4	2.0	19.8	1.6	25.1	1.3	44.3	0.3	15.7	0.8	9.6	0.7	9.6	0.9	25.1
	Mg^{2+}	2.9	43.0	1.2	11.7	2.4	48.7	3.2	35.4	9.3	28.8	2.2	49.8	1.8	21.4	4.9	15.0	7.2	36.6
	Ca^{2+}	7.8	131.6	5.7	33.5	9.1	55.6	11.6	58.2	28.4	93.7	14.5	84.1	17.6	44.4	15.1	29.3	15.1	47.8
	Cl^-	16.5	133.1	0.4	80.4	5.5	90.7	8.6	99.1	17.6	94.7	4.8	323.5	4.7	108.7	5.9	75.2	22.3	169.1
	NO_3^-_N	0.4	24.9	0.0	3.9	0.0	21.1	0.0	27.0	0.1	14.1	0.0	4.7	0.1	24.9	0.0	9.4	0.0	9.2
	PO_4^-_P	0.0	1.0	0.0	1.0	0.0	5.4	0.1	6.4	0.0	8.3								
	SO_4^{2-}	2.2	348.0	0.1	59.7	0.4	117.0	6.0	103.1	6.2	272.4	1.1	189.9	1.3	53.4	0.5	13.7	1.2	93.5
	HCO_3^-	54.9	109.8	67.1	420.9	42.7	542.9	48.8	402.6	122.0	579.5	73.2	256.2	85.4	317.2	122.0	219.6	109.8	585.6

The percentage of groundwater EC exceeding NDWQS limit (1500 µS/cm) is also high in the dry season (8.54%) in relative to the wet season (4.71%) (Figure 114). Groundwater from the Bishnumati, Bagmati and Manahara Rivers; and Godawari Khola exceeds limit of NDWQS in the wet season. Similarly, groundwater of Manahara, Godawari and Balkhu Khola exceeds limit during the dry season (Figure 115). EC shows strong positive correlation with most dominant ions.

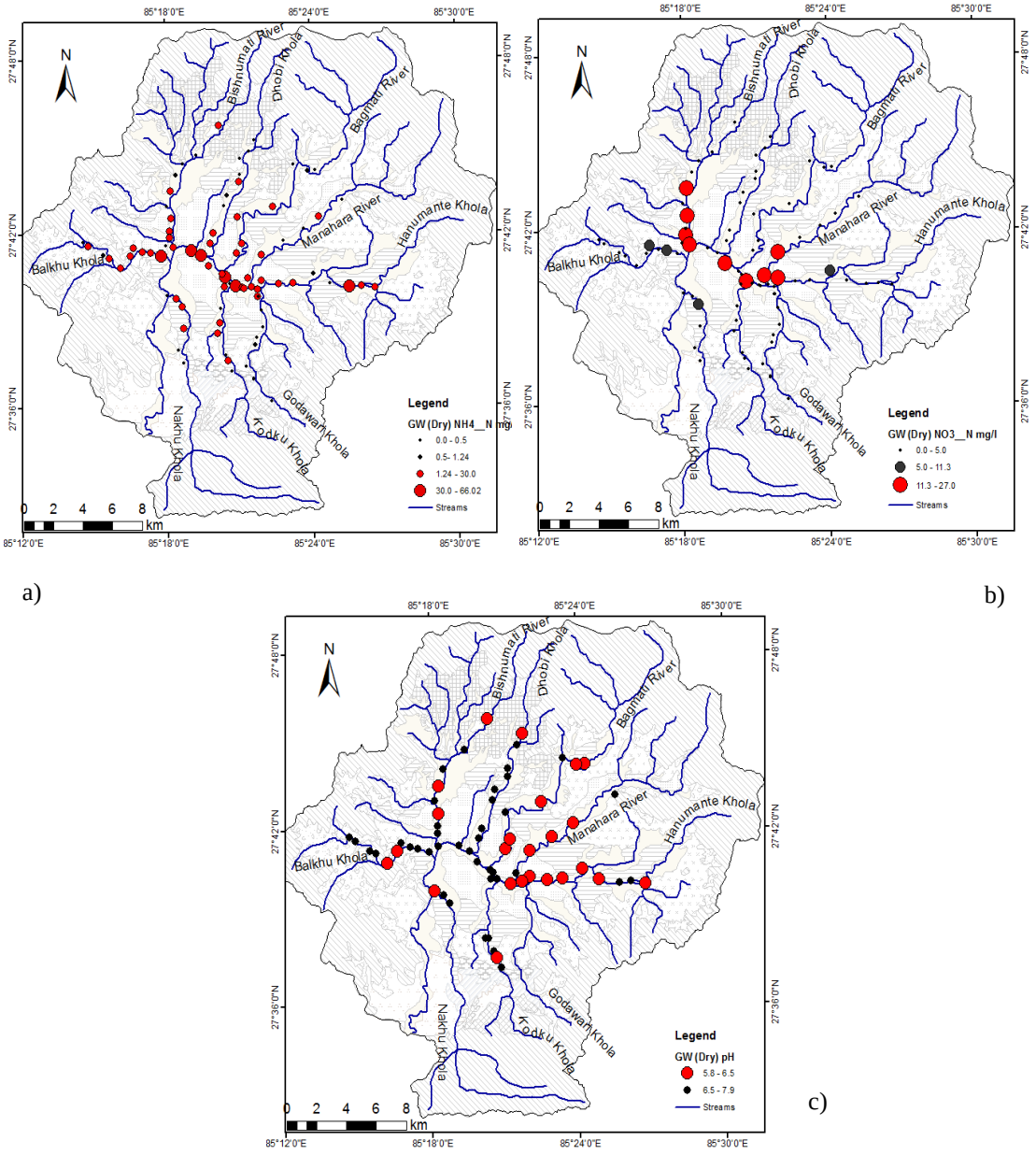

Figure 116: Spatial distribution of chemical parameters exceeding NDWQS a) NH_4-N b) NO_3-N and c) pH

Groundwater is basically dominant of Ca^{2+}, Na^{+} and HCO_3^{-} ions in the wet and dry seasons (Figure 117). Geologically, the dominant rock composition of the northern and

southern parts of the Kathmandu Valley is different. The northern hills of the valley are mainly composed of gneiss rocks. The fluvial deposits as well as river banks also have dominant gravels composed of gneiss rocks. In the case of the southern part, the hills are composed of limestone and the gravels of terrace deposits have also similar composition. However, the rock and gravel composition of the valley is different, the groundwater from the northern and southern parts shows similar dominant ions in both seasons (Figure 117). The dominance of groundwater is also classified as Ca-HCO_3 type in the wet and dry seasons. Only certain sites from the Bishnumati, Dhobi, and Godawari rivers are classified as Ca-SO_4 type in the wet season. Similarly, certain sites from all corridors show water types of Ca-SO_4, Na-K- HCO_3 and Ca-Cl-SO_4 (Appendix 5 and Figure 119).

Generally, the water type of groundwater is dependent on the geological material through which the water flows and the residence time of contact with these materials. Most of the previous research discusses water-rock reaction effects on groundwater chemistry (Elango and Kannan, 2007; Panno Hackley, 2010; Baba and Gunduz, 2017). Shakya *et al*., (2019a) also present the effects of geological material from the northern part of the Kathmandu Valley to the deep groundwater. They presented that the Na-K-HCO_3 water type of deep groundwater is the result of the weathered minerals of gneiss and long-term residence time. But in the present study, the water type from the northern tributaries like the Bishnumati, Dhobi and Bagmati Rivers (Figure 1) is classified as Ca-HCO_3 type which differs from the water type of deep groundwater defined by Shakya *et al*. (2019a). Basically, the Ca-HCO_3 water type is formed by the dissolution of calcite (Elango and Kannan, 2007) which is not available in the northern part. This indicates that the chemical concentration of northern shallow groundwater has less reflection of geological material.

The groundwater from the southern corridors (Godawari, Kodku and Nakhu) is also classified as Ca-HCO_3 type. The dominancy of Ca^{2+} and HCO_3^- is possibly from the dissolution of carbonate rocks of the southern terrain. These results show a distinct reflection of geological materials on the northern and southern shallow groundwater of the Kathmandu Valley. The gneiss rock, dominant in northern terrain, basically has high resistance to chemical weathering while the southern terrain dominant carbonate rock has low resistance to chemical weathering (Elango and Kannan, 2007). In the meantime, the groundwater collected from shallow dug wells (1.1 to 15.7 m) has very low

residence time to interact with geological materials. Some of the dug wells are completely dry during the dry season. As a result, the northern shallow groundwater reflects less effect of the water-rock reaction on groundwater chemistry compared to the southern groundwater.

Table 26: Correlation matrix of groundwater in wet and dry season

Groundwater wet season														
Parameters	DO	EC	Temp	pH	Na^+	NH_4^+-N	K^+	Mg^{2+}	Ca^{2+}	Cl^-	NO_3^--N	PO_4^--P	SO_4^{2-}	HCO_3^-
DO	1													
EC	-0.17	1												
Temp	-0.13	-0.21	1											
pH	.390**	-0.13	.266*	1										
Na^+	-0.20	.665**	-0.04	-0.17	1									
NH_4^+-N	-.246*	.469**	-0.15	0.10	0.21	1								
K^+	-0.17	.331**	0.16	-0.05	.553**	0.12	1							
Mg^{2+}	-0.06	.690**	-0.19	-0.05	.823**	.311**	.454**	1						
Ca^{2+}	-0.08	.694**	-0.17	-0.21	.843**	0.15	.493**	.795**	1					
Cl^-	-0.09	.612**	-0.14	-0.07	.912**	0.17	.423**	.843**	.801**	1				
NO_3^--N	-0.02	.264*	0.09	-0.10	.626**	-0.18	.423**	.527**	.587**	.605**	1			
PO_4^--P	-0.17	-0.10	0.08	.482*	-0.04	.456*	0.03	0.03	-0.12	-0.07	-0.14	1		
SO_4^{2-}	-0.01	.531**	-0.16	-.255*	.626**	0.09	.499**	.606**	.791**	.543**	.355**	0.01	1	
HCO_3^-	-0.20	.679**	-0.17	0.03	.578**	.565**	.262*	.664**	.607**	.527**	0.05	-0.15	.269*	1
Groundwater dry season														
Parameters	DO	EC	Temp	pH	Na^+	NH_4^+-N	K^+	Mg^{2+}	Ca^{2+}	Cl^-	NO_3^--N	PO_4^--P	SO_4^{2-}	HCO_3^-
DO	1													
EC	-0.16	1												
Temp	-0.21	.226*	1											
pH	.246*	.294**	-0.12	1										
Na^+	-0.10	.694**	0.12	0.14	1									
NH_4^+-N	-.303**	.541**	.319**	0.15	.447**	1								
K^+	-0.14	.536**	.269*	0.04	.523**	.489**	1							
Mg^{2+}	-0.12	.651**	0.06	0.18	.819**	.332**	.382**	1						
Ca^{2+}	-0.06	.471**	0.13	-0.05	.371**	0.06	.380**	.404**	1					
Cl^-	-0.06	.586**	0.05	0.10	.917**	.277*	.383**	.795**	.304**	1				
NO_3^--N	0.19	.266*	0.05	0.05	.383**	-0.10	.299**	.429**	.348**	.276*	1			
PO_4^--P	-.398*	0.33	.424*	0.23	0.17	.723**	.391*	0.25	0.22	-0.11	0.02	1.00		
SO_4^{2-}	0.07	.366**	0.01	-0.06	.305**	-0.09	.220*	.300**	.813**	.240*	.317**	-0.21	1.00	
HCO_3^-	-.344**	.588**	.299**	0.15	.524**	.880**	.561**	.497**	0.14	.347**	-0.03	.758**	-0.18	1
*. Correlation is significant at the 0.05 level (2-tailed).														
**. Correlation is significant at the 0.01 level (2-tailed).														

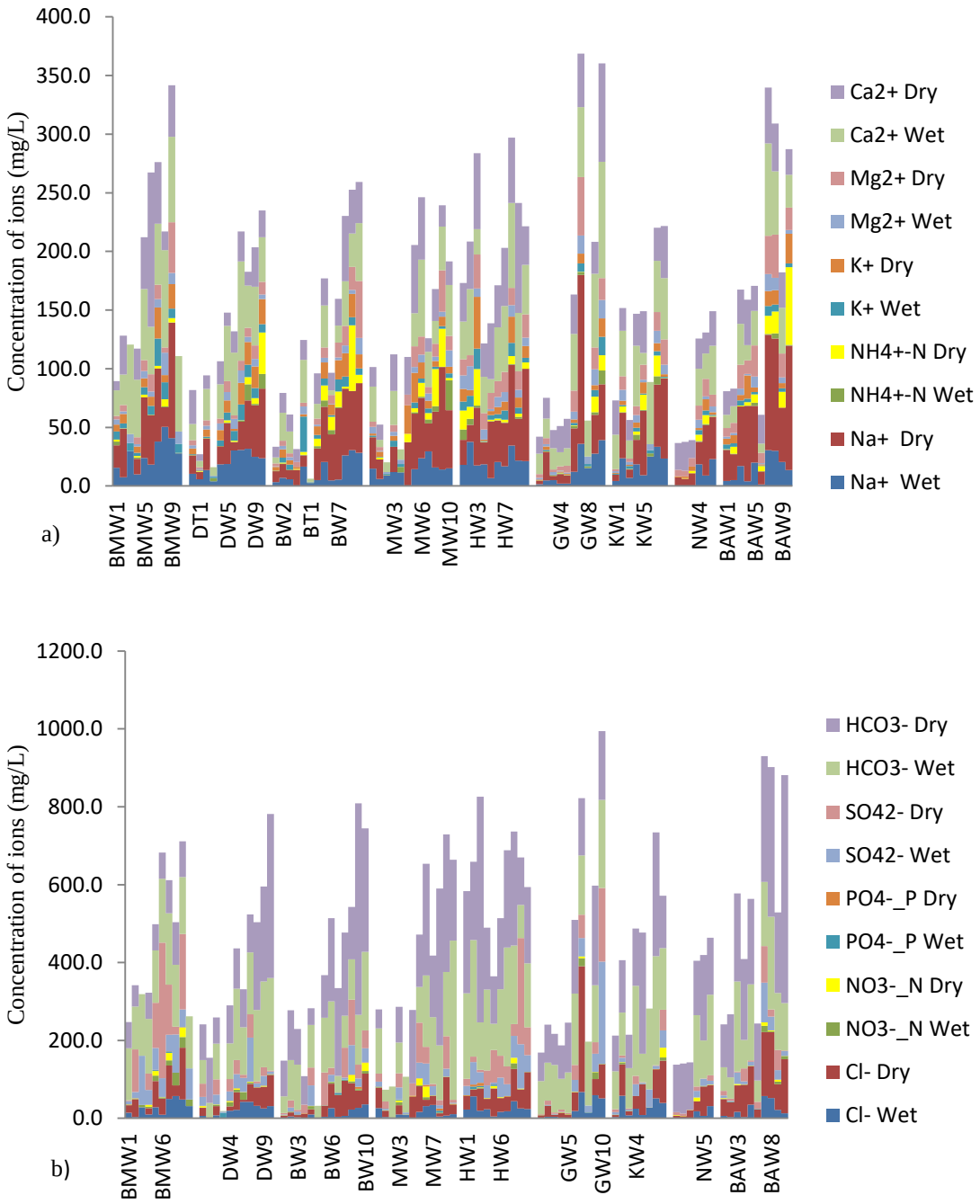

Figure 117: Spatial-temporal variation of cation (a) and anion (b) in the Kathmandu Valley groundwater

Additionally, the Ca-HCO_3 water type represents the recent infiltration of freshwater (Al-Khatib and Al-Najar, 2011). The plotting of groundwater, except for certain sites, close or near to the LMWL in δD versus $\delta^{18}O$ also signifies rainfall as a major recharge source for these dug wells. The surficial sediment variation along the river corridors (earlier described in 4.1.1 sediment distribution pattern map) also presents the possibility of rainfall infiltration to the groundwater. Furthermore, the result obtained from the interconnection suggests the effects of polluted river water on shallow

groundwater chemistry in the dry season. The change in water type in certain sites also represents a mixture of recharge sources during the dry season.

The concentration of ions is spatial and temporally variable (Figure 117). The groundwater sampled from the downstream section, especially located in core urban areas has a higher concentration. The groundwater collected from the upstream rural section of the Nakhu and Godawari Kholas exhibits a very lower concentration while groundwater from the downstream urban section of the Godawari Khola shows a higher concentration of ions. The significant positive correlation of Na^+, K^+, NH_4^+-N, Ca^{2+}, Mg^{2+}, Cl^-, HCO_3^- and SO_4^{2-} between each other (Table 26) indicate an influence of anthropogenic pollution on groundwater chemistry. In the case of temporal variation, only fewer ions show significant variation (paired t-test within 95% confidence level) while the type of ions changed with different river corridors. Basically, Mg^{2+}, Na^+, K^+ and Cl^- possess significant increments in the Bagmati River and the Hanumante, Godawari, and Balkhu Khola. The concentration of SO_4^- and Cl^- is increased in a few groundwaters of the Godawari and Hanumante Khola exceeding limits of NDWQS (250 mg/L) (Figure 114 and Figure 115).

The concentration of PO_4^--P is nearly absent in the southern corridors like Godawari, Kodku, Nakhu and Balkhu Kholas (Table 25) in both seasons. Contrarily, concentration is drastically increased in some wells of the northern corridors both in the wet (1 to 12.7 mg/L) and dry seasons (1 to 8 mg/L). The PO_4^--P concentration can be increased by detergent and industrial wastes (Soltan 1991) together with sewage and fertilizers (Karafistan *et al*., 2002). The rapid growth of urbanization (Ishtiaque *et al*., 2017), sewer leakage and the use of detergent for households may be one of the responsible reasons to obtain higher concentrations from specific sites of the northern corridors. But in the case of southern corridors, cultivated land is still dominated along the river corridors. The absence of PO_4^--P in southern groundwater indicates that agricultural activities such as fertilizers and pesticides have a lower effect on the PO_4^--P concentration of groundwater as compared to human wastes obtained in central and northern areas of the valley. In addition, the absence of the PO_4^--P concentration reflects that the sewage source is not closely located with dug wells (Warner *et al*., 2008).

In the case of NH_4^+-N and NO_3^--N, concentrations are abruptly increased in some specific sites of river corridors, exceeding limits (1.24 and 11.3 mg/L respectively) of

NDWQS. The percentage of groundwater, exceeding the limit of NH_4^+-N is increased by double in the dry season (60.98%) as compared to the wet season (30.5%) (Figure 114). A certain percentage of groundwater from all the river corridors exceeds the limit of NDWQS. But a higher percentage exceeding the limit is observed from the groundwater along the Manahara, Hanumante, Godawari and Kodku corridors in the wet season while from the Bagmati, Manahara, Hanumante, and Balkhu corridors during the dry seasons (Figure 115 and Figure 116a). The observed value range is low in the groundwater of the Bishnumati and Nakhu corridors in both seasons (Appendix 4). Except for certain sites, almost groundwater from nine corridors shows higher NH_4^+-N during the dry season (Figure 117a) even though the presence of different geological materials. Contrarily, Shakya *et al*., (2019b) explained that the NH_4^+-N concentration is higher in gravel aquifers during the dry season and nearly constant in the clay aquifer throughout the wet and dry seasons. They also reported that the high concentration of NH_4^+-N during the dry season is the result of the mineralization of organic matter such as the continued loading of solid and liquid wastes. The occurrences of higher NH_4^+-N concentration at the core central area of the Kathmandu Valley (Figure 116a) reveal similar types of NH_4^+-N sources for shallow groundwater. An analysis of NH_4^+-N in Kathmandu's sewer by Nakamura *et al*., (2014) also reported a very high-value range (46 to 175 mg/L). On the other hand, the observation of lower concentration during the wet season may be the effect of oxidation of NH_4^+-N from the infiltrated oxygen-enriched rainfall.

Compared to NH_4^+-N, the groundwater percentage exceeding the limit of NO_3^--N (NDWQS) is lower in both seasons (Figure 114). The exceeding percentage of groundwater collected from the Bishnumati corridor has higher relative to the remaining corridors (Figure 115). The value range of NO_3^--N is varied from 0 to 32.2 mg/L in the wet season and 0 to 27.9 mg/L in the dry season (Figure 117 and Table 25). Though this study period shows a high concentration of NO_3^--N, previous research reported a slightly decreasing trend over the period from 1990 to 2008 (Pathak *et al*., 2011). During both seasons, higher values are recorded from the northern and central areas of the Kathmandu Valley (Figure 116b). Pathak *et al*., (2013) and Bittner (2000) also presented a higher value of 26 mg/L and 63.3 mg/L respectively from the northern shallow groundwater of the valley. The previous research found that the concentration of NO_3^--N of shallow groundwater of the Kathmandu Valley is higher in the wet season

relative to the dry season (Pathak *et al*., 2013; Shakya *et al*., 2019b). In contrast, this study shows mix types of increments in the wet and dry seasons indicating site-specific conditions. For example, the dominant groundwater collected from the Bishnumati has a higher concentration of NO_3^--N in the wet season while some sites from other rivers have higher concentrations in the dry season (Appendix 4). But the overall areas which show higher concentration is located at the core urban areas of the valley (Figure 116b) which is similar to the result presented by Pathak *et al*., (2009). This result exhibits that urban sources contribute more nitrate contamination than agricultural activities. An analysis of nitrate-nitrogen and oxygen isotopes by Nakamura *et al*., (2014) also signifies that human waste is the dominating source of NO_3^--N in the shallow groundwater of the Kathmandu Valley.

The shallow groundwater shows a weak negative correlation between NH_4^+-N and NO_3^--N (Table 26). This result shows that the higher NH_4^+-N and NO_3^--N concentration of shallow groundwater near to river corridor of the Kathmandu Valley may be due to anthropogenic activities like leakage of the sewage system (Bo¨hlke, 2006 and Lindenbaum, 2012) (Figure 118) rather than the nitrification of ammonia. At the same time, a strong positive correlation between Na^+, Mg^{2+} and Cl^- also indicates the influence of anthropogenic activities (Kumar, 2019) because there is no evidence of halite deposits in the study area.

Figure 118: Surrounding condition of wells

Quality of groundwater can also be affected by river-groundwater interaction. Comparing with individual corridors, 40 to 50% of groundwater from the Manahara, Hanumante, Godawari and Kodku Khola exceeds NDWQS in concentration of NH_4-N^- in the wet season (Figure 115a). Meantime, Figure 106 presents about 68% of sites show an absence of interconnection. The Manahara and Hanumante Rivers have only one

groundwater site which shows interconnection with river sites. This result indicates that the chemical concentration of groundwater in the wet season is not directly reflected by river-groundwater interconnection. Furthermore, the plotting of dominant sites close or near to the LMWL in δD versus $\delta^{18}O$ reflects that the chemical concentration can be added through percolation of rainfall. During percolation through soil media, it has possibility to dissolve natural material along with mixing with sewer leakage.

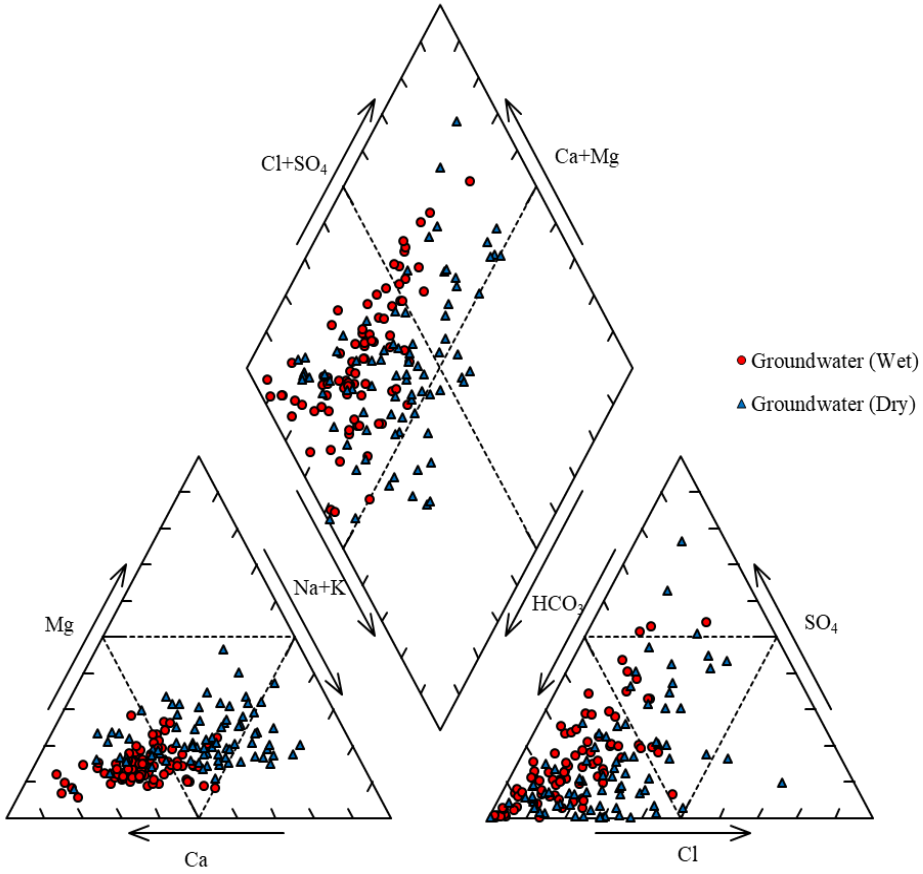

Figure 119: Piper diagram of groundwater in the wet and dry season

However, in the case of the dry season, river water can contribute total of 54% of groundwater sites by infiltrating directly from adjacent river water (35%) or infiltration from upstream river sites (19%) (Figure 108). At the same time, river water possesses high concentrations of ions of Na^+, NH_4-N^-, Cl^-, PO_4^--P indicating pollution. Groundwater site also exceeds NDWQS by twofold than that of the wet season. Groundwater sites from the Bagmati, Manahara, Hanumante and Balkhu Khola have dominancy of influent condition as exchange flow (Figure 108) and these rivers also show a higher percentage of sites exceeding NDWQS in the concentration of NH_4^--N

(Figure 115). This indication signifies that the shallow groundwater quality of river peripheral areas of the Kathmandu Valley is highly affected by contaminated river water during the dry season. Previous research conducted in different countries also presented the effects of contaminated surface water on groundwater quality (Brindha *et al*., 2014; Huang and Han, 3015; Sakakibara *et al*., 2016; Singh, 2013; Zhang *et al*., 2016). Thus the groundwater nearby river channel are unsuitable for human consumption without any treatment.

This research emphasizes the important of river-groundwater interconnection investigation for water quality monitoring of river as well as peripheral shallow groundwater, river restoration projects and policy making of quantity and quality of groundwater.

CHAPTER 5

CONCLUSION AND RECOMMENDATION

5.1 Conclusion

The connection condition of groundwater and river water in the Kathmandu Valley is analyzed by using multivariate method, HCA with hydro-chemical and isotopic composition along with surficial sediment distribution and subsurface lithological variation. The major findings of this research are given as follow:

5.1.1. River-groundwater interconnection:

1. Interconnection of river water and groundwater shows spatially and temporally variable. Different exchange processes are categorized based on the flow direction of water. As this research lack of measuring water level in river channel, the exchange process is defined based on comparative isotopic composition of river-groundwater, water level in wells and field verification of locations. Exchange process is categorized as influent; influent from upstream; effluent; effluent to downstream or effluent from upstream; combination of influent and effluent.
2. During the wet season, 68% of sampling sites show absence of interconnection. The non-connected sites are basically situated at the core urban areas.
3. In contrast, the areas of interconnection are focused on the southern tributaries of the Kathmandu Valley which has lower urbanization. This indicates that unmanaged urbanization effects on river-groundwater interconnection.
4. River-groundwater interconnection is spatially more variable in the dry season. Only 11% of sites shows absence of interconnection. Remaining sites shows influent and influent from upstream condition as dominant exchange processes (54%) indicating tendency to contribute of river water for adjacent and downstream groundwater even during low discharge.

5.1.2 Seasonal variation in interconnection:

1. Temporal variation is noticeable in river-groundwater interconnection. Observation of only 9% of sites possessing absence of interconnection in both wet and dry seasons signifies that whole rivers of the Kathmandu Valley are interconnected with shallow groundwater.

2. Dominant sites from core urbanized area have changed exchange process from non-connected (in wet season) to influent from upstream condition (in dry season).

5.1.3 Status of river water quality:

1. Quality of rivers is reflected by concentrations of chemical ions dissolved in the river water. Ions of river water show significant temporal variation with drastic increment in concentration at the dry season. It also shows increment towards downstream section and possess unsuitable environment for aquatic habitat.
2. Based on dry season chemical data, HCA classify two major clusters A and B. River sites grouped in Cluster A possess less polluted river section and river sites enclosed in cluster B indicates highly contaminated section. Comparing with nine rivers, the Hanumante Khola is one of the heavily contaminated river in the Kathmandu Valley whereas the Godawari Khola is least polluted.
3. The correlation between different chemical ions of river water has been analyzed. Strong positive correlation between chemical ions indicates that river water is highly influenced by anthropogenic pollution such as direct discharge of municipal and industrial sewage and leachate of solid waste disposal near the river channel during the dry season.
4. Wet season river water is classified as Ca-HCO_3. The water type is remained same for water from the Godawari Khola and some other river section; others are changed to Na-K-HCO_3, Ca-SO_4, Na-Cl-SO_4 type during the dry season.

5.1.4 Status of groundwater quality:

1. The quality status of dug wells has been analyzed using the NDWQS limits. The parameters, namely, pH, EC, Cl^-, Ca^{2+}, SO_4^{2-}, NH_4^+-N and NO_3^--N are used to compare limits with NDWQS.
2. The percentage of groundwater from dug wells exceeding NH_4^+-N limit is 30.6% in the wet season and 60.9% in the dry season. Exceeding percentage of NO_3^--N is similar in both seasons (10.5 to 10.9%). Percentage of EC is nearly double in the dry season (8.5%) in relative to wet season (4.7%) whereas exceeding pH has increased up to ten times in the dry season (10.4%). About 80% of dug wells exceed limit of NH_4^+-N from the Manahara River and

Hanumante and Balkhu Khola in the dry season showing sever anthropogenic contamination on shallow aquifer. This indicates that the shallow aquifers nearby these river channels are unsuitable for drinking purpose.

5. Groundwater quality can also be affected by river-groundwater interconnection. During the wet season, dominant of sites possess non-connected with river. Even though, groundwater sites exceeding NDWQS in wet season indicates the chemical concentration of groundwater is not directly reflected by river-groundwater interconnection in the wet season.
6. In the dry season, 54% of sites are interconnected with rivers and about 60% of groundwater exceed NDWQS in NH_4^+-N. This indicates that groundwater quality of river peripheral areas of the Kathmandu Valley are affected by contaminated river water.

5.1.5 Isotopic composition of river and groundwater:

1. The isotopic composition (δD and $\delta^{18}O$) of river water of the Kathmandu Valley shows lighter value in the wet season. The discharges on the rivers are basically from the rainfall with some other additional sources. Some river samples from the Bagmati River, and Hanumante and Godawari Khola suggests possibility of evaporation during the dry season as they plotted below LMWL with enriched isotopic composition.
2. The isotopic composition of groundwater shows wide spatial variation. The meteoric water is the main recharge source in the wet season and rainfall with some additional surface water sources during the dry season. Spatial variation in composition indicates presence of elevation and amount effect on rainfall isotopic composition.

5.2 Recommendation

Based on the study of interconnection of groundwater and river water using cluster analyses (hydro-chemical and isotopic composition), following recommendations are prepared which can be useful for water resource management and policy development:

1. Presence of river interconnection with surrounding aquifers, in both wet and dry seasons, emphasizes importance of incorporation of groundwater and river water interconnection during river restoration or water system management and policy making, taking both of it as a single source.

2. The upstream section of the Bagmati river, Dhobi, Godawari and Nakhu Kolas shows influent condition in both seasons. Thus these areas can be used for bank storage during rainy season to minimize local scale water scaricity.
3. The measurement of river channel water level and site specific lithology is important in the study of interconnection to compare hydraulic head and find out lateral and vertical subsurface material variation respectively. Present study unable to such information. Therefore, for the similar type of research, it needs to incorporate such types of data so that it can be easy to find out direction of water flow.
4. Contamination in shallow groundwater exceeding limits of NDWQS, are harmful for human health. Shallow aquifers nearby major rivers exceed limits of NDWQS. Thus, for consumption of groundwater, located within 100 m from the river channels, needs to purify for reduction in chemical ions.
5. Similar types of researches are necessary for other valley or basin to identify connection condition of river-groundwater. Only knowing about the connection condition, one can develop water management projects and can make policies by government.

CHAPTER 6

SUMMARY

The Kathamandu Valley is one of the most populated and urbanized city in Nepal. Increased population growth expands urbanization towards major river corridors, affecting river quality by dumping solid and sewer effluent to the rivers. The polluted rivers adversely effects on nearby groundwater, as they are interconnected with each other. The interconnection of river is not only exchange water but also toxic contents included with water. Condition of exchange is dependent on climatic factors and lithology of river channel and bank materials. During the wet season, river stage has increased and water infiltrates through bank materials, recharging surrounding aquifer. In contrast, dry season has lower water stage and has low tendency to infiltrate bank material, thus presenting effluent condition from groundwater. This indicates that the condition of exchange is temporally as well as spatially variable.

The river water quality of previously studied research presented degrading condition at urbanized areas. Similarly, shallow groundwater quality also reported higher concentration of nitrate, iron, EC, chloride and turbidity with coliform bacteria. But there are rare research related with interconnection of groundwater and river. Therefore, the present study is focused on the connection condition as well as their temporal and spatial variation.

The composition of isotope and chemicals are major analytic methods applied to achieve targeted goals. HCA is interpretative method to identify connection condition between groundwater and river with additional information from surficial and sub-surface lithological distribution pattern.

Preparation of dug well inventory is preliminary phase of this research. Total 237 dug wells are recorded from major tributaries of the Bagmati River. In-situ parameters along with water level depth has recorded from all dug well in April and August of 2017 to record seasonal variation. The lowest water level variation has recorded in the Nakhu Khola (3.6 m) and the highest obtained in the Dhobi Khola (10.7 m) in dry season; and 2.5 m in the Nakhu Khola and 6.3 m in the Kodku Khola during wet season. Average EC value ranged from 614.2 to 1123.9 µS/cm in dry season and then decreased to 613.0

and 916.1 µS/cm in the wet season. In both seasons, the highest value observed in the Balkhu Khola corridor and the lowest in the Nakhu Khola corridor. In each river, EC at upstream segments well presents lower comparing with the downstream urbanized area. EC is also high near to (<30 m) river channel.

The isotopic composition (δD and $\delta^{18}O$) of river water of the Kathmandu Valley shows lighter values in relative to dry season. Comparing to GMWL and LMWL, wet season river water have precipitation source and dry season indicates presence of additional source for river discharge. Enriched isotopic composition from the Bagmati River, and Hanumante and Godawari Khola suggests possibility of evaporation during the dry season. Groundwater isotopic composition shows spatially variable in both seasons. The variation range of δD and $\delta^{18}O$ is high in the wet season (-81.7 to -34.7‰ for δD and -11.4 to -4.8‰ for $\delta^{18}O$) comparing to the range of the dry season (-65.3 to -42.9‰ for δD and -9.3 to -6.3‰ for $\delta^{18}O$). Relation with GMWL and LMWL, wet groundwater presents meteoric water as recharge source whereas dry groundwater indicates presence of additional recharge sources. Some groundwater samples from the Bishnumati and Bagmati Rivers; and Nakhu Khola possesseing enrich isotopic composition indicates possibility of evaporation during the dry season.

The apparent resistivity observed from ERT survey categorizes subsurface material from clay to sandy gravels. Gravelly sand and sandy gravels are observed at upstream section of the rivers. Thick deposits of clay and silt are observed at the bottom of each ERT profiles, except upstream one from the Bishnumati River. However, the elevation of upper surface of clay and silt layer is different. Highest elevation of around 1332 m existed in upstream profile of the Nakhu Khola and lowest elevation of around 1275 m occur in downstream profile of the Manahara River. Profiles from the Bishnumati River exhibits tentative similar elevation of 1284 m.

Interconnection condition of the groundwater and river water has been identified using multivariate method, HCA. The composition of δD**,** $\delta^{18}O$, Na^+ and Cl^- are used as major parameter for clustering. The grouping of samples in single cluster indicates similarity or interconnection in groundwater and river water. The interconnection between groundwater and river is observed in all river corridors of the Kathmandu Valley both in the wet and dry seasons. Wet season shows dominancy in non-connected sites while dry season presents dominancy of influent condition indicating tendency to recharge

adjacent groundwater. The non-connected areas is mainly concentrated on the core urban areas of the Central Groundwater District. While influent condition is observed from the upstream section of southern and northern tributaries.

The river water possesses dominancy of Ca^{2+} and HCO_3^- ions in the wet season and Na^+ and HCO_3^- during the dry season. Significant increment of NH_4^+-N and $PO_4^{—}$P and strong positive correlation of Na^+, K^+, NH_4^+-N, Ca^{2+}, Mg^{2+}, Cl^-, HCO_3^-, PO_4^--P, and SO_4^{2-} between each other, indicates anthropogenic influences in river water. Strong positive correlation existence of PO_4^--P with SO_4^{2-}, NH_4^+-N and NO_3^- - N in most of rivers also suggests the influence of fertilizer used in the cultivated land of river peripheral areas. Wet season river water is classified as Ca-HCO_3. The water type is remained same for the Godawari Khola and few other river sections; and others are changed to Na-K-HCO_3, Ca-SO_4, Na-Cl-SO_4 type during the dry season. Cluster analysis of dry river data implies that the Hanumante Khola is one of heavily contaminated while the Godawari Khola is least polluted among the rivers in the Kathmandu Valley.

Groundwater is dominant of Ca^{2+}, Na^+ and HCO_3^- ions in the wet and dry season. However, fewer ions show significant temporal variation (paired t-test within 95% confidency level), type of ions are changed with different river corridors. Mostly, concentration of PO_4^--P is nearly absent in the southern corridors like Godawari, Kodku, Nakhu and Balkhu Kholas. The percentage of dug wells, exceeding limit of NH_4^+-N is increased by double in the dry season (60.98%) as compared to the wet season (30.5%). The higher concentration of NH_4^+-N and NO_3^- - N and strong positive correlation between Na^+, Mg^{2+} and Cl^- signify that the groundwater near to river corridor of the Kathmandu Valley is contaminated by anthropogenic activities. Presence of interconnection of river-groundwater as influent and influent from upstream condition in dry season implies that degradation of groundwater is the result of river recharge to adjacent and downstream groundwater.

REFERRENCES

Adhikari, B., & Tamrakar, N.K. (2006). Bank Instability and Erosion Problems in Bishnumati River, Kathmandu, Nepal. *Journal of Nepal Geological Society*, **34**: 109-116.

Adhikari, N., Gao, J., Yao, T., Yang, Y. & Dai, D. (2020). The Main Controls of the Precipitation Stable Isotopes at Kathmandu, Nepal. *Tellus B: Chemical and Physical Meteorology*, **72** (1): 1-17. Doi: 10.1080/16000889.2020.1721967.

Al-Khatib, M., & Al-Najar, H. (2011). Hydro-Geochemical Characteristics of Groundwater Beneath the Gaza Strip. *J. Water Resour. Prot*., **3**: 341–348.

Ali, K.K., & Ajeena, A.R. (2016). Assessment of Interconnection Between Surface Water and Groundwater in Sawa Lake Area, Southern Iraq, Using Stable Isotope Technique. *Arab. J. Geosci.*, **9**: 648. Doi:10.1007/s12517-016-2673-6.

Awad, M., Arabi, N.E. & Hamza, M.S. (1997). Use of Solute Chemistry and Isotopes to Identify Sources of Ground-Water Recharge in the Nile Aquifer System, Upper Egypt. *Ground Water*, **35** (2).

Aytekin, H., & Bayraktaroglu, N. (2014). An Investigation on the Quality of Natural Spring Waters in Zonguldak Provinance (Turkey) Academic Library Collections in Korea. *J. Korean Libr. Inf. Sci. Soc.*, **45**: 277–308. Doi: 10.16981/kliss.45.4.201412.277.

Baba, A., & Gunduz, O. (2017). Effect of Geogenic Factors on Water Quality and Its Relation on Human Healh around Mount Ida, Turkey. *Water*, **9**, 66. Doi:10.3390/w9010066

Bajracharya, R., & Tamrakar, N.K. (2007). Environmental Status of Manahara River, Kathmandu. Nepal, *Bull. Dep. Geol*., **10**: 21–32. Doi:10.3126/bdg.v10i0.1417.

Bajracharya, R., Nakamura, T., Shakya, B.M., Nishida, K., Shrestha, S.D., & Tamrakar, N.K. (2018). Identification of River Water and Groundwater Interaction at Central Part of the Kathmandu Valley, Nepal Using Stable Isotope Tracers. *Int. J. Adv. Sci. Tech. Res*., **3** (8): 29–41. Doi:10.26808/rs.st.i8v3.04.

Bajracharya, R., Tamrakar, N.K., Shrestha, M., & Bohara, B. (2018). Status of Shallow Wells along Major Rivers of the Kathmandu Valley, Central Nepal. *J. Nepal Geol. Soc.*, **56** (1): 31–42. Doi:10.3126/jngs.v56i1.22697.

Banks, E.W., Simmons, C.T., Love, A.J., & Shand, P. (2011). Assessing Spatial and Temporal connectivity between Surface Water and Groundwater in a Regional Catchment: Implication for Regional Scale Water Quantity and Quality. *Journal of Hydrology*, **404**:30-49. Doi: 10.1016/j.jhydrol.2011.04.017.

Barrie, C.J., Rasmussen, T.C., Trollner, E.W., Golladay, S.W., & Brantley, S.T. (2022). Steady vs Dynamis Stream-Aquifer Interaction:Lower Flint River Basin, Southwest Georgia, USA. *Journal of Hydrology: Regional Studies*, **40**:101046. Doi: 10.1016/j.ejrh.2022.101046.

Bhat, S.A., Meraj, G., Yaseen, S., & Pandit, A.K. (2014). Statistical Assessment of Water Quality Parameters for Pollution Source Identification in Sukhnag Stream : An Inflow Stream of Lake Wular (Ramsar Iite), Kashmir Himalaya. *J. Ecosystem.*, **18.** Doi:10.1155/2014/898054.

Bhatta, B.P., & Pandey, R.K. (2020). Bhaktapur Urban Flood Related Disaster Risk and Strategy after 2018. *J. APA command and Staff College,* **3** (1): 72-89.

Bhandari, P., Banjara, M.R., Singh, A., KAndel, S., Rawal, D.S., & Pant, B.R. (2021). Water Quality Status of Groundwater and Municipal Water Supply (Tap Water) from Bagmati River Basin in Kathmandu Valley, Nepal. *Journal of Water, Sanitation and Hygiene for Development*, **11** (1). Doi: 10.2166/washdev.2020.190.

Binnie & Partners. (1973). Kathmandu Water Supply and Sewerage Scheme. Appendix 4.5. *Groundwater Investigation, World Health Organization Project Nepal 0025*. Unpublished.

Bishara, A.J., & Hittner, J.B. (2012). Testing the Significance of a Correlation with Nonnormal Data: Comparision of Pearson, Spearman, Transformation, and Resampling Approaches. *Psychol. Methods*, **17**: 399-417. Doi:10.1037/a0028087.

Bittner, A. (2000). Nepal Drinking Water Quality Assessment: Nitrate and Ammonia.

Thesis of Master of Engineering, Massachusetts Institute of Technology, 70p.

Blair, T.C., & McPherson, J.G. (1999). Grain-Size and Textural Classification of Coarse Sedimentary Particles. *J. Sed. Res.,* **69** (1): 6-19.

Brenot, A., Petelet-Giraud, E., & Gourcy, L. (2015). Insight from Surface Water-Groundwater Interactions in an Alluvial Aquifer: Contributions of $\delta^{2}H$ and $\delta^{18}O$ of Water, $\delta^{34}SSO_4$ and $\delta^{18}OSO_4$ of Sulfates, $^{87}Sr/^{86}Sr$ Ratio. *Procedia Earth Planet. Sci*., **13**: 84–87. Doi:10.1016/j.proeps.2015.07.020.

Brindha, K., Neena Vaman, K.V., Srinivasan, K., Sathis Babu, M., & Elango, L. (2014). Identification of Surface Water-Groundwater Interaction by Hydrogeochemical Indicators and Assessing its Suitability for Drinking and Irrigational Purposes in Chennai, Southern India. *Appl. Water Sci*., **4**: 159–174.

Brownbill, R.J., Lamontagne, S., Williams, R.M., Cook, P.G., Simmons, C.T., & Merrick, N. (2011). Interconnection of Surface and Groundwater Systems-River Losses from Losing-Disconnected Streams. *Technical final report, NSW office of water, Sydney*, 48p.

Brunke, M.; & Gonser, T. (1997). The Ecological Significance of Exchange Processes between Rivers and Groundwater. *Freshwater Biol*., **37**: 1–33.

Brunner, P., Cook, P.G., & Simmons, C.T. (2009a). Hydrogeological Controls on Disconnection between Surface Water and Groundwater. *Water Resources Research,* **45**. Doi: 10.1029/2008wr006953.

Brunner, P., Simmons, C.T., & Cook, P.G. (2009b). Spatial and Temporal Aspects of the Transition from Connection to Disconnection between Rivers, Lakes and Groundwater. *Journal of Hydrology*, **376**: 159-169.

Chambers, J.E., Wilkinson, P.B., Weller, A., Meldrum, P.I., Kuras, O., Ogilvy, R.D., Aumonier, J., Bailey, E., Griffiths, N., Matthews, B., Penn, S., & Wardrop, D. (2011). Characterizing Sand and Gravel Deposits Using Electrical Resistivity Tomography (ERT): Case Histories from England and Wales. *Proceeding of the 16th Extractive Industry Geology Conference,* 166-172.

Chhetri, T.B., Yao, T., Yu, W., Ding, L., Joswiak, D., Tian, L., Devkota, L.P., & Qu,

D. (2014). Stable Isotopic Composition of Precipitation Events from Kathmandu, Southern Slope of the Himalayas. *Chin.sci.Bull.,* **59**: 4838-4846. Doi: 10.1007/s11434-014-0547-4.

Craig, H. (1961). Isotopic Variations in Meteoric Waters. *Science,* **133** (3465): 1702–1703. Doi:10.1126/science.133.3465.1702.

Darling, W.G., Bath, A.H., Gibson, J.J., & Rozanski, K. (2005). Isotopes in Paleoenvironmental Research. *Springer, Dordrecht, The Netherlands*.

Davids, J.C., Rutten, M.M., Shah, R.D.T., Shah, D.N., Devkota, N., Izeboud, P., Pandey, A., & Giesen, N. (2018). Quantifying the Connections – Linkage between Land-use and Water in the Kathmandu Valley, Nepal. *Environ Monit Assess*, **190**: 304. Doi: 10.1007/s10661-018-6687-2.

Derx, J., Blaschke, A.P., & Bloschl, G. (2010). Three-dimensional Flow Patterns at the River-Aquifer Interface-A Case Study at the Danube. *Adv. Water Resour*. **33**: 1375-1387. Doi:10.1016/j.advwatres.2010.04.013

Devkota, D.C., & Watanabe, K. (2005). Impact of Solid Waste on Water Quality of Bishnumati River and Surrounding Areas in Kathmandu, Nepal. *J. Nepal Geol. Soc.* **31**: 19–24. Doi:10.3126/jngs.v31i0.253.

Dhakal, S. (2006). Study on Physiochemical Parameters and Benthic Macroinvertibrates of Balkhu Khola in Kathmandu Valley, Central Nepal. *Paper presentation on Management of Water, Wastewater and Environment: Challenges for the developing countries.*

Dhital, M.R. (2015). Geology of the Nepal Himalaya: Regional Perspective of the Classical Collided Orogen. *Switzerland: Springer International Publishing*, USA.

Diwakar, J., Yami, K.D., & Prasai, T. (2010). Assessment of Drinking Water of Bhaktapur Municipality Area in Pre-monsoon Season. *Sci. World*, **6**: 94–98. Doi: 10.3126/sw.v6i6.2642

DMG, 1998. Engineering and Environmental Geological Map of the Kathmandu Valley. *Department of Mines and Geology, Kathmandu*.

Duwal, S., Upadhyay, S., Silwal, P., Thapa, A.B., & Prajapati, R. (2019). Shallow Grounddwater Level Variation in the Kathmandu Valley: A GIS-based Study. *KEC conference*

Edokpayi, J.N., Odiyo, J.O., Msagati, T.A.M., & Potgieter, N. (2015). Temporal Variations in Physico-Chemical and Microbiological Characteristics of Mvudi River, South Africa. *Int.L.Environ.Res.Public Health,* **12**: 4128-4140. Doi: 10.3390/ijerph120404128.

Elango, L. & Kannan, R. (2016). Rock-Water Interaction and Its Control on Chemical Composition of Groundwater. *Development of Environmental Science,* **5**, 229-242. Doi:10.1016/S1474-8177(07)05011-5

Environmental protection Agency (EPA) CADDIS Volume **2**.

Epstein, S., & Mayeda, T.K. (1953). Variation of ^{18}O Contents of Waters from Natural Sources. *Geochim. Cosmochim,* Ac. **4**: 213-224

Epting, J., Huggenberger, P., Radny, D., Hammes, F., Hollender, J., Page, R.M., Weber, S., Banninger, D., & Auckenthaler, A. (2018). Spatiotemporal Scales of River-Groundwater Interaction-The Role of Local Interaction Processes and Regional Groundwater Regimes. *Sci. Total Environ,* **618**: 1224–1243.

El Alfy, M., & Merkel, B. (2004). Assessment of Human Impact on Quaternary Aquifers of Rafah Area , NE Sinai , Egypt. *Int. J. Econ. Environ. Geol.*, **1**: 1–9.

Ezugwu, C.N., & Apeh, S. (2017). Groundwater and Surface Water as One Resource: Connectivity and Interaction. *J. Mech. Civil Eng.,* **14** (3): 54-59.

Fleckenstein, J.H., Krause, S., Hannah, D.M., & Boano, F. (2010). Groundwater-Surface Water Interactions: New Methods and Models to Improve Understanding of Processes and Dynamics. *Adv. Water Resour.,* **33** (11): 1291–1295. doi:10.1016/j.advwatres.2010.09.011.

Fundamentals of Envirnmental Measurements (2015). Dissolved Oxygen - Environmental Measurement Systems. *Fundam. Envirnmental Meas*.

Gajurel, A.P., France-Lanord, C., Huyghe, P., Guilmette, C., & Gurung, D. (2006). C and O Isotope Compositions of Modern Fresh-water Mollusc Shells and River

Waters from the Himalaya and Ganga Plain. *Chem. Geol.*, **233** (1–2): 156–183. Doi:10.1016/j.chemgeo.2006.03.002.

Ganiyu, S.A., Badmus, B.S., Olurin, O.T., & Ojekunle, Z.O. (2018). Evaluation of Seasonal Variation of Water Quality using Multivariate Statistical Analysis and Irrigation Parameter Indices in Ajakanga Area , Ibadan, Nigeria. *Appl. Water Sci.*, **8**: 35. Doi:10.1007/s13201-018-0677-y.

Gao, Z., Liu, W., Liu, J., Wang, Z., & Wnag, S. (2022). Study on the Relationship between River Water and Groundwater under Different Aquifer Mediums. *Water*, **14**, 1134. Doi: 10.3390/w14071134

Gardi, S.Q. S. (2014). 2D Electrical Resistivity Tomography Survey for Shallow Environmental Study at Wastewater Valley of Southestern Erbil City, Iraqi Kurdistan Region. *Research Journal of Environmental and Earth Sciences* **6** (5): 266-277.

Gat, J.R. (1995). The Relatioship Between the Isotopic Composition of Precipitation, Surface Runoff and Groundwater for Semiarid and Arid Zones. *Appl. Tracesrs in Arid Zone Hydrol.*, **232**: 409-416.

Gautam, D., & Prajapati, R.N. (2014). Drawdown and Dynamics of Groundwater Table in Kathmandu Valley , Nepal. *Open Hydrol. J.* **8**: 17–26. Doi: 10.2174/18743 78101408010017.

Gautam, R., Shrestha, J.K., & Shrestha, G.K.C. (2013). Assessment of River Water Intrusion at the Periphery of Bagmati River in Kathmandu Valley. *Nepal J. Sci. Technol.,***14** (1): 137–146. Doi:10.3126/njst.v14i1.8934.

Ghimire, G., Adhikari, B., & Pradhan, M. (2013). Bacteriological Analysis of Water of Kathmandu Valley. *MJSBH,* **12**: 19-22.

Ghimire, S., Pokhrel, N., Pant, S., Gyawali, T., Koirala, A., Mainali, B., Angove, M., & Paudel, S.R. (2022). Assessment of Technologies for Water Quality Control of the Bagmati River In Kathmandu Valley, Nepal. *Groundwater for Sustainable Development*, **18**:100770.

Gotway, C.A., Helsel, D.R., & Hirsch, R.M. (1994). Statistical Methods in Water Resources. *Technometics*, 323 p. Doi:10.2307/1269385.

Giri, U. (2018). Evaluation of Stable Isotope Ratios within Meteoric , Surface , and Groundwater within the Kathmandu Valley. *Thesis, Georgia State University*, 48 p. http://scholarwork.gsu.edu/geoscience_theses/116.

Gurung, J.K., Ishiga, H., Khadka, M.S., & Shrestha, N.R. (2007). Characterization of Groundwater in the Reference of Arsenic and Nitrate Mobilization, Kathmandu Basin, Nepal.

Guggenmos, M.R., Daughney, C.J., Jackson, B.M., & Morgenstern, U. (2011). Regional-scale Identification of Groundwater-Surface Water Interaction using Hydrochemistry and Multivariate Statistical Methods , Wairarapa Valley, New Zealand. *Hydrol. Earth Syst. Sci.*, **15**: 3383–3398. Doi:10.5194/hess-15-3383-2011.

Guzman, P., Anibas, C., Batelaan, O., Huysmans, M., & Wyseure, G. (2016). Hydrological Connectivity of Alluvial Andean Valleys: A Groundwater/Surface-Water Iinteraction Case Study in Ecuador. *Hydrogeol J*., Doi: 10.1007/s100040-015-1361-z.

Hada, R., Lupker, M., Gajurel, A.P., &Shakya, N. (2019). Assessment on Connection between Shallow and Deep Aquifers of Siraha and Saptari District using Isotope Analysis. *Journal of Nepal Geological Society*, **59**: 65-72. Doi: 10.3126/jngs.v59i0.24989.

Hanisch, Jorg., Busch, K., Kerntke, M., & Jager, S. (1999). A Geo-Environmental Map for the Sustainable Development of the Kathmandu Valley, Nepal. *GeoJournal*, **49**: 165-172.

Hoehn, E., & Scholtis, A. (2011). Exchange between a River and Groundwater, Assessed with Hydrochemical Data. *Hydrol. Earth Syst.Sci.*, **15**: 983-988. Doi: 10.5194/hess-15-983-2011.

Huang, P., & Han, S. (2016). Assessment by Multivariate Analysis of Groundwater – Surface Water Interactions in the Coal-Mining Exploring District, China. *Earth Sci. Res. J.*, **20** (1): 1–8.

Hunt, R.J., Strand, M., & Walker, J.F. (2006). Measuring Groundwater-Surface Water Interaction and Its Effect on Wetland Stream Benthic Productivity, Trout Lake

Watershed, Northern Wisconsin, USA. *J. Hydrol.*, **320** (3–4): 370–384, Doi:10.1016/j.jhydrol.2005.07.029.

Idoko, O.M., & Oklo, A. (2010). Seasonal Variation in Physico-Chemical Characeristics of Rural Groundwater of Benue State, Nigeria. *Journal of Asian Scientific Research,* **2** (10): 574-586.

Ishtiaque, A., Shrestha, M., & Chhetri, N. (2017). Rapid Urban Growth in the Kathmandu Valley, Nepal: Monitoring Land Use Land Cover Dynamics of a Himalayan City with Landsat Imageries. *Environments*, **4**, 72, Doi: 10.3390/environments4040072

Islam, M.S., Uddin, M.K., Tareq, S.M., Shammi, M., Kamal, A.K.I., Sugano, T., Kurasaki, M., Saito, T., Tanaka, S., & Kuramitz, H. (2015). Alteration of Water Pollution Level with the Seasonal Changes in Mean Daily Discharge in Three Main Rivers around Dhaka City, Bangladesh. *Environments*, **2**: 280-294. Doi: 10.3390/environments2030280.

Ito, Y., Shrestha Malla, S., Bhattarai, A.P., Haramoto, E., Shindo, J., & Nishida, K. (2020). Waterborne Diarrhoeal Infection rist from Multiple Water Sources and the Impact of n Earthquake. *Journal of Water and Health*, **18** (4): 464-476. Doi: 10.2166/wh.2020.223.

Japan International Cooperation Agency (JICA) (1990). Groundwater Management Project in the Kathmandu Valley. Unpublished.

Kalbus, E., Reinstorf, F., & Schirmer, M.(2006). Measuring Methods for Groundwater-Surface Water Interactions: A Review. *Hydrol. Earth Syst. Sci.*, **10** (6): 873–887. doi:10.5194/hess-10-873-2006.

Kannel, P.R., Lee, S., Kanel, S.R., Khan, S.P., & Lee, Y. (2007). Spatial-Temporal Variation and Comparative Assessment of Water Qualities of Urban River System: A Case Study of the River Bagmati (Nepal). *Environ monit Assess*., **129**: 433-459. Doi:10.1007/s10661-006-9375-6.

Karafistan, A., Martin, J.M., Rixen, M., & Beckers, J.M. (2002). Space and Time Distribution of Phosphate in the Mediterranean Sea. *Deep-sea Research I*, **49,** 67-82

Karki, S.S., & Tamrakar, N.K. (2016). Fluvial Morphology and Dynamics of Godawari Khola, Southeast Kathmandu, Central Nepal. *Bulletin of the Department of Geology,* **19**: 15-28.

Katz, B.G., Coplen, T.B., Bullen, T.D., & Hal Davis, J. (1997). Use of Chemical and Isotopic Tracers to Characterize the Interactions Between Groundwater and Surface Water in Mantled Karst. G*round Water*, **35** (6): 1014–1028. Doi:10.1111/j.1745-6584.1997.tb00174.x.

Khadka, M.S. (1993). The Groundwater Quality Situation in Alluvial Aquifer of the Kathmandu Valley, Nepal. *AGSO Journal of Australian Geology and Geophysics,* **14**: 207-211.

Krishna, G., Singh, S., Sharma, A., Sandhu, C., Kumar, S., CP, K., &Gurjar, S. (2017). Assessment of River Yamuna and Groundwater Interaction using Isotopes in Agra and Mathura Area of Uttar Pradesh, India. *International Journal of Hydrology*, **1** (3): 86-89.

Kumar, M., Ramanathan, A., & Keshari, A.K. (2009). Understanding the Extent of Interactions Between Groundwater and Surface Water Through Major Ion Chemistry and Multivariate Statistical Techniques. *Hydrol. Process*, **23**: 297–310. Doi: 10.1002/hyp.7149

Kumar, P.J.S. (2019). Hydrogeochemical and Multivariate Statistical Appraisal of Pollution Sources in the Groundwater of the Lower Bhavani River Basin in Tamil Nadu. *Geology, Ecology and Landscapes*, Doi:10.1080/24749508.2019.1574156.

Lachniet, M.S., & Patterson, W.P. (2009). Oxygen Isotope Values of Precipitation and Surface Waters in Northern Central America (Belize and Guatemala) are Dominated by Temperature and Amount Effects. *Earth Planet. Sci. Lett.*, **284**: 435–446. Doi: 10.1016/j.epsl.2009.05.010.

Lamichane, S., & Shakya, N.M. (2019). Alteration of Groundwater Recharge Areas due to Land Use/Cover Change in Kathmandu Valley, Nepal. *Journal of Hydrology: Regional Studies*, **26**: 100635. Doi: 10.1016/j.ejrh.2019.100635.

Lee, K.S., & Kim, Y. (2007). Determining the Seasonality of Groundwater Recharge

Using Water Isotopes: A Case Study from the Upper North Han River Basin, Korea. *Environ. Geol*., **52**: 853–859.

Li, X., Tang, C., Han, Z., Cao, Y. (2016). Hydrochemical Characteristic and Interaction Process of Surface and Groundwater in Mid-Lower Reach of Hanjiang River, China. *Environ Earth Sci.,* **75**: 418. Doi: 10.1007/s12665-015-5175-z.

Ling, T.Y., Gerunsin, N., Soo, C.L., Nyant, L., Sim, S.F., & Grinang, J. (2017). Seasonal Changes and Spatial Variation in Water Quality of a Large Young Tropical Reservoir and its Downstream River. Hindawi: *Journal of Chemistry,* **8153246**: 16p. Doi: 10.1155/2017/8153246.

Liu, Y., & Yamanaka, T. (2012). Tracing Groundwater Recharge Sources in a Mountain-plain Transitional Area using Stable Isotopes and Hydrochemistry. *J. Hydrol*., **464–465**: 116–126. Doi:10.1016/j.jhydrol.2012.06.053.

Li, X., Tang, C., Han, Z., & Cao, Y. (2016). Hydrochemical Characteristic and Interaction Process of Surface and Groundwater in Mid-lower Reach of Hanjiang River, China. *Environ. Earth Sci.*, **75** (418): 1–12. Doi:10.1007/s12665-015-5175-z.

Loke, M.H. (1994). Geotomo Software. Geoelectrical Imaging 2D & 3D. www.geoelectrical.com.

Loke, M.H. (1997). RES2DINV ver. 3.3 for Windows 3.1, 95 and NT, *Advanced Geosciences*, Inc, 66p.

Loke, M.H. (2000). Electrical Imaging Survey for Environmental and Engineering Studies: *A practical guide to 2D and 3D surveys*, 67p.

Mahananda, M.R., Mohanty, B.P., & Behera, N.R. (2010). Physico-Chemical Analysis of Surface and Groundwater of Bargarh District, Orissa, India. *IJRRAS* **2**(3)

Maharjan, B., & Tamrakar, N.K. (2010). Morpho-hydraulic Parameters and Existing Stability Condition of Nakhu River, Southern Kathmandu, Central Nepal. *Bulletin of the Department of Geology,* **13:** 1-12.

Maharjan, B., & Tamrakar, N.K. (2011). Deterioration of the Nakhu River: Impairment on Dynamic and Recreational Functions of the River. *Journal of Nepal*

Geological Society, **43:** 225-240.

Maharjan, N. (2018). Groundwater Quality Assessment Along Bagmati River Corridor, Kathmandu, Nepal. *Master Dissertation submitted to Central Department of Geology, TU,* 132p.

Malla, R., Shrestha, S., Chapagain, S.K., Shakya, M., & Nakamura, T. (2015). Physico-Chemical and Oxygen-Hydrogen Isotopic Assessment of Bagmati and Bishnumati Rivers and the Shallow Groundwater along the River Corridors in Kathmandu Valley, Nepal. *J. Water Resour. Prot.,* **7** (17): 1435–1448. Doi:10.4236/jwarp.2015.717117.

Matheswaran, K., Khadka, A., & Dhaubanjar, S. (2019). Delineation of Spring Recharge Zones using Environmental Isotopes to Support Climate-resilient Interventions in two Mountainous Catchments in Far-Western Nepal. *Hydrogeol. J.*, **27**: 2181–2197.

McLachlan, P.J., Chambers, J.E., Uhlemann, S.S., & Binley, A. (2017). Geophysical Characterisation of the Groundwater–Surface Water Interface. *Adv. Water Resour.,* **109**: 302–319. Doi:10.1016/j.advwatres.2017.09.016.

Menció, A., & Mas-Pla, J. (2008). Assessment by Multivariate Analysis of Groundwater-Surface Water Interactions in Urbanized Mediterranean Streams. *J. Hydrol*., **352** (3–4): 355–366. Doi:10.1016/j.jhydrol.2008.01.014.

Meyerhoff, S.B., Maxwell, R.M., Revil, A., Martin, J.B., Karaoulis, M., & Graham, W.D. (2014). Characterization of Groundwater and Surface Water Mixing in a Semiconfined Karst Aquifer using Time-Lapse Electrical Resistivity Tomography. *Water Resour. Res.,* **50** (3): 2566–2585. Doi:10.1002/2013WR013991.

Mishra, B.K., Regmi, R.K., Masago, Y., Fukushi, K., Kumar, P., & Saraswat, C.)2017). Assessment of Bagmati River Pollution in Kathmandu Valley: Scenario-based Modeling and Analysis for Sustainable Urban Development. *Sustainable of Water Quality and Ecology.* Doi: 10.1016/j.swaqe.2017.06.001

Modie, L.T., Kenabatho, P.K., Stephens, M., & Mosekiemang, T. (2022). Investigating Groundwater and Surface Water Interactions using Stable Isotopes and

Hydrochemistry in the Notwane River Catchment, South East Botswana. *Journal of Hydrology: Regional Studies*, **40**: 101014. Doi:10.1016/j.ejrh.2022.101014.

Mohammed, A.M., Krishnamurthy, R. V, Kehew, A.E., Crossey, L.J., & Karlstrom, K.K. (2016). Factors Affecting the Stable Isotopes Ratios in Groundwater Impacted by Intense Agricultural Practices: A Case Study from the Nile Valley of Egypt. *Sci. Total Environ.*, **573**: 707–715. Doi:10.1016/j.scitotenv.2016.08.095.

Moog, O., & Sharma, S.(2005). Biological Rapid Assessment of Water Quality in the Bagmati River and its Tributaries, Kathmandu. *International Conferenc on Ecology of High Mountain Areas-Water quality and Limnological Issue*, 609-621.

Naaz, A., & Anshumali (2015). Seasonal Variation in pH and Alkalinity of Groundwater in Sidhi District, Central India. *Current World environment*, **10** (3). Doi: 10.12944/CWE.10.3.34.

Nakamura, T., Nishida, K., Kazama, F., Osaka, K., & Chapagain, S.K. (2014). Nitrogen Contamination of Shallow Groundwater in Kathmandu Valley, Nepal. *J.Jpn. Assoc. Hydrol. Sci.*, **44**:197-206.

Nakamura, T., Nishida, K., & Kazama, F. (2017). Influence of a Dual Monsoon System and two Sources of Groundwater Recharge on Kofu Basin Alluvial Fans, Japan. *Hydrol. Res*., **48** (4): 1071–1087. Doi:10.2166/nh.2016.208.

Neupane, S., Gajurel, A.P., Shakya, N., Lupker, M., & Hada, R. (2019). Assessment on Connection between Shallow and Deep Aquifers using Isotopic Analysis of Surface Water and Groundwater in Sunsari and Morang Districts. *Journal of Nepal Geological Society*, **59**:73-78. Doi: 10.3126/jngs.v59i0.24991.

Ngabirano, H., Byamugisha, D., & Ntambi, E. (2016). Effects of Seasonal Variations in Physical Parameters on Quality of Gravity Flow Water in Kyanamira Sub-County, Kabale District, Uganda. *J. Water Resour. Prot.*, **8**: 1297–1309. Doi: 10.4236/jwarp.2016.813099

Nienie, A. B., Sivalingam, P., Laffite, A., Ngelinkoto, P., Otamonga, J. p., Matand, A.,

Mulaji, C. K., Mubedi, J. I., Mpiana, P. T., & Pote, J. (2017). Seasonal Variability of Water Quality by Physicochemical Indexes and Traceble Metals in Suburban Area in Kikwit, Democratic Repubic of the Congo. *International Soil and Water Conservation Research,* **5**: 158-165.

Oyem, H.H., Oyem, I.M., & Ezeweali, D. (2014). Temperature, pH, Electrical Conductivity, Total Dissolved Solids and Chemical Oxygen Demand of Groundwater in Boji-BojiAgbor/Owa Area and Immediate Suburbs. *Environmental Sciences. Res. J. Environ. Sci.,* **8**: 444–450.

Ozel, S., Yilmaz, A., & Candansayar, M.E. (2017). The Examination of the Spread of the Leachates Coming out of a Solid Waste Disposal Area on the Ground with Geophysical and Geochemical Methods (Sivas, Turkey). *Journal of Applied Geophysics*, **123**: 40-49

Pandey, S. (2006). Water Pollution and Health. *Kath. Uni. Med. J.,* **4** (13): 128–134.

Pandey, V.P., Chapagain, S.K., & Kazama, F. (2010). Evaluation of Groundwater Environment of Kathmandu Valley. *Environ. Earth Sci.,* **60**: 1329–1342. Doi: 10.1007/s12665-009-0263-6.

Pandey, V.P., & Kazama, F. (2011). Hydrogeologic Characteristics of Groundwater Aquifers in Kathmandu Valley, Nepal. Environ Earth Sci, 62: 1723-1732. Doi: 10.1007/s12665-010-0667-3.

Pandey, V.P., Shrestha, S., & Kazama, F. (2012). Groundwater in the Kathmandu Valley : Development Dynamics , Consequences and Prospects for Sustainable Management. *Eur. Water,* **37**: 3–14.

Panno, S.V. & Hackley, K.C. (2010). Geologic Influences on Water Quality.

Pant, R.R., Zhang, F., Rehman, F.U., Wang, G., Ye, M., Zeng, C., & Tang, H. (2018). Spatiotemporal Variations of Hydrogeochemistry and its Controlling Factors in the Gandaki River Basin , Central Himalaya Nepal. *Sci. Total Environ.***, 622–623**: 770-782. Doi:10.1016/j.scitotenv.2017.12.063.

Pant, B.R. (2011). Ground Water Quality in the Kathmandu Valley of Nepal. *Environ. Monit. Assess.*, **178**: 477–485. Doi:10.1007/s10661-010-1706-y

Pathak, D.R., Hiratsuka, A., & Awata, I. (2009). Assessment of Nitrate Contamination in Groundwater of a Shallow Aquifer in Kathmandu, Nepal. *Trends and Sustainability of Groundwater in Highly Stresses Aquifer (Proc. Of Symposium JS. 2 at the Joint IAHS & IAH Convention, Hyderabad, India), IAHS Publ.,* **329:** 178-183

Pathak, D.R., & Hiratsuka, A. (2010). An Investigation of Nitrate and Iron Concentration and their Relationship in Shallow Groundwater System of Kathmandu. *Desalination and Water Treatment,* **19**: 191-197.

Pathak, D.R., Yatabe, R., & Bhandary, N.P. (2013). Statistical Analysis of Factors Affecting Groundwater Quality in Shallow Aquifer of Kathmandu, Nepal. *International Journal of Water Research*, **1** (1): 12-20.

Pathak, D.R., Yatabe, R., & Bhandary, N.P. (2015). Indentification of Major Affecting Spatial and Temporal Variation of Water Quality in Kathmandu Basin, Nepal, Using Multivariate Statistical Analysis. *Int. J. Water*, **9** (3): 209-225. Doi: 10.1504/IJW.2015.070357.

Paudyal, R., Kang, S., Sharma, C.M., Tripathee, L., & Sillanpaa, M. (2016). Variations of Physicochemical Parameters and Metal Levels and Their Risk Assessment in Urbanized Bagmati River, Kathmandu, Nepal. *Journal of Chemistry*, 6025905. Doi: 10.1155/2016/6025905.

Poudel, S. (2013). Assessment of Community Vulnerability to Flood in Hanumante River, Bhaktapur, Nepal: Finding the Causes and Mitigation Approaches. *Int.J.Lsld.Env.*, **1**(1), 77-78.

Prajapati, R., Upadhyay, S., Talchabhadel, R., Thapa, B.R., Ertis, B., Silwal, P., & Davids, J.C. (2021a). Investigating the Nexus of Groundwater Levels, Rainfall and Land Use in the Kathmandu Valley. *Groundwater for Sustainable Development,* **14**: 100584. Doi: 10.1016/j.gsd.2021.100584.

Prajapati, R., Overkamp, N.N., Moesker, N., Happee, K., Bentem, R.V., Danegulu, A., Manandhar, B., Devkota, N., Thapa, A.B., Upathya, S., Talchabhadel, R., Thapa, B.R., Malla, R., Pandey, V.P., &Davids, J.C. (2021b). Stream, Sewage, and Shallow Groundwater: Stream-Aquifer Interaction in the Kathmandu

Valley, Nepal. *Sustainable Water Resoueces Management*, **7**: 72. Doi: 10.1007/s40899-021-00542-8.

Prasai, T., Lekhak, B., Joshi, D. R., & Baral, M. P. (2007). Microbiological Analysis of Drinking Water of Kathmandu Valley. *Scientific World*, **5** (5).

Prasai, T., Lekhak, B., Joshi, D.R., & Baral, M.P. (2010). Microbiological Analysis of Drinking Water of Kathmandu Valley. *Sci. World*, **5**: 112–114. Doi: 10.3126/sw.v5i5.2667

Quichimbo, E.A., Singer, M.B., & Cuthbert, M.O. (2020). Characterising Groundwater-Surface water Interactions in Idealised Ephemeral Stream Systems. *Hydrological Processes*,**34**: 3792-3806. Doi: 10.1002/hyp.13847.

Ramamohan, H., & Sudhakar, I. (2014). Evaluation of Groundwater Quality for the Pre and Post-Monsoon Variations in Physico-Chemical Characteristics of North East Coast of Srikakulam District, A.P., India. **3**: 124–131.

Saad, R., Nawawi, M.N.M. (2012). Groundwater Detection in Alluvium using 2-D Electrical Resistivity Tomigraphy (ERT). *Electrical Journal of Geotechnical Engineering*, **17.**

Sada, R. (2014). Trajectory of Urban River Degradation:Initiatives for Conservation and Restoration (A Case Study of Hamunante River in Bhaktapur, Nepal). *South Asisn water studies*, **4**: (2).

Sakai, T., Gajurel, A.P., Tabata, H., Ooi, N., Takaawa, T., Kitagawa, H., & Upreti, B.N. (2008). Revised Lithostrtigraphy of Fluvio-Lacustrine Sediments Comprising Northern Kathmandu Basin in Central Nepal. *Journal of Nepal Geological Society*, **37**: 25-44.

Sakakibara, K., Tsujimura, M., Song, X., & Zhang, J. (2016). Interaction Between Surface Water and Groundwater Revealed by Multi-Tracer and Statistical Approaches in the Baiyangdian Lake Watershed, North China Plain *Hydrol. Res. Lett*., **10** (2): 74–80.

Sarkar, B., Mitchell, E., Frisbie, S., Grigg, L., Adhikari, S., & Byanju, R.M. (2022). Drinking Water Quality and Public Health in the Kathmandu Valley, Nepal:

Coliform Bacteria, Chemical Contaminations, and Health Status of Consumers. *Journal of Environmental and Public Health*, **2022**: 3895859, 21. Doi:10.1155/2022/3895859.

Shakya, B.M., Nakamura, T., Shrestha, S. Das, & Nishida, K. (2019a). Identifying the Deep Groundwater Recharge Processes in an Intermountain Basin Using the Hydrogeochemical and Water Isotope Characteristics. *Hydrol. Res*., **50** (5): 1216–1229.

Shakya, B.M., Nakamura, T., Kamei, T., Shrestha, S. Das, & Nishida, K. (2019b). Seasonal Groundwater Quality Status and Nitrogen Contamination in the Shallow Aquifer System of the Kathmandu Valley, Nepal. *Water*, **11**:2184. Doi:10.3390/w11102184.

Shrestha, O.M., Koirala, A., Hanisch, J., Blusch, K., Kerntke, M., & Jager, S. (1999). A Geo-Environmental Map for the Sustainable Development of the Kathmandu Valley, Nepal. *GeoJournal*, **49**: 165-172.

Shrestha, P. (2010). Climate Change Impact on River Dynamics of the Bagmati Basin , Kathmandu Nepal. *Report submitted to National Adaptation Program of Action to Climate Change Project, GoN* , 36 p.

Shrestha, P., & Tamrakar, N.K. (2011). Effects of Human Disturbances and Climate on Morphological Changes of Bagmati River, Central Nepal. *Journal of Nepal Geological Society*, **43:** 205-218.

Shrestha, S., & Kazama, F. (2007). Assessment of Surface Water Quality using Multivariate Statistical Techniques: A Case Study of the Fuji River Basin, Japan. *Environ. Model. Softw*., **22** (4): 464–475. Doi:10.1016/j.envsoft.2006.02.001.

Shrestha, S., & Shah, S. (2014). Shallow aquifer mapping of Kathmandu Valley. *A final report submitted to Groundwater Resources Development Board.*

Shrestha, N., Lamsal, A., Regmi, R.K., & Mishra, B.K. (2015). Current Status of Water Environment in Kathmandu Valley, Nepal. *Water and Urban Initiative Working Paper Series*, **3**

Shrestha, G., Shakya, B.M., Shrestha, M.B., & Khadka, U.R. (2023). Water Infiltration

rate in the Kathmandu Valley of Nepal Admist Present Urbanization and Land-Use Change. *H_2 Open Journal*, **6** (1): 1. Doi: 10.2166/h2oj.2023.044.

Shrestha, S., Haramoto, E., Malla, R., & Nishida, K. (2015). Rist of Diarrhoea from Shallow Groundwater Contaminated with Enteropathogens in the Kathmandu Valley, Nepal. *Journal of Water and Health*, **13** (1): 259-269. Doi: 10.2166/wh.2014.036

Singh, A.K., & Kumar, S.R. (2015). Quality Assessment of Groundwater for Drinking and Irrigation Use in Semi-Urban Area of Tripura , India. *Eco. Env.&Cons.*, **21** (1): 97-108.

Siriwardana, C., Cooray, A.T., Liyanage, S.S., & Koliyabandara, S.M.P.A. (2019). Seasonal and Spatial Variation of Dissolved Oxygen and Nutrients in Padaviya Reservoirs, Sri Lanka. *Journal of Chemistry*, **5405016**:11. Doi: 10.1155/2019/5405016.

Shrestha, S., Semkuyu, D.J., & Pandey, V.P (2016). Assessment of Groundwater Vulnerability and Risk to Ppollution in Kathmandu Valley, Nepal. *Science of the Total Environment*, **556**: 23-35. Doi: 10.1016/j.scitotenv.2016.03.021.

Stocklin, J. & Bhattarai, K.D. (1977). Geology of Kathmandu Area and Central Mahabharat Range Nepal. *In: Himalaya report Department of Mines and Geology, Kathmandu, Nepal*, 86.

Stocklin, J. (1980). Geology of Nepal and Its Regional Frame. *Journal of Geological Society London*, **137:** 1-34

Soltan, M.E. (1991). Study of River Nile Pollution. *PhD Thesis*. Fac.Sci.Aswan, Assiut University, Egypt.

Sophocleous, M. (2002). Interaction between Groundwater and Surface Water: The State of the Science. *Hydrol. J.*, **10**: 52–67.

Song, X.; Liu, X.; Xia, J.; Yu, J.; & Tang, C. (2006). A Study of Interaction Between Surface Water and Groundwater Using Environmental Isotope in Huaisha River Basin. Sci. China Ser. *D Earth Sci*., **49:** 1299–1310.

Tamrakar, C,S., & Shakya, P.R. (2013). Physio-Chemical Assessment of Deep

Groundwater Quality of Various Sites of Kathmandu Metropolitan City, Nepal. *Research Journal of Chemical Science*, **3** (8): 78–82.

Tamrakar, N.K. (2004). Disturbances and Instabilities in the Bishnumati River Corridor, Kathmandu Basin. *JUSAN*, **9** (16): 7-18.

Tamrakar, N.K. (2009). Riverbed-Material Texture and Composition of Bishnumati River, Kathmandu, Nepal; Implication in Provenance Analysis. *Bulletin of the Department og Geology*, **12:** 55-62.

Tamrakar, N.K., & Bajracharya, R. (2012). Basinal and Planform Characteristics of the Kodku and the Godawari Rivers, Kathmandu, Central Nepal. *Bulletin of the Department of Geology*,**15**: 15-22.

Tamrakar, N.K., Bajracharya, R., Thapa, I., Sapkota, S., & Paudel, P.N. (2013). Morpho-Hydraulic Parameters and Classification of the Kodku River for Stream Stability Assessment, Southern Kathmandu, Central Nepal. *Bulletin of the* stability *Geology*, **16**: 1-20.

Terwey, J.L. (1984). Isotopes in Groundwater Hydrology. *Challenge in African Hydrology and Water Resources*, **144**, 155–160.

Thapa, B.R., Ishidaira, H., Pandey, V.P & Shakya, N.M. (2016). Impact Assessment of Gorkha Earthquake 2015 on Portable Water Supply in Kathmandu Valley: Preliminary Analysis. *J. Japan Soc. Civil Eng.*, **72:** 61-66.

Tonina, D., Buffington, J.M. (2009). Hyporheic Exchange in Mountain Rivers: Mechanics and Environmental Effects. *Geography Compass* **3 (**3): 1063-1086.

Uchengbulam, O., & Ayolabi, E.A. (2014). Application of Electrical Resistivity Imaging in Investigating Groundwater Pollution in Sapele Area, Nigeria. *Journal of Water Resources and Protection*, **6:** 1369-1379. Doi: 10.4236/jwarp.2014.614126.

Uhlemann, S., Kuras, O., Richards, L.A., Naden, E., & Polya, D.A. (2017). Electrical Resistivity Tomography Determines the Spatial Distribution of Clay Layer Thickness and Aquifer Vulnerability, Kandal Province, Cambodia. *Journal of Asian Earth Sciences*, **147:** 402-414.

Vanderzalm, J.L., Jeuken, B.M., Wischusen, J.D. H., Pavelic, P., Salle, C.L. G.L., Knapton, A., & Dillon, P.J. (2011). Recharge Sources and Hydrogeological Evolution of Groundwater in Alluvial Basins in Arid Central Australia. *Journal of Hydrology,* **397:** 71-82. Doi: 10.1016/j.jhydrol.2010.11.035.

Vrzel, J., Kip Solomon, D., Blazeka, Z., & Ogrinc, N. (2018). The Study of Interactions Between Groundwater and Sawa River Water in the Ljubljansko Polje Aquifer System (Slovenia). *Journal of Hydrology*, **556:** 384-396. Doi:10.1016/j.jhydrol.2017.11.022

Wang, W., Dai, Z., Zhao, Y, Li, J., Duan, L., Wang, Z., & Zhu, L. (2016). A Quantitative analysis of Hydraulic Interraction Processes in Stream-Aquifer systems. *Scientific Report*, **6**: 19876. Doi: 10.1038/srep19876.

Ward, J.H. (1963). Hierarchical Grouping to Optimize an Objective Function. *J. Am. Stat. Assoc.*, **58** (301): 236–244, Doi:10.1080/01621459.1963.10500845.

Ward A.S., Gooseff, M.M., & Singha, K. (2010). Characterizing Hyporheic Transport Processes-Interpretation of Electrical Geophysical Data in Coupled Stream-Hyporheic Zone System during Solute Tracer Studies. *Advances in Water Resources*, **33**: 1320-1330.

Warner, N.R., Levy, J., Harpp, K., & Farruggia, F. (2008). Drinking Water Quality in Nepal's Kathmandu Valley: A Survey and Assessment of Selected Controlling Site Characteristics. *Hydrogeol. J.*, **16**: 321–334. https://doi.org/10.1007/s10040-007-0238-1

Wen, R., Tian, L., Weng, Y.B., Liu, Z.F., & Zhao, Z.P. (2012). The Altitude Effect of $\delta^{18}O$ in Precipitation and River Water in the Southern Himalayas. *Chin Sci. Bull.*, **57**: 1693-1698. Doi:10.1007/s11434-012-4992-7.

WHO Nepal, 2005. National Drinking Water Quality Standards 22.

Winter, T.C., Harvey, J.W., Franke, O.L., & Alley, W.M. (1998). Ground Water and Surface Water: A Single Resource. *U.S. Geological Survey Circular 1139*, 79p.

Woessner, W.W. (2000). Stream and Fluvial Plain Groundwater Interaction: Rescaling Hydroecologic Thought. *Ground Water*, **38**: 423–429.

Yoshida, M., & Igarashi, Y. (1984). Neogene to Quaternary Lacuastrine Sediments in

the Kathmandu Valley, Nepal. *Jour. Nepal Geological Society, Special Issue,* **4**: 73-100

Yoshida, M., & Igarashi, Y. (1984). Neogene to Quaternary Lacustrine Sediment in the Kathmandu Valley, Nepal. *J. Nepal Geol. Soc.*, Special issue, **4**: 37-100.

Yang, L., Song, X., Zhang, Y., Han, D., Zhang, B., & Long, D. (2012). Characterizing Interactions between Surface Water and Groundwater in the Jialu River Basin using Major Ion Chemistry and Stable Isotopes. *Hydrol. Earth Syst. Sci.,* **16** (11): 4265–4277. Doi:10.5194/hess-16-4265-2012.

Yang, K., Han, G., Liu, M., Li, X., Liu J., & Zhang, Q. 92018). Spatial and Seasonal Variation of O and H Isotopes in the Jiulong River, Southeast China. *Water*, **10**:1677. Doi: 10.3390/w10111677.

Zhong, M., Zhang, H., Sun, X., Wang, Z., Tian, W., & Huang, H. (2018). Analyzing the Significant Environmental Factors on the Spatial and Temporal Distribution of Water Quality Utilizing Multivariate Statistical Techniques: A Case Study in the Balihe Lake, China. *Environ. Sci. Pollut. Res*., **25** (29): 29418–29432. Doi:10.1007/s11356-018-2943-9.

Zhang, B., Song, X., Zhang, Y., Ma, Y., Tang, C., Yang, L., & Wang, Z.L. (2016). The Interaction between Surface Water and Groundwater and Its Effect on Water Quality in the Second Songhua River Basin, Northeast China. *J. Earth Syst. Sci.*, **125** (7): 1495–1507. Doi:10.1007/s12040-016-0742-6.

Zhou, P., Li, M., & Lu, Y. (2017). Hydrochemisry and Isotope Hydrology for Groundwater Sustainability of the Coastal Multilayered Aquifer System (Zhanjian, China). Hindawi: *Geofluids*, **7080346**, 19. Doi: 10.1155/2017/7080346.

Zhu, M., Wang, S., Kong, X., Zheng, W., Feng, W., Zhang, X., Yuan, R., Song, X., & Sprenger, M. (2019). Interaction of Surface Water and Groundwater Influenced by Groundwater Over-Extraction, Waste Water Discharge and Water Transfer in Xiong'an New area, China. *Water*, **11**:539. Doi:10.3390/w11030539.

APPENDIX 1

LIST OF PUBLICATIONS RELATED TO PHD RESEARCH

Appendix 1A International Journal with impact factor

Bajracharya,R., Nakamura, T., Ghimire, S., Shakya, B.M., & Tamrakar, N.K. (2020). Identifying groundwater and river water interconnections using hydrochemistry, stable isotopes, and statistical methods in Hanumante River, Kathmandu Valley, Central Nepal. Water, 12 (6),1524,doi:10.3390/w12061524.

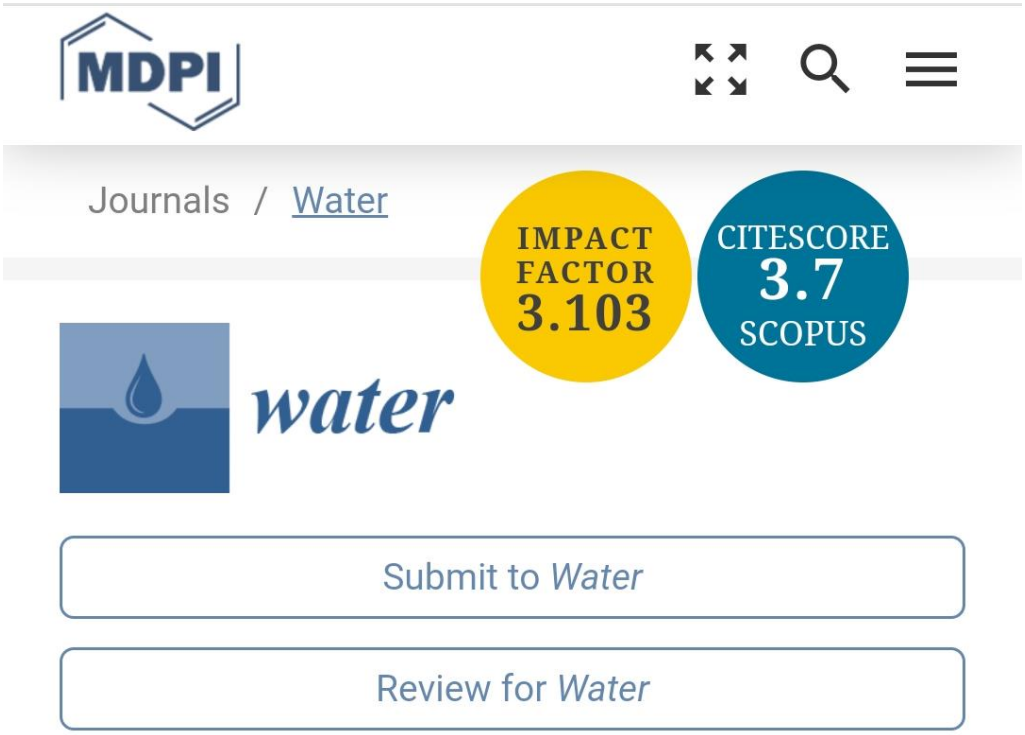

water

MDPI

Article

Identifying Groundwater and River Water Interconnections Using Hydrochemistry, Stable Isotopes, and Statistical Methods in Hanumante River, Kathmandu Valley, Central Nepal

Ramita Bajracharya [1], Takashi Nakamura [2,*], Subesh Ghimire [1], Bijay Man Shakya [2] and Naresh Kazi Tamrakar [1]

[1] Central Department of Geology, Tribhuvan University, Kirtipur, Kathmandu 44613, Nepal; bajrarami@yahoo.com (R.B.); shghimire2001@gmail.com (S.G.); nktam555@gmail.com (N.K.T.)
[2] Interdisciplinary Centre for River Basin Environment (ICRE), University of Yamanashi, 4-4-37 Takeda, Kofu, Yamanashi 400-8511, Japan; inform.bj76@gmail.com
* Correspondence: tnakamura@yamanashi.ac.jp

Received: 24 April 2020; Accepted: 23 May 2020; Published: 27 May 2020

Abstract: Interconnection between river water and groundwater plays an important role in maintaining water quantity and quality in hydrological systems. Furthermore, the exact interconnection is often difficult to observe and measure. This study attempts to explain river and shallow groundwater interconnection in urbanized areas of the Kathmandu Valley, Nepal. Isotopic (δD and $\delta^{18}O$) and chemical analyses were performed on river and groundwater samples, and the results were analyzed using statistical methods to identify areas of interconnection between river water and groundwater. Higher concentrations and positive strong correlations of Na^+ with K^+, NH_4^+-N, Cl^-, HCO_3^-, and PO_4^--P, and a change of water type from Ca-HCO_3 during the wet season to Na-K-HCO_3 during the dry season indicate higher contamination in river water during the dry season. Hierarchical cluster analysis was used in grouping water samples into clusters on the basis of isotopic and chemical (Na+ and Cl^-) composition. Grouping of river and groundwater samples in one–one clusters from wet and dry seasons shows the presence of interconnection, indicating the contribution of river water in recharging shallow groundwater. These results imply that shallow groundwater found near rivers is chemically contaminated by polluted river water through bank infiltration, in both wet and dry seasons.

Keywords: stable isotopes; chemical ions; hierarchical cluster analysis; groundwater-river water interconnection; Hanumante River

1. Introduction

Interconnection of river water and groundwater is a process of exchange between waters located on the river channel with those in the rocks/sediments under the surface. The exchange rate of water is controlled by hydraulic conductivities of the river channel and aquifer sediments; the relative stage of the river channel and nearby groundwater level; and geometry of the river channel within the alluvial plain [1,2]. The presence of a clogging layer on an aquifer and a riverbed or bank can decrease or stop the water flow exchange [3]. Interconnection of river water and groundwater also depends on the distance from a river channel, the geological conditions, and climatic factors [4]. Understanding of groundwater and surface water interconnection is very important to develop effective water resource management and policy as it can change the water quality and quantity of both water systems [5,6].

Studies related to the interconnection between river water and groundwater has increased in most developing countries during the last few decades. Utmost studies have been carried out to the assess areas of interconnection and the presence of exchange flow between river and groundwater on a regional as well as local scale [7–9]. Essentially, two types of exchange flow conditions are involved in the river and groundwater interaction: (1) the influent condition and (2) the effluent condition. Based on the condition of exchange flow, several studies specify that base flow in the river during the dry season is the result of effluent flow from shallow groundwater [5,10–13]. Furthermore, the condition of the exchange process can be affected by anthropogenic activities that alter the exchange processes, reduce connectivity, and lead to chemical or biological contaminations [2,14]. Increased sewage load into the rivers running through the urbanized cities can transfer toxic contamination to surrounding shallow groundwater in influent reaches. The decline of water table in a nearby shallow aquifer due to over-extraction can increase groundwater recharge from polluted river water [15,16]. The anthropogenic activities driven by increased urbanization and population growth affect river water quality, which adversely reflects on nearby groundwater quality.

Previous research conducted in the Kathmandu Valley reported the presence of an interconnection between river water and groundwater, showing a recharge of the groundwater by river water [17–19]. Additionally, a number of previous studies on river water quality have also reported heavy contamination of the downstream section of major rivers [20–23], inducing the occurrence of various water-borne diseases such as diarrhea, cholera, and dysentery among the people of riverside areas [24].

Methods such as heat tracer, solute tracer, direct measurement of water flux, and environmental tracer methods including isotope and geochemistry have been used to determine the interconnections of groundwater and surface water [25–30]. Similarly, numerical modeling, geophysical methods, and statistical methods have also been used to describe interaction processes [31–34]. Basically, water flux measurement mostly used a direct method to get exchange flow conditions involved in interacting processes. The recharging source for groundwater or river water is dependent on the direction of exchange flow [35]. Further, stable isotopes of hydrogen and oxygen along with Na and Cl ions have been widely used to determine river and groundwater interconnections. Similarity in isotopic values and chemical ions between nearby groundwater and river water indicate the presence of river and groundwater interconnection [13,36]. Additionally, hierarchical cluster analysis (HCA), one of the multivariate methods, has been widely used to determine the interaction of river water and groundwater at the absence of a water flux dataset [37]. HCA can be used to analyze regional-scale as well as local small datasets. Several previous studies used HCA as a major statistical method and suggested similarities in chemical and isotopic compositions between river water and their nearby groundwater representing the presence of river and groundwater interaction [9,34,37].

The present study will focus on the application of stable isotope values, chemical compositions of the river and groundwater samples, followed by statistical analysis for one of the contaminated rivers in urban areas of the Kathmandu valley. Thus, identifying the occurrence of the spatial and seasonal interconnectivity and possible contamination load from the river to river periphery groundwater are major goals of this study.

2. Materials and Methods

2.1. Study Area

The Hanumante River is a centripetal river and is one of the most polluted tributaries of the Bagmati River in the Kathmandu Valley, Central Nepal [20,38]. It is the only river that drains from the eastern part of the Kathmandu Valley and confluences with the Manahara River (a major tributary of the Bagmati River) at Jadibuti (Figure 1). This sixth-order river extends up to 18.29 km, covering nearly 97 km^2 of watershed areas [39]. The Godawari Khola, Tabyakhusi Khola, and Chakkhu Khola are major tributaries of this river.

The quality of the Hanumante River water is deteriorating as urbanization increases downstream, having lower dissolved oxygen (0-7 mg/L) and higher biological oxygen demand (3.5–79.9 mg/L), chemical oxygen demand (128 mg/L), ammonia (0.4-25 mg/L), and phosphorous (0.09-1.71 mg/L), such that the river water is harmful for domestic purposes [38]. Direct disposal of sewage and solid waste effluent from industries converts the Hanumante River into an open sewer during the dry season [40]. The sole municipal drinking water supply organization, namely, Kathmandu Upatyaka Khanepani Limited (KUKL), cannot fulfill the total water demands of the Kathmandu Valley [41], compelling it to fulfill the water deficit by extracting groundwater from shallow as well as deep aquifers. Meanwhile, Gautam et al. [17] discussed the high possibility of shallow aquifer contamination by polluted river water in the peripheral part of the rivers in the Kathmandu Valley.

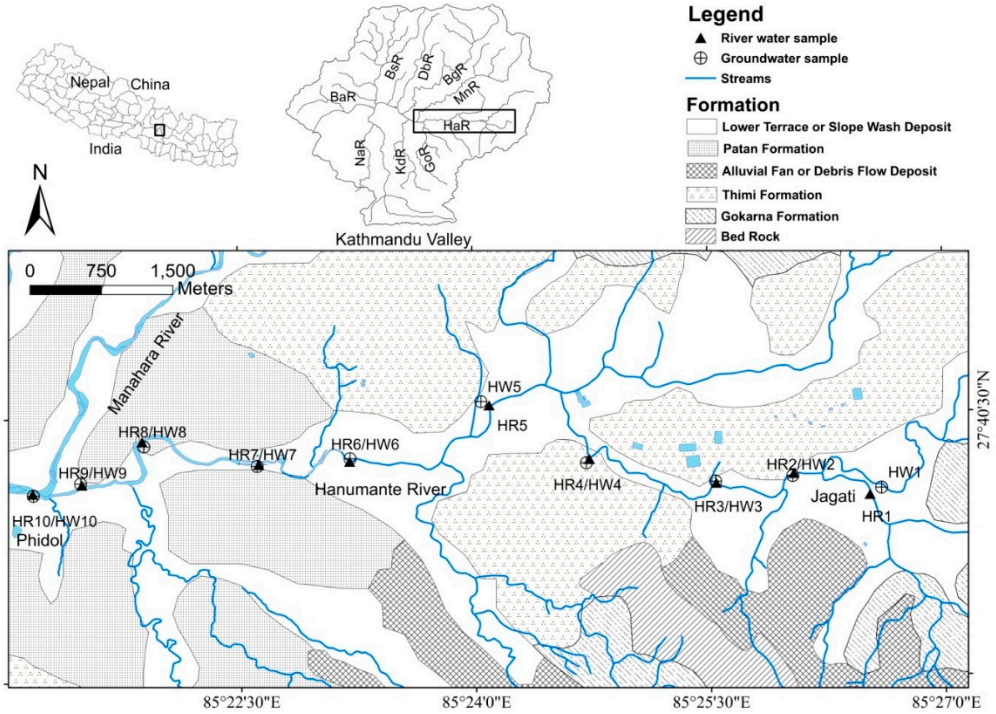

Figure 1. Sedimentological map showing study area and sampling locations along the Hanumante River corridor (modified from Yoshida and Igarashi [42], Sakai et al. [43], and Dhital [44]); BsR = Bishnumati, DbR = Dhobi, BgR = Bagmati, MnR = Manahara, HaR = Hanumante, GoR = Godawari, KdR = Kodku, NaR = Nakhhu, and BaR = Balkhu river.

Geologically, Plio-Pleistocene fluvial, fluvio-lacustrine, and fluvio-deltaic sediments comprise the Kathmandu Valley [42,43]. The study area presented in Figure 1 is characterized by four formations, namely, the Gokarna Formation, Patan Formation, Thimi Formation, and Lower Terrace Deposit [44]. The upstream section of the study area is composed of the Gokarna Formation, containing dark brown colored, laminated arkosic sand, silty clay, and peat. The middle section of the study area is covered by the Thimi Formation, which consists of sand, silt, clay, peat, and gravel composed of granite and gneiss derived from the Shivapuri Range. Similarly, the lower section of the study area is dominated by the Patan Formation, which contains deposits of fluvial-lacustrine composed of sand, silt, clay, and peat. The Lower Terrace Deposit along the river corridor consists of micaceous sand, pebbles, and granules [44].

To use chemical and isotopic analysis to investigate any interconnectivity between river and groundwater, samples were collected from 20 locations—10 from rivers and 10 from dug wells (Figure 1) during the wet (August 2017) and dry seasons (February 2018).

2.2. FieldMeasurement and Water Sampling

Groundwater was collected from dug wells which are located within 10 to 100 m from the river channel, with the depth ranging between 1.5 and 15.7 m. Sampling was carried out in two seasons—August 2017 (wet season) and February 2018 (dry season)—where the samples were collected from 20 locations, 10 from rivers and 10 from dug wells (Figure 1) in the consecutive seasons, respectively. Water samples were collected in 100 mL polyethylene bottles. Each bottle was rinsed three times with the same water before sample collection. Groundwater samples were collected after removing a quantity of water using an installed hand pump or with the help of rope and a plastic bucket. The collected water samples were stored at −4°C at a laboratory until the chemical and isotope analyses were performed

Additionally, during the sample collection, well depth, water level depth, electrical conductivity (EC), dissolved oxygen(DO), pH, and water temperature were measured at each sampling location.

Well depth was measured using a measuring tape and was verified with the dug well owner. A water depth logger was deployed for the water table measurement. In situ parameters were measured by using portable devices, namely, a DO meter (Mettler Toledo SG3-ELK, Greifensee, Zurich, Switzerland) and a pH/EC meter (Mettler Toledo Duo, Greifensee, Zurich, Switzerland). The location of the water samples is shown in Figure 1, and Table 1 presents the data measured during the field survey.

2.3. Chemical and Isotopic Analysis

The Interdisciplinary Center for River Basin Environment, University of Yamanashi (ICRE-UY), Japan provided laboratory facilities to carry out chemical and isotopic analyses. As per the laboratory procedure, collected water samples were first filtered through 0.2 µm filter paper to prepare final samples for further laboratory analyses. The dominant chemical ions, including cations (Na^+, K^+, NH_4-N^+, Ca^{2+}, and Mg^{2+}) and anions (Cl^-, $NO_3{}^-$-N, $PO_4{}^-$-P, and $SO_4{}^{2-}$), were determined by using ion chromatography (ICS-1100, Dionex, Waltham, MA, USA with an analytical error of 5%. The bicarbonate ion ($HCO_3{}^-$) concentrations were measured by using a titration method with 0.01N sulfuric acid.

The stable isotopes of hydrogen (δD) and oxygen ($\delta^{18}O$) were analyzed using cavity ring-down spectroscopy (L1102-i, Picarro, Santa Clara, CA, USA). VSMOW (Vienna Standard Mean Ocean Water) is the standard water used to calculate isotopic ratios (δ) of D and ^{18}O of water samples. The results were reported in parts per thousand (per mill deviation) with respect to these standards with precision 0.5‰ for δD and 0.1‰ for $\delta^{18}O$. The isotopic ratios of hydrogen and oxygen were calculated by using the formula given by Craig [45]:

$$\delta = [(R_{sample} - R_{standard})/R_{standard}] \times 1000 \ (‰)$$

R is defined as D/H or $^{18}O/^{16}O$ in sampled water (R_{sample}) and standard mean ocean water ($R_{standard}$).

2.4. Statistical Analysis

Temporal variations of chemical variables were evaluated using a paired t-test for significant difference in parameters [46,47] within a 95% confidence level. Spearman's rho correlation analysis [48] was adopted to establish any relationship among different variables. Hierarchical cluster analysis (HCA) was used to examine any similarity in chemical as well as isotopic composition between river water and groundwater. Cluster analysis is useful in distinguishing water showing similar chemical or isotopic composition from dissimilar ones [37,49,50]. HCA was performed based on Ward's linkage method [51] with squared Euclidean distances as a measure of similarity between samples [11,40]. Statistical Package for Social studies version 25 (SPSS Inc., Chicago, IL, USA) was used for statistical analyses.

3. Results

3.1. InSitu Parameters

Table 1 presents locations of sample points, the depth of water level at different wells, and the measured in situ parameters in wet and dry seasons. All sample wells had shallow water depth in the wet season, which may imply high recharge and lower extraction rates during wet seasons, with a maximum fluctuation of 3.60 m and a minimum fluctuation of 0.65 m at HW9 and HW6, respectively (Table 1).

In situ parameters, namely, temperature, pH, EC, and DO, in river water and groundwater were measured in wet and dry seasons. The temperature of river water ranged from 22.3 °C to 24.3 °C in the wet season, while in the dry season the range was 14.0–17.9 °C. The temperature range of groundwater was 20.7–24.1°C in the wet season and 13.4–20.5 °C in the dry season (Table 1). The pH value slightly decreased during the dry season in both river water and groundwater (Table 1). EC measured in groundwater ranged from 290 to 934 µS/cm in the wet season, and from 576 to 1323µS/cm in the dry season. Groundwater exhibited higher EC in the dry season relative to the wet season, except at HW1, HW2, and HW4 (Figure 1, Table 1). However, in the case of river water, the value of EC was low (164.2 to 247 µS/cm) in the wet season and abruptly increased by up to eight times (604 to 2060 µS/cm) in the dry season. DO was high in river water during the wet season and abruptly decreased below the value measured in groundwater during the dry season (Table 1).

3.2. Hydro-Chemical Parameters

Figure 2 presents spatial and temporal variations of the chemical parameters analyzed from river water and groundwater. Na^+, K^+, NH_4^+-N, Ca^{2+}, Mg^{2+}, Cl^-, HCO_3^-, NO_3^--N, PO_4^--P, and SO_4^{2-} are considered as chemical parameters in this study.

Ca^{2+} and HCO_3^- were the most dominant ions of river water in the wet season, with values ranging from 7.3 to 17.0 mg/L and 24.4 to 73.2 mg/L, respectively (Figure 2). The major cations had an order of $Ca^{2+} > Na^+ > K^+ > Mg^{2+}$ in the wet season, which changed to the order $Na^+ > NH_4^+ > Ca^{2+} > K^+ > Mg^{2+}$ in the dry season. Similarly, for anions, HCO_3^- was dominant, followed by SO_4^{2-} and Cl^- in the wet season, and Cl^- and SO_4^{2-} in the dry season. Except for NO_3^--N, all other parameters showed strong significant seasonal variation ($p < 0.01$). Concentrations of all these parameters increased in the dry season, but the rate of increment varied for different parameters. NH_4^+-N and PO_4^--P concentration was insignificant (<1 mg/L) in the wet season and significantly increased in the dry season, ranging from 10.3 to 102.9 mg/L (for NH_4^+-N) and from 2.4 to 31.7 mg/L (for PO_4^--P). Similarly, concentrations of Na^+, K^+, Cl^-, and HCO_3^- increased by more than ten times than in the wet season (Figure 2). Based on piper plot from the chemical analyses, the Hanumante River can be categorized as Ca-HCO_3 type in the wet season and Na-K-HCO_3 type in the dry season (Figure 3).

Table 1. In situ measured parameters of groundwater and river water in the wet (7 August 2017) and dry (18 February 2018) seasons.

Sampling ID	N	E	River Bank	Distance from River (m)	Well Depth (m)	Water Level Depth (m)			EC (µs/cm)		pH		DO (mg/L)		Water Temp (°C)	
						Wet	Dry	Difference WLD	Wet	Dry	Wet	Dry	Wet	Dry	Wet	Dry
HW1	27.66936	85.44028	Right	100	3.3	1	2.82	1.82	839	797	7.03	6.40	2.05	0.44	22.3	20.5
HW2	27.6696	85.43617	Left	10	15.7	1	1.97	0.97	934	820	8.05	7.35	1.54	0.51	20.7	18.9
HW3	27.66915	85.42796	Right	15	8.2	0.9	4.1	3.2	784	1323	7.22	6.79	1.14	0.52	23.6	19.0
HW4	27.67104	85.41425	Left	60	1.5	0.6	1.74	1.14	681	576	7.16	6.40	2.38	2.27	22.0	13.4
HW5	27.67638	85.40083	Right	80	5	1	3.38	2.38	290	637	7.75	6.09	3.16	1.27	24.1	17.5
HW6	27.67166	85.38907	Right	20	2.8	1.7	2.35	0.65	520	611	7.06	6.13	2.56	1.25	22.8	17.5
HW7	27.67103	85.37917	Left	30	7	4.3	5.8	1.5	591	856	7.52	6.48	2.45	1.97	22.7	17.6
HW8	27.673	85.36717	Left	35	5	3.6	4.5	0.9	889	1192	7.25	6.39	4.10	1.82	22.6	20.4
HW9	27.67027	85.3619	Right	20	2.8	0.8	4.4	3.6	769	964	6.73	6.28	3.00	2.08	21.0	18.3
HW10	27.66843	85.35531	Left	10	2.4	0.1	1.9	1.8	623	1168	7.61	6.70	3.29	1.65	22.8	16.2
HR1	27.66722	85.44194							164.2	604	8.00	7.45	6.48	5.54	22.3	14.9
HR2	27.66916	85.43388							171.6	1340	8.06	6.84	6.30	1.67	22.4	16.5
HR3	27.66833	85.42555							186.6	2010	7.22	7.02	5.50	0.51	23.0	16.6
HR4	27.67083	85.41222							226	1780	7.78	6.88	4.43	0.67	23.0	14.0
HR5	27.67583	85.40166							224	2060	7.85	6.75	4.59	0.55	23.9	15.6
HR6	27.67083	85.38666							227	1924	7.81	7.00	4.26	0.24	24.3	17.2
HR7	27.67055	85.37694							240	1998	7.96	7.00	3.99	0.32	23.5	16.7
HR8	27.67277	85.36472							237	1955	7.80	6.99	4.03	0.15	23.5	17.1
HR9	27.66861	85.35805							247	1960	6.70	7.00	4.05	0.07	23.0	17.9
HR10	27.66805	85.35305							239	1985	7.96	6.98	4.25	0.44	23.4	16.4

HW = Hanumante well water, HR = Hanumante river water, WLD = water level depth.EC = electrical conductivity, DO = dissolved oxygen.

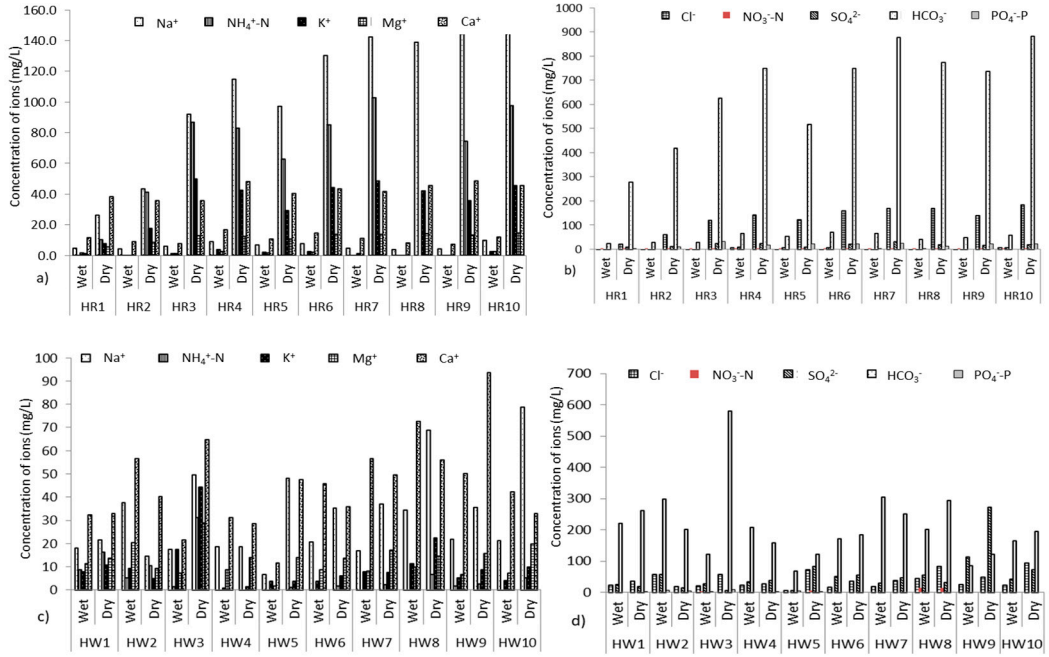

Figure 2. Bar diagram showing temporal and spatial variation of chemical parameters in river water (**a**,**b**) and groundwater (**c**,**d**). HR = Hanumante river water and HW = Hanumante groundwater.

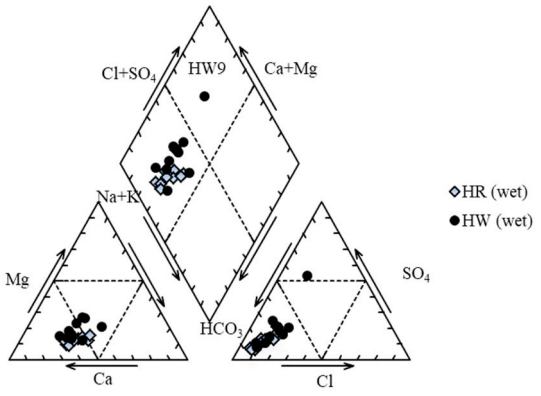

(**a**)

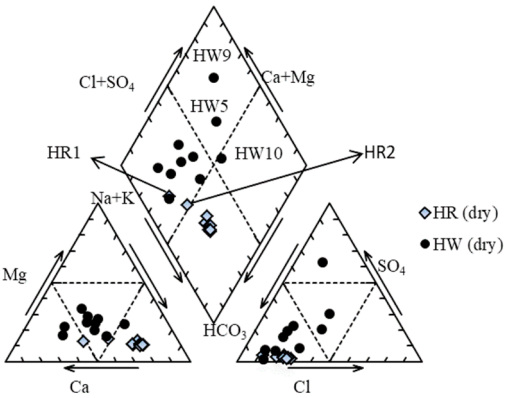

(**b**)

Figure 3. Piper diagram of major ions of groundwater and river water in (**a**) wet season (**b**) dry season. HR = Hanumante river water, HW = Hanumante groundwater.

Likewise, Ca^{2+} and HCO_3^- were the most dominant ions of groundwater in both wet and dry seasons. Concentration of Ca^{2+} ranged from 11.7 to 72.5 mg/L in the wet season and from 28.4 to 93.7 mg/L in the dry season. In the case of HCO_3^-, 67.1-305.0 mg/L was the range in the wet season, which increased to 122.0–579.5 mg/L in the dry season. Statistical analysis (paired t-test within a 95% confidence level) showed no significant temporal variation in K^+, NH_4^+-N, Ca^{2+}, HCO_3^-, NO_3^--N, and SO_4^{2-} in groundwater. However, for Na^+, Mg^{2+}, and Cl^-, temporal variation was significant, with a *p*-value of 0.03. In general, groundwater showed lesser increments in concentration compared with river water during the dry season (Figure 2) and is classified as Ca-HCO_3 type in both dry and wet seasons, except at HW5, HW9, and HW10. Water samples collected from HW5 and HW10 changed slightly from Ca-HCO_3 (in the wet season) to Ca-SO_4, and Na-Cl-SO_4, respectively, during the dry season (Figure 3). Groundwater collected from HW9 in both seasons is of Ca-SO_4 type.

Determination of water types using a piper diagram suggests the origin of the water [52]. Ca-HCO_3 type represents recent infiltration of freshwater, whereas Ca-SO_4 and Na-K-HCO_3 types indicate water exhibiting simple dissolution or mixing and ion exchange, respectively [53]. Groundwater and river water from the wet season of Ca-HCO_3 type thus represents recent rainfall infiltration or runoff as a major contributing source for groundwater recharge and river discharge. Changes in river water type during the dry season reflect the presence of different water sources for river discharge, including direct discharge of untreated sewage from municipal and industrial sources [16].

The Spearman's rho correlation matrix between different chemical parameters in river water and groundwater is presented in Table 2. In river water, DO has a strong negative correlation ($r = -0.60$ to -0.86) with all parameters except pH and NO_3^--N. The negative correlation of DO indicates that the presence of a higher concentration of chemical parameters decreases the amount of dissolved oxygen in river water. In contrast, EC has a strong positive correlation with parameters which have a negative correlation to DO, suggesting full dependence of conductivity of river water on dissolved ion concentrations [50]. The higher value of EC and positive correlation with most ions also indicate higher anthropogenic contamination during the dry season [54] (Table 1 and Figure 2). There is also a strong positive correlation of Na^+, K^+, NH_4^+-N, Ca^{2+}, Mg^{2+}, Cl^-, HCO_3^-, PO_4^{-}P, and SO_4^{2-} between each other ($r = 0.67$ to 0.98), indicating that the river water is highly influenced by anthropogenic pollution [11] such as direct discharge of municipal and industrial sewage and leachate of solid waste disposal near the river channel during the dry season [40]. Strong positive correlation of PO_4^--P with SO_4^{2-}, NH_4^+-N, and NO_3^--N also suggests the influence of fertilizer and pesticides used in the cultivated land of river peripheral areas [54–56].

Correlations of chemical parameters of groundwater are similar to those of river water. As in the case of EC, it has strong positive correlation with Na^+, K^+, NH_4^+-N, Ca^{2+}, Mg^{2+}, Cl^-, and PO_4^--P. Strong positive correlation between Na^+, Mg^{2+} and Cl^- (0.94) in groundwater indicates the influence of anthropogenic activities [57] because there was no evidence of halite deposits in the study area [58]. The negative correlation between NH_4^+-N and NO_3^--N represents nitrification of NH_4^+-N into NO_3^--N [59]. Positive correlation of K^+, NH_4^+-N, and PO_4^--P represents agricultural impact from the surrounding cultivated land.

Table 2. Correlation matrix of different chemical parameters.

(a) River Water												
Parameters	**DO**	**EC**	**pH**	**Na^+**	**$NH4^+$-N**	**K^+**	**Mg^{2+}**	**Ca^{2+}**	**Cl^-**	**NO_3-N**	**PO_4-P**	**SO_4^{2-}**	**HCO_3^-**
DO	1.00												
EC	−0.86	1.00											
pH	0.64 **	−0.72	1.00										
Na^+	−0.77	0.76 **	−0.54	1.00									
$NH4^+$-N	−0.83	0.87 **	−0.61	0.87 **	1.00								
K^+	−0.72	0.80 **	−0.49	0.92 **	0.92 **	1.00							
Mg^{2+}	−0.78	0.81 **	−0.54	0.98 **	0.90 **	0.95 **	1.00						
Ca^{2+}	−0.73	0.74 **	−0.49	0.94 **	0.82 **	0.87 **	0.92 **	1.00					
Cl^-	−0.77	0.79 **	−0.57	0.98 **	0.91 **	0.95 **	0.98 **	0.92 **	1.00				
NO_3-N	0.14	−0.30	0.30	0.15	−0.09	0.13	0.12	0.02	0.13	1.00			
PO_4-P	−0.61	0.93 **	−0.37	0.67 *	0.89 **	0.88 **	0.69 *	0.40	0.66 *	0.70 *	1.00		
SO_4^{2-}	−0.70	0.77 **	−0.50	0.92 **	0.89 **	0.98 **	0.94 **	0.88 **	0.93 **	0.12	0.75 **	1.00	
HCO_3^-	−0.85	0.86 **	−0.62	0.92 **	0.92 **	0.90 **	0.95 **	0.90 **	0.94 **	−0.05	0.68 *	0.89 **	1.00
(b) Groundwater													
Parameters	**DO**	**EC**	**pH**	**Na^+**	**$NH4^+$-N**	**K^+**	**Mg^{2+}**	**Ca^{2+}**	**Cl^-**	**NO_3-N**	**PO_4-P**	**SO_4^{2-}**	**HCO_3^-**
DO	1.00												
EC	−0.39	1.00											
pH	0.36	−0.18	1.00										
Na^+	−0.26	0.66 **	−0.53	1.00									
$NH4^+$-N	−0.72	0.74 **	−0.26	0.38	1.00								
K^+	−0.38	0.75 **	−0.03	0.42	0.63 **	1.00							
Mg^{2+}	0.00	0.69 **	−0.46	0.78 **	0.57 **	0.40	1.00						
Ca^{2+}	0.10	0.51 *	−0.07	0.55*	0.22	0.42	0.42	1.00					
Cl^-	−0.32	0.71 **	−0.54	0.94 **	0.44	0.47 *	0.81 **	0.49 *	1.00				
NO_3-N	0.30	−0.10	−0.28	0.11	−0.45	0.07	−0.10	0.14	0.18	1.00			
PO_4-P	−0.19	0.74 *	0.69	0.14	0.64	0.64	0.25	0.50	0.00	−0.54	1.00		
SO_4^{2-}	0.25	0.12	−0.36	0.54 *	−0.21	−0.12	0.24	0.45 *	0.47 *	0.19	−0.48	1.00	
HCO_3^-	−0.33	0.48	0.12	0.26	0.45 *	0.48 *	0.49 *	0.36	0.27	−0.21	0.55	−0.33	1.00

* Correlation is significant at the 0.05 level (two-tailed); ** Correlation is significant at the 0.01 level (two-tailed), DO = dissolved oxygen, EC = Electrical conductivity, NH_4^+-N = ammonium nitrogen, NO_3^--N = nitrate nitrogen, PO_4^--P = phosphate phosphorous.

3.3. Isotopic Composition

Fewer studies regarding isotopic analysis of meteoric water have been carried out on a local scale [60–62]. The local meteoric water line (LMWL), established by Gajurel et al. [60] and Giri [61], has a similar slope and intercept value as the global meteoric water line (GMWL) reported by Craig [45]. In this study, GMWL is used as a reference of meteoric water. The $\delta^{18}O$ verses δD plot (Figure 4) presents variations in stable isotopic compositions of groundwater and river water during both wet and dry seasons.

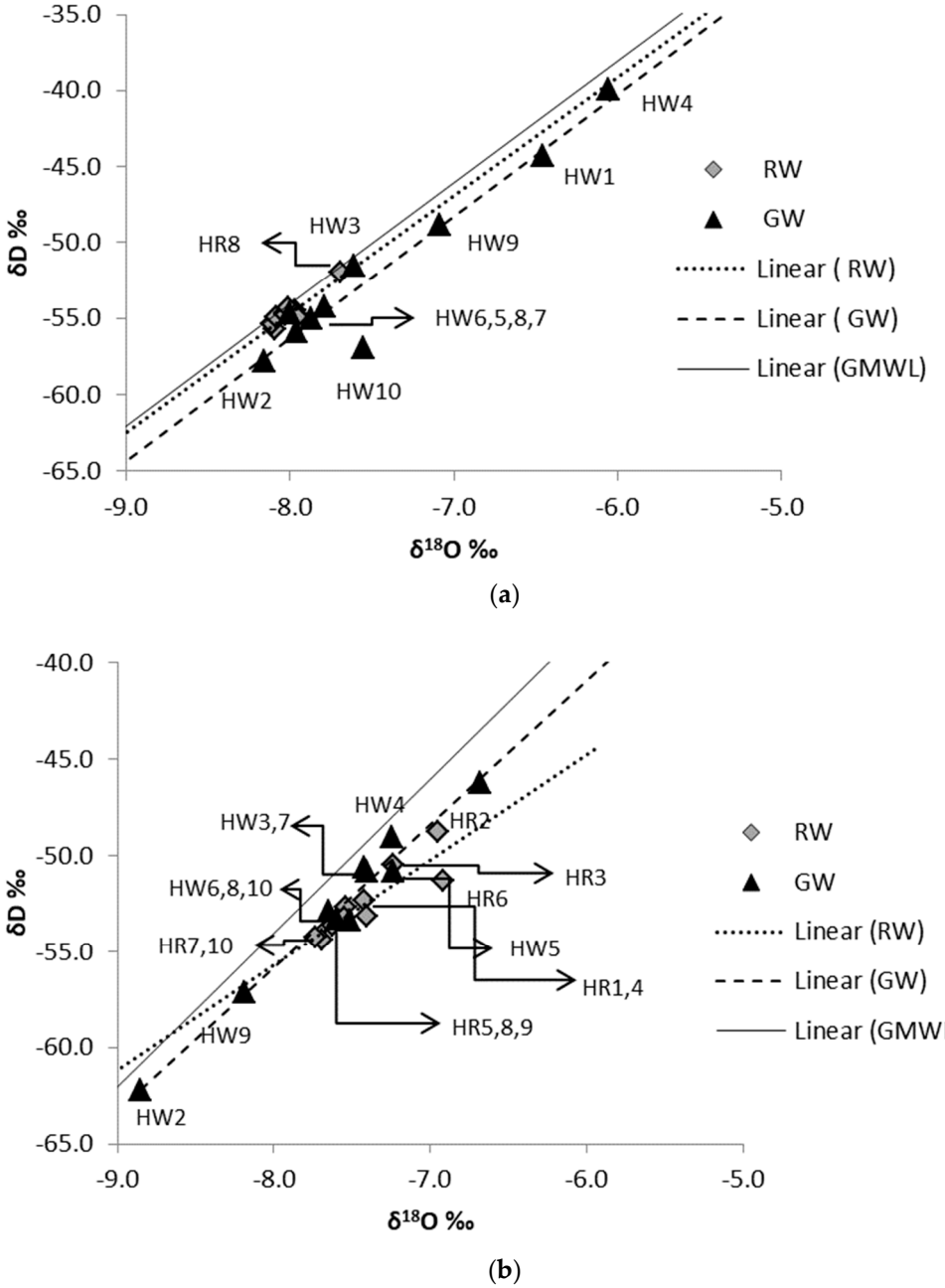

Figure 4. δD verses $\delta^{18}O$ plots of groundwater and river water in (**a**) wet season and (**b**) dry season. HW = Hanumante groundwater, HR = Hanumante river water. GMWL represents global meteoric water line [45]; linear (RW) = trend line of river water; linear (GW) = trend line of groundwater.

During the wet season, almost all river samples showed similar isotopic compositions of $\delta^{18}O$ (−8.0 to −8.1‰) and δD (−54.3 to −55.7‰) except HR8, which had a heavier isotopic composition

(Figures 1 and 4). Composition of isotopes slightly changed to heavier with wider value range during the dry season, showing a range from −6.91 to −7.73‰ for $\delta^{18}O$ and −48.75 to −54.41‰ for δD. Research work by Yang et al. [63] in the Jiulong River also presents a narrow and wider value range for the wet and dry season, respectively. Wet season river samples are plotted near the GMWL and have a similar slope and intercept (R^2 = 0.86) as the GMWL (Figure 4a), indicating recent meteoric water as a major source for river discharge [4,8,34,58]. Ca-HCO_3 water type, defined from piper diagram and lighter isotopic composition of rainfall during wet season [62,64], also suggests a similar water source. However, there was no evidence of evaporation in a previous study in the Kathmandu Valley [58,60]; dry season river samples plotted below the GMWL with lower slope (slope = 5.46 with R^2 = 0.79; Figure 4b) as compared with the GMWL may indicate a possibility of evaporation [26,65].

Large spatial variation of $\delta^{18}O$ and δD in water from dug wells was observed in both wet and dry seasons (Figure 4b). The $\delta^{18}O$ of groundwater ranged from −6.1‰ to −8.2‰ in the wet season and from−6.68‰ to −8.85‰ in the dry season. However, the overall range of $\delta^{18}O$ was similar in both seasons, with samples from HW3, HW5, HW6, HW7, HW8, and HW10 showing lighter composition in the wet season. In both seasons, HW1 had the heaviest isotopic value, whereas HW2 had the lightest isotopic composition. Groundwater samples plot below the GMWL, with a similar slope ($R^2 > 0.9$) in both wet and dry seasons (Figure 4b), indicating recent meteoric water as a major recharge source for these dug wells [12]. Although meteoric water is a major source for dug wells, spatial variation is noticeable in groundwater since isotopic composition of precipitation is dependent on rainfall amount, elevation, and source of water vapor of rainfall [62,64,66].

3.4. Clustering of River Water and Groundwater

Isotopic composition is a reliable source to identify recharge sources of groundwater, while the concentration of Na^+ and Cl^- can be used as an indicator of the presence of contamination through increased urbanization [36]. Thus, for HCA, δD, $\delta^{18}O$, Na^+, and Cl^- are used as major parameters to identify similarity or interconnection between river water and groundwater [4,30]. All 20 water samples from river water and groundwater of both seasons are managed separately for HCA. In the wet season, three clusters, namely A, B, and C, are observed in a dendrogram (Figure 5a). Cluster A consists of the water samples with lower concentration of Na^+, and Cl^-. It includes one dug well site (HW5) with all river sites and indicates minor influence of sewage discharge in wet season river water. The clusters B and C consist entirely of groundwater locations (Figure 5a) with higher concentration of Na^+ and Cl^- and different isotopic compositions compared with that of river water locations.

Two major clusters, D and E, are categorized from a dendrogram of the dry season (Figure 5b). Cluster D consists only of river sites (eight sites), whereas Cluster E contains a combination of river and groundwater sites, indicating similarity in selected parameters [56,67]. Cluster E has two subgroups, E1 and E2. Six dug well sites and one river site (HR1) are contained in Cluster E1. Similarly, four dug well sites and one river site (HR2) are grouped in Cluster E2. These two river samples, which are clustered with groundwater in Cluster E, are located at the uppermost section of the river (Figure 1), having lower concentrations of Na^+ and Cl^- and classified as Ca-HCO_3 type. However, in the case of the river sites of Cluster D, they have the highest concentration of Na^+ and Cl^-, and it is categorized as aNa-K-HCO_3 water type, which indicates pronounced effects of sewage discharge. Continued discharge of sewage in river water can develop an organic clogging layer on the riverbed [2], which will drastically reduce water exchange from the river channel to groundwater [3]. The absence of groundwater samples grouping with river samples in Cluster D may indicate the possibility of clogging layer formation within the river bed. However, the clusters combining river water and groundwater, Cluster A from the wet season (Figure 5a) and Cluster E from the dry season (Figure 5b), show similarity in selected parameters and indicate interconnection between river and groundwater [9,11,37].

However, the current research has a limitation in the methodological approach where the river channel stage could not be developed comparing relative river water and groundwater level.

The HCA along with hydraulic head between river water and groundwater can give a clearer view of interconnection between river and groundwater.

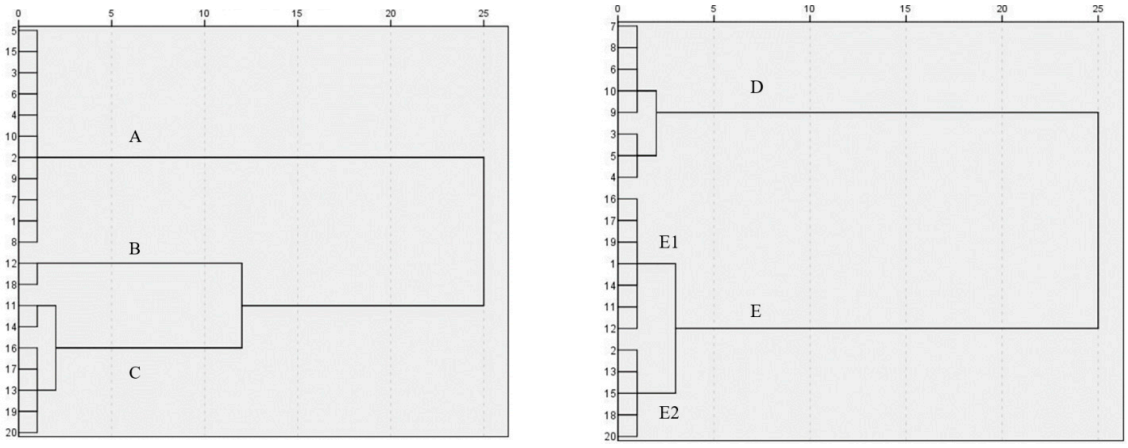

(**a**) (**b**)

River water		Groundwater	
Sampling Id	Cluster No.	Sampling Id	Cluster No.
HR1	1	HW1	11
HR2	2	HW2	12
HR3	3	HW3	13
HR4	4	HW4	14
HR5	5	HW5	15
HR6	6	HW6	16
HR7	7	HW7	17
HR8	8	HW8	18
HR9	9	HW9	19
HR10	10	HW10	20

(c)

Figure 5. Dendrogram based on hierarchical clustering (Ward's method) in (**a**) wet season and (**b**) dry season. (**c**) Relation of Hanumante river water (HR) and Hanumante groundwater (HW) with cluster number in dendrogram.

3.5. Identifying Areas of River Water and Groundwater Interconnection

Results from HCA imply interconnection between river water and groundwater in both wet and dry seasons. Cluster A from the wet season combines all river water with one groundwater (HW5), showing the similar water type Ca-HCO_3. HW5 has shallow well depth (5 m) with water level depth at 1 m. It is located in permeable lower terrace deposits (Figure 1), generally used for cultivation. Many flooding events were recorded for the Hanumante River [68], with a major one recently in July 2018 [69] which inundated the entire area from Jagati to Madhyapur Thimi, along with HW2, HW5, and HW6 (Figure 1). However, HW5 is the only groundwater sample that was grouped with all river sites in Cluster A (Figure 5); HR5 is closest site to HW5 (80 m away; Figure 1). Identical isotopic compositions of $\delta^{18}O$ (−8.0‰) and δD (−54.7‰) observed in HW5 and HR5 suggest possible recharge of groundwater in HW5. Similar concentration of Na^+ and Cl^- with HR5, along with drastic dilution

of these concentrations (Figure 2) at HW5, supports bank infiltration [4,18,19,70] as the mechanism recharging HW5 during the wet season (August of 2017). Similar types of results are presented by previous research conducted in developing countries for local scale [36] as well as for regional scale [37], indicating river water can recharge nearby groundwater.

In the dry season, dug wells HW1, HW2, HW4, HW6, HW7, and HW9 are grouped with the river site HR1 in Cluster E1, whereas dug wells HW3, HW5, HW8, and HW10 grouped with HR2 are clustered in E2. However, Cluster E from the dry season (Figure 5b) is suggestive of possible interaction between river water (HR1 and HR2) and groundwater. As HR1 and HR2 are located at the uppermost section of the river channel compared with grouped groundwater sites (Figure 1), there is a higher possibility of downstream groundwater recharge by HR1 and HR2 in the dry season. But differences in isotopic compositions of river water and nearby groundwater samples (Figure 4b) imply the possibility of other recharge sources besides river water. Further, groundwater samples exhibited similar trends of isotopic composition as that of the GMWL, suggesting dry season rainfall as one of the alternative sources of recharge for these dug wells.

Dug wells HW2, HW3, HW9, and HW10 are located within 20 m of HR2, HR3, HR9, and HR10, respectively (Figure 1). However, no single cluster formed includes this entire sampling site. These results indicate that interaction between river water and groundwater not only depends on distance from the river channel to groundwater sites, it also depends on well depth, water level depth, topography of well location, water level in river channel, and sedimentological formation of the areas.

3.6. River Water Contribution to Groundwater

Dug wells recharged by river water have a mixture of water, including river water (RW) and original groundwater (GW). During the study period, only HW5 showed interconnection with river water during the wet season. The proportion of river water to groundwater can be estimated using a mass balance approach equation [18,36]:

$$f = [(CS - CGW)/(CRW - CGW)] \times 100\%$$

where CS is the Cl^-, δD, or $\delta^{18}O$ (mg/L or ‰) of mixed water (HW5 in the wet season); CRW is the Cl^-, δD, or $\delta^{18}O$ of river water (HR5 in the wet season), and CGW is the Cl^-, δD, or $\delta^{18}O$ of original groundwater (HW5 in the dry season) which has not been influenced by river water recharge.

The calculated fractional contribution is nearly 100% for Cl^-, δD, or $\delta^{18}O$, indicating the contribution of river water (HR5) to recharge HW5 during the wet season (August 2017). This is the only well which had an identical isotopic value as in HR5 with much diluted water during the wet season.

The existence of interconnection between the Hanumante River and shallow groundwater shows that the surrounding shallow groundwater is contaminated by polluted river water. As river water deterioration continues with increasing urbanization, groundwater contamination is expected. It is very important to maintain river water quality for the improvement of peripheral shallow groundwater quality.

4. Conclusions

This study analyzes chemical and isotopic compositions of river water and groundwater to investigate interconnectivity between river water and shallow aquifers. Hydro-chemical parameters of river water exhibit significant temporal variations compared with groundwater. Groundwater and river water reveal a Ca-HCO_3 type with similar trends of isotopic composition as that of the GMWL, confirming freshwater as a major source for groundwater recharge and river discharge during the wet season. Water types shifted from Ca-HCO_3 to Na-K-HCO_3, and strong positive correlations between Na^+, K^+, NH_4^+-N, Ca^{2+}, Mg^{2+}, Cl^-, HCO_3^-, PO_4-P, and SO_4^{2-} indicate anthropogenic activities as a major source of contamination in dry season river water. Slight deviations of isotopic compositions

from GMWL with a lower slope may suggest the possibility of evaporation in river water during the dry season.

Clusters formed by combinations of river water and groundwater, both in wet (Cluster A) and dry (Cluster E) seasons, indicate the presence of interconnectivity between river water and shallow groundwater. The wet season included one groundwater sample with all the river samples, including one well which was near the riverside (within 80 m). Identical isotopic composition and similar concentrations of Na^+ and Cl^- in groundwater and river water suggest almost 100% of water recharge through bank infiltration comes from river to shallow groundwater during the wet season. Grouping of two upstream river samples with all downstream shallow groundwater implies that upstream river water is one of the sources of recharge for downstream shallow groundwater during the dry season.

This research concluded that polluted river water is one of the contamination sources for shallow groundwater around riverside areas. Such types of studies can be applied in other highly contaminated rivers to give a clear view about the contamination source for river peripheral groundwater. Higher extents of similar studies in rivers of the most urbanized areas are very important for groundwater management of the river peripheral area.

Author Contributions: T.N., N.K.T. and S.G. supervised this work. R.B. designed the field work for sample collection; R.B., T.N., and B.M.S. were involved in lab analyses; R.B. performed statistical analysis and prepared the manuscript; S.G., T.N., and B.M.S. revised the manuscript. All authors have read and agreed to the published version of the manuscript.

Funding: This research was funded by University Grant Commission (UGC), Nepal (Award No. 73/74/S & T-06).

Acknowledgments: The authors are grateful to ICRE-UY, Japan for providing lab facilities and Ramesh Raj Pant for his support in statistical discussions. The authors would like to acknowledge the support of Science and Technology Research Partnership for Sustainable Development (SATREPS), Japan International Co-operation Agency (JICA), Japan Science and Technology Agency (JST), and Grants-in-Aid for Scientific Research (KAKENHI No. 18K11617).

Conflicts of Interest: The authors declare no conflict of interest.

References

1. Woessner, W.W. Stream and fluvial plain grondwater interaction: Rescaling hydroeologic thought. *Ground Water* **2000**, *38*, 423–429. [CrossRef]
2. Sophocleous, M. Interaction between groundwater and surface water: The state of the science. *Hydrol. J.* **2002**, *10*, 52–67. [CrossRef]
3. Derx, J.; Blaschke, A.P.; Bloschl, G. Three-dimensional flow patterns at the river-aquifer interface—A case study at the Danube. *Adv. Water Resour.* **2010**, *33*, 1375–1387. [CrossRef]
4. Liu, Y.; Yamanaka, T. Tracing groundwater recharge sources in a mountain-plain transitional area using stable isotopes and hydrochemistry. *J. Hydrol.* **2012**, *464–465*, 116–126. [CrossRef]
5. Winter, T.C.; Harvey, J.W.; Franke, O.L.; Alley, W.M. *Ground Water and Surface Water: A Single Resource*; DIANE Publishing Inc.: Darby, PA, USA, 1998; Volume 79.
6. Ezugwu, C.N.; Apeh, S. Groundwater and surface water as one resource: Connectivity and interaction. *J. Mech. Civil Eng.* **2017**, *14*, 54–59. [CrossRef]
7. Song, X.; Liu, X.; Xia, J.; Yu, J.; Tang, C. A study of interaction between surface water and groundwater using environmental isotope in Huaisha River basin. *Sci. China Ser. D Earth Sci.* **2006**, *49*, 1299–1310. [CrossRef]
8. Ali, K.K.; Ajeena, A.R. Assessment of interconnection between surface water and groundwater in Sawa lake area, Southern Iraq, using stable isotope technique. *Arab. J. Geosci.* **2016**, *9*, 648. [CrossRef]
9. Huang, P.; Han, S. Assessment by Multivariate Analysis of groundwater – surface water interactions in the coal-mining exploring district, China. *Earth Sci. Res. J.* **2016**, *20*, 1–8. [CrossRef]
10. Lee, K.S.; Kim, Y. Determining the seasonality of groundwater recharge using water isotopes: A case study from the upper North Han River basin, Korea. *Environ. Geol.* **2007**, *52*, 853–859. [CrossRef]
11. Menció, A.; Mas-Pla, J. Assessment by multivariate analysis of groundwater-surface water interactions in urbanized mediterranean streams. *J. Hydrol.* **2008**, *352*, 355–366. [CrossRef]

12. Li, X.; Tang, C.; Han, Z.; Cao, Y. Hydrochemical characteristic and interaction process of surface and groundwater in mid-lower reach of Hanjiang River, China. *Environ. Earth Sci.* **2016**, *75*, 1–12. [CrossRef]
13. Zhang, B.; Song, X.; Zhang, Y.; Ma, Y.; Tang, C.; Yang, L.; Wang, Z.L. The Interaction between surface water and groundwater and its effect on water quality in the Second Songhua River Basin, Northeast China. *J. Earth Syst. Sci.* **2016**, *125*, 1495–1507. [CrossRef]
14. Brunke, M.; Gonser, T. The ecological significance of exchange processes between rivers and groundwater. *Freshwater Biol.* **1997**, *37*, 1–33. [CrossRef]
15. Brindha, K.; Neena Vaman, K.V.; Srinivasan, K.; Sathis Babu, M.; Elango, L. Identification of surface water-groundwater interaction by hydrogeochemical indicators and assessing its suitability for drinking and irrigational purposes in Chennai, Southern India. *Appl. Water Sci.* **2014**, *4*, 159–174. [CrossRef]
16. Zhu, M.; Wang, S.; Kong, X.; Zheng, W.; Feng, W.; Zhang, X.; Yuan, R.; Song, X.; Sprenger, M. Interaction of surface water and groundwater influenced by groundwater over-extraction, waste water discharge and water transfer in Xiong'an New area, China. *Water* **2019**, *11*, 539. [CrossRef]
17. Gautam, R.; Shrestha, J.K.; Shrestha, G.K.C. Assessment of river water intrusion at the periphery of Bagmati River in Kathmandu Valley. *Nepal J. Sci. Technol.* **2013**, *14*, 137–146. [CrossRef]
18. Malla, R.; Shrestha, S.; Chapagain, S.K.; Shakya, M.; Nakamura, T. Physico-chemical and oxygen-hydrogen isotopic assessment of Bagmati and Bishnumati rivers and the shallow groundwater along the river corridors in Kathmandu Valley, Nepal. *J. Water Resour. Prot.* **2015**, *7*, 1435–1448. [CrossRef]
19. Bajracharya, R.; Nakamura, T.; Shakya, B.M.; Nishida, K.; Shrestha, S.D.; Tamrakar, N.K. Identification of river water and groundwater interaction at central part of the Kathmandu Valley, Nepal using stable isotope tracers. *Int. J. Adv. Sci. Tech. Res.* **2018**, *3*, 29–41. [CrossRef]
20. Moog, O.; Sharma, S. Biological rapid assessment of water quality in the Bagmati River and its tributaries, Kathmandu. In Proceedings of the Ecohydrology Conference on High Mountain Areas, Kathmandu, Nepal, 24–28 March 1996; pp. 23–26.
21. Devkota, D.C.; Watanabe, K. Impact of solid waste on water quality of Bishnumati River and surrounding areas in Kathmandu, Nepal. *J. Nepal Geol. Soc.* **2005**, *31*, 19–24. [CrossRef]
22. Bajracharya, R.; Tamrakar, N.K. Environmental status of Manahara River, Kathmandu, Nepal. *Bull. Dep. Geol.* **2007**, *10*, 21–32. [CrossRef]
23. Bajracharya, R.; Tamrakar, N.K.; Shrestha, M.; Bohara, B. Status of shallow wells along major rivers of the Kathmandu Valley, Central Nepal. *J. Nepal Geol. Soc.* **2018**, *56*, 31–42. [CrossRef]
24. Pandey, S. Water pollution and health. *Kath. Uni. Med. J.* **2006**, *4*, 128–134.
25. Kalbus, E.; Reinstorf, F.; Schirmer, M. Measuring methods for groundwater—Surface water interactions: A review. *Hydrol. Earth Syst. Sci.* **2006**, *10*, 873–887. [CrossRef]
26. Terwey, J.L. Isotopes in groundwater hydrology. *Chall. Afr. Hydrol. Water Resour.* **1984**, *144*, 155–160.
27. Katz, B.G.; Coplen, T.B.; Bullen, T.D.; Hal Davis, J. Use of chemical and isotopic tracers to characterize the interactions between ground water and surface water in mantled karst. *Ground Water* **1997**, *35*, 1014–1028. [CrossRef]
28. Hunt, R.J.; Strand, M.; Walker, J.F. Measuring groundwater-surface water interaction and its effect on wetland stream benthic productivity, Trout Lake Watershed, Northern Wisconsin, USA. *J. Hydrol.* **2006**, *320*, 370–384. [CrossRef]
29. Brenot, A.; Petelet-Giraud, E.; Gourcy, L. Insight from surface water-groundwater interactions in an alluvial aquifer: Contributions of δ^2H and $\delta^{18}O$ of water, $\delta^{34}SSO_4$ and $\delta^{18}OSO_4$ of sulfates, $^{87}Sr/^{86}Sr$ Ratio. *Procedia Earth Planet. Sci.* **2015**, *13*, 84–87. [CrossRef]
30. Mohammed, A.M.; Krishnamurthy, R.V.; Kehew, A.E.; Crossey, L.J.; Karlstrom, K.K. Factors affecting the stable isotopes ratios in groundwater impacted by intense agricultural practices: A case study from the Nile Valley of Egypt. *Sci. Total Environ.* **2016**, *573*, 707–715. [CrossRef]
31. Fleckenstein, J.H.; Krause, S.; Hannah, D.M.; Boano, F. Groundwater-surface water interactions: New methods and models to improve understanding of processes and dynamics. *Adv. Water Resour.* **2010**, *33*, 1291–1295. [CrossRef]
32. Meyerhoff, S.B.; Maxwell, R.M.; Revil, A.; Martin, J.B.; Karaoulis, M.; Graham, W.D. Characterization of groundwater and surface water mixing in a semiconfined karst aquifer using time-lapse electrical resistivity tomography. *Water Resour. Res.* **2014**, *50*, 2566–2585. [CrossRef]

33. McLachlan, P.J.; Chambers, J.E.; Uhlemann, S.S.; Binley, A. Geophysical characterisation of the groundwater–surface water interface. *Adv. Water Resour.* **2017**, *109*, 302–319. [CrossRef]
34. Sakakibara, K.; Tsujimura, M.; Song, X.; Zhang, J. Interaction between surface water and groundwater revealed by multi-tracer and statistical approaches in the Baiyangdian Lake watershed, North China Plain. *Hydrol. Res. Lett.* **2016**, *10*, 74–80. [CrossRef]
35. Epting, J.; Huggenberger, P.; Radny, D.; Hammes, F.; Hollender, J.; Page, R.M.; Weber, S.; Banninger, D.; Auckenthaler, A. Spatiotemporal scales of river-groundwater interaction—The role of local interaction processes and regional groundwater regimes. *Sci. Total Environ.* **2018**, *618*, 1224–1243. [CrossRef] [PubMed]
36. Yang, L.; Song, X.; Zhang, Y.; Han, D.; Zhang, B.; Long, D. Characterizing interactions between surface water and groundwater in the Jialu River Basin using major ion chemistry and stable isotopes. *Hydrol. Earth Syst. Sci.* **2012**, *16*, 4265–4277. [CrossRef]
37. Guggenmos, M.R.; Daughney, C.J.; Jackson, B.M.; Morgenstern, U. Regional-scale identification of groundwater-surface water interaction using hydrochemistry and multivariate statistical methods, Wairarapa Valley, New Zealand. *Hydrol. Earth Syst. Sci.* **2011**, *15*, 3383–3398. [CrossRef]
38. Sada, R. Trajectory of urban river degradation:Initiatives for conservation and restoration (a case study of Hamunante River in Bhaktapur, Nepal). *South Asisn Water Stud.* **2014**, *4*, 2.
39. Shrestha, P. *Climate Change Impact on River Dynamics of the Bagmati Basin, Kathmandu Nepal*; Report Submitted to National Adaptation Program of Action to Climate Change Project; Government of Nepal: Kathmandu, Nepal, 2010; Volume 36.
40. Pathak, D.R.; Yatabe, R.; Bhandary, N.P. Indentification of major affecting spatial and temporal variation of water quality in Kathmandu Basin, Nepal, using multivariate statistical analysis. *Int. J. Water* **2015**, *9*, 209–225. [CrossRef]
41. Thapa, B.R.; Ishidaira, H.; Pandey, V.P.; Shakya, N.M. Impact assessment of Gorkha earthquake 2015 on portable water supply in Kathmandu Valley: Preliminary analysis. *J. Jpn. Soc. Civ. Eng.* **2016**, *72*, 61–66. [CrossRef]
42. Yoshida, M.; Igarashi, Y. Neogene to quaternary lacustrine sediment in the Kathmandu Valley, Nepal. *J. Nepal Geol. Soc.* **1984**, *4*, 37–100.
43. Sakai, T.; Gajurel, A.P.; Tabata, H.; Ooi, N.; Takagawa, T.; Kitagawa, H.; Upreti, B.N. Revised lithostratigraphy of fluvial-lacustrine sediments comprising northern Kathmandu basin in central Nepal. *J. Nepal Geol. Soc.* **2008**, *37*, 25–44.
44. Dhittal, M.R. *Geology of Nepal Himalayas: Regional Perspective of the Classic Collided Orogeen*; Springer: New York, NY, USA, 2015.
45. Craig, H. Isotopic variations in meteoric waters. *Science* **1961**, *133*, 1702–1703. [CrossRef] [PubMed]
46. Gotway, C.A.; Helsel, D.R.; Hirsch, R.M. Statistical methods in water resources. *Technometics* **1994**, 323. [CrossRef]
47. Pant, R.R.; Zhang, F.; Rehman, F.U.; Wang, G.; Ye, M.; Zeng, C.; Tang, H. Spatiotemporal variations of hydrogeochemistry and its controlling factors in the Gandaki River Basin, Central Himalaya Nepal. *Sci. Total Environ.* **2018**, *622–623*, 770–782. [CrossRef] [PubMed]
48. Bishara, A.J.; Hittner, J.B. Testing the significance of a correlation with nonnormal data: Comparision of Pearson, Spearman, transformation, and resampling approaches. *Psychol. Methods* **2012**, *17*, 399–417. [CrossRef] [PubMed]
49. Kumar, M.; Ramanathan, A.; Keshari, A.K. Understanding the extent of interactions between groundwater and surface water through major ion chemistry and multivariate statistical techniques. *Hydrol. Process* **2009**, *23*, 297–310. [CrossRef]
50. Ganiyu, S.A.; Badmus, B.S.; Olurin, O.T.; Ojekunle, Z.O. Evaluation of seasonal variation of water quality using multivariate statistical analysis and irrigation parameter indices in Ajakanga area, Ibadan, Nigeria. *Appl. Water Sci.* **2018**, *8*, 35. [CrossRef]
51. Ward, J.H. Hierarchical grouping to optimize an objective function. *J. Am. Stat. Assoc.* **1963**, *58*, 236–244. [CrossRef]
52. Singh, A.K.; Kumar, S.R. Quality assessment of groundwater for drinking and irrigation use in semi-urban area of Tripura, India. *Ecol. Environ. Cons.* **2015**, *21*, 97–108.
53. Al-Khatib, M.; Al-Najar, H. Hydro-geochemical characteristics of groundwater beneath the Gaza Strip. *J. Water Resour. Prot.* **2011**, *3*, 341–348. [CrossRef]

54. Bhat, S.A.; Meraj, G.; Yaseen, S.; Pandit, A.K. Statistical assessment of water quality parameters for pollution source identification in Sukhnag Stream: An inflow stream of Lake Wular (Ramsar iite), Kashmir Himalaya. *J. Ecosyst.* **2014**, *2014*, 18. [CrossRef]
55. El Alfy, M.; Merkel, B. Assessment of human impact on quaternary aquifers of Rafah Area, NE Sinai, Egypt. *Int. J. Econ. Environ. Geol.* **2004**, *1*, 1–9.
56. Zhong, M.; Zhang, H.; Sun, X.; Wang, Z.; Tian, W.; Huang, H. Analyzing the significant environmental factors on the spatial and temporal distribution of water quality utilizing multivariate statistical techniques: A case study in the Balihe Lake, China. *Environ. Sci. Pollut. Res.* **2018**, *25*, 29418–29432. [CrossRef] [PubMed]
57. Kumar, P.J.S. Hydrogeochemical and multivariate statistical appraisal of pollution sources in the groundwater of the lower Bhavani River basin in Tamil Nadu. *Geol. Ecol. Landsc.* **2019**. [CrossRef]
58. Shakya, B.M.; Nakamura, T.; Shrestha, S.D.; Nishida, K. Identifying the deep groundwater recharge processes in an intermountain basin using the hydrogeochemical and water isotope characteristics. *Hydrol. Res.* **2019**, *50*, 1216–1229. [CrossRef]
59. Shakya, B.M.; Nakamura, T.; Kamei, T.; Shrestha, S.D.; Nishida, K. Seasonal groundwater quality status and nitrogen contamination in the shallow aquifer system of the Kathmandu Valley, Nepal. *Water* **2019**, *11*, 2184. [CrossRef]
60. Gajurel, A.P.; France-Lanord, C.; Huyghe, P.; Guilmette, C.; Gurung, D. C and O isotope compositions of modern fresh-water mollusc shells and river waters from the Himalaya and Ganga Plain. *Chem. Geol.* **2006**, *233*, 156–183. [CrossRef]
61. Giri, U. Evaluation of Stable Isotope Ratios within Meteoric, Surface, and Groundwater within the Kathmandu Valley. Master's Thesis, Georgia State University, Atlanta, GA, USA, 2018. Available online: http://scholarwork.gsu.edu/geoscience_theses/116 (accessed on 10 November 2019).
62. Matheswaran, K.; Khadka, A.; Dhaubanjar, S. Delineation of spring recharge zones using environmental isotopes to support climate-resilient interventions in two mountainous catchments in far-western Nepal. *Hydrogeol. J.* **2019**, *27*, 2181–2197. [CrossRef]
63. Yang, K.; Han, G.; Liu, M.; Li, X.; Liu, J.; Zhang, Q. Spatial and seasonal variation of O and H isotopes in the Jiulong River, Southeast China. *Water* **2018**, *10*, 1677. [CrossRef]
64. Lachniet, M.S.; Patterson, W.P. Oxygen isotope values of precipitation and surface waters in northern Central America (Belize and Guatemala) are dominated by temperature and amount effects. *Earth Planet. Sci. Lett.* **2009**, *284*, 435–446. [CrossRef]
65. Gat, J.R. The relatioship between the isotopic composition of precipitation, surface runoff and groundwater for semiarid and arid zones. *Appl. Tracesrs Arid Zone Hydrol.* **1995**, *232*, 409–416.
66. Wen, R.; Tian, L.; Weng, Y.B.; Liu, Z.F.; Zhao, Z.P. The altitude effect of $\delta^{18}O$ in precipitation and river water in the Southern Himalayas. *Chin. Sci. Bull.* **2012**, *57*, 1693–1698. [CrossRef]
67. Shrestha, S.; Kazama, F. Assessment of surface water quality using multivariate statistical techniques: A case study of the Fuji River Basin, Japan. *Environ. Model. Softw.* **2007**, *22*, 464–475. [CrossRef]
68. Poudel, S. Assessment of community vulnerability to flood in Hanumante River, Bhaktapur, Nepal: Finding the causes and mitigation approaches. *Int. J. Lsld. Environ.* **2013**, *1*, 77–78.
69. Bhatta, B.P.; Pandey, R.K. Bhaktapur urban flood related disaster risk and strategy after 2018. *J. APF Command Staff Coll.* **2020**, *3*, 72–89. [CrossRef]
70. Nakamura, T.; Nishida, K.; Kazama, F. Influence of a dual monsoon system and two sources of groundwater recharge on Kofu Basin alluvial fans, Japan. *Hydrol. Res.* **2017**, *48*, 1071–1087. [CrossRef]

Appendix 1B Index Journal

Bajracharya, R., Tamrakar, T., Shrestha, M., & Bohara, B. (2018). Status of shallow wells along major rivers of the Kathmandu Valley, Central Nepal. Journal of Neal Geological Society, v.56, 31-42. DOI: https://doi.org/10.3126/jngs.v56i1.22697

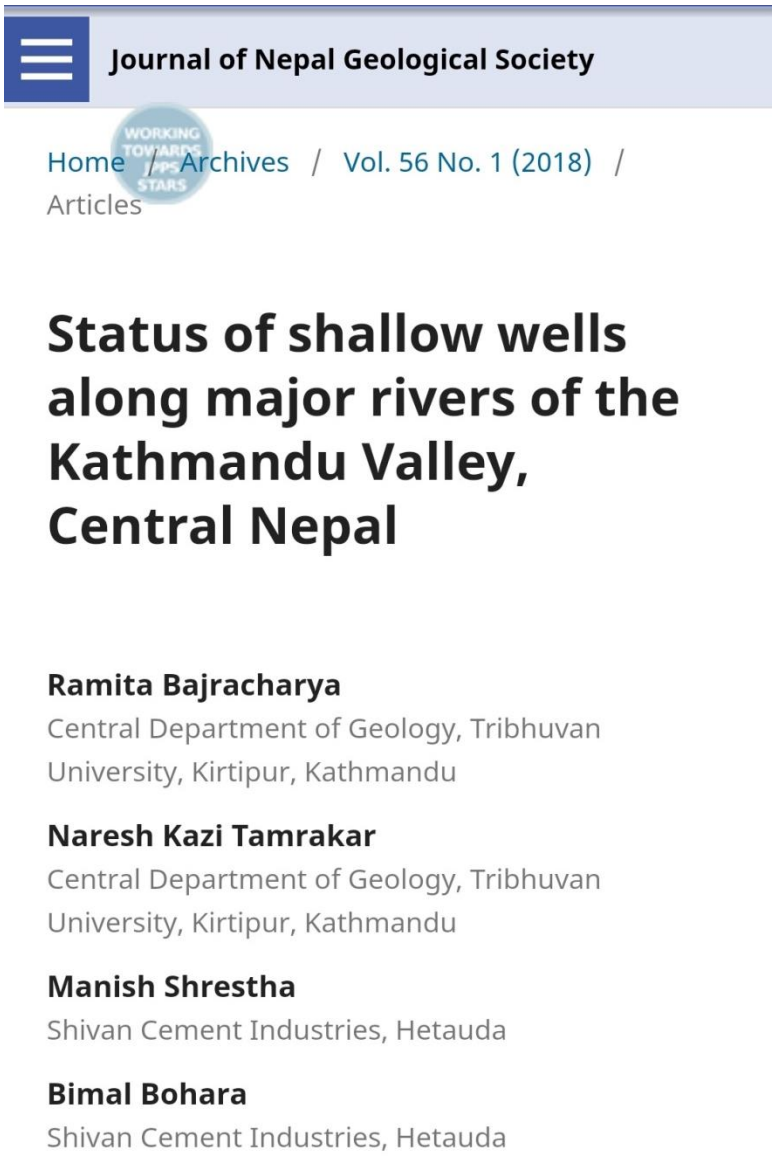

Journal of Nepal Geological Society

Home / Archives / Vol. 56 No. 1 (2018) / Articles

Status of shallow wells along major rivers of the Kathmandu Valley, Central Nepal

Ramita Bajracharya
Central Department of Geology, Tribhuvan University, Kirtipur, Kathmandu

Naresh Kazi Tamrakar
Central Department of Geology, Tribhuvan University, Kirtipur, Kathmandu

Manish Shrestha
Shivan Cement Industries, Hetauda

Bimal Bohara
Shivan Cement Industries, Hetauda

Journal of Nepal Geological Society, 2018, vol. 56, pp. 31–42

Status of shallow wells along major rivers of the Kathmandu Valley, Central Nepal

***Ramita Bajracharya[1], Naresh Kazi Tamrakar[1], Manish Shrestha[2], and Bimal Bohara[2]**

[1]Central Department of Geology, Tribhuvan University, Kirtipur, Kathmandu, Nepal
[1]Shivan Cement Industries, Hetauda, Nepal
**Corresponding author: bajrarami@gmail.com*

ABSTRACT

Groundwater is one of the important natural resources to which people of the Kathmandu Valley rely on for their daily purpose. The rate of extraction of groundwater from shallow as well as deep aquifers has increased in the river corridor with the increased urbanization towards the major river corridors in the valley. Wells located within 100 m from the rivers of the Kathmandu Valley were focused in the present study. Altogether 237 wells were recorded from the Bagmati, Manahara and the Bishnumati River corridors of the northern Kathmandu basin, and the Dhobi, Hanumante, Godavari, Kodku, Nakhu and the Balkhu Khola corridors of the southern Kathmandu basin. This research was based on field measurements of well dimension (well diameter, well depth and water level depth) and physical parameters (electrical conductivity, dissolve oxygen, pH and temperature) in April and August of year 2017. The lowest water level was measured in the Nakhu Khola and the highest was measured in the Dhobi Khola in dry season. Average EC ranged between 614.2 µS/cm and 1123.9 µS/cm in dry season, and between 613.0 µS/cm and 916.1 µS/cm in wet season. DO also varied from 1.46 mg/L to 2.46 mg/L in dry season and increased to 1.67–2.53 mg/L in wet season. The lower DO and higher EC in the Balkhu Khola corridor indicates the most contaminated wells in the Kathmandu Valley. Average values of pH and temperature increased in wet season compared to dry season. Average high values of EC and low values of DO were recorded within 30 m distance from the rivers, and EC increased and DO decreased as the distance from river channel increased.

Keywords: Water quality, Well dimension, Dissolved oxygen, Kathmandu Valley, River corridor, Bagmati River

Paper Received: 22 Mar 2018 **Paper Accepted:** 21 May 2018

INTRODUCTION

Groundwater is one of the important natural resources to which majority of the world's population depend on for their daily lives. In Nepal, it is the major source of drinking water in both urban and rural areas. In the Kathmandu valley, the government authorized institution; Kathmandu Upatyaka Khanepani Limited (KUKL) could not fulfill the total amount of water (around 370 million/day) needed. The demand has been largely contributed from groundwater source (Panday et al. 2012). The dependency towards the use of groundwater in the valley has been increasing with the growth of population and industrial activity (Panday et al. 2010). The rapid growth of urbanization for last one decade has also increased settlements along the river corridors. These increased settlements contribute to contaminate the river and surface water through solid waste disposal, industrial waste and agriculture waste which have further increased the dependency toward the groundwater use. The overexploitation of the groundwater and change of land use by clearing vegetation and forming impervious surfaces have decreased groundwater table and minimized groundwater recharge (Panday et al. 2010; Gautam and Prajapati, 2014).

Rapid urbanization along the river corridors exploits groundwater from both shallow and deep aquifers. Housing, industries and large colonies mostly exploit groundwater from deep aquifer whereas individual houses fulfill their water demand by digging dug wells and shallow tube wells. Consequently, the shallow aquifer has higher possibility of being contaminated by anthropogenic activities which were also reported in previous researches that the shallow aquifer has higher concentration of nitrate, EC, iron, chloride and turbidity exceeding Nepal standard (Warner et al., 2008; Prasai et al., 2010; Diwakar et al., 2010; Pant, 2011). But there are very few researches, which were conducted based on shallow aquifer extraction rate, shallow well inventory and water level as well as fluctuations of major physio-chemical parameters (Shrestha and Shah, 2014). Many researches were conducted including combined groundwater quality of shallow and deep aquifer; stone spots and spring water (Khadka, 1993; Pathak and Hiratsuka, 2010; Ghimire et al., 2013). As shallow aquifers near the rivers are often the most exploited and are the ones being possibly contaminated by the polluted river water and riverbank areas, the present study tried to include most of dug wells which are located within 100 m spans from both right and left banks of the corridors of major rivers of the Kathmandu Valley. This study was totally focused on in situ field measurement data such as well dimension (well diameter, well depth and water level depth) and some parameters like electrical conductivity, dissolved oxygen, pH and temperature. The aims of this study were to find out (i) status of dug wells based on well dimension and physical parameter,

(ii) seasonal variation in water level depth and physical parameter, and (iii) relation between proximity from rivers and physical parameters.

GEOLOGICAL SETTING

The Kathmandu Valley is located between latitudes 27°32'13" and 27°49'10" north and longitudes 85°11'31" and 85°31'38" east covering area about 650 sq. km. The bowl-shaped valley extends for 30 km towards E-W and 25 km towards N-S. The valley has average elevation of 1350 m and enclosed by peaks of the Shivapuri, Chandragiri and the Phulchauki ranges from the north, the south, and the west, respectively. The Bagmati River is the only one outlet drainage of the valley, and has many tributaries such as Bishnumati River, Dhobi Khola, Manahara River, Hanumante River, Godawari River, Kodku River, Nakhu River and Balkhu River.

The surrounding mountain ranges of the valley are composed of sedimentary and metamorphic rocks with gneiss and migmatites (Stöcklin, 1980) whereas the valley fill consists of Plio-Pleistocene fluvial, fluvial lacustrine and fluvio-deltaic sediments (Yoshida and Igarashi, 1984; Shrestha et al., 1998; Sakai et al., 2008). The lacustrine and fluvial deposits of the valley contain peat, clay, carbonaceous clay, sand, gravel and boulders. They lie unconformably on the rocks of the Phulchauki Group and the Bhimphedi Group. The basin-fill sediments were divided into different units (Table 1).

Within the Kathmandu Valley, the present study area was located on the major river corridors which include basin fill sediments of the Lower Terrace Deposits, Alluvial Fan or Debris Flow Deposit, Lukundol Formation, Gokarna Formation, Thimi Formation and the Patan Formation (Fig. 1). Based on observed lithological data of different location, the Kathmandu Valley was divided into three groundwater districts as northern, central and southern groundwater districts (JICA, 1990). As per sub-surface layer data, the Northern Groundwater District is considered as recharge belt of the Kathmandu valley.

METHODOLOGY

Dug wells which were located within 100 m from the corridors of the major 9 tributaries; the Bishnumati, Manahara and the Bagmati Rivers, and the Dhobi, Hanumante, Godavari, Kodku, Nakhu and the Balkhu Kholas in the Kathmandu Valley were selected for this study. This study tried to include all those dug wells which were located within 100 m from river corridor but some was not possible due to absence of owner at the time of survey. GPS location, well dimension (well depth, well diameter and water level depth) and some parameters such as electrical conductivity (EC), dissolved oxygen (DO), pH and water temperature was measured in situ at each well location.

Well depth, well diameter and water level depth of each well were measured by using measuring tape and water depth logger for water level depth. The total well depth was also noted in the field through owner information or from direct measurement. And parameters such as EC, DO, pH and water temperature were measured by using portable measuring devices such as DO-meter (Mettler Toledo SG3-ELK) and pH/EC meter

Table 1: Stratigratigraphic units of valley-fill sediments (Yoshida and Igarashi, 1984 and Sakai et al., 2008)

Stratigraphic unit	Geological Age	Composition
River Flood Plain	Holocene	Sand, silt and clay.
Lower Terrace deposits	Holocene	Micaceous sand, pebbles and gravel
Patan Formation	Pleistocene	Laminated arkosic sand, silt, clay and peat layers.
Kalimati Formation	Pleistocene	Black clay or silt (kalimati) beds with thin beds of very fine sands.
Thimi Formation	Pleistocene	Arkosic sand, silt clay, peat and gravel, gravel are mainly of gneiss and granite.
Tokha Formation	Pleistocene	Pale green silty sand and gravel lenses with black silt and thin diatomite.
Gokarna Formation	Pleistocene	Laminated arkosic sand, silt clay and peat.
Boregaon Terrace deposit	Pleistocene	Rounded gravel with silt and sand laminated, gravel composed of limestone, metasandstone.
Chapagaon Terrace Deposit	Pleistocene	Subrounded cobbles and pebbles of metasandstone, limestone and phyllite
Pyangaon Terrace deposit	Pleistocene	Rounded to sub rounded cobbles and pebbles of meta-sandstone, limestone and phyllite.
Dharmasthali Formation	Plio-Pleistocene	Silt beds with intercalation of gravel and sand.
Lukundol Formation	Plio-Pleistocene	Weakly consolidated clay, silt and beds with lignite layers. Subdivided into Basal Conglomerate, lignite and laminated silt members

(Mettler Toledo Duo). All these data were measured at each well site after removing some water by using rope and plastic bucket.

The well number was given based on the name of river such as BMW for Bishnumati corridor well; DW for Dhobi; BW for Bagmati; MW for Manahara; HW for Hanumante; GW for Godavari; KW for Kodku; NW for Nakhhu and BAW for Balkhu corridor wells. Measurement of well dimension and physio-chemical parameters were carried out in dry (April 2017) and wet (August 2017) seasons.

RESULTS AND DISCUSSIONS

The numbers of wells recorded for different river corridor was different and was given in Table 2. The total numbers of recorded wells from nine river corridors were 237 among which 117 dug wells were from northern rivers (Bishnumati, Dhobi, Bagmati and Manahara) and 120 were from southern rivers (Hanumante, Godavari, Kodku, Nakhhu and Balkhu) of the valley (Fig. 1).

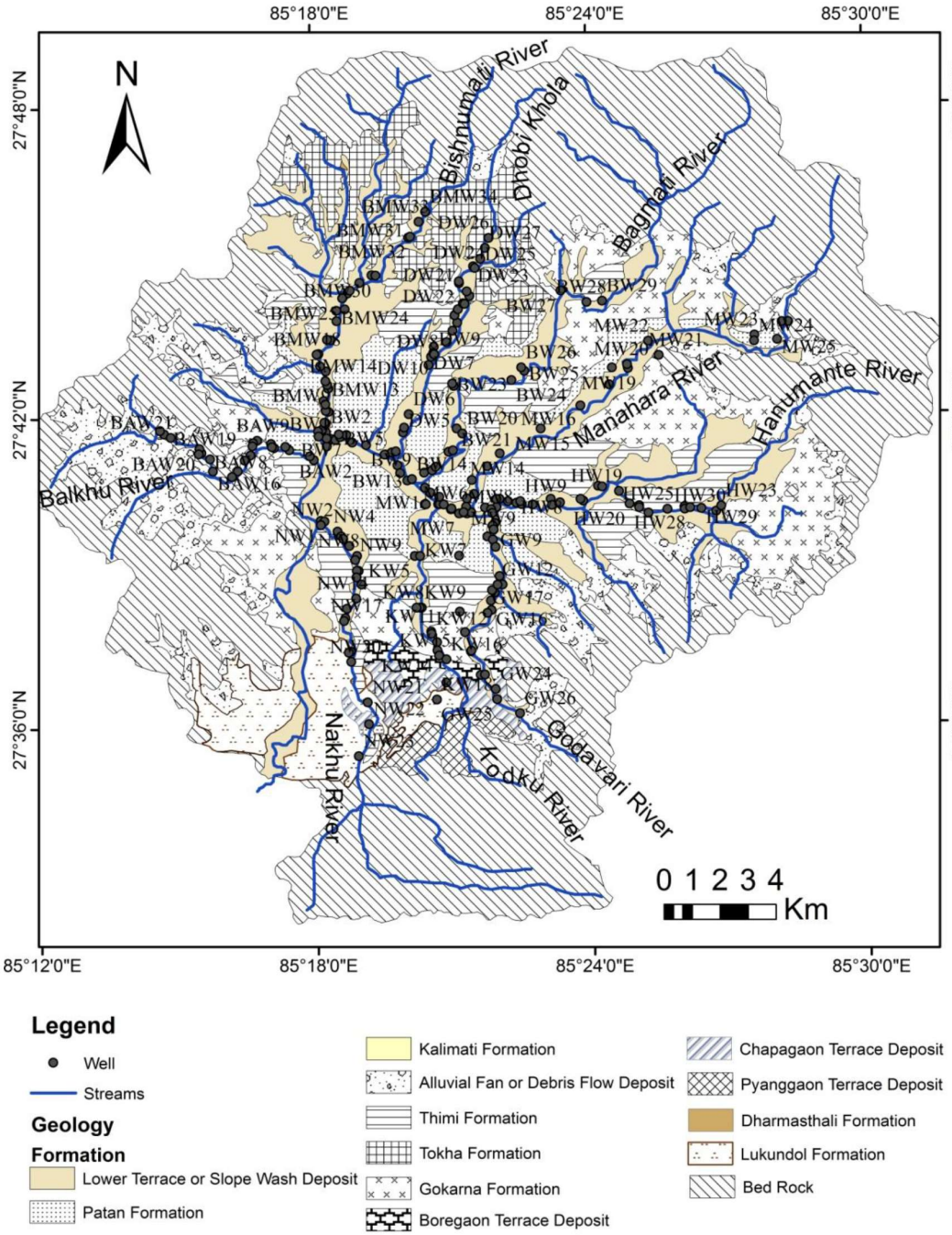

Fig. 1: Well location on geological map of the Kathmandu valley (Compilation of Yoshida & Igarashi, 1984; Shrestha et al., 1998; Sakai et al., 2008 and Dhital, 2015)

Table 2: Value ranges of well dimension and elevation

Name of tributaries	No. of Wells	Elevation (m)	Well Diameter (m)	Well Depth (m)	Water level Depth (m)	
					Dry	Wet
Bishnumati River	34	1280 – 1309	0.8 – 1.2	2.2–7.1	0.9 –6.8	0.4 –4.2
Dhobi Khola	27	1277 – 1329	0.9 – 1.2	2.3–12.2	1.1 –11.8	0.1 –3.1
Bagmati River	29	1267 – 1329	0.8 – 1.6	1.9–8.45	0.9 –5.8	0.6 –5.7
Manahara River	28	1276 –1390	0.8 –1.2	1.15–7.65	0.6 –5.7	0.1 –5.0
Hanumante Khola	30	1280 –1315	0.8 –1.2	1.5–15.7	1.1 –6.3	0.1 –5.6
Godavari Khola	26	1293 –1429	0.9 –1.3	1.5–10.4	0.45 –8.3	0.1 –4.5
Kodku Khola	18	1288 –1430	0.9 –2.3	2.3–9.9	0.4 –8.3	0.1 –6.4
Nakhu Khola	23	1263 –1400	0.6 –1.2	1.4–14.4	0.2 –3.8	0.1 –2.6
Balkhu Khola	23	1267 –1345	0.8 –1.2	2.8–10.8	1.3 –8.1	0.1 –3.0

Well dimension and water level depth

The well diameter, well total depth and water level depth were measured in each well. The maximum and minimum ranges for each measurement were presented in Table 2. In all nine rivers, minimum well diameter was ranged from 60 to 90 cm where as maximum was from 120 to 230 cm. These wells were located at different elevation. The highest elevation was observed at upstream sections of the Godavari Khola, Kodku Khola and the Nakhu Khola (1400 to 1430 m) and the lowest was at downstream sections of all tributaries (1263 to 1293 m).

The total well depth was very much variable along and among wells of different tributaries. The shallowest well depth was observed at the Manahara River (1.15 m) whereas the deepest one was noted from the Hanumante Khola (15.7 m). Wells of the Bishnumati River and the Manahara River corridors have the lowest well depth (Fig. 2). In the study area, depths of wells which were located on the Lower Terrace Deposit, Chapagaon Terrace Deposit and Boreaon Terrace Deposit have lower well depth as compared with those wells which were located on the Patan Formation and Thimi Formation. The Terrace Deposits mainly consists of gravels, pebbles, sand whereas Patan and Thimi Formation contain sand, silt, clay and peat layers. This indicates that depth of wells depends on the subsurface lithology of well location.

Water level depth varied from 0.2 to 11.8 m in dry month. Lower water level was noticed from well near to the Nakhu River and higher depth was from well near to the Dhobi Khola (Fig. 3). Except in few wells, all other wells have lower water level depths (from 0.1 to 6.4 m) in wet season as compared to dry season. Comparing well along northern and southern corridors, most of southern wells have lower water level (0.1–0.3 m) in wet season. Water level depth was variable for wells located within a single tributary as well as among different tributaries. The lowest level of variation was recorded in the Nakhu Khola (3.6 m) and the highest was obtained in the Dhobi Khola (10.7 m) in dry season which was changed to 2.5 m in the Nakhu Khola and 6.3 m in the Kodku Khola during wet season (Fig. 4 and Table 2).

Comparing among wells distributed in nine different corridors of the northern and the southern regions of the Kathmandu Valley, the Nakhu Khola has the lowest water level depth in the study period (Fig. 3). But comparing water level depth with lithology of well location, it can be found that most of wells which were located on Lower Terrace Deposit have lower water level depth. The wells of northern and southern corridors located on the terrace deposit have different water level depth. Rate of urbanization along river corridors was higher in northern river such as the Bishnumati, Dhobi and the Bagmati Rivers as compared to the southern rivers, Nakhhu, Kodku and Godavari. Increased urbanization can also increased withdraw of water from wells which can increase water level depth and thus withdraw rate may be one possible reason for lower water level depth in southern river corridor wells.

Physical parameters

Some parameters of water such as temperature, pH, electrical conductivity (EC) and dissolved oxygen (DO) were measured in each well in dry and wet season. Minimum, maximum and average data of these parameters for each nine rivers are presented in Table 3.

Temperature

Groundwater temperature is one of important parameters as it can affect physical, chemical and biological activities. Increase in temperature can decrease solubility of gases such as O_2, CO_2 and N_2 (Yilmaz and Koc, 2014). Higher temperature also increases taste, odour, colour and corrosion problem due to growth of microorganism (UNICEF, 2008). Increase in temperature also decreases the amount of dissolved oxygen, accelerates nitrification and oxidation of ammonia to nitrates and create oxygen deficient water environment (Ngabirano et al., 2016). Groundwater average temperature in dry season varied from 17.6 to 19.8^{o}C in which the lowest was measured from wells near to the Kodku Khola whereas the highest one was measured from the wells near to the Dhobi Khola. Variation in temperature among nine river corridor wells may be due to

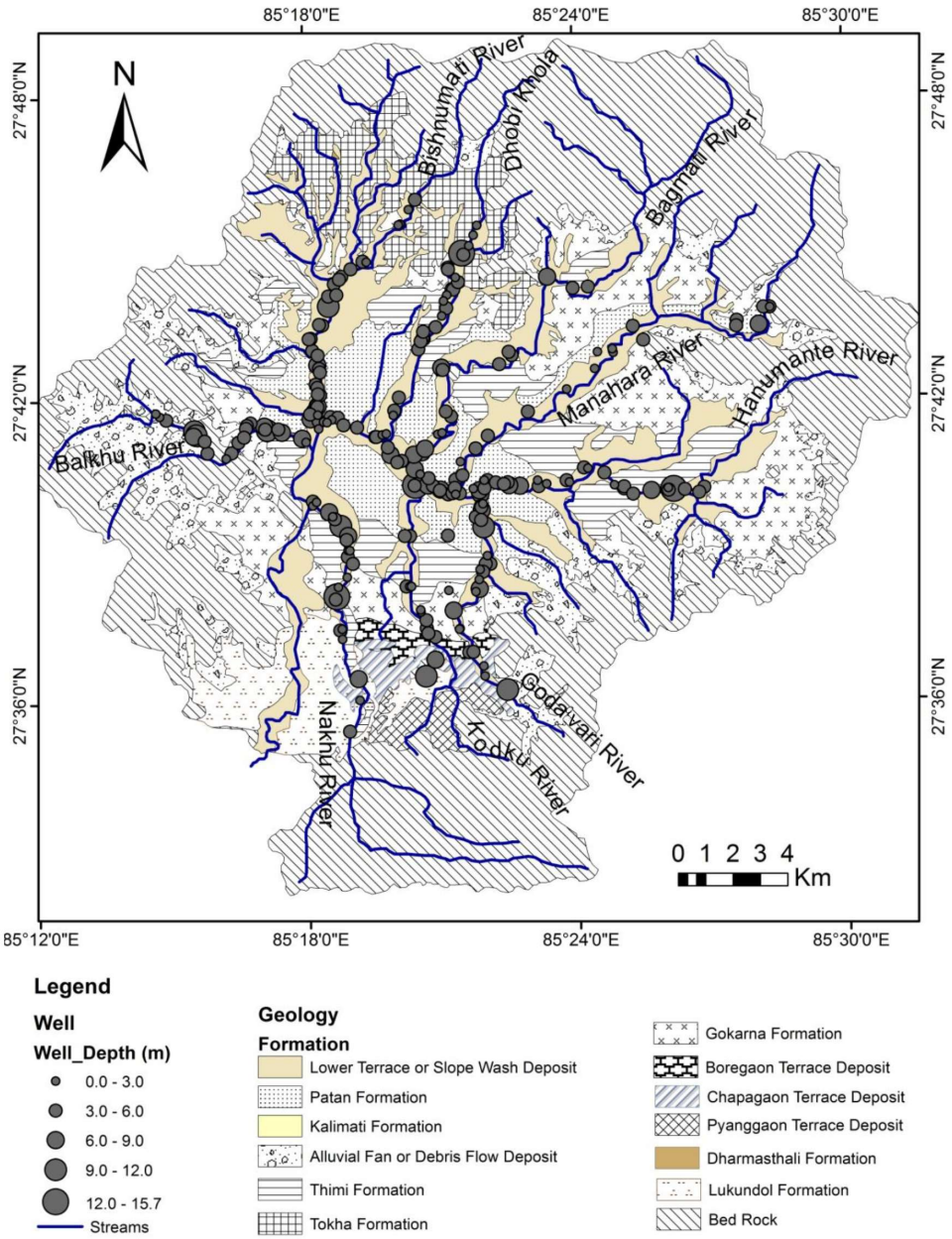

Fig. 2: Well depth variation on wells

change in depth of water, different timing of sample collection and mixing whether cold or warm from the surrounding rocks and soils in the plumes (Ngabirano et al., 2016). Seasonal variation was also occurred in wet season with value ranging from 22.59 to 23.66ºC.

pH

The pH indicates hydrogen concentration in the water which is affected by dissolved gases and salts. Average value of pH ranged from 6.69 to 7.33 in dry season but very low pH was measured in some wells near to the Hanumante, Manahara and the Kodku tributaries as 5.67, 5.96 and 6.16, respectively which were below permissible limit of NWQDS (WHO Nepal, 2005). A water sample with less than 7 pH is considered as acidic and can corrosive metal such as copper, zinc, lead from pipes causing increasing level of toxic metal in water (Aytekin and Bayraktaroglu, 2014). Higher pH was noted in well near to the Bishnumati River (8.5) which is disadvantage in order to treat with chlorine (Oyem et al., 2014). Except in few wells, pH has changed to slightly basic in the wet season with average value ranging from 7.19 to 7.41 (Table 3 and Fig. 5) indicating wet seasons has greater pH as compared to dry season (Ramamohan and Sudhakar, 2014; Zhou et al., 2015).

Electrical Conductivity (EC)

Electrical conductivity (EC) is the measure of ionic component dissolved in the water and gives an indication of

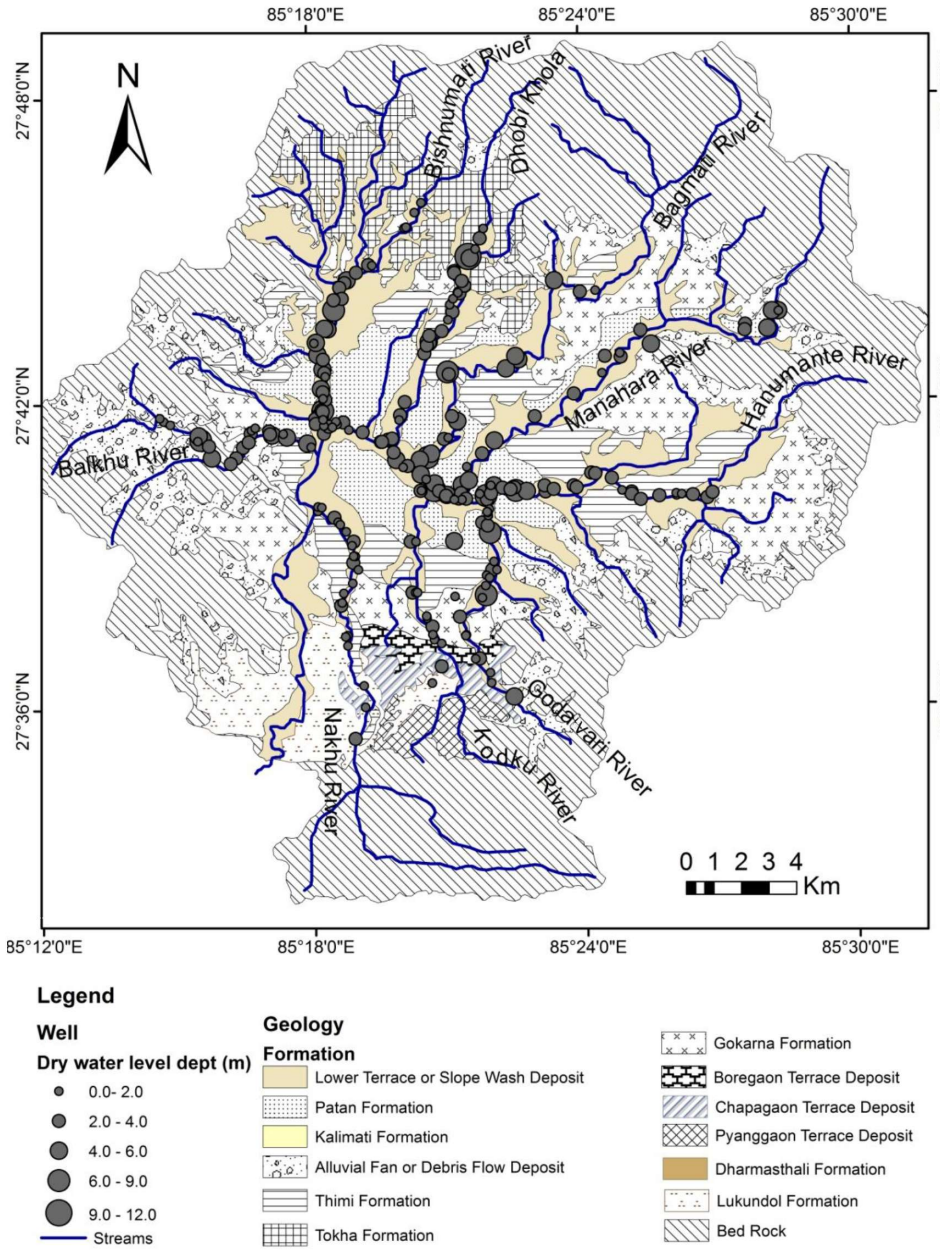

Fig. 3: Water level depth variation in dry season (April 2017)

the amount of total dissolved substitution in water (Yilmaz and Koc, 2014). EC was spatially and temporally very much variable (Table 3). Average EC value ranged from 614.2 to 1123.9 µS/cm in dry season and then decreased to 613.0 and 916.1 µS/cm in wet season. In both seasons, the highest value was observed in the wells of the Balkhu Khola corridor and the lowest was in the wells of the Nakhu Khola corridor (Fig. 6). Except in few wells, all other wells have lower EC in wet as compared to dry season. Evaporation rate generally is higher in dry season increasing ions concentration and hence increase EC but in the case of wet season there is dilution of ions due to rainwater infiltration and can increase water volumes resulting in a decrease in EC (Ngabirano et al., 2016).

In each river, wells located in the upstream segments of the tributaries have the lowest EC value as compared with the wells of the downstream segments indicating higher values towards downstream urbanized area (Fig. 7). The higher EC indicates higher concentration of dissolved ions. These ionic substances were available to groundwater by infiltration of solid wastes, industrial wastes, agricultural wastes, leakage of safety tank and sewer pipes (Pant, 2011).

When the EC is compared among the wells located in different corridors, the samples from the downstream of the Balkhu Khola corridor has the highest EC but the samples from the Nakhu Khola and the Dhobi Khola corridors have the least values both in wet and dry seasons (Table 3). Wells of the Nakhu and the Dhobi Khola corridors only were within permissible

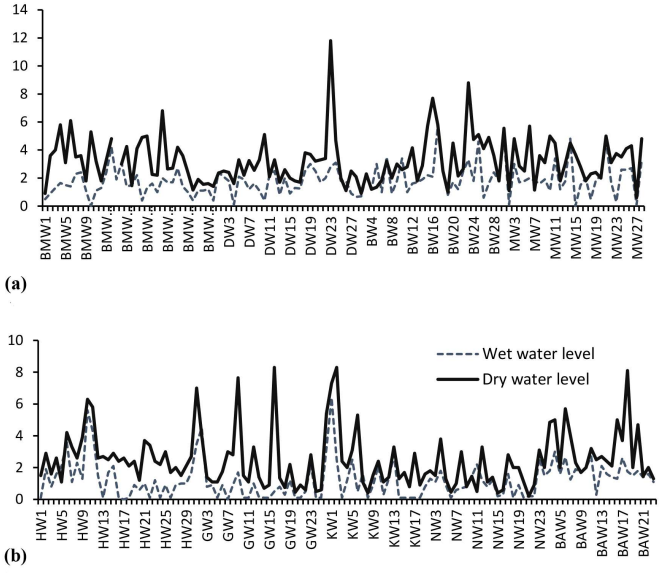

Fig. 4: Water level depth in wet and dry seasons at (a) Northern tributaries (Bishnumati, BMW; Dhobi, DW; Bagmati, BW and Manahara, MW), and (b) Southern tributaries (Hanumante, HW; Godavari, GW; Kodku, KW; Nakhu, NW andBalkhu, BAW) rivers

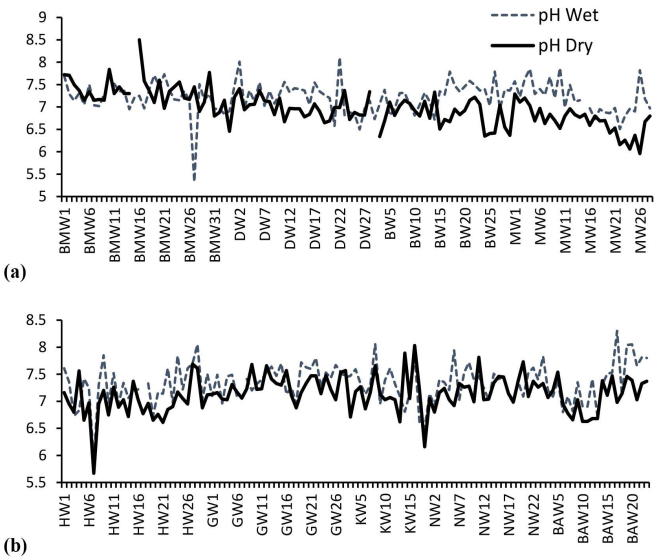

Fig. 5: pH variation in wells of a) northern and b) southern river corridors in wet and dry seasons

Table 3: Maximum, minimum and average value of physical parameters of wells

River corridor Name		EC		pH		DO		Temperature	
		Dry	Wet	Dry	Wet	Dry	Wet	Dry	Wet
Bishnumati River	Min	260	334	6.46	5.33	0.26	0.33	16.2	21.6
	Max	2150	2090	8.5	7.73	5.93	6.34	21.6	25.8
	Average	1014	851.73	7.33	7.19	2.39	2.18	18.74	23.4
Dhobi Khola	Min	231	162.5	6.65	6.5	0.37	0.48	18.4	21.8
	Max	1481	1199	7.41	8.11	6.06	4.88	21.2	24.8
	Average	745	656.91	6.98	7.24	2.46	2.18	19.83	23.29
Bagmati River	Min	149.6	121.7	6.34	6.71	0.19	0.26	17.1	20.7
	Max	2280	1949	7.34	7.79	4.8	8.55	23.4	25.8
	Average	963	872.16	6.84	7.24	1.48	2.16	19.69	23.34
Manahara River	Min	119.8	148.5	5.96	6.51	0.37	0.52	16.9	20.2
	Max	2070	1922	7.29	7.87	5.43	6.36	20.9	27.6
	Average	692	666.28	6.69	7.19	2.31	2.27	18.90	23.60
Hanumante Khola	Min	549	228	5.67	5.92	0.54	0.55	18.1	20.7
	Max	1546	2158	7.69	8.05	4.67	4.88	20.7	24.7
	Average	892	852.90	6.96	7.26	1.72	2.53	19.37	22.82
Godavari Khola	Min	303	299	6.88	6.96	0.5	0.77	15.3	19.6
	Max	2090	1575	7.68	7.8	5.78	5.21	24	25.6
	Average	707	622.40	7.26	7.41	2.26	1.93	18.07	23.38
Kodku Khola	Min	230	183	6.16	6.51	0.09	0.42	15.5	20
	Max	1840	1568	8.03	8.06	5.45	5.04	22	24.9
	Average	710	749.44	7.18	7.29	1.67	1.94	17.67	22.59
Nakhu Khola	Min	242	244	6.8	6.92	0.5	0.19	18.2	21.6
	Max	1131	1540	7.81	7.94	5.7	5.05	20.9	25.1
	Average	614	613.04	7.22	7.34	2.15	2.11	19.51	23.42
Balkhu Khola	Min	553	385	6.63	6.73	0.11	0.33	18.4	21.7
	Max	2860	3030	7.54	8.3	3.46	3.64	20.6	25.2
	Average	1124	916.18	7.08	7.39	1.46	1.67	19.46	23.66

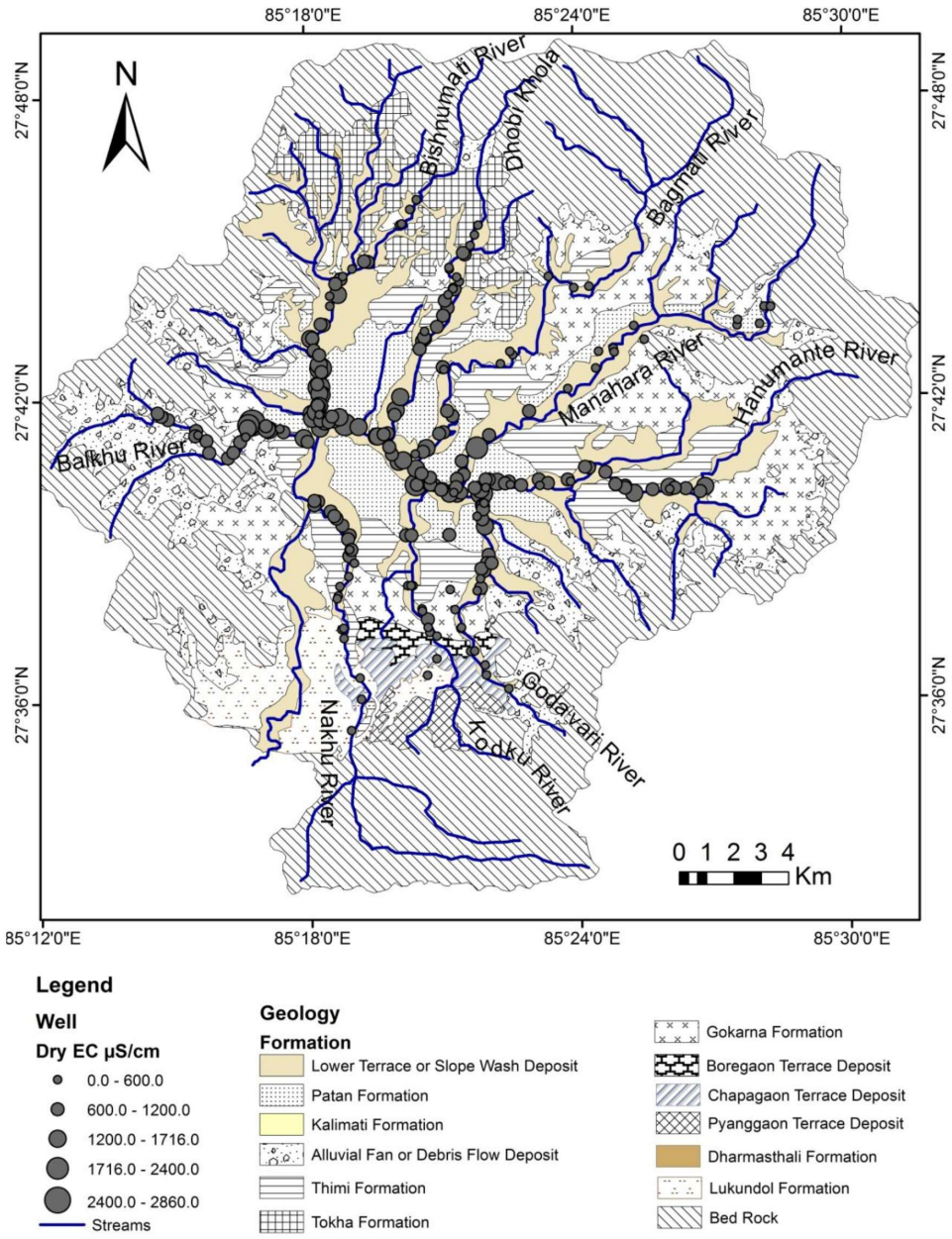

Fig. 6: Variation of EC in dry season

limit of NDWQS (1500 µS/cm). The EC values in the samples from the downstream of other seven tributaries exceeds limit of NDWQS and indicate unsuitability for drinking purpose.

Dissolve Oxygen (DO)

Dissolved oxygen refers to the level of free, non-compound oxygen present in water. It is an important parameter in assessing water quality because of its influence on the organism living within a body of water. DO variation depends on temperature, pressure and salinity of water (Fundamentals of Envirnmental Measurements, 2015). The average DO varied from 1.46 to 2.46 mg/L in dry season and increased to 1.67 and 2.53 mg/L in wet season. Most of the wells have higher DO during wet season. The highest DO was recorded in the samples from the upstream section of all rivers, and DO decreased in samples lying towards core areas of the Kathmandu Valley. In the study area, DO increased as temperature and EC decreased.

Comparing nine rivers, minimum value was obtained from the downstream of the Kodku Khola (0.09 mg/L) and maximum value was found in the sample fromthe upstream of the Dhobi Khola (6.06 mg/L) in dry season (Fig. 8). In wet season, minimum (0.26 mg/L) and maximum (8.55 mg/L) values of DO was recorded in samples from the downstream and the upstream segments of the Bagmati River (Fig. 9).

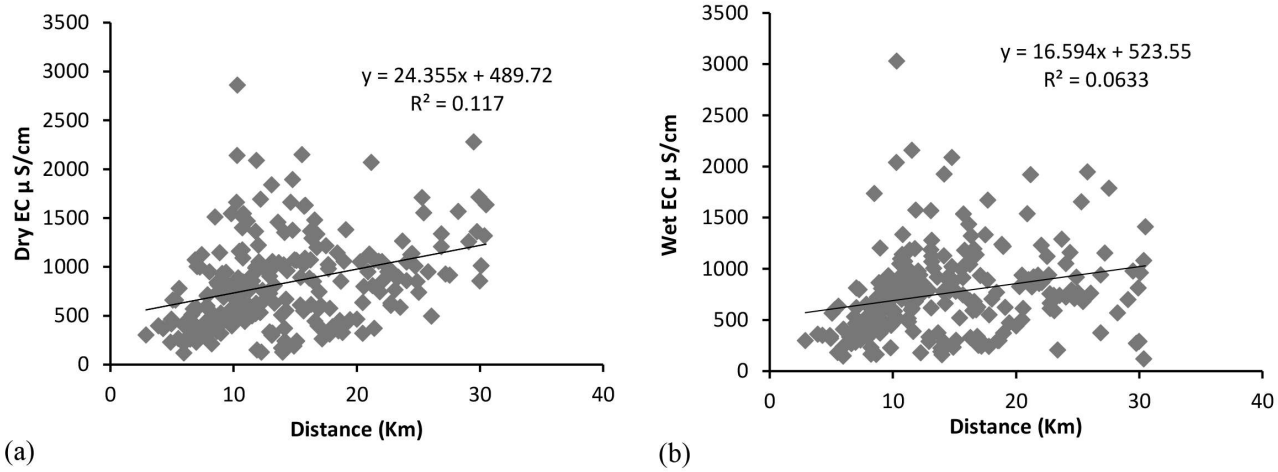

Fig. 7: EC verses downstream distance of well location from the origin of each river in a) dry season and b) wet season

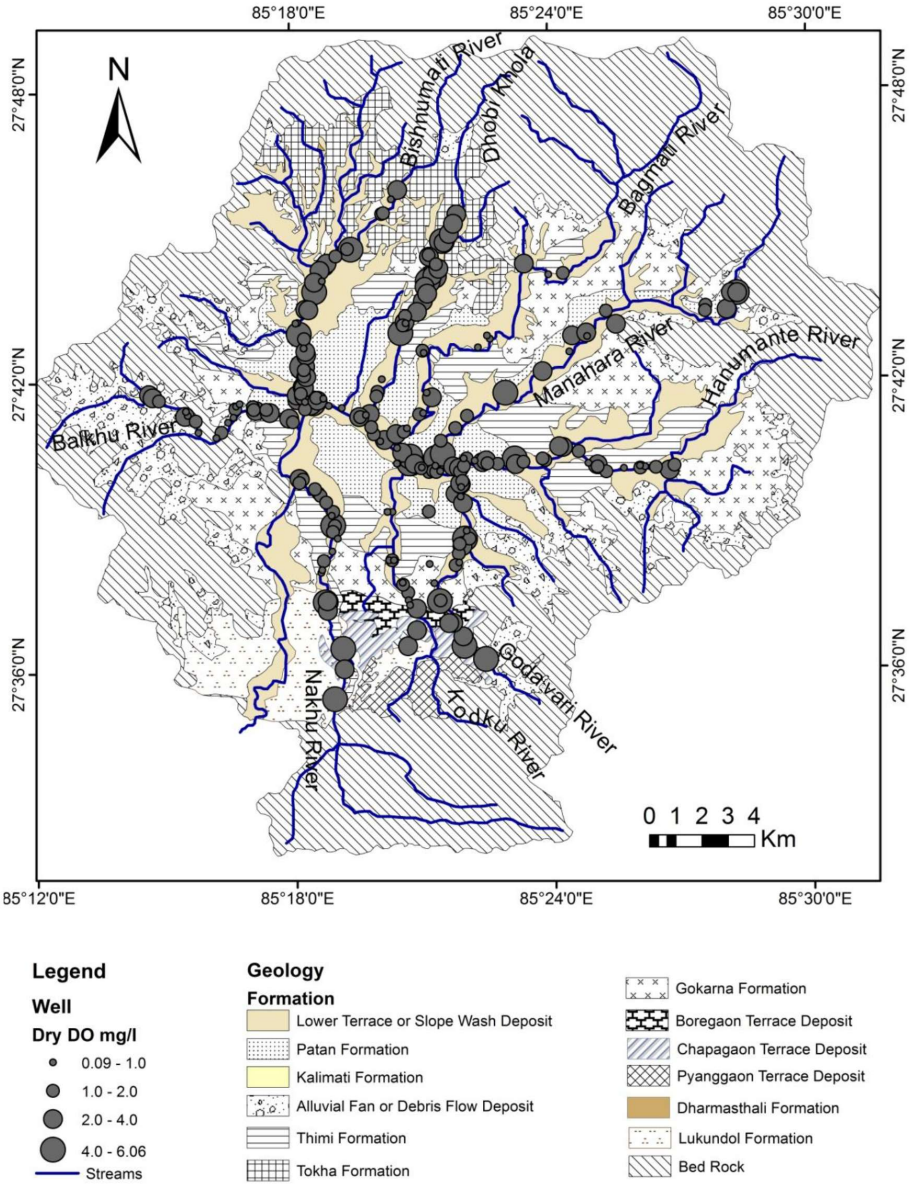

Fig. 8: DO variation in dry season

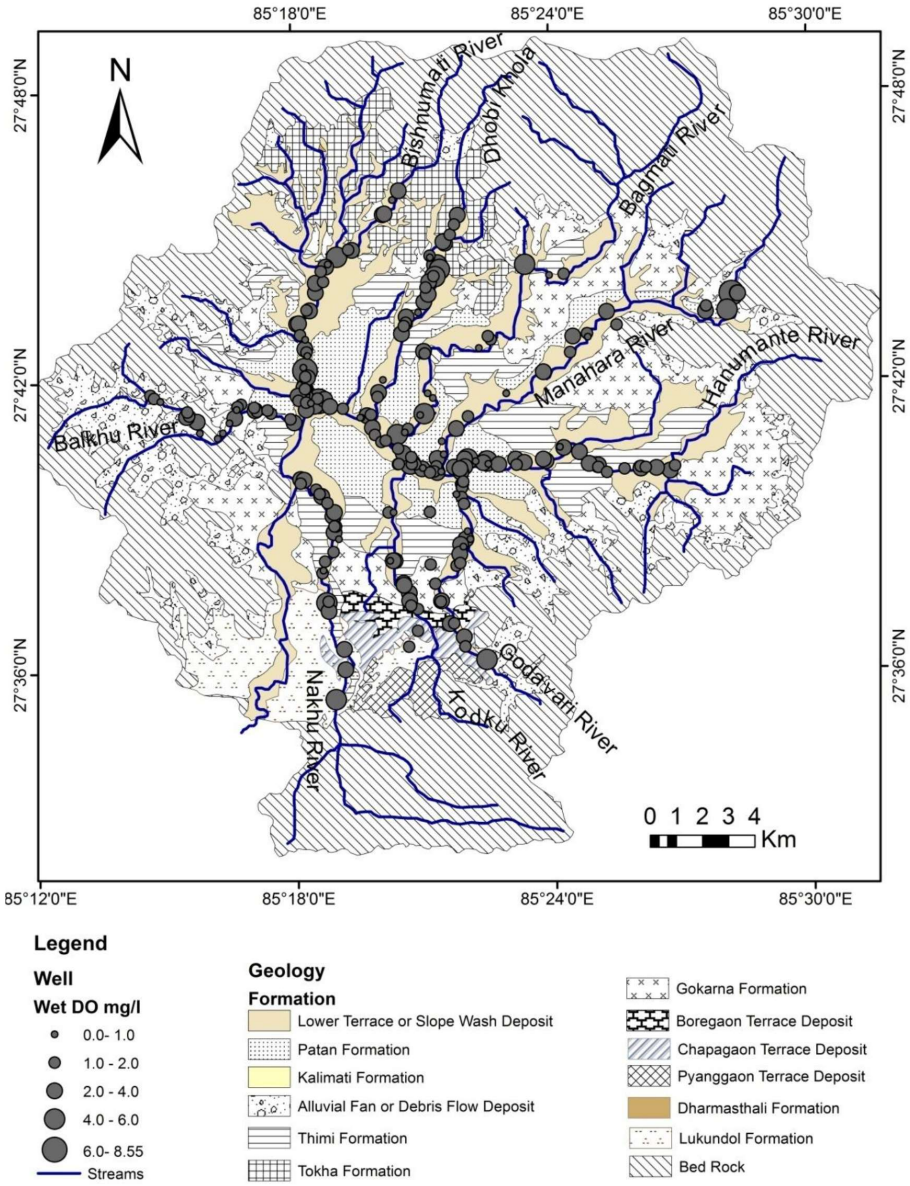

Fig. 9: DO variation in wet season

Relation between physical parameter of water and distance from river channel to well location

In present investigation, wells which were located within 100 m from major rivers of the Kathmandu valley were used. Wells were divided into 4 categories as 0–30 m, 30–60 m, 60–90 m and above 90 m from river channel. Variation of EC, DO, temperature and pH related with the distance were studied in this part.

EC was found highest in those wells which were located within 30 m from river channels having average value 878.2 µS/cm. EC values decreased to 858.1 µS/cm, 727.2 µS/cm and 378.1 µS/cm as the distance from river channel increased to 30–60 m, 60–90 m and above 90 m, respectively in dry season (Table 4). But within 30 m distance also, there was wide range of values with minimum of 231 µS/cm and maximum 2860 µS/cm. The minimum value was recorded from upstream section whereas maximum value was noted from downstream section. Average EC value was decreased to 765.6 µS/cm in wet season which was located within 30 m but other wells located between 30–60m, 60–90 m and above 90 m have higher EC as compared to dry season. The average pH and temperature were similar in wet and dry season in all 4 categorical ranges of distances. There was no any difference observed in relation to distance from river channel. But in the case of DO, the lowest average value (1.9 mg/L) was found within 30 m and increased to 2.1 m/L as the distance from river increased. The combined information on EC and DO suggests two possibility: (1) recharge from the polluted river water to the groundwater and contaminated groundwater (Gautam et al., 2013) and (2) leachate from solid waste, sewer and industrial disposal near the river banks contaminated the groundwater of shallow wells.

Table 4: Physical parameters and distance from river channel

Parameters		Distance from river channel							
		0– 30		30–60		60– 90		>90	
		Dry	Wet	Dry	Wet	Dry	Wet	Dry	Wet
EC	Min	231	121.7	126.8	160.5	169.9	190	119.8	148.5
	Max	2860	2090	2090	2158	1637	1413	1092	1142
	Average	878.2	765.6	858.1	817.0	727.2	646.0	378.1	475.0
pH	Min	6.46	5.33	6.35	6.73	5.67	5.92	5.96	6.51
	Max	8.5	8.3	7.73	7.85	8.03	7.87	7.23	7.82
	Average	7.1	7.3	7.1	7.3	7.0	7.2	6.5	7.2
DO	Min	0.09	0.19	0.19	0.36	0.11	0.59	0.31	1.02
	Max	5.93	8.55	6.06	4.81	4.75	3.88	4.61	6.36
	Average	1.9	2.2	2.1	2.0	2.0	1.9	2.1	2.8
Temp.	Min	15.3	19.6	15.5	21	15.4	21	18.8	20.2
	Max	21.6	25.8	23.4	25.8	24	27.6	16	24.1
	Average	19.0	23.3	19.3	23.5	18.9	23.4	19.7	23.0

CONCLUSIONS

All physical parameter and water level depth was spatially and seasonally variable. Water level depth was the least in the wells of the Nakhu Khola corridor in both dry and wet season whereas the highest values were recorded in the wells of the Dhobi Khola and the Kodku Khola corridors in dry and wet seasons, respectively. Average temperature and pH value ranged from 17.67 to 19.83oC and 6.16 to 7.33 in dry season which increased to the range from 22.8 to 23.6°C and 7.19 to 7.41 in wet season, respectively. Similarly, DO average value was obtained within 1.46 to 2.46 mg/L in dry season and was found to increase to 1.67 and 2.53 mg/L in wet season. But in the case of EC, it decreased from dry season (614.2 and 1123.9 µS/cm) to wet season (613.0 and 916.1 µS/cm) indicating dilution in ionic concentration due to rainfall infiltration. EC and DO show inverse relation and both indicate that wells located at the core or urbanized area have been more contaminated than those of the outer regions due to greater anthropogenic activities in the core area.

Average EC of wells located within 30 m from the river channel has the highest value as compared with other wells. These wells also showed lower DO indicating higher possibility of contamination near river banks due to leachate of solid waste, industrial and sewer disposal. There is also possibility of recharge from the polluted river water to shallow groundwater which was close to river bank (approx 0–60 m) through bank infiltration.

ACKNOWLEDGMENTS

Authors are thankful to the Central Department of geology for providing test kits and suitable environment for research. Authors are also thankful to Prof. Dr. Suresh Das Shrestha for providing valuable suggestion and comments during this research work and Ms. Mamata Sayami for supporting preparation of maps in GIS.

REFERENCES

Aytekin, H. and Bayraktaroglu, N., 2014, An investigation on the quality of natural spring waters in Zonguldak Provinance (Turkey) Academic Library Collections in Korea. J. Korean Libr. Inf. Sci. Soc. v. 45, pp. 277–308. https://doi.org/10.16981/kliss.45.4.201412.277

Diwakar, J., Yami, K.D., and Prasai, T., 2010, Assessment of drinking water of Bhaktapur Municipality area in pre-monsoon season. Sci. World, v. 6, pp. 94–98.

Dhital, M.R., 2015, Geology of the Nepal Himalaya: Regional perspective of the classical collided orogen. Switzerland: Springer International Publishing, pp. 448–453

Fundamentals of envirnmental measurements, 2015. Dissolved oxygen-environmental measurement systems. Fundam. Envirnmental Meas.

Gautam, D. and Prajapati, R.N., 2014, Drawdown and dynamics of groundwater table in Kathmandu Valley , Nepal. Open Hydrol. J., v. 8, pp. 17–26. https://doi.org/10.2174/1874378101408010017

Gautam, R., Shrestha, J.K., Kumar, G., and Shrestha, C., 2013, Assessment of river water intrusion at the periphery of Bagmati River in Kathmandu Valley. Nepal J. Sci. Technol., v. 14, pp.137–146.

Ghimire, G., Adhikari, B., and Pradhan, M., 2013, Bacteriological analysis of water of Kathmandu Valley. MJSBH, v. 12, pp. 19–22

Khadka, M.S., 1993, The groundwater quality situation in alluvial aquifer of the Kathmandu Valley, Nepal. AGSO Journal of Australian Geology and Geophysics, v. 14, pp. 207–211

Ngabirano, H., Byamugisha, D., and Ntambi, E., 2016, Effects of seasonal variations in physical parameters on quality of gravity flow water in Kyanamira Sub-County, Kabale District, Uganda. J. Water Resour. Prot., v. 8, pp.1297–1309. https://doi.org/10.4236/jwarp.2016.813099

Oyem, H.H., Oyem, I.M., and Ezeweali, D., 2014, Temperature, pH, electrical conductivity, total dissolved solids and chemical oxygen demand of groundwater in Boji-BojiAgbor/Owa Area and Immediate suburbs. Environmental Sciences. Res. J. Environ. Sci., v. 8, pp. 444–450. https://doi.org/10.3923/ryes.2014.444.450

Pandey, V.P., Chapagain, S.K., and Kazama, F., 2010, Evaluation of groundwater environment of Kathmandu valley. Environ. Earth Sci., v. 60, pp. 1329–1342.

Pandey, V.P., Shrestha, S., and Kazama, F., 2012. Groundwater in the Kathmandu Valley: Development dynamics , consequences and prospects for sustainable management. Eur. Water, v. 37, pp. 3–14.

Pant, B.R., 2011. Ground water quality in the Kathmandu valley of Nepal. Environ. Monit. Assess., v. 178, pp. 477–485. https://doi.org/10.1007/s10661-010-1706-y

Pathak, D.R. and Hiratsuka, A., 2010, An investigation of nitrate and iron concentration and their relationship in shallow groundwater system of Kathmandu. Desalination and Water Treatment, v. 19, pp.191–197.

Prasai, T., Lekhak, B., Joshi, D.R., and Baral, M.P., 2010, Microbiological analysis of drinking water of Kathmandu Valley. Sci. World, v. 5, pp. 112–114. https://doi.org/10.3126/sw.v5i5.2667

Ramamohan, H. and Sudhakar, I., 2014, Evaluation of ground water quality for the pre and post-monsoon variations in physico-chemical characteristics of North East Coast of Srikakulam District, A.P., India, v. 3, pp. 124–131.

Sakai, T., Gajurel, A.P., Tabata, H., Ooi, N., Takaawa, T., Kitagawa, H., and Upreti, B.N., 2008, Revised lithostrtigraphy of fluvio-lacustrine sediments comprising northern Kathmandu Basin in Central Nepal. Journal of Nepal Geological Society, v. 37, pp. 25–44.

Shrestha,O.M., Koirala, A., Hanisch, Jorg., Busch, K., Kerntke, M., and Jager, S., 1999, A Geo-environmental map for the sustainable development of the Kathmandu Valley, Nepal. GeoJournal, v. 49, pp. 165–172

Shrestha, S. and Shah, S., 2014, Final report on shallow aquifer mapping of Kathmandu Valley. submitted to Groundwater Resources Development Board, Babarmahal, Kathmandu, 49 p.

Stocklin, J., 1980, Geology of Nepal and its regional frame. Journal of Geological Society of London, v. 137, pp. 1–34

Warner, N.R., Levy, J., Harpp, K., and Farruggia, F., 2008, Drinking water quality in Nepal's Kathmandu Valley: A survey and assessment of selected controlling site characteristics. Hydrogeol. J., v. 16, pp. 321–334. https://doi.org/10.1007/s10040-007-0238-1

WHO Nepal, 2005. National drinking water quality standards,22p http://mowss.gov.np/article/34/national-drinking-water-quality-standards-2062.html,

Yoshida, M. and Igarashi, Y., 1984, Neogene to quaternary lacuastrine sediments in the Kathmandu Valley, Nepal. Jour. Nepal Geological Society, Special Issue, v. 4, pp. 73–100.

APPENDIX 2

PARTICIPATION IN CONFERENCES

Appendix 2A:

International Conference on Water, Environment and Climate Change (WECC): Knowledge Sharing and Partnership, organized from April 10-12, 2018 at Hotel Yak and Yeti, Kathmandu, Nepal.

CERTIFICATE OF APPRECIATION

Awarded to

Ms. Ramita Bajracharya in recognition of invaluable contribution as Poster Presenter during the International Conference on "Water, Environment and Climate Change: Knowledge Sharing and Partnership".

10-12 April, 2018

Kathmandu, Nepal

Er. Tej Raj Bhatt
Director General
Department of Water Supply & Sewerage (DWSS), GoN

Er. Ramdeep Sah
Chairman
Society of Public Health Engineers, Nepal (SOPHEN)

Er. Hare Ram Shrestha
Chairman
Nepal Engineers' Association (NEA)

Appendix 2B:

9th Nepal Geological Congress, organized from 19-21 November 2018 at Hotel Yak and Yeti, Kathmandu, Nepal.

Appendix 2C:

35th Himalaya-Karakorum-Tibet (HKT) Workshop, organized from 2-4 November 2022 in Pokhara Nepal.

Appendix 2D:

Ph.D Festival, organized from 9-10 October 2023 in Tribhuvan University, Kirtipur, Nepal.

TRIBHUVAN UNIVERSITY
INSTITUTE OF SCIENCE & TECHNOLOGY
Kirtipur, Kathmandu

PARTICIPATION CERTIFICATE

AWARDED TO

RAMITA BAJRACHARYA

With appreciation and good wishes for participation with a poster presentation in the

Ph.D. Festival 2023

Held on 9-10 October, 2023 (22-23 Asoj 2080) in University Campus, Kirtipur, Nepal.

Prof. Dr. Binil Aryal
Dean, IoST, TU, Nepal

Organized by
Institute of Science & Technology, TU

Prof. Dr. Shiva Lal Bhusal
Rector, TU, Nepal

APPENDIX 3

Inventory data of dug wells from rivers

Appendix 3A: Inventory data of the Bishnumati river

S.No	Well ID	Location	Elevation (m)	Northing	Easting	Distance from river (m)	Bank	Well Depth (m)	Well Diameter (m)	Water Depth (m)		EC (µS/cm)		pH		DO (mg/l)		Temperature (°C)	
										Dry	Wet	Dry	Wet	Dry	Wet	Dry	Wet	Dry	Wet
1	BMW1	Teku dovan	1280	27.69242	85.3025	60	Left	5	1	0.9	0.5	1198	600	7.7	7.7	0.3	1.5	18.4	25.8
7	BMW2	Kuleshwor	1285	27.69306	85.2995	10	Right	6.9	0.9	3.6	0.9	1336	1139	7.7	7.3	3.8	1.9	18.4	23.2
6	BMW3	Kuleshwor	1285	27.69467	85.2994	35	Right	4.1	1	4.0	1.3	1341	1111	7.5	7.1	3.7	2.4	20.4	21.8
2	BMW4	Capital Hill College	1283	27.69522	85.3009	50	Left	6.6	1	5.8	1.7	1294	1323	7.4	7.3	1.5	3.3	18.1	23.2
4	BMW5	Kalimati pul	1288	27.69708	85.3021	28	Left	4.5	1	3.1	1.5	1072	1043	7.2	7.1	3.8	1.5	17.7	21.6
3	BMW6	Kalimati pul	1288	27.69731	85.3022	25	Left	7.1	0.9	6.1	1.4	1366	689	7.3	7.5	3.0	3.7	17.9	24.1
5	BMW7	Kalimati pul	1288	27.69747	85.3017	15	Right	4.6	0.9	3.5	2.3	885	1436	7.2	7.0	3.0	3	18.7	21.7
8	BMW8	Paropakar Road	1283	27.70097	85.3031	35	Left	5	0.9	3.6	2.4	1630	1182	7.2	7.0	2.7	2	19	22.5
9	BMW9	Bishumati Pul	1283	27.70128	85.3023	7	Right	3.2	1.2	1.8	1.1	1621	1536	7.2	7.3	1.4	1.1	18.2	23.7
10	BMW10	Dallu	1286	27.70447	85.3015	25	Right	5.8	1	5.3	AB	893		7.8		4.1		19.2	
11	BMW11	Dallu	1284	27.70339	85.3021	1	Left	4	0.8	3.2	1.1	2150	997	7.3	7.5	1.3	6.3	20.2	24.7
12	BMW12	Dallu	1287	27.7085	85.3031	12	Left	4.2	1	1.8	1.3	1071	880	7.5	7.4	3.7	0.3	16.7	23.2
13	BMW13	Dallu	1287	27.70967	85.3028	8	Left	4.8	0.8	3.3	2.4	1895	2090	7.3	7.4	2.1	1.2	20.7	23.5
21	BMW14	Gongabu	1290	27.71083	85.3022	10	Right	7.8	1	4.8	4.2	1662	789	7.3	7.0	0.7	2.4	20.2	22.7
14	BMW15	Dallu	1288	27.71181	85.3025	5	Left	3.8	1		1.9		553		7.2		2.5		23.5
15	BMW16	Shovabagwati	1291	27.71406	85.3024	12	Left	3.9	1	3.0	3.1	962	908	8.5	7.3	1.7	0.5	19.7	23.7
20	BMW17	Chamati	1289	27.71567	85.3004	50	Right	4.85	1	4.3	1.4	1020	779	7.6	7.0	4.2	1.5	18.8	23.5
19	BMW18	Khusibu	1289	27.7195	85.2991	20	Right	3.1	1	1.5	1.5	1457	920	7.4	7.4	0.5	3.4	17.7	22.8

16	BMW19	Chamati	1289	27.71967	85.2998	20	Left	4.8	0.9	4.1	2.2	1042	374	7.1	7.7	0.7	2.3	17.5	25
18	BMW20	Balaju	1289	27.72425	85.303	40	Right	5.1	1	4.9	0.4	729	334	7.6	7.5	3.1	1.6	19.4	23.3
17	BMW21	Balaju	1290	27.72403	85.3042	50	Left	5.6	1	5.0	1.3	905	794	7.0	7.7	2.1	2.1	19.9	23.9
22	BMW22	Gongabu	1290	27.73397	85.3095	230	Left	3.4	1	2.3	1.6	1364	935	7.4	7.4	0.7	1.6	18.3	23.3
23	BMW23	Ganga hall	1290	27.73356	85.3065	15	Right	4.6	1	2.2	1.0	521	740	7.5	7.2	2.6	2.2	18.3	23.6
24	BMW24	Gongabu	1291	27.73022	85.3065	30	Right	9.5	1	6.8	2.0	533	733	7.6	7.2	4.3	2.3	21.6	23.2
26	BMW25	Baniyatar	1293	27.73756	85.3087	7	Right	5	1	2.7	1.7	761	482	7.2	7.4	2.7	1.1	19.9	23.8
25	BMW26	Machhapokhari	1293	27.73911	85.3106	7	Left	4.2	0.9	2.7	1.7	807	735	7.2	7.1	3.3	2.4	17.8	22.7
28	BMW27	Baniyatar	1291	27.74	85.3114	28	Right	4.9	0.9	4.2	2.7	488	1074	7.5	5.3	3.3	0.7	20.6	21.6
27	BMW28	Baniyatar	1290	27.74244	85.3149	20	Left	4.35	1	3.6	1.4	489	1048	6.9	7.5	1.6	5.1	19.5	23.5
29	BMW29	Baniyatar	1296	27.74492	85.3194	25	Left	3.4	0.9	2.4	1.0	665	587	7.1	7.2	1.1	1.6	18.1	23
30	BMW30	Tokha Road	1296	27.74478	85.3208	20	Right	2.2	0.9	1.2	0.4	754	468	7.8	7.3	5.9	2.6	16.7	23.5
31	BMW31	Tokha	1296	27.75692	85.3328	5	Left	2.5	0.9	1.9	1.1	582	655	6.8	7.0	1.4	2.8	18.7	23.4
32	BMW32	Tokha	1309	27.75719	85.3335	5	Right	2.9	0.9	1.6	1.1	317	471	6.9	7.0	1.4	2.7	18	23.5
33	BMW33	Tokha	1303	27.76197	85.3366	30	Right	2.2	0.9	1.6	1.2	397	368	7.2	6.8	0.6	0.5	16.2	24.7
34	BMW34	Budhanilkantha	1307	27.76519	85.3391	25	Left	3.97	1	1.4	0.4	260	334	6.5	6.9	2.7	2.1	17.9	25

AB=Abandoned

Appendix 3 B: Inventory data of the Dhobi Khola

S.No	Well ID	Location	Elevation (m)	Northing	Easting	Well Depth (m)	WD (m)	Distance from river (m)	Bank	Water Depth (m)		EC (µS/cm)		pH		DO (mg/l)		Temperature (°C)	
										Dry	Wet	Dry	Wet	Dry	Wet	Dry	Wet	Dry	Wet
35	DW1	Thapathali	1283	27.687	85.3238	3.3	0.9	50	Right	2.4	2.4	1481	1196	7.2	7.5	1.4	0.7	20.6	22.4
36	DW2	Buddhanagar	1285	27.68767	85.326	3.0	1	15	Left	2.5	2.1	616	328	7.4	8.0	0.4	3.7	18.4	23.1
37	DW3	Buddhanagar	1286	27.68799	85.3275	2.7	1	20	Right	2.4	1.8	1088	1034	6.9	7.0	3.3	1.9	20.3	22.8
38	DW4	Bijuli bazar	1291	27.69411	85.3302	2.8	0.9	60	Left	1.6	0.1	1066	780	7.1	7.4	1.4	1.2	19.2	23.6
39	DW5	Baneshwor	1295	27.69567	85.3306	4.3	0.9	15	Left	3.3	2.1	1376	1023	7.1	7.1	1.5	3.3	19.1	22.3
40	DW6	Rudramati marga	1294	27.69994	85.3323	4.7	1	20	Right	2.2	1.9	1353	1128	7.4	7.6	0.6	0.5	19.9	22.8
41	DW7	Chabahil bulbule	1304	27.71577	85.3397	5.4	1.2	80	Left	3.3	1.2	760	843	7.1	7.0	4.8	3.8	20.5	23.2
42	DW8	Bhatkya pul	1300	27.71842	85.3406	4.4	1		Left	2.6	1.6	1052	978	7.1	7.4	1.8	1.0	19.7	23.9
43	DW9	Bhatkya pul	1300	27.71917	85.3418	5.5	0.9	10	Left	3.3	1.1	1003	703	6.8	7.1	0.5	1.4	19.9	23.8
44	DW10	Hadigaun	1300	27.7196	85.3414	5.4	0.9	60	Right	5.1	0.4	989	1199	7.2	7.3	2.6	1.4	20.1	24.8
45	DW11	Gopikrishna hall	1300	27.72163	85.3416	3.1	1.1	80	Right	2.1	2.2	561	389	6.7	7.6	2.0	2.3	20.1	24.0
46	DW12	Gopikrishna hall	1305	27.72308	85.3462	4.3	0.9	10	Left	3.3	2.5	834	999	7.0	7.3	2.3	0.6	20.2	22.4
47	DW13	Sukedhara	1303	27.72673	85.3485	2.3	1	40	Right	1.7	0.8	719	702	7.0	7.4	3.3	3.4	20.7	23.4
48	DW14	Dalanepul	1304	27.72929	85.3502	3.5	0.9	5	Left	2.6	2	888	515	7.0	7.4	2.2	2.6	19.0	21.8
49	DW15	Nelopul	1304	27.73167	85.3493	2.7	1.1	10	Left	2	0.9	676	737	6.8	7.4	2.4	1.1	20.2	23.5
50	DW16	Rudramati chowk	1306	27.73362	85.3505	3.0	1.1	40	Right	1.8	1.3	396	448	6.8	7.1	4.2	3.0	19.6	24.0
51	DW17	Miteripul	1306	27.73555	85.3524	6.0	0.9	5	Right	1.7	1.3	430	769	7.1	7.6	3.4	1.2	21.2	24.7
52	DW18	Miteripul	1309	27.73537	85.3529	4.2	1.1	50	Left	3.8	2.5	802	802	6.9	7.4	4.3	4.4	19.1	22.3
53	DW19	Ekatabasti	1308	27.73787	85.3547	4.1	1	15	Right	3.7	3	511	473	6.7	7.3	2.0	4.5	20.3	22.5
54	DW20	Ekatabasti	1309	27.7394	85.3538	3.0	0.9	15	Left	3.2	2.5	501	404	6.7	7.2	1.0	4.9	20.1	23.6
55	DW21	Baluwakhani	1310	27.74203	85.351	3.4	1	25	Left	3.3	1.7	496	497	7.0	6.6	3.7	1.0	19.7	23.4
56	DW22	Mandikhatar	1309	27.74261	85.351	3.7	0.9	20	Right	3.4	2	341	163	7.0	8.1	1.1	1.5	20.2	24.5
57	DW23	Bhangal	1310	27.7474	85.3562	12.2	1	40	Right	12	2.8	602	381	7.4	6.8	6.1	2.1	18.6	22.7
58	DW24	Bhangal	1315	27.74689	85.3568	5.5	0.9	10	Left	4.7	3.1	703	357	6.7	6.9	2.9	3.2	18.6	22.3
59	DW25	Chunkhel	1311	27.74981	85.3589	2.4	1	10	Left	2	1.8	341	304	6.9	6.8	2.8	1.2	20.4	24.2
60	DW26	Nayabasti	1319	27.75652	85.3619	3.0	1.1	30	Left	1.1	1.8	297	302	6.8	6.5	2.5	2.0	20.2	23.3
61	DW27	Tankal	1315	27.75334	85.3606	2.6	0.9	15	Right	2.5	0.9	231	283	6.8	7.0	2.2	1.1	19.5	23.6

WD = Well diameter

Appendix 3C: Inventory data of the Bagmati river

S.No	Well ID	Location	Elevation	Northing	Easting	Well Depth (m)	WD (m)	Distance from river (m)	Bank	Water Depth (m)		EC (µS/cm)		pH		DO (mg/L)		Temperature (°C)	
										Dry	Wet	Dry	Wet	Dry	Wet	Dry	Wet	Dry	Wet
62	BW1	Kalopul, Teku	1282	27.69213	85.30428	2.2	1	40	Left	2.1	0.7	1319	1081	7.3	7.1	4.3	0.4	18	23.4
63	BW2	TekuDobhan	1280	27.69444	85.30222	2.6	0.9	30	Right	0.9	0.7		122		6.7		3.6		24.1
64	BW3	TekuDobhan	1281	27.68987	85.30247	2.75	1	70	Left	2.3	2.2	1637	1413	6.3	7.1	1.5	2.4	17.9	22.6
65	BW4	Rajtirtha	1285	27.69188	85.30561	1.25	1	60	Left	1.2	1.2	1013	963	6.7	7.4	4.8	4.8	19.4	23.8
66	BW5	HanumanGhat	1281	27.69371	85.3069	3.8	1	25	Right	1.4	3	855	291	7.1	6.8	2.0	2.0	19.9	23.3
67	BW6	Gusingal	1280	27.69283	85.30734	2.1	0.9	10	Left	1.9	1	1716	814	6.8	7.0	2.1	8.6	19.4	24.1
68	BW7	Bansitar,Teku	1285	27.69349	85.3096	3.7	0.9	60	Right	3.2	3.5	1360	273	7.0	7.3	0.4	3.7	18.9	21.4
69	BW8	Kupondol	1282	27.691	85.31169	3.3	1	25	Left	2.0	0.9	2280	979	7.2	7.3	0.2	2.1	18.9	25.6
70	BW9	Thapathali	1282	27.69016	85.31674	3.2	1	20	Right	3.0	1.8	1259	701	7.1	7.1	0.5	1.4	19.4	24.5
71	BW10	Rudreshwor mahadev	1282	27.68699	85.3234	3.6	1	20	Right	2.6	3.4	1569	570	6.9	6.8	2.6	0.4	19	21.5
72	BW11	Jwagal	1284	27.68352	85.32802	3.45	0.8	20	Left	2.8	1	916	1787	6.8	7.1	1.2	2.0	19.4	23.5
73	BW12	Sankhamul	1288	27.681	85.32898	6.5	1	80	Left	4.2	1.6	926	1155	7.1	7.3	1.4	1.9	18.9	24.7
74	BW13	Sankhamul Temple	1284	27.67856	85.33149	3.2	1.6	50	Left	1.8	1.7	1337	942	6.8	7.1	0.4	1.7	20.3	24.4
75	BW14	Sankhamul yoga park	1285	27.67899	85.33318	3.4	0.9	20	Right	2.9	1.9	1207	374	7.3	6.7	2.8	1.0	19.2	21.8
76	BW15	Koteshwor, Sahayogi nagar	1288	27.68103	85.33766	6.3	1.1	25	Left	5.7	2.2	495	761	6.5	7.4	2.7	4.2	21.4	25.8
77	BW16	Mahadevsthan	1291	27.68179	85.34058	8.6	1	20	Left	7.7	2.1	951	1949	6.7	7.3	1.1	0.6	19.6	21.1
78	BW17	Sahayogi Nagar	1289	27.68294	85.34184	6.1	1	30	Right	5.8	5.7	1553	681	6.7	7.8	0.7	1.9	19.6	20.7
79	BW18	Gairigaon	1293	27.68773	85.34661	2.7	0.9	25	Left	2.5	2.5	852	918	7.0	7.5	1.3	0.3	18.2	21.9
80	BW19	Tinkune,Gairigaon	1290	27.68815	85.34818	1.9	0.8	10	Left	1.0	0.8	1136	793	6.8	7.3	0.5	4.7	19.1	22.8
81	BW20	Jagriti Nagar	1295	27.69355	85.35163	4.9	0.9	30	Right	4.5	1.7	895	207	6.9	7.5	2.3	0.5	19.1	25.1
82	BW21	Jagriti Nagar	1294	27.69518	85.34963	4.2	1	2	Right	2.2	1.2	766	592	7.2	7.6	0.5	0.8	17.1	23.2
83	BW22	PashupatinathTemple	1300	27.70889	85.34866	3.45	1.1	5	Left	2.7	2.5	371	922	7.2	7.5	0.4	1.8	19.2	23.3
84	BW23	PashupatinathTemple	1309	27.70967	85.34817	9	1.5	50	Right	8.8	3.3	808	825	7.1	7.4	1.7	2.3	21	22
85	BW24	Gothatar, Airport	1311	27.7106	85.36965	5.35	0.9	50	Left	4.8	1.8	329	124	6.4	7.4	0.8	0.5	19.1	25.2
86	BW25	Gothatar	1311	27.71358	85.3743	5.9	1.1	50	Left	5.1	4.6	388	705	6.4	7.0	0.6	1.5	19.4	22.6
87	BW26	Nayabasti, Jorpati	1308	27.71468	85.37321	4.3	1.1	40	Right	4.1	0.6	311	243	6.4	7.8	0.2	1.3	23.4	25.7
88	BW27	GokarnaTemple	1323	27.73931	85.38779	6.5	1.1	20	Right	4.9	1.6	242	193	7.0	7.0	2.8	4.4	19	21.7

89	BW28	Uttar gaya Temple	1324	27.73554	85.39717	4.3	1.1	40	Right	3.6	2.4	323	113	6.6	7.4	0.6	0.6	19	24.3
90	BW29	Namgyal	1322	27.73591	85.40282	3.2	0.8	80	Right	1.8	1.8	150	94.2	6.4	7.4	1.1	1.6	19.4	22.7

WD = Well diameter

Appendix 3D: Inventory data of the Manahara river

S.No	Well ID	Location	Elevation (m)	Northing	Easting	Well Depth (m)	WD (m)	Distance from river (m)	Bank	Water Depth (m)		EC (µS/cm)		pH		DO (mg/l)		Temperature (°C)	
										Dry	Wet	Dry	Wet	Dry	Wet	Dry	Wet	Dry	Wet
91	MW1	Sankhamul Jhulungepul	1286	27.6762	85.3379	7.1	1.1	35	Right	5.6	5	1711	1656	7.3	7.6	0.6	1.5	20.3	21
92	MW2	Balkumari	1283	27.6746	85.3399	1.15	0.9	10	Left	1.1	0.1	741	768	7.1	7.2	3.5	2.2	19.4	24.5
93	MW3	Balkumari	1289	27.6732	85.343	5.1	0.9	70	Right	4.8	3	1010	712	7.2	7.6	4	1.1	18.8	23.3
94	MW4	Mahalaxmi	1287	27.6707	85.3446	6	0.9	45	Left	2.9	1.7	1126	1160	7	7.9	3.3	1.7	18.5	24
95	MW5	Imadol	1285	27.6691	85.3472	3.1	1.1	20	Left	2.5	1.8	859	1052	6.7	7.3	1.5	2.9	19.1	23.8
96	MW6	Narephat	1287	27.6694	85.3474	7.65	1.1	20	Right	5.7	2	1049	724	7	7.4	0.4	0.8	20.9	24.7
97	MW7	Imadol	1288	27.6678	85.3502	5.65	1.1	30	Left	1.2	1.8	1264	1290	6.6	7.3	1.7	1.3	17.8	22.6
98	MW8	Narephat	1287	27.6682	85.3518	3.9	0.9	10	Right	3.6	1.6	588	740	6.8	7.7	1.6	1.6	20.2	24.5
99	MW9	Nilopul	1288	27.6699	85.3527	3.6	1.1	25	Left	3.1	1.9	914	740	6.7	7.2	0.5	1.7	17.8	22.7
100	MW10	Jadibuti Narephat	1288	27.6726	85.353	5.3	1.1	90	Right	5	1.1	949	756	6.5	7.9	4.1	2.1	20.8	25.7
101	MW11	Jadibuti	1292	27.674	85.3556	4.8	1	40	Left	4.5	3.4	950	1123	6.8	7	4	0.5	19.8	21.7
102	MW12	Jadibuti	1293	27.6785	85.3549	2.15	0.8	50	Right	1.8	1.2	1054	1230	7	7.5	1.4	0.8	18.6	23.7
103	MW13	Pepsicola	1291	27.6829	85.3605	3.3	0.9	50	Right	3	1.8	2070	1922	6.8	7.1	1.8	2.8	19.7	24.3
104	MW14	Pepsicola	1296	27.687	85.3651	5.4	1.2	15	Right	4.5	4.8	801	612	6.8	7.2	1.1	1.2	20.5	21.9
105	MW15	Kadaghari, Harhar mahadev	1304	27.6949	85.3801	4.6	1.1	60	Right	3.7	AB	854		6.8		5.4		18	
106	MW16	Mulpani	1313	27.7022	85.3946	2.6	1	50	Left	2.8	1.5	445	681	6.6	7	2.3	2.9	18.7	24.2
107	MW17	Mulpani	1317	27.7089	85.405	2.3	1.1	90	Right	1.8	2	190	235	6.8	6.7	0.5	1.9	17.5	24.2
108	MW18	Risheswor mahadev	1321	27.7144	85.4061	2.8	1.1	80	Right	2.3	0.5	508	227	6.7	7	2.5	3	19.2	27.6
109	MW19	Mulpani	1319	27.7141	85.4119	2.8	0.9	60	Left	2.4	1.8	127	161	6.7	6.9	0.6	0.7	17.2	24.9
110	MW20	Mulpani	1319	27.7153	85.4116	2.4	1.1	80	Right	2	2.2	170	190	6.4	6.9	2	2	16.9	24.8
111	MW21	Changunarayan	1321	27.7182	85.4231	5.35	0.9	30	Left	5	4.7	302	620	6.5	7	3.1	2	18.4	21.9
112	MW22	Bhairavsthan	1322	27.7228	85.4193	3.4	1.1	280	Right	3.1	1.7	127	181	6.2	6.5	1.6	4	18.8	24.1
113	MW23	Shankarapur, salambutar	1368	27.7244	85.4579	4	0.9	260	Right	3.8	0.3	214	232	6.3	6.8	2	1.6	18.7	23.8
114	MW24	Sakhu, salmutar	1366	27.7225	85.4577	4	0.9	150	Right	3.5	2.6	426	168	6.1	7	1.8	3.4	19.5	23.3
115	MW25	Sakhu, chattitar	1360	27.723	85.4661	6.15	1.1	260	Right	4.1	2.6	342	269	6.4	6.9	3.2	5.7	19.1	23.8
116	MW26	Sakhu	1380	27.7287	85.4678	4.6	1.2	180	Right	4.3	2.7	218	149	6	7.8	3.2	6.4	18.9	23.3
117	MW27	Sakhu	1387	27.7286	85.4702	2.8	1	150	Left	0.6	0.1	120	154	6.7	7.2	2.5	2.6	18.4	22.7
118	MW28	Sakhu	1384	27.7287	85.4701	6	1	140	Left	4.8	3.3	244	239	6.8	7	4.6	3.1	17.8	20.2

AB = Abandoned, WD = Well Diameter

Appendix 3E: Inventory data of the Hanumante Khola

S.No	Well ID	Location	Elevation (m)	Northing	Easting	Well Depth (m)	WD (m)	Distance from river (m)	Bank	Water Depth (m)		EC (µS/cm)		pH		DO (mg/l)		Temperature (°C)	
										Dry	Wet	Dry	Wet	Dry	Wet	Dry	Wet	Dry	Wet
119	HW1	Bogateswor Mahadev	1280	27.6684	85.3553	2.4	0.9	10	Left	1.5	0.1	1382	623	7.2	7.6	1.5	3.3	19.1	22.8
120	HW2	Lokanthali	1281	27.6687	85.3569	6	1.1	5	Right	2.9	1.9	1059	1221	7	7.4	0.6	1	20.1	22.4
121	HW3	Lokanthali,Budathokigaun	1283	27.6703	85.3619	2.8	0.9	20	Right	1.6	0.8	1142	769	6.8	6.7	3.3	3	19.2	21
122	HW4	Lokanthali	1290	27.6704	85.366	4.3	1.1	2	Left	2.6	1.6	576	551	7.6	6.8	1.1	3	18.6	22.2
123	HW5	Kausaltar	1282	27.673	85.366	2.4	0.9	8	Right	1.1	2.1	982	1671	6.7	7.4	1	3	20.1	23.7
124	HW6	Balkot	1296	27.673	85.3672	5	0.9	25	Left	4.2	3.6	1023	889	7	7.3	1.8	4.1	20.2	22.6
125	HW7	Sagbari	1284	27.6722	85.3702	4.6	1.1	70	Right	3.3	1.1	1217	1334	5.7	5.9	0.7	0.6	19.7	23.8
126	HW8	Balkot	1285	27.6717	85.3733	3.2	0.9	5	Left	2.6	2.3	604	935	7	7.3	2.3	2.1	19.6	23.3
127	HW9	Sarbari,phalamepul	1284	27.6722	85.3747	4.5	1.1	25	Right	3.9	1.3	746	252	7.2	7.9	2.1	4.9	19.4	24.5
128	HW10	Gathaghar	1291	27.6712	85.3752	6.7	1.2	25	Left	6.3	5.6	571	627	6.8	7	1.1	0.6	20.7	20.7
129	HW11	Balkot	1284	27.671	85.3792	7	1	30	Left	5.8	4.3	852	591	7.3	7.5	1.9	2.5	18.8	22.7
130	HW12	Madhyapur thimi	1295	27.6728	85.3857	2.8	0.9	25	Right	2.6	1.5	1023	745	6.9	6.9	4.7	3.8	18.9	22.2
131	HW13	Dadhikot	1289	27.6709	85.3861	3.6	1.1	20	Left	2.7	0.1	549	915	7	7.3	2.2	1.1	19.4	22.5
132	HW14	Madhepur thimi	1288	27.6717	85.3891	2.8	1	20	Right	2.5	1.7	609	520	6.7	7.1	1.6	2.6	19.5	22.8
133	HW15	Tappa bagar	1286	27.6727	85.3965	3.3	1	40	Right	2.9	2.1	670	662	7.4	7.2	1.3	2.9	19.6	22.3
134	HW16	Sano chokhu	1288	27.6721	85.3975	2.7	1	60	Left	2.4	0.1	553	801	7	7.2	1.8	3.2	19.6	24.2
135	HW17	Shyam shyam dham								2.6	AB	630		6.8		2.6		20	
136	HW18	Shyam shyam dham	1289	27.6766	85.4045	2.8	0.9	25	Left	2.1	0.1	812	1006	7	7.3	3.6	3.8	19.2	23.8
137	HW19	Sallaghari	1292	27.6751	85.4105	3.8	1.1	20	right	2.4	0.9	661	849	6.7	6.7	1.3	3.9	18.9	22.9
138	HW20	Sallaghari	1309	27.671	85.4143	1.5	0.8	60	Left	1.2	0.6	627	681	6.8	7.2	0.7	2.4	18.4	22
139	HW21	Tabakay	1296	27.6705	85.4178	5.3	1	15	Right	3.7	1	921	613	6.6	7.1	2.6	3.2	18.8	23.1
140	HW22	Chundevi albu	1293	27.6698	85.4178	5.5	1.1	40	Left	3.4	0.1	855	2158	6.9	7.6	1.1	1.3	18.1	24.7
141	HW23	khusibu	1300	27.6701	85.4475	4.7	1.1	50	Right	2.4	1.2	1512	1736	6.9	7	1.9	1.8	19	22.1
142	HW24	Chundevi	1300	27.668	85.4211	3.6	1.1	30	Left	2.2	0.1	1468	699	7.2	7.8	1.8	1.3	18.3	23.5
143	HW25	Mangatitha	1300	27.6692	85.428	8.2	1.1	15	Right	3	0.9	1160	784	7.1	7.2	0.6	1.1	19.9	23.6

144	HW26	Siddhipur	1301	27.6699	85.4341	2.9	0.9	35	Right	1.7	0.1	1546	228	7	7.6	0.5	2	19.3	23.8
145	HW27	Siddhipur hospital	1315	27.6692	85.4343	4.8	1.2	10	Left	2	0.9	571	481	7.7	7.7	1.1	3.7	19.5	23.5
146	HW28	Hanumanghat	1306	27.6696	85.4362	15.7	1.2	10	Left	1.5	1	804	934	7.6	8.1	0.7	1.5	18.9	20.7
147	HW29	Jagati	1302	27.6694	85.4403	3.3	1	2	Left	2.1	1	824	839	6.9	7	1.9	2.1	19.8	22.3
148	HW30		1303	27.6684	85.4456	4.5	1	90	Right	2.7	1.7	816	620	7.1	7.5	2.5	3.9	20.4	22.2

AB = Abandoned

Appendix 3F: Inventory data of the Godawari Khola

S.No	Well ID	Location	Elevation (m)	Northing	Easting	Well Depth (m)	WD (m)	Distance from river (m)	Bank	Water Depth (m)		EC (µS/cm)		pH		DO (mg/l)		Temperature (°C)	
										Dry	Wet	Dry	Wet	Dry	Wet	Dry	Wet	Dry	Wet
149	GW1		1297	27.6697	85.3641	7.1	1	18-20	Right	7	3.5	1222	856	7.1	7.1	2.5	2.9	19	21.3
150	GW2		1298	27.6685	85.3645	8.53	1	50	Right	4	4.5	2090	1575	7.2	7.5	1.7	2.9	20	21.9
151	GW3		1293	27.6653	85.3654	2.6	0.9	15	Left	1.4	0.8	498	599	7	7	1.7	1.3	15	24.5
152	GW4		1293	27.6641	85.3648	3.3	0.9	10	Left	1.1	0.9	810	923	7	7.5	2.5	1.9	18	24.4
153	GW5		1293	27.6644	85.3645	3.5	0.9	50	Left	1.1	0.1	840	815	7.3	7.5	2.5	1.9	18	24.2
154	GW6		1293	27.6632	85.3649	8.5	0.9	65	Right	1.8	0.9	608	515	7.2	7.1	0.7	1.5	18	23.5
155	GW7									3	AB	441		7.1		3.8		24	
156	GW8		1315	27.6599	85.3646	3.06	0.9	160	Right	2.8	0.9	620	779	7.2	7.4	0.6	1.3	17	21.3
157	GW9		1301	27.6575	85.3655	9.15	1	82	Right	7.7	1.7	1525	1099	7.7	7.2	2.1	1.3	20	22
158	GW10		1306	27.6481	85.3669	3	1	50	Left	1.5	0.1	944	876	7.2	7.3	0.7	0.8	17	23.6
159	GW11		1303	27.6454	85.3679	4.1	1	90	Right	1.1	0.1	741	809	7.2	7.4	1.2	1	17	23.7
160	GW12		1317	27.6454	85.3661	3.7	0.9	50	Left	3.3	1	932	848	7.7	7.5	5	3	17	25.2
161	GW13		1313	27.6436	85.3641	2.6	0.9	30	Left	1.4	0.2	747	725	7.4	7.6	1.1	2.9	15	25.6
162	GW14		1312	27.6428	85.3651	3.3	0.9	80	Right	0.7	0.1	838	697	7.3	7.5	2.3	0.8	15	24.6
163	GW15	Bishnu Tol	1297	27.6402	85.3637	1.85	1	35	Right	0.9	0.1	512	405	7.3	7.7	1.3	2.1	18	25.2
164	GW16	Charghare	1302	27.6372	85.3639	8.55	0.9	45	Right	8.3	0.5	951	550	7.6	7.1	0.5	1	19	22.3
165	GW17		1307	27.6363	85.3624	1.4	0.9	80	Left	1.4	0.8	422	331	7.1	7.3	1.2	1.7	18	22.9
166	GW18	Taukhel	1370	27.6368	85.3524	2.8	1.2	55	Right	0.8	0.3	459	325	6.9	7	0.8	1.3	18	23.5
167	GW19	Bagarphat,khusibu	1321	27.6301	85.3542	6.2	1	80	Left	2.2	1.2	406	346	7.2	7.7	0.6	1	18	24
168	GW20	Thaiba	1343	27.6239	85.3562	1.75	1.3	5	Left	0.5	0.1	428	405	7.3	7.6	4.6	1.5	21	24
169	GW21	Thaiba	1344	27.6242	85.3564	2.3	1	25	Right	0.9	0.1	400	409	7.5	7.6	1	2.1	19	24.5
170	GW22	Badegaun	1400	27.6163	85.3597	4.2	0.9	80	Left	0.6	0.5	464	340	7.5	7.8	2.6	2.9	16	22.5
171	GW23	Thaiba	1370	27.6164	85.3613	4.2	0.9	25	Right	2.8	2.2	418	322	7.1	7.3	3.6	1.8	17	23.6
172	GW24	Godamchour	1390	27.6117	85.3651	1.5	0.9	40	Right	0.5	0.1	369	350	7.5	7.5	4	3	20	23.2
173	GW25	Putali ghat	1399	27.6084	85.3655	1.5	0.9	25	Left	0.6	0.1	398	362	7.2	7.4	5.8	1.2	17	23.4
174	GW26	Rachantar,Godawari	1429	27.6038	85.3738	10.4	1.2	20	Right	5.4	3.2	303	299	7	7.7	4.5	5.2	20	19.6

AB = Abandoned, WD = Well Diameter

Appendix 3G: Inventory data of the Kodku Khola

S.No	Well ID	Location	Elevation (m)	Northing	Easting	Well Depth (m)	WD (m)	Distance from river (m)	Bank	Water Depth (m)		EC (µS/cm)		pH		DO (mg/l)		Temperature (°C)	
										Dry	Wet	Dry	Wet	Dry	Wet	Dry	Wet	Dry	Wet
175	KW1		1288	27.67151	85.34496	7.5	1	4.1	Left	7.3	6.4	1054	1072	7.5	7.6	5.4	5	15.9	20
176	KW2		1288	27.67151	85.34549	9	0.9	10	Right	8.3	2.5	1021	1279	7.6	7.4	5.5	1.2	15.9	22.5
177	KW3		1310	27.67151	85.3401	4.2	1	120	Left	2.4	0.1	1840	1568	6.7	7.5	0.3	1.3	16	23.8
178	KW4		1294	27.67151	85.34046	13	1	10	Right	2	1.2	977	1187	7.2	7.6	0.9	1.1	17.3	24.8
179	KW5		1294	27.65484	85.33626	4.4	0.9	24	Right	3.1	2.5	847	872	7.3	7.3	0.4	1.5	18.2	22.5
180	KW6		1294	27.65484	85.35229	6	1.1	160	Left	5.3	0.5	1092	1142	6.9	7.1	1.3	1.2	19.7	22.1
181	KW7		1296	27.65484	85.33821	6	1	20	Right	1.1	1.6	804	945	7.2	7.3	0.6	0.4	16.2	23.3
182	KW8		1304	27.63818	85.3386	1.8	1.2	2	Left	0.4	0.1	528	371	7.7	8.1	0.1	3.6	15.9	24.9
183	KW9		1310	27.63818	85.3379	2.05	0.9	45	Right	1.6	0.9	320	516	7.1	7	1.1	2.8	15.5	24.2
184	KW10		1315	27.63818	85.33671	3.6	1	20	Left	2.4	2.1	416	1204	7	7.4	0.9	0.5	16.8	22
185	KW11	Harrisiddhi,Daar	1316	27.63039	85.3419	1.25	1	15	Right	1.1	0.3	455	421	7.1	7.6	0.5	2.6	17.8	23.7
186	KW12	Dhapakhel	1316	27.6297	85.34202	2.3	0.9	30	Left	1.4	1.3	294	432	7	7.3	1.4	2.2	17.2	23.3
187	KW13	Dhapakhel	1321	27.62696	85.344	4	1	90	Left	3.3	2.8	999	796	6.6	7.1	1.4	2.9	18.6	21
188	KW14	Dhapakhel	1323	27.62435	85.34408	5.1	1	75	Left	1.3	0.1	568	468	7.9	6.8	0.8	2.2	17.5	21.2
189	KW15	Thaiba	1325	27.62263	85.34467	3.3	1	20	Left	1.7	0.1	570	312	7.1	7.2	0.5	1.3	17.8	21.4
190	KW16	Thaiba	1331	27.62143	85.3473	3.45	1	70	Right	0.8	0.1	511	375	8	7.9	3.1	1.9	20.8	23
191	KW17	Jharawashi	1384	27.61392	85.34721	6.25	1.1	50	Left	2.9	0.1	267	183	7.2	6.6	2.5	1.2	19	21.6
192	KW18	Jharawashi	1430	27.60845	85.3437	9.9	2.3	70	Left	0.9	0.1	230	347	6.2	6.5	3.7	2	22	21.3

WD = Well Diameter

Appendix 3H: Inventory data of the Nakhu Khola

S.No	Well ID	Location	Elevation (m)	Northing	Easting	Well Depth (m)	WD (m)	Distance from river (m)	Bank	Water Depth (m)		EC (µS/cm)		pH		DO (mg/l)		Temperature (°C)	
										Dry	Wet	Dry	Wet	Dry	Wet	Dry	Wet	Dry	Wet
193	NW1	Bagdol	1267	27.6665	85.30235	3.1	1	15	Right	1.6	0.8	608	612	7.1	7.1	3	2.7	20.3	24.7
194	NW2	Bhaisepati	1263	27.6651	85.30235	2.7	1	30	Left	1.8	1.3	629	666	6.8	6.9	1.4	1	18.7	21.6
195	NW3	Bagdol	1269	27.6663	85.30369	2.5	1.1	15	Right	1.5	1.1	978	940	7.2	7.4	1.6	2.5	20.2	23.5
196	NW4	Nakkhupul	1270	27.663	85.30835	7.2	1	20	Left	3.8	1.8	856	867	7.2	7.4	1	1.9	18.4	21.8
197	NW5	Nakkhu	1272	27.6614	85.3097	2.4	1.1	15	Left	1.3	0.9	745	856	7	7.2	2	1.9	19	22.6
198	NW6	Nakkhu	1272	27.6606	85.31043	3.2	1.1	30	Right	0.5	0.1	1058	937	6.9	7.9	1.3	2.5	20.3	24.6
199	NW7	Kusunti	1271	27.6583	85.3126	11.3	1.1	10	Left	1	0.6	1068	870	7.3	7	1.2	1	19.4	24.9
200	NW8	Kusunti	1281	27.6551	85.31532	7.2	1	35	Right	3	0.7	1131	895	7.3	7.5	1.7	2.3	19.2	24
201	NW9	Nakhidol	1267	27.6538	85.31469	3.5	0.7	3	Left	0.8	0.8	950	1540	7.3	7.7	0.7	2.9	20.6	23
202	NW10	Nakhipot	1280	27.6502	85.31589	2.65	0.9	15	Right	1.5	1.5	635	501	7	7.4	1.8	1.4	20.4	24.1
203	NW11	Nakhidol	1281	27.6503	85.31522	2.8	0.9	15	Left	0.5	2.2	320	938	7.8	7.5	4.6	1.2	19.8	22.5
204	NW12	Kantipur colony	1288	27.6482	85.31509	4.6	1.1	25	right	3.3	1.2	1052	827	7	7.3	1.3	3.6	18.9	24.1
205	NW13		1294	27.6458	85.31692	3.7	0.9	25	Right	1.1	0.8	464	443	7	7	0.6	1	19	23.7
206	NW14	Kirat chowk	1299	27.6414	85.31484	1.9	0.7	15	Left	1.4	1.2	458	472	7.3	7.5	0.8	1.2	19.3	24.4
207	NW15		1302	27.6381	85.31149	1.4	0.9	50	Right	0.4	0.2	401	373	7.5	7.4	1.1	1	20.2	24.3
208	NW16	Sunakothi,Nakkhu	1302	27.635	85.31088	14.4	1.2	10	Right	0.6	0.3	452	299	7.5	7.5	0.5	0.2	19.8	22.5
209	NW17	Sunakothi	1312	27.6341	85.31045	4.8	1.1	65	Right	2.8	1.6	345	300	7.1	7.1	0.6	1.1	19.2	22.6
210	NW18	Thecho	1321	27.6243	85.31274	2.3	1.1	80	Right	2	0.1	264	244	7	7	2.8	1.6	19.5	21.6
211	NW19	Thecho	1330	27.6239	85.31199	4.5	1.1	8	Right	2	0.9	370	300	7.4	7.4	4.2	4.3	18.2	23.1
212	NW20	Kaule	1330	27.6209	85.31285	1.5	0.8	50	Right	1.1	0.1	396	340	7.7	7.1	3.5	3.2	19.1	23.4
213	NW21	Thecho	1354	27.6078	85.31863	6.3	1.1	40	Right	0.2	0.2	242	303	7.1	7.5	5.7	2.7	20.9	23.1
214	NW22	Tikabhairav,Chapagaun	1370	27.6008	85.31905	2.7	1.1	40	Right	0.9	0.2	371	286	7.4	7.6	2.8	2.2	19.7	25.1
215	NW23	Chapagaun	1400	27.5905	85.31522	3.5	1.1	20	Right	3.1	2.6	335	291	7.3	7.4	5.4	5.1	18.7	23.4

Appendix 3I: Inventory data of the Balkhu Khola

S.No	Well ID	Location	Elevation (m)	Northing	Easting	Well Depth (m)	WD (m)	Distance from river (m)	Bank	Water Depth (m)		EC (µS/cm)		pH		DO (mg/l)		Temperature (°C)	
										Dry	Wet	Dry	Wet	Dry	Wet	Dry	Wet	Dry	Wet
216	BAW1	Balkhu	1284	27.6861	85.3	2.8	0.9	5	Left	2	1.5	992	859	7.3	7.8	1.8	3.6	19.5	23.3
217	BAW2	Balkhu,Mohargaun	1271	27.6873	85.2987	7.2	1.1	5	Right	4.9	1.8	1694	942	7.1	7.2	3	1.3	18.7	23.7
218	BAW4	Khasibazar	1277	27.6894	85.2912	7.7	1	5	Left	5	3	896	1184	7.2	7.1	2.2	1.4	20.3	22.8
219	BAW5	Sunar gaun	1285	27.6905	85.2898	5.85	0.9	15	Left	2	1.6	553	886	7.5	7.4	1.6	1.2	20.6	23.9
220	BAW6	Khasibazar	1278	27.6901	85.2857	9.4	1	20	Right	5.7	2.7	1544	1335	7	6.8	3.5	2	19.8	21.7
221	BAW7	Kalanki	1278	27.6914	85.2846	6.4	1	30	Left	4	1.3	1174	837	6.8	7.1	1.7	2	20	23.8
222	BAW8	Kalanki	1267	27.6904	85.2849	5	1	5	Right	2.3	1.9	1401	785	6.7	6.8	1.3	2.8	18.6	24.9
223	BAW9	Kalanki	1285	27.6926	85.2795	4.7	0.9	2	Left	1.7	1.7	2860	3030	7	7.4	0.4	2	20.3	23.3
224	BAW10	Tinthana	1329	27.6918	85.2782	4.7	1	10	Left	2	2	2140	2040	6.6	6.9	0.4	1.3	19.6	23.9
225	BAW11	Tinthana	1317	27.6908	85.2779	3.8	0.9	15	Left	3.2	2.7	1661	859	6.6	6.9	1	0.8	19.8	24.2
226	BAW12	Maitrinagar	1284	27.6879	85.2771	3.4	0.9	30	Right	2.5	0.3	583	579	6.7	7.4	0.5	2.9	19.9	25.2
227	BAW13	Civil home	1297	27.6862	85.275	4	1	40	Right	2.7	2.1	797	685	6.7	6.7	0.7	0.9	19.9	23.5
228	BAW14	Kritipur ghat	1313	27.6827	85.2724	4.6	1.2	1	Right	2.4	1.6	689	589	7.4	7.3	1.3	0.3	18.5	24
229	BAW15	Sangam nayabasti	1316	27.6809	85.2704	2.8	0.9	70	Right	2.1	1.4	1145	865	7.1	7.5	0.1	0.7	18.4	24
230	BAW16	Bishnu devi	1320	27.6828	85.2635	5.2	1.2	5	Right	5	1.3	714	523	7.5	7.5	0.5	1	18.4	24.3
231	BAW17	Sapradi Naikap	1324	27.6867	85.2625	3.8	0.8	10	Left	3.7	2.6	1127	385	7	8.3	2	2.7	20.1	24.5
232	BAW18	Naikap	1332	27.6887	85.2594	10.4	1.1	20	Left	8.1	1.8	577	622	7.1	7.1	0.6	1.8	20.6	23
233	BAW19	Naikap	1324	27.6884	85.2584	7.2	1	20	right	2	1.5	1005	814	7.5	8	2.6	2.3	18.9	23.5
234	BAW20	Bacchap	1333	27.69	85.2587	10.8	1.1	25	Left	4.7	1.8	1071	531	7.4	8.1	0.5	1.7	18.6	22.3
235	BAW21	Balambu	1339	27.6938	85.2483	5.85	0.9	40	Right	1.5	1.4	781	635	7	7.7	1.1	0.4	19.1	22.6
236	BAW22	Balambu	1345	27.6949	85.2459	2.5	1.1	10	Right	2	1.6	661	603	7.3	7.8	2.6	1.7	19	23.5
237	BAW23	Balambu	1338	27.696	85.2445	1.9	1	25	Left	1.3	1.1	661	568	7.4	7.8	3	1.9	19.5	24.6

WD = Well Diameter

APPENDIX 4

Chemical concentration of groundwater and river water in wet and dry season

Appendix 4A: Chemical concentration of river and groundwater of Bishnumati River in wet (August 2017) and dry (Feb 2018) seasons

Sampling ID	Na^+ (mg/l)		$NH4^+$-N(mg/l)		K^+(mg/l)		Mg^{2+}(mg/l)		Ca^{2+}(mg/l)		Cl^-(mg/l)		$NO3^-$_N(mg/l)		$PO4^-$_P(mg/l)		$SO4^{2-}$(mg/l)		$HCO3^-$(mg/l)	
	Wet	Dry	Wet	Dry	Wet	Dry	Wet	Dry	Wet	Dry	Wet	Dry	Wet	Dry	Wet	Dry	Wet	Dry	Wet	Dry
BMW1	15.5	19.3	3.3	1.5	6.9	5.9	4.3	2.9	22.1	7.8	14.0	19.2	1.5	0.5	ND	0.3	8.3	2.2	134.2	67.1
BMW2	7.4	41.5	ND	0.3	4.2	8.0	2.2	5.4	25.9	33.2	3.3	46.1	0.8	1.0	ND	0.1	16.6	109.2	109.8	54.9
BMW3	29.9		ND		6.8		7.5		76.3		28.6		6.0		ND		126.0		158.6	
BMW4	9.9	13.3	1.3	1.1	2.7	5.4	2.2	5.8	49.2	26.4	10.0	16.5	3.4	4.6	ND	0.5	37.4	42.7	140.3	67.1
BMW5	23.9	51.7	0.1	2.1	6.4	7.6	6.2	9.3	60.7	44.1	28.1	67.3	14.5	11.6	2.5	0.7	55.9	116.3	134.2	67.1
BMW6	18.2	42.2	0.0	0.3	7.7	7.7	4.4	14.8	40.4	131.6	9.0	41.3	3.0	0.8	0.7	0.0	48.1	348.0	164.7	67.1
BMW7	37.9	62.2	0.2	2.1	23.3	26.7	7.0	12.3	51.9	52.5	49.5	86.4	13.3	19.2	3.0	1.0	41.9	129.0	183	85.4
BMW8	50.4	16.8	0.6	6.2	14.6	5.9	19.3	4.4	82.9	15.8	57.2	27.5	32.2	0.4	ND	ND	98.3	19.9	158.6	109.8
BMW9	40.7	98.6	0.1	3.8	8.1	20.7	9.8	43.0	73.0	44.0	48.6	133.1	27.2	24.9	ND	0.3	45.8	193.4	146.4	91.5
BMW10	27.9		0.4		7.8		10.4		64.2		31.2		17.5		ND		79.4		134.2	
BMR1	9.9	10.8	0.9	3.6	2.1	3.3	1.3	1.6	7.5	13.0	6.4	12.2	0.7	0.3	ND	2.7	3.9	3.6	54.9	85.4
BMR2	10.6	63.6	1.6	23.4	2.7	19.0	1.8	8.3	11.1	26.0	8.5	69.2	0.5	0.0	0.2	3.6	6.6	36.8	73.2	262.3
BMR3	13.5	58.7	1.7	30.1	4.0	17.7	2.0	6.7	11.1	21.2	11.7	64.7	0.6	0.0	0.8	8.7	7.4	30.4	67.1	329.4
BMR4	10.3	76.8	1.5	54.8	2.6	24.4	2.1	7.7	16.1	21.9	7.8	90.8	0.9	0.0	0.5	10.3	9.8	35.0	73.2	420.9
BMR5	13.9	74.6	2.7	49.2	3.8	22.5	2.1	8.1	12.7	25.7	11.5	86.7	ND	0.0	1.0	11.9	7.6	30.8	96.38	366.0
BMR6	13.9	91.7	3.0	66.5	3.9	29.2	2.0	8.6	10.3	22.8	12.4	107.8	0.1	0.0	ND	11.8	7.8	37.3	91.5	372.1
BMR7	15.6	105.1	3.3	83.6	4.1	32.8	2.2	9.6	12.9	24.6	13.6	127.7	0.1	0.0	ND	15.2	8.5	41.1	42.7	530.7
BMR8	16.8	100.4	3.8	70.1	4.8	27.6	2.7	7.9	15.5	25.0	15.6	115.8	0.0	0.0	ND	13.5	9.4	38.8	103.7	372.1
BMR9	18.5	108.2	4.5	66.7	5.4	32.3	2.6	8.7	16.8	25.8	18.0	129.3	0.0	0.0	2.4	13.8	9.8	41.5	109.8	481.9
BMR10	14.1		3.7		4.0		2.3		14.7		14.0		0.1		ND		8.2		103.7	

BMW = Bishnumati well water, BMR = Bishnumati river water, ND = Not Detected

Appendix 4B: Chemical concentration of river and groundwater of Dhobi Khola in wet (August 2017) and dry (Feb 2018) seasons

Sampling ID	Na^+ mg/l		NH_4-N^+ mg/l		K^+ mg/l		Mg^+ mg/l		Ca^+ mg/l		Cl^- mg/l		NO_3_N^- mg/l		PO_4_P^- mg/l		SO_4^{2-} mg/l		HCO_3^- mg/l	
	Wet	Dry	Wet	Dry	Wet	Dry	Wet	Dry	Wet	Dry	Wet	Dry	Wet	Dry	Wet	Dry	Wet	Dry	Wet	Dry
DR1	6.4	21.1	0.3	7.9	1.3	7.3	0.9	2.8	7.2	18.2	3.2	21.7	0.7	0.8	0.3	3.8	2.7	8.0	61	122
DR2	6.1	30.3	0.5	11.5	0.4	10.3	0.7	3.6	5.5	16.5	2.9	34.3	0.3	0.3	0.3	3.7	1.9	11.1	61	158.6
DR3	9.7		1.1		2.1		1.3		8.0		6.1		0.7		ND		4.3		61	
DR4	10.7	71.3	1.6	33.1	2.6	19.6	1.6	7.1	11.4	25.6	7.8	79.4	0.5	0.0	1.1	9.8	5.5	37.6	73.2	317.2
DR5	10.7	81.1	3.4	39.1	3.3	21.7	1.7	7.8	13.6	25.4	10.6	96.0	ND	0.0	1.9	11.2	6.3	41.8	91.5	341.6
DR6	14.0	98.8	3.5	56.7	3.9	26.7	1.8	7.8	11.5	22.1	12.9	103.5	ND	0.0	1.9	14.7	7.6	47.7	103.7	408.7
DR7	15.5	57.6	3.7	24.5	4.1	17.1	2.0	5.9	15.2	16.4	13.8	67.4	ND	0.0	2.4	11.6	8.3	24.8	109.8	262.3
DR8	22.0	100.6	6.0	70.9	6.7	32.0	2.8	8.2	14.5	20.8	22.6	111.8	ND	0.0	2.6	15.3	11.6	45.0	115.9	469.7
DR9	20.0	105.4	6.4	80.0	6.5	34.7	2.6	6.8	13.1	21.8	20.2	127.0	0.0	0.0	2.1	16.2	10.1	44.7	140.3	530.7
DR10	19.5	99.9	10.2	77.4	6.8	32.4	3.3	7.3	21.7	20.6	23.5	119.7	ND	0.0	3.0	14.0	8.1	38.1	170.8	494.1
DW1	10.5	15.6	0.1	0.1	0.7	5.0	2.6	4.4	13.8	28.8	6.5	20.8	0.3	3.9	ND	0.3	23.1	33.9	61	91.5
DT1	5.6	6.2	0.4	0.4	0.4	0.7	1.1	1.2	5.4	5.7	0.5	0.4	0.0	0.0	1.0	0.9	ND	0.1	36.6	115.9
DW2	13.5	27.0	0.1	0.2	1.2	6.1	3.3	4.6	26.9	11.4	8.0	23.6	3.9	0.4	ND	ND	25.5	38.9	91.5	67.1
DW3	4.0		2.7		1.3		0.7		7.5		1.3		0.1		12.7		3.2		1.22	
DW4	18.6	15.3	0.1	0.1	4.8	8.9	5.5	4.3	29.0	19.8	19.9	10.7	11.2	2.7	ND	0.1	24.4	32.2	91.5	97.6
DW5	18.7	34.9	0.4	1.9	6.7	10.4	7.1	9.4	47.1	11.3	22.1	45.0	6.5	3.4	ND	0.0	36.3	36.5	183	103.7
DW6	30.4	7.1	0.3	1.0	8.2	1.8	8.5	2.9	53.4	18.3	42.4	4.9	19.9	0.0	ND	ND	36.3	8.2	122	97.6
DW7	30.7	24.0	1.0	0.4	13.3	18.5	10.6	8.3	84.6	25.5	42.8	45.3	5.0	1.5	ND	ND	113.1	59.7	158.6	97.6
DW8	31.6	41.4	13.6	6.2	10.5	19.3	4.6	7.5	36.3	11.7	32.4	46.8	0.2	0.1	ND	0.1	10.3	5.3	183	225.7
DW9	24.9	44.0	1.1	5.1	8.6	18.4	6.2	11.7	50.0	33.5	25.6	55.1	1.3	1.9	ND	0.0	25.3	22.4	219.6	244
DW10	23.6	59.5	12.5	35.4	7.0	21.4	3.9	10.8	38.2	22.7	31.1	80.4	1.0	0.1	ND	1.0	6.7	2.2	237.9	420.9

ND = Not Detected

Appendix 4C: Chemical concentration of river and groundwater of Bagmati River in wet (August 2017) and dry (Feb 2018) seasons

Sampling ID	Na^+ mg/l		NH_4-N^+mg/l		K^+ mg/l		Mg^+ mg/l		Ca^+ mg/l		Cl^- mg/l		NO_3_N^- mg/l		PO_4_P^- mg/l		SO_4^{2-} mg/l		HCO_3^- mg/l	
	Wet	Dry	Wet	Dry	Wet	Dry	Wet	Dry	Wet	Dry	Wet	Dry	Wet	Dry	Wet	Dry	Wet	Dry	Wet	Dry
BR1	3.5	13.0	0.1	0.1	0.2	1.7	0.4	2.0	2.7	4.6	1.1	4.3	0.1	0.2	ND	ND	0.6	4.4	18.3	54.9
BR2	3.8	12.4	0.1	0.2	0.6	2.1	0.5	1.9	2.3	4.8	1.2	4.9	0.1	0.2	ND	ND	0.9	4.3	18.3	67.1
BR3	3.4	18.0	0.2	2.0	0.7	3.6	0.6	2.4	3.7	9.1	1.3	10.1	0.1	0.2	ND	0.4	1.0	5.2	36.6	91.5
BT1R		20.9		3.0		4.0		3.0		19.9		15.1		0.1		1.2		33.6		91.5
BR4	3.9	49.2	0.4	20.5	0.4	12.1	0.5	4.8	3.3	15.6	1.8	49.0	0.1	0.0	ND	6.0	1.1	22.0	18.3	244
BR5	6.3	26.1	0.5	8.8	1.5	6.9	0.9	3.5	5.0	10.9	3.2	22.9	0.3	0.0	0.3	1.2	2.5	13.4	42.7	134.2
BR6	6.1	69.8	1.3	26.0	1.4	17.9	0.9	6.0	6.6	15.8	4.5	77.6	0.2	0.0	0.7	10.4	2.5	29.1	48.8	274.5
BR7	7.9	101.6	1.6	36.3	1.8	23.5	1.0	7.2	6.2	21.5	5.4	95.8	0.2	0.0	0.8	12.5	3.4	32.8	42.7	396.5
BR8	15.7	94.9	1.6	57.5	1.8	26.6	2.1	9.2	12.2	29.6	10.0	101.6	0.2	0.0	0.7	14.4	5.6	27.9	73.2	481.9
BR9	14.4	53.1	3.5	34.1	4.3	16.4	2.1	6.9	12.3	24.6	14.1	70.3	ND	0.0	1.9	15.1	7.6	18.9	85.4	366
BR10	11.3	97.3	2.2	69.1	3.4	29.5	2.7	9.7	15.1	32.3	10.6	112.1	0.2	ND	ND	17.8	7.9	29.3	97.6	536.8
BW1	3.3	9.3	0.0	0.1	0.2	3.1	0.5	2.4	5.2	9.1	1.0	6.0	0.2	0.3	ND	ND	2.5	3.8	42.7	91.5
BW2	6.9	11.8	0.6	0.7	4.1	7.2	2.8	4.5	23.9	16.7	4.9	10.6	0.9	0.1	0.6	0.1	10.7	18.1	103.7	128.1
BW3	5.7	8.1	0.0	0.0	4.5	3.6	2.9	3.1	18.7	14.6	2.7	5.5	0.3	0.0	0.5	0.0	8.3	4.8	115.9	91.5
BT1W		13.9		0.5		1.9		4.1		11.0		12.5		0.0		0.0		22.5		73.2
BW4	16.7	9.5	0.5	2.5	30.1	2.0	6.6	3.3	36.4	16.9	10.1	13.1	8.5	0.5	ND	ND	52.5	45.7	109.8	42.7
BT1	2.7		0.4		0.1		0.4		2.6		1.6		ND		ND		0.1		30.5	
BW5	4.9	27.0	2.0	6.4	3.2	7.5	1.5	5.0	12.5	26.1	3.8	28.1	0.0	0.2	0.2	ND	0.5	84.8	140.3	109.8
BW6	20.6	47.0	5.4	12.7	5.8	13.8	4.1	8.8	35.7	23.1	26.5	62.3	3.6	1.3	0.8	ND	17.7	17.6	170.8	213.5
BT2	4.8	39.2	3.8	11.3	1.4	8.9	0.5	7.6	4.1	15.0	3.8	56.3	ND	0.0	5.3	ND	0.1	0.4	42.7	225.7
BW7	5.5	60.8	1.0	13.4	10.3	16.4	2.3	12.8	14.4	22.8	6.2	90.7	0.1	0.0	2.5	ND	5.0	77.0	81.74	213.5
BW8	26.1	56.9	0.1	1.6	8.7	19.8	6.7	16.7	38.0	55.6	22.3	68.3	4.0	17.1	ND	0.3	75.7	117.0	103.7	134.2
BW9	30.7	50.5	ND	55.8	7.0	19.8	3.5	19.6	28.5	37.3	27.3	44.1	3.5	0.1	0.6	5.4	21.4	35.5	128.1	542.9
BW10	28.4	59.3	0.1	7.0	5.4	11.9	14.0	48.7	49.2	35.2	35.9	78.7	6.8	21.1	ND	0.9	36.2	46.3	201.3	317.2

ND = Not Detected

Appendix 4D: Chemical concentration of river and groundwater of Manahara River in wet (August 2017) and dry (Feb 2018) seasons

Sampling ID	Na^+ mg/l		NH_4-N^+mg/l		K^+ mg/l		Mg^+ mg/l		Ca^+ mg/l		Cl^- mg/l		NO_3_N^- mg/l		PO_4_P^- mg/l		SO_4^{2-} mg/l		HCO_3^- mg/l	
	Wet	Dry	Wet	Dry	Wet	Dry	Wet	Dry	Wet	Dry	Wet	Dry	Wet	Dry	Wet	Dry	Wet	Dry	Wet	Dry
MR1	4.3	7.9	0.1	ND	0.5	1.9	0.7	1.6	3.7	8.9	1.5	3.7	0.3	0.9	ND	0.1	1.1	3.1	24.4	97.6
MR2	7.6	8.4	ND	0.1	0.2	2.0	0.8	1.7	4.0	6.3	2.1	4.4	0.3	0.9	ND	0.1	1.3	3.6	48.8	48.8
MR3	5.3	23.5	ND	0.1	ND	3.2	0.6	2.9	4.9	28.6	1.2	15.6	0.2	1.0	ND	0.0	1.6	24.0	36.6	97.6
MR4	7.0	14.3	0.1	0.2	0.2	2.9	0.8	2.7	3.9	14.1	2.3	9.4	0.4	0.4	0.4	0.1	1.9	11.7	36.6	97.6
MR5	6.7	45.2	0.7	15.6	1.7	11.7	1.1	5.3	5.5	24.4	3.7	47.3	0.5	0.1	ND	6.0	2.7	22.9	54.9	237.9
MR6	4.8	45.1	0.3	22.9	0.2	13.3	0.6	6.1	3.9	22.9	2.1	53.1	0.1	0.0	ND	6.0	1.1	20.3	36.6	286.7
MR7	8.2	50.3	0.5	17.0	0.9	10.1	1.0	5.1	5.4	15.4	4.4	52.7	0.4	0.0	0.5	1.7	2.2	20.2	36.6	219.6
MR8	12.2	91.8	1.6	54.9	2.7	25.0	2.4	9.1	12.0	24.8	10.2	101.3	0.4	0.0	0.8	11.9	6.6	19.0	67.1	488.0
MR9	8.1	102.0	1.5	63.6	1.3	28.0	1.7	10.7	9.7	32.0	6.4	110.0	0.2	0.0	0.9	12.2	3.9	24.8	61.0	567.3
MR10	11.8	79.1	1.9	37.1	2.1	18.5	2.0	9.7	12.0	35.2	11.8	80.9	0.2	ND	1.1	12.5	5.7	18.3	73.2	433.1
MW1	14.7	26.9	0.1	0.2	1.2	1.6	5.6	4.4	29.9	16.8	26.1	52.3	2.2	0.1	ND	0.1	13.3	21.1	115.9	48.8
MW2	6.0	16.6	0.2	1.7	0.3	4.6	0.8	3.2	6.2	12.8	3.3	16.6	0.3	0.6	ND	ND	4.2	18.0	30.5	
MB1	9.1		0.6		0.6		1.6		8.3		1.1		0.1		0.5		0.4		79.3	
MW3	12.0	21.4	0.1	0.1	5.2	4.1	3.4	5.8	29.1	31.1	9.9	23.8	7.7	4.9	1.7	0.9	30.2	36.6	79.3	91.5
MB2	11.6		4.6		2.6		3.5		8.9		8.8		1.4		ND		5.3		91.5	
MW4		37.3		7.1		24.3		9.3		32.0		56.5		1.2		0.4		31.3		189.1
MW5	14.4	47.2	1.2	3.5	5.0	25.1	5.1	17.7	28.1	58.2	16.6	65.7	2.0	18.2	ND	0.8	39.5	103.1	91.5	134.2
MW6	23.7	51.4	0.9	12.0	3.6	13.8	6.7	15.4	65.6	53.2	31.5	16.5	6.5	27.0	ND	5.1	54.3	42.9	183.0	286.7
MW7	29.6	23.8	3.4	5.4	3.8	6.8	6.0	5.7	30.0	11.6	34.6	23.4	0.8	0.3	ND	ND	23.6	6.0	170.8	158.6
MW8	15.9	47.6	4.5	31.7	2.0	5.1	3.5	11.1	19.3	27.3	4.6	8.6	1.3	0.0	5.0	6.4	7.5	13.9	140.3	402.6
MW9	14.1	87.4	0.1	32.5	2.1	8.2	4.2	35.4	37.4	18.1	6.7	99.1	0.9	0.1	ND	ND	20.6	83.3	164.7	353.8
MW10	15.1	49.6	25.4	2.1	3.8	5.7	13.9	12.3	43.5	19.9	10.4	25.7	ND	1.1	ND	0.1	2.9	7.8	408.7	207.4

ND- Not detected

Appendix 4E: Chemical concentration of river and groundwater of Hanumante Khola in wet (August 2017) and dry (Feb 2018) seasons

Sampling ID	Na^+ mg/l		NH_4-N^+mg/l		K^+ mg/l		Mg^+ mg/l		Ca^+ mg/l		Cl^- mg/l		NO_3_N^- mg/l		PO_4_P^- mg/l		SO_4^{2-} mg/l		HCO_3^- mg/l	
	Wet	Dry	Wet	Dry	Wet	Dry	Wet	Dry	Wet	Dry	Wet	Dry	Wet	Dry	Wet	Dry	Wet	Dry	Wet	Dry
HR1	4.9	26.4	0.3	10.3	1.6	7.6	1.2	5.7	11.6	38.3	3.3	23.7	0.6	0.1	ND	2.4	6.2	10.2	24.4	280.6
HR2	4.2	43.7	0.3	41.2	0.6	17.7	0.8	8.5	8.9	35.9	2.2	63.0	0.4	0.3	ND	9.8	4.1	13.8	30.5	420.9
HR3	6.2	92.2	0.5	87.0	1.4	50.0	1.1	13.1	7.9	35.9	4.3	120.7	0.7	0.5	ND	31.7	5.6	26.4	30.5	628.3
HR4	9.2	115.2	0.8	83.0	4.0	42.7	2.4	12.5	17.0	48.1	8.0	142.6	1.1	0.5	ND	17.7	9.8	25.5	67.1	750.3
HR5	7.0	97.3	0.7	63.0	2.1	29.1	1.8	10.8	10.7	40.5	5.3	124.8	0.6	0.3	ND	22.4	7.3	11.1	54.9	518.5
HR6	7.5	130.7	0.6	85.5	2.5	44.2	2.1	13.7	14.5	43.5	6.1	161.6	0.7	0.5	ND	20.7	7.9	21.8	73.2	750.3
HR7	4.7	142.7	0.5	102.9	0.8	48.8	1.2	13.9	11.0	42.0	3.1	172.0	0.3	0.5	0.2	24.3	4.4	31.8	67.1	878.4
HR8	4.0	139.2	0.9	ND	0.7	42.4	0.7	14.1	8.0	45.7	3.0	171.1	0.2	0.5	0.6	13.2	2.5	20.5	42.7	774.7
HR9	4.1	151.9	0.5	74.8	0.5	35.6	0.9	13.4	7.3	48.6	2.7	142.4	0.3	0.5	ND	21.0	2.9	18.5	48.8	738.1
HR10	9.9	151.9	0.8	97.8	2.5	45.8	2.4	14.7	12.2	45.6	8.7	186.3	1.2	0.6	ND	23.0	8.5	19.4	61.0	884.5
HW1	18.1	21.4	8.7	16.1	7.8	10.8	11.4	13.7	32.2	32.9	22.5	36.0	ND	0.2	ND	0.6	24.2	18.1	219.6	262.3
HW2	37.6	14.4	5.3	10.3	9.3	4.9	20.4	9.3	56.6	40.3	56.6	17.6	0.6	0.1	6.3	5.3	58.0	14.1	298.9	201.3
HW3	17.6	49.4	1.5	31.3	17.3	44.3	7.2	28.8	21.7	64.7	19.5	57.0	3.1	0.6	2.8	8.3	27.1	6.2	122.0	579.5
HW4	18.6	18.6	0.2	0.4	0.7	1.3	8.6	13.8	31.1	28.4	23.3	26.7	0.9	0.9	ND	0.1	32.6	38.9	207.4	158.6
HW5	6.7	48.2	0.5	1.1	3.9	3.6	1.6	13.8	11.7	47.6	4.8	71.7	0.7	6.0	3.7	0.2	5.0	83.7	67.1	122
HW6	20.5	35.3	0.2	1.6	3.7	6.0	8.7	13.6	45.8	35.7	16.4	35.8	ND	1.9	ND	ND	50.6	55.7	170.8	183
HW7	16.8	37.0	0.4	2.3	7.9	7.5	8.0	17.2	56.4	49.4	18.1	38.8	ND	0.5	ND	ND	30.0	46.3	305.0	250.1
HW8	34.5	68.9	0.6	6.7	11.4	22.4	9.8	14.6	72.5	55.9	44.3	82.5	14.8	14.1	ND	ND	55.8	30.8	201.3	292.8
HW9	21.8	35.5	1.7	2.7	5.2	8.6	6.7	15.6	50.0	93.7	25.6	48.8	0.5	1.5	ND	ND	113.8	272.4	85.4	122
HW10	21.1	78.8	0.1	5.2	4.0	10.0	7.3	19.7	42.3	33.0	23.6	94.7	0.7	0.5	ND	ND	42.5	71.5	164.7	195.2

ND- Not detected

Appendix 4F: Chemical concentration of river and groundwater of Godawari Khola in wet (August 2017) and dry (Feb 2018) seasons

Sampling ID	Na^+ mg/l		NH_4-N^+mg/l		K^+ mg/l		Mg^+ mg/l		Ca^+ mg/l		Cl^- mg/l		NO_3_N^- mg/l		PO_4_P^- mg/l		SO_4^{2-} mg/l		HCO_3^- mg/l	
	Wet	Dry	Wet	Dry	Wet	Dry	Wet	Dry	Wet	Dry	Wet	Dry	Wet	Dry	Wet	Dry	Wet	Dry	Wet	Dry
GR1	1.6	6.0	0.1	1.1	0.2	2.3	1.5	4.1	9.3	20.6	1.2	9.5	0.4	0.6	ND	ND	1.0	2.3	36.6	109.8
GR2	3.6	8.9	0.1	0.1	0.5	1.7	2.0	3.9	11.9	21.6	2.9	9.8	0.4	1.0	ND	ND	1.4	3.1	42.7	109.8
GR3	2.6	8.2	ND	0.0	0.3	1.2	1.4	3.9	11.8	18.2	2.1	9.3	0.2	0.5	ND	ND	1.4	3.4	91.5	109.8
GR4	2.8	11.5	0.0	1.2	0.4	3.1	1.8	4.2	15.3	14.6	2.1	15.3	0.1	0.8	ND	ND	1.6	5.0	91.5	85.4
GR5	4.2	9.2	0.1	0.2	0.5	1.2	2.4	3.8	16.2	12.6	4.1	13.8	ND	0.6	ND	ND	2.9	6.1	122	67.1
GR6	3.6	10.0	0.0	0.6	0.6	1.4	2.3	4.3	14.9	15.3	3.3	14.3	0.1	0.2	ND	ND	2.4	5.0	109.8	103.7
GR7	2.62	26.4	0.07	8.8	0.4	3.8	1.53	5.6	10.9	23.6	2.82	36.2	0.10	0.1	ND	ND	2.5	28.6	97.6	152.5
GR8/GW9	7.03	24.1	0.10	1.7	1.1	2.4	3.75	7.5	19.2	20.1	7.41	42.9	0.29	0.1	ND	ND	5.6	19.5	103.7	97.6
GR10	7.93		0.01		1.0		4.18		18.0		9.28		0.28		ND.		6.9		91.5	
GW1	1.7	2.6	ND	0.1	0.2	0.9	1.5	3.2	17.3	14.5	1.7	6.3	0.2	0.8	ND	ND	0.3	1.1	85.4	73.2
GW2	4.9	24.4	0.0	0.4	1.1	3.1	1.9	5.2	16.8	17.7	3.8	28.2	0.0	0.0	ND	ND	2.6	11.1	97.6	97.6
GW3	4.9	3.8	0.0	0.2	0.4	0.3	2.2	2.2	18.1	15.4	4.3	4.8	ND	0.0	ND	ND	2.3	4.0	122	79.3
GW4	2.1	8.2	0.1	0.7	0.5	0.9	0.8	3.6	12.2	22.1	1.5	12.8	0.0	0.6	ND	ND	1.6	5.9	79.3	85.4
GW5	2.2	7.1	ND	0.3	0.0	0.7	1.1	5.9	14.8	25.2	1.0	9.3	0.0	0.1	ND	ND	0.5	3.1	103.7	128.1
GW6	12.0	37.1	2.1	0.4	2.3	2.8	6.6	18.0	48.4	33.6	18.9	48.3	0.3	0.5	ND	ND	30.4	38.7	183	189.1
GW7	35.9	144.2	2.3	0.3	7.03	8.3	15.6	49.8	59.6	45.6	67.2	323.5	20.36	4.7	0.43	ND	46.8	60.0	152.5	146.4
GW8	15.2		1.7		1.9		6.3		30.7		14.1		0.13		0.65		17.7		164.7	
GW9	27.7	33.1	2.2	13.4	5.5	4.3	13.5	18.6	63.0	27.1	59.3	41.8	17.74	0.3	ND	ND	47.0	29.1	146.4	256.2
GW10	39.1	47.5	11.9	13.0	15.6	15.7	15.7	18.6	99.2	84.1	51.5	87.8	0.13	0.1	ND	ND	262.5	189.9	225.7	176.9

ND- Not detected

Appendix 4G: Chemical concentration of river and groundwater of Kodku Khola in wet (August 2017) and dry (Feb 2018) seasons

Sampling ID	Na^+ mg/l		NH_4-N^+mg/l		K^+ mg/l		Mg^+ mg/l		Ca^+ mg/l		Cl^- mg/l		NO_3_N^- mg/l		PO_4_P^- mg/l		SO_4^{2-} mg/l		HCO_3^- mg/l	
	Wet	Dry	Wet	Dry	Wet	Dry	Wet	Dry	Wet	Dry	Wet	Dry	Wet	Dry	Wet	Dry	Wet	Dry	Wet	Dry
KR1	4.5	6.66	0.0	0.29	0.1	1.99	1.4	4.30	10.0	19.25	2.3	7.87	0.1	0.33	ND	ND	1.9	5.23	73.2	73.2
KR2	8.2	7.75	0.2	0.36	0.5	1.47	2.6	3.38	12.5	16.04	7.0	9.93	0.3	0.14	ND	ND	3.2	3.16	97.6	91.5
KR3	11.5	13.32	0.3	0.33	1.2	2.08	3.7	4.57	15.7	15.04	12.0	16.40	0.5	0.19	ND	ND	4.4	4.32	109.8	109.8
KR4	7.7	15.55	0.2	0.38	0.8	2.42	2.4	5.37	13.2	18.04	8.2	20.42	0.3	0.17	ND	ND	3.2	4.47	91.5	79.3
KR5	10.4	35.02	0.1	10.40	1.5	6.84	1.4	7.25	18.4	31.57	7.0	45.36	1.8	0.14	ND	2.26	9.5	9.85	91.5	219.6
KR6	19.2		2.2		3.9		6.0		24.0		22.8		0.6		ND		8.4		158.6	
KR7	20.3	94.48	3.3	63.38	4.4	24.74	5.3	11.41	18.7	39.66	25.4	116.88	0.2	0.42	ND	13.31	10.0	22.73	176.9	536.8
KR8	13.1	89.48	2.8	59.90	2.8	23.36	3.7	11.91	17.7	42.90	15.4	110.00	ND	0.40	ND	10.46	6.9	19.73	134.2	585.6
KW1	4.3	5.4	0.0	0.1	0.6	0.8	1.5	1.8	29.6	29.1	3.5	4.7	0.5	0.8	ND	ND	6.1	7.7	97.6	91.5
KW2	23.6	38.9	0.6	4.8	1.2	3.7	9.4	11.6	38.6	19.6	58.3	80.0	4.5	1.4	0.0	ND	11.3	6.3	109.8	134.2
KW3	6.9	7.2	0.3	0.2	2.5	1.0	2.4	2.7	15.5	17.6	7.9	10.2	0.5	0.3	ND	ND	3.8	2.8	103.7	85.4
KW4	18.6	20.8	4.5	2.6	3.0	4.5	6.5	7.6	51.4	27.2	24.8	32.2	ND	0.1	ND	ND	30.7	21.1	231.8	146.4
KW5	9.1	55.1	0.8	12.9	0.9	9.6	2.4	12.6	10.2	35.4	8.7	78.5	0.3	0.2	ND	ND	3.7	1.3	73.2	311.1
KW6	25.0		2.9		2.5		5.2		53.1		27.9		0.2		ND		46.1		207.4	
KW7	33.5	52.9	7.1	17.8	3.5	6.9	10.6	15.9	43.8	28.1	51.1	75.2	ND	0.7	ND	ND	7.8	1.3	280.6	317.2
KW8	23.4	68.4	0.1	0.4	0.8	2.2	8.3	21.4	52.5	44.4	39.4	108.7	8.1	24.9	ND	ND	44.3	53.4	158.6	134.2

ND- Not detected

Appendix 4H: Chemical concentration of river and groundwater of Nakhu Khola in wet (August 2017) and dry (Feb 2018) seasons

Sampling ID	Na^+ mg/l		NH_4-N^+ mg/l		K^+ mg/l		Mg^+ mg/l		Ca^+ mg/l		Cl^- mg/l		NO_3_N^- mg/l		PO_4_P^- mg/l		SO_4^{2-} mg/l		HCO_3^- mg/l	
	Wet	Dry	Wet	Dry	Wet	Dry	Wet	Dry	Wet	Dry	Wet	Dry	Wet	Dry	Wet	Dry	Wet	Dry	Wet	Dry
NR1		5.73		0.05		1.30		3.96		14.49		4.78		0.35		ND		3.98		91.5
NR2		6.65		0.16		1.72		4.59		19.86		5.93		0.39		ND		4.50		115.9
NR3		7.26		0.17		1.74		4.46		17.73		7.42		0.38		ND		4.14		91.5
NR4	3.7	12.42	0.2	1.22	0.6	2.80	1.6	5.99	11.7	15.97	2.3	13.00	0.2	0.33	ND	ND	1.7	5.42	115.9	103.7
NR5	14.8	36.79	0.7	8.30	3.2	ND	4.5	8.35	20.3	29.08	15.2	43.64	ND	0.21	ND	ND	ND	10.67	109.8	237.9
NR6	7.6	98.10	0.8	61.24	2.0	25.57	2.6	10.99	12.3	44.12	6.8	114.05	1.0	0.35	ND	10.84	6.2	50.67	158.6	494.1
NW1		7.5		0.1		0.7		5.5		22.8		7.3		1.5		ND		6.8		122
NW2		6.3		0.5		1.5		4.9		24.5		5.9		0.0		ND		6.4		128.1
NW3		10.9		1.9		3.7		7.4		15.1		20.8		0.4		ND		0.5		122
NW4	18.6	19.0	0.9	5.2	4.0	1.8	7.1	12.0	31.3	25.9	17.9	25.7	0.5	9.4	ND	ND	17.0	11.1	183	140.3
NW5	8.8	43.1	1.0	7.6	3.8	9.6	2.4	15.0	21.8	17.7	6.5	75.2	1.2	0.2	ND	ND	18.6	0.7	97.6	219.6
NW6	23.0	36.0	0.3	0.4	1.0	2.1	4.8	10.3	41.6	29.3	31.6	53.6	1.0	0.4	ND	ND	9.9	13.7	207.4	146.4

ND- Not detected

Appendix 4I: Chemical concentration of river and groundwater of Balkhu Khola in wet (August 2017) and dry (Feb 2018) seasons

Sampling ID	Na^+ mg/l		NH_4-N_mg/l		K^+ mg/l		Mg^+ mg/l		Ca^+ mg/l		Cl^- mg/l		NO_3_N^- mg/l		PO_4_P^- mg/l		SO_4^{2-} mg/l		HCO_3^- mg/l	
	Wet	Dry	Wet	Dry	Wet	Dry	Wet	Dry	Wet	Dry	Wet	Dry	Wet	Dry	Wet	Dry	Wet	Dry	Wet	Dry
BAR1	8.6	18.9	0.6	0.8	2.5	3.2	2.1	4.4	12.9	15.0	8.3	23.5	ND	0.3	ND	ND	ND	4.3	91.5	103.7
BAR2	13.1	29.3	1.0	1.5	5.0	5.3	3.6	6.5	22.6	21.3	14.8	35.4	2.0	0.2	ND	ND	11.1	4.4	140.3	128.1
BAR3	10.8	16.0	1.1	6.0	4.1	3.7	2.9	3.5	21.5	37.5	11.5	20.6	1.5	0.2	ND	2.81	9.2	2.5	115.9	183
BAR4	7.1	67.3	0.7	26.3	1.6	18.2	1.5	9.3	12.2	40.6	6.1	87.9	0.7	0.3	ND	7.27	5.0	8.8	109.8	372.1
BAR5	7.2	55.4	0.7	18.4	2.0	13.5	2.1	7.6	18.3	37.3	6.7	72.4	0.8	0.2	ND	3.05	7.2	4.9	109.8	329.4
BAR6	4.9	79.6	0.4	27.7	0.2	18.7	0.9	10.8	9.0	43.6	3.2	98.1	0.3	0.3	ND	4.66	3.0	9.2	85.4	451.4
BAR7	9.6	77.3	0.8	37.3	2.9	20.0	3.0	12.2	20.0	39.4	10.1	101.8	1.1	0.3	ND	2.60	10.8	11.1	109.8	433.1
BAR8	10.1	95.1	1.9	54.4	3.4	27.5	3.2	13.1	20.1	52.2	11.7	121.4	1.1	0.4	ND	9.71	12.5	13.4	128.1	634.4
BAR9	6.5	105.3	1.0	60.5	3.0	30.2	2.0	13.3	11.3	53.7	7.4	132.3	0.9	0.4	ND	11.40	6.5	14.4	79.3	622.2
BAR10	3.4	120.3	0.7	81.5	0.6	34.8	0.8	15.0	10.1	51.0	3.0	158.6	0.3	0.5	ND	13.49	3.5	11.9	67.1	793
BAW1	4.3	26.5	0.6	0.1	3.9	4.9	1.8	7.2	11.4	20.2	6.6	42.8	1.2	1.5	ND	ND	6.5	11.7	61	109.8
BAW2	5.0	22.0	0.5	6.1	2.7	7.0	1.9	8.5	14.3	15.1	3.6	37.5	0.1	0.1	0.9	ND	2.2	6.2	54.9	161.65
BAW3	17.0	50.8	0.1	0.6	4.5	4.5	5.5	20.4	34.8	29.2	16.7	67.8	1.2	2.5	ND	ND	29.8	1.9	231.8	225.7
BAW4	4.0	64.4	0.1	3.0	2.8	19.8	1.4	11.6	12.8	38.7	3.0	83.4	0.3	1.1	ND	ND	7.6	33.0	73.2	207.4
BAW5	20.0	48.4	2.5	7.2	2.0	3.9	9.3	26.5	29.6	21.3	35.3	98.6	0.6	0.6	ND	ND	9.9	3.8	195.2	219.6
BAW6	1.4	11.0	0.2	4.6	0.4	0.9	1.0	8.8	7.9	24.5	0.8	22.3	0.1	0.1	0.3	ND	1.3	17.5	54.9	146.4
BAW7	30.5	98.4	0.7	15.5	8.2	13.0	14.3	32.7	78.7	47.8	57.4	163.9	16.1	9.2	ND	ND	101.9	93.5	164.7	323.3
BAW8	30.1	95.5	4.6	18.6	5.7	12.4	10.7	36.6	54.1	40.7	52.2	169.1	2.5	1.6	ND	ND	35.7	18.3	237.9	384.3
BAW9	20.5	46.2	ND	13.5	3.1	4.3	4.9	20.5	39.0	30.3	21.8	65.8	6.6	5.5	ND	ND	23.7	51.8	146.4	207.4
BAW10	13.5	106.1	0.9	66.0	3.4	25.1	3.2	19.2	27.8	21.9	12.9	138.9	8.2	0.0	ND	ND	12.6	1.2	122	585.6

ND- Not detected

APPENDIX 5

Piper diagram of major ions of the river and groundwater

Appendix 5A: Piper diagram of major ions of the Bishnumati River

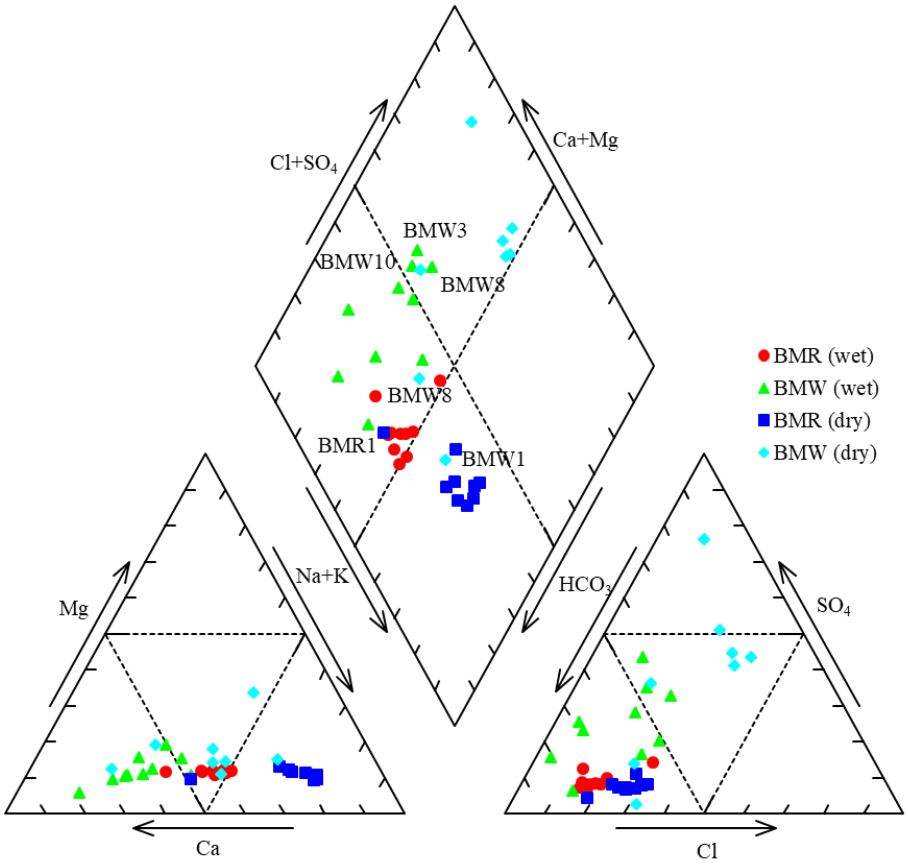

Appendix 5B: Piper diagram of major ions of the Dhobi Khola

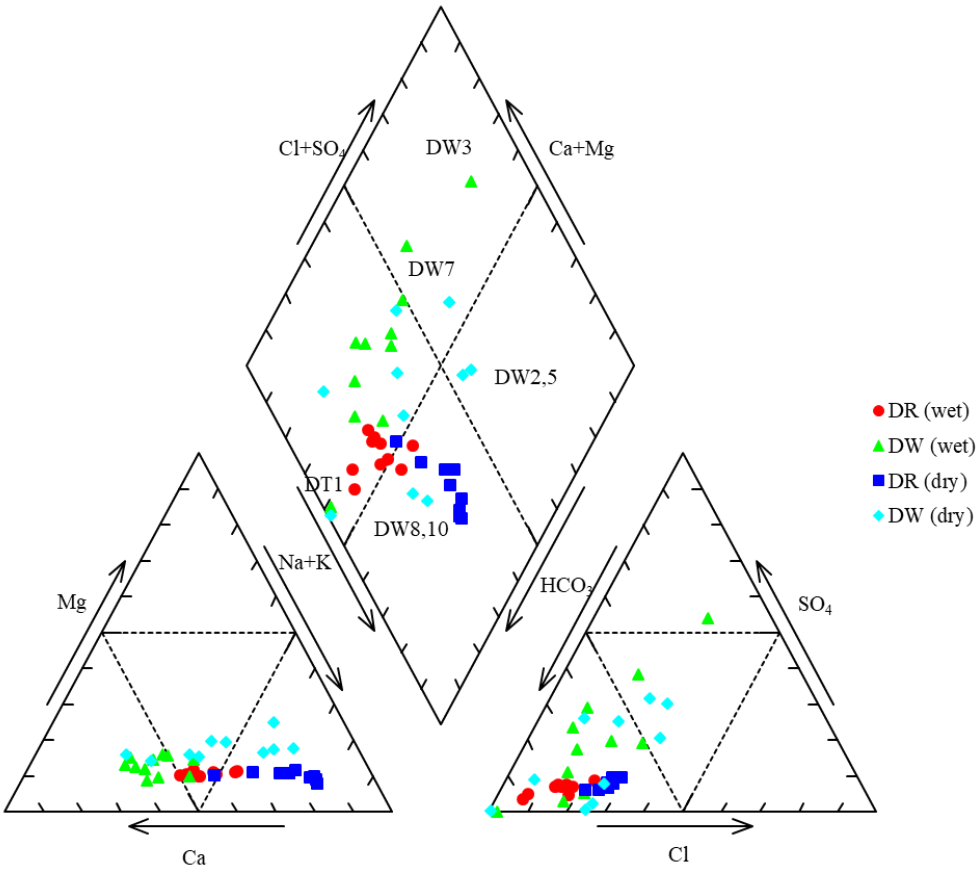

Appendix 5C: Piper diagram of major ions of the Bagmati River

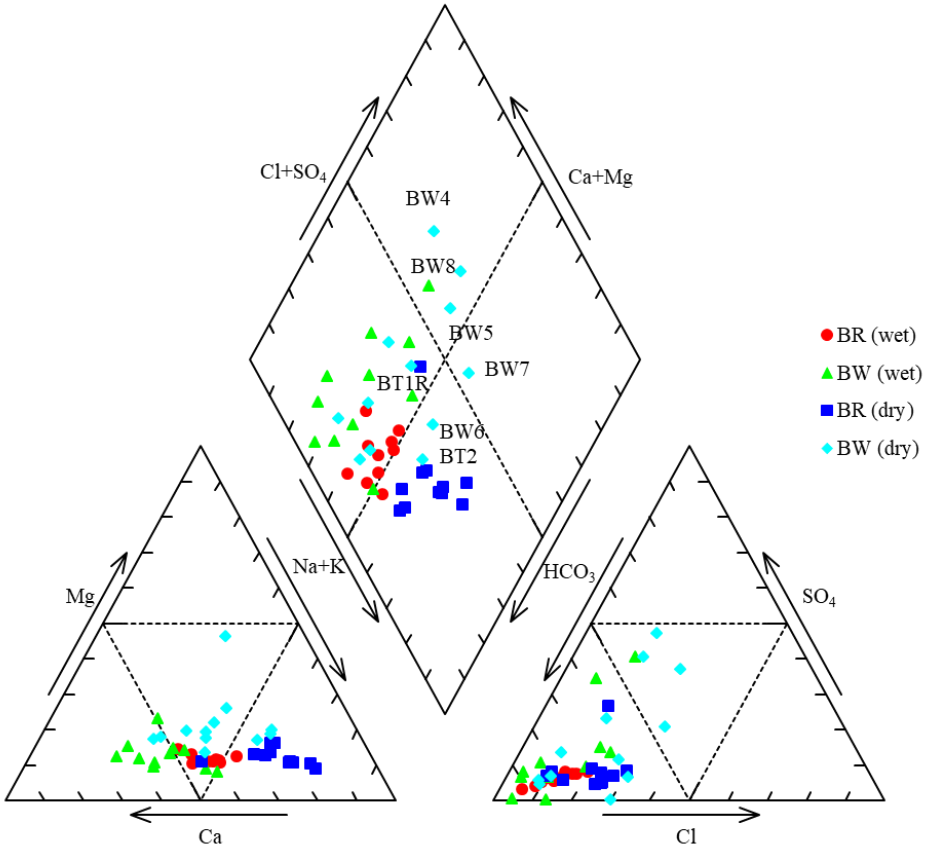

Appendix 5D: Piper diagram of major ions of the Manahara River

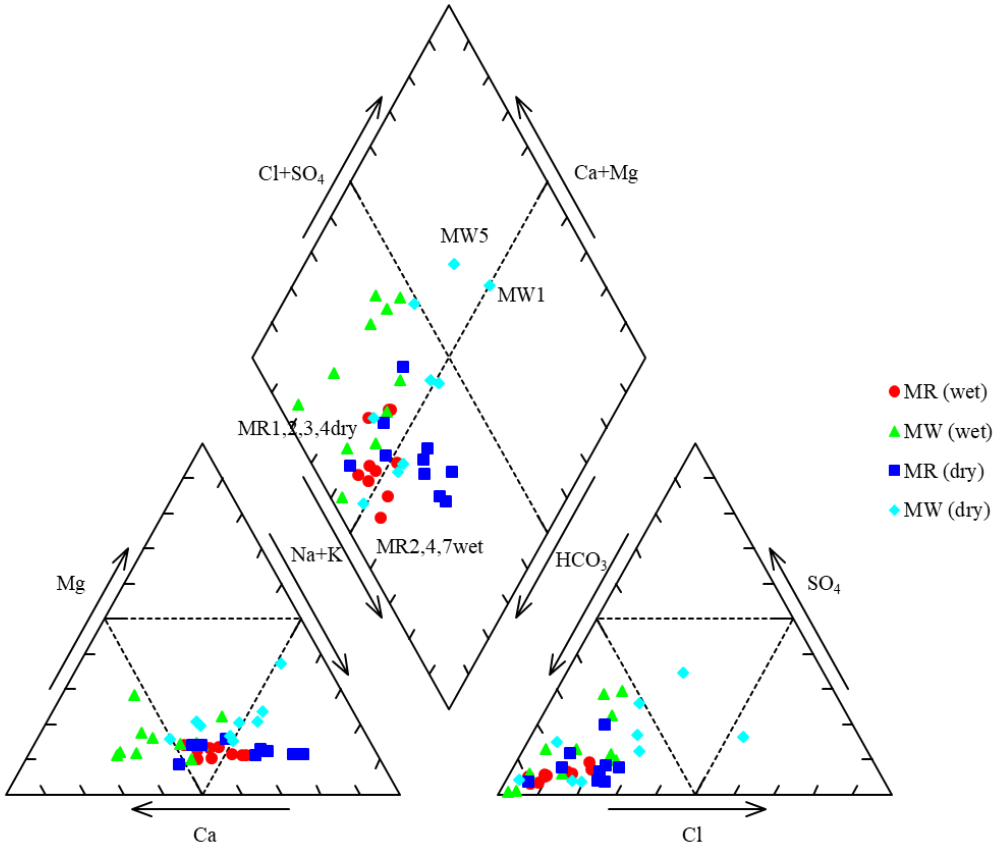

Appendix 5E: Piper diagram of major ions of the Hanumante Khola

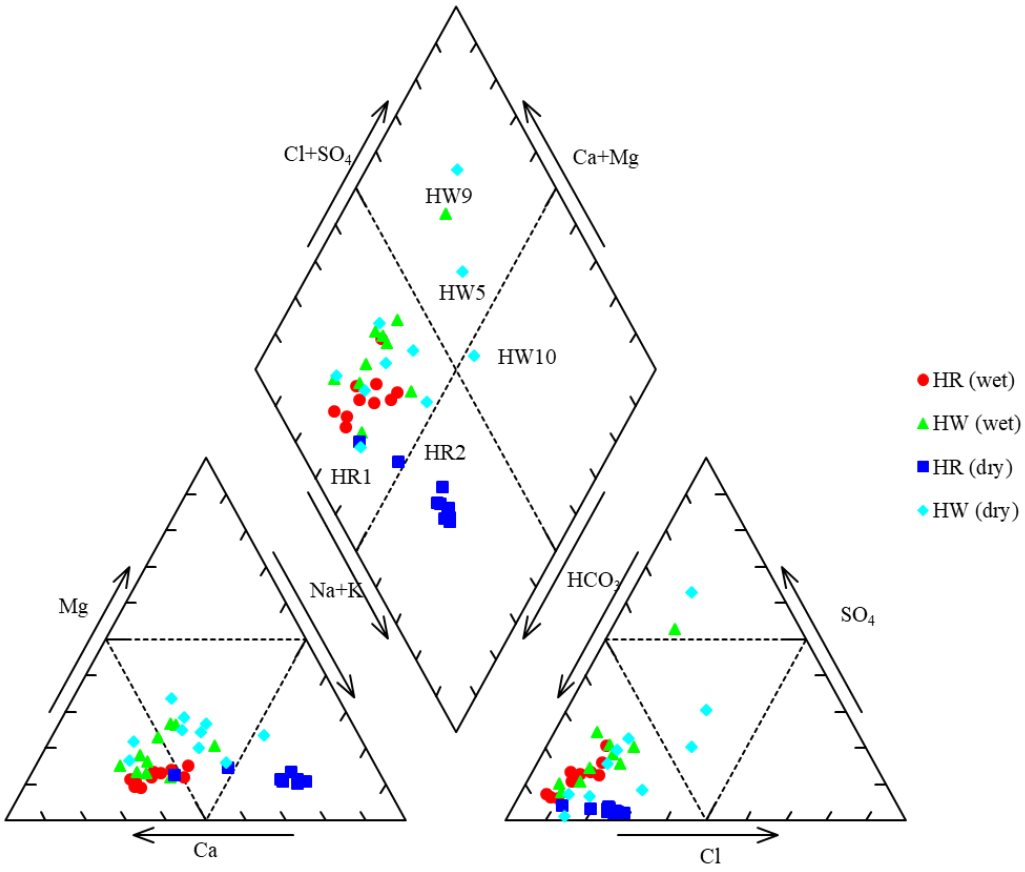

Appendix 5F: Piper diagram of major ions of the Godawari Khola

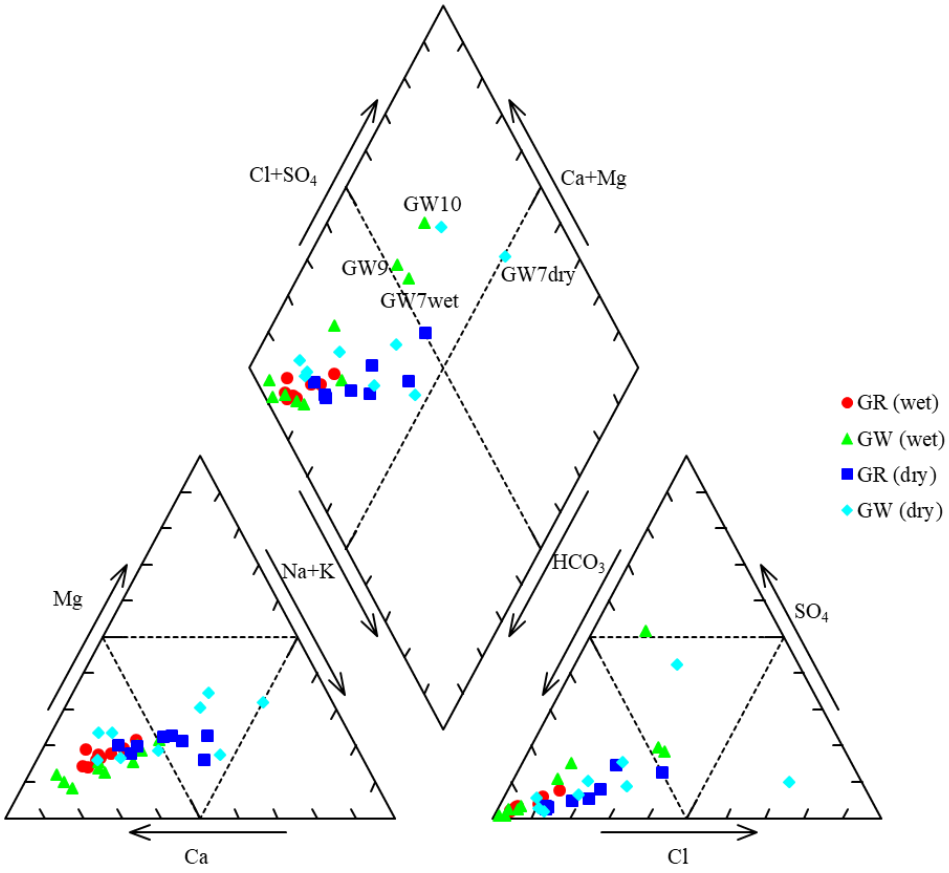

Appendix 5G: Piper diagram of major ions of the Kodku Khola

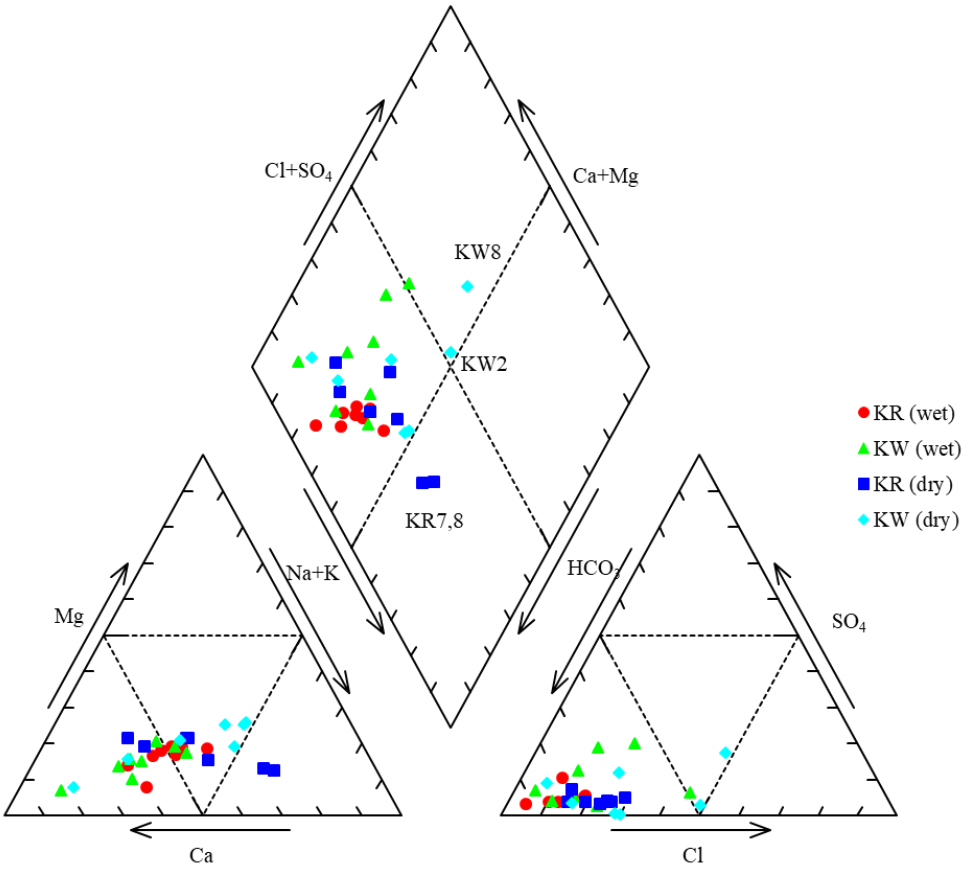

Appendix 5H: Piper diagram of major ions of the Nakhu Khola

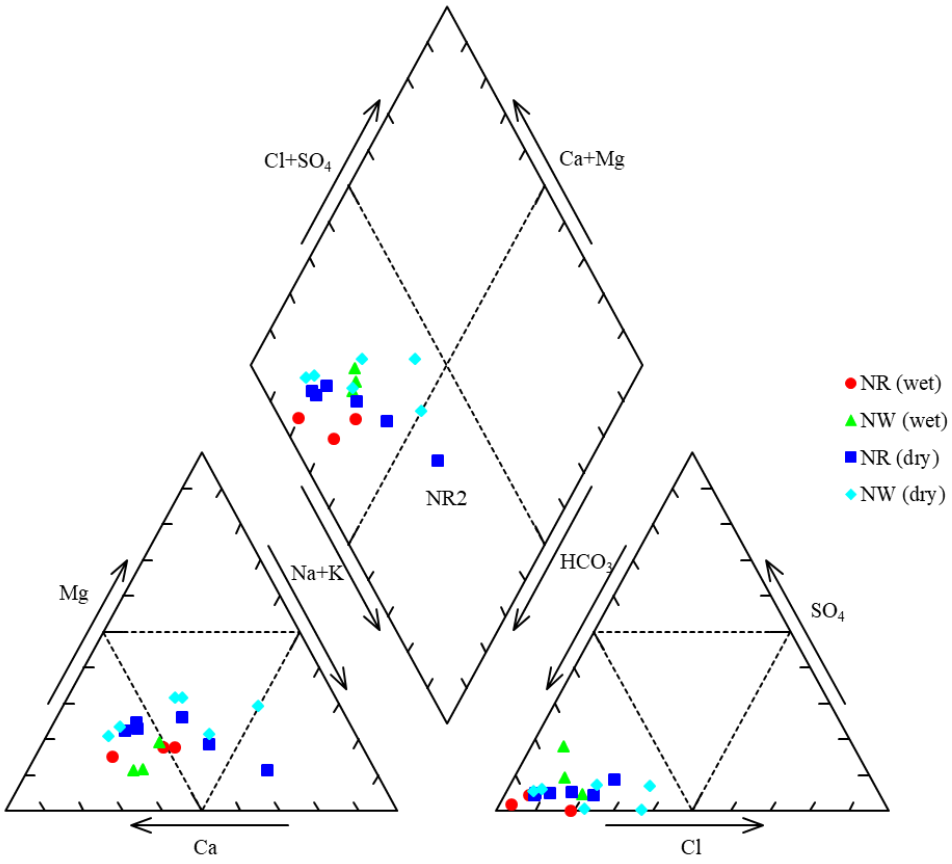

Appendix 5I: Piper diagram of major ions of the Balkhu Khola

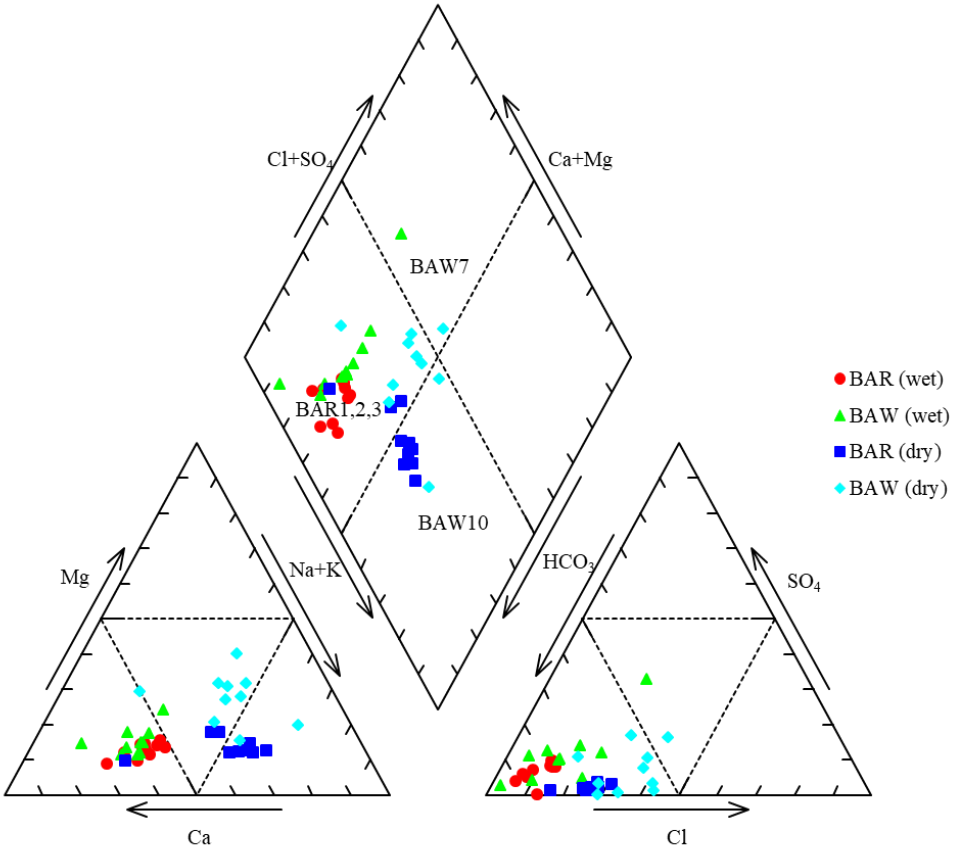

APPENDIX 6

Isotopic composition of groundwater and river water

Appendix 6A: Isotopic composition of Bishnumati river water and groundwater

Sampling ID	$\delta^{18}O$ (‰)		δD (‰)		d-excess (‰)	
	Wet	Dry	Wet	Dry	Wet	Dry
BMR1	-8.0	-8.28	-53.1	-56.72	11.1	9.56
BMR2	-8.1	-7.80	-54.2	-54.87	10.6	7.53
BMR3	-8.2	-7.90	-55.0	-56.22	10.5	6.96
BMR4	-7.8	-7.79	-53.1	-55.17	9.4	7.13
BMR5	-8.1	-8.00	-55.1	-56.47	9.8	7.57
BMR6	-8.0	-7.83	-53.9	-55.27	10.3	7.33
BMR7	-8.1	-7.82	-54.5	-55.24	10.1	7.33
BMR8	-8.1	-7.98	-55.0	-56.14	9.6	7.73
BMR9	-8.2	-8.02	-55.1	-58.36	10.8	5.76
BMR10	-8.1		-54.6		10.5	
BMW1	-6.8	-8.00	-44.8	-54.73	9.3	9.27
BMW2	-8.8	-7.13	-60.9	-51.24	9.7	5.79
BMW3	-7.7	WD	-51.6		9.6	
BMW4	-5.9	-6.61	-40.5	-50.23	6.5	2.68
BMW5	-6.7	-7.24	-44.2	-49.86	9.3	8.05
BMW6	-7.7	-7.67	-50.7	-53.17	11.2	8.23
BMW7	-7.6	-7.60	-51.2	-52.44	9.7	8.34
BMW8	-5.5	-7.36	-34.7	-50.06	9.3	8.79
BMW9	-7.6	-6.72	-53.5	-46.24	7.5	7.54
BMW10	-5.5		-34.4		9.9	

Appendix 6B: Isotopic composition of Dhobi Khola river water and groundwater

Sampling ID	$\delta^{18}O$		δD		d-excess	
	Wet	Dry	Wet	Dry	Wet	Dry
DR1	-8.4	-7.94	-55.3	-54.40	12.1	9.14
DR2	-7.8	-7.66	-54.1	-53.07	8.1	8.19
DR3	-8.4		-55.2		11.9	
DR4	-8.3	-7.59	-55.1	-53.07	11.1	7.67
DR5	-8.2	-7.61	-55.5	-53.08	10.3	7.81
DR6	-8.3	-7.69	-54.9	-53.21	11.4	8.34
DR7	-8.1	-8.30	-54.6	-57.37	10.4	9.04
DR8	-8.1	-7.90	-54.8	-54.66	10.1	8.56
DR9	-8.5	-7.86	-56.1	-54.44	11.8	8.46
DR10	-7.8	-7.92	-53.5	-54.46	9.1	8.86
DW1	-6.0	-8.09	-37.4	-55.18	10.4	9.56
DT1	-8.2	-8.35	-59.1	-60.19	6.7	6.64
DW2	-4.8	-7.22	-34.7	-47.70	3.5	10.08
DW3	-9.3		-65.3		8.9	
DW4	-6.6	-8.66	-43.7	-60.65	8.9	8.67
DW5	-7.4	-8.38	-48.1	-57.40	11.1	9.63
DW6	-7.1	-7.87	-47.1	-54.17	9.5	8.82
DW7	-7.4	-8.10	-48.1	-55.27	11.2	9.52
DW8	-6.8	-8.14	-44.3	-54.62	10.2	10.52
DW9	-7.5	-8.13	-50.1	-55.25	9.5	9.77
DW10	-5.8	-7.99	-35.7	-54.46	10.9	9.42

Appendix 6C: Isotopic composition of Bagmati river water and groundwater

Sampling ID	$\delta^{18}O$ (‰)		δD (‰)		d-excess (‰)	
	Wet	Dry	Wet	Dry	Wet	Dry
BR1	-8.9	-8.32	-58.1	-57.31	13.2	9.2
BR2	-9.0	-8.24	-59.4	-57.05	12.4	8.9
BR3	-8.9	-8.04	-60.2	-54.56	10.6	9.7
BT1R		-7.89		-54.87		8.3
BR4	-9.1	-7.88	-60.8	-54.36	11.9	8.7
BR5	-9.1	-7.75	-60.7	-53.48	12.1	8.5
BR6	-9.1	-7.78	-61.0	-53.46	11.6	8.8
BR7	-8.9	-7.90	-60.4	-53.36	10.4	9.9
BR8	-9.0	-7.75	-63.5	-52.32	8.8	9.6
BR9	-9.0	-7.93	-61.2	-53.97	10.6	9.5
BR10	-9.0	-7.55	-63.1	-53.16	9.2	7.2
BW1	-9.2	-6.91	-66.2	-51.04	7.1	4.3
BW2	-8.5	-8.28	-62.3	-57.60	5.9	8.7
BW3	-7.8	-8.57	-49.5	-56.06	12.7	12.5
BT1W		-7.89		-55.22		7.9
BW4	-7.7	-7.33	-51.9	-48.88	9.5	9.8
BT1	-7.9		-54.6		8.4	
BW5	-8.4	-8.05	-55.1	-52.99	12.3	11.4
BW6	-6.4	-8.00	-40.3	-52.92	11.2	11.1
BT2	-7.6	-8.14	-49.8	-53.75	10.8	11.3
BW7	-8.7	-7.24	-61.7	-47.86	8.1	10.1
BW8	-7.7	-7.94	-52.2	-50.16	9.6	13.4
BW9	-7.1	-7.90	-47.2	-51.28	9.9	11.9
BW10	-7.3	-7.58	-49.3	-48.97	9.4	11.7

Appendix 6D: Isotopic composition of Manahara river water and groundwater

Sampling ID	$\delta^{18}O$ (‰)		δD (‰)		d-excess (‰)	
	Wet	Dry	Wet	Dry	Wet	Dry
MR1	-8.4	-7.9	-57.1	-53.1	10.42	9.9
MR2	-8.5	-8.0	-57.7	-51.2	10.46	12.5
MR3	-8.4	-7.6	-56.9	-53.1	9.98	7.8
MR4	-8.4	-7.6	-56.8	-53.0	10.56	7.6
MR5	-8.3	-7.5	-57.8	-53.2	8.68	7.2
MR6	-8.4	-7.5	-56.7	-52.3	10.58	7.9
MR7	-8.5	-7.6	-56.7	-53.8	10.9	7.0
MR8	-8.3	-7.3	-57.4	-52.1	9.32	6.6
MR9	-8.5	-7.4	-57.9	-52.8	9.78	7.6
MR10	-7.7	-7.7	-56.1	-54.1	5.42	6.6
MW1	-6.6	-6.8	-43.1	-44.3	9.54	9.7
MW2	-6.7		-47.2		6.16	
MB1	-8.3		-60.0		6.48	
MW3	-5.3	-7.7	-32.8	-54.5	9.68	7.5
MB2	-8.4		-61.2		6.16	
MW4		-7.8		-53.8		8.3
MW5	-7.8	-7.6	-54.6	-53.6	8.04	7.1
MW6	-7.1	-7.8	-47.6	-53.8	9.28	8.7
MW7	-7.5	-7.3	-52.7	-50.4	7.54	8.2
MW8	-7.7	-8.1	-52.8	-56.2	8.64	8.5
MW9	-7.0	-6.3	-47.9	-42.9	7.86	7.4
MW10	-7.5	-7.9	-51.7	-55.8	8.62	7.4

Appendix 6E: Isotopic composition of Hanumante Khola river water and groundwater

Sampling ID	$\delta^{18}O$ (‰)		δD (‰)		d-excess (‰)	
	Wet	Dry	Wet	Dry	Wet	Dry
HR1	-8.1	-7.42	-55.7	-52.35	9.0	7.0
HR2	-8.1	-6.95	-55.4	-48.75	9.5	6.9
HR3	-8.0	-7.24	-54.5	-50.49	9.3	7.4
HR4	-8.1	-7.41	-54.9	-53.15	9.7	6.1
HR5	-8.0	-7.69	-54.7	-54.41	9.5	7.1
HR6	-8.0	-6.91	-54.8	-51.33	9.4	4.0
HR7	-8.0	-7.73	-54.3	-54.26	9.8	7.6
HR8	-7.7	-7.54	-52.0	-52.69	9.5	7.6
HR9	-8.0	-7.55	-54.8	-53.23	8.9	7.2
HR10	-8.0	-7.63	-54.9	-53.64	8.7	7.4
HW1	-6.5	-6.68	-44.3	-46.23	7.4	7.2
HW2	-8.2	-8.85	-57.8	-62.22	7.5	8.6
HW3	-7.6	-7.42	-51.5	-50.59	9.4	8.8
HW4	-6.1	-7.25	-39.9	-49.06	8.6	8.9
HW5	-8.0	-7.24	-54.7	-50.84	9.3	7.1
HW6	-7.8	-7.60	-54.2	-53.26	8.1	7.6
HW7	-8.0	-7.41	-55.9	-50.83	7.8	8.4
HW8	-7.9	-7.65	-55.0	-52.91	8.0	8.3
HW9	-7.1	-8.19	-48.8	-57.14	7.9	8.4
HW10	-7.6	-7.51	-56.9	-53.38	3.5	6.7

Appendix 6F: Isotopic composition of Godawari Khola river water and groundwater

Sampling ID	$\delta^{18}O$ (‰)		δD (‰)		d-excess (‰)	
	Wet	Dry	Wet	Dry	Wet	Dry
GR1	-8.8	-8.8	-59.6	-58.5	11.0	11.96
GR2	-8.6	-8.6	-59.3	-57.9	9.3	10.57
GR3	-8.5	-8.5	-58.5	-57.3	9.5	10.35
GR4	-8.8	-8.4	-60.4	-58.0	9.8	9.37
GR5	-8.2	-8.3	-57.1	-56.3	8.7	9.79
GR6	-8.5	-8.0	-57.9	-56.0	9.7	7.82
GR7	-8.1	-6.2	-55.9	-46.0	8.8	3.55
GR8/GW9	-8.4	-6.5	-57.4	-47.4	9.6	4.38
GR10	-8.0		-55.5		8.8	
GW1	-9.2	-9.2	-62.4	-62.1	10.9	11.43
GW2	-7.9	-8.0	-56.6	-55.1	6.8	8.76
GW3	-8.3	-7.8	-57.3	-55.3	8.7	7.41
GW4	-8.5	-8.5	-58.5	-59.5	9.5	8.59
GW5	-8.0	-7.9	-59.9	-56.5	4.3	6.85
GW6	-7.7	-7.7	-53.8	-52.3	8.0	9.13
GW7	-7.5	-7.1	-50.1	-49.5	9.7	6.99
GW8	-7.7		-52.1		9.5	
GW9	-7.4	-7.2	-50.8	-49.4	8.4	8.17
GW10	-8.5	-7.0	-58.6	-48.4	9.6	7.67

Appendix 6G: Isotopic composition of Kodku Khola river water and groundwater

Sampling ID	$\delta^{18}O$ (‰)		δD (‰)		d-excess (‰)	
	Wet	Dry	Wet	Dry	Wet	Dry
KR1	-8.4	-8.73	-58.3	-59.78	8.5	10.0
KR2	-8.1	-8.63	-56.1	-59.41	8.3	9.7
KR3	-7.9	-8.77	-56.7	-60.71	6.7	9.5
KR4	-7.9	-8.24	-56.4	-57.44	7.1	8.4
KR5	-8.3	-8.17	-58.0	-56.73	8.0	8.7
KR6	-8.0		-56.3		7.8	
KR7	-7.9	-7.86	-56.2	-54.55	7.2	8.4
KR8	-7.9	-8.03	-55.5	-56.43	7.4	7.8
KW1	-9.3	-9.34	-63.8	-65.26	10.3	9.5
KW2	-7.6	-7.89	-53.7	-55.28	6.8	7.9
KW3	-8.7	-8.53	-61.8	-59.42	8.0	8.8
KW4	-7.0	-8.66	-48.6	-59.59	7.7	9.7
KW5	-7.9	-8.02	-56.3	-55.43	6.7	8.7
KW6	-7.6		-52.8		7.8	
KW7	-7.0	-7.85	-49.2	-54.32	6.8	8.5
KW8	-7.7	-7.93	-53.5	-55.03	8.1	8.4

Appendix 6H: Isotopic composition of Nakhu Khola river water and groundwater

Sampling ID	$\delta^{18}O$ (‰)		δD (‰)		d-excess (‰)	
	Wet	Dry	Wet	Dry	Wet	Dry
NR1		-8.62		-59.53		9.39
NR2		-8.57		-59.15		9.40
NR3		-8.37		-58.23		8.75
NR4	-9.0	-8.21	-62.4	-57.06	9.3	8.60
NR5	-9.0	-7.95	-61.9	-55.47	9.7	8.15
NR6	-8.9	-8.00	-61.6	-55.36	9.2	8.60
NW1		-8.16		-57.12		8.20
NW2		-8.41		-58.34		8.90
NW3		-7.78		-54.85		7.43
NW4	-8.6	-7.56	-62.0	-53.32	6.9	7.13
NW5	-9.2	-7.97	-66.9	-55.31	7.0	8.43
NW6	-7.6	-7.83	-53.3	-54.65	7.2	8.01

Appendix 6I: Isotopic composition of Balkhu Khola river water and groundwater

Sampling ID	$\delta^{18}O$ (‰)		δD (‰)		d-excess (‰)	
	Wet	Dry	Wet	Dry	Wet	Dry
BAR1	-8.2	-8.24	-56.9	-56.46	8.7	9.45
BAR2	-8.3	-7.72	-57.8	-52.98	8.8	8.75
BAR3	-8.5	-7.54	-59.5	-52.33	8.5	8.02
BAR4	-8.4	-7.75	-59.0	-53.33	8.4	8.71
BAR5	-8.5	-7.62	-59.6	-53.43	8.4	7.51
BAR6	-8.4	-7.51	-58.4	-51.52	8.5	8.60
BAR7	-8.6	-7.45	-60.3	-50.82	8.7	8.77
BAR8	-8.6	-7.36	-59.6	-50.90	9.3	7.96
BAR9	-9.0	-7.37	-61.6	-50.86	10.8	8.10
BAR10	-8.7	-7.20	-60.3	-50.14	9.2	7.50
BAW1	-9.6	-8.06	-67.0	-55.30	9.6	9.18
BAW2	-9.4	-8.08	-66.1	-54.27	9.1	10.35
BAW3	-8.9	-7.65	-61.0	-51.27	9.8	9.91
BAW4	-10.2	-7.72	-72.1	-52.26	9.7	9.48
BAW5	-7.7	-6.83	-53.0	-47.09	8.4	7.57
BAW6	-11.4	-7.51	-81.7	-51.13	9.3	8.95
BAW7	-9.0	-7.12	-61.2	-47.87	10.6	9.06
BAW8	-8.0	-7.18	-53.7	-47.74	10.3	9.67
BAW9	-8.3	-7.62	-56.0	-51.49	10.4	9.51
BAW10	-9.2	-7.41	-63.9	-50.16	9.7	9.15

APPENDIX 7

Correlation matrix of the river and groundwater

Appendix 7A: Correlation matrix of river and groundwater of the Bishnumati River

Bishnumati River water														
Parameters	DO	EC	Temp	pH	Na^+	NH_4^+-N	K^+	Mg^{2+}	Ca^{2+}	Cl^-	NO_3^--N	PO_4^--P	SO_4^{2-}	HCO_3^-
DO	1													
EC	-.660**	1												
Temp	0.19	-.678**	1											
pH	0.24	-.779**	.942**	1										
Na^+	-.611**	.989**	-.699**	-.791**	1									
NH_4^+-N	-.606**	.977**	-.680**	-.757**	.981**	1								
K^+	-.613**	.984**	-.715**	-.791**	.997**	.982**	1							
Mg^{2+}	-.621**	.950**	-.752**	-.795**	.972**	.934**	.977**	1						
Ca^{2+}	-.652**	.906**	-.692**	-.748**	.906**	.848**	.904**	.949**	1					
Cl^-	-.608**	.990**	-.703**	-.792**	.999**	.986**	.998**	.968**	.901**	1				
NO_3^--N	.808**	-.586*	0.35	0.32	-.589*	-.545*	-.594**	-.620**	-.631**	-.587*	1			
PO_4^--P	-.846**	.978**	-.598*	-.704**	.960**	.978**	.959**	.901**	.841**	.966**	-.722**	1		
SO_4^{2-}	-.608**	.953**	-.719**	-.791**	.978**	.935**	.978**	.992**	.943**	.973**	-.596**	.894**	1	
HCO_3^-	-.603**	.965**	-.728**	-.787**	.975**	.968**	.982**	.963**	.891**	.979**	-.591**	.963**	.960**	1
Bishnumati Groundwater														
Parameters	DO	EC	Temp	pH	Na^+	NH_4^+-N	K^+	Mg^{2+}	Ca^{2+}	Cl^-	NO_3^--N	PO_4^--P	SO_4^{2-}	HCO_3^-
DO	1													
EC	0.01	1												
Temp	-.561*	-0.18	1											
pH	0.20	-0.18	0.36	1										
Na^+	0.42	.552*	-0.41	-0.02	1									
NH_4^+-N	-0.19	0.36	-0.17	-.524*	0.12	1								
K^+	0.06	.484*	-0.22	0.01	.727**	0.05	1							
Mg^{2+}	0.17	.556*	-0.23	0.04	.888**	0.21	.559*	1						
Ca^{2+}	0.10	0.42	0.09	0.01	0.31	-0.49	0.14	0.31	1					
Cl^-	0.39	.554*	-0.42	-0.03	.985**	0.23	.754**	.869**	0.21	1				
NO_3^--N	0.07	0.37	0.19	0.26	.655**	-0.17	.572*	.629**	0.37	.655**	1			
PO_4^--P	-0.61	-0.26	.747*	0.41	-0.17	-0.34	0.35	-0.24	0.01	-0.10	0.39	1		
SO_4^{2-}	0.37	.553*	-0.45	-0.18	.602**	-0.12	0.27	.576*	.757**	.519*	0.14	-0.42	1	
HCO_3^-	-.631**	0.01	.878**	0.18	-0.20	-0.23	0.11	-0.11	0.19	-0.22	0.31	.772**	-0.34	1
*. Correlation is significant at the 0.05 level (2-tailed).														
**. Correlation is significant at the 0.01 level (2-tailed).														

Appendix 7B: Correlation matrix of river and groundwater of the Dhobi Khola

Dhobi River water														
Parameters	DO	EC	Temp	pH	Na^+	NH_4^+-N	K^+	Mg^{2+}	Ca^{2+}	Cl^-	NO_3^--N	PO_4^--P	SO_4^{2-}	HCO_3^-
DO	1													
EC	-.696**	1												
Temp	0.16	-.659**	1											
pH	0.40	-.811**	.944**	1										
Na^+	-.572*	.942**	-.723**	-.842**	1									
NH_4^+-N	-.531*	.915**	-.649**	-.783**	.972**	1								
K^+	-.584**	.948**	-.721**	-.847**	.991**	.987**	1							
Mg^{2+}	-.626**	.938**	-.760**	-.867**	.967**	.893**	.946**	1						
Ca^{2+}	-.677**	.789**	-.676**	-.771**	.775**	.691**	.762**	.865**	1					
Cl^-	-.583**	.951**	-.727**	-.847**	.997**	.974**	.994**	.964**	.783**	1				
NO_3^--N	.887**	-.807**	0.37	.604*	-.764**	-.689**	-.740**	-.785**	-.640*	-.766**	1			
PO_4^--P	-.556*	.963**	-.723**	-.847**	.987**	.954**	.981**	.958**	.752**	.985**	-.719**	1		
SO_4^{2-}	-.587**	.915**	-.698**	-.810**	.986**	.929**	.960**	.975**	.803**	.977**	-.778**	.969**	1	
HCO_3^-	-.602**	.953**	-.684**	-.823**	.987**	.989**	.996**	.939**	.769**	.992**	-.757**	.975**	.957**	1
Dhobi Groundwater														
Parameters	DO	EC	Temp	pH	Na^+	NH_4^+-N	K^+	Mg^{2+}	Ca^{2+}	Cl^-	NO_3^--N	PO_4^--P	SO_4^{2-}	HCO_3^-
DO	1													
EC	-0.19	1												
Temp	-.581**	-0.03	1											
pH	-.460*	0.09	.741**	1										
Na^+	0.04	.825**	-0.09	-0.04	1									
NH_4^+-N	-0.31	.672**	0.02	0.10	.672**	1								
K^+	0.19	.812**	-0.24	0.02	.887**	.532*	1							
Mg^{2+}	0.32	.663**	-0.11	-0.04	.858**	0.33	.851**	1						
Ca^{2+}	0.00	0.33	0.43	0.29	0.28	-0.01	0.27	.526*	1					
Cl^-	0.11	.806**	-0.10	0.04	.964**	.641**	.918**	.906**	0.35	1				
NO_3^--N	0.10	-0.18	0.35	0.20	0.07	-0.25	-0.04	0.30	.484*	0.14	1			
PO_4^--P	-0.57	-0.37	.826**	.882**	-0.41	-0.06	-0.40	-0.47	-0.36	-0.38	-0.36	1		
SO_4^{2-}	.519*	-0.04	0.09	0.04	0.07	-0.37	0.20	.461*	.665**	0.18	0.30	-0.41	1	
HCO_3^-	-0.21	.830**	-0.05	-0.04	.811**	.806**	.714**	.626**	0.32	.775**	-0.10	-0.41	-0.18	1
**. Correlation is significant at the 0.01 level (2-tailed).														
*. Correlation is significant at the 0.05 level (2-tailed).														

Appendix 7C: Correlation matrix of river and groundwater of the Bagmati River

Bagmati River water														
Parameters	DO	EC	Temp	pH	Na^+	NH_4^+-N	K^+	Mg^{2+}	Ca^{2+}	Cl^-	NO_3^--N	PO_4^--P	SO_4^{2-}	HCO_3^-
DO	1													
EC	-.800**	1												
Temp	0.02	-.469*	1											
pH	0.21	-.493*	.846**	1										
Na^+	-.763**	.949**	-.530*	-.530*	1									
NH_4^+-N	-.742**	.946**	-.451*	-.437*	.942**	1								
K^+	-.787**	.968**	-.491*	-.500*	.988**	.978**	1							
Mg^{2+}	-.776**	.974**	-.511*	-.519*	.965**	.960**	.981**	1						
Ca^{2+}	-.763**	.914**	-0.35	-0.40	.867**	.890**	.894**	.941**	1					
Cl^-	-.800**	.975**	-.484*	-.504*	.989**	.968**	.997**	.976**	.889**	1				
NO_3^--N	.676**	-.727**	0.40	.618**	-.721**	-.730**	-.741**	-.700**	-.578**	-.753**	1			
PO_4^--P	-.808**	.987**	-.595*	-0.45	.923**	.956**	.960**	.958**	.893**	.969**	-.779**	1		
SO_4^{2-}	-.675**	.820**	-.532*	-.648**	.860**	.758**	.834**	.855**	.864**	.843**	-.642**	.709**	1	
HCO_3^-	-.784**	.982**	-.488*	-.485*	.970**	.983**	.991**	.989**	.921**	.987**	-.720**	.975**	.814**	1
Bagmati Groundwater														
Parameters	DO	EC	Temp	pH	Na^+	NH_4^+-N	K^+	Mg^{2+}	Ca^{2+}	Cl^-	NO_3^--N	PO_4^--P	SO_4^{2-}	HCO_3^-
DO	1													
EC	0.32	1												
Temp	-0.18	-0.03	1											
pH	-0.01	0.14	.679**	1										
Na^+	-0.10	.407*	-.460*	-0.21	1									
NH_4^+-N	-0.03	0.28	-0.20	-0.20	.527**	1								
K^+	-0.13	0.19	-0.03	0.09	.626**	.417*	1							
Mg^{2+}	0.29	.431*	-.489*	-0.07	.745**	0.35	.431*	1						
Ca^{2+}	-0.12	.430*	0.08	0.11	.636**	0.22	.624**	.537**	1					
Cl^-	-0.10	0.38	-.522**	-0.22	.971**	0.41	.536**	.719**	.537**	1				
NO_3^--N	0.15	0.21	-0.15	0.24	.532*	-0.11	.438*	.781**	.688**	.497*	1			
PO_4^--P	0.22	0.05	0.12	0.28	0.12	.669*	0.28	0.07	-0.08	0.03	-0.13	1		
SO_4^{2-}	-0.19	0.23	-0.22	-0.14	.624**	0.10	.566**	.407*	.711**	.566**	.517*	-0.12	1	
HCO_3^-	0.08	.477*	-0.28	-0.14	.708**	.872**	.509*	.663**	.477*	.615**	0.21	0.44	0.17	1
*. Correlation is significant at the 0.05 level (2-tailed).														
**. Correlation is significant at the 0.01 level (2-tailed).														

Appendix 7D: Correlation matrix of river and groundwater of the Manahara River

Manahara River water														
Parameters	DO	EC	Temp	pH	Na^+	NH_4^+-N	K^+	Mg^{2+}	Ca^{2+}	Cl^-	NO_3^--N	PO_4^--P	SO_4^{2-}	HCO_3^-
DO	1													
EC	-.762**	1												
Temp	0.40	-.537*	1											
pH	.571**	-.526*	.815**	1										
Na^+	-.800**	.907**	-.630**	-.670**	1									
NH_4^+-N	-.764**	.886**	-.538*	-.573**	.977**	1								
K^+	-.793**	.890**	-.636**	-.657**	.991**	.988**	1							
Mg^{2+}	-.811**	.902**	-.690**	-.683**	.986**	.953**	.981**	1						
Ca^{2+}	-.662**	.780**	-.758**	-.689**	.856**	.763**	.830**	.899**	1					
Cl^-	-.821**	.902**	-.623**	-.659**	.997**	.981**	.995**	.984**	.838**	1				
NO_3^--N	.843**	-.520*	-0.004	0.19	-.539*	-.566**	-.539*	-.516*	-0.29	-.573**	1			
PO_4^--P	-.777**	.904**	-.564**	-.538*	.954**	.955**	.961**	.960**	.821**	.956**	-.576**	1		
SO_4^{2-}	-.683**	.685**	-.792**	-.823**	.815**	.703**	.788**	.832**	.926**	.804**	-0.30	.695**	1	
HCO_3^-	-.786**	.896**	-.645**	-.647**	.991**	.983**	.995**	.988**	.848**	.992**	-.533*	.968**	.784**	1
Manahara Groundwater														
Parameters	DO	EC	Temp	pH	Na^+	NH_4^+-N	K^+	Mg^{2+}	Ca^{2+}	Cl^-	NO_3^--N	PO_4^--P	SO_4^{2-}	HCO_3^-
DO	1													
EC	-0.36	1												
Temp	-0.34	-0.04	1											
pH	-0.11	0.28	.537*	1										
Na^+	-0.18	.544*	-.489*	-0.19	1									
NH_4^+-N	-0.35	.684**	-0.16	0.18	.625**	1								
K^+	-0.18	0.20	-0.27	-.567**	.504*	0.14	1							
Mg^{2+}	-0.27	.747**	-0.37	-0.02	.904**	.724**	.454*	1						
Ca^{2+}	-0.17	.564**	-0.03	-0.15	0.19	0.05	.459*	0.26	1					
Cl^-	0.10	0.37	-0.39	-0.20	.749**	0.29	.543*	.742**	0.18	1				
NO_3^--N	-0.09	0.18	-0.16	-0.36	0.27	-0.06	.542*	0.25	.644**	0.09	1			
PO_4^--P	-0.21	0.11	0.05	-0.06	0.22	0.38	0.10	0.06	0.14	-0.28	0.37	1		
SO_4^{2-}	-0.14	0.43	-0.15	-0.26	.614**	0.17	.628**	.659**	.576**	.743**	.539*	-0.05	1	
HCO_3^-	-0.42	.814**	-0.20	0.16	.607**	.902**	0.20	.684**	0.33	0.20	0.07	0.38	0.14	1
*. Correlation is significant at the 0.05 level (2-tailed).														
**. Correlation is significant at the 0.01 level (2-tailed).														

Appendix 7E: Correlation matrix of river and groundwater of the Hanumante Khola

Hanumante River water														
Parameters	DO	EC	Temp	pH	Na^+	NH_4^+-N	K^+	Mg^{2+}	Ca^{2+}	Cl^-	NO_3^--N	PO_4^--P	SO_4^{2-}	HCO_3^-
DO	1													
EC	-.949**	1												
Temp	.726**	-.864**	1											
pH	.765**	-.775**	.731**	1										
Na^+	-.916**	.957**	-.786**	-.698**	1									
NH_4^+-N	-.926**	.975**	-.818**	-.719**	.971**	1								
K^+	-.919**	.967**	-.815**	-.706**	.956**	.993**	1							
Mg^{2+}	-.930**	.985**	-.867**	-.735**	.974**	.983**	.979**	1						
Ca^{2+}	-.853**	.934**	-.935**	-.710**	.919**	.899**	.896**	.958**	1					
Cl^-	-.928**	.970**	-.808**	-.719**	.990**	.990**	.975**	.982**	.916**	1				
NO_3^--N	0.12	-0.20	0.37	0.32	-0.11	-0.14	-0.10	-0.14	-0.21	-0.12	1			
PO_4^--P	-.854**	.917**	-0.56	-.766**	.799**	.934**	.912**	.868**	.676*	.828**	.767**	1		
SO_4^{2-}	-.826**	.871**	-.767**	-.601**	.870**	.925**	.944**	.911**	.844**	.886**	0.02	.806**	1	
HCO_3^-	-.920**	.968**	-.853**	-.728**	.983**	.987**	.976**	.990**	.946**	.989**	-0.16	.820**	.915**	1
Hanumante Groundwater														
Parameters	DO	EC	Temp	pH	Na^+	NH_4^+-N	K^+	Mg^{2+}	Ca^{2+}	Cl^-	NO_3^--N	PO_4^--P	SO_4^{2-}	HCO_3^-
DO	1													
EC	-0.39	1												
Temp	0.39	-0.28	1											
pH	0.34	-0.24	.666**	1										
Na^+	-0.24	.740**	-.459*	-0.43	1									
NH_4^+-N	-.631**	.632**	-0.13	-0.12	0.25	1								
K^+	-0.40	.736**	0.01	-0.09	.447*	.802**	1							
Mg^{2+}	-.542*	.772**	-.580**	-0.35	.684**	.665**	.638**	1						
Ca^{2+}	0.11	.497*	-0.11	-0.17	0.35	0.16	0.32	0.42	1					
Cl^-	-0.28	.727**	-.488*	-0.43	.970**	0.25	0.40	.697**	0.37	1				
NO_3^--N	0.33	0.25	0.20	-0.13	0.38	-0.16	0.21	-0.07	0.35	0.38	1			
PO_4^--P	-0.23	0.65	0.31	0.62	0.27	0.59	0.65	0.48	0.54	0.09	-0.45	1		
SO_4^{2-}	0.15	0.14	-0.25	-0.36	0.19	-0.26	-0.18	0.10	.643**	0.24	-0.02	-0.41	1	
HCO_3^-	-0.43	.633**	-0.09	0.03	0.35	.800**	.789**	.733**	0.32	0.31	0.03	0.68	-0.35	1

**. Correlation is significant at the 0.01 level (2-tailed).

*. Correlation is significant at the 0.05 level (2-tailed).

Appendix 7F: Correlation matrix of river and groundwater of the Godawari Khola

Godawari River water													
Parameters	DO	EC	Temp	pH	Na^+	NH_4^+-N	K^+	Mg^{2+}	Ca^{2+}	Cl^-	NO_3^- -N	SO_4^{2-}	HCO_3^-
DO	1												
EC	0.04	1											
Temp	-0.43	-0.36	1										
pH	-0.46	-0.24	.623**	1									
Na^+	0.24	.913**	-0.44	-0.33	1								
NH_4^+-N	0.45	.553*	-0.25	-0.39	.785**	1							
K^+	0.38	.730**	-.625**	-.605*	.844**	.757**	1						
Mg^{2+}	0.06	.896**	-.528*	-0.39	.900**	.506*	.804**	1					
Ca^{2+}	0.03	.535*	-0.35	-0.46	.663**	.528*	.695**	.739**	1				
Cl^-	0.15	.937**	-0.44	-0.25	.982**	.701**	.799**	.916**	.604*	1			
NO_3^- -N	0.32	-0.14	-.673**	-0.37	-0.10	-0.24	0.25	0.07	0.12	-0.14	1		
SO_4^{2-}	0.25	.821**	-0.23	-0.22	.948**	.883**	.741**	.759**	.601*	.914**	-0.313	1	
HCO_3^-	0.10	0.43	-0.06	-0.48	0.48	.540*	.498*	0.42	.751**	0.40	-0.18	.502*	1
Godawari Groundwater													
Parameters	DO	EC	Temp	pH	Na^+	NH_4^+-N	K^+	Mg^{2+}	Ca^{2+}	Cl^-	NO_3^- -N	SO_4^{2-}	HCO_3^-
DO	1												
EC	-0.21	1											
Temp	-0.06	0.03	1										
pH	0.39	-0.19	.690**	1									
Na^+	-0.30	0.41	-0.19	-.484*	1								
NH_4^+-N	0.01	.932**	0.13	0.03	0.19	1							
K^+	-0.24	.765**	0.05	-0.28	.580**	.753**	1						
Mg^{2+}	-0.26	.502*	-0.18	-.493*	.981**	0.28	.599**	1					
Ca^{2+}	-0.27	.701**	0.19	-0.17	0.45	.657**	.926**	.500*	1				
Cl^-	-0.28	0.31	-0.17	-.477*	.986**	0.09	.506*	.957**	0.389	1			
NO_3^- -N	-0.19	0.01	0.25	-0.02	0.23	-0.09	0.21	0.27	0.37	0.26	1		
SO_4^{2-}	-0.14	.718**	0.09	-0.15	0.40	.752**	.948**	0.420	.910**	0.31	0.03	1	
HCO_3^-	-0.19	.849**	0.17	-0.02	0.39	.754**	.604**	.511*	.649**	0.27	0.09	.591**	1
**. Correlation is significant at the 0.01 level (2-tailed).													
*. Correlation is significant at the 0.05 level (2-tailed).													

Appendix 7G: Correlation matrix of river and groundwater of the Kodku Khola

Kodku River water														
Parameters	DO	EC	Temp	pH	Na^+	NH_4^+-N	K^+	Mg^{2+}	Ca^{2+}	Cl^-	NO_3^--N	PO_4^--P	SO_4^{2-}	HCO_3^-
DO	1													
EC	-.691**	1												
Temp	-0.24	-0.32	1											
pH	0.26	-.651**	.831**	1										
Na^+	-.675**	.988**	-0.36	-.694**	1									
NH_4^+-N	-.624*	.991**	-0.36	-.651**	.988**	1								
K^+	-.663**	.993**	-0.37	-.688**	.997**	.993**	1							
Mg^{2+}	-.612*	.905**	-0.48	-.782**	.939**	.894**	.933**	1						
Ca^{2+}	-.711**	.912**	-0.42	-.763**	.940**	.898**	.934**	.948**	1					
Cl^-	-.668**	.985**	-0.39	-.718**	.999**	.982**	.995**	.952**	.945**	1				
NO_3^--N	-0.22	-0.02	0.38	0.24	-0.02	-0.01	-0.02	-0.19	0.05	-0.06	1			
PO_4^--P	-0.97	0.97	0.38	0.14	0.98	0.98	0.98	0.94	0.86	0.99	0.98	1		
SO_4^{2-}	-.792**	.945**	-0.22	-.609*	.950**	.926**	.952**	.880**	.932**	.944**	0.20	1.000*	1	
HCO_3^-	-.710**	.988**	-0.30	-.650**	.990**	.984**	.990**	.924**	.930**	.987**	-0.02	0.93	.943**	1
Kodku Groundwater														
Parameters	DO	EC	Temp	pH	Na^+	NH_4^+-N	K^+	Mg^{2+}	Ca^{2+}	Cl^-	NO_3^--N	SO_4^{2-}	HCO_3^-	
DO	1													
EC	-0.13	1												
Temp	-0.13	0.17	1											
pH	0.21	-0.24	.601*	1										
Na^+	0.18	.706**	-0.18	-0.40	1									
NH_4^+-N	-0.31	0.51	-0.12	-0.39	.608*	1								
K^+	-0.33	0.44	-0.15	-0.48	.648**	.878**	1							
Mg^{2+}	0.23	.710**	-0.20	-0.41	.968**	0.512	.519*	1						
Ca^{2+}	-0.21	.733**	0.21	0.05	0.33	0.06	0.03	0.35	1					
Cl^-	0.27	.699**	-0.19	-0.47	.962**	0.50	.544*	.971**	0.29	1				
NO_3^--N	.619*	0.43	-0.11	0.07	.571*	-0.23	-0.17	.671*	0.46	.595*	1			
SO_4^{2-}	0.10	0.45	0.08	0.07	0.28	-0.31	-0.24	0.33	.744**	0.25	.694**	1		
HCO_3^-	-0.46	.742**	0.08	-0.24	.616*	.881**	.806**	.523*	0.46	0.48	-0.09	0.01	1	
*. Correlation is significant at the 0.05 level (2-tailed).														
**. Correlation is significant at the 0.01 level (2-tailed).														

Appendix 7H: Correlation matrix of river and groundwater of the Nakhu Khola

Nakhu River water													
Parameters	DO	EC	Temp	pH	Na^+	NH_4^+-N	K^+	Mg^{2+}	Ca^{2+}	Cl^-	NO_3^--N	SO_4^{2-}	HCO_3^-
DO	1												
EC	-.854**	1											
Temp	-0.02	-0.25	1										
pH	0.58	-0.66	.762*	1									
Na^+	-.864**	.993**	-0.21	-0.63	1								
NH_4^+-N	-.792*	.983**	-0.20	-0.56	.978**	1							
K^+	-.870**	.996**	-0.20	-0.62	1.000**	.996**	1						
Mg^{2+}	-.799**	.885**	-0.51	-.851**	.894**	.810**	.909**	1					
Ca^{2+}	-.796*	.942**	-0.35	-0.66	.960**	.906**	.965**	.942**	1				
Cl^-	-.866**	.993**	-0.22	-0.64	1.000**	.974**	1.000**	.900**	.963**	1			
NO_3^--N	0.10	-0.13	0.49	0.40	-0.169	-0.12	-0.11	-0.31	-0.27	-0.18	1		
SO_4^{2-}	-.797*	.987**	-0.17	-0.58	.981**	.998**	.999**	.823*	.918**	.977**	-0.07	1	
HCO_3^-	-.874**	.985**	-0.12	-0.56	.981**	.970**	.984**	.828**	.921**	.981**	-0.06	.972**	1
Nakhu Groundwater													
Parameters	DO	EC	Temp	pH	Na^+	NH_4^+-N	K^+	Mg^{2+}	Ca^{2+}	Cl^-	NO_3^--N	SO_4^{2-}	HCO_3^-
DO	1												
EC	0.26	1											
Temp	0.36	0.47	1										
pH	0.31	0.60	.835**	1									
Na^+	0.13	0.52	-0.01	-0.09	1								
NH_4^+-N	0.14	.719*	-0.17	0.12	0.56	1							
K^+	0.38	0.53	0.02	0.27	0.59	.745*	1						
Mg^{2+}	0.15	0.56	-0.31	-0.13	.784*	.830**	0.581	1					
Ca^{2+}	-0.25	0.06	0.58	0.21	0.13	-0.43	-0.49	-0.25	1				
Cl^-	0.09	0.45	-0.18	-0.20	.978**	0.64	0.65	.824**	-0.03	1			
NO_3^--N	-0.06	0.53	0.02	0.13	-0.07	0.39	-0.25	0.31	0.05	-0.09	1		
SO_4^{2-}	0.19	0.28	.732*	0.53	-0.14	-0.43	-0.32	-0.40	0.50	-0.32	0.15	1	
HCO_3^-	0.06	0.43	0.31	0.22	.732*	0.42	0.47	0.51	0.43	.695*	-0.15	-0.21	1
*. Correlation is significant at the 0.05 level (2-tailed).													
**. Correlation is significant at the 0.01 level (2-tailed).													

Appendix 7I: Correlation matrix of river and groundwater of the Balkhu Khola

Balkhu River water														
Parameters	DO	EC	Temp	pH	Na^+	NH_4^+-N	K^+	Mg^{2+}	Ca^{2+}	Cl^-	NO_3^--N	PO_4^--P	SO_4^{2-}	HCO_3^-
DO	1													
EC	-.844**	1												
Temp	0.37	-.717**	1											
pH	.561*	-.770**	.880**	1										
Na^+	-.819**	.944**	-.691**	-.746**	1									
NH_4^+-N	-.839**	.935**	-.563**	-.659**	.964**	1								
K^+	-.844**	.944**	-.624**	-.712**	.991**	.982**	1							
Mg^{2+}	-.797**	.925**	-.722**	-.778**	.987**	.934**	.974**	1						
Ca^{2+}	-.762**	.938**	-.741**	-.782**	.927**	.880**	.923**	.928**	1					
Cl^-	-.819**	.949**	-.697**	-.749**	.999**	.966**	.991**	.988**	.927**	1				
NO_3^--N	0.22	-0.42	.650**	0.38	-0.40	-0.32	-0.31	-0.37	-0.32	-0.40	1			
PO_4^--P	-.736*	.886**	0.27	-.787*	.817*	.896**	.877**	.736*	.904**	.817*	.930**	1		
SO_4^{2-}	-.656**	.519*	-0.02	-0.25	.591**	.618**	.654**	.618**	.587**	.584**	0.37	.723*	1	
HCO_3^-	-.835**	.952**	-.625**	-.707**	.984**	.987**	.992**	.960**	.929**	.984**	-0.33	.885**	.622**	1
Balkhu Groundwater														
Parameters	DO	EC	Temp	pH	Na^+	NH_4^+-N	K^+	Mg^{2+}	Ca^{2+}	Cl^-	NO_3^--N	SO_4^{2-}	HCO_3^-	
DO	1													
EC	-.524*	1												
Temp	.597**	-.572**	1											
pH	.709**	-.536*	.829**	1										
Na^+	-.515*	.921**	-.663**	-.618**	1									
NH_4^+-N	-.481*	.611**	-0.44	-0.39	.725**	1								
K^+	-.454*	.755**	-.492*	-0.40	.827**	.754**	1							
Mg^{2+}	-.477*	.833**	-.659**	-.650**	.866**	0.45	.480*	1						
Ca^{2+}	-0.13	.548*	0.01	-0.09	0.34	-0.01	0.27	0.39	1					
Cl^-	-.504*	.926**	-.667**	-.637**	.974**	.635**	.730**	.937**	0.38	1				
NO_3^--N	-0.05	0.34	0.17	0.06	0.12	-0.10	0.04	0.20	.764**	0.15	1			
SO_4^{2-}	-0.10	.554*	-0.01	-0.10	0.30	-0.04	0.21	0.37	.826**	0.34	.825**	1		
HCO_3^-	-.511*	.803**	-.536*	-.471*	.890**	.871**	.790**	.705**	0.30	.834**	0.00	0.14	1	
*. Correlation is significant at the 0.05 level (2-tailed).														
**. Correlation is significant at the 0.01 level (2-tailed).														